ISSN 0021-9673

VOL. 555 NOS. 1 + 2 AUGUST 30, 1991

JOURNAL OF CHROMATOGRAPHY

INCLUDING ELECTROPHORESIS AND OTHER SEPARATION METHODS

ELSEVIER

JOURNAL OF CHROMATOGRAPHY

Scope. The *Journal of Chromatography* publishes papers on all aspects of chromatography, electrophoresis and related methods. Contributions consist mainly of research papers dealing with chromatographic theory, instrumental development and their applications. The section *Biomedical Applications*, which is under separate editorship, deals with the following aspects: developments in and applications of chromatographic and electrophoretic techniques related to clinical diagnosis or alterations during medical treatment; screening and profiling of body fluids or tissues with special reference to metabolic disorders; results from basic medical research with direct consequences in clinical practice; drug level monitoring and pharmacokinetic studies; clinical toxicology; analytical studies in occupational medicine.

Submission of Papers. Manuscripts (in English; *four* copies are required) should be submitted to: Editorial Office of *Journal of Chromatography*, P.O. Box 681, 1000 AR Amsterdam, The Netherlands, Telefax (+31-20) 5862 304, or to: The Editor of *Journal of Chromatography, Biomedical Applications*, P.O. Box 681, 1000 AR Amsterdam, The Netherlands. Review articles are invited or proposed by letter to the Editors. An outline of the proposed review should first be forwarded to the Editors for preliminary discussion prior to preparation. Submission of an article is understood to imply that the article is original and unpublished and is not being considered for publication elsewhere. For copyright regulations, see below.

Publication. The *Journal of Chromatography* (incl. *Biomedical Applications*) has 38 volumes in 1991. The subscription prices for 1991 are:

J. Chromatogr. (incl. *Cum. Indexes, Vols. 501–550*) + *Biomed. Appl.* (Vols. 535–572):
Dfl. 7220.00 plus Dfl. 1140.00 (p.p.h.) (total *ca.* US$ 4400.00)

J. Chromatogr. (incl. *Cum. Indexes, Vols. 501–550*) only (Vols. 535–561):
Dfl. 5859.00 plus Dfl. 810.00 (p.p.h.) (total *ca.* US$ 3510.00)

Biomed. Appl. only (Vols. 562–572):
Dfl. 2387.00 plus Dfl. 330.00 (p.p.h.) (total *ca.* US$ 1430.00).

Subscription Orders. The Dutch guilder price is definitive. The US$ price is subject to exchange-rate fluctuations and is given as a guide. Subscriptions are accepted on a prepaid basis only, unless different terms have been previously agreed upon. Subscriptions orders can be entered only by calender year (Jan.–Dec.) and should be sent to Elsevier Science Publishers, Journal Department, P.O. Box 211, 1000 AE Amsterdam, The Netherlands, Tel. (+31-20) 5803 642, Telefax (+31-20) 5803 598, or to your usual subscription agent. Postage and handling charges include surface delivery except to the following countries where air delivery via SAL (Surface Air Lift) mail is ensured: Argentina, Australia, Brazil, Canada, Hong Kong, India, Israel, Japan*, Malaysia, Mexico, New Zealand, Pakistan, PR CHina, Singapore, South Africa, South Korea, Taiwan, Thailand, USA. * For Japan air delivery (SAL) requires 50% additional charge of the normal postage and handling charge. For all other countries airmail rates are available upon request. Claims for missing issues must be made within three months of our publication (mailing) date, otherwise such claims cannot be honoured free of charge. Back volumes of the *Journal of Chromatography* (Vols. 1–534) are available at Dfl. 208.00 (plus postage). Customers in the USA and Canada wishing information on this and other Elsevier journals, please contact Journal Information Center, Elsevier Science Publishing Co. Inc., 655 Avenue of the Americas, New York, NY 10010, USA, Tel. (+1-212) 633 3750, Telefax (+1-212) 633 3990.

Abstracts/Contents Lists published in Analytical Abstracts, Biochemical Abstracts, Biological Abstracts, Chemical Abstracts, Chemical Titles, Chromatography Abstracts, Clinical Chemistry Lookout, Current Contents/Life Sciences, Current Contents/Physical, Chemical & Earth Sciences, Deep-Sea Research/Part B: Oceanographic Literature Review, Excerpta Medica, Index Medicus, Mass Spectrometry Bulletin, PASCAL-CNRS, Pharmaceutical Abstracts, Referativnyi Zhurnal, Research Alert, Science Citation Index and Trends in Biotechnology.

See inside back cover for Publication Schedule, Information for Authors and information on Advertisements.

0021-9673/91/$03.50

Printed in The Netherlands

VOL. 555 NOS. 1+2 JOURNAL OF CHROMATOGRAPHY AUGUST 30, 1991

CONTENTS

(Abstracts/Contents Lists publishes in Analytical Abstracts, Biochemical Abstracts, Biological Abstracts, Chemical Abstracts, Chemical Titles, Chromatography Abstracts, Current Contents/Life Sciences, Current Contents/Physical, Chemical & Earth Sciences, Deep-Sea Research/Part B: Oceanographic Literature Review, Excerpta Medica, Index Medicus, Mass Spectrometry Bulletin, PASCAL-CRNS, Referativnyi Zhurnal, Research Alert and Science Citation Index)

REGULAR PAPERS

Column Liquid Chromatography

(Continued overleaf)

SHORT COMMUNICATIONS

(Continued overleaf)

BOOK REVIEW

In articles with more than one author, the name of the author to whom correspondence should be addressed is indicated in the article heading by a 6-pointed asterisk (*)

JOURNAL OF CHROMATOGRAPHY

VOL. 555 (1991)

JOURNAL of CHROMATOGRAPHY

INCLUDING ELECTROPHORESIS AND OTHER SEPARATION METHODS

ELSEVIER

AMSTERDAM — LONDON — NEW YORK — TOKYO

J. Chromatogr., Vol. 555 (1991)

0021-9673/91/$03.50

Printed in The Netherlands

Journal of Chromatography, 555 (1991) 1–19
Elsevier Science Publishers B.V., Amsterdam

CHROM. 23 436

Computer simulation of gradient elution separation

Accuracy of predictions for non-linear gradients

DIANA D. LISI and JAMES D. STUART*
Department of Chemistry, U-60, University of Connecticut, Storrs, CT 06269 (USA)
and
LLOYD R. SNYDER
LC Resources Inc., 3182 C Old Tunnel Road, Lafayette, CA 94549 (USA)
(First received February 19th, 1991; revised manuscript received May 6th, 1991)

ABSTRACT

An experimental study was carried out for the separation of a series of homologous 2-ketoalkanes by reversed-phase gradient elution. Both linear and non-linear gradients were used. Computer simulation was applied to these same separations, and comparisons were made between experimental and predicted results (values of retention time, retention time difference and bandwidth). Errors in the predicted separation were generally small and similar for both linear and non-linear gradients. Somewhat larger errors (retention time differences) were found in non-linear gradient separations for bands eluting after a change in gradient steepness. This can be attributed to the dispersion (rounding) of the gradient as it passes through the high-performance liquid chromatographic equipment. Computer simulation was demonstrated to provide predictions that are adequate for the purposes of developing an optimized gradient separation.

INTRODUCTION

Computer simulation based on DryLab software has been shown to be a useful tool for high-performance liquid chromatography (HPLC) method development [1–3]. The ability to predict separation as a function of experimental conditions allows the chromatographer to explore a much wider range of conditions than would normally be possible in the laboratory. The accuracy of such simulations in practical applications has been documented by a number of different workers [4–8]. Several studies [9–12] have also discussed potential errors in computer simulation from a theoretical standpoint.

In the present investigation, we have examined errors in computer simulation that can arise from the use of non-linear gradients, *e.g.*, segmented or step gradients. A few samples of computer simulation for the prediction of separation based on non-linear gradients have been reported [2,5–8], but no systematic study of the errors associated with these kinds of gradients has yet been reported. Our findings are also

0021-9673/91/$03.50

relevant to the use of microbore columns, where gradient elution imposes special requirements for the equipment used for these separations [13,14].

THEORY

Gradient equipment

The theory of computer simulation for gradient elution has been described [9,15–17]. The use of non-linear gradients introduces additional complexity, but these

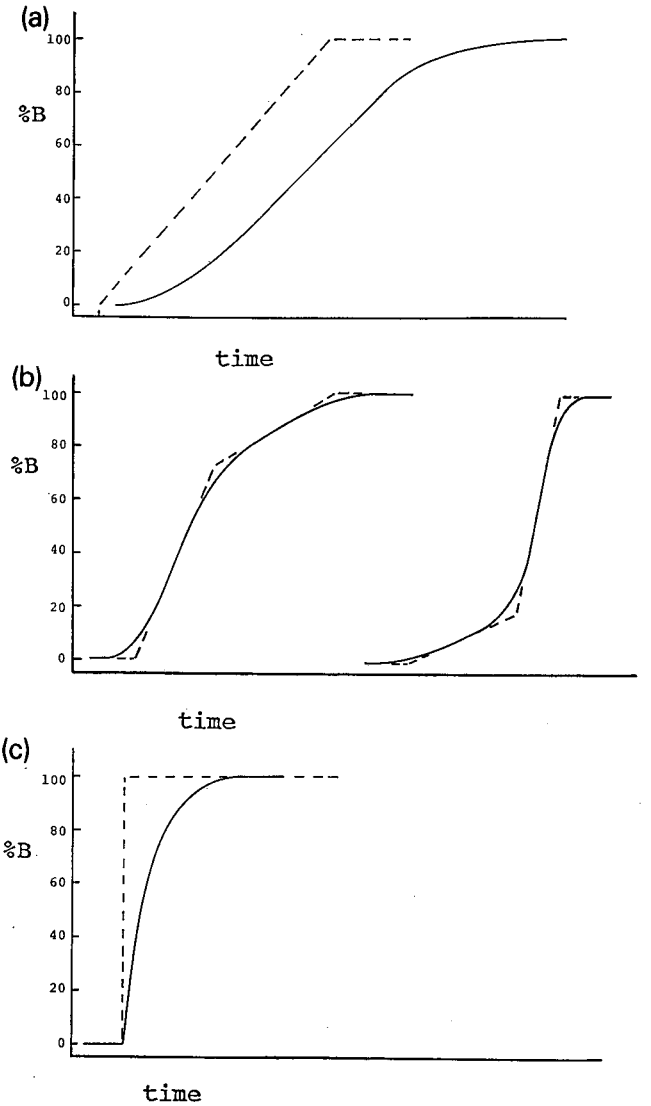

Fig. 1. Hypothetical examples of gradient distortion due to the equipment. (a) Gradient delay and rounding for a linear gradient; (b) gradient rounding for two-segment gradients; (c) gradient rounding for a step-gradient. ——— = Experimental gradient; – – – = input (intended) gradient. See text for further details.

effects can be accounted for by the basic model on which DryLab G software is based; see the discussion of refs. 17 and 18. Further complications are created by the use of "non-ideal" equipment, which produces gradients that do not conform exactly to the desired gradient [19,20]. Every gradient system can be considered "non-ideal" to some degree, but continued advances in equipment design have reduced the importance of these effects.

Fig. 1a illustrates the most common consequences of "non-ideal" gradient equipment. Here the dashed curve is the gradient selected by the user, while the solid curve is the actual gradient delivered by the system. The actual gradient is delayed by a time t_D (the equipment "dwell time"), and the ends of this gradient are rounded by dispersion within the equipment. The effects of gradient dwell time on the separation are easily described and are accounted for in the DryLab G software [20]. Gradient rounding has been discussed in detail for linear gradients [19]; this equipment non-ideality usually has only a minor effect on separations that make use of linear gradients [20], because only bands that elute at the beginning or the end of the gradient are affected. DryLab G/plus does not correct for the effects of gradient rounding by the equipment.

Fig. 1b illustrates the rounding of two representative non-linear (segmented) gradients. In this case, the dashed curves correspond to the input gradients (with correction for the dwell time t_D), and the solid curves are the actual gradients. In this figure it is seen that a decrease in steepness of the second gradient segment leads to low %B values near the point that joins the two segments, and *vice versa* for the case where the second segment is steeper. This should result in simulated retention times that are too small for the first case and too large for the second case —in the region where gradient steepness changes. Sample bands are more likely to be present near the middle of the chromatogram than at its ends, so that errors in predicted retention times due to gradient rounding should be more important in the examples of Fig. 1b than in 1a.

Step gradients as in Fig. 1c can lead to larger deviations of actual %B values (solid curve) from the input gradient (dashed curve). Gradients of this kind are used less often; one example is a step gradient at the end of a separation, in order to remove strongly retained sample components (late eluters) from the column. This application is not usually intended to separate the late eluters from each other, but rather to remove them from the column as quickly as possible. In this situation, errors in predicted retention times (computer simulation) are generally unimportant.

Quantitative relationships (linear or segmented gradients). The rounding of the ends of a linear gradient (Fig. 1a) can be described exactly, as discussed in ref. 19. The maximum deviation in %B for the actual gradient (δ%, see Fig. 2b) occurs at the beginning (or end) of the intended gradient. This deviation is related[a] to the so-called mixing volume V_M of the gradient equipment and the gradient volume ($V_G = t_G F$, where t_G is gradient time and F is flow-rate)

$$\delta\% = 37 V_M / V_G \tag{1}$$

[a] Eqn. 1 can be obtained from Table I of ref. 19 (see values of δ% as a function of V_M/V_G).

The deviation of the actual from intended gradients at other times during the separation is always less than $\delta\%$ and can be predicted if values of V_M and V_D are known for the equipment [19].

The effect of gradient rounding on predicted retention times for linear gradient elution should be minor for values of $V_M/V_G < 0.1$. This means that such effects are avoidable either by selecting equipment with a small value of V_M or by increasing V_G (by using higher flow-rates or longer gradient times).

Gradient rounding near the juncture of two gradient segments (Fig. 1b) is more difficult to describe in mathematical form, and an explicit solution for this case has not been reported. Intuitively it seems obvious that the maximum deviation in the gradient ($\delta\%$) will be less than for the corresponding linear-gradient case, *i.e.*, $\delta\%$ for the steeper segment, since $\delta\%$ approaches zero as the steepness of the two segments becomes more similar, and $\delta\%$ approaches the value for the steeper segment as the difference in steepness for the two segments becomes large.

Quantitative relationships (step gradients). The shape of an actual step gradient as in Fig. 1c can be related to the mixing volume V_M [21]

$$\%B = 100\ (e^{V/V_M} - 1)/e^{V/V_M} \tag{2}$$

Here V is the delivered volume of mobile phase following the start of the gradient (equal to tF, where t is time), and the dwell time is ignored. Correcting for the dwell time we have

$$\%B = 100\ [e^{(V-V_D)/V_M} - 1]/e^{(V-V_D)/V_M} \tag{3}$$

where the dwell volume $V_D = t_D F$. When the actual gradient in Fig. 1c equals 63% B, $V/V_M = 1$ (eqn. 2). This allows a convenient measurement of V_M for the equipment, based on a blank step-gradient run.

Other distortions of the gradient. Aside from the effect of equipment characteristics on gradient distortion, other processes within the column can lead to gradient rounding [22]. Since the column pressure typically varies during a gradient run, solvent compressibility can lead to corresponding changes in flow. The strong solvent component (B) is also selectively adsorbed by the column packing (solvent demixing), leading to a further lag in the experimental *vs.* input gradients. Solvent demixing works in an opposite direction to gradient rounding (causing a decrease in %B; *cf.* Fig. 2b), so as to partially cancel its consequences.

EXPERIMENTAL

Equipment

An LC/9533 ternary-gradient liquid chromatograph (IBM Instruments, Danbury, CT, USA) was used with a Model 7125 sample injector (Rheodyne, Cotati, CA, USA) having a 20-μl loop. A circulating water bath controlled the temperature of the column compartment at 23 ± 0.2°C. A variable-wavelength UV detector (Model 9523, IBM Instruments) was used at 274 nm. Chromatograms were processed with a 3390A reporting integrator (Hewlett-Packard, Palo Alto, CA, USA), which supplied values of retention times, band areas and area/height ratios. The area/height ratio was used to determine bandwidths and plate number (N) values [23].

The equipment dwell volume V_D was determined from (a) blank gradients as in Fig. 1a and (b) comparisons of simulated *vs.* experimental retention times; see refs. 12 and 20 for details. Measurement of blank gradients with flow-rates of 1 or 2 ml/min gave values of V_D = 4.1–4.5 ml. Retention time measurements for an isocratic mobile phase of 73% B were also compared with values predicted by DryLab G/plus (10–100% B in 20 and 60 min used as input). The latter procedure gave V_D = 3.9 ml. An average of these three measurements was assumed: V_D = 4.2 ml. The extra-column band broadening of the HPLC system was reported in ref. 12; σ_{ec} = 0.04 ml.

Materials

Columns were Zorbax C_8 (25 × 0.46 cm I.D., 5-μm particles, MacMod Analytical, Chadds Ford, PA, USA). Column plate number was evaluated at frequent intervals using a test mixture of uracil, acetophenone, nitrobenzene, methyl benzoate and toluene (acetonitrile–water, 70:30, as mobile phase, 0.8 ml/min). The plate number for new columns (toluene solute) was N $\approx$ 14000. The column dead time t_0 was measured from the retention time of sodium nitrate (methanol–water, 70:30, as mobile phase): t_0 = 1.43 min at F = 1.5 ml/min.

The sample used in the present study was a homologous series of nine 2-ketoalkanes: C_5–C_{13} (Aldrich, Milwaukee, WI, USA, or Fluka, Ronkonkoma, NY, USA). The large differences in retention for adjacent bands permitted accurate measurements of retention time and width (or N) for each band, *i.e.*, all bands were well resolved.

The following gradient separations used 0.1% H_3PO_4 (J. T. Baker, Phillipsburg, PA, USA) in water (distilled and deionized [24]) for solvent A, and 0.1% H_3PO_4 in acetonitrile (Fisher Scientific, Fair Lawn, NJ, USA) for solvent B. Methanol was obtained from Burdick & Jackson (Muskegon, MI, USA).

Computer simulations

DryLab G/plus software (LC Resources, Lafayette, CA, USA) was used with a liquid chromatography simulator (IBM-PC/XT personal computer plus a 8087 math coprocessor, also from LC Resources). Simulations of bandwidth required values of the column parameters x = 0.75 and y = 0.40 (see ref. 12 for details). Values of the Knox-parameter A for these columns were determined by means of DryLab G/plus and data for the 2-ketoalkane sample: A = 0.90. For additional details on the simulation and measurement of bandwidth and plate number values, see ref. 12.

RESULTS AND DISCUSSION

Mixing volume V_M of the present HPLC system

Fig. 2a and b shows a blank gradient for the equipment used in these studies. The value of δ% from Fig. 2b equals 6.1%, from which V_M = 0.8 ml was determined from Eqn. 1 (F = 0.5 ml/min, t_G = 10 min). The gradient volume V_G = 5 ml for Fig. 2a and b was deliberately small, in order to magnify the effects of gradient rounding and facilitate the measurement of V_M.

The blank gradient of Fig. 2c is composed of two segments of differing steepness; it shows the expected rounding of the gradient at a time after starting the gradient of about 16 min (where the two segments join). The magnitude of this

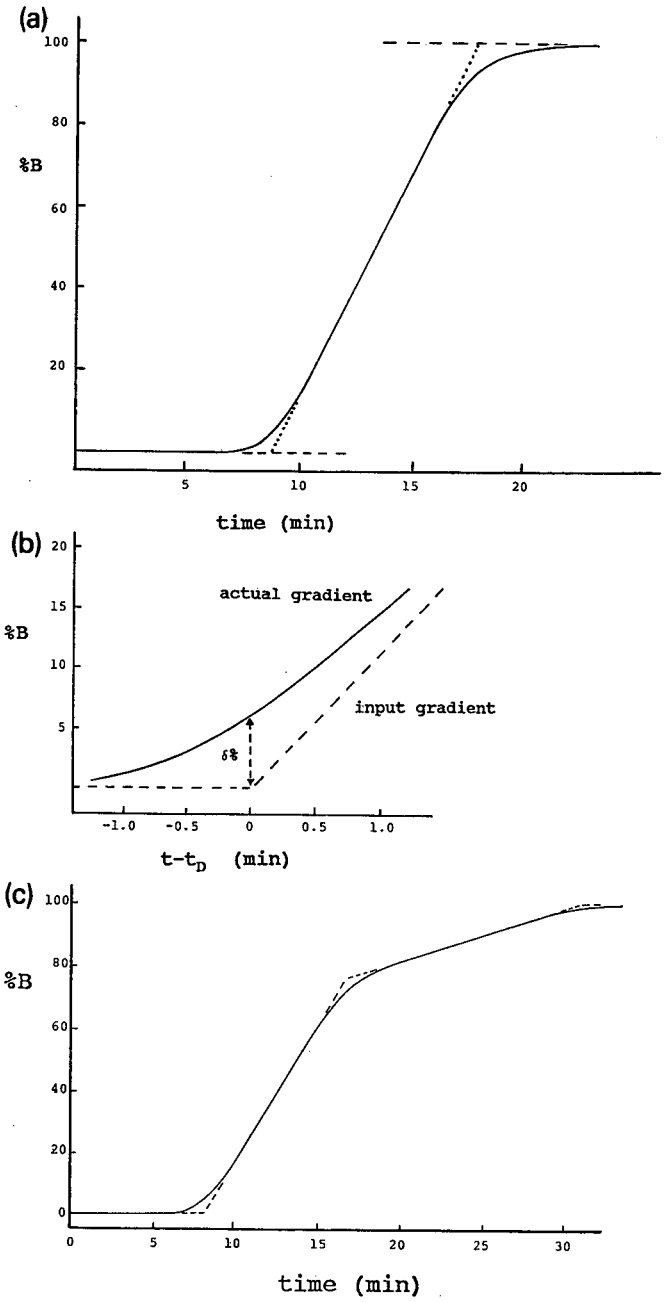

Fig. 2. Experimental examples of gradient distortion by the present HPLC system. (a) Gradient rounding for a linear gradient; 0–100% B in 10 min, 0.5 ml/min; (b) expansion of initial gradient from (a); (c) gradient rounding in a two-step gradient; 0–75–100% B in 0–10–27 min, 0.5 ml/min.

rounding (value of δ%) is comparable to that for the beginning of the initial (steeper) segment, as predicted (see discussion of Theory section). Again, a small gradient volume was used for the first segment of Fig. 2c, in order to magnify the effects of gradient rounding.

Computer simulations for linear gradients

Our primary goal in the present study was to evaluate possible errors in computer simulations for non-linear gradient systems. We wished to compare these errors (for non-linear gradients) with the well-understood [8–11] errors that arise in computer simulations for linear gradient systems. Therefore we first investigated the computer simulation of representative linear gradient separations of the 2-ketoalkane sample. Conditions were selected for these experiments (with one exception) so that sample components were not eluted near the beginning or end of the gradient. In this way, errors due to the rounding of the gradient at its ends were minimized.

Retention time errors. Table I summarizes data for a run with a very steep gradient: 10–100% B in 6 min (15% B/min). There is generally good agreement (Fig. 3) between experimental and calculated (simulated) retention times (t_g), except for the last three bands. The errors in t_g for the latter bands are seen to increase from C_{11} to C_{13}. These errors in t_g have an even larger effect on the retention time differences Δt_g for adjacent bands (values of Δt_g are proportional to resolution R_s). Consequently, the average error in predicted values of Δt_g is rather large ($\pm$ 23%; see Table I). This is

TABLE I

COMPARISON OF EXPERIMENTAL AND PREDICTED RETENTION TIMES FOR THE SEPARATION OF THE 2-KETOALKANE SAMPLE BY LINEAR GRADIENT ELUTION (DATA OF FIG. 3)

Conditions: 10–100% B, 1.5 ml/min; other conditions as in Experimental section. All simulations based on 20- and 60-min gradient runs as input.

Band	Retention times (min)		Retention time errors (min)[a]	
	Expt.	Calc.	t_g	Δt_g
C_5	7.33	7.48	0.15	−0.06
C_6	8.06	8.15	0.09	−0.07
C_7	8.66	8.68	0.02	−0.03
C_8	9.19	9.16	−0.03	−0.02
C_9	9.67	9.62	−0.05	−0.07
C_{10}	10.14	10.02	−0.12	−0.10
C_{11}	10.61	10.39	−0.22	−0.18
C_{12}	11.11	10.71	−0.40	−0.29
C_{13}	11.67	10.98	−0.69	
Average error[b]			±0.20 (2.2%)	±0.10 (23%)

[a] Difference between experimental and predicted (DryLab) values; t_g is the retention time; Δt_g is the retention time difference for adjacent bands (proportional to resolution R_s).

[b] Average absolute error; % error is average absolute error divided by average retention time or retention time difference.

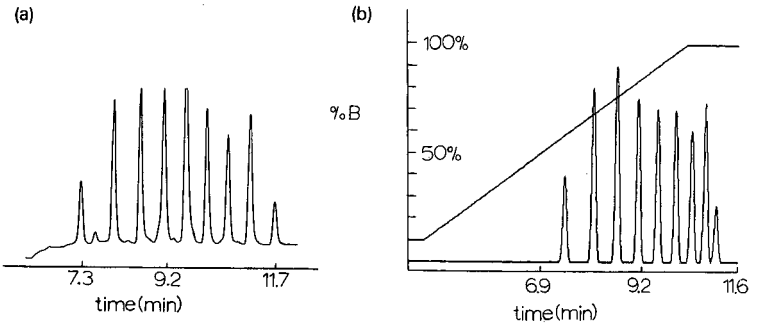

Fig. 3. (a) Experimental and (b) simulated chromatograms for separation of a 2-ketoalkane sample with a linear gradient in 6 min. Conditions: 10–100% B, 1.5 ml/min, other conditions in Experimental section. Simulations based on 20- and 60-min runs as input.

also apparent in Fig. 3, where the simulated chromatogram shows much less resolution of the last two bands than is found experimentally.

The larger errors in t_g and Δt_g for the last three bands of Fig. 3 are due to a combination of effects. First, for this rather steep gradient (15% B/min), there is a considerable rounding of the end of the gradient. The maximum error δ% can be estimated equal to 3.4% B for this separation. Second, as can be seen in Fig. 3b, the last three bands are eluted after the completion of the linear gradient (during the subsequent gradient hold at 100% B). Bands that elute near or after the end of the gradient will be particularly affected by gradient rounding.

When gradient steepness is reduced for the separation of the 2-ketoalkane sample, gradient rounding becomes less severe. Less steep gradients also result in the earlier elution of all bands, so that all bands elute before the end of the gradient. This

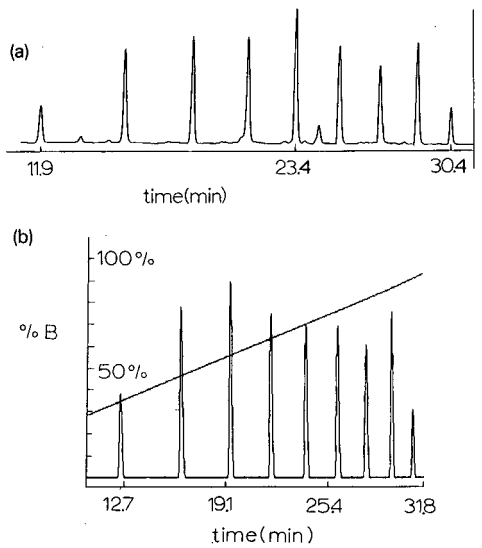

Fig. 4. (a) Experimental and (b) simulated chromatograms for separation of a 2-ketoalkane sample with a linear gradient in 30 min. Conditions: 10–100% B, 1.5 ml/min, other conditions in Experimental section. Simulations based on 20- and 60-min runs as input.

TABLE II

SUMMARY OF COMPARISONS OF EXPERIMENTAL AND PREDICTED RETENTION TIMES FOR THE SEPARATION OF THE 2-KETOALKANE SAMPLE BY LINEAR GRADIENT ELUTION (AS IN FIG. 3)

Conditions as in Fig. 3. All simulations based on 20- and 60-min runs as input.

Gradient conditions		Average t_g (min)	Errors	
t_G (min)	%B/min		t_g (%)	Δt_g (%)
6	15	9.5	±2.2	±23
12	7.5	13	1.7	3
30	3	22	2.8	1
90	1	46	1.3	2
150	0.6	65	1.1	3
Average errors (%)			±1.8 (±1.7)[a]	± 6 (±2)[a]

[a] "Best" values, excluding 6-min run.

is illustrated in Fig. 4 for separation of this sample in a time t_G = 30 min (3% B/min). Now the last band (t_g = 30 min) elutes well before the end of the gradient ($30 + t_0 + t_D$ = 34.5 min). As a result of earlier sample elution plus reduced gradient rounding, the experimental retention times for the last three bands agree much more closely than in Fig. 3, and the average error in predicted values of Δt_g is now only ±1% (*vs.* ±23% in Fig. 3).

Table II summarizes data for several gradient runs of varying steepness. With the exception of the (very steep) 6-min gradient, the average error in retention times is ±1.7%, and the error in values of Δt_g is only ±2%. This represents reasonable agreement between experimental and predicted retention times, when compared with previous examples of computer simulation for linear gradients [5–8,11,12].

Isocratic separations. DryLab G/plus can also be used to predict isocratic separation as a function of %B, based on the same gradient input data used in Figs. 3 and 4 and Tables I and II. Comparison of experimental and predicted retention times for isocratic runs is relevant to the present study of non-linear gradient elution, since some (non-linear) gradients consist of an initial gradient followed by a hold (or *vice versa*). In the latter cases, some sample bands may be eluted under isocratic conditions. Fig. 5 shows experimental and simulated chromatograms for isocratic separation of the 2-ketoalkane sample with 65% B as the mobile phase. Retention times agree within ±8.2%, and Δt_g values agree within ±12% (average values). Similar data for other isocratic separations are summarized in Table III.

The accuracy of these isocratic predictions (Table III) is poorer than for corresponding predictions of gradient separation (Table II). Additional errors in computer simulation are introduced by the conversion of gradient (input) to isocratic (predicted) data (see discussion of refs. 19 and 22). The even larger errors in Table III for B > 70% are due to excessive extrapolation of data derived from the input gradient runs. If the latter data are excluded, the average error is ±8% for retention times and ±11% for Δt_g and resolution. This is adequate for the purpose of method development based on computer simulation.

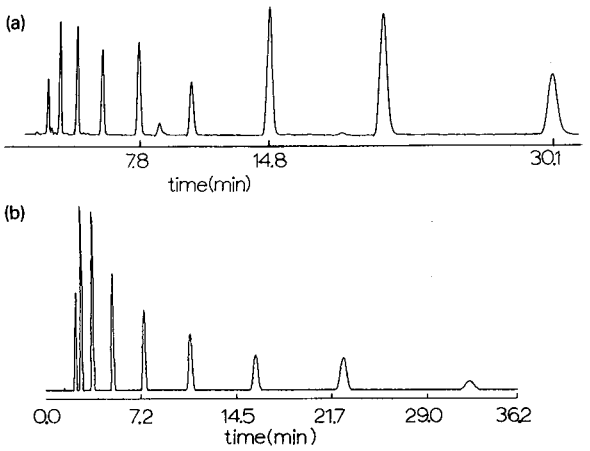

Fig. 5. (a) Experimental and (b) simulated chromatograms for separation of a 2-ketoalkane sample isocratically. Conditions: 65% B, other conditions as in Fig. 3. Simulation based on 20- and 60-min runs as input.

Bandwidth errors. Errors in bandwidths for the various linear gradient and isocratic runs of Tables II and III are summarized in Table IV. The average error in predicted values of bandwidth is about ±10%. These errors are similar to those observed in a preceding study of the separation of *o*-phthalaldehyde-derivatized amino acids by gradient elution [12] and are also adequate for method development purposes.

Computer simulations for non-linear gradients

Additional experiments as in Tables II–IV were carried out for the separation of the 2-ketoalkane sample using non-linear gradients of various types: two-segment gradients, partial gradients with isocratic holds, step gradients and more complex gradients. In each case, comparisons were made of experimental and simulated data

TABLE III

SUMMARY OF COMPARISONS OF EXPERIMENTAL AND PREDICTED RETENTION TIMES (t_R) FOR THE SEPARATION OF THE 2-KETOALKANE SAMPLE BY ISOCRATIC ELUTION (AS IN FIG. 5)

All simulations based on 20- and 60-min runs as input.

B (%)	Average t_g (min)	Errors	
		t_R (%)	Δt_R (%)
60	16	7	9
70	8.4	9	13
80	5.2	14	18
90	3.8	21	23
Average errors (%)		±13	±16

TABLE IV

SUMMARY OF COMPARISONS OF EXPERIMENTAL AND PREDICTED BANDWIDTHS FOR THE SEPARATION OF THE 2-KETOALKANE SAMPLE BY LINEAR GRADIENT OR ISOCRATIC ELUTION (FOR RUNS OF TABLES II AND III)

Conditions: as given in table; other conditions as in Fig. 3. All simulations based on 20- and 60-min runs as input.

Conditions	Bandwidth data[a]	
	Average value (min)	Error[b] (%)
Linear gradients (min)		
6	0.40	±11
12	0.43	5
30	0.60	6
90	1.20	7
150	1.61	18
Average error (%)		± 9
Isocratic runs (%B)		
60	1.42	±12
70	0.81	11
80	0.54	12
90	0.46	15
Average error (%)		±12

[a] Baseline bandwidth.
[b] Average of absolute errors; % error is average absolute error divided by average bandwidth.

for retention time, retention time difference and bandwidth. Attempts were also made to relate unusually large errors to gradient rounding effects, wherever the latter were known to be significant.

Non-linear gradients: retention data. Several separations that involved non-linear gradients were carried out and verified by computer simulation. Typical two-segment gradients are illustrated in Figs. 6 and 7, while Figs. 8–10 show a linear gradient with an initial isocratic hold, a step gradient, and a complex gradient, respectively. Comparisons of experimental and simulated runs are summarized in Tables V (retention data) and VI (bandwidth data), respectively.

Table V shows that the overall accuracy of computer simulation for these ten non-linear gradient separations was ±3.4% for retention times t_g and ±10% for retention time differences Δt_g. These values can be compared with the average errors for linear gradients (Table II): ±1.7% for t_g and ±2% for Δt_g (data for 6-min run excluded). Thus, computer simulation for non-linear gradients is less accurate *vs.* linear gradients, but still adequate for method development purposes.

A distinction should be made between segmented gradients and the other non-linear gradients of Table V. The latter gradients include isocratic holds and are therefore expected to yield somewhat less accurate predictions; thus the data of Table III for isocratic separation suggest ±13% in t_R and ±16% in Δt_R. For the non-linear

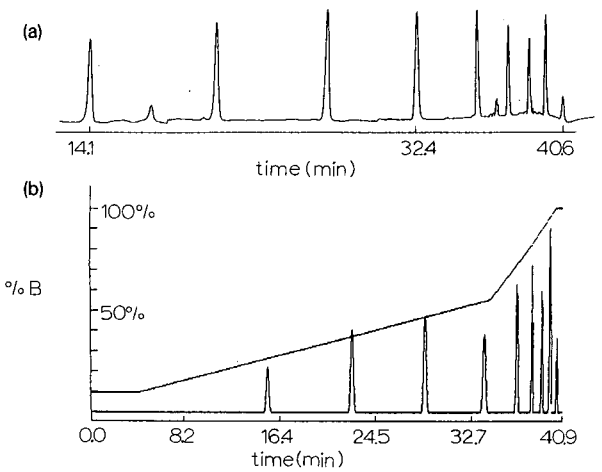

Fig. 6. (a) Experimental and (b) simulated chromatograms for separation of a 2-ketoalkane sample with a two-segment gradient. Conditions: 10–55–100% B in 0–30–36 min; other conditions as in Fig. 3. Simulation based on 20- and 60-min runs as input.

gradient separations of Table V which do not include an isocratic hold (two-segment gradients), the accuracy of predicted retention times ($\pm 2.4\%$ in t_g, $\pm 4\%$ in Δt_g) is not very different from the accuracy of linear gradient simulations ($\pm 1.7\%$ in t_g, $\pm 2\%$ in Δt_g; Table II).

Non-linear gradients: bandwidth data. A comparison of experimental and predicted bandwidths for these non-linear gradient separations is given in Table VI. The

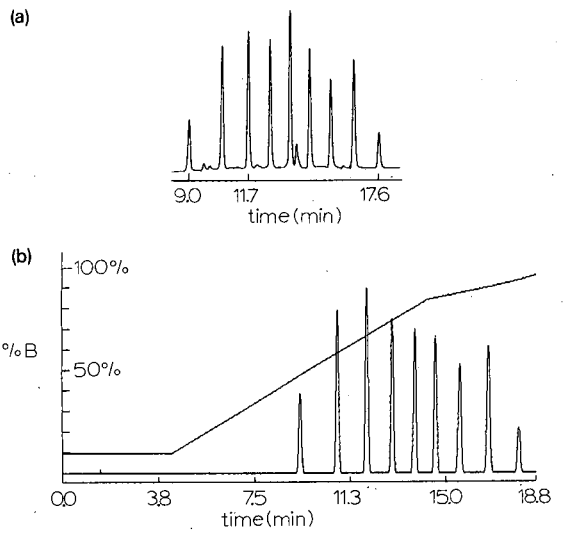

Fig. 7. (a) Experimental and (b) simulated chromatograms for separation of a 2-ketoalkane sample with a two-segment gradient. Conditions: 10–85–100% B in 0–10–20 min; other conditions as in Fig. 3. Simulation based on 20- and 60-min runs as input.

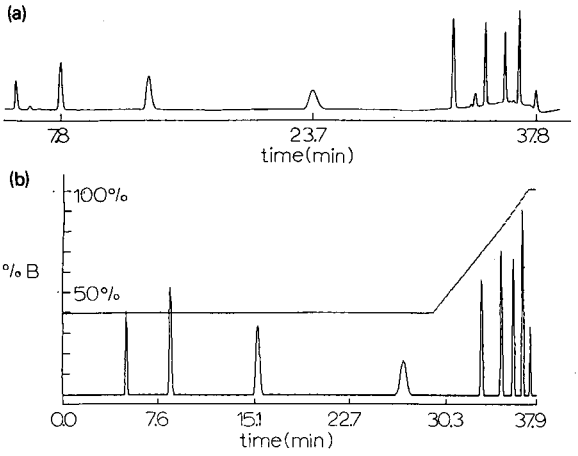

Fig. 8. (a) Experimental and (b) simulated chromatograms for separation of a 2-ketoalkane sample with an initial isocratic hold followed by a linear gradient. Conditions: 40–40–100% B in 0–25–33 min; other conditions as in Fig. 3. Simulation based on 20- and 60-min runs as input.

average error in predicted bandwidths for all ten runs is ± 11%, which is similar to the 9–12% error found for linear gradient or isocratic separation (Table IV). It appears that bandwidths are predicted as accurately for non-linear gradient elution as for separations based on linear gradients.

Further analysis of data of Tables V and VI. If gradient rounding or other "non-ideal" effects contribute to error in non-linear gradient elution, larger relative errors would be expected for bands that elute in that part of the chromatogram where

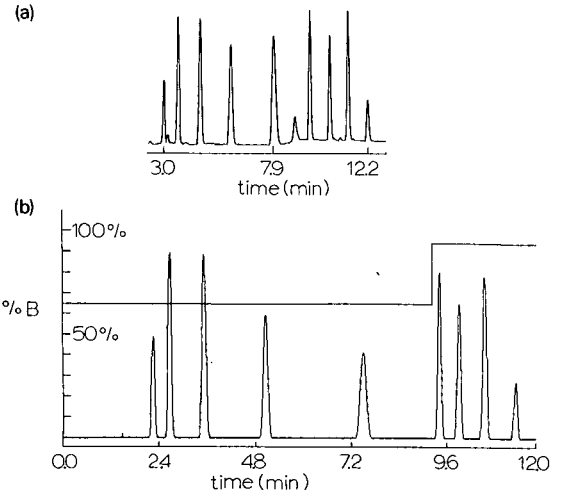

Fig. 9. (a) Experimental and (b) simulated chromatograms for separation of a 2-ketoalkane sample with a step gradient. Conditions: 65–65–95–95% B in 0–5–5–60 min; other conditions as in Fig. 3. Simulation based on 20- and 60-min runs as input.

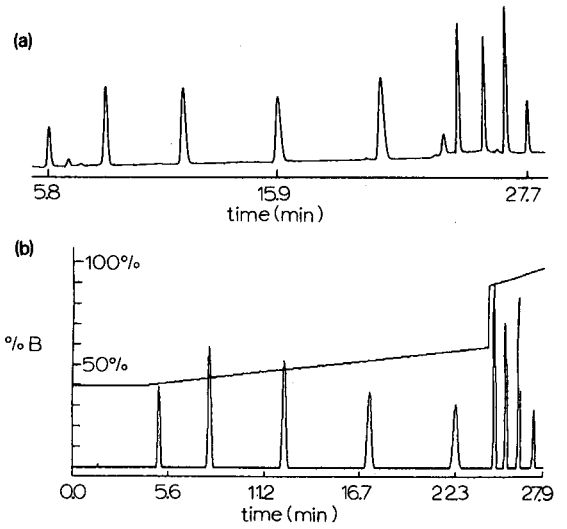

Fig. 10. (a) Experimental and (b) simulated chromatograms for separation of a 2-ketoalkane sample with a complex gradient. Conditions: 40–60–90–100% B in 0–20–20–30 min; other conditions as in Fig. 3. Simulation based on 20- and 60-min runs as input.

TABLE V

SUMMARY OF COMPARISONS OF EXPERIMENTAL AND PREDICTED RETENTION TIMES FOR THE SEPARATION OF THE 2-KETOALKANE SAMPLE BY NON-LINEAR GRADIENT ELUTION (AS IN FIGS. 6–10)

Conditions as listed in table; other conditions as in Fig. 3. All simulations based on 20- and 60-min runs as input.

Gradient conditions	Average t_g (min)	Errors	
		t_g (%)	Δt_g (%)
Two-segment gradient			
10–85–100% B in 0–10–20 min	31	±1.5	± 5
10–55–100% B in 0–30–36 min	31	2.5	6
10–75–100% B in 0–14–25 min	17	2.6	2
10–70–100% B in 0–26–33 min	26	3.1	3
Gradient hold			
40–40–100% B in 0–25–33 min	25	3.3	21
10–85–85% B in 0–10–20 min	14	0.9	6
Step gradient			
65–65–75–75% B in 0–5–5–60 min	9	5.2	10
65–65–95–95% B in 0–5–5–60 min	8	8.8	22
Complex gradient			
40–75–90–100% B in 0–5–5–15 min	9	2.2	6
40–60–90–100% B in 0–20–20–30 min	18	3.5	14
Average errors (all data)		±3.4	±10
(Two-segment gradients)		±2.4	± 4

TABLE VI

SUMMARY OF COMPARISONS OF EXPERIMENTAL AND PREDICTED BANDWIDTHS FOR THE SEPARATION OF THE 2-KETOALKANE SAMPLE BY NON-LINEAR GRADIENT ELUTION (FOR RUNS OF TABLE V)

Conditions as given in table; other conditions as in Fig. 3. All simulations based on 20- and 60-min runs as input.

Gradient conditions	Bandwidth data[a]	
	Average value (min)	Error (%)
Two-segment gradient		
10–85–100% B in 0–10–20 min	0.47	± 8
10–55–100% B in 0–30–36 min	0.71	9
10–75–100% B in 0–14–25 min	0.53	7
10–70–100% B in 0–26–33 min	0.67	8
Gradient hold		
40–40–100% B in 0–25–33 min	0.90	14
10–85–85% B in 0–10–20 min	0.50	8
Step gradient		
65–65–75–75% B in 0–5–5–60 min	0.71	11
65–65–95–95% B in 0–5–5–60 min	0.50	16
Complex gradient		
40–75–90–100% B in 0–5–5–15 min	0.46	9
40–60–90–100% B in 0–20–20–30 min	0.71	11
Average errors (all data)		±11
(Two-segment gradients)		± 8
(Other gradients)		±10

[a] Baseline bandwidths.

the gradient changes steepness. We will refer to this time during the gradient as the "critical" time t_c. For various reasons, it can be argued that errors in Δt_g (expressed in %) provide a good measure of the inaccuracy of simulated retention times. Errors in Δt_g are also much more significant in method development than are errors in t_g. Fig. 11 summarizes the dependence of retention errors measured in this way as a function of retention time (position of the bands in the chromatogram) relative to the critical time t_c. The x-axis of Fig. 11 is in units of $(t - t_c)/t_G$, which is a measure of normalized retention relative to t_c. The data of Fig. 11 are from the four two-segment gradient separations of Table V.

It is obvious from Fig. 11 that errors in Δt_g are consistently larger for bands eluting after the critical time t_c. Based on gradient rounding effects, it might be assumed that these errors should reach a maximum when the average band retention $t = t_c$, but this is clearly not the case. The larger errors for bands eluting after t_c can be rationalized in terms of the elution history of each band as it migrates through the column. That is, a band eluting at a time $t_g = t_c$ has been exposed only to the gradient (mobile phase) preceding t_c, so that (small) errors in this part of the gradient will

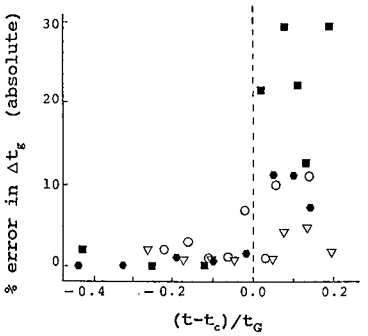

Fig. 11. Error in predicted values of Δt_g as a function of when the two bands elute from the column. The vertical dashed line corresponds to an elution time equal to the "critical" time t_c. Data for two-segment runs of Table V. (○) 10–85–100% B in 0–10–20 min; (■) 10-55–100% B in 0–30–36 min; (▽) 10–75–100% B in 0–14–25 min; (●) 10–70–100% B in 0–26–33 min. Other conditions as in Fig. 3.

result in less error in predicted values of t_g. However, bands eluting after a time t_c are affected to a greater extent by errors in the gradient before and after t_c. That is, the error in t_g (and Δt_g) is a summation of errors in that part of the gradient (preceding t_g) that causes the migration of the band through the column (see Discussion of ref. 15). The rather sharp rise in error that occurs for bands that have eluted just after a time t_c (Fig. 11) is nevertheless rather remarkable.

It is interesting to examine the average error for each of the runs of Fig. 11, for the case where bands elute after the critical time t_c. These average errors for bands eluting after t_c in each of the four runs of Fig. 11 are summarized in Table VII. Retention errors caused by gradient rounding (Fig. 1b, first example) should lead to increasingly negative errors in t_g as $t_g - t_c$ increases (beyond $t_g \approx t_c$). This should result in negative errors in Δt_g when the second gradient segment is steeper, and *vice versa* when the first segment is steeper. This is observed for all four separations of Table VII. Similarly, these errors should be larger for a bigger change in steepness (%B/min) between the two gradient segments; again this is confirmed in Table VII. Thus the correlations of Fig. 11 can be explained in terms of gradient rounding effects.

TABLE VII

AVERAGE ERROR IN VALUES OF Δt_g AND RESOLUTION R_s FOR TWO-SEGMENT GRADIENTS OF TABLE V FOR BANDS ELUTING AFTER THE CRITICAL TIME t_c

Gradient conditions (%/min)		Average error[a] (%)	
1st segment	2nd segment	Δt_g	R_s
7.5	1.5	+ 7	+10
1.5	7.5	−23	−14
4.6	2.3	+ 4	− 1
2.3	4.3	−11	− 4

[a] Actual (not absolute) values.

If this explanation of the post-t_c errors of Fig. 11 is correct, we should also expect to see corresponding errors in predicted bandwidths, *e.g.*, a decrease in an experimental t_g value due to rounding (elution of the band in a higher %B) should lead to a decrease in bandwidth, so that the error in resolution is less than predicted from the error in Δt_g. This is observed, as seen in Table VII, for errors in R_s; the latter are generally smaller than are errors in Δt_g. Finally, it is seen in Table VII that errors in predicted values of R_s are seldom greater than $\pm 10\%$.

Mobile phase demixing (in the absence of gradient rounding) would lead to a qualitatively similar correlation of errors and band retention (Fig. 11). However, errors due to demixing should increase gradually for increasing values of $t_g - t_c$, beginning at $t_g = t_c$. This is not observed in Fig. 11, suggesting that gradient rounding is the major factor in these larger errors for later-eluting band pairs.

Gradient elution using microbore columns and equipment

The preceding discussion suggests that gradient rounding will become significant (in terms of its effect on separation), when the mixing volume $V_M > 1$ ml (for a column whose diameter is 0.46 cm). Reliable predictions of gradient-elution separation based on computer simulation therefore require $V_M < 1$ ml. As the column diameter d_c is decreased, flow-rates must be decreased by a factor of d_c^2, if a similar separation is to be maintained. This in turn means a reduction of gradient volume V_G by the same factor. If gradient rounding is to be held at the same level, the equipment mixing volume V_M must be reduced by a similar factor. This means that mixing volumes must be less than 50 μl for a microbore system ($d_c = 0.1$ cm). This is a rather severe requirement, requiring careful design of the gradient system [13,14].

CONCLUSIONS

Computer simulation based on DryLab G/plus software was evaluated for non-linear gradients of various kinds. Errors in retention time, retention time differences (proportional to resolution R_s) and bandwidth were generally small and similar in magnitude to those found for linear gradients. These results suggest that computer simulation is sufficiently accurate as a tool for developing methods based on non-linear gradients.

An analysis of observed errors in predicted retention time differences showed that larger errors are found for bands eluting after the "critical" time t_c, where t_c is the time during the gradient when gradient steepness changes. These larger errors appear to be due to gradient rounding caused by dispersion of the gradient within the HPLC equipment. This suggests that gradient equipment which exhibits less dispersion of the gradient (a smaller "mixing volume" V_M) should provide experimental data which are in better agreement with computer simulation, since DryLab G/plus ignores gradient rounding. Computer simulation should therefore prove less reliable for the prediction of segmented-gradient separations (when gradient steepness changes by more than $\pm 4\%$/min between segments), if gradient equipment with $V_M > 1$ ml is used.

For the special case of microbore gradient elution, rounding of the gradient is a potentially more serious problem, because of very small values of the gradient volume V_G (due to low flow-rates). Unless the mixing volume V_M (gradient dispersion) for

microbore systems is reduced to a very small value (< 50 μl), observed separations will be less predictable and computer simulation can be seriously in error.

The present study provides additional confirmation of the general theory of gradient elution as applied to non-linear gradient systems [18].

SYMBOLS

B	solvent B in mobile phase A–B; acetonitrile or methanol in present study
d_c	column internal diameter (cm)
F	mobile phase flow-rate (ml/min)
N	column plate number
R_s	resolution of two adjacent bands
t	average value of t_g for two adjacent bands (Fig. 11; min)
t_c	"critical" time for a non-linear gradient (min); time at which gradient steepness (measured at outlet of column) changes (min)
t_D	dwell time of gradient HPLC system (min)
t_g	retention time in gradient elution (min)
t_G	gradient time (min)
t_0	column dead time (min)
t_R	retention time in isocratic elution (min)
V	volume of mobile phase at some time after the start of the gradient (eqn. 2)
V_D	dwell volume of gradient HPLC system; equal to $t_D F$ (ml)
V_G	gradient volume, equal to Ft_G (ml)
V_M	mixing volume of gradient HPLC system (ml)
$\delta\%$	change in %B at beginning of gradient due to rounding (see Fig. 2b)
Δt_g	difference in t_g values for two adjacent bands; proportional to resolution R_s (min)
Δt_R	difference in t_R values for two adjacent bands; proportional to resolution R_s (min)
σ_{ec}	extra-column band broadening of gradient system (ml)

REFERENCES

1 L. R. Snyder, J. W. Dolan and D. C. Lommen, *J. Chromatogr.*, 485 (1989) 65.
2 J. W. Dolan, D. C. Lommen and L. R. Snyder, *J. Chromatogr.*, 485 (1989) 91.
3 L. R. Snyder, J. W. Dolan and D. C. Lommen, *J. Chromatogr.*, 553 (1990) 75.
4 P. E. Shaw and C. W. Wilson, III, *J. Chromatogr. Sci.*, 26 (1988) 478.
5 R. G. Lehmann and J. R. Miller, *J. Chromatogr.*, 485 (1989) 581.
6 D. J. Thompson and W. D. Ellenson, *J. Chromatogr.*, 485 (1989) 607.
7 W. Markowski, T. H. Dzido and E. Soczewinski, *J. Chromatogr.*, 523 (1990) 81.
8 B. F. D. Ghrist, B. S. Cooperman and L. R. Snyder, in K. M. Gooding and F. E. Regnier (Editors), *HPLC of Biological Macromolecules*, Marcel Dekker, New York, 1990, p. 403.
9 M. A. Quarry, R. L. Grob and L. R. Snyder, *Anal. Chem.*, 58 (1986) 907.
10 L. R. Snyder and M. A. Quarry, *J. Liq. Chromatogr.*, 10 (1987) 1789.
11 B. F. D. Ghrist, B. S. Cooperman and L. R. Snyder, *J. Chromatogr.*, 459 (1988) 1.
12 J. D. Stuart, D. D. Lisi and L. R. Snyder, *J. Chromatogr.*, 485 (1989) 657.
13 K. Potter and J. Tehrani, *LC/GC Mag.*, 8 (1990) 862.
14 K. Nugent and K. Olson, personal communication, 1991.
15 L. R. Snyder, in Cs. Horváth (Editor), *High-Performance Liquid Chromatography —Advances and Perspectives*, Vol. 1, Academic Press, New York, 1980, p. 207.

16 L. R. Snyder and M. A. Stadalius, in Cs. Horváth (Editor), *High-Performance Liquid Chromatography —Advances and Perspectives*, Vol. 4, Academic Press, New York, 1986, p. 195.
17 J. W. Dolan, L. R. Snyder and M. A. Quarry, *Chromatographia*, 24 (1987) 261.
18 P. Jandera and J. Churacek, *Gradient Elution in Column Liquid Chromatography*, Elsevier, Amsterdam, 1985, Ch. 6.
19 M. A. Quarry, R. L. Grob and L. R. Snyder, *J. Chromatogr.*, 285 (1984) 1.
20 J. W. Dolan and L. R. Snyder, *LC/GC Mag.*, 8 (1990) 524.
21 L. R. Snyder, *Chromatogr. Rev.*, 7 (1965) 1 (Eqn. 14).
22 M. A. Quarry, R. L. Grob and L. R. Snyder, *J. Chromatogr.*, 285 (1984) 19.
23 B. L. Karger, L. R. Snyder and Cs. Horváth, *An Introduction to Separation Science*, Wiley-Interscience, New York, 1973, p. 137.
24 M. Eslami, J. D. Stuart and K. A. Cohen, *J. Chromatogr.*, 411 (1987) 121.

Journal of Chromatography, 555 (1991) 21–31
Elsevier Science Publishers B.V., Amsterdam

CHROM. 23 378

Application of solute and mobile phase partition coefficient to describe solute retention in reversed-phase high-performance liquid chromatography

HASMUKH B. PATEL[a], DAVID N. KING and TERENCE M. JEFFERIES*
School of Pharmacy and Pharmacology, University of Bath, Bath BA2 7AY (UK)
(First received September 14th, 1990; revised manuscript received March 5th, 1991)

ABSTRACT

The calculated partition coefficient, log P_{sm} (logarithm of partition coefficient of solvent mixture), of aqueous mobile phases containing either methanol, acetonitrile or tetrahydrofuran, may be used as a quantitative parameter for solvent strength instead of the commonly used term, Φ (volume fraction of solvent in water). This has permitted the development of a new relationship that expresses the retention behaviour of non-ionised solutes based solely on the hydrophobic parameter of the solute (log P) and the mobile phase (log P_{sm}). This statistically derived relationship has not only given a highly significant fit to the data, but also provided regression coefficients that were consistent for different, but related chromatographic (reversed-phase liquid chromatography) systems. One unique advantage offered by this approach is that it allows all retention data, for all solutes analysed under different solvent systems, to be combined in a single expression. It is suggested that this expression could be used to determine the initial solvent conditions in the optimisation of chromatographic mobile phases or as a general model for quantitative structure–retention relationship.

INTRODUCTION

The prediction of the conditions required in reversed-phase high-performance liquid chromatography (RP-HPLC) for the adequate resolution of a particular group of analytes is still a difficult task for most chromatographers. The most commonly used 'trial-and-error' or systematic but empirical approach may be used to arrive at the optimum conditions so that adequate resolution is achieved with reasonable analysis time. Ideally, it should be possible to calculate the retention parameter of a given analyte in the chosen column–mobile phase system from the physico-chemical properties of the analyte, mobile phase and stationary phase. In practice, this has not yet been achieved although much progress is being made through the development of systematic methods. These approaches include the use of one or more gradient run(s) in order to select an optimum isocratic composition [1–3] or an iterative method [4]

[a] Present address: K-11-3019 Pharmaceutical Analysis, Schering-Plough Research, 2000 Galloping Hill Road, Kenilworth, NJ 07033, USA.

0021-9673/91/$03.50

and automated sequential simplex approach [5,6]. These methods do not require *a priori* knowledge of the physico-chemical properties of the analytes.

Other workers have approached the problem by considering the physico-chemical properties of the analytes and using semi-deterministic or semi-empirical techniques, generally known as quantitative structure–retention relationship (QSRR) [7–12]. This type of modeling is commonly based upon the principles of linear free energy relationships, as used in quantitative structure–activity relationships (QSAR) in drug design. Commonly used parameters for the QSRR studies are: (1) hydrophobic parameter, π [9,12], (2) partition coefficient, P [9–11], (3) correlation factor, F [11,12], (4) molecular connectivity index, χ [10–12], (5) length over breadth shape parameter of a molecule, L/B [11] and (6) Van der Waals volume, V_W [10–12].

In an earlier study [13] we had shown that the logarithm of partition coefficient (1-octanol/water) of a solvent, log P_s, could be used as a "solvent strength" parameter in RP-HPLC. Strength of a solvent refers to its eluotropic potential. Two solvents are iso-eluotropic if they elute a given solute with same elution volume (V_R) under identical chromatographic conditions.

In view of the well understood influence of hydrophobicity in RP-HPLC, the aim of this study was to examine whether the partition coefficients of the analytes as well as the mobile phase could be used to describe the retention behaviour of non-ionised analytes under those conditions.

THEORETICAL

Many physico-chemical parameters of a solute influence its retention in RP-HPLC, and some may be estimated from the retention parameter, k' [14]. However, it has been suggested that in RP-HPLC the interaction between solute and hydrocarbonaceous stationary phase is the major factor for the retention in absence of organic modifiers [15], *i.e.*, the process is governed by the so-called hydrophobic effect in which the cohesive density of water is responsible [16]. This theory has also been employed to describe the effect of solvents on certain chemical events [17,18] and does not restrict a solvophobic effect to aqueous media. Additionally, it has been observed that water is not a unique solvent in terms of its chromatographic property [19] and that the hydrophobic selectivity of different solvents is approximately independent of their chemical nature [20]. In other words, the total solvophobic force of solvent mixture is governing the solvation of molecule. Therefore, it is apparent that in the ion-suppressed mode of RP-HPLC, the solvophobic effect could be considered to be the most influential parameter.

The retention of solutes in RP-HPLC has been described by eqn. 1 [14,21].

$$\ln k' = a' + b' \log P \tag{1}$$

$$\ln k' = a + b\varphi + c\varphi^2 \tag{2}$$

where k' = peak capacity factor, log P = logarithm of octanol/water partition coefficient, φ = volume fraction of the organic modifier in mobile phase and a', b', a, b and c are system-dependent coefficients. These equations are applicable under certain conditions only, for example retention data of a given analyte for a given column

analysed under *different* solvents may not be combined to obtain a single expression such as eqns. 1 and 2. Furthermore, a general expression is not available to describe the retention behaviour of a variety of solutes analysed employing different mixed solvents of different compositions in isocratic mode. The major difficulty for obtaining such a correlation lies in accurately defining the "solvent strength" of the mobile phase containing a mixture of solvents from chemically different classes.

A variety of approaches have been suggested for calculating solvent strength parameters. In our previous study [13] we have shown that partition coefficient of a solvent (log P_s, subscript "s" indicates that log P value refers to the solvent and not analyte) can be used as a "strength" parameter. In this study a number of currently available parameters were compared with log P_s. Solvent strength parameters, *viz.*, P' [22], S [23], δ_T [24] and log P_s [13], are listed in Table I and a comparison of the accuracy of prediction of solvent strength of mixed solvents using these parameters is given in Table II. It is apparent that parameter log P_s is able to predict solvent strength more accurately as compared to others for the experimental data under consideration. Therefore the log P_s parameter was employed to derive an expression (eqn. 3) for calculating the strength of a mixed solvent system, which is given below:

$$\log P_{sm} = \sum_{i}^{n} x_i \log P_{s,i} \tag{3}$$

where, m indicates that the parameter is for solvent mixture, x_i is the mole fraction of the ith solvent component, log $P_{s,i}$ is logarithm of the partition coefficient of the ith solvent and n is the total number of pure solvents present in the solvent mixture. Therefore, according to eqn. 3, the eluotropic strength of a solvent mixture is a sum of the partition coefficient times the mole fraction of each solvent. Solvent strengths of water–methanol, water–acetonitrile and water–tetrahydrofuran were calculated and compared with experimental data as well as another study [21]. The experimental and predicted values compared very well [13]. It was found that the use of log P_{sm} as a strength parameter resulted in better predictions as compared to other parameters and approaches [13]. The major advantage of this method of strength parameter

TABLE I

STRENGTH PARAMETERS FOR SOME HPLC SOLVENTS

P' = polarity index [23]; S = solvent strength [24]; δ_T = total solubility [25]; log P_s = n-octanol/water log partition coefficients obtained from ref. 22.

Solvent	P'	S	δ_T	log P_s
Water	10.2	0.0	25.52	−1.38
Methanol	5.1	3.0	15.85	−0.82
Acetonitrile	5.8	3.1	13.15	−0.34
Ethanol	4.3	3.6	13.65	−0.31
Dioxane	4.8	3.5	10.65	−0.27
Acetone	5.1	3.4	10.51	−0.24
Propan-2-ol	3.9	4.2	12.37	+0.30
Tetrahydrofuran	4.0	4.4	9.88	+0.46

TABLE II

COMPARISON OF ACCURACY OF SOLVENT STRENGTH PREDICTIONS BY DIFFERENT PARAMETERS

Parameter	S.D.[a]	r^2 (%)[a]
S	5.938	66.1
P'	5.885	66.7
φ_T	4.997	76.0
Empirical[b]	4.572	79.9
log P_s	4.517	80.4

[a] Standard deviation (root mean square of the fit) and coefficients of determination (adjusted to degree of freedom) between experimental and predicted solvent compositions (% $\text{solvent}_{\text{exp.}} = c + m \cdot \%\ \text{solvent}_{\text{pred.}}$) [13].
[b] Empirical transfer equations of Schoenmaker *et al.* [3].

calculation is that a single quantitative value can be readily calculated for the solvent mixtures commonly employed in RP-HPLC. Our interest was then to see whether this parameter could be used as strength parameter instead of the φ term in eqn. 2. For the solvents water, methanol, acetonitrile and tetrahydrofuran it was found that a highly significant relationship existed between the volume fraction of solvent (φ) and reciprocal of computed solvent partition coefficient ($1/P_{sm}$) as compared to x_i and $1/P_{sm}$. Statistical analysis for the relationship between φ and $1/P_{sm}$ (eqn. 4) is presented in Table III.

$$\varphi = A' + B' \frac{1}{P_{sm}} \tag{4}$$

where A' and B' are regression coefficients. It is apparent from Table III that φ and $1/P_{sm}$ are highly correlated ($r^2 \geqslant 99.6\%$). This correlation suggests that the volume

TABLE III

STATISTICS FOR THE RELATIONSHIP BETWEEN φ AND $1/P_{sm}$ (SEE EQN. 4)
φ values were selected in the range of 0–1 with an interval of 0.01 and the corresponding P_{sm} values were back-calculated using eqn. 3.

Solvent	A	B	n[a]	r^2 (%)[b]	s[c]	F[d]
Methanol	1.40	−0.0569	101	0.998	0.015	42 816
Acetonitrile	1.07	−0.0439	101	0.999	0.005	> 51 069
Tetrahydrofuran	0.92	−0.0378	101	0.999	0.066	> 37 714

[a] Number of selected solvent compositions.
[b] Coefficient of determination.
[c] Standard deviation (root mean square of fit).
[d] F-ratio [28].

fraction term (φ) can be substituted by a solvent strength term ($1/P_{sm}$) in eqn. 2 to provide eqn. 5.

$$\ln k' = A'' + B'' \frac{1}{P_{sm}} + C'' \frac{1}{P_{sm}^2} \quad (5)$$

where A'' and B'' and C'' are regression coefficients. This equation has been examined for a relationship with eqn. 1 in order to express the well known dependence of solute retention in RP-HPLC upon solute log P and mobile phase strength. A number of equations (derived from eqns. 1 and 2) were generated and subjected to statistical analysis using two sets of experimental data from the literature (data sets 1 and 2) and two sets of experimental data (data sets 3 and 4) from our laboratory.

EXPERIMENTAL

Data set 1

Hypersil silica (Shandon, Cheshire, UK) was chemically bonded in house to form an *n*-octyl end-capped material and packed into a 150 mm × 4.6 mm I.D. column. It was used at 30°C to analyse sixteen non-ionic polar substances and non-polar aromatic compounds employing methanol–water (50:50, v/v), acetonitrile–water (30:70, v/v) and tetrahydrofuran–water (25:75, v/v) by Tanaka *et al.* [25]. The compounds were benzene, toluene, ethylbenzene, benzamide, benzyl alcohol, phenol, benzaldehyde, benzonitrile, 2-phenylethanol, phenyl methyl lactone, nitrobenzene, methoxybenzene, methyl benzoate, chlorobenzene, ethyl benzoate and isopropyl benzoate.

Data set 2

A 300 × 4.6 mm I.D. column was packed with Merck RP-18 material (Merck, Darmstadt, Germany) and used at 25°C and a flow-rate of 1.5 ml/min^{-1}, with 32 non-ionic aromatic compounds in aqueous systems containing 10–90% of methanol, acetonitrile or tetrahydrofuran as organic modifiers under isocratic conditions, by Schoenmakers *et al.* [26]. The analytes were acetophenone, anethole, aniline, anisole, anthracene, benzaldehyde, benzene, benzonitrile, benzophenone, benzyl alcohol, biphenyl, chlorobenzene, *o*-cresol, diethyl *o*-phthalate, N,N-dimethylaniline, 2,4-dimethylphenol, dimethyl *o*-phthalate, *m*-dinitrobenzene, diphenyl ether, ethylbenzene, N-methylaniline, naphthalene, *p*-nitroacetophenone, *o*-nitroaniline, nitrobenzene, *m*-nitrophenol, phenol, 1-phenylethanol, 2-phenylethanol, 3-phenylpropanol, quinolone and toluene.

Data sets 3 and 4

Equipments. Chromatographic studies were performed using either a Spectra-Physics Model SP8100 liquid chromatograph with Model SP8440 UV–VIS detector and Model SP4200 computing integrator (Spectra-Physics, St. Albans, UK) or a modular system assembled from a Constametric III pump (Milton Roy, Stone, UK), Rheodyne 7125 injection valve, and a UV–LC detector (Pye-Unicam, UK). Methanol, acetonitrile and tetrahydrofuran were HPLC grade (Fisons, UK) and HPLC-grade water was obtained from a Milli-Q water system (Millipore, Harrow, UK).

Data set 3. A 50 × 4.6 mm I.D. column was packed with 3 μm Hypersil-ODS (Shandon) and used at a flow-rate of 1.0 ml/min^{-1} and a temperature of 40°C, with UV detection at 254 nm. For the methanol–water mixture five compositions were used, *viz.*, 28, 42, 58, 74 and 90% (v/v) methanol. The five iso-eluotropic equivalent mobile phases containing acetonitrile and tetrahydrofuran were calculated [13] and used for analysis under the same conditions. Five non-ionisable solutes were chosen in order to give a range of log P values (log P values for solutes of data sets 1–4 were obtained from ref. 27, namely, benzyl alcohol (log P = 1.10), benzonitrile (1.56), benzene (2.15), chlorobenzene (2.84) and benzophenone (3.58). These solutes were dissolved in 25% methanol and injected individually, in triplicate.

Data set 4. A 150 × 4.6 mm I.D. column was packed with 6-μm Zorbax-ODS (Du Pont) and used at a flow-rate of 1 ml/min^{-1} and a temperature of 35°C, with UV detection at 254 nm. For the methanol–25 mM buffer (phosphate, pH 6.9) mixtures, three compositions were used, namely 50, 60 and 70% (v/v) of methanol, and their isoeluotropic equivalent solvents containing acetonitrile and tetrahydrofuran. The five related non-ionisable solutes were benzonitrile (log P = 1.56), benzene (2.15), toluene (2.72), naphthalene (3.2) and biphenyl (4.0), dissolved in 50% methanol and injected individually, in triplicate.

Data processing and computing was done using statistical software (MINITAB®) with Honewell 68 DPS Level 2 via RJE or GEC 63/40 computers.

RESULTS AND DISCUSSION

A number of relevant equations were statistically examined that incorporated relationships expressed by eqns. 1 and 5, using the four sets of data described in Experimental. In order to select the equation that was best able to describe the data, we compared F-ratio (weighted according to number of experimental data points), correlation coefficients (r) and standard deviation (s) about the regression line. On this basis, two equations were considered to be most suitable. These equations are given below.

$$\ln k' = A + B\frac{\log P}{P_{sm}} + C\frac{1}{P_{sm}^2} \tag{6}$$

$$\ln k' = A^0 + B^0\frac{\log P}{P_{sm}} + C^0\frac{\log P}{P_{sm}^2} \tag{7}$$

where A, B, C, A^0, B^0 and C^0 are regression coefficients. The results of statistical analysis are presented in Table IV. An examination of Table IV under "All data" shows that both equations gave significant "fit" to the experimental data as judged from the F-ratios ($F > 337$) when compared to the tabulated [28] value ($F < 8.09$ at 99.9% confidence level). Since experimental data may include some accidentally large errors a "trimming" step was carried out in order to eliminate such observations. Those observations which showed Studentised Residual values greater than 2 were considered to be outliers. Statistical analysis was again performed for the "trimmed" data and the results appear in Table IV under "Data after outliers removed". It was

TABLE IV

RESULTS OF STATISTICAL ANALYSIS ON EQNS. 6 AND 7 FOR FOUR DATA SETS
Symbols n, r, s and F are defined in Table III.

Eqn.	Data set	All data				Data after outliers removed			
		n	r	s	F	n	r	s	F
6	1	131	0.973	0.235	1113	127	0.976	0.222	1232
	2	1176	0.967	0.611	8054	1125	0.981	0.428	13 013
	3	145	0.969	0.311	1040	138	0.973	0.267	1211
	4	45	0.971	0.223	337	42	0.979	0.181	443
7	1	131	0.972	0.238	1112	129	0.974	0.231	1147
	2	1176	0.913	0.987	2869	1106	0.945	0.738	5043
	3	145	0.974	0.286	1313	138	0.984	0.226	2081
	4	45	0.972	0.217	360	41	0.987	0.150	694

found that there were few outliers, and removing them did not change the correlation (r) and standard deviation (s) statistics considerably as compared to "untrimmed" data, but F ratios (F) were improved. Eqn. 6 was prefered over eqn. 7 because of higher F-ratios for larger data sets. Further support for eqn. 6 as more appropriate model comes from an examination of regression coefficients and the error associated with their estimation. These coefficients and corresponding t-ratios appear in Table V. It is evident that the coefficients (A, B and C) for eqn. 6 are consistent in magnitude and sign for all data sets, in contrast to those for eqn. 7. Such consistency of the estimated coefficients implies that a common "trend" of chromatographic process is occurring in different but related systems, as measured by the hydrophobic parameters of the solutes and solvents. Further evidence in favour of eqn. 6 over eqn. 7 is provided by the greater values of t-ratio (t_a, t_b and t_c) for each coefficient (see Table V). This indicates that the coefficients for eqn. 6 can be estimated with less error as compared to those for eqn. 7, therefore a higher confidence limit could be assigned to

TABLE V

REGRESSION COEFFICIENTS AND t STATISTIC FOR EQNS. 6 AND 7 FOR FOUR DATA SETS
A, B and C are regression coefficients. t_a, t_b and t_c are t-ratio (ratio of coefficient and standard deviation) for coefficients A, B and C, respectively.

Eqn.	Data set	A	t_a	B	t_b	C	t_c
6	1	−2.0585	−17.77	0.0849	45.49	0.0024	05.84
	2	−1.5866	−70.34	0.0667	71.71	0.0057	55.11
	3	−0.7013	−13.13	0.0459	22.80	0.0061	24.51
	4	−1.2222	−08.52	0.0567	24.81	0.0055	08.05
7	1	−1.4205	−22.66	0.0459	05.65	0.0024	05.32
	2	−1.4974	−37.67	0.1050	93.93	−0.0009	−00.11
	3	0.2180	04.28	−0.0244	−05.05	0.0056	27.62
	4	−0.1854	−02.39	−0.0052	−00.77	0.0045	10.87

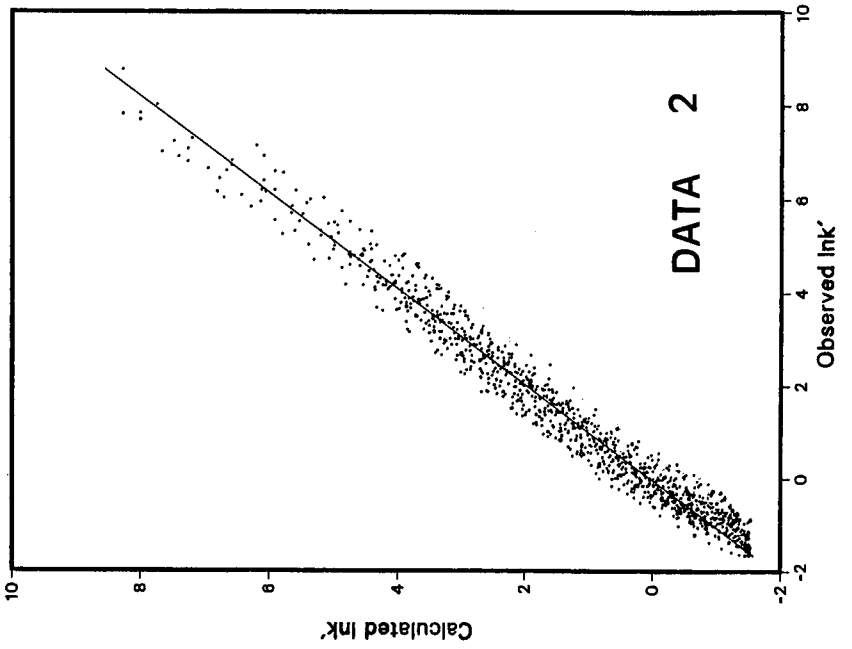
DATA 2
Observed lnk'
Calculated lnk'
-2
0
2
4
6
8
10

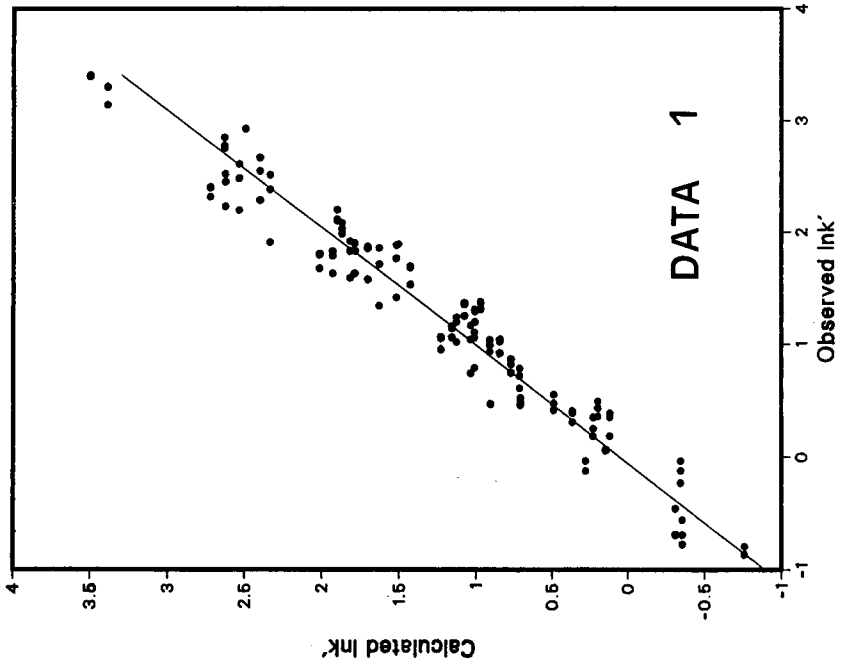
DATA 1
Observed lnk'
Calculated lnk'
-1
0
1
2
3
4
-0.5
0
0.5
1
1.5
2
2.5
3
3.5

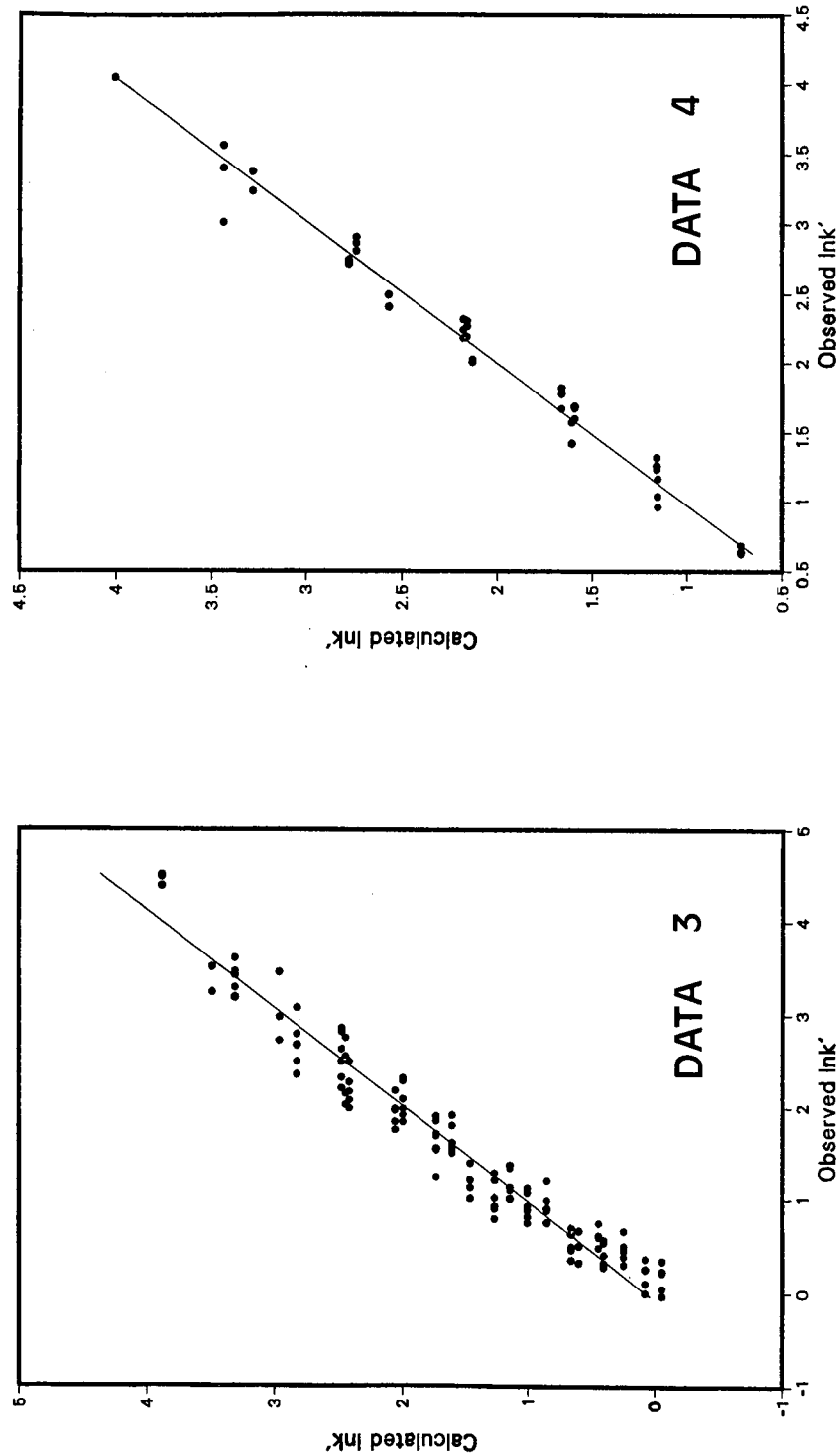

Fig. 1. Plots for the four data sets (1–4) showing the correlation between the observed and calculated ln k' values obtained using eqn. 6. The statistical analyses for these plots are given in Tables IV and V. Fractions of the organic solvents and their chemical nature used in the studies were: Data set 1, φ(MeOH) = 0.50, φ(ACN) = 0.30, φ(THF) = 0.25; Data set 2, φ(MeOH) = 0.10–0.90, φ(ACN) = 0.07–0.69, φ(THF) = 0.06–0.60; Data set 3, φ(MeOH) = 0.28–0.90, φ(ACN) = 0.20–0.69, φ(THF) = 0.18–0.60 and Data set 4, φ(MeOH) = 0.50–0.70, φ(ACN) = 0.37–0.52, φ(THF) = 0.32–0.46.

the predictions from eqn. 6. Plots of the experimental and calculated retentions (ln k'), according to eqn. 6, appear in Fig. 1 for the four data sets. It is evident that good correlation between observed and predicted solute retentions has been achieved. It is important to emphasise at this stage that though the predictions may not by very accurate, because of the use of only one physico-chemical parameter for solute (log P) and solvent (log P_{xm}), eqn. 6 does provide a general and consistent model relating retention and solute and solvent property for physically different but chromatographically similar reversed-phase systems.

Having established that eqn. 6 is a statistically sound, chromatographically appropriate and a general model, it was of interest to examine the significance of each term. The terms in eqn. 6 represent a number of familiar observations in RP-HPLC. For example, the direct proportionality of ln k' to log P shows the commonly observed phenomenon that retention is dependent on the hydrophobic parameter of the solute [14]. The quadratic dependance of ln k' on $1/P_{sm}$ reflects the relationship given in eqn. 2 which was derived semi-empirically based on regular solution theory [3]. Additionally, the inverse proportionality of ln k' to P_{sm} shows that P_{sm} is an appropriate solvent strength parameter, because the greater the solvent strength (P_{sm}), the shorter is the retention (ln k'). The interrelationship between solute log P and mobile phase strength, $1/P_{sm}$, expressed as the ratio (log P)/($1/P_{sm}$), again shows the commonly observed fact that the greater the hydrophobicity of the solute (log P), the greater is the solvent strength required to obtain the same retention.

The relationship provided by eqn. 6 may be used practically to obtain useful but approximate prediction of solute retention in many RP materials by the analysis of a few solutes sufficiently different in their log P values, under different strengths using the $1/P_{sm}$ scale, for different solvents. This will permit the estimation of the coefficients of eqn. 6 for a given chromatographic system. It is further suggested that eqn. 6 can be of value as a starting point in the development of solvent optimisation procedures, or in the development of other equations that are able to define solute retention more accurately by incorporating additional physico-chemical parameters. This study has shown that for non-ionic solutes chromatographed in a RP system, using data generated from four different RP materials, that the retention is very largely determined by solute hydrophobicity (log P) and mobile phase hydrophobicity (log P_{sm}).

CONCLUSIONS

(1) The calculated partition coefficient, log P_{sm}, of aqueous–organic mobile phases containing either methanol, acetonitrile or tetrahydrofuran has been found to be a quantitative parameter for eluotropic strength and to have a highly significant relationship with Φ, the volume fraction of solvent in water (eqn. 2).

(2) Eqn. 2 has permitted the development of a relationship (eqn. 6), using experimental data, that expresses the retention behaviour of non-ionic solutes based solely on the hydrophobic parameter of both the solute (log P) and the solvent (log P_{sm}).

(3) The relationship shown by eqn. 6 was found to be statistically sound and gave consistent regression coefficients when applied to four different experimental data sets, indicating a common type of retention and solute–solvent property relationship.

(4) A distinct advantage offered by eqn. 6 is that the retention data for different solutes analysed under different solvent compositions (qualitative and quantitative) may be combined in a single expression.

ACKNOWLEDGEMENTS

One of the authors (H.B.P.) would like to thank Professor E. Tomlinson and Dr. K. Petrak for their suggestions and support, and also to thank Ciba-Geigy Pharmaceuticals (Horsham, UK) for providing facilities.

REFERENCES

1 M. A. Quarry, L. R. Grob and L. R. Snyder, *J. Chromatogr.*, 285 (1984) 1.
2 P. Jandera and J. Churachek, *J. Chromatogr.*, 91 (1974) 223.
3 P. J. Schoenmakers, H. A. H. Billiet and L. de Galan, *J. Chromatogr.*, 205 (1981) 13.
4 S. Sekulic, P. R. Hadad and C. J. Lamberton, *J. Chromatogr.*, 363 (1986) 125.
5 M. W. Watson and P. W. Carr, *Anal. Chem.*, 51 (1979) 1835.
6 J. C. Berridge, *J. Chromatogr.*, 244 (1982) 1.
7 W. Melander and Cs. Horvath, *Chromatographia*, 15 (1982) 86.
8 T. L. Hafkenscheid, *Ph. D. Thesis*, University of Amsterdam, Amsterdam, 1983.
9 K. Jinno and K. Kawasaki, *J. Chromatogr.*, 298 (1984) 326.
10 K. Jinno and K. Kawasaki, *Chromatographia*, 17 (1983) 337.
11 K. Jinno and K. Kawasaki, *Chromatographia*, 17 (1983) 445.
12 K. Jinno and K. Kawasaki, *Chromatographia*, 18 (1984) 90.
13 H. B. Patel and T. M. Jefferies, *J. Chromatogr.*, 389 (1987) 21.
14 T. L. Hafkenscheid and E. Tomlinson, *Adv. Chromatogr.*, 25 (1985) 1.
15 Cs. Horvath, W. Melander and I. P. Molnar, *J. Chromatogr.*, 125 (1976) 129.
16 C. Tanford, *The Hydrophobic Effect*, Wiley-Interscience, New York, 1973.
17 O. Sinanoglu, in B. Pullman (Editor), *Molecular Associations in Biology*, Academic Press, New York, 1968, p. 427.
18 O. Sinanoglu and S. Abdulnur, *Fed. Proc. Fed. Am. Soc. Exp. Biol.*, 24 No. 2 (1965) 12.
19 N. Tanaka and E. R. Thornton, *J. Am. Chem. Soc.*, 99 (1977) 7300.
20 B. L. Karger, J. R. Gant, A. Hartkopf and P. Weiner, *J. Chromatogr.*, 128 (1978) 519.
21 P. J. Schoenmakers, H. A. H. Billiet, R. Tijsen and L. de Galan, *J. Chromatogr.*, 149 (1978) 519.
22 L. R. Snyder, *J. Chromatogr. Sci.*, 16 (1978) 223.
23 L. R. Snyder, J. W. Dolan and J. R. Gant, *J. Chromatogr.*, 165 (1979) 3.
24 R. Tijssen, H. A. H. Billiet and P. J. Schoenmakers, *J. Chromatogr.*, 122 (1976) 185.
25 N. Tanaka, H. Goodel and B. L. Karger, *J. Chromatogr.*, 158 (1978) 233.
26 P. J. Schoenmakers, H. A. H. Billiet and L. de Galan, *J. Chromatogr.*, 185 (1979) 179.
27 C. Hansch and A. Leo, *Substituent Constants for Correlation Analysis in Chemistry and Biology*, Wiley-Interscience, New York, 1979.
28 H. R. Neave, *Elementary Statistics Tables*, George Allen & Unwin, London, 1981, p. 22.

Journal of Chromatography, 555 (1991) 33–51
Elsevier Science Publishers B.V., Amsterdam

CHROM. 23 368

Experimental model for predicting solute retention time as a function of mobile phase composition in ternary reversed-phase high-performance liquid chromatography

MINGGAO XIE*, CHUNFENG ZHOU, ZHONGJIAO REN and TIANSHUN LUO
Department of Chemistry, South-Central Institute for National Minorities, Wuhan 430074 (China)
(Received February 18th, 1991)

ABSTRACT

It was observed that the variance of the solute retention time with the mobile phase composition in ternary reversed-phase high-performance liquid chromatography (RP-HPLC) approximately obeys a simple exponential model that is involved in the Snyder solvent strength theory. Using Newton or Marquardt algorithms, the values of the unknown non-linear parameters in the model were obtained, and further used to predict the retention time of solute as a function of ternary solvent composition to a good approximation, based upon three isocratic HPLC runs only. No dead time is needed for the prediction here. To test the model further, four sets of experimental data published by other groups were used. Three of the sets of experimental data conformed well with this model, but the other set showed serious deviations. In the latter instance, however, all the mobile phases used contained 5 m*M* heptanesulphonate and 1% acetic acid in addition to methanol, acetonitrile and water. For practical use, some problems in the non-linear least-squares estimation are discussed.

INTRODUCTION

The prediction of solute retention in polynary reversed-phase high-performance liquid chromatography (RP-HPLC) is of significance, because the location of the optimum mobile phase composition for certain separations under polynary conditions is very difficult or even impossible by using trial-and-error methods. Therefore, models describing the relationship between the solute retention and mobile phase composition in binary, ternary and quaternary RP-HPLC with a variety of automated optimization techniques for RP-HPLC separations have been continuously proposed since the 1970s [1–12]. With computers, these approaches have been used more and more widely.

In ternary RP-HPLC, a typical model to describe the relationship between solute retention and mobile phase composition is of the following form [7]:

$$\ln k' = a_1x_1 + a_2x_2 + a_3x_3 + a_{12}x_1x_2 + a_{13}x_1x_3 + a_{23}x_2x_3 + a_{123}x_1x_2x_3 \quad (1)$$

where x_1, x_2 and x_3 are the fraction of each component in the ternary mobile phase and a_1–a_{123} are the coefficients to be calculated. Certainly eqn. 1 has given a fairly complex description of solute–solvent behaviour. However, much experimentation would be

0021-9673/91/$03.50

needed for acquiring good estimates of the coefficients because there are seven unknown coefficients in the model. Generally, seven HPLC runs would be required. In addition, measurements of the dead times under different mobile phase compositions are essential in order to calculate the capacity factors, which could be difficult to measure accurately and be subject to variations depending on the solvent composition [2,13].

In this paper, we report an experimental model for the prediction of retention times of solutes as a function of mobile phase composition in ternary RP-HPLC. Experiments have shown that most of the relative deviations between the experimental and the predicted retention times for all the solutes tested using this model are within 3%, the maximum being not greater than 6.5%.

We used four other sets of experimental data to examine this model, published out by Bartha *et al.* [14], Issaq *et al.* [15] and Sekulic *et al.* [16]. The results examined are basically in agreement with ours.

We consider that the major merits of this experimental model are that only three RP-HPLC runs are needed for predicting solute retention times to a first approximation as a function of mobile phase composition in ternary RP-HPLC, and dead times are no longer needed for the prediction of solute retention times.

THEORETICAL

In RP-HPLC separations, it is generally observed that there is a linear relationship between log k' and mobile phase composition for certain organic modifiers [1,2]:

$$\log k' = \log k_w + S\varphi \tag{2}$$

where k' is the capacity factor of the solute, k_w is the extrapolated value of k' for pure water as mobile phase, φ is the volume fraction of the organic modifier in the mobile phase and S is a constant for a given solute and organic modifier. According to Snyder *et al.* [17], the coefficient S is related to the strength of the mobile phase; the solvent strength can be an approximate measure of the ability of a solvent to elute a solute from a column [18,19]. Hence, it could be suggested that eqn. 2 be expressed as the following form:

$$\log k' = A + BST \tag{3}$$

where A and B are constants for a given solute, column and solvent system and ST is the total solvent strength of the mobile phase, which can be calculated by using Snyder's appraoch [17–19]:

$$ST = s_1\varphi_1 + s_2\varphi_2 + \ldots \tag{4}$$

where s is the solvent strength weighting factor of each component in the mobile phase, being 0 for water, 2.6 for methanol, 3.2 for acetonitrile and 4.5 for tetrahydrofuran [20,21]; φ is the volume fraction of each solvent in the mobile phase. Because the value of s for water is zero, we could rewrite eqn. 2, based on eqn. 4, as

$$\log k' = A + Bs\varphi \tag{5}$$

where s and φ are the solvent strength weighting factor and the volume fraction of the organic modifier only in the binary solvent system of water and the organic component, respectively. The product of s and φ here represents the total solvent strength of the mobile phase. Actually, eqn. 5 is the same as eqn. 2, and both will result in an identical value of the capacity factor in any case in binary RP-HPLC.

Theory predicts that mobile phases of same solvent strength will produce approximately equal ranges of capacity factors [19]. Therefore, the solute capacity factor in ternary RP-HPLC could possibly be expressed as a function of the total solvent strength of the mobile phase. We assume that this function has a similar form to eqn. 3. Substituting eqn. 4 in eqn. 3, we obtain

$$\log k' = A + B(s_1\varphi_1 + s_2\varphi_2) \tag{6}$$

where s and φ refer to the solvent strength weighting factors and the volume fractions of organic modifiers 1 and 2 in the mobile phase consisting of water and two organic solvents, respectively.

On comparing eqn. 6 with eqn. 2, we find that eqn. 6 is not a simple linear combination of two individual binary retention equations, because this kind of linear combination would have the following form:

$$\log k' = A' + S_1\varphi_1 + S_2\varphi_2 \tag{7}$$

or

$$\log k' = A' + B_1s_1\varphi_1 + B_2s_2\varphi_2 \tag{7'}$$

where A', S_1, S_2, B_1 and B_2 are constants.

Using eqn. 6 and the relationship between the retention time and the capacity factor of a solute:

$$t_R = \frac{L}{u}(1 + k') \tag{8}$$

we can obtain the following equation:

$$t_R = a \exp [b(s_1\varphi_1 + s_2\varphi_2)] + c \tag{9}$$

where the linear velocity of the mobile phase is assumed to be constant. In eqns. 8 and 9, t_R is the retention time of the solute, L is the column length and u is the linear velocity of the mobile phase; a, b and c are constants for a given solute, column and ternary solvent system. From eqn. 9, it could be seen that there are only three unknown parameters, and therefore it is possible to use three RP-HPLC runs to predict the retention time of a solute as a function of mobile phase composition.

EXPERIMENTAL

A Model LC-4A liquid chromatographic system (Shimadzu, Kyoto, Japan) with an SPD-2AS UV spectrophotometric detector (Shimadzu) set at 254 nm was used in

TABLE I

COEFFICIENTS OF EXPONENTIAL CURVE FITTING OF RETENTION TIMES *VS.* MOBILE PHASE COMPOSITIONS FOR THE SOLUTES IN GROUP 1 WITH TERNARY SOLVENT MIXTURES CONSISTING OF METHANOL, ACETONITRILE AND WATER, USING THE SOLVENT STRENGTH WEIGHTING FACTORS IN RP-HPLC

Solute	*a*	*b*	*c*
p-Chloronitrobenzene	290.7344	−2.4904	0.5296
8-Hydroxyquinoline	85 127.6833	−5.5284	1.3039
Benzophenone	335.1216	−2.3112	−0.2481
Naphthalene	572.9292	−2.5280	0.0062
Phenergan	738.7899	−2.6006	−0.5138
Diazepam	−4.1073	0.6115	17.0027
Dibutyl phthalate	9249.3730	−3.3599	−4.2784
Phenanthrene	557.1322	−1.8788	−6.5645
Acetanilide	3.9642	−0.8168	0.8501

the ternary RP-HPLC experiments. A Model C-R2AX data processing system (Shimadzu) was employed to record the experimental data. The non-linear least-squares fitting programs of the Newton [22] and Marquardt [23] algorithms were written in Pascal and BASIC, which were run on an AST computer (AST Research, Irvine, CA, USA) and an Apple II plus, respectively.

A stainless-steel column (150 × 4 mm I.D.) was packed with 10-μm YWG-$C_{18}H_{37}$ material (Second Chemical Reagent Factory, Tianjing, China). Methanol (CH_3OH), acetonitrile (ACN), tetrahydrofuran (THF) and water were used for two ternary mobile phase systems; nineteen solutes were eluted by one or another ternary solvent mixture. The flow-rate of the mobile phase was fixed at 1.0 ml/min.

Three mobile phase compositions were taken as the raw experimental data sampling points, where the values of the retention times of the solutes of interest were recorded by the C-R2AX data system. Therefore, we can obtain three sets of raw

TABLE II

COEFFICIENTS OF EXPONENTIAL CURVE FITTING OF RETENTION TIMES *VS.* MOBILE PHASE COMPOSITIONS FOR THE SOLUTES IN GROUP 2 WITH TERNARY SOLVENT MIXTURES OF METHANOL, TETRAHYDROFURAN AND WATER IN RP-HPLC, USING THE SOLVENT STRENGTH WEIGHTING FACTORS IN RP-HPLC

Solute	*a*	*b*	*c*
Toluene	−57.3852	0.0227	63.9574
Ethylbenzene	62.8576	−0.0468	−52.0560
Biphenyl	34.4027	−0.5650	−4.3960
Nitrobenzene	−0.00046	2.4683	2.4528
Chlorobenzol	−2.3026	0.2984	7.9513
p-Dichlorobenzene	−3.6346	0.3402	12.4137
o-Dichlorobenzene	−55.2138	0.0459	65.2931
m-Dichlorobenzene	−22.2652	0.1184	33.9193
Methyl salicylate	9.3597	−0.8188	1.3190
Benzyl acetate	103.2134	−2.8445	2.1003

experimental data about the retention times and the corresponding mobile phase compositions for each solute. The choice of the raw experimental data points will be discussed below.

The three sets of raw experimental data for each solute mentioned above were used to fit eqn. 9. This is the so-called non-linear least-squares fitting. Hence Newton [22] or Marquardt [23] algorithms can be used to find the values of a, b and c. Generally, the problem here is the choice of the initial values of a, b and c before the iteration. This is discussed below.

TABLE III

COMPARISON BETWEEN EXPERIMENTAL AND CALCULATED RETENTION TIMES OF THE SOLUTES IN GROUP 1 WITH TERNARY MOBILE PHASES CONSISTING OF METHANOL, ACETONITRILE AND WATER USING THE SOLVENT STRENGTH WEIGHTING FACTORS IN RP-HPLC

Solute	Parameter[a]	Retention time (min)						
		1	2	3	4	5	6	7
p-Chloronitrobenzene	Exp.	2.167	2.337	2.850	3.506	4.315	4.693	5.940
	Calc.	2.167	2.375	2.873	3.506	4.310	4.790	5.940
	r.d. (%)	0	−1.62	−0.81	0	0.12	−2.06	0
8-Hydroxyquinoline	Exp.	2.167	2.352	3.433	4.557	7.025	8.833	13.565
	Calc.	2.167	2.429	3.217	4.557	6.835	8.516	13.565
	r.d. (%)	0	−3.29	6.28	0	2.71	3.59	0
Benzophenone	Exp.	2.490	2.750	3.567	4.520	5.910	6.465	8.055
	Calc.	2.490	2.811	3.571	4.520	5.704	6.403	8.055
	r.d. (%)	0	−2.23	−0.12	0	3.48	0.96	0
Naphthalene	Exp.	2.988	3.350	4.322	5.476	7.012	7.958	10.040
	Calc.	2.988	3.373	4.297	5.476	6.978	7.878	10.040
	r.d. (%)	0	−0.68	0.57	0	0.48	1.01	0
Phenergan	Exp.	2.792	3.183	4.198	5.657	7.400	8.600	11.005
	Calc.	2.792	3.232	4.294	5.657	7.407	8.460	11.005
	r.d. (%)	0	−1.52	−2.28	0	−0.09	1.63	0
Diazepam	Exp.	2.350	2.633	3.485	4.350	5.385	5.402	6.077
	Calc.	2.350	2.774	3.585	4.350	5.071	5.416	6.077
	r.d. (%)	0	−5.35	−2.87	0	5.82	−0.27	0
Dibutyl phthalate	Exp.	4.253	5.475	9.378	14.830	23.218	26.493	38.520
	Calc.	4.253	5.746	9.562	14.830	22.103	26.721	38.520
	r.d. (%)	0	−4.95	−1.96	0	4.80	−0.86	0
Phenanthrene	Exp.	4.625	5.522	7.715	11.000	15.307	17.100	21.007
	Calc.	4.625	5.681	8.101	11.000	14.472	16.457	21.007
	r.d. (%)	0	−2.88	−5.01	0	5.46	3.76	0
Acetanilide	Exp.	1.575	1.590	1.683	1.732	1.850	1.875	1.923
	Calc.	1.575	1.604	1.665	1.732	1.804	1.842	1.923
	r.d. (%)	0	−0.88	1.04	0	2.49	1.76	0
Mobile phase composition (%)								
CH_3OH		80.0	72.0	56.0	40.0	24.0	16.0	0
ACN		0	5.0	15.0	25.0	35.0	40.0	50.0
Water		20.0	23.0	29.0	35.0	41.0	44.0	50.0

[a] r.d. (%) = 100 (exp. − calc.)/exp.

RESULTS AND DISCUSSION

In Tables I and II, the values of the non-linear parameters in eqn. 9 are listed for the solutes in two groups eluted by two different ternary solvent systems. The

TABLE IV

COMPARISON BETWEEN EXPERIMENTAL AND CALCULATED RETENTION TIMES OF THE SOLUTES IN GROUP 2 WITH TERNARY MOBILE PHASES CONSISTING OF METHANOL, TETRAHYDROFURAN AND WATER, USING THE SOLVENT STRENGTH WEIGHTING FACTORS IN RP-HPLC

Solute	Parameter[a]	Retention time (min)						
		1	2	3	4	5	6	7
Toluene	Exp.	4.157	3.890	3.690	3.558	3.458	3.173	2.953
	Calc.	4.157	3.918	3.678	3.558	3.437	3.196	2.953
	r.d. (%)	0	−0.72	0.32	0	0.59	−0.72	0
Ethylbenzene	Exp.	5.667	5.158	4.773	4.490	4.247	3.792	3.337
	Calc.	5.667	5.193	4.723	4.490	4.257	3.795	3.337
	r.d. (%)	0	−0.68	1.04	0	−0.25	−0.09	0
Biphenyl	Exp.	7.908	6.595	5.421	5.200	4.458	3.703	3.088
	Calc.	7.908	6.743	5.689	5.200	4.735	3.870	3.088
	r.d. (%)	0	−2.25	−4.95	0	−6.20	−4.52	0
Nitrobenzene	Exp.	2.412	2.398	2.400	2.332	2.328	2.195	2.095
	Calc.	2.412	2.390	2.356	2.332	2.303	2.221	2.095
	r.d. (%)	0	0.34	1.85	0	1.09	−1.19	0
Chlorobenzol	Exp.	3.988	3.758	3.583	3.432	3.290	2.992	2.798
	Calc.	3.988	3.774	3.549	3.432	3.312	3.062	2.798
	r.d. (%)	0	−0.43	0.95	0	−0.66	−2.33	0
p-Dichlorobenzene	Exp.	5.663	5.100	4.800	4.573	4.492	3.822	3.307
	Calc.	5.663	5.246	4.804	4.573	4.335	3.836	3.307
	r.d. (%)	0	−2.87	−0.88	0	3.50	−0.37	0
o-Dichlorobenzene	Exp.	5.267	4.865	4.300	4.042	3.757	3.248	2.792
	Calc.	5.267	4.780	4.289	4.042	3.794	3.295	2.792
	r.d. (%)	0	1.75	0.26	0	−0.99	−1.45	0
m-Dichlorobenzene	Exp.	6.300	5.605	5.238	4.823	4.525	3.833	3.267
	Calc.	6.300	5.718	5.125	4.823	4.518	3.899	3.267
	r.d. (%)	0	−2.02	2.16	0	0.15	−1.73	0
Methyl salicylate	Exp.	3.428	3.175	2.908	2.790	2.680	2.495	2.345
	Calc.	3.428	3.145	2.900	2.790	2.688	2.504	2.345
	r.d. (%)	0	0.95	0.28	0	−0.29	−0.36	0
Benzyl acetate	Exp.	2.683	2.408	2.295	2.267	2.223	2.150	2.148
	Calc.	2.683	2.454	2.314	2.267	2.230	2.179	2.148
	r.d. (%)	0	−1.89	−0.85	0	−0.32	−1.35	0
Mobile phase composition (%)								
CH_3OH		70.0	56.0	42.0	35.0	28.0	14.0	0
THF		0	12.0	24.0	30.0	36.0	48.0	60.0
Water		30.0	32.0	34.0	35.0	36.0	38.0	40.0

[a] r.d. (%) = 100 (exp. − calc.)/exp.

experimental and the calculated solute retention times with seven ternary mobile phase compositions are compared in Tables III and IV. In these cases, points 1, 4 and 7 are the raw experimental data sampling points, at which the calculated retention times of the solutes are the fitted values; points 2, 3, 5 and 6 are the random points which were used to examine this experimental model.

TABLE V

USING THE EXPERIMENTAL DATA OF BARTHA *ET AL.* [14]: RESULTS OF EXPONENTIAL CURVE FITTING OF SOLUTE RETENTION TIMES *VS.* MOBILE PHASE COMPOSITIONS AND COMPARISON BETWEEN EXPERIMENTAL AND CALCULATED SOLUTE RETENTION TIMES USING THE SOLVENT STRENGTH WEIGHTING FACTORS IN RP-HPLC

Solute	Parameter[a]	Retention time (min)					Fitted coefficients
		1	2	3	4	5	
Benzyl alcohol	Exp.	4.02	3.34	3.51	3.40	3.45	$a = 4.50 \cdot 10^{-7}$
	Calc.	4.02	3.341	3.49	3.399	3.431	$b = 8.3573$
	r.d. (%)	0	−0.022	0.63	0.03	0.55	$c = 3.2390$
Dimethyl phthalate	Exp.	4.79	5.49	4.75	5.03	4.94	$a = 2.71 \cdot 10^{10}$
	Calc.	4.77	5.48	4.88	5.06	4.97	$b = -16.5096$
	r.d. (%)	0.32	0.19	−2.84	−0.50	−0.55	$c = 4.7621$
Phenol	Exp.	6.20	3.72	4.39	4.05	4.18	$a = 8.73 \cdot 10^{-4}$
	Calc.	6.20	3.72	4.47	4.05	4.21	$b = 4.8394$
	r.d. (%)	0	0	−1.74	0	−0.68	$c = 2.6197$
Benzonitrile	Exp.	6.29	5.49	5.33	5.36	5.33	$a = 4.92 \cdot 10^{-17}$
	Calc.	6.288	5.42	5.46	5.43	5.44	$b = 21.7654$
	r.d. (%)	0.03	1.27	−2.45	−1.31	−2.04	$c = 5.4162$
p-Cresol	Exp.	7.71	4.51	5.40	5.00	5.33	$a = 0.0110$
	Calc.	7.71	4.51	5.58	5.00	5.22	$b = 3.6112$
	r.d. (%)	0	0	−3.32	0	1.98	$c = 2.2435$
Diethyl phthalate	Exp.	8.19	9.76	8.16	8.87	8.73	$a = 4.85 \cdot 10^{9}$
	Calc.	8.19	9.76	8.48	8.87	8.67	$b = -14.7940$
	r.d. (%)	0	0	−3.89	0	0.67	$c = 8.1462$
3,4-Dimethylphenol	Exp.	9.37	5.49	6.67	6.13	6.33	$a = 0.0489$
	Calc.	9.37	5.49	6.86	6.13	6.42	$b = 2.9352$
	r.d. (%)	0	0	−2.84	0	−1.36	$c = 1.7787$
Benzene	Exp.	11.91	8.42	9.07	8.80	8.73	$a = 6.14 \cdot 10^{-5}$
	Calc.	11.91	8.42	9.32	8.80	8.99	$b = 6.5021$
	r.d. (%)	0	0	−2.80	0	−3.02	$c = 7.5206$
2,4-Dimethylphenol	Exp.	11.48	6.21	7.87	7.09	7.39	$a = 0.0829$
	Calc.	11.48	6.21	8.09	7.09	7.48	$b = 2.8220$
	r.d. (%)	0	0	−2.76	0	−1.24	$c = 0.8854$
Mobile phase composition (%)							
ACN		0	46.1	26.1	35.7	32.3	
THF		38.2	0	16.6	8.6	11.5	
Water		61.8	53.9	57.3	55.7	56.2	

[a] r.d. (%) = 100 (exp. − calc.)/exp.

Tables III and IV indicate that each ternary solvent system actually consisted of two binary solvent systems of an organic modifier and water. The mobile phase compositions at the three raw experimental data sampling points 1, 4 and 7 were 100:0, 50:50 and 0:100, representing the ratios of the volume fractions of two binary solvent mixtures in the ternary solvent systems. From the tables, it can be seen that the maximum relative deviation between the experimental and the calculated solute

TABLE VI

USING THE EXPERIMENTAL DATA OF BARTHA *ET AL.* [14]: RESULTS OF EXPONENTIAL CURVE FITTING OF SOLUTE RETENTION TIME *VS.* MOBILE PHASE COMPOSITIONS AND COMPARISON BETWEEN EXPERIMENTAL AND CALCULATED VALUES OF SOLUTE RETENTION TIMES USING THE SOLVENT STRENGTH WEIGHTING FACTORS IN TERNARY RP-HPLC

Solute	Parameter[a]	Retention time (min)					Fitted coefficients
		1	2	3	4	5	
Benzyl alcohol	Exp.	4.33	3.77	4.17	3.95	4.02	$a = -628.257$
	Calc.	4.33	3.77	4.08	3.95	3.98	$b = -5.0666$
	r.d. (%)	0	0	2.06	0	1.06	$c = 5.2077$
Dimethyl phthalate	Exp.	6.95	7.23	7.75	7.53	7.81	$a = -2.3 \cdot 10^{-19}$
	Calc.	6.96	7.39	7.31	7.36	7.35	$b = 32.4709$
	r.d. (%)	−0.15	−2.18	5.62	2.23	5.84	$c = 7.4068$
Phenol	Exp.	4.33	4.35	4.49	4.30	4.49	$a = 400.212$
	Calc.	4.320	4.332	4.325	4.328	4.327	$b = -8.2249$
	r.d. (%)	0.23	0.42	3.680	−0.64	3.63	$c = 4.3109$
Benzonitrile	Exp.	5.95	7.23	6.63	6.85	7.04	$a = 133.610$
	Calc.	5.95	7.23	6.55	6.85	6.78	$b = -2.6355$
	r.d. (%)	0	0	1.21	0	3.72	$c = 1.5763$
p-Cresol	Exp.	6.33	5.70	6.35	6.00	6.25	$a = -1.5 \cdot 10^{10}$
	Calc.	6.33	5.70	6.16	6.00	6.04	$b = -19.7860$
	r.d. (%)	0	0	3.06	0	3.42	$c = 6.4373$
Diethyl phthalate	Exp.	17.15	15.55	18.92	17.51	18.48	$a = -2.8 \cdot 10^{19}$
	Calc.	17.54	15.77	17.29	16.90	17.02	$b = -36.8231$
	(r.d. (%)	−2.28	−1.40	8.62	3.47	7.89	$c = 17.5922$
3,4-Dimethylphenol	Exp.	9.23	7.23	8.87	8.11	8.54	$a = -8.26 \cdot 10^{8}$
	Calc.	9.23	7.23	8.61	8.11	8.24	$b = -16.3428$
	r.d. (%)	0	0	2.96	0	3.48	$c = 9.7412$
Benzene	Exp.	11.43	11.80	11.42	11.52	11.91	$a = 4.5 \cdot 10^{18}$
	Calc.	11.41	11.79	11.47	11.55	11.52	$b = -36.5770$
	r.d. (%)	0.16	0.09	−0.40	−0.25	3.25	$c = 11.4005$
2,4-Dimethylphenol	Exp.	10.80	8.58	10.41	9.50	10.07	$a = -5.43 \cdot 10^{7}$
	Calc.	10.80	8.58	10.05	9.50	9.64	$b = -13.9296$
	r.d. (%)	0	0	3.41	0	4.22	$c = 11.5699$
Mobile phase composition (%)							
CH_3OH		49.9	0	24.4	13.2	15.0	
ACN		0	37.5	19.2	27.6	26.3	
Water		50.1	62.5	56.4	59.2	58.7	

[a] r.d. (%) = 100 (exp. − calc.)/exp.

TABLE VII

USING THE EXPERIMENTAL DATA OF ISSAQ *ET AL.* [15]: RESULTS OF EXPONENTIAL CURVE FITTING OF SOLUTE RETENTION TIMES *VS.* TERNARY MOBILE PHASE COMPOSITIONS AND COMPARISON BETWEEN EXPERIMENTAL AND CALCULATED RETENTION TIMES OF THE SOLUTES USING THE SOLVENT STRENGTH WEIGHTING FACTORS IN RP-HPLC

Solute	Parameter[a]	Retention time (min)					Fitted coefficients
		1	2	3	4	5	
Anthraquinone	Exp.	7.23	8.26	9.57	11.65	16.44	$a = 1.12 \cdot 10^{15}$
	Calc.	7.23	8.09	9.57	12.10	16.44	$b = -17.9503$
	r.d. (%)	0	2.03	0	3.88	0	$c = 6.0213$
2-Methylanthraquinone	Exp.	8.98	10.30	11.98	14.75	21.20	$a = 5.81 \cdot 10^{15}$
	Calc.	8.98	10.07	11.98	15.33	21.20	$b = -18.7129$
	r.d. (%)	0	2.23	0	−3.93	0	$c = 7.5331$
Naphthalene	Exp.	7.23	9.16	11.30	14.67	22.41	$a = 2.13 \cdot 10^{14}$
	Calc.	7.23	8.76	11.30	15.49	22.41	$b = -16.7368$
	r.d. (%)	0	4.32	0	−5.58	0	$c = 4.8771$
2-Ethylanthraquinone	Exp.	10.94	13.27	15.82	19.98	30.19	$a = 2.56 \cdot 10^{15}$
	Calc.	10.94	12.74	15.82	21.11	30.19	$b = -18.0000$
	r.d. (%)	0	4.02	0	−5.66	0	$c = 8.4306$
Biphenyl	Exp.	8.98	11.77	15.13	20.38	34.03	$a = 1.19 \cdot 10^{16}$
	Calc.	8.98	11.21	15.13	22.00	34.03	$b = -18.7119$
	r.d. (%)	0	4.72	0	−7.93	0	$c = 6.0135$
Mobile phase composition (%)							
ACN		60.0	45.0	30.0	15.0	0	
THF		0	10.0	20.0	30.0	40.0	
Water		40.0	45.0	50.0	55.0	60.0	

[a] r.d. (%) = 100 (exp. − calc.)/exp.

TABLE VIII

COEFFICIENTS OF EXPONENTIAL CURVE FITTING OF RETENTION TIMES *VS.* MOBILE PHASE COMPOSITIONS FOR THE SOLUTES IN GROUP 1 WITH TERNARY SOLVENT MIXTURES OF METHANOL, ACETONITRILE AND WATER, USING THE SOLVENT POLARITY PARAMETERS IN RP-HPLC

Solute	*a*	*b*	*c*
p-Chloronitrobenzene	102.0783	−1.0129	0.5296
8-Hydroxquinoline	8333.9404	−2.2488	1.3039
Benzophenone	126.8513	−0.9401	−0.2482
Naphthalene	197.9749	−1.0283	0.0062
Phenergan	247.6103	−1.0579	−0.5138
Diazepam	−5.3106	0.2487	17.0021
Dibutyl phthalate	2253.0161	−1.3667	−4.2784
Phenanthrene	252.9215	−0.7642	−6.5646
Acetanilide	2.8122	−0.3323	0.8500

TABLE IX

COMPARISON BETWEEN EXPERIMENTAL AND CALCULATED RETENTION TIMES OF THE SOLUTES IN GROUP I WITH TERNARY MOBILE PHASES CONSISTING OF METHANOL, ACETONITRILE AND WATER, USING THE SOLVENT POLARITY PARAMETERS IN RP-HPLC

Solute	Parameter[a]	Retention time (min)						
		1	2	3	4	5	6	7
p-Chloronitrobenzene	Exp.	2.167	2.337	2.850	3.506	4.315	4.693	5.940
	Calc.	2.167	2.375	2.873	3.506	4.310	4.790	5.940
	r.d. (%)	0	−1.62	−0.81	0	0.12	−2.06	0
8-Hydroxyquinoline	Exp.	2.167	2.352	3.433	4.557	7.025	8.833	13.565
	Calc.	2.167	2.429	3.217	4.557	6.835	8.516	13.565
	r.d. (%)	0	−3.29	6.28	0	2.71	3.59	0
Benzophenone	Exp.	2.490	2.750	3.567	4.520	5.910	6.465	8.055
	Calc.	2.490	2.811	3.571	4.520	5.704	6.403	8.055
	r.d. (%)	0	−2.23	−0.12	0	3.48	0.96	0
Naphthalene	Exp.	2.988	3.350	4.322	5.476	7.012	7.958	10.040
	Calc.	2.988	3.373	4.297	5.476	6.978	7.878	10.040
	r.d. (%)	0	−0.68	0.57	0	0.48	1.01	0
Phenergan	Exp.	2.792	3.183	4.198	5.657	7.400	8.600	11.005
	Calc.	2.792	3.232	4.294	5.657	7.407	8.460	11.005
	r.d. (%)	0	−1.52	−2.28	0	−0.09	1.63	0
Diazepam	Exp.	2.350	2.633	3.485	4.350	5.385	5.402	6.077
	Calc.	2.350	2.774	3.585	4.350	5.071	5.416	6.077
	r.d. (%)	0	−5.35	−2.87	0	5.82	−0.27	0
Dibutyl phthalate	Exp.	4.253	5.475	9.378	14.830	23.218	26.493	38.520
	Calc.	4.253	5.746	9.562	14.830	22.103	26.720	38.520
	r.d. (%)	0	−4.95	−1.96	0	4.80	−0.86	0
Phenanthrene	Exp.	4.625	5.522	7.715	11.000	15.307	17.100	21.007
	Calc.	4.625	5.681	8.101	11.000	14.472	16.457	21.007
	r.d. (%)	0	−2.88	−5.01	0	5.46	3.76	0
Acetanilide	Exp.	1.575	1.590	1.683	1.732	1.850	1.875	1.923
	Calc.	1.575	1.604	1.665	1.732	1.804	1.842	1.923
	r.d. (%)	0	−0.88	1.04	0	2.49	1.76	0
Mobile phase composition (%)								
CH_3OH		80.0	72.0	56.0	40.0	24.0	16.0	0
ACN		0	5.0	15.0	25.0	35.0	40.0	50.0
Water		20.0	23.0	29.0	35.0	41.0	44.0	50.0

[a] r.d. (%) = 100 (exp. − calc.)/exp.

retention time [the r.d. (%) values in the tables] is not greater than 6.5%, and most are within 3%.

The results in Tables V–VII are based on experimental data published by Bartha *et al.* [14] and Issaq *et al.* [15]. In Tables V and VI, points 1, 2 and 4 were the raw experimental data sampling points and points 3 and 5 were used as the test points. In

Table VII, points 1, 3 and 5 were the raw experimental data points and points 2 and 4 were used as the test points. The tables show that the prediction model for the solute retention time described in this paper really does work. In some instances, *e.g.*, in Table V, the r.d. (%) values are even better than our experimental results.

An interesting fact is that a similar model to eqn. 9 will also be effective for predicting solute retention times, which could have the following form:

$$t_R = a' \exp [b'(P'_1\varphi_1 + P'_2\varphi_2)] + c' \quad (10)$$

where P' refers to the Snyder solvent polarity parameter of the organic modifier in mobile phases, being 5.1 for CH_3OH, 5.8 for ACN, 4.0 for THF (and 10.2 for water) [18,19]. In Tables VIII–XI are given the non-linear least-squares fitted coefficients and a comparison of the experimental and calculated retention times of the solutes by using Snyder polarity parameters based on our experimental data. Tables XII–XIV give the fitted coefficients and a comparison between the predicted and experimental retention times of the solutes by using the experimental data reported by Bartha *et al.* [14] and Issaq *et al.* [15], based on Snyder solvent polarity parameters. From the tables, it can be seen that the solute retention times predicted by using the solvent strength weighting factors are mostly close to those obtained by using the solvent polarity parameters with the same compositions of the mobile phase, although the fitted coefficients are different from each other.

However, no ternary solvent system conforms with eqn. 9. For instance, some systems containing supplementary chemicals in a ternary mobile phase of water, CH_3OH, ACN or THF show serious deviations from eqn. 9. Table XV gives typical results based on the experimental data reported by Sekulic *et al.* [16] by using Snyder solvent polarity parameters. In their experiment, all the mobile phases contained 5 m*M* heptanesulphonate and 1% acetic acid in addition to water, CH_3OH and ACN. Nevertheless, the situation would be even more serious if the solvent polarity parameters were replaced with the solvent strength weighting factors. Because of the

TABLE X

COEFFICIENTS OF EXPONENTIAL CURVE FITTING OF RETENTION TIMES *VS.* MOBILE PHASE COMPOSITIONS FOR THE SOLUTES IN GROUP 2 WITH TERNARY SOLVENT MIXTURES OF METHANOL, ACETONITRILE AND WATER, USING THE SOLVENT POLARITY PARAMETERS IN RP-HPLC

Solute	*a*	*b*	*c*
Toluene	−63.5506	−0.1704	63.9574
Ethyl benzene	50.9036	0.0352	−52.0560
Biphenyl	2.6993	9.4249	−4.3961
Nitrobenzene	−30.8040	−1.8565	2.4528
Chlorobenzol	−8.8305	−0.2244	7.9512
p-Dichlorobenzene	−16.8285	−0.2559	12.4131
o-Dichlorobenzene	−67.9021	−0.3453	65.2930
m-Dichlorobenzene	−37.8762	−0.0893	33.8358
Methyl salicylate	0.2340	0.6158	1.3190
Benzyl acetate	0.0003	2.1394	2.1003

TABLE XI

COMPARISON BETWEEN EXPERIMENTAL AND CALCULATED RETENTION TIMES OF THE SOLUTES IN GROUP 2 WITH TERNARY MOBILE PHASES CONSISTING OF METHANOL, TETRAHYDROFURAN AND WATER, USING THE SOLVENT POLARITY PARAMETERS IN RP-HPLC

Solute	Parameter[a]	Retention time (min)						
		1	2	3	4	5	6	7
Toluene	Exp.	4.157	3.890	3.690	3.558	3.458	3.173	2.953
	Calc.	4.157	3.918	3.678	3.558	3.437	3.196	2.953
	r.d. (%)	0	−0.72	0.32	0	0.59	−0.72	0
Ethylbenzene	Exp.	5.667	5.158	4.773	4.490	4.247	3.792	3.337
	Calc.	5.667	5.193	4.723	4.490	4.257	3.795	3.337
	r.d. (%)	0	−0.68	1.04	0	−0.25	−0.09	0
Biphenyl	Exp.	7.908	6.595	5.421	5.200	4.458	3.703	3.088
	Calc.	7.908	6.743	5.689	5.200	4.735	3.870	3.088
	r.d. (%)	0	−2.25	−4.95	0	−6.20	−4.52	0
Nitrobenzene	Exp.	2.412	2.398	2.400	2.332	2.328	2.195	2.095
	Calc.	2.412	2.390	2.356	2.332	2.303	2.221	2.095
	r.d. (%)	0	0.34	1.85	0	1.09	−1.19	0
Chlorobenzol	Exp.	3.988	3.758	3.583	3.432	3.290	2.992	2.798
	Calc.	3.988	3.774	3.549	3.432	3.312	3.062	2.798
	r.d. (%)	0	−0.43	0.95	0	−0.66	−2.33	0
p-Dichlorobenzene	Exp.	5.663	5.100	4.800	4.573	4.492	3.822	3.307
	Calc.	5.663	5.246	4.804	4.573	4.335	3.836	3.307
	r.d. (%)	0	−2.87	−0.88	0	3.50	−0.37	0
o-Dichlorobenzene	Exp.	5.267	4.865	4.300	4.042	3.757	3.248	2.792
	Calc.	5.267	4.780	4.289	4.042	3.794	3.295	2.792
	r.d. (%)	0	1.75	0.26	0	−0.99	−1.45	0
m-Dichlorobenzene	Exp.	6.300	5.605	5.238	4.823	4.525	3.833	3.267
	Calc.	6.300	5.718	5.125	4.823	4.518	3.899	3.267
	r.d. (%)	0	−2.02	2.16	0	0.15	−1.73	0
Methyl salicylate	Exp.	3.428	3.175	2.908	2.790	2.680	2.495	2.345
	Calc.	3.428	3.145	2.900	2.790	2.688	2.504	2.345
	r.d. (%)	0	0.95	0.28	0	−0.29	−0.36	0
Benzyl acetate	Exp.	2.683	2.408	2.295	2.267	2.223	2.150	2.148
	Calc.	2.683	2.454	2.314	2.267	2.230	2.179	2.148
	r.d. (%)	0	−1.89	−0.85	0	−0.32	−1.35	0
Mobile phase composition (%)								
CH_3OH		70.0	56.0	42.0	35.0	28.0	14.0	0
THF		0	12.0	24.0	30.0	36.0	48.0	60.0
Water		30.0	32.0	34.0	35.0	36.0	38.0	40.0

[a] r.d. (%) = 100 (exp. − calc.)/exp.

interaction between the solvents and the supplementary chemicals, the calculation of the total solvent strength of the mobile phase may become more complex. Therefore, some modification to eqn. 9 might be needed if this kind of ternary mobile phase is used.

TABLE XII

USING THE EXPERIMENTAL DATA OF BARTHA *ET AL.* [14]: RESULTS OF EXPONENTIAL CURVE FITTING OF SOLUTE RETENTION TIMES *VS.* TERNARY MOBILE PHASE COMPOSITIONS AND COMPARISON BETWEEN EXPERIMENTAL AND CALCULATED VALUES OF SOLUTE RETENTION TIMES, USING SNYDER'S SOLVENT POLARITY PARAMETERS IN RP-HPLC

Solute	Parameter[a]	Retention time (min)					Fitted coefficients
		1	2	3	4	5	
Benzyl alcohol	Exp.	4.02	3.34	3.51	3.40	3.45	a = 33.9121
	Calc.	4.02	3.34	3.48	3.40	3.43	b = −2.4664
	r.d. (%)	0	0	0.72	0	0.73	c = 3.2372
Dimethyl phthalate	Exp.	4.79	5.49	4.75	5.03	4.94	a = $1.22 \cdot 10^{-6}$
	Calc.	4.79	5.49	4.88	5.03	4.96	b = 5.6449
	r.d. (%)	0	0	−2.69	0	−0.44	c = 4.7833
Phenol	Exp.	6.20	3.72	4.39	4.05	4.18	a = 34.0663
	Calc.	6.20	3.72	4.44	4.05	4.17	b = −1.4867
	r.d. (%)	0	0	−1.16	0	0.20	c = 2.6866
Benzonitrile	Exp.	6.29	5.49	5.33	5.36	5.33	a = 3138.2
	Calc.	6.289	5.42	5.45	5.43	5.43	b = −5.3613
	r.d. (%)	0.01	1.23	−2.20	−1.27	−1.92	c = 5.4206
p-Cresol	Exp.	7.71	4.51	5.40	5.00	5.33	a = 29.5279
	Calc.	7.71	4.51	5.54	5.00	5.17	b = −1.1238
	r.d. (%)	0	0	−2.67	0	2.95	c = 2.4072
Diethyl phthalate	Exp.	8.19	9.76	8.16	8.87	8.73	a = $6.79 \cdot 10^{-5}$
	Calc.	8.19	9.76	8.49	8.87	8.71	b = 4.2867
	r.d. (%)	0	0	−4.09	0	0.21	c = 8.1427
3,4-Dimethylphenol	Exp.	9.37	5.49	6.67	6.13	6.33	a = 29.8979
	Calc.	9.37	5.49	6.82	6.13	6.35	b = −0.9241
	r.d. (%)	0	0	−2.19	0	−0.32	c = 2.0853
Benzene	Exp.	11.91	8.42	9.07	8.80	8.73	a = 89.2399
	Calc.	11.91	8.42	9.29	8.80	8.95	b = −1.9784
	r.d. (%)	0	0	−2.44	0	−2.50	c = 7.5679
2,4-Dimethylphenol	Exp.	11.48	6.21	7.87	7.09	7.39	a = 39.5542
	Calc.	11.48	6.21	8.03	7.09	7.392	b = −0.8906
	r.d. (%)	0	0	−2.01	0	−0.02	c = 1.3124
Mobile phase composition (%)							
ACN		0	46.1	26.1	35.7	32.3	
THF		38.2	0	16.6	8.6	11.5	
Water		61.8	53.9	57.3	55.7	56.2	

[a] r.d. (%) = 100 (exp. − calc.)/exp.

Although eqn. 9 is based on eqn. 6, the precision of the prediction of capacity factors using eqn. 6 is not as good as that for retention times in some instances. This could be due to the fact that the dead time is not easy to measure exactly and is subject to variations with the mobile phase composition [2,13]. Tables XVI–XIX show that the relative deviations between the experimental and calculated capacity factors are

TABLE XIII

USING THE EXPERIMENTAL DATA OF BARTHA *ET AL.* [14]: RESULTS OF EXPONENTIAL CURVE FITTING OF SOLUTE RETENTION TIMES *VS.* MOBILE PHASE COMPOSITIONS AND COMPARISON BETWEEN EXPERIMENTAL AND CALCULATED VALUES OF SOLUTE RETENTION TIMES USING THE SOLVENT POLARITY PARAMETERS IN TERNARY RP-HPLC

Solute	Parameter[a]	Retention time (min)					Fitted coefficients	
		1	2	3	4	5		
Benzyl alcohol	Exp.	4.33	3.77	4.17	3.95	4.02	a =	−30.6719
	Calc.	4.33	3.77	4.08	3.95	3.98	b =	−1.4320
	r.d. (%)	0	0	2.06	0	1.06	c =	5.1318
Dimethyl phthalate	Exp.	6.95	7.23	7.75	7.53	7.81	a =	$-1.8 \cdot 10^{-14}$
	Calc.	6.954	7.38	7.34	7.37	7.37	b =	12.1074
	r.d. (%)	−0.06	−2.13	5.25	2.09	5.65	c =	−3.4654
Phenol	Exp.	4.33	4.35	4.49	4.30	4.49	a =	1.7983
	Calc.	4.323	4.330	4.326	4.328	4.327	b =	−0.0110
	r.d. (%)	0.17	0.47	3.65	−0.65	3.62	c =	2.5739
Benzonitrile	Exp.	5.95	7.23	6.63	6.85	7.04	a =	28.1515
	Calc.	5.95	7.23	6.55	6.85	6.79	b =	−0.7897
	r.d. (%)	0	0	1.21	0	3.55	c =	2.1771
p-Cresol	Exp.	6.33	5.70	6.35	6.00	6.25	a =	−78 604.9
	Calc.	6.33	5.70	6.16	6.00	6.04	b =	−5.3260
	r.d. (%)	0	0	3.06	0	3.42	c =	6.4321
Diethyl phthalate	Exp.	17.15	15.55	18.92	17.51	18.48	a =	$-5.6 \cdot 10^{19}$
	Calc.	17.44	15.60	17.39	17.17	17.25	b =	−19.5712
	r.d. (%)	1.67	−0.32	8.10	1.92	6.68	c =	17.4385
3,4-Dimethylphenol	Exp.	9.23	7.23	8.87	8.11	8.54	a =	−36 734.4
	Calc.	9.23	7.23	8.61	8.11	8.22	b =	−4.4142
	r.d. (%)	0	0	2.96	0	3.72	c =	9.7156
Benzene	Exp.	11.43	11.80	11.42	11.52	11.91	a =	$4.27 \cdot 10^{10}$
	Calc.	11.42	11.795	11.46	11.53	11.51	b =	−11.6984
	r.d. (%)	0.09	0.04	−0.35	−0.13	3.33	c =	11.4150
2,4-Dimethylphenol	Exp.	10.80	8.58	10.41	9.50	10.07	a =	−10 867.7
	Calc.	10.80	8.58	10.05	9.50	9.62	b =	−3.7755
	r.d. (%)	0	0	3.44	0	4.45	c =	11.5299
Mobile phase composition (%)								
CH_3OH		49.0	0	24.4	13.2	15.0		
ACN		0	37.5	19.2	27.6	26.3		
Water		50.1	62.5	56.4	59.2	58.7		

[a] r.d. (%) = 100 (exp. − calc.)/exp.

usually greater than those for the retention times, although the correlation coefficient (R) and remainder standard deviation (S.D.) are statistically acceptable. Hence we suggest that eqn. 9 be used instead of eqn. 6 in practice.

From the fitted and the regression coefficients of the same solutes in Tables I and XVI using the solvent strength weighting factors, and in Tables VIII and XVIII using

TABLE XIV

USING THE EXPERIMENTAL DATA OF ISSAQ *ET AL.* [15]: FITTING RESULTS OF SOLUTE RETENTION TIME *VS.* MOBILE PHASE COMPOSITION AND COMPARISON BETWEEN EXPERIMENTAL AND CALCULATED RETENTION TIMES OF THE SOLUTES BY USING THE SOLVENT POLARITY PARAMETERS IN TERNARY RP-HPLC

Solute	Parameter[a]	Retention time (min)					Fitted coefficients
		1	2	3	4	5	
Anthraquinone	Exp.	7.23	8.26	9.57	11.65	16.44	a = 65.1583
	Calc.	7.23	8.09	9.57	12.10	16.44	b = −1.1458
	r.d. (%)	0	2.03	0	3.88	0	c = 6.0213
2-Methylanthraquinone	Exp.	8.98	10.30	11.98	14.75	21.20	a = 92.3943
	Calc.	8.98	10.07	11.98	15.33	21.20	b = −1.1944
	r.d. (%)	0	2.23	0	−3.93	0	c = 7.5331
Naphthalene	Exp.	7.23	9.16	11.30	14.67	22.41	a = 96.8694
	Calc.	7.23	8.76	11.30	15.49	22.41	b = −1.0683
	r.d. (%)	0	4.32	0	−5.58	0	c = 4.8770
2-Ethylanthraquinone	Exp.	10.94	13.27	15.82	19.98	30.19	a = 136.7754
	Calc.	10.94	12.74	15.82	21.11	30.19	b = −1.1489
	r.d. (%)	0	4.02	0	−5.66	0	c = 8.4306
Biphenyl	Exp.	8.98	11.77	15.13	20.38	34.03	a = 189.3861
	Calc.	8.98	11.21	15.13	22.00	34.03	b = −1.1944
	r.d. (%)	0	4.72	0	−7.93	0	c = 6.0135
Mobile phase composition (%)							
ACN		60.0	45.0	30.0	15.0	0	
THF		0	10.0	20.0	30.0	40.0	
Water		40.0	45.0	50.0	55.0	60.0	

[a] r.d. (%) = 100 (exp. − calc.)/exp.

the solvent polarity parameters, it is found that there is no potential correlation between the values of b in eqn. 9 and B in eqn. 6. In theory, they could be expected to be identical. The values of c could represent the dead time, so all the values of c for the solutes eluted using same column and solvent system must be identical. In fact, however, these values are different from each other. This might be due to the fact that the approximative solution of eqn. 9 is not unique for the Newton or Marquardt algorithm [24]. Often, the iteration results are relevant to the initial values of a, b and c in eqn. 9 [24], even though the Marquardt algorithm is not as restricted as the Newton iteration in assuming the initial values for the iteration. In our experience, the initial values of a, b and c could be assumed by taking advantage of the Taylor expansion of eqn. 9 with the Lagrange remainder item at the three raw experimental data sampling points, no matter what algorithm is used, which could be:

$$b' = \frac{2 \ln \left| \frac{[t_R(3) - t_R(2)][x(2) - x(1)]}{[x(3) - x(2)][t_R(2) - t_R(1)]} \right|}{x(3) - x(1)} \quad (11)$$

TABLE XV

USING THE EXPERIMENTAL DATA OF SEKULIC *ET AL.* [16]: FITTED PARAMETERS AND COMPARISON BETWEEN EXPERIMENTAL AND CALCULATED RETENTION TIMES OF THE SOLUTES USING THE SOLVENT POLARITY PARAMETERS IN RP-HPLC[a]

Solute[b]	Parameter[c]	Retention time (min)						Fitted coefficients
		1	2	3	4	5	6	
PPA	Exp.	2.13	1.03	2.18	1.67	1.78	1.67	$a = -1.06 \cdot 10^{19}$
	Calc.	2.16	1.06	1.95	1.61	1.73	1.61	$b = -20.6478$
	r.d. (%)	−1.31	−2.66	10.63	3.31	2.83	3.31	$c = 2.1579$
PEA	Exp.	2.23	1.10	2.30	1.81	1.94	1.81	$a = -1.62 \cdot 10^{12}$
	Calc.	2.30	1.23	1.93	1.62	1.71	1.62	$b = -13.2459$
	r.d. (%)	−3.12	−11.44	16.04	10.59	11.60	10.59	$c = 2.3030$
MePEA	Exp.	2.20	1.16	2.42	1.89	2.04	1.89	$a = -1.98 \cdot 10^{13}$
	Calc.	2.28	1.29	1.97	1.68	1.77	1.68	$b = -14.4677$
	r.d. (%)	−3.71	−11.47	18.44	11.13	13.12	11.13	$c = 2.2836$
AMPH	Exp.	2.70	1.14	2.86	2.06	2.26	2.06	$a = -1.46 \cdot 10^{19}$
	Calc.	2.74	1.18	2.45	1.97	2.14	1.97	$b = -20.6342$
	r.d. (%)	−1.62	−3.78	14.47	4.21	5.49	4.21	$c = 2.7439$
DiMePEA	Exp.	2.10	1.23	2.46	1.98	2.08	1.98	$a = -7.77 \cdot 10^{15}$
	Calc.	2.21	1.37	2.00	1.74	1.83	1.74	$b = -17.3663$
	r.d. (%)	−5.04	−11.15	18.77	11.97	12.17	11.97	$c = 2.2063$
BuPEA	Exp.	4.10	1.86	5.35	4.08	4.52	4.08	$a = -5.62 \cdot 10^{17}$
	Calc.	4.46	2.28	3.99	3.32	3.54	3.32	$b = -18.9375$
	r.d. (%)	−8.82	−22.58	25.51	18.62	21.60	18.62	$c = 4.4624$
DiPEA	Exp.	7.25	1.84	8.96	5.33	6.20	5.33	$a = -5.62 \cdot 10^{17}$
	Calc.	7.50	2.09	6.47	4.83	5.40	4.83	$b = -20.7051$
	r.d. (%)	−3.45	−13.36	27.74	9.31	12.92	9.31	$c = 7.5011$
Mobile phase composition (%)								
CH_3OH		50.0	0	22.5	15.0	17.5	15.0	
ACN		0	36.5	18.1	23.9	21.9	23.9	
Water		50.0	63.5	59.4	60.1	60.6	60.1	

[a] All mobile phases contained 5 m*M* heptanesulphonate and 1% acetic acid.

[b] PPA = phenylpropanolamine; PEA = phenethylamine; MePEA = N-methyl-2-phenethylamine; AMPH = amphetamine; DiMePEA = N,N-dimethyl-2-phenethylamine; BuPEA = N-*n*-butyl-2-phenethylamine; DiPEA = 2,2′-diphenylethylamine.

[c] r.d. (%) = 100 (exp. − calc.)/exp.

TABLE XVI

REGRESSION COEFFICIENTS FOR CAPACITY FACTORS OF THE SOLUTES IN GROUP 1 *VS.* MOBILE PHASE COMPOSITION IN TERNARY SOLVENT SYSTEM OF METHANOL, ACETONITRILE AND WATER, USING SNYDER'S SOLVENT STRENGTH WEIGHTING FACTORS IN RP-HPLC

Solute	*A*	*B*	*R*[a]	S.D.[a]
p-Chloronitrobenzene	7.6131	−3.7986	−0.9988	0.0626
8-Hydroxyquinoline	11.6661	−5.7629	−0.9999	0.1753
Benzophenone	8.1797	−3.9201	−0.9978	0.1344
Naphthalene	8.1232	−3.7378	−0.9991	0.1445
Phenergan	8.9823	−4.2004	−0.9978	0.1724
Diazepam	7.1939	−3.4766	−0.9815	0.2306
Dibutyl phthalate	12.5494	−5.5757	−0.9950	0.3404
Phenanthrene	9.4033	−4.0186	−0.9954	0.1311
Acetanilide	3.4977	−2.3284	−0.9996	0.3704

[a] *R* = Correlation coefficient; S.D. = remainder standard deviation.

TABLE XVII

COMPARISON BETWEEN EXPERIMENTAL AND CALCULATED CAPACITY FACTORS OF THE SOLUTES IN GROUP 1 WITH TERNARY MOBILE PHASES CONSISTING OF METHANOL, ACETONITRILE AND WATER, USING SNYDER'S SOLVENT STRENGTH WEIGHTING FACTORS IN RP-HPLC

Solute	Parameter[a]	Capacity factor						
		1	2	3	4	5	6	7
p-Chloronitrobenzene	Exp.	0.731	0.992	1.375	1.964	2.474	3.298	4.526
	Calc.	0.750	0.900	1.296	1.866	2.687	3.224	4.643
	r.d. (%)	−2.59	9.33	5.77	4.99	−8.59	2.23	−2.59
8-Hydroxyquinoline	Exp.	0.731	1.005	1.861	2.852	4.656	7.089	11.619
	Calc.	0.726	0.957	1.664	2.893	5.031	6.634	11.536
	r.d. (%)	0.71	4.80	10.59	−1.44	−8.05	6.42	0.71
Benzophenone	Exp.	0.989	1.344	1.973	2.821	3.758	4.920	6.493
	Calc.	1.025	1.237	1.802	2.626	3.826	4.619	6.729
	r.d. (%)	−3.64	7.99	8.62	6.90	−1.80	6.13	−3.64
Naphthalene	Exp.	1.387	1.856	2.602	3.629	4.646	6.288	8.340
	Calc.	1.417	1.695	2.427	3.475	4.975	5.953	8.522
	r.d. (%)	−2.19	8.65	6.70	4.24	−7.09	5.32	−2.19
Phenergan	Exp.	1.230	1.714	2.498	3.782	4.958	6.875	9.237
	Calc.	1.278	1.564	2.340	3.503	5.242	6.413	9.598
	r.d. (%)	−3.96	8.75	6.33	7.39	−5.72	6.72	−3.91
Diazepam	Exp.	0.877	1.245	1.904	2.677	3.336	3.947	4.653
	Calc.	0.963	1.138	1.589	2.219	3.098	3.661	5.111
	r.d. (%)	−9.84	8.55	16.54	17.12	7.13	7.25	−9.84
Dibutyl phthalate	Exp.	2.397	3.668	6.815	11.536	17.694	23.261	34.833
	Calc.	2.591	3.386	5.782	9.876	16.867	22.043	37.647
	r.d. (%)	−8.08	7.69	15.15	14.39	4.68	5.24	−8.08
Phenanthrene	Exp.	2.694	3.708	5.429	8.298	11.324	14.659	18.541
	Calc.	2.842	3.447	5.070	7.456	10.966	13.299	19.561
	r.d. (%)	−5.50	7.03	6.62	10.15	3.16	9.28	−5.50
Acetanilide	Exp.	0.258	0.355	0.403	0.464	0.490	0.717	0.789
	Calc.	0.260	0.291	0.364	0.455	0.569	0.637	0.796
	r.d. (%)	−0.95	18.08	9.52	1.87	16.33	11.19	−0.95
Mobile phase composition (%)								
CH_3OH		80.0	72.0	56.0	40.0	24.0	16.0	0
ACN		0	5.0	15.0	25.0	35.0	40.0	50.0
Water		20.0	23.0	29.0	35.0	41.0	44.0	50.0

[a] r.d. (%) = 100 (exp. − calc.)/exp.

$$a' = \frac{\dfrac{t_R(3) - t_R(2)}{x(3) - x(2)}}{b' \exp\{b'[x(3) + x(2)]/2\}} \tag{12}$$

$$c' = t_R(2) - a' \exp\{b'[x(1) + x(3)]/2\} \tag{13}$$

where a', b' and c' represent the initial values of a, b and c in eqn. 9 when the iteration process started; $x(i) = s_1\varphi_1(i) + s_2\varphi_2(i)$ $(i = 1, 2, 3)$, where $\varphi_1(i)$ and $\varphi_2(i)$ are the

TABLE XVIII

RESULTS OF REGRESSION ANALYSIS OF EQN. 2 FOR THE SOLUTES IN GROUP 1 WITH TERNARY SOLVENT MIXTURES CONSISTING OF METHANOL, ACETONITRILE AND WATER, USING SNYDER'S SOLVENT POLARITY PARAMETERS IN RP-HPLC

Solute	A	B	R^a	S.D.[a]
p-Chloronitrobenzene	6.0164	−1.5452	−0.9988	0.0626
8-Hydroxyquinoline	9.2437	−2.3442	−0.9999	0.1033
Benzophenone	6.5317	−1.5949	−0.9978	0.1355
Naphthalene	6.5521	−1.5205	−0.9991	0.1455
Phenergan	7.2167	−1.7086	−0.9978	0.1732
Diazepam	5.7326	−1.4142	−0.9815	0.2879
Dibutyl phthalate	10.2057	−2.2681	−0.9950	0.3451
Phenanthrene	7.7141	−1.6347	−0.9954	0.3691
Acetanilide	2.5190	−0.9472	−0.9996	0.3699

[a] R = Correlation coefficient; S.D. = remainder standard deviation.

TABLE XIX

COMPARISON BETWEEN EXPERIMENTAL AND CALCULATED CAPACITY FACTORS OF THE SOLUTES IN GROUP 1 WITH TERNARY MOBILE PHASES CONSISTING OF METHANOL, ACETONITRILE AND WATER, USING THE SOLVENT POLARITY PARAMETERS IN RP-HPLC

Solute	Parameter[a]	Capacity factor						
		1	2	3	4	5	6	7
p-Chloronitrobenzene	Exp.	0.731	0.992	1.375	1.964	2.474	3.298	4.526
	Calc.	0.750	0.900	1.296	1.866	2.687	3.224	4.643
	r.d. (%)	−2.59	9.33	5.77	4.99	−8.59	2.23	−2.59
8-Hydroxyquinoline	Exp.	0.731	1.005	1.861	2.852	4.656	7.089	11.619
	Calc.	0.726	0.957	1.664	2.893	5.031	6.634	11.536
	r.d. (%)	0.71	4.80	10.59	−1.44	−8.05	6.42	0.71
Benzophenone	Exp.	0.989	1.344	1.973	2.821	3.758	4.920	6.493
	Calc.	1.025	1.237	1.802	2.626	3.826	4.619	6.729
	r.d. (%)	−3.64	7.99	8.62	6.90	−1.80	6.13	−3.64
Naphthalene	Exp.	1.387	1.856	2.602	3.629	4.646	6.288	8.340
	Calc.	1.417	1.695	2.427	3.475	4.975	5.953	8.522
	r.d. (%)	−2.19	8.65	6.70	4.24	−7.09	5.32	−2.19
Phenergan	Exp.	1.230	1.714	2.498	3.782	4.958	6.875	9.237
	Calc.	1.278	1.564	2.340	3.503	5.242	6.413	9.598
	r.d. (%)	−3.96	8.75	6.33	7.39	−5.72	6.72	−3.91
Diazepam	Exp.	0.877	1.245	1.904	2.677	3.336	3.947	4.653
	Calc.	0.963	1.138	1.589	2.219	3.098	3.661	5.111
	r.d. (%)	−9.84	8.55	16.54	17.12	7.13	7.25	−9.84
Dibutyl phthalate	Exp.	2.397	3.668	6.815	11.536	17.694	23.261	34.833
	Calc.	2.591	3.386	5.782	9.876	16.867	22.043	37.647
	r.d. (%)	−8.08	7.69	15.15	14.39	4.68	5.24	−8.08
Phenanthrene	Exp.	2.694	3.708	5.429	8.298	11.324	14.659	18.541
	Calc.	2.842	3.447	5.070	7.456	10.966	13.299	19.561
	r.d. (%)	−5.50	7.03	6.62	10.15	3.16	9.28	−5.50
Acetanilide	Exp.	0.258	0.355	0.403	0.464	0.490	0.717	0.789
	Calc.	0.260	0.291	0.364	0.455	0.569	0.637	0.796
	r.d. (%)	−0.95	18.08	9.52	1.87	16.33	11.19	−0.95
Mobile phase composition (%)								
CH_3OH		80.0	72.0	56.0	40.0	24.0	16.0	0
ACN		0	5.0	15.0	25.0	35.0	40.0	50.0
Water		20.0	23.0	29.0	35.0	41.0	44.0	50.0

[a] r.d. (%) = 100 (exp. − calc.)/exp.

volume percentages of organic modifiers 1 and 2 in the mobile phase at raw experimental data point i; and $t_R(i)$ ($i = 1, 2, 3$) is the retention time of a solute at the ith raw experimental data sampling point. If the above choice of a', b' and c' cannot make the iteration continue or the obtained a, b and c values result in unacceptable r.d. (%) values, possibly another choice for the initial values of a, b and c is needed [24]. Generally, the Marquardt method is likely to be more powerful than the Newton algorithm in our experience. However, the former would take much more computer time than the latter.

In order to improve further the prediction of retention times, we tried to modify eqn. 9. For example, we added a solvent interaction term:

$$t_R = a \exp [b(s_1\varphi_1 + s_2\varphi_2 + G\, s_1\varphi_1 s_2\varphi_2)] + c \qquad (14)$$

where G is a weighting factor. We tried many different values of G, including the positive and negative values, but the r.d. (%) values using eqn. 14 were always poorer than those using eqn. 9. From eqn. 9, we can see that the b is likely to connect $s_1\varphi_1$ and $s_2\varphi_2$. In other words, it belongs to two organic modifiers simultaneously. Hence it can be questioned whether b in eqn. 9 is involved in the interaction between the solvents. Certainly this aspect needs to be investigated further.

REFERENCES

1 L. R. Snyder, *Anal. Chem.*, 46 (1974) 1384.
2 L. R. Snyder and M. A. Quarry, *J. Liq. Chromatogr.*, 10 (1987) 1789.
3 P. J. Schoenmakers, H. A. H. Billiet, R. Tijssen and L. de Galan, *J. Chromatogr.*, 149 (1978) 519.
4 P.-C. Lu and X.-M. Lu, *Sepu*, 2 (1984) 102.
5 P. J. Schoenmakers, H. A. H. Billiet and L. de Galan, *J. Chromatogr.*, 218 (1981) 261.
6 A.-J. Hsu, R. J. Laub and S. J. Madden, *J. Liq. Chromatogr.*, 7 (1984) 615.
7 J. W. Weyland, C. H. P. Bruins and D. A. Doornbos, *J. Chromatogr. Sci.*, 22 (1984) 31.
8 P. J. Schoenmakers, H. A. H. Billiet and L. de Galan, *J. Chromatogr.*, 282 (1983) 107.
9 A. K. Smilde, C. H. P. Bruins, D. A. Doornbos and J. Vink, *J. Chromatogr.*, 410 (1987) 1.
10 P. M. J. Coenegracht, A. K. Smilde, H. J. Metting and D. A. Doornbos, *J. Chromatogr.*, 485 (1989) 195.
11 E. Marengo, C. Baicch, M. C. Gennaro and P. Bortolo, *Chromatographia*, 27 (1989) 19.
12 P. M. J. Coenegracht, A. K. Smilde and A. Knevelman, *J. Liq. Chromatogr.*, 12 (1989) 77.
13 R. A. Djerki and R. J. Laub, *J. Liq. Chromatogr.*, 10 (1987) 1749.
14 A. Bartha, H. A. H. Billiet and L. de Galan, *J. Chromatogr.*, 458 (1988) 371.
15 H. J. Issaq, G. M. Muschik and G. M. Janini, *J. Liq. Chromatogr.*, 6 (1983) 259.
16 S. Sekulic, P. R. Haddad and C. J. Lamberton, *J. Chromatogr.*, 363 (1986) 125.
17 L. R. Snyder, J. W. Dolan and J. R. Gant, *J. Chromatogr.*, 165 (1979) 3.
18 L. R. Snyder, *J. Chromatogr. Sci.*, 16 (1978) 223.
19 J. C. Berridge, *Techniques for the Automated Optimization of HPLC Separations*, Wiley, Chichester, 1985, pp. 55–57 and 72–74.
20 R. L. Lehrer, *Int. Lab.*, 11 (1981) 76.
21 S. J. Ziegler and O. Sticher, *J. Liq. Chromatogr.*, 12 (1989) 199.
22 G. R. Deily, *Commun. ACM*, 2 (1966) 85.
23 D. W. Marquardt, *J. Soc. Ind. Appl. Math.*, 11 (1963) 431.
24 T. E. Shoup, *Numerical Methods for the Personal Computer*, Prentice-Hall, New York, 1983; Chinese Edition, translated by X.-Z. Liu, Science Press, Beijing, 1989, pp. 63–70.

Journal of Chromatography, 555 (1991) 53–64
Elsevier Science Publishers B.V., Amsterdam

CHROM. 23 379

Retention behavior and chiral recognition of β-cyclodextrin-derivative polymer adsorbed on silica for warfarin, structurally related compounds and Dns-amino acids

N. THUAUD*, B. SEBILLE, A. DERATANI and G. LELIEVRE
Laboratoire de Physico-Chimie des Biopolymères, U.M. 27, CNRS-Université Paris XII, 2 Rue H. Dunant, 94320 Thiais (France)
(Received March 22nd, 1991)

ABSTRACT

Warfarin enantiomers that have previously been reported to be difficult to separate on cyclodextrin bonded high-performance liquid chromatographic supports can be easily and completely resolved on a stationary phase obtained by deposition on silica of an epichlorohydrin–β-cyclodextrin polymer derivative. The separation of other hydroxy-coumarin analogues and Dns-amino acids is also demonstrated. Studying the influence of the pH and methanol content of the aqueous mobile phase allows the conditions required to separate these compounds to be optimized.

INTRODUCTION

Cyclodextrins (CD) have been succesfully used as chiral liquid chromatography stationary phases for the separation of enantiomers. First, cross-linked β-CD–polymers beads were used to resolve the enantiomers of mandelic acid derivatives [1] and indole alkaloids [2] in conventional chromatography. Then, the grafting of β-CD to silica by Armstrong [3] gave rise to Cyclobond stationary phases. These supports exhibit excellent properties, allowing the enantiomeric resolution of numerous compounds such as alkaloids, amino acid derivatives, organometallic compounds, mandelic acid and drugs [3–6]. However, no chiral stationary phase is universally effective for the resolution of all types of enantiomers. For example warfarin, a 3-substituted 4-hydroxycoumarin derivative, could not be resolved on a β-CD bound column [7].

There are a number of requirements for chiral recognition by the β-CD cavity. In addition to inclusion of a part of the molecule, the chiral center or one of its substituents must be near and interact with the mouth of the β-CD cavity. So, computer models of *d* and *l* isomers of the anticoagulant warfarin demonstrate that the phenyl group of the drug is too far from the CD rim to achieve differential complexation [7].

To extend the range of chiral recognition separation, derivatization of the secondary hydroxyl groups of β-CD has been carried out in order to provide additional interactions. Several isomer separations that are not possible on high-performance

0021-9673/91/$03.50

liquid chromatographic (HPLC) supports bearing native CD residues have been achieved on acetylated [4] or hydroxypropyl-substituted β-CD phases [8].

β-CD silica supports can also be obtained by non-covalent coating of β-CD polymers to the mineral surface. In a previous study [9] we grafted native β-CD to polyethyleneimine to prepare a water-soluble polymer easily adsorbed at the silica surface, the amine functions providing a tightly adsorbed coating as a result of strong interactions with silanol groups. This liquid chromatographic support was able to separate structural isomers but no specific drug chiral recognition was observed for warfarin, which was eluted as a single peak, as on Cyclobond phases [7].

The present work deals with the properties of a new HPLC support for enantiomer separations that we have described recently [10]. It is based on adsorption onto silica of a soluble epichlorohydrin–β-CD polymer bearing ammonium substituents. The efficiency of these supports in resolving warfarin and related coumarin enantiomers was examined. Moreover the separation of Dns-amino acids (Dns = dansyl = 5-dimethylaminonaphthalene-1-sulphonyl) already described on immobilized native [11] or modified β-CD [12], was investigated to compare the chromatographic properties of our β-CD polymer phase with previous ones.

EXPERIMENTAL

Materials

β-CD (Ringdex B) was a gift from Orsan (Paris, France). The coumarin anticoagulants, sodium warfarin (Merrel Dow, Bourgoin-Jallieu, France), coumachlor and acenocoumarol (Ciba-Geigy, Rueil-Malmaison, France) and phenprocoumon (Hoffman-La Roche, Basle, Switzerland) were used as supplied by the manufacturers and are listed in Table I.

Dns-amino acids were obtained from Sigma (St. Louis, MO, USA).

LiChrospher Si-100, 5 μm particle diameter, was obtained from Merck (Darmstadt, Germany).

Preparation of the enantiomers of warfarin

Warfarin was resolved by the method of West *et al.* [13] to yield optically pure *R*-warfarin ($[\alpha]_D^{25} = +149.0$) and *S*-warfarin ($[\alpha]_D^{25} = -148.7$) (concentration = 1 *M*, 0.5 *M* sodium hydroxide).

Preparation of the chromatographic supports

Several soluble epichlorohydrin–β-CD polymers bearing ammonium substituents (EP–β-CD-N^+) were obtained as previously described [10]. Firstly we prepared EP–β-CD derivatives by reacting epichlorohydrin and β-CD. By varying the molar ratio of these compounds, β-CD polymers with different amounts of dihydroxypropyl groups as substituents and hydroxypropyl groups as bridges linking β-CD were obtained. It has been previously determined by ^{13}C-NMR spectra that the hydroxypropyl substitutions take place at the C-2, C-3 and even C-6 positions of β-CD [14,15]. Then, by reacting the polymers with 2,3-epoxypropyltrimethylammonium chloride we obtained EP–β-CD-N^+ derivatives containing about one hydroxypropylammonium group (N^+) per β-CD moiety. The supposed structure is illustrated in Fig. 1.

TABLE I

COUMARIN ANTICOAGULANTS AND THEIR FORMULAE

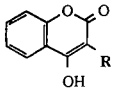

Drug	R
Warfarin D,L-3-(α-Acetonyl-4-benzyl)-4 hydroxycoumarin	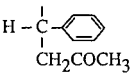
Acenocoumarol D,L-3-(α-Acetonyl-4-nitrobenzyl)-4 hydroxycoumarin	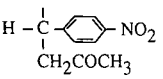
Coumachlor D,L-3-(α-Acetonyl-4-chlorobenzyl)-4 hydroxycoumarin	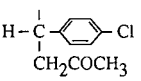
Phenprocoumon D,L-3-(α-Ethyl-benzyl)-4 hydroxycoumarin	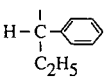

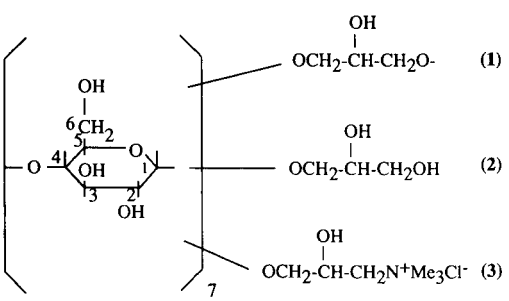

(1) hydroxypropyl bridge
(2) dilhydroxypropyl substituent } *OHP GROUPS*

(3) hydroxypropylammonium substituent *N+ GROUP*

Fig. 1. Proposed structure of EP–β-CD-N^+.

The number of ammonium substituents was determined by anion argentimetric titration. The number of β-CD cavities was evaluated by spectroscopic measurement of the decoloration of phenolphthalein solutions at pH 10.5, which form a very stable complex with β-CD [16].

The 2-hydroxy-3-trimethylammonium β-CD derivative (β-CD-N^+), compound **6**, was prepared as described previously [17], with 1.1 ammonium substituents per β-CD residue.

Solutions of compounds **1–6** in distilled water (6%, v/v), were adsorbed on LiChrospher Si-100 at room temperature, stirred with a vortex mixer for 24 h, then filtered, washed and dried under vacuum.

The composition of compounds **1–6** and the carbon content of supports are summarized in Table II.

TABLE II

COMPOSITION OF β-CD DERIVATIVES AND CHARACTERIZATION OF SUPPORTS

EP–β-CD-N^+ polymer	N^+–β-CD ratio	OHP[a]–β-CD ratio	Support carbon content (%)
1	1.76	12.6	4.67
2	0.93	9.3	4.46
3	1.39	7.6	4.11
4	1.16	5.8	4.07
5	1.46	1.2	2.07
β-CD-N^+			
6	1.1	0	1.15

[a] OHP is the sum of mono- and dihydroxypropylgroups present in the CD polymer.

Chromatographic experiments

Stainless-steel columns (10 cm × 4.6 mm I.D.) were filled with the supports by a slurry packing technique. Phosphate buffer (0.1 *M*) of various pH was used as eluent. Methanol was used as organic modifier. The flow-rate was 1 ml/min. Samples of 20 μl of 10 μ*M* coumarin derivatives and dansyl amino acid solutions were injected.

The apparatus was the same as described previously [9].

RESULTS AND DISCUSSION

Influence of the OHP–β-CD ratio on the chromatographic behavior of coumarin derivatives

Fig. 2a, b and c presents the chromatographic profiles of racemic warfarin on columns **IV–VI** filled with the supports obtained by impregnation of silica with 6% solutions of compounds **4–6**, respectively. A mixture of 20% methanol and 80% phosphate buffer (pH 4) was used as mobile phase. Note that the chromatographic profile of warfarin depends on the value of OHP–β-CD ratios and also on the amount of β-CD derivative deposited (from carbon content results in Table II). An increase in warfarin retention was observed with an increase in the amount of β-CD derivative adsorbed. So excellent separation of warfarin enantiomers (resolution factor R_s = 2.0) is observed in Fig. 2a, while poor resolution is observed in Fig. 2b and neither

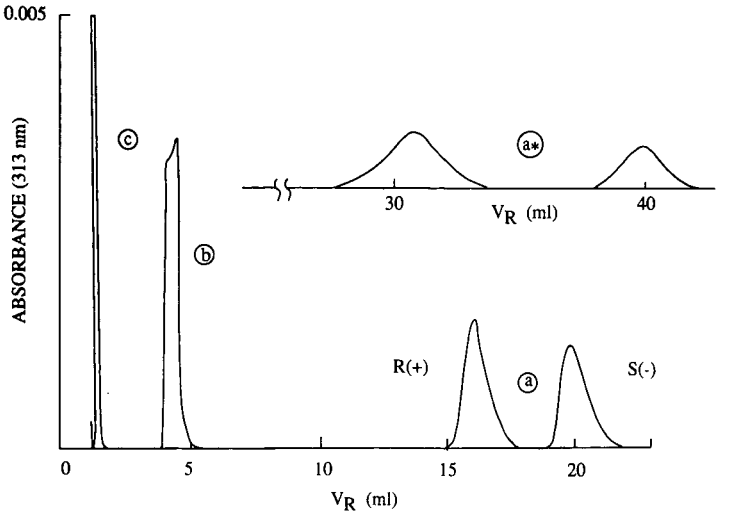

Fig. 2. Elution profiles (V_R = elution volume) of racemic warfarin on 10 cm × 4.6 mm I.D. columns **IV–VI**, filled respectively with LiChrospher Si-100 coated with β-CD derivatives **4–6**. Silica was impregnated with 6% solutions of (a) EP–β-CD-N^+ derivative **4**, (b) EP–β-CD-N^+ derivative **5** and (c) β-CD-N^+ derivative **6** and (a*) a 12% solution of β-CD derivative **4**. Eluent: methanol–0.1 *M* phosphate buffer (pH 4) (20:80).

retention nor separation in Fig. 2c, which corresponds to a support without an OHP group. So there is a minimum OHP–β-CD ratio that is needed to obtain sufficient adsorption of the β-CD derivative on silica and consecutive resolution of warfarin enantiomers.

An additional experiment presented in Fig. 2a* was done on column **IV*** filled with silica impregnated with a 12% solution of compound **4**. Stronger retentions of warfarin isomers are noticed on this support. The result of elemental analysis (C = 7.82%) indicates that saturation of silica was not reached when impregnated with a 6% solution of β-CD derivative (Table II, carbon content results). But as it appears that the separation properties of column **IV** are high enough to assure a complete resolution of warfarin enantiomers, the subsequent experiments were done on this column.

Moreover we injected separately the enantiomers of warfarin. The *R*(+) isomer is eluted first (Fig. 1a), thus the presence of OHP groups on β-CD reinforces the *S*(−) isomer complexation.

Fig. 3 shows the separation on column **IV** of three other coumarin anticoagulant enantiomers which all contain one phenyl group substituent on the chiral C atom. They are well resolved with factors of resolution which are not related to their retention volumes: warfarin and phenprocoumon R_s values are respectively 2.0 and 0.8, while the latter compound has a retention volume 4.5 times greater than that of warfarin. The R_s values of acenocoumarol and coumachlor are 0.5 and 1.5, respectively. The diversity of the R_s values demonstrates the influence of the various substituents near the chiral center, a nitro group being less favorable than a chloro group.

We can conclude that the presence of hydroxypropyl groups bonded to β-CD is responsible for the additional interactions with the chiral group outside the cavity,

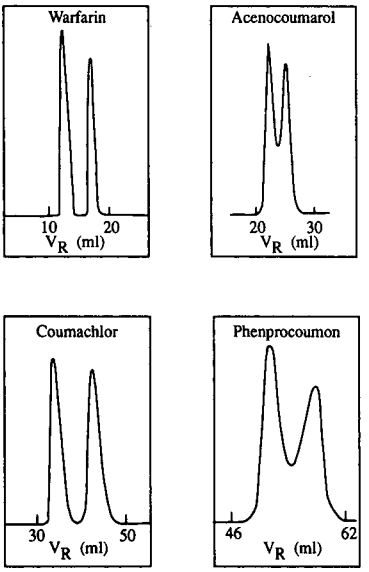

Fig. 3. Separation of structurally related coumarin isomers on column **IV**. Eluent: methanol–pH 4 phosphate buffer (20:80).

resulting in the ability of these derivatives to bind preferentially to one of the enantiomers. This assumption is supported by a recent paper [8] describing the separation of coumachlor (R_s = 0.6) on *S* and rac-2 hydroxypropyl bonded support [mobile phase: triethylammonium acetate buffer (pH 7)–acetonitrile (95:5)].

However, it can be seen that the presence of OHP groups at OHP–β-CD ratios higher than 5.8 does not change the elution profiles of warfarin, acenocoumarol and coumachlor. This is not the case for phenprocoumon, the enantiomers of which could not be resolved on column **III** (Fig. 4b), and the retention time of which remains about the same as on column **IV** (Fig. 4a). The role of the number of OHP sub-

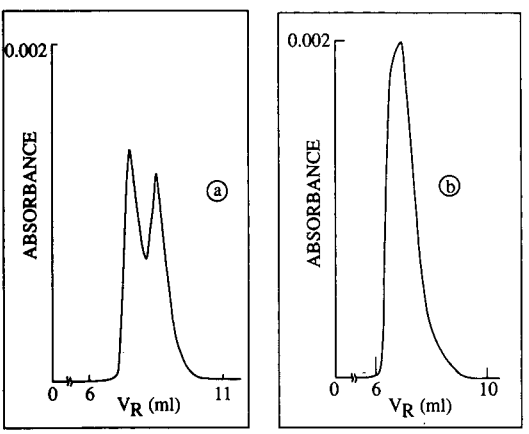

Fig. 4. Racemic phenprocoumon elution profiles on columns **III** (a) and **IV** (b) filled respectively with silica coated with β-CD derivatives **3** and **4**. Eluent: methanol–pH 4 phosphate buffer (40:60).

stituents per β-CD is demonstrated, the chiral recognition of phenprocoumon disappearing when it exceeds a value of *ca.* 7. A steric hindrance, resulting from the higher degree of substitution on β-CD, probably prevents the separation of phenprocoumon enantiomers.

The rest of the study was therefore performed on supports made from the impregnation of silica with a 6% solution of the β-CD derivative No. **4** (OHP–β-CD = 5.5).

Effect of methanol content and pH of the mobile phase on the separation of coumarin derivative enantiomers

The capacity factors (k') and resolutions of the coumarin derivatives were measured by changing the methanol–phosphate buffer ratio in the mobile phase (at pH 4), from 10:90 to 60:40. We observed a decrease in the capacity factor of the enantiomers as the percentage of methanol increased. A plot of k' *vs.* percentage methanol for the *R*- and *S*-warfarin enantiomers is shown in Fig. 5 in order to illustrate this general behavior.

At the same time a decrease in the resolution factor was observed (Table III), and the enantiomers could not be resolved with mobile phases containing more than 60% methanol. Thus an increase in the methanol content causes a loss of β-CD inclusion properties, the organic modifier reducing the interaction between the solute and the CD cavity. This behavior is usually observed on β-CD bonded columns [18].

Significant decreases of retention and selectivity were observed when the pH of the mobile phase was changed from 4 to 5.5, as shown in Fig. 6 for a fixed 30% methanol content. A smaller change occurred between pH 5.5 and 7. At pH 7 only phenprocoumon enantiomers were separated when the methanol content of the mobile phase was 30%. With mobile phases containing smaller amounts of methanol, warfarin and coumachlor isomers were also separated at this pH, but with a resolution less than that obtained at pH 4 with a methanol content giving similar retention.

The studied coumarin derivatives are only slightly soluble in aqueous solution

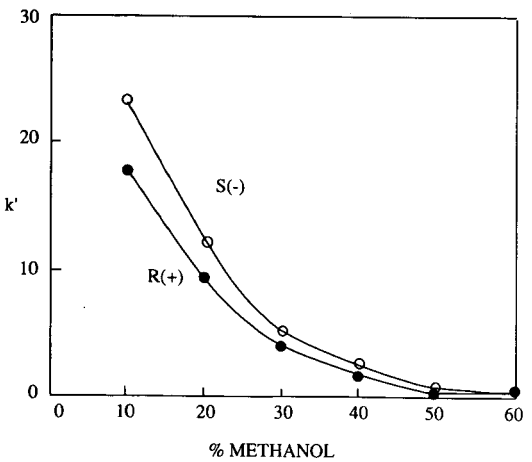

Fig. 5. Variation in the capacity factors of warfarin enantiomers on column **IV** as a function of the methanol content of the mobile phase (at fixed pH 4).

TABLE III

EFFECT OF METHANOL CONTENT IN THE pH 4 MOBILE PHASE ON THE COLUMN **IV** RETENTION AND RESOLUTION PARAMETERS OF COUMARIN DERIVATIVES

Compounds	Capacity factors		Separation factor ($\alpha = k'_2/k'_1$)	Resolution factor (R_s)	Mobile phase methanol content (%)
	k'_1	k'_2			
Warfarin	9.00	11.90	1.32	2.0	20
	4.30	5.40	1.26	1.3	30
	1.82	2.28	1.25	0.8	40
	0.14	0.14	1.00	0	60
Acenocoumarol	15.64	17.85	1.14	0.6	20
	8.23	8.97	1.09	0.4	30
	3.15	3.40	1.08	0.2	40
	0.36	0.36	1.00	0	60
Coumachlor	23.20	32.02	1.38	1.5	20
	8.88	11.14	1.25	1.1	30
	3.00	3.43	1.14	0.7	40
	0.32	0.32	1.00	0	60
Phenprocoumon	35.78	40.43	1.13	0.9	20
	13.33	15.14	1.13	0.8	30
	4.50	5.04	1.12	0.5	40
	0.54	0.54	1.00	0	60

in their non-ionized form. Their pK_a values are in the range 4.3–5.1 [19]. Inclusion of the drug in the hydrophobic cavity of β-CD is reinforced at low pH as the non-ionized moieties are preferentially complexed by β-CD [20]. This phenomenon is responsible for the increased retentions observed at pH 4. At higher pH, the increased hydration

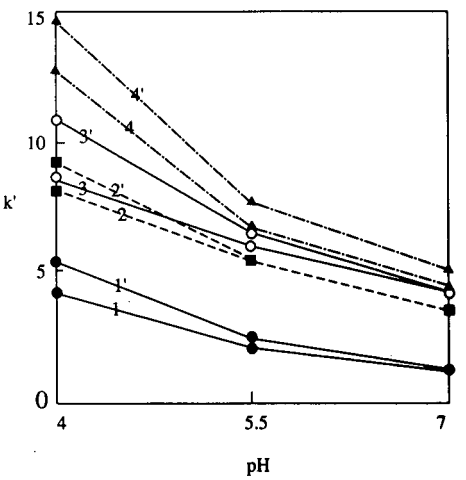

Fig. 6. Variation in the capacity factors of the coumarin derivatives on column **IV** as a function of the pH of the mobile phase, at fixed methanol content (30%). The curves relative to the first and second isomers of warfarin are respectively, 1 and 1′ (●), acenocoumarol 2 and 2′ (■), coumachlor 3 and 3′ (○), and phenprocoumon 4 and 4′ (▲).

of the ionized moiety is unfavorable for complex formation, and this explains the lower retention and resolution of the coumarin derivatives.

In order to explain the origin of the relative retention of these anticoagulants on the supports impregnated with β-CD derivatives, we compared their relative capacity factors with the apparent partition coefficients (*n*-octanol to water) previously reported by Otagiri *et al.* [19], these being 7.94, 10.9 and 17.1 for acenocoumarin, warfarin and phenprocoumon, respectively. We noticed that these are in good agreement for warfarin and phenprocoumon. Conversely the value of the acenocoumarol partition coefficient indicates that this compound is less hydrophobic than warfarin, while its retention volume on column **IV** is higher. Otagiri's previous results have shown that the complexation constant of native β-CD with these drugs increases with their partition coefficient [19]. We assume that the nitro substituent on the phenyl ring of acenocoumarol is responsible for an additional interaction with the hydroxypropyl groups outside the cavity, as it may be possible for the oxygen of the nitro group which has electron pairs to form hydrogen bonds [21].

Separation of dansyl amino acid enantiomers

Column **IV** exhibits enantioselectivity for certain dansyl amino acids (Dns-amino acids) using water–methanol mobile phases. Fig. 7 presents the chromatograms obtained under optimized mobile phase conditions. As can be seen, separations were achieved for threonine, leucine and phenylalanine D,L pairs with R_s values of, respectively, 1.18, 0.95 and 1.28. The L-enantiomers elute first. Their capacity coefficients increase with increasing hydrophobicity of the side chain on the chiral carbon atom, as previously reported [11,12].

Excellent enantioselectivities have been found on native β-CD bonded columns, the dimethylaminonaphthyl group penetrating tightly in the cavity and the chiral center with its substituents being close to the hydroxyl groups on the CD rim where hydrogen bonds can be formed with the carboxylate and amine moieties [11]. It has been reported recently [12] that modification of the hydroxyl groups on the β-CD molecule with a hydrophobic substituent results in a reduction in the ability to form

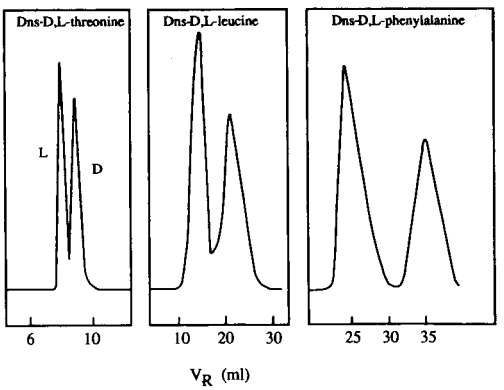

Fig. 7. Separation of Dns-amino acids enantiomers on column **IV**, using methanol–phosphate buffer mixtures as mobile phases. Methanol–pH 4 buffer (20:80) for Dns-threonine, methanol–pH 5.5 buffer (30:70) for Dns-leucine and Dns-phenylalanine.

TABLE IV

EFFECT OF METHANOL CONTENT IN THE pH 4 MOBILE PHASE ON THE COLUMN **IV** RETENTION AND RESOLUTION PARAMETERS OF Dns-AMINO ACIDS

Compounds	Capacity factors		Separation factor ($\alpha = k'_2/k'_1$)	Resolution factor (R_s)	Mobile phase methanol content (%)
	k'_1	k'_2			
Threonine	4.7	5.43	1.15	1.18	20
	2.28	2.57	1.13	0.40	30
	0.57	0.57	1.00	0	50
Tryptophan	10.00	10.00	1.00	0	30
	3.50	3.50	1.00	0	40
Leucine	15.78	20.43	1.29	1.00	30
	8.00	10.96	1.37	0.80	40
	3.14	4.57	1.45	0.80	50
	0.93	1.39	1.49	0.54	60
Phenylalanine	18.64	28.64	1.54	1.50	30
	10.50	15.00	1.43	1.50	40
	4.28	6.64	1.58	0.88	50
	1.16	1.80	1.55	0.70	60

an inclusion complex with all Dns-amino acids and consequently a reduction in their ability to resolve their enantiomers. This was interpreted as being due to a change in the depth of the cavity in which the phenylcarbamoyl or propylcarbamoyl substituents of β-CD may penetrate [12]. Owing to their hydrophilicity, the hydroxypropyl substituents of the EP–β-CD-N^+ polymers have no tendency to penetrate the hydrophobic cavity of β-CD. This explains why the enantiomers of Dns-leucine are separated on column **IV** (Fig. 7) while they were not on previous 6-*O*-phenyl or propyl carbamoylated β-CD stationary phases [12].

Moreover, we have noticed, as have previous authors [11,12], that Dns-D,L-tryptophan cannot be resolved under any mobile phase conditions while its retention volume is superior to that of Dns-threonine (Table IV). It has been suggested that the side chain on the chiral atom of Dns-tryptophan and the Dns group are included at the same extent, preventing a chiral recognition, such a mechanism being supported by the fact that this enantiomeric resolution could be achieved by replacing β-CD by larger γ-CD [12].

Table IV shows the capacity coefficients and resolution factors for different Dns-D,L-amino acids as a function of the methanol content of the mobile phase at fixed pH 4. k' and R_s values decreased with the increase of methanol content, as in the case of coumarin derivatives. However, note that for a methanol content lower than 30%, Dns-leucine and -phenylalanine were retained more strongly and the peaks were asymmetric, leading to a loss of resolution.

Table V compares the retention and separation parameters of the Dns-amino acids at pH 4, 5.5 and 7, with a 30% methanol content. Increasing the pH of the mobile phase lowers the k' values. Dns-threonine was resolved only at pH 4 because its k' value was too low at higher pH. The other amino acids were resolved even at pH 7. pH 5.5 leads to better resolution, pH 4 giving stronger retentions and large peaks.

TABLE V

EFFECT OF MOBILE PHASE pH ON THE COLUMN IV RETENTION AND RESOLUTION PARAMETERS OF Dns-AMINO ACIDS AT FIXED 30% METHANOL CONTENT

Compounds	Capacity factors		Separation factor ($\alpha = k'_2/k'_1$)	Resolution factor (R_s)	Mobile phase, pH
	k'_1	k'_2			
Threonine	2.28	2.57	1.13	0.40	4.0
	1.40	1.40	1.00	0.00	5.5
	0.80	0.80	1.00	0.00	7.0
Leucine	10.07	15.07	1.50	0.95	5.5
	6.85	11.14	1.63	0.85	7.0
Phenylalanine	16.10	25.00	1.55	1.28	5.5
	11.85	18.28	1.54	1.20	7.0

In conclusion, our columns can be used for optical resolution of Dns-D,L-amino acids. The presence of hydrophilic hydroxypropyl substituents on the β-CD polymer does not prevent the separation of their enantiomers.

Finally it is important to note the reproducibility of the above experiments. We noticed that after about 6 l of eluents of different pH and methanol content there was a decrease in all the retention volumes. The carbon content of the support of column IV decreased to 2.8%, indicating a loss of polymer adsorbed onto silica. In these conditions all the enantiomers were still resolved with a decrease of R_s. The cross-linking of the polymer adsorbed on silica is under study in order to avoid the leaching of the active adsorbed layer.

β-CD polymer-coated support represents a good candidate for enantiomeric separations as it is cheap and very easy to use. Therefore its applicability to preparative chromatography is under investigation.

CONCLUSIONS

In summary, the described β-CD derivative polymers have been shown to be convenient for the preparation of stationary phases able to recognize enantiomers. It is observed that the chiral recognition properties of the packings are different to those of native β-CD supports because of the presence of hydroxy and dihydroxy substituents on the β-CD, allowing the separation of warfarin and related compounds.

REFERENCES

1 A. Harada, M. Furue and S. Nozakura, *J. Polym. Sci.*, 16 (1978) 189.
2 B. Zsadon, L. Décsei, M. Szilasi, F. Tudos and J. Szejtli, *J. Chromatogr.*, 270 (1983) 127.
3 D. W. Armstrong, *J. Liq. Chromatogr.*, 7 (1984) 353.
4 T. J. Ward and D. W. Armstrong, *J. Liq. Chromatogr.*, 9 (1986) 407.
5 W. L. Hinze, T. E. Riehl, D. W. Armstrong, W. DeMond, A. Alak and T. Ward, *Anal. Chem.*, 57 (1985) 237.
6 D. W. Armstrong, Y. I. Han and S. M. Han, *Anal. Chim. Acta*, 208 (1988) 275.
7 D. W. Armstrong, T. J. Ward, R. D. Armstrong and T. E. Beesley, *Science*, 232 (1986) 1132.
8 A. M. Stalcup, S. Chang, D. W. Armstrong and J. Pitha, *J. Chromatogr.*, 513 (1990) 181.

9 B. Sébille, N. Thuaud, J. Piquion, N. Behar, *J. Chromatogr.*, 409 (1987) 61.
10 A. Deratani, B. Sébille, N. Thuaud, G. Lelièvre, *Patent pending,* France, 1990.
11 W. L. Hinze, T. E. Riehl, D. W. Armstrong, W. DeMond, A. Alak and T. Ward, *Anal. Chem.*, 57 (1985) 239.
12 K. Fujimura, S. Suzuki, K. Hayashi and S. Masuda, *Anal. Chem.*, 62 (1990) 2198.
13 B. D. West, S. Preis, C. H. Schroeder and K. P. Link, *J. Am. Chem. Soc.*, 83 (1961) 2676.
14 N. Wiedenhof, J. N. J. J. Lammers and C. L. van Panthaleon van Eck, *Staerke*, 21 (1969) 119.
15 A. Harada, M. Furue and S. Nozakura, *Polymer J.*, 13 (1981) 777.
16 R. P. Rohrbach, L. J. Rodriguez, E. M. Eyring and J. F. Wojcik, *J. Phys. Chem.*, 81 (1977) 944.
17 A. Deratani, G. Lelièvre, T. Maraldo and B. Sébille, *Carbohydr. Res.*, 192 (1989) 215.
18 D. W. Armstrong, W. DeMond and B. Czech, *Anal. Chem.*, 57 (1985) 481.
19 M. Otagiri, J. G. Fokkens, G. E. Hardee and J. H. Perrin, *Pharm. Acta Helv.*, 53 (1978) 241.
20 M. Otagiri, T. Miyaji, K. Uekama and K. Ikeda, *Chem. Pharm. Bull*, 24 (1976) 1146.
21 W. A. Schroeder, *J. Am. Chem. Soc.*, 73 (1951) 1122.

Journal of Chromatography, 555 (1991) 65–71
Elsevier Science Publishers B.V., Amsterdam

CHROM. 23 367

Determination of volatile and non-volatile organic acids in technical sugar solutions by ion-exclusion chromatography

CARLA ALBERTA ACCORSI* and GABRIELLA BLO
Department of Chemistry, University of Ferrara, Via L. Borsari 46, 44100 Ferrara (Italy)
(First received October 18th, 1990; revised manuscript received March 27th, 1991)

ABSTRACT

Volatile and non-volatile organic acids present in sugar process juices were separated by ion-exclusion chromatography on an HPICE-AS1 cation-exchange column (H^+ form) using both dilute hydrochloric acid and 2-propanol–water solutions of tridecafluoroheptanoic acid. Coupled with an anion-exchange micromembrane suppressor, a conductivity detector made it possible to reveal citric, tartaric, gluconic, malic, lactic, succinic, glycolic, formic, acetic and pyrrolidonecarboxylic acid in the presence of inorganic acids and non-ionic organic matter. In sugar process juices subjected to alkaline and/or oxidative treatment, increasing concentrations of the major acid components, *i.e.*, acetic, formic and lactic acid, can be measured. The analysis is performed in the presence of sucrose and a simple clean-up by rapid batch treatment with a cation exchanger (H^+ form) is sufficient to remove proteins and cations. The multiple standard addition procedure is used for calibration.

INTRODUCTION

Organic acids can be successfully determined in sugar process juices by anion-exchange high-performance liquid chromatography (HPLC) using either a differential refractometer or a UV detector if, and only if, the acid fraction is isolated by an appropriate but tedious pretreatment of the sample [1–4].

The problems related to co-elution and quantification in the analysis of cane sugar juices are overcome by using a dual-column system in which each column is equilibrated at two temperatures [3]. Interference of sucrose with the acid elution profile is observed with a refractive index detector and the results for lactic, formic and acetic acid are found to have a high relative standard deviation (R.S.D.) [1]. Interference from inorganic anions (nitrates) is also evident [5].

In all chromatographic applications [HPLC and gas chromatography (GC)], analysis of the previously isolated acid fraction requires treatment with cation- and anion-exchange resins with subsequent recovery by elution from the anion exchanger. Preconcentration by vacuum evaporation of the eluate is always necessary. The volatile acids are removed to different extents, rendering their accurate determination impossible [1–4,6–8]. In this paper, a method is described for the determination of volatile and non-volatile organic acids in sugar process juices. The method, employ-

0021-9673/91/$03.50

ing ion-exclusion chromatography, does not require any previous isolation of the acid fraction.

Ion-exclusion chromatography on a high-capacity cation-exchange resin, using either water or a dilute acid as eluent, is a valuable technique for separating weakly acidic compounds [9–12]. Ionized solutes are excluded from the exchanger matrix by the Donnan potential and eluted faster than non-ionic compounds, retained by partition through Van der Waals or other forces. Weakly ionized compounds are eluted according to their pK_1 value and hydrophobic character. Size exclusion dominates the separation mechanism for polycarboxylic acids.

A conductivity detector, the response of which is enhanced by an anion-exchange micromembrane suppressor, offers a sensitivity and selectivity higher than those of the UV and refractive index detectors currently employed in HPLC for the matrices considered here.

EXPERIMENTAL

Analyses were performed by using a Dionex (Sunnyvale, CA, USA) Qic ion chromatograph equipped with a conductivity detector and a 50-μ sample loop. The separation column contained Dionex HPICE-AS1, a totally sulphonated cation-exchange resin with polystyrene–divinylbenzene as support material (degree of cross-linking 9%, capacity 5 mequiv./g). The eluents were dilute hydrochloric acid or solutions of tridecafluoroheptanoic acid (TDFHA). A Dionex anion-exchange micromembrane suppressor for ion-exclusion chromatography (AMMS-ICE) was inserted between the column and the detector in order to enhance the detection of organic acids in standard solutions and sugar juice samples. The regenerant was 5 m*M* tetrabutylammonium hydroxide (TBA), flowing at 2 ml/min for the continuous regeneration of the cation-exchange sites within the suppressor. The exchange between H^+ and TBA^+ reduced the background conductivity of the acidic eluent generated by hydrochloric acid or TDFHA in 2-propanol–water to values of about 100 and 40 μS, respectively. All determinations were performed at room temperature. The eluent flow-rate was always 0.8 ml/min (column pressure 62 bar).

All the reagents were of analytical-reagent grade. The water used in eluent preparation and sample dilution was obtained from a Milli-Q water purification system (Millipore–Waters, Milford, MA, USA).

Standard and sample treatment

Concentrated standard solutions in water were prepared by dissolving weighed amounts of the acids or their salts. The sugar juice samples and standards were diluted with water or eluent, when TDFHA was used, in order to prevent system peak interferences. To prevent the contamination of the analytical column with proteins and to avoid cation-exchange processes that could modify the elution profiles of the acids, both the standard solutions and suitably diluted samples were batch treated with a strong cationic exchanger (H^+ form), IR-120 (exchange capacity 1.8 mequiv./ml). To avoid dilution effects, the exchanger was first liberated from the excess of water by filtration. Subsequently, an amount corresponding to 2 ml of wet product was added to 100 ml of the solution to be analysed. The solution was passed through a Millipore 0.45-μm membrane filter before injection.

RESULTS AND DISCUSSION

Influence of the eluent

Various concentrations of hydrochloric acid (0.5–2 m*M*) were tested as the first eluent. Good resolution was achieved for the main acids involved in the oxidative process studied (formic, lactic and acetic) only with a 2 m*M* concentration of hydrochloric acid. As a relatively high background conductivity was obtained by using hydrochloric acid, a second eluent was considered, *viz.*, TDFHA in 2-propanol–water solutions, which provides lower background conductivity values. The 2-propanol, added to eluent to solubilize the TDFHA, has no significant effect on the acid retention. A 5% concentration of 2-propanol in water was used, as this does not endanger the analytical column but is sufficient to solubilize the TDFHA.

In Fig. 1 the capacity factor k' [$k' = (t_R - t_0)/t_0$] is plotted against eluent concentration. The dead time, t_0, is the retention time for dissociated inorganic species. With increasing TDFHA concentration in the eluent, the pH decreases from 3.7 (0.1 m*M* TDFHA) to 2.4 (2 m*M* TDFHA). The ionized acid molecule fraction together with the capacity factor varies with the pH according to the various pK_1 values of the acids (Table I). With concentrations of TDFHA between 0.1 and 0.5 m*M*, formic, malic and pyrrolidonecarboxylic acid show a greater increase in k', as the respective pK_1 values fall within this range and the variation of the dissociated/undissociated species ratio is maximum. At pH 3.7 the dissociated fraction has the highest relative value and the elution is principally affected by Donnan exclusion. When the degree of association increases because of a decrease in pH, the electrostatic repulsion forces progressively diminish and other effects start to influence the elution process, such as adsorption by the matrix and steric exclusion. The dominant role of these effects is reflected, for example, in the elution of lactic and formic acid.

Although not involved in the oxidative reaction, PCA cannot be ignored because it is the most prominent acid in sugar beet process juices. This acid demonstrates peculiar behaviour: its retention time at low pH is higher even than that of acetic acid. This behaviour is probably determined by the interaction between the fixed negative charges on the matrix ($-SO_3^-$) and the positive charge of the polar form of amide group, resulting from the partial double bond character of the C–N bond. Further, in an acidic environment, as revealed by NMR spectra, the O-protonated

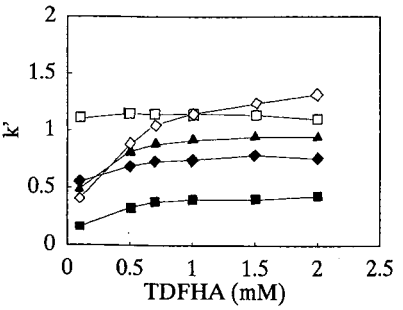

Fig. 1. Plots of capacity factors (k') *vs.* TDFHA concentration. Conditions: column, HPICE-AS1; eluent, TDFHA in 5% 2-propanol–water; flow-rate; 0.8 ml/min. ■ = Malic acid; ◆ = lactic acid; ▲ = formic acid; □ = acetic acid; ◇ = pyrrolidonecarboxylic acid (PCA).

TABLE I

CAPACITY FACTORS (k') AND pK_1 VALUES FOR DIFFERENT ACIDS

Column: HPICE-AS1; eluent, 2 m*M* TDFHA in 5% 2-propanol–water; flow-rate, 0.8 ml/min.

Acid	k'	pK_1	Acid	k'	pK_1
Oxalic	0.00	1.04	Succinic	0.75	4.00
Citric	0.23	2.87	Glycolic	0.82	3.63
Tartaric	0.30	2.82	Formic	0.95	3.55
Gluconic	0.36	3.56	Acetic	1.10	4.56
Malic	0.42	3.20	PCA	1.32	3.13
Lactic	0.75	3.66			

form is more frequent than the N-protonated form. The electrostatic interaction is positive in this instance and the elution process is consequently slowed.

In order to establish the optimum separation conditions, the selectivity coefficients for possible acid pairs were determined. In the window diagram in Fig. 2 [13], where selectivity is plotted against TDFHA concentration, the acids under study provided well separated peaks at three different TDFHA concentrations, 0.3, 0.65 and 2 m*M*. As small concentration variations around 0.3 and/or 0.65 m*M* are sufficient to modify the elution sequence, 2 m*M* TDFHA solution was chosen as the eluent. This concentration provided both optimum selectivity and equally well separated peaks.

We also studied the retention of other organic acids, generally present in the sugar beet process juice samples in negligible amounts. Their k' values in standard solutions, reported in Table I, together with the corresponding pK_1 values, show how the main acids involved in the present study can be determined. Possible co-elutions refer to the gluconic–malic, and succinic–lactic pairs. Fortunately, the amount of succinic acid normally found in technical sugar juices is negligible. In fact, this acid is used as an external standard in GC determinations (via trimethylsilyl derivatives) in this type of sample. Gluconic acid also is present in small amounts and provides a lower conductimetric response.

Fig. 3 shows the chromatogram obtained from the analysis of a technical sugar juice sample suitably diluted and treated as described above.

The identities of the peaks were confirmed by eluting samples to which the

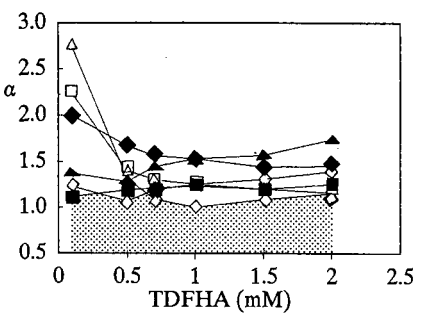

Fig. 2. Window diagram for organic acid pairs. Conditions as in Fig. 1. ▲ = Lactic–PCA; ◆ = lactic–acetic; ◇ = formic–PCA; ■ = lactic–formic; □ = formic–acetic; △ = acetic–PCA.

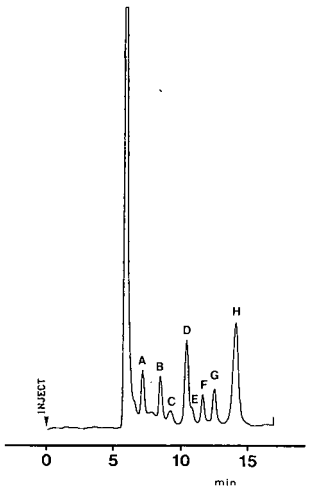

Fig. 3. Typical chromatogram of acids in a sugar beet juice sample. Conditions: column, HPICE-AS1; eluent, 2 m*M* TDFHA in 5% 2-propanol–water; flow-rate, 0.8 ml/min. A = Citric acid; B = malic acid; C = not identified; D = lactic acid; E = glycolic acid; F = formic acid; G = acetic acid; H = PCA.

various acids were added stepwise. This was necessary because of small but not negligible variations of the retention time during the measurements. All the peaks were identified except one, which appeared in all the technical solutions analysed and which lay between the malic and lactic acid peaks. Because of the Donnan exclusion, the inorganic anions elute together with the column void volume. The presence of citric acid, in addition to malic acid, is confirmed among the polycarboxylic acids with selectivity factors that conform to the pK_1 values, whereas oxalic acid, strongly excluded by the Donnan effect, co-elutes with the inorganic anions.

Because of the high lactic acid concentrations in the samples, the peaks of lactic and glycolic acid also overlap. The latter elutes as shoulder peak but it does not interfere because its concentration in the samples is generally low.

Quantitative analysis

Calibration graphs with correlation coefficients higher than 0.999 were obtained for all the pure standard acids in the concentration range 0–120 ppm (injection volume 50 μl). Quantitative analysis was performed by measuring peak heights, which proved better than peak areas. The repeatability of the analysis as relative standard deviation (R.S.D.) was calculated from five replicate analyses. The R.D.S.s for malic, lactic, formic and acetic acid and PCA were 2.5, 3.4, 3.2, 4.0 and 1.1%, respectively.

Significant differences between the slopes of the regression line calculated in recovery experiments on different juice samples and that of the calibration line for pure standards were obtained (confidence interval 95%) [14], thus confirming the expected matrix effect. Considering this effect and that the aim of this work was to determine concentration variations, the multiple standard addition procedure [15] was employed for quantitative analysis.

TABLE II

EXTRAPOLATED AMOUNTS OF DIFFERENT ACIDS IN SUGAR BEET PROCESS JUICES AND RELATIVE STANDARD DEVIATIONS

Malic acid		Formic acid		Lactic acid		Acetic acid		PCA	
Amount (ppm)	R.S.D. (%)	Amount (ppm)	R.S.D. (%)	Amount (ppm)	R.S.D. (%)	Amount (ppm)	R.S.D. (%)	Amount (ppm)	R.S.D. (%)
5.8	3.1	3.8	7.6	16.1	8.1	5.0	5.8	11.1	9.0
7.1	1.4	4.0	3.0	35.1	1.0	7.3	1.0	64.8	3.0
9.1	2.0	5.0	3.2	46.9	2.9	7.6	3.4	81.4	4.5
16.4	2.3	6.5	2.3	62.6	5.4	13.8	1.2	95.8	4.4
36.8	1.8	9.5	3.0	80.5	1.0	17.0	1.0	100.7	1.1

For calibration, five different known amounts ranging from 5 to 50 ppm (10 to 100 ppm for PCA and lactic acid) of each analyte were added to the samples under the condition of constant volume. Regression analysis yielded a linear plot with correlation coefficients higher than 0.999 in all instances.

The differences between the slopes of the regression lines from different samples (thin juices, thick juices, molasses) were also significant. The presence of different amounts of sucrose, the main component in these solutions, alters their physical properties, *i.e.*, viscosity and dielectric constant, and consequently the intensity of the detector signal.

The amounts of organic acids in the tested samples were determined by using the calculated regression coefficients [16]. The R.S.D.s of the extrapolated concentration values for five juice samples (0.5–1.0 g per 100 ml) are reported in Table II.

The PCA response factor is relatively low in comparison with the other acids determined, so the determination of PCA, of which the concentration is normally greater than that of the other acids, does not require excessive dilution of the samples.

CONCLUSION

Ion-exclusion chromatography offers a rapid method for determining oxy acids and organic acids in sugar process juices. The procedure described here, with the multiple standard addition method for calibration, is faster than other techniques such as HPLC and GC. No preliminary separation is required and the only pretreatment consists in the addition of a cation exchanger in the H^+ form to the solution before injection to protect the column life. The main advantage is the possibility of simultaneously determining volatile and non-volatile products. In particular cases, *e.g.*, when one is studying the behaviour of solutions having a high monosaccharide content, possible interference between glycolic and lactic acid must be carefully taken into consideration. Such situations are commonly encountered when processing sugar cane juices but are not usual in beet sugar factories.

ACKNOWLEDGEMENT

This work was partially supported by the Italian Ministero dell'Università e della Ricerca Scientifica e Tecnologica (MURST 60%), Rome.

REFERENCES

1 D. F. Charles, *Int. Sugar J.*, 83 (1981) 195.
2 J. M. de Bruijn, A. P. G. Kieboom, H. van Bekkum and P. W. van der Poel, *Int. Sugar J.*, 86 (1984) 195.
3 M. A. Clarke and W. S. C. Tsang, *Int. Sugar J.*, 86 (1984) 215.
4 J. D. Blake and M. L. Clarke, *J. Chromatogr.*, 398 (1987) 265.
5 S. Rokushika, Z. L. Sun and H. Hatano, *J. Chromatogr.*, 253 (1982) 84.
6 R. M. Sequeira, *J. Am. Soc. Sugar Beet Technol.*, 16 (1970) 136.
7 J. F. T. Oldfield, R. Parslow and M. Shore, *Int. Sugar J.*, 75 (1973) 44.
8 E. Reinefeld, K.-M. Bliesener, A. Reinefeld and L. Rexilius, *Zucker*, 28 (1975) 472.
9 K. Kihara, S. Rokushika and H. Hatano, *J. Chromatogr.*, 410 (1987) 103.
10 Y. Hanaoka, T. Muryama, S. Muramoto, T. Matsuura and A. Nanba, *J. Chromatogr.*, 239 (1982) 537.
11 J. Haginaka, J. Wakai, H. Yasuda and T. Nomura, *J. Chromatogr.*, 447 (1988) 373.
12 D. T. Gjerde and J. S. Fritz, *Ion Chromatography*, Hüthig, New York, 2nd ed., 1987.
13 R. J. Laub and J. H. Purnell, *J. Chromatogr.*, 112 (1975) 71.
14 P. D. Lark, B. R. Craven and R. C. L. Bosworth, *The Handling of Chemical Data*, Pergamon Press, Oxford, 1st ed., 1968.
15 D. L. Massart, B. G. M. Vandengiste, S. N. Deming, Y. Michotte and L. Kaufmann, *Chemometrics: a Textbook (Data Handling in Science and Technology, No. 2)*, Elsevier, Amsterdam, 1988.
16 J. C. Miller and J. N. Miller, *Statistics for Analytical Chemistry*, Ellis Horwood, Chichester, 1984.

Journal of Chromatography, 555 (1991) 73–80
Elsevier Science Publishers B.V., Amsterdam

CHROM. 23 402

Simultaneous determination of prostaglandins E_1, A_1 and B_1 by reversed-phase high-performance liquid chromatography for the kinetic studies of prostaglandin E_1 in solution

KANG CHOON LEE[a] and PATRICK P. DeLUCA*
University of Kentucky, College of Pharmacy, Rose Street, Lexington, KY 40536-0082 (USA)
(First received August 1st, 1990; revised manuscript received April 16th, 1991)

ABSTRACT

A method for the simultaneous determination of prostaglandins E_1, A_1 and B_1 (PGE_1, PGA_1 and PGB_1) in solution has been developed by reversed-phase high-performance liquid chromatography using a 3 μm C_{18} column. The mobile phase consisted of 35% acetonitrile in 0.002 *M* phosphate buffer (pH 3.5) and its flow-rate was 1.5 ml/min. Quantitative measurement was performed using a photodiode array detector system at 190, 220 and 280 nm for PGE_1, PGA_1 and PGB_1, respectively. The method has been applied to the primary kinetic studies for reaction profile for $PGE_1 \rightarrow PGA_1 \rightarrow PGB_1$ at 60°C in pH 2.0, 7.2, 10.0 and 12.0 buffer solutions.

INTRODUCTION

Prostaglandin E_1 (PGE_1), having a β-hydroxylketone moiety, readily undergoes dehydration in acidic and basic aqueous solutions to produce prostaglandin A_1 (PGA_1) which further isomerizes to prostaglandin B_1 (PGB_1) in alkaline conditions as shown in Fig. 1 [1–3]. Kinetic information on the solution stability of PGE_1 in terms of these dehydration and internal rearrangement reactions has been limited because of the lack of a practical separation method for PGE_1, PGA_1 and PGB_1 [2–4].

PGA_1 and PGB_1 are structurally very similar and have similar polarities. PGE_1 on the other hand is significantly more polar. Normal- and reversed-phase isocratic high-performance liquid chromatography (HPLC) methods have so far not provided adequate kinetic data for PGE_1 due to poor resolution of PGA_1 and PGB_1 as well as long retention times [5–6]. An anion-exchange column with a mobile phase containing β-cyclodextrin was adopted for the simultaneous determination of PGE_1, PGA_1 and PGB_1, but the resolution between them was marginal [7].

The naphthacyl ester derivatization technique was shown to be effective in separating PGA_1 and PGB_1, but was not capable of simultaneously separating PGE_1, PGA_1 and PGB_1 [8]. Derivatization with fluorescent reagents of 3-bromo-

[a] Present address: Chonnam National University, Korea.

0021-9673/91/$03.50

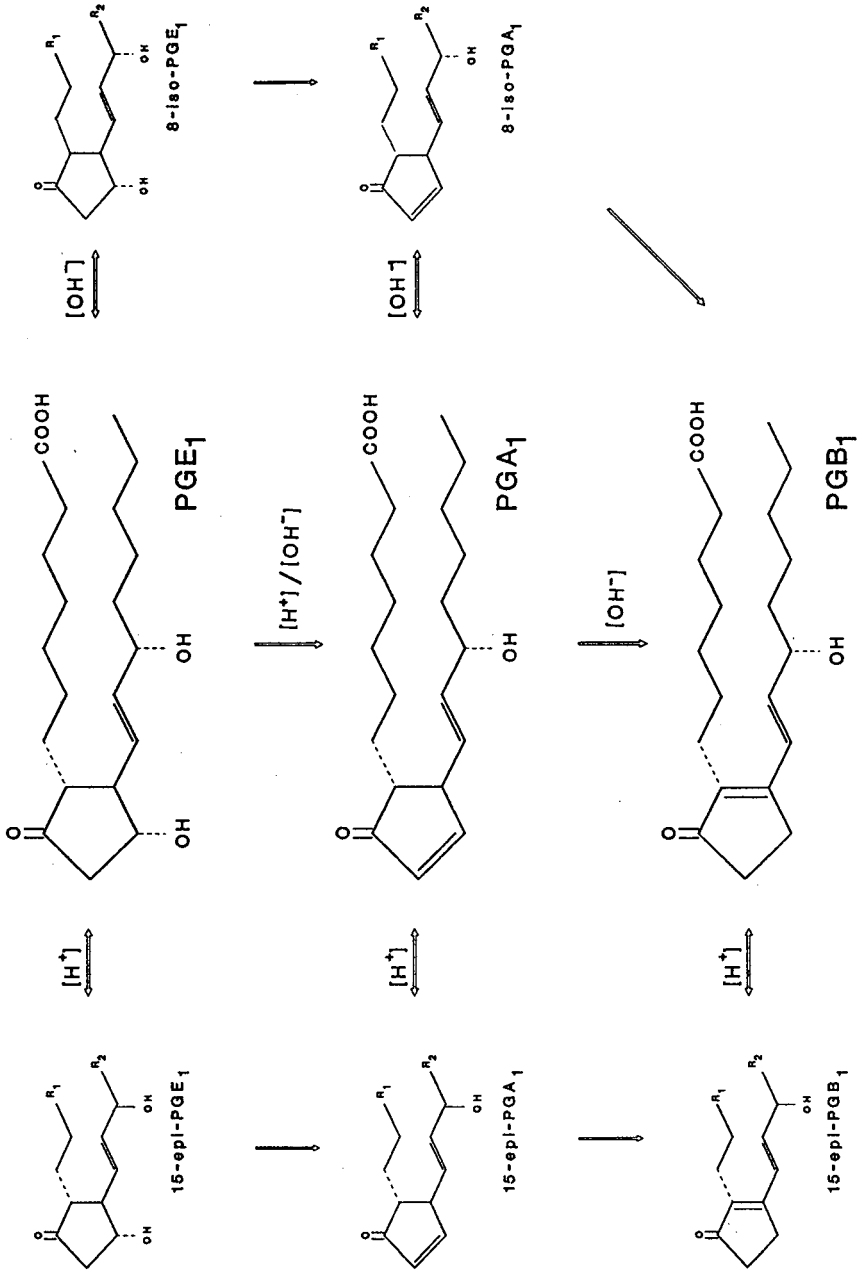

Fig. 1. The major degradation pathway of PGE_1 in solution.

methyl-6,7-dimethoxy-1-methyl-2(1H)-quinoxalinone [9] and 4-bromomethyl-7-methoxy coumarin [10] were also studied. The former method failed to resolve the peaks for PGA_1 and PGB_1 by any proportions of the solvent and the latter method was not practical due to the long retention times (over 4 h for PGA_1 and PGB_1). In fact, any derivatization technique may not be suitable for kinetic studies of PGE_1, because the derivative conditions, *i.e.*, high temperature and long reaction time, could accelerate the dehydration or internal rearrangement reactions.

The purpose of this research was to develop a simple and simultaneous separation method for PGE_1, PGA_1 and PGB_1 in order to study the stability of PGE_1 in solution.

MATERIALS AND METHODS

Materials

PGE_1 was used as received from Upjohn (Kalamazoo, MI, USA). PGA_1 and PGB_1 were purchased from Sigma (St. Louis, MO, USA). Acetonitrile and methanol were HPLC grade from Fisher (Pittsburgh, PA, USA) and all other materials were of reagent grade.

Chromatography

A modular HPLC system consisting of two LC6-A pumps, a SIL-6B autoinjector, a SPD-6AV UV detector, SCL-6B system controller and CR-601 integrator (Shimadzu, Columbia, MD, USA) was operated at ambient temperature. A 990 photodiode array detection (PAD) system (Waters, Milford, MA, USA) was connected between the analytical column and UV detector for the quantitative analysis of chromatograms and spectra.

An LC-18 column (3 μm, 15 cm × 4.6 mm I.D.; Supelco, Bellefonte, PA, USA) was used with a mobile phase of 35% acetonitrile in 0.002 *M* phosphate buffer (pH 3.5). The flow-rate was 1.5 ml/min and the injection volume was 5 μl.

Stock solutions of 5 mg/ml of PGE_1, PGA_1 and PGB_1 were prepared in methanol and stored in nitrogen gas-filled vials at 4°C. The working solution of PGE_1, PGA_1 and PGB_1 was prepared from the respective stock solution and diluted in methanol to contain 20 μg/ml each of PGE_1, PGA_1 and PGB_1.

Chromatograms were recorded by both UV detection at a fixed wavelength of 195 nm and PAD in the scanning wavelength range of 190–350 nm. Quantitation of PGE_1, PGA_1 and PGB_1 was achieved by measurement of the peak areas at 190, 220 and 280 nm, respectively.

Kinetic studies

PGE_1 solutions at a concentration of 50 μg/ml were prepared at pH 2.0, 7.2, 10 and 12 by placing 0.1 ml of 0.5 mg/ml PGE_1–methanol solution and 0.9 ml of the appropriate buffer into the screw cap vials of the autoinjector. Buffers used were 0.05 *M* hydrochloric acid–potassium chloride (pH 2.0), 0.002 *M* sodium dihydrogenphosphate–sodium hydroxide (pH 7.2), sodium bicarbonate–sodium hydroxide (pH 10.0) and sodium hydrogenphosphate–sodium hydroxide (pH 12.0). The vials were placed in a 60°C water bath. At specific times each vial was removed, cooled to room temperature and 5 μl of the solution were injected into the HPLC system using an autoinjector. The vial was then returned to the water bath.

RESULTS AND DISCUSSION

Simultaneous assay of PGE_1, PGA_1 and PGB_1

Fig. 2 shows a chromatogram which illustrates the simultaneous separation of PGE_1, PGA_1 and PGB_1. The chromatogram was obtained by UV detection at a fixed wavelength of 195 nm. The retention times for PGE_1, PGA_1 and PGB_1 were 4.9, 14.4 and 15.4 min respectively, and the separation factors of PGE_1 and PGA_1 were 3.14 and 1.07 in comparison with PGB_1. The concentration ratio between PGE_1, PGA_1 and PGB_1 (up to 60 μg/ml of each) and the variation of mobile phase pH in the range pH 3.0–4.5, at which PGE_1 is considered to be relatively stable [4], had no significant influence on the separation efficiency.

Fig. 3 shows the adsorption spectra in the scanning range of 190–350 nm with the PADS. The optimum detection wavelengths for PGE_1, PGA_1 and PGB_1 were found to be 190, 220 and 280 nm, respectively. This suggests that, to detect PGE_1, PGA_1 and PGB_1 together using one measuring wavelength, a wavelength of under 200 nm would be both preferable and suitable.

Fig. 4 shows the chromatograms of PGE_1 PGA_1 and PGB_1 measured with PAD at the three different wavelengths. All three were detected at 190 and 220 nm, while at 280 nm only PGB_1 was detected. However, the detector response to PGE_1 and PGB_1 was extremely poor at 220 nm. Therefore, using a wavelength of 220 nm for the quantitation of PGA_1 in stability and kinetic studies of PGE_1 by both UV spectrophotometry [1,3,11] and HPLC with poor resolution between PGA_1 and PGB_1 [5,7] might lead to erroneous results.

The detection limit, defined by a signal-to-noise ratio of *ca.* 3:1, was 0.5 μg/ml

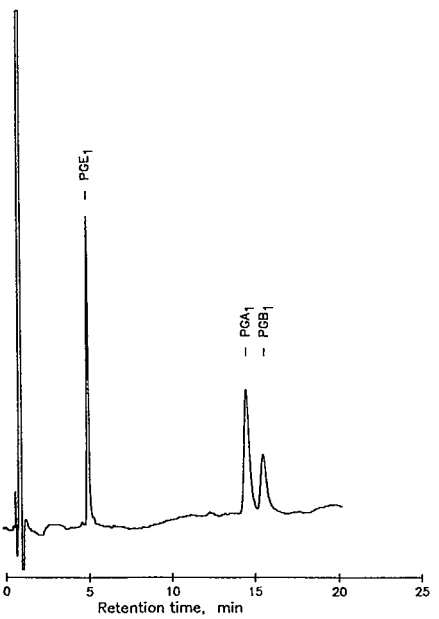

Fig. 2. Chromatograms measured by UV detection at 195 nm. Concentrations; 100 ng each of PGE_1, PGA_1 and PGB in 5 μl. Attenuation: 3.

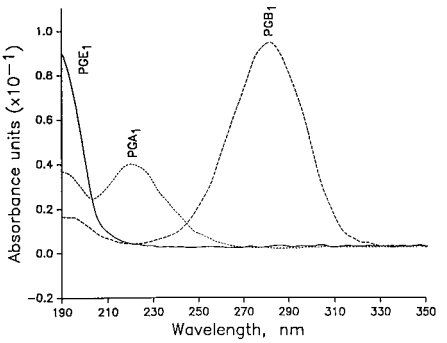

Fig. 3. Absorption spectra measured directly at the peaks of PGE_1, PGA_1 and PGB_1 in the flow cells, respectively, by PAD. Concentrations: 100 ng of each PGE_1, PGA_1 and PGB_1 in 5 μl.

for PGE_1, PGA_1 and PGB_1 with PAD at wavelengths of 190, 220 and 280 nm, respectively, while that measured by UV at 195 nm was 2 μg/ml for both PGE_1 and PGA_1 and 5 μg/ml for PGB_1. With PAD the correlation of peak area ratio with concentration was linear in the range 1–60 μg/ml and the correlation coefficients for the standard calibration curves were better than 0.999.

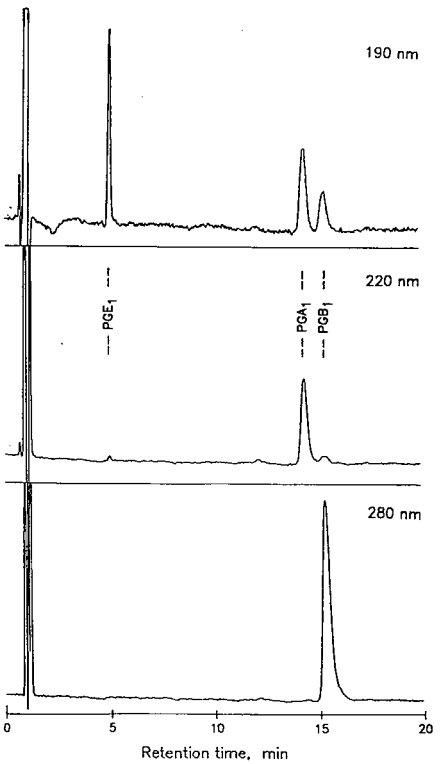

Fig. 4. Chromatograms measured by PAD at 190, 220 and 280 nm, respectively. Concentrations; 100 ng of each PGE_1, PGA_1 and PGB_1 in 5 μl. Full scale: 0.01 A.U.

Aqueous solution kinetics

Fig. 5 shows the reaction profiles for PGE_1 at different pH values at 60°C. The mole percents were plotted as a function of time beginning with 100% PGE_1. At all pH, PGE_1 degraded rapidly and was essentially exhausted in 40 h. In Fig. 6 the total mole percents of PGE_1, PGA_1 and PGB_1 are plotted *versus* time in the same buffers. At pH 2.0, the main degradation product was only PGA_1 and the conversion ratio from PGE_1 to PGA_1 was negligible compared with those at the higher pH conditions. The total mole percent of PGE_1 and PGA_1 was sharply decreased. At the higher pH, the reaction rate of dehydration and isomerization was accelerated as described previously [1,4]. However, the total mole percents of PGE_1, PGA_1 and PGB_1 were not maintained at essentially 100% of initial PGE_1 as reported previously [1,3,7], but decreased to a range of about 50–60%. At pH 12.0, the reaction was completed within 1 h to produce PGB_1 at about 50% of initial PGE_1. Moreover, the total mole percents of PGE_1, PGA_1 and PGB_1 in pH 7.2 and 10.0 were inclined to approach 50% shown in Fig. 6. Therefore, it is assumed that the major final degradation product of PGE_1 in basic solution was PGB_1 with a conversion ratio of about 50% of initial PGE_1 and also the remaining 50% was considered to degrade to unidentified products or analogs of prostaglandins other than PGA_1 and PGB_1.

Fig. 7 shows the chromatograms of PGE_1 solution measured by UVD at a fixed

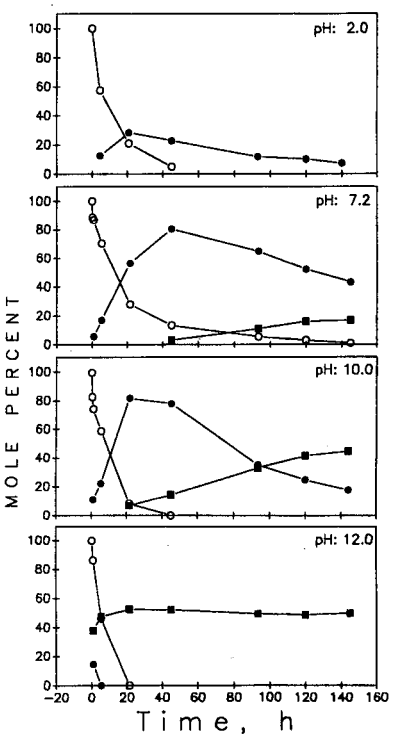

Fig. 5. Dehydration and rearrangement reaction profiles of PGE_1 as a function of time at 60°C at different pH conditions. Initial concentration of PGE_1: 50 μl/ml. ○ = PGE_1, ● = PGA_1; ■ = PGB_1.

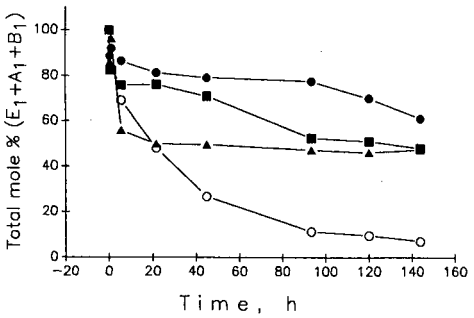

Fig. 6. Total mole percent of PGE_1, PGA_1, and PGB_1 as a function of time at 60°C at different pH conditions. Initial concentration of PGE_1: 50 μg/ml. pH: ○ = 2.0; ● = 7.2; ■ = 10.0; ▲ = 12.0.

wavelength of 195 nm after 6 days at 60°C in the buffer solutions. Besides typical peaks of PGA_1 and PGB_1, the chromatograms show several additional peaks of unknown degradation products, which have been assigned as peaks 1–6. Peaks 2 and 3 were detected at all conditions, peak 1 was detected at pH 7.2 and above and peaks 4–6 appeared only at pH 2.0. The identification of these peaks remains to be determined.

The findings suggest that in addition to PGA_1 and PGB_1 a variety of degrada-

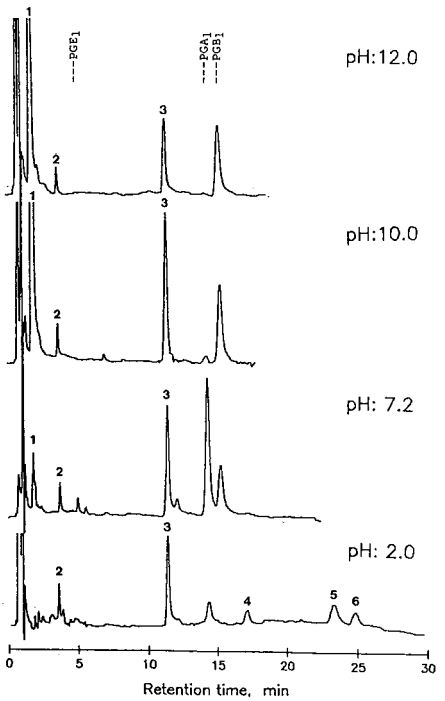

Fig. 7. Typical chromatograms measured after 6 days at 60°C at different pH conditions measured by UV detection at 195 nm. Initial concentration of PGE_1: 50 μg/ml. Attenuation: 3.

tion products occur with time at various pH values. In addition to the main degradation pathway of $PGE_1 \rightarrow PGA_1 \rightarrow PGB_1$, the formation of epimers at C-15 or C-18 of PGE_1, PGA_1 and PGB_1 have been considered with limited evidence [1,2,12] as illustrated in Fig. 1. A highly conjugated 13,15-dehydration product of PGA_1 in acidic solution [2] and 11-dehydration product of PGA_1 [13] have also been considered as possible degradation products. Based on Fig. 1, an experimental kinetic model had been proposed [2], but the appropriate separation techniques for the reaction products have not been established. A better understanding of the chromatograms of Fig. 7 could help to explain the complex kinetic behaviour of PGE_1 in solution.

In summary, the simultaneous separation of PGE_1, PGA_1 and PGB_1 was possible by using a 3 μm C_{18} column without any modification and derivatization procedures. The primary kinetic studies of PGE_1 using this method suggest that the kinetic behaviours of PGE_1 in solution could be traced more correctly than before with respect to PGE_1, PGA_1 and PGB_1.

REFERENCES

1 D. C. Monkhouse, L. van Campen and A. J. Aguiar, *J. Pharm. Sci.*, 62 (1973) 576–580.
2 R. G. Stehle and T. O. Oesterling, *J. Pharm. Sci.* 66 (1977) 1590–1595.
3 N. H. Andersen, *J. Lipid Research*, 10 (1969) 320–325.
4 D. L. Teagarden, B. D. Anderson and W. J. Petre, *Pharm. Res.*, 6 (1989) 210–215.
5 S. Inayama, H. Hori and T. Shibata, *J. Chromatogr.*, 194 (1980) 85–88.
6 A. Terragno, R. Rydzik and N. A. Terragno, *Postaglandins*, 21 (1981) 101–112.
7 K. Uekama, F. K. Hirayama, K. Ikeda and K. Inaba, *J. Pharm. Sci.* 66 (1977) 706–710.
8 P. H. Zoutemdam, P. B. Bowman, J. L. Rumph and T. M. Ryan, *J. Chromatogr.*, 283 (1984) 281–287.
9 M. Yamaguchi, K. Fukada, S. Hara and M. Nakamura, *J. Chromatogr.*, 380 (1986) 257–265.
10 V. L. McGuffin and R. N. Zare, *Proc. Natl. Acad. Sci. USA*, 82 (1985) 8315–8319.
11 E. W. Younger and R. M. Szabo, *Prostaglandins*, 31 (1986) 923–927.
12 J. E. Pike, F. H. Lincoln and W. P. Schneider, *J. Org. Chem.*, 34 (1969) 3552–3557.
13 H. K. Lee, H. J. Lambert and R. L. Schowen, *J. Pharm. Sci.*, 73 (1984) 306–310.

Journal of Chromatography, 555 (1991) 81–95
Elsevier Science Publishers B.V., Amsterdam

CHROM. 23 355

High-performance liquid chromatographic separation of DL-amino acids derivatized with chiral variants of Sanger's reagent[a]

HANS BRÜCKNER* and CARMEN GAH
Institute of Food Technology, University of Hohenheim, W-7000 Stuttgart 70 (Germany)
(First received October 11th, 1990; revised manuscript received February 11th, 1991)

ABSTRACT

Substitution of one fluorine atom in 1,5-difluoro-2,4-dinitrobenzene by L-alanine amide yields N^2-(5-fluoro-2,4-dinitrophenyl)-L-alanine amide (FDNP-Ala-NH_2, "Marfey's reagent"). This reagent (or analogues, termed FDNP reagents, in which Ala is replaced with other chiral α-amino acids (AAs), oligopeptides or amino components) might be considered as a chiral variant of "Sanger's reagent" (1-fluoro-2,4-dinitrobenzene). The remaining fluorine atom in FDNP reagents can be substituted by chiral AAs to furnish diastereomeric derivatives which are separable by high-performance liquid chromatography (HPLC). A number of chiral variants of Sanger's reagent have been synthesized with the general structures (a) FDNP-Val-NHR (R = H, *tert.*-butyl, chiral aralkyl, phenyl, *p*-nitrophenyl), (b) FDNP-Val-OR (R = H, CH_3, *tert.*-butyl), (c) FDNP-$(Ala)_n$-NH_2, $n = 1,2$, and (d) FDNP-NHR (R = aralkyl and hydroxyalkyl), and their ability to resolve certain DL-AAs as diastereomers in reversed-phase HPLC was investigated. Reagents with the structures (a), (b) and (c), but not (d), made possible the separation of DL-AAs as diastereomers. From the results obtained and from observations of Corey–Pauling–Koltun (CPK) space-filling molecular models of the diastereomers, it is concluded that the AA side-chains and the carboxy and carboxamide substituents in the reagents have an influence on the retention times of diastereomers and that the differences in free energy as a result of the formation of an intramolecular hydrogen bridge in the L–L and non-formation in the D–L diastereomers (first letter refers to the configuration of the amino acid to be analysed) are in particular responsible for large differences in the retention times of certain diastereomers in HPLC.

INTRODUCTION

In 1945, Sanger [1] reported that 1-fluoro-2,4-dinitrobenzene (FDNB, later called "Sanger's reagent") was a highly suitable compound for the masking of free amino groups in insulin and that the respective dinitrophenyl amino acids (DNP-AAs) released under the conditions of acidic total hydrolysis were separable chromatographically and could be identified by comparison with authentic samples of the

[a] Parts of this paper were presented at the *21st European Peptide Symposium, Playa d'Aro, September 2–8, 1990*, and at the *10th International Symposium on HPLC of Peptides, Proteins, and Polynucleotides, Wiesbaden, October 29–31, 1990*.

0021-9673/91/$03.50

DNP-AAs. Continuation of this work finally led to the sequence determination of insulin [2], the first sequence of a protein to be elucidated. Encouraged by this work, many attempts were undertaken in the following years to increase the sensitivity of the reagent and to alter the polarity by synthesizing substituted fluorodinitrobenzenes [3–5].

Zahn [6] and Zahn and Meienhofer [7] were the first to use a bifunctional variation of Sanger's reagent, namely 1,5-difluoro-2,4-dinitrobenzene (DFDNB), for the cross-linking of proteins such as wool, silk and insulin. DFDNB was later also used, *e.g.*, for the intramolecular cross-linking of bovine pancreatic ribonuclease A [8] and basic myelin protein [9]. It is noteworthy that Zahn and Meienhofer [7] prepared by reaction of DFDNB with AA esters monofunctional, bifunctional and mixed bifunctional derivatives which were investigated by paper chromatography. They also reported on attempts to separate certain diastereomeric derivatives by fractionated crystallization [7].

Marfey [10] showed that monosubstitution of DFDNB by L-alanine amide yielded a chiral variant of Sanger's reagent, namely 1-fluoro-2,4-dinitrophenyl-5-L-alanine amide {N^2-(5-fluoro-2,4-dinitrophenyl)-L-alanine amide [11], FDNP-Ala-NH_2; *cf.*, Fig. 1i}. The remaining reactive fluorine atom in this reagent was susceptible to nucleophilic substitution by DL-AAs to furnish the respective diastereomeric derivatives which could be separated by high-performance liquid chromatography (HPLC). This reagent, referred to as "Marfey's reagent" in this paper, has been used for the separation of (3*R*)- and (3*S*)-β-leucine [11], in racemization studies of AAs and peptides [12,13], for the determination of the enantiomeric error frequency of aspartase aminotransferase via quantification of the racemization of L- and D-glutamate [14] and for the HPLC resolution of a mixture of twenty L-AAs [15].

We have used this reagent for the HPLC separation of diastereomers of non-proteinogenic α-hydroxymethyl-α-amino acids and α-alkyl-α-amino acids (AAAs) [16,17], which were also separable as diastereomeric esters by gas–liquid chromatography [18]. It was found that the diastereomers of AAAs formed with Marfey's reagent, like those of proteinogenic AAs, showed exceptionally large differences in retention times (Δt_R) in HPLC in comparison with other methods such as the formation of diastereomers by derivatization with *o*-phthaldialdehyde and chiral thiols [19,20].

In continuation of the above work, we have recently synthesized a series of new, systematically modified chiral variants of Sanger's reagent by substitution of one fluorine atom of 1,5-difluoro-2,4-dinitrobenzene with selected L-AA amides (*viz.*, H-Val-NH_2, H-Phe-NH_2 and H-Pro-NH_2) and showed that FDNP-Val-NH_2 in particular gave large Δt_R values for diastereomers of many DL-AAs [21]. With the aims of determining the structural parameters responsible for the large Δt_R values of AA diastereomers and to design new reagents for the optimum separation of certain AAs, we now report the syntheses of a number of substituted FDNP-Val amides, FDNP-Val esters, FDNP-amines and an FDNP-dipeptide amide (*cf.*, Fig. 1) and the HPLC investigation of the diastereomers formed by reaction of these novel FDNP reagents with selected DL-AAs.

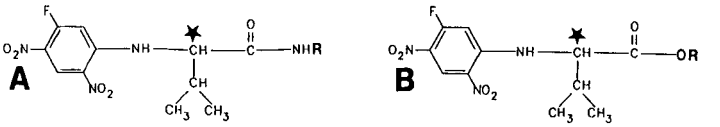

Reagent R

(a) FDNP-Val-NH_2 -H

(b) FDNP-Val-NHtBu

(c) FDNP-Val-PEA

(d) FDNP-Val-AN

(e) FDNP-Val-pNA

(f) FDNP-Val-OH -H

(g) FDNP-Val-OMe $-CH_3$

(h) FDNP-Val-OtBu

(i) FDNP-Ala-NH_2

(j) FDNP-Ala-Ala-NH_2

(k) FDNP-PEA

(l) FDNP-valol

Fig. 1. Formulae of FDNP reagents of the structure (A) FDNP-Val-NHR and (B) FDNP-Val-OR, residues R in (a)–(e) FDNP-Val-NHR and (f)–(h) FDNP-Val-OR, and structures of (i) FDNP-Ala-NH_2, (j) FDNP-Ala-Ala-NH_2, (k) FDNP-PEA and (l) FDNP-valol. Asterisks indicate chiral centres in reagents; letters (a)–(l) in parentheses correspond to those used in Fig. 2 and Table I.

EXPERIMENTAL

Instruments

A Jasco (Kyoto, Japan) HPLC system was used, consisting of a Model 880 PU single-head pump with active damper, a Model 880-02 low-pressure gradient unit, a Model 801-SC system controller, a Model 875-UV variable-wavelength spectroscopic detector and a Model D-2000 integrator from Merck–Hitachi (Darmstadt, Germany).

Sample injection was carried out with a Rheodyne (Cotati, CA, USA) Model 7125 injection valve equipped with a 20-μl sample loop.

Amino acids and chemicals

DL- and L-amino acids were purchased from either Sigma (St. Louis, MO, USA) or Fluka (Buchs, Switzerland); *tert.*-butyloxycarbonyl-L-valine hydroxysuccinimide ester (Boc-Val-OSu), L-alanyl-L-alanine amide hydrochloride (H-Ala-Ala-NH_2 · HCl), L-valine *p*-nitroanilide (H-Val-pNA), L-valine *tert.*-butyl ester hydrochloride (H-Val-OtBu · HCl) and L-valine *tert.*-butylamide hydrochloride (H-Val-NHtBu · HCl) were from Bachem (Bubendorf, Switzerland); N-methyl-DL-valine (NMe-Val-OH) was from Sigma; 1,5-difluoro-2,4 dinitrobenzene (DFDNB or FFDNB) was from Fluka, N^2-(5-fluoro-2,4-dinitrophenyl)-L-alanine amide (Marfey's reagent) was synthesized in our laboratory [21] and is also obtainable from Pierce (Rockford, IL, USA), Serva (Heidelberg, Germany) or Sigma; dimethyl sulphoxide (DMSO), trifluoroacetic acid (TFA), acetonitrile (ACN), methanol (CH_3OH), dichloromethane (DCM), light petroleum (b.p. 40–60°C), diethyl ether, N-methylmorpholine (NMM), N,N-dimethylformamide (DMF) and orthophosphoric acid (85%) of analytical-reagent grade were from Merck; triethylamine (puriss.) and L-valinol (valol) were from Fluka, (S)(−)-phenylethylamine (PEA) was from Aldrich (Steinheim, Germany) and aniline (AN) was from Sigma; DL-valine methyl or isopropyl ester [H-Val-OMe (iPrp)] were synthesized by reaction of 3 mg of DL-Val with 500 μl of 2 *M* hydrochloric acid in methanol (or isopropanol) for 1 h at 100°C.

Stationary phase and preparation of eluents for HPLC

The column (250 × 4 mm I.D.) was packed with Spherisorb ODS 2, 5 μm (Shandon, Queensferry, UK) and the precolumn (4 × 4 mm I.D.) with Microspher 100 RP-18, 5 μm (Merck).

For gradient elution, a linear gradient from 0 to 100% B in 45 min was used for separations; flow-rate, 1 ml/min at ambient temperature; absorbance (*A*), 340 nm; the mobile phase hold-up time t_0 (CH_3OH) was 1.75 min under these conditions. To prepare triethylammonium phosphate buffer (TEAP), 6.93 ml (50 m*M*) of triethylamine were dissolved in 950 ml doubly distilled water, the pH was adjusted to 3 by addition of orthophosphoric acid (85%, *ca.* 4 ml) and the volume was made up to 1 l by addition of doubly distilled water. For eluent A, 900 ml of TEAP were mixed with 100 ml of ACN; for eluent B, 200 ml of TEAP were mixed with 800 ml of ACN. In one instance (*cf.*, Fig. 2f, upper trace), the TEAP buffer was adjusted to pH 2; in another instance (*cf.*, Fig. 2c, upper trace), gradient elution was performed under the following conditions: Eluent A, 13 m*M* aqueous TFA (900 ml) and ACN (100 ml); eluent B, 13 m*M* aqueous TFA (200 ml) and ACN (800 ml); linear gradient from 0 to

100% B in 45 min; flow-rate 1 ml/min; t_0 (CH_3OH), 1.85 min. Buffers were filtered prior to use (Millipore HVLPO 4700 filter, pore size 0.45 μm) and degassed by sonification for *ca.* 15 min (Eurosonic Cobra 44 sonicator).

Corey–Pauling–Koltun (CPK) molecular models were obtained from Ealing Beck (Watford, UK).

Characterization of chiral variants of Sanger's reagent

All FDNP reagents (for syntheses see below) were found to be pure by HPLC and by thin-layer chromatography (TLC) using precoated plates (Kieselgel 60 F_{254}; Merck) and were characterized by their electron impact (EI) mass spectra (MS), usually at 70 eV, using a Varian 311 A mass spectrometer. Melting points were determined on a Büchi (Flawil, Switzerland) Model B 520 melting point apparatus. R_F values were determined at 24°C on TLC plates in glass chambers (Desaga, Heidelberg, Germany) coated with filter-paper; the distance from the start to the front on the TLC plates was 10 cm. The solvent systems were as follows (v/v): (I) ethyl acetate–light petroleum–methanol–acetic acid (30:70:14:9); (II), acetone–ethyl acetate–*n*-hexane (10:10:20); (III), chloroform–*n*-hexane–acetic acid (80:20:20). UV spectra were determined by photodiode-array detection and HPLC using instruments described elsewere [19].

Syntheses and characterization of reagents

The general procedure was as follows. Under protection from light, DFDNB was dissolved in acetone and distilled water was added; 0.5–0.7 equiv. of the amino component were dissolved in 0.6 *M* $NaHCO_3$ (in subsequent text, $NaHCO_3$ refers to this concentration unless stated otherwise) and the solution was slowly added dropwise (*ca.* 30 min) at room temperature (RT) to the vigorously stirred solution of DFDNB and heated for 1–2 h at 40–50°C (see below.) In the course of the reaction the products precipitated either as solids or oils or remained in solution. Acetone was removed *in vacuo* and the remaining aqueous phase was diluted by addition of water. Precipitated solids were isolated by filtration, washed several times with water and dried in an desiccator over P_2O_5 and KOH pellets *in vacuo* (*ca.* 0.02 mmHg). When oily products formed in the course of the reaction or after addition of water the supernatant was discarded, the oil was dissolved in ethyl acetate (EA) and the organic phase was washed three times each with about half of the volume of aqueous $NaHCO_3$ (5%), $KHSO_4$ (5%) and water. The organic phase was dried over anhydrous Na_2SO_4, evaporated to dryness and the residue was precipitated or crystallized from organic solvents (see below.) In those instances where the product remained in solution after addition of water the reaction mixture was extracted three times with EA and the combined extracts were washed and treated as described above. Reagents and solutions were stored at 4°C and protected from light. The reagents synthesized were pure according to TLC and HPLC and were characterized as described below.

Individual syntheses of reagents are given below; for structures of reagents, see Fig. 1; for syntheses of FDNP-Ala-NH_2 and FDNP-Val-NH_2 see ref. 21. FDNP-Val-NH_2 is obtainable form Novabiochem (Läufelfingen, Switzerland) on request; letters (a)–(l) in parentheses for the synthetic compounds correspond to the designations of the FDNP reagents in Table I and Fig. 2; AAs and derivatives are abbre-

viated as usual in peptide chemistry [22], consequently FDNP is considered as an amino blocking group. Syntheses were not optimized with respect to highest yields.

(a) N^2-(5-Fluoro-2,4-dinitrophenyl)-L-valine amide (FDNP-Val-NH_2). For syntheses, see ref. 20.

(b) N^2-(5-Fluoro-2,4-dinitrophenyl)-L-valine tert.-butylamide (FDNP-Val-NHtBu). A 122.5 mg (0.6 mmol) amount of DFDNB was dissolved in 2 ml of acetone and 0.5 ml of water, 62.7 mg (0.3 mmol) of H-Val-L-NHtBu · HCl in 2 ml of $NaHCO_3$ were added and the mixture was stirred for 18 h at 40°C. On addition of 10 ml of water a yellow oil precipitated, which was then treated according to the general procedure above. The remaining yellow oil yielded an amorphous powder after being stirring with light petroleum. Yield, 73 mg (68.3%); m.p. 103°C; R_F (I) 0.80, R_F (II) 0.62, R_F (III) 0.84; UV (nm), 335, 215, 263; MS, *m/z* 357 (MH^+), 256, int. (M − $COOCMe_3$), 284/285 (M − $OCMe_3$).

(c) N^2-(5-Fluoro-2,4-dinitrophenyl)-L-valine phenylethylamide (FDNP-Val-PEA). To 816.4 mg (4 mmol) of DFDNB in 30 ml of acetone, 10 ml of water and 896 mg (2.7 mmol) of H-Val-PEA · TFA (n) in 20 ml of $NaHCO_3$ were added dropwise; (c) started to precipitate during the addition. After 1 h at 40°C, 60 ml of water were added, the precipitate was filtered and washed as described under the general procedure above. Yield, 978 mg (89.6%); m.p. 189°C; R_F (I) 0.79, R_F (II) 0.58, R_F (III) 0.85; UV (nm), 213, 334, 263; MS, *m/z* 405 (MH^+), 257, int. (M − $CONHCH(Me)C_6H_5$ + H].

(d) N^2-(5-Fluoro-2,4-dinitrophenyl)-L-valine anilide (FDNP-Val-AN). A 408.2 mg (2 mmol) amount of DFDNB was dissolved in 10 ml of acetone and 4 ml of water and 420 mg (1.4 mmol) of H-Val-AN · TFA (p) in 10 ml of $NaHCO_3$ were added. An orange oil formed immediately. After 1 h at 40°C the mixture was treated as described under the general procedure above, yielding a dark orange oil which slowly crystallized. The product was dissolved in CH_3OH and recrystallized by addition of diethyl ether and light petroleum. Yield, 504 mg (95.6%); m.p. 156°C; R_F (I) 0.79, R_F (II) 0.58, R_F (III) 0.79; UV (nm), 237, 333, 264 (shoulder); MS, *m/z* 376 (M^+), 257, int. (M − $CONHC_6H_5$ + H).

(e) N^2-(5-Fluoro-2,4-dinitrophenyl)-L-valine p-nitroanilide (FDNP-Val-pNA). To 122.5 mg (0.6 mmol) of DFDNB in 2 ml of acetone and 0.5 ml of water a suspension of 71.2 mg (0.3 mmol) of H-Val-pNA in 2 ml of $NaHCO_3$ was added with stirring and the mixture was heated for 3 h at 40°C. A yellow oil was formed which crystallized after being stirred overnight. The fine crystal needles were collected by centrifugation. Yield, 98 mg (77.5%); m.p. 224°C; R_F (I) 0.77, R_F (II) 0.51, R_F (III) 0.56; UV (nm), 329, 226; 266; MS, *m/z* 422 (MH^+), 256 (M − $CONHC_6H_5NO_2$).

(f) N^2-(5-Fluoro-2,4-dinitrophenyl)-L-valine (FDNP-Val-OH). A 1.0 g (2.8 mmol) amount of FDNP-Val-OtBu was dissolved in 15 ml of DCM, 15 ml of TFA were added and the solution was stirred at RT for 90 min. Solvents were removed *in vacuo,* the residue was dissolved in diethyl ether and the product was precipitated by addition of light petroleum. Yield, 666 mg (79%); m.p. 129°C; UV (nm), 338, 216, 264; R_F (I) 0.62, R_F (III) 0.59; MS, *m/z* 301 (MH^+), 256, int. (M − COOH).

(g) N^2-(5-Fluoro-2,4-dinitrophenyl)-L-valine methyl ester (FDNP-Val-OMe). To 20 mg (0.07 mmol) of FDNP-Val-OH in 200 µl of CH_3OH, 4 ml of a solution of diazomethane in diethyl ether were added and the solvents were removed after 10 min in a stream of nitrogen; completeness of reaction was checked by TLC. R_F (I) 0.80; R_F (II) 0.65; MS, *m/z* 316 (MH^+), 255 (M − COOMe).

(h) N^2-(5-Fluoro-2,4-dinitrophenyl)-L-valine tert.-butyl ester (FDNP-Val-O-tBu). A 682 mg (3.27 mmol) amount of H-Val-OtBu · HCl was dissolved in 10 ml of $NaHCO_3$ and 0.36 ml (3.27 mmol) of NMM in 3 ml of $NaHCO_3$ and 1.33 g (6.5 mmol) of DFDNB in 45 ml of acetone were added. The product precipitated as an oil. The mixture was stirred for 18 h at 40°C and the oil was treated as described under the general procedure above. The dark yellow oil obtained was dissolved in 5 ml of acetone and the product was precipitated by dropwise addition of water. Yield, 1.09 g (93.3%) (yellow solid); m.p., 82°C; R_F (I) 0.85, R_F (II) 0.72; UV (nm), 330, 263, 225; MS, *m/z* 357 (M^+), 302 (M − CMe_3), 285 (M − $OCMe_3$), 255, int. [M − $COOC(Me)_3$].

(i) N^2-(5-Fluoro-2,4-dinitrophenyl)-L-alanine amide (FDNP-Ala-NH_2). See refs. 10 and 21.

(j) N^2-(5-Fluoro-2,4-dinitrophenyl)-L-alanyl-L-alanine amide (FDNP-Ala-Ala-NH_2). A 122.5 mg (0.6 mmol) amount of DFDNB was dissolved in 2 ml of acetone and 0.5 ml of water and 58.7 mg (0.35 mmol) of H-Ala-Ala-NH_2 · HCl in 2 ml of $NaHCO_3$ were added. The mixture was heated for 1 h at 40°C, 10 ml of distilled water were added and the crystalline precipitate was treated as described under the general procedure above. Yield, 83.3 mg (69.4%); m.p. >244°C (decomp.); R_F (I) 0.53, R_F (II) 0.06, R_F (III) 0.15.; UV (nm), 336, 212, 264; MS, *m/z* 344 (MH^+), 300 (M − $CONH_2$), 228, int. (M − $CONHCH(CH_3)$-$CONH_2$.

(k) N^2-(5-Fluoro-2,4-dinitrophenyl)-(S)(−)-phenylethylamide (FDNP-PEA). A 408.2 mg (2 mmol) amount of DFDNB was dissolved in 5 ml of acetone, mixed with 15 ml of $NaHCO_3$ and 129 µl (1 mmol) of (*S*)(−)-phenylethylamine in 10 ml acetone were added to the suspension. After 20 h at RT the solution was treated as described under the general procedure above, the resultant yellow residue was dissolved in ethanol and the product was precipitated by addition of light petroleum ether. Yield, 199 mg (65.2%), amorphous powder; m.p. >290°C (decomp.); R_F (I) 0.59; UV (nm), 345, 232, 257; MS, *m/z* 305 (M^+), 228 (M − C_6H_5), 202, int. (M − $CHCH_3C_6H_5$ + 2H).

(l) N-(5-Fluoro-2,4-dinitrophenyl)-L-valinol (FDNP-valol). To 408.2 mg (2 mmol) of DFDNB in 15 ml of acetone and 15 ml of $NaHCO_3$ a solution of 103.2 mg (1 mmol) of L-valinol in 10 ml of $NaHCO_3$ were added and the mixture was heated for 1 h at 40°C. Solvents were removed *in vacuo*, the residue was dissolved in ethanol and the compound was crystallized by addition of light petroleum. Yield, 164 mg (57.1%); m.p. >200°C (decomp.); R_F (I) 0.59, R_F (III) 0.83; UV (nm), 343, 227, 258; MS, *m/z* 256, int. (M − CH_2OH).

(m) N^2-tert.-Butyloxycarbonyl-L-valine phenylethyl amide (Boc-Val-PEA). To 943 mg (3 mmol) of Boc-Val-OSu in 10 ml of ACN, 774 µl (6 mmol) of PEA in 3 ml of ACN were added. After 20 h at RT the solvents were removed *in vacuo*, EA was added and the organic phase was washed as described under the general procedure above. Yield, 884 mg (92%) (white crystals). The product was used without further characterization for the synthesis of (n).

(n) L-Valine phenylethylamide trifluoroacetate (H-Val-PEA · TFA). A 938 mg (2.93 mmol) amount of Boc-Val-PEA (m) was dissolved in 5 ml of DCM and 15 ml of TFA were added. The solvent was removed *in vacuo* and the oily residue was stirred with diethyl ether and light petroleum. The solvents were removed *in vacuo*, leaving a white foam. Yield, 941 mg (96%); the product was used for the synthesis of (c).

(o) N^2-tert.-Butyloxycarbonyl-L-valine 5-fluoro-2,4-dinitroanilide (Boc-Val-AN). To 943 (3 mmol) of Boc-Val-OSu in 20 ml of ACN, 1.70 g (18.3 mmol) of aniline in 3 ml of ACN were added and the mixture was heated for 20 h at 40°C. The solvents were removed *in vacuo*, EA was added and the organic phase was washed as described under the general procedure above. As the material obtained after removal of EA contained unreacted Boc-Val-OSu according to TLC, it was treated with a mixture of 50 ml of aqueous Na_2CO_3 (10%) and 25 ml of CH_3OH for 1 h at RT. EA was added and the organic phase was washed as described under the general procedure above. Yield, 447 mg (51%). The product was used for the synthesis of (p).

(p) L-Valine anilide trifluoroacetate (H-Val-AN · TFA). To 482 mg (1.65 mmol) of Boc-Val-AN (o) in 5 ml of DCM, 10 ml TFA were added and the solvents were removed *in vacuo* after 30 min at RT. The oily residue was dissolved in diethyl ether, light petroleum was added and the mixture was stirred overnight at RT. Yield, 463 mg (91.7%) (white crystals); the product was used for the synthesis of (d).

Preparation of stock solutions and standards

Chiral reagents. Solutions (100 m*M*) of chiral reagents in acetone were prepared with the exceptions of FDNP-Ala-NH_2, FDNP-Ala-Ala-NH_2 and FDNP-Val-PEA, for which 33.3 m*M* solutions in acetone were used.

DL-amino acids. Standards of 200 m*M* AA in 1 *M* HCl were prepared.

Derivatization of DL-amino acids with chiral reagents

A volume of 25 µl (5µmol) of DL-amino acid standard solution, 25 µl of 1 *M* $NaHCO_3$, 50 µl (or 150 µl in the cases of 33.3 m*M* reagent solutions) (5 µmol) of reagent solutions and further 40 µl of 1 *M* $NaHCO_3$ were heated for 1 h at 40°C, then 20 µl of 2 *M* HCl were added and the mixture was dried for 18 h *in vacuo* over $KOH–P_2O_5$. The residue was dissolved in 1 ml of DMSO, filtered (Anotop 0.2-µm filter, Merck) and a 1-µl aliquot was used for HPLC (this corresponds to 2.5 nmol of the respective diastereomers calculated for a 100% derivatization yield).

RESULTS AND DISCUSSION

Derivatization of DL-amino acids with FDNP-Val-NHR and FDNP-Val-OR

From the Δt_R values of diastereomers obtained by reaction of DL-AAs with reagents of the structure FDNP-L-AA-NH_2 (AA = Ala, Val, Phe, Pro) [21], it was concluded that exchange of further AAs in FDNP-AA amides would not lead to reagents giving rise to substantially larger Δt_R values for DL-AAs.

As FDNP-Val-NH_2 gave the largest Δt_R value for many diastereomers of DL-AAs [21], substituted FDNP-Val amides and esters of the structures FDNP-Val-NHR (R = *tert.*-butyl; H_2NR = phenylethylamine, aniline, *p*-nitroaniline), FDNP-L-Val-OR (R = H, methyl, *tert.*-butyl) and FDNP-L-Ala-L-Ala-NH_2 were synthesized. Furthermore, FDNP reagents were synthesized by substitution of one fluorine atom of DFDNB with the chiral amines (*S*)(−)-phenylethylamine and L-valinol (Fig. 1.).

The reagents were used for the derivatization of selected DL-AAs, *viz.*, DL-Val (branched, neutral side-chain), Ser (neutral side-chain with hetereoatom), Glu (trifunctional, acidic AA) and Lys (trifunctional, basic AA). Net retention times, t'_R, and

Δt_R values calculated therefrom, determined under same gradient conditions by HPLC, were compared with those of FDNP-Val-NH_2 and FDNP-Ala-NH_2 as shown in Table I; sections of the chromatograms of the diastereomers of DL-Val (which are best resolved in most cases) are shown in Fig. 2a–h. The HPLC investigation of the diastereomers formed by reaction of selected analyte DL-AAs with FDNP reagents (*cf.*, Table I) is discussed below.

Resolution of DL-Val

By derivatization of DL-Val with reagents (a)–(j) (Table I), all diastereomers formed were baseline resolved with Δt_R values from 1.36 to 8.78 min. The largest Δt_R values were obtained by derivatization with FDNP-Val-OH and FDNP-Val-NH_2 and the smallest by derivatization with FDNP-Val-NHtBu and FDNP-Val-OtBu. Derivatization with FDNP-Val-OtBu and FDNP-Val-PEA gave rise to intense reagent peaks in the chromatograms, indicating that the reactions are less complete in comparison with the other reagents as a result of steric hindrance. Kinetic discrimination is also a feasible explanation that the peak areas of certain diastereomers are not equal (*cf.*, Fig. 2). In several instances, such as derivatization of DL-Val with FDNP-Val-PEA and FDNP-Val-pNA, the peak of the hydrolysed reagent and one of the diastereomers formed eluted together under the conditions used (Fig. 2c, lower trace, and Fig. 2e, respectively). Diastereomers and reagent were separated, however, using a TFA gradient (Fig. 2c, upper trace; for conditions see Experimental). Derivatization of DL-Val with FDNP-Val-OH resulted in the elution of the diastereomer formed with D-Val (but not with L-Val) as a very broad and asymmetric peak in HPLC using the TEAP pH 3 buffer (Fig. 2f, lower trace). The peak symmetry was improved considerably by adjusting the buffer to pH 2, probably as a result of the protonation of carboxy groups (Fig. 2f, upper trace). For a discussion of the resolution mechanisms, it is crucial that diastereomers of DL-Ala, DL-Val, DL-Ser and DL-Glu, obtained by derivatization with FDNP-PEA, and FDNP-valol, were not resolved under the HPLC conditions used (for HPLC of diastereomers of these reagents formed with DL-Val, see Fig. 2k–l).

Resolution of DL-Glu

Baseline separation of DL-Glu was achieved for diastereomers formed by reactions with most reagents, with the exception of FDNP-Val-OH, FDNP-Val-OMe and FDNP-Val-OtBu, which gave unsatisfactory resolution under the HPLC conditions used. With the exception of FDNP-Val-NHtBu, FDNP-Val-pNA and FDNP-Ala-Ala-NH_2, intense peaks of hydrolysed reagents appeared in the chromatograms, indicating low derivatization yields for the other reagents.

Resolution of DL-Ser

Baseline separation of DL-Ser was possible by formation of the diastereomers obtained with FDNP-Ala-NH_2 and FDNP-Val-NH_2, and almost beaseline separation occurred by derivatization with FDNP-Val-OH and FDNP-Val-pNA. Unsatisfactory resolution was obtained by derivatization with FDNP-Val-OMe and FDNP-Val-PEA, and no or only very slight separation was obtained with FDNP-Val-NHtBu, FDNP-Ala-Ala-NH_2, FDNP-Val-AN and FDNP-Val-OtBu. Relatively low derivatization yields were realized with the use of FDNP-Val-OtBu, FDNP-Val-PEA

TABLE I

NET RETENTION TIMES OF FIRST ($t'_{R(L-L)}$) AND SECOND ($t'_{R(D-L)}$) ELUTED DIASTEREOMER FORMED BY REACTION OF DL-Val, DL-Glu, DL-Ser, AND DL-Lys WITH CHIRAL FDNP REAGENTS, AND DIFFERENCES IN ELUTION TIMES (Δt_R).

For monosubstituted DL-Lys net retention times $t'_{R1,2,3}$ are given. Experiments were carried out under same gradient elution conditions in HPLC (*cf.*, Experimental). mono., di. = Mono- and disubstituted Lys, respectively.

FDNP reagent[b]		Retention time (min)														
		Analyte amino acid														
		DL-Val			DL-Glu			DL-Ser			DL-Lys (mono.)[a]			DL-Lys (di.)		
		$t'_{R(L-L)}$	$t'_{R(D-L)}$	Δt_R	$t'_{R(L-L)}$	$t'_{R(D-L)}$	Δt_R	$t'_{R(L-L)}$	$t'_{R(D-L)}$	Δt_R	t'_{R_1}	t'_{R_2}	t'_{R_3}	$t'_{R(L-L)}$	$t'_{R(D-L)}$	Δt_R
(a)	FDNP-Val-NH_2	19.31	24.47	5.16	15.80	16.92	1.12	14.94	15.72	0.78	12.89	13.03	14.57	27.62	29.45	1.83
(b)	FDNP-Val-NHtBu	33.33	34.96	1.63	22.08	22.94	0.86	21.98	21.98	0.00	17.64	17.98	19.04	41.57	42.13	0.56
(c)	FDNP-Val-PEA	33.91	36.13	2.22	24.31	25.18	0.87	23.81	24.13	0.32	19.79	20.75	–	42.35	42.94	0.59
(d)	FDNP-Val-AN	33.73	35.99	2.26	23.75	25.80	2.05	24.09	24.31	0.22	19.25	20.04	20.46	41.32	42.68	1.36
(e)	FDNP-Val-pNA	34.13	37.00	2.87	25.52	27.81	2.29	24.79	26.48	1.69	21.01	21.60	22.16	40.57	42.91	2.34
(f)	FDNP-Val-OH	22.68	31.46	8.78	17.73	18.08	0.35	16.63	17.49	0.86	13.88	15.67	–	29.99	32.18	2.19
(g)	FDNP-Val-OMe	33.02	34.95	1.93	21.87	22.05	0.18	21.42	21.85	0.43	17.49	17.68	18.69	–	–	–
(h)	FDNP-Val-OtBu	40.29	41.65	1.36	29.66	29.95	0.29	30.40	30.58	0.18	22.96	23.75	–	49.94	50.93	0.99
(i)	FDNP-Ala-NH_2	17.49	20.27	2.78	12.57	13.68	1.11	11.15	11.81	0.66	9.86	11.36	–	18.57	19.73	1.16
(j)	FDNP-Ala-Ala-NH_2	16.76	18.49	1.73	12.50	13.67	1.17	11.37	11.31	0.00	10.00	11.60	–	20.62	21.76	1.14
(k)	FDNP-PEA[c]	22.35	22.35	0.00												
(l)	FDNP-valol[c]	23.07	23.07	0.00												

[a] Δt_R not calculated.

[b] Amino acids in reagents are of the L-configuration, for abbreviations and structures, *cf.*, Experimental and Fig. 1, respectively.

[c] Δt_R = 0.00 for DL-Glu, DL-Ser, DL-Lys and DL-Ala; – = t'_{R_3} not found under conditions used; t_0 (CH_3OH) 1.75 min under HPLC conditions used (*cf.*, Experimental); first letter in diastereomers L–L and D–L, respectively, refers to the configuration of the amino acid to be analyzed, second to that of the amino acid in FDNP reagent.

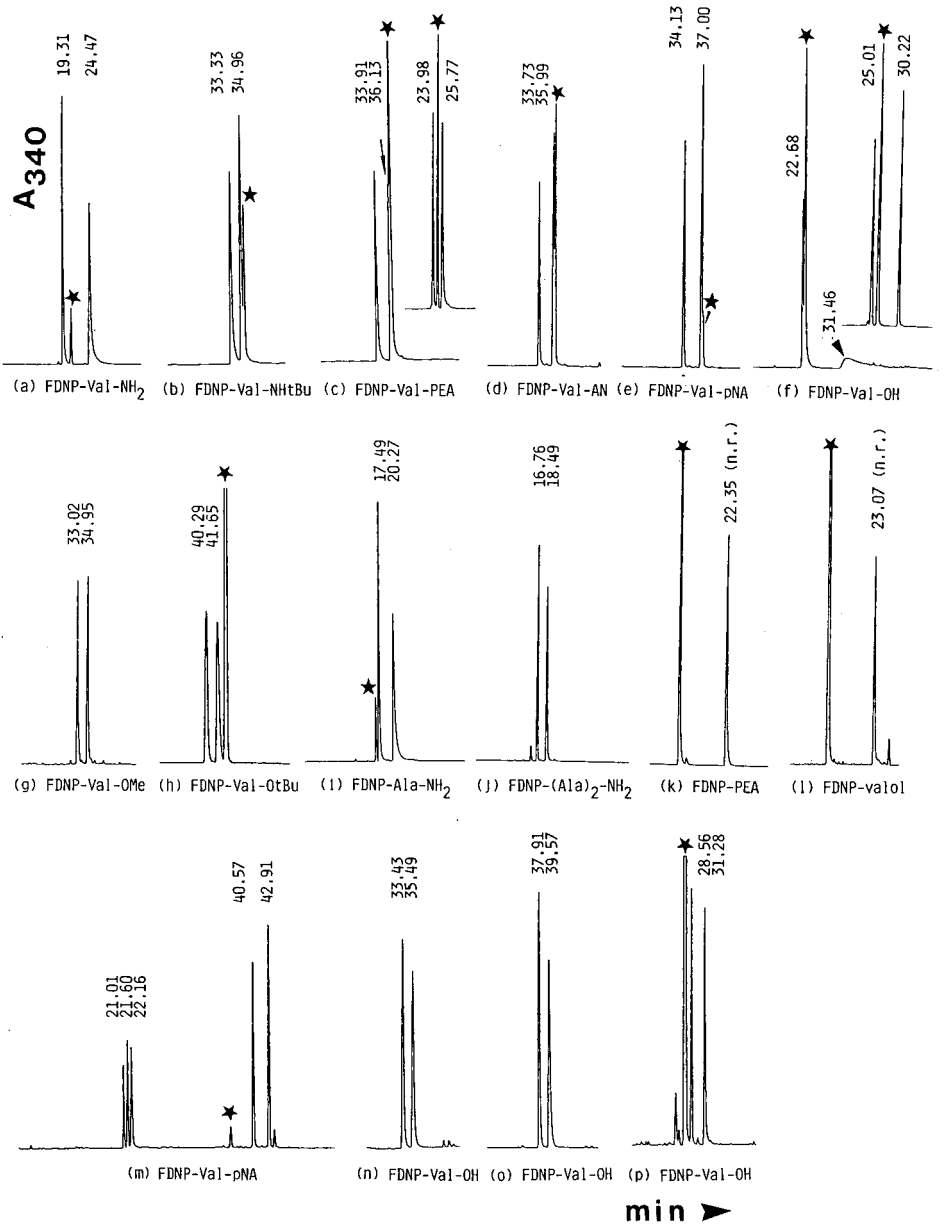

Fig. 2. Sections of chromatograms of the HPLC separation of diastereomers obtained by reaction of (a)–(l) FDNP reagents (*cf.*, Table I) with DL-Val, (m) FDNP-Val-pNA with DL-Lys and of (n)–(p) FDNP-Val-OH with (n) DL–Val-OMe, (o) DL-Val-iPrp and (p) NMe-DL-Val-OH. Net retention times, t'_R, of diastereomers are given; diastereomers of (k)–(l) are not resolved (n.r.); asterisks indicate peaks of hydrolysed reagents which are shown in chromatograms if eluted close to diastereomers. Chromatograms were taken under same standard gradient elution conditions (*cf.*, Experimental); upper traces in (c) and (f) show elution with TEAP pH 2 buffer and TFA gradient, respectively (for details, see Experimental). For structures of reagents, see Fig. 1.

and FDNP-Val-AN, as indicated by intense peaks of hydrolysed reagent in the chromatograms.

Diastereomers formed by derivatization of DL-Ser are eluted much earlier than those of DL-Val (*cf.*, Table I). This is explained by the higher polarity (hydrophilicity) of the respective derivatives; the shorter retention times might also contribute to smaller Δt_R values.

Derivatization of DL-Lys

As Lys has reactive ε- and α-amino groups, the formation of mono- and disubstituted derivatization products is, in principle, possible. The respective diastereomers are baseline separated by application of FDNP reagents (a)–(j) (Table I; FDNP-Val-OMe tested only in a less than equivalent amount yielded monosubstituted Lys).

It is of interest that derivatization of DL-Lys with certain FDNP reagents (*cf.*, Table I) gives rise to three signals at relatively low retention times in the chromatograms, assigned to monosubstitution products, and to two signals at relatively higher retention times, assumed to be disubstituted products [12] (in addition, peaks of hydrolysed reagents are seen in the chromatograms; see derivatization of DL-Lys with FDNP-Val-pNA as an example, Fig. 2m).

With monosubstitution products, the formation of four diastereomers from DL-Lys is possible, *viz.*, L–L_α, D–L_α, L–L_ε and D–L_ε (the first letter refers to the configuration of the analyte AA and the second letter to the substitution position α or ε in Lys by the reagent L-AA).

With disubstitution products, the formation of two diastereomers from DL-Lys is possible, *viz.*, L–L_α–L_ε and D–L_α–L_ε. Derivatization of either L- or D-Lys with the reagents gives two signals of monosubstitution products at relatively lower retention times. It is feasible, therefore to assume that the monosubstitution products are the unresolved diastereomeric pairs obtained by reaction of the reagents with the α- and ε-amino group, respectively, of Lys giving rise to two signals in the chromatogram. In instances where three peaks of monosubstitution products are detected in the chromatograms, one diastereomeric pair is separated and the other is not (*cf.*, Fig. 2m).

That FDNP reagents are, in principle, also suitable for the separation of DL-AA esters and N-methyl-DL-AAs is demonstrated by the resolution of diastereomers obtained by derivatization of H-DL-Val-OMe(iPrp) (Fig. 2n and o) and NMe-DL-Val-OH (Fig. 2p) with FDNP-Val-OH.

Model for resolution of diastereomers

From the results presented it is obvious that, in principle, all DL-AAs are separable as the diastereomers formed by reaction with reagents of the general structures FDNP-AA-NHR [AA = chiral AA or oligopeptides such as Ala-Ala; R = H, alkyl such as *tert.*-butyl (tBu), aralkyl such as phenylethyl, phenyl, *p*-nitrophenyl] and by derivatization with FDNP-AA-OR (R = tBu, CH_3, iPr). However, no separation of DL-AAs is achieved by derivatization with reagents of the structure FDNP-NHR (R = chiral hydroxyalkyl or chiral aralkyl).

Marfey [10] found that after derivatization of DL-AAs with FDNP-Ala-NH_2 the L-AAs (*i.e.*, L–L diastereomers) are eluted before D-AAs (*i.e.*, D–L diastereomers; the first letter refers to the configuration of the amino acid to be analysed and the

second to the L-configuration of the AA amide). He postulated that the carboxy group in the diastereomers of the respective D-AAs forms stronger intramolecular hydrogen bridges to the carboxamide group than do L-AAs. The twelve-membered ring in the respective D–L diastereomer thus formed was assumed to be more hydrophobic than the L–L diastereomer. The more hydrophobic molecule was supposed to interact more strongly with the reversed-phase, leading to higher retention times for D–L diastereomers as compared with L–L diastereomers.

From space filling Corey–Pauling–Koltun (CPK) molecular models of diastereomers (Fig. 3), however, and from experimental results, the following conclusions on the resolution mechanisms of diastereomers by RP-HPLC are drawn.

(1) It is assumed that the dinitrobenzene ring forms a stable, planar conformation. CPK models show that in L–L diastereomers the carboxy group of the analyte L-AA, and not of the D-AA, is positioned very near to the carboxamide group of the reagent L-AA amide, thus probably forming hydrogen bridges. Models also show that the formation of such an intramolecular hydrogen bridge is not possible to such an extent in the case of the D–L diastereomers (Fig. 3). This will count for an enthalpy difference of *ca.* 4 kcal/mol of diastereomers.

(2) CPK models also show that C^{β}-branching of AA side-chains, as in the case of Val, in the diastereomers further reduce the (in the case of Ala already very low) conformational freedom of the diastereomers formed. The formation (non-formation) of intramolecular hydrogen bridges of the L–L (D–L) diastereomer as pointed out above, however, is influenced to a minor extent by the structures of AA side-chains.

(3) The models also demonstrate that all reagents with the formulae FDNP-L-

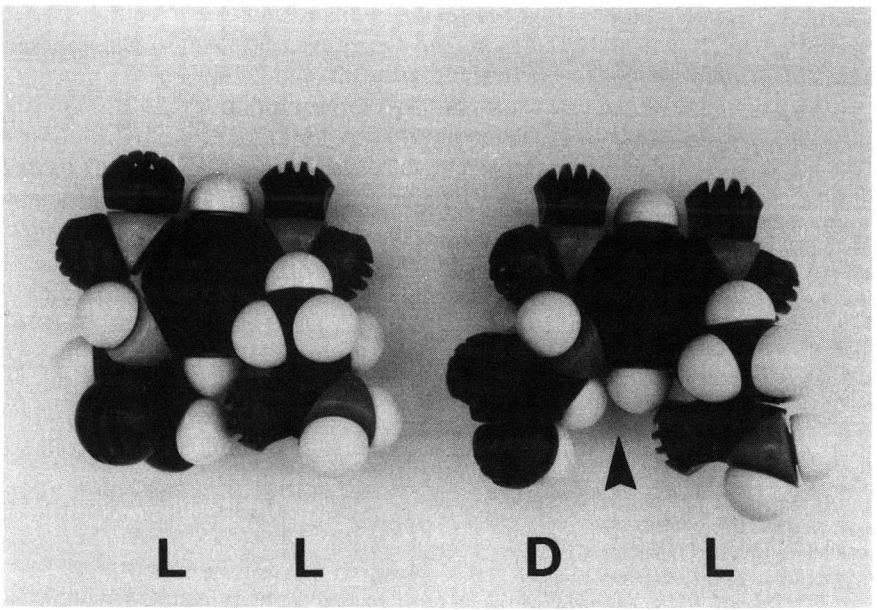

Fig. 3. Corey–Pauling–Koltun (CPK) molecular models of L–L and D–L diastereomers obtained by derivatization of L- and D-Ala with FDNP-L-Ala-NH_2. The arrow indicates the gap in the model of the D–L diastereomer.

AA-NHR, FDNP-L-AA-OR or FDNP-L-Ala-Ala-NH_2 have resolution capability as diastereomers formed by reaction with DL-AAs, as in all instances an intramolecular hydrogen bridge can be formed for the L–L diastereomer. This is not the case with reagents with the structures FDNP-NHR. The moiety R, however, alters the electronegativity of the carboxy group in CONHR and COOR residues and also the hydrophobicities of diastereomers. The model also explains that large Δt_R values are obtained by diastereomers formed by reaction of H-L-Val-OH with FDNP-L-Val-OH, since in the resulting L–L diastereomer the carboxy groups of amino acids can form hydrogen bridges to each other.

(4) The non-hydrogen-bonded, free carboxy group of the D-AA in the D–L diastereomer and the less symmetrical form of the molecule as a result of the gap in the D–L diastereomer as compared with the hydrogen-bridged, more compact L–L diastereomer (*cf.*, Fig. 3) might also explain the elution order of the respective diastereomers in HPLC. In comparison with the L–L diastereomer, the D–L diastereomer is assumed to interact more strongly with the alkyl chains of the reversed phase. It should be mentioned, however, that a CPK model is also constructable in which an intramolecular hydrogen bond is formed in the D–L diastereomer from the carboxy group of the analyte D-amino acid to the *ortho*-situated nitro group. In this instance, nevertheless, the less symmetrical shape and the gap in the D–L diastereomer remain.

In conclusion, and taking the proposed resolution mechanisms into account, under optimized separation conditions some of the new FDNP reagents might be of interest for the specific resolution of certain amino acids using the diastereomeric approach. This is also shown with the separation of DL-Val esters and NMe-DL-Val-OH by derivatization with FDNP-Val-OH (Fig. 2n–p). It is also realized that the reverse approach, *i.e.*, derivatization of DL-AA derivatives with the structures H-AA-NHR and H-AA-OR with reagents with the structures FDNP-AA-OH and subsequent HPLC separation of diastereomers is possible.

REFERENCES

1 F. Sanger, *Biochem. J.*, 39 (1945) 507.
2 F. Sanger, *Science*, 129 (1959) 1340.
3 O. Neunhoeffer and W. Ruske, *Justus Liebigs Ann. Chem.*, 610 (1957) 143.
4 E. D. Bergmann and M. Bentov, *J. Org. Chem.*, 26 (1960) 1480 and references cited therein.
5 R. L. Munier, A. M. Drapier, S. Meunier and P. Le Xuan, *Chromatographia*, 14 (1981) 289.
6 H. Zahn, *Kolloid-Z.* 121 (1951) 40.
7 H. Zahn and J. Meienhofer, *Makromol. Chem.*, 26 (1958) 126.
8 P. S. Marfey, H. Nowak, M. Uziel and D. A. Yphantis, *J. Biol. Chem.*, 240 (1965) 3264.
9 E. E. Gold and P. E. Braun, *J. Biol. Chem.*, 253 (1978) 8171.
10 P. Marfey, *Carlsberg Res. Commun.*, 49 (1984) 591.
11 D. J. Aberhart, J.-A. Cotting and H.-J. Lin, *Anal. Biochem.*, 151 (1985) 88.
12 G. Szókán, G. Mező and F. Hudecz, *J. Chromatogr.*, 444 (1988) 115.
13 G. Szókán, G. Mező, F. Hudecz, Z. Majer, I. Schön, O. Nyéki, T. Szirtes and R. Dölling, *J. Liq. Chromatogr.*, 12 (1989) 2855.
14 S. Kochhar and P. Christen, *Eur. J. Biochem.*, 175 (1988) 433.
15 S. Kochhar and P. Christen, *Anal. Biochem.*, 178 (1989) 17.
16 H. Brückner, I. Bosch, S. Kühne and S. Zivny, in G. R. Marshall (Editor), *Peptides: Chemistry and Biology*, Escom Science, Leiden, 1988, p. 195.
17 H. Brückner, S. Kühne, S. Zivny, M. Langer, Z. J. Kamiński and M. T. Leplawy, in A. Aubry, M. Marraud and B. Vitoux (Editors), *Second Forum on Peptides*, John Libbey Eurotext, London, 1988, p. 291.

18 H. Brückner and M. Langer, *J. Chromatogr.*, 542 (1991) 161.
19 H. Brückner, R. Wittner and H. Godel, *J. Chromatogr.*, 476 (1989) 73.
20 H. Brückner, C. Keller-Hoehl, H. Godel and R. Wittner, in E. Giralt and D. Andreu (Editors), *Peptides 1990*, Escom Science, Leiden, 1991, p. 334.
21 H. Brückner and C. Keller-Hoehl, *Chromatographia*, 30 (1990) 621.
22 G. C. Barrett (Editor), *Chemistry and Biochemistry of Amino Acids*, Chapman & Hall, London, 1985.

Journal of Chromatography, 555 (1991) 97–107
Elsevier Science Publishers B.V., Amsterdam

CHROM. 23 361

High-performance membrane chromatography of proteins, a novel method of protein separation

T. B. TENNIKOVA, M. BLEHA and F. ŠVEC*
Institute of Macromolecular Chemistry, Czechoslovak Academy of Sciences, 162 06 Prague (Czechoslovakia)
and
T. V. ALMAZOVA and B. G. BELENKII
Institute of Macromolecular Compounds, Academy of Sciences of the USSR, 199 004 Leningrad (USSR)
(First received December 14th, 1989; revised manuscript received April 14th, 1991)

ABSTRACT

Macroporous polymeric membranes, approximately 1 mm thick, were synthesized from poly(glycidyl methacrylate-co-ethylene dimethacrylate). The epoxide groups were further derivatized to add different functional groups which are commonly used as stationary phases in column chromatography. Separations of model mixtures of proteins were carried out on membranes modified with sulpho, C4 or C8 groups; the results were similar to those obtained using a column separation in the ion-exchange mode and in hydrophobic interaction chromatography. The advantage of high-performance membrane chromatography (HPMC) is that the pressure used is lower by as much as two orders of magnitude than that required to reach the same flow-rate in a packed column, although a high loading capacity can still be achieved. This makes HPMC suitable for both analytical and preparative separations.

INTRODUCTION

New methods for the separation of proteins should combine high selectivity and a high loading capacity [1]. The methods should also have the potential to be scaled up and be able to work at the low pressures required by membrane technology.

The way to obtain a membrane with the same properties as a chromatographic column is to use the Bio-Rex ion-exchange membranes (Bio-Rad) for fast separations. These consist of 90% standard chromatographic media in a bead form based on a styrene–divinylbenzene ion-exchange resin embedded in a web of poly(tetrafluoroethylene) [2]. Dominick Hunter Filters, now part of Millipore, have introduced the technique of shallow bed liquid chromatography. In this method the cartridge is filled with several sheets (up to a 10 mm layer) of modified cellulose paper supporting weak ion-exchange groups [3]. CUNO has developed a technique called Zetachromatography, which uses similar cellulose sheets consisting of a cross-linked vinyl polymer supporting ion-exchange groups [4]. Cellulose membranes with attached Protein A, Protein G or other ligands for affinity chromatography are also commercially avail-

0021-9673/91/$03.50

able (Memsep from Millipore, MAC Discs from Memtek and AbSorbent G from Genex [5]). However, membrane chromatographic techniques using hydrophobic interactions are currently not available commercially, and all the "membranes" used for the chromatographic separation of proteins are based on cellulose, which is characterized by a fibrous texture.

Calculations of the optimum particle diameter and length of a column for the separation of different molecular weight proteins suggest a bead size considerably less than 1 μm, a column $\leqslant 1$ cm in length and a pore size exceeding the Stokes diameter of the separated molecule by at least three-fold [6]. Gradient elution effects as a function of factors such as column length and gradient steepness have been investigated both theoretically [6–9] and experimentally [8–11].

The objective of this paper is to describe the use of modified macroporous polymeric flat bodies (thick membranes), prepared by a free radical bulk polymerization, for the chromatographic separation of proteins.

EXPERIMENTAL

Characterization of membranes

The membranes were synthesized by a free radical co-polymerization of glycidyl methacrylate and ethylene dimethacrylate in the presence of pores producing solvents using a procedure similar to that used for the synthesis of beads [12]. The polymerization took place in a space formed between two heated plate moulds separated by a silicone rubber gasket, the thickness of which corresponded to the required thickness of the membrane. The sheets obtained in this manner, from which membranes of the desired shape and size were cut, were washed with methanol, a methanol–water mixture (1:1, v/v) and water to remove the residue of unreacted compounds. The membranes were then stored without drying.

The permeability of the membranes to water was measured by a method described elsewhere [13] using an ultrafiltration cell (Amicon) and was calculated using Poiseuille's equation. Micro-photographs of the internal structure of the membrane were obtained with a JEOL JSM 35 scanning electron microscope. The specific surface area was calculated using the dynamic desorption of nitrogen obtained with a Quantasorb apparatus (Quantachrome).

A chemical modification of the epoxide groups of the polymer has been described elsewhere [14,15].

Sorption measurements

To determine the static sorption capacity, a 2 cm diameter, 1 mm thick membrane, with an area of 3.14 cm^2, was made from a macroporous copolymer with a specific density of 1.3 ml/g. The membrane was immersed in a 1 mg/ml protein solution. The concentration changes were monitored spectrophotometrically until equilibrium was reached. The amount adsorbed per membrane was recalculated to give the sorption per square metre of a membrane by multiplying the weight of sorbed protein by 3185. This value was obtained by dividing 1 m^2 (10 000 cm^2) by the area of the 2 cm diameter membrane (3.14 cm^2). The surface area covered by the protein was calculated as a percentage of the specific surface area of the porous polymer, divided by the sum of the known cross-section areas of the sorbed protein molecules.

The dynamic sorption data were determined on the same set of membranes with the membrane located in a chromatographic cell. A 10-ml volume of buffered protein solution (1 mg/ml) was passed through the membrane at a flow-rate of 1 ml/min, adjusted by a pressure of approximately 0.2 MPa. The effluent was collected and the overall protein content was determined photometrically. The difference between the starting and final protein concentrations gave the amount of protein sorbed on the membrane.

Chromatography[a]

Membrane chromatography of proteins was performed in a special magnetically stirred cell, 5.5 ml in volume, with a membrane at the bottom. The cell has an inlet capillary for the supply of the mobile phase and an outlet, in which the solution which has passed through the membrane is collected and then transmitted through a capillary to a UV detector (LKB, Sweden). The mobile phase is pumped into the cell using an 300 pump (Laboratory Instruments Works, Czechoslovakia). In a typical experiment the mixture of proteins dissolved in the initial buffer solution is injected into the cell and a buffer solution the same as mobile phase A is pumped into the cell. As they pass through the membrane, the proteins are sorbed onto the solid phase; the non-adsorbed protein is washed through. This process is monitored by a UV detector. After the signal has returned to baseline, the mobile phase is changed to solution B. With respect to the final volume of the cell, phase A is gradually diluted with phase B, and the change in the composition of the mobile phase entering the membrane has an exponential gradient. During the formation of the concentration gradient, the individual components of the original mixture are desorbed, depending on the interaction with the groups localized on the inner surface of the membrane, and separation is achieved.

RESULTS AND DISCUSSION

Current theories for the separation of large molecules by high-performance liquid chromatography (HPLC) favour small particles and short columns. The reduction in volume, which lowers the loading of very short columns, can be compensated by using a large diameter column, *i.e.* a flat or shallow bed column. In such a column the thin layer of polymer particles can be replaced by continuous material with properties close to those of a column packing. This continuous bed will not contain the interstitial spaces characteristic of a filled column containing spherical beads. These interstitial spaces amount at least 26% of the column volume; this volume will not contribute to the separation and causes peak broadening.

An early approach to this problem was the use of modified paper sheets to replace the modified cellulose sorbents (porous beads or microcrystalline fibres). This was widely used in biochemistry but was not established as a standard HPLC method.

Most packings for column HPLC consist of macroporous beads of both inorganic and organic origin. Each individual particle consists of mutually connected spherical entities called globules [16], the size of which is usually in the range 100–300 nm. Voids between the globules are permanent pores representing the macroporosity.

[a] The HMPC cartridges Quick Disc are now available from Säulentechnik Knauer, Berlin, Germany.

TABLE I

BASIC CHARACTERISTICS OF CHROMATOGRAPHIC MEMBRANES

Abbreviations: GMA = glycidyl methacrylate; EMDA = ethylene dimethacrylate; S_g = specific surface area; L = specific permeability; r_p = mean pore radius.

Membrane	Polymerization feed (wt. %)		S_g (m^2/g)	L (1/h m^2 MPa)	r_p (nm)
	GMA	EDMA			
G-5	5	95	250	–	5[a]
G-25	25	75	139	390	10[b]
G-40	40	60	80	1120	17[b]
G-50	50	50	60	1940	23[b]
G-60	60	40	43	–	25[a]

[a] Mean pore radius measured on beads of identical composition.
[b] Mean pore radius calculated from L.

The particles are synthesized by a suspension process which automatically yields beads from droplets of the dispersed liquid phase. The suspension polymerization is, in fact, a bulk polymerization, in which each dispersed polymerizing droplet is regarded as an individual block. This is why it is easy to move from this suspension polymerization to a polymerization of the same monomer mixture in a system not containing any continuous dispersion phase (water phase). The patented process of Švec and co-workers [17,18] yields a single piece of sorbent, which resembles a flat board polymerized in a bulk layer. The properties of this board are the same as those of a standard beaded sorbent. Macroporous membranes which match the conditions for chromatographic use are cut from this board.

Membrane properties

Characteristic data for a series of membranes prepared using different monomer mixtures are summarized in Table I. The table shows that the properties can be easily varied by changing the ratio of the monomers, *i.e.* the monovinylic glycidyl methacrylate and the divinylic cross-linking agent ethylene dimethacrylate. Earlier studies of the suspension polymerization of the same set of monomers showed that the structure and properties of a macroporous matrix are also affected by the amount and composition of the inert pores producing solvent in the organic phase, the initiator concentration, the reaction temperature and the polymerization time [12,19].

With respect to their permeability to the liquid, the membranes behave in a similar manner to the common ultrafiltration membranes. Their basic feature is a linear permeability *versus* pressure relationship (Fig. 1). The slope of this dependence is inversely proportional to the fraction of the cross-linking agent in the polymerization mixture. A high ethylene dimethacrylate concentration causes an increase in the specific surface area and moves the pore size distribution towards smaller values. To use a 2 cm diameter membrane containing 75% ethylene dimethacrylate at a flow-rate 1 ml/min, a pressure of over 0.75 MPa is required whereas only 0.1 MPa is needed for a membrane with 50% cross-linking. Any direct comparison with the permeability of a chromatographic column is incorrect. The permeability of a mem-

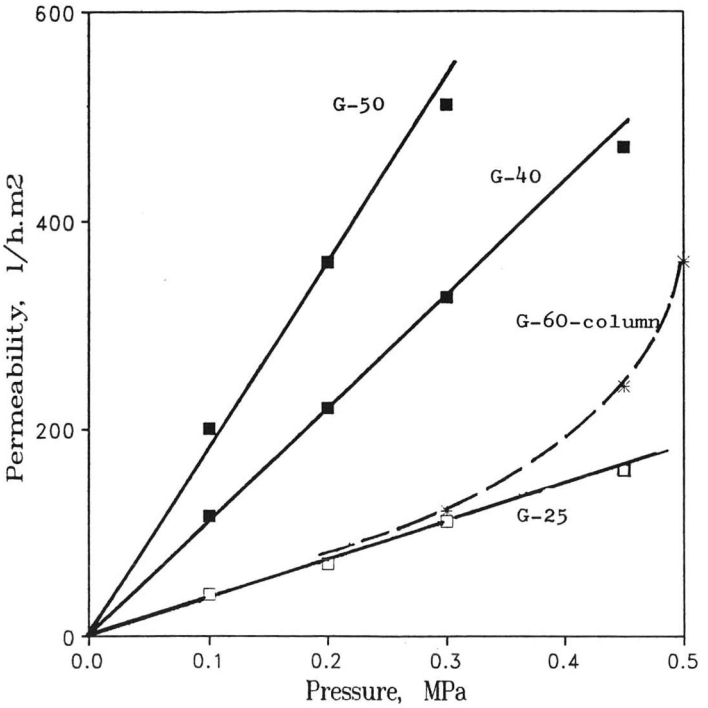

Fig. 1. Pressure dependence of flow through a 1 mm thick membrane made from poly(glycidyl methacrylate–ethylene dimethacrylate) copolymers with various glycidyl methacrylate contents. The results are compared with a 300 × 8 mm column packed with 5–7-μm beads of the copolymer containing 60% glycidyl methacrylate.

brane represents the flow through the pores, whereas the flow through a column proceeds via the interconnected interstitial voids. The pressure drop in a column depends on the particle size and particle size distribution of the sorbent, the packing efficiency, the column diameter and column length but, except in perfusion chromatography [19,20], does not depend on the porous properties of the packing material. It is possible to project the properties of a column down to the size of a membrane, but the physical properties of both are so different that any comparison is not relevant. A simplified direct comparison shows that a 1 mm thick membrane is more "permeable" than a 300 mm long column packed with 5–7 μm particles of identical composition, even when the diameter is recalculated to the same size (Fig. 1).

The mechanical stability of the membrane is equal to that of macroporous beads [21] which resist a column pressure of up to 30 MPa without damage. A detailed study of the mechanical properties of membranes has been published elsewhere [22].

A comparison between permeability and the mean pore size obtained by chromatographic measurements indicates that the pore size distribution is broad [23]. The membranes contain both relatively large transport pore (canals) and small separation pores. The former ensure a high flow-rate at low pressures, whereas the latter mainly contribute to the high specific surface area. From this point of view membrane chro-

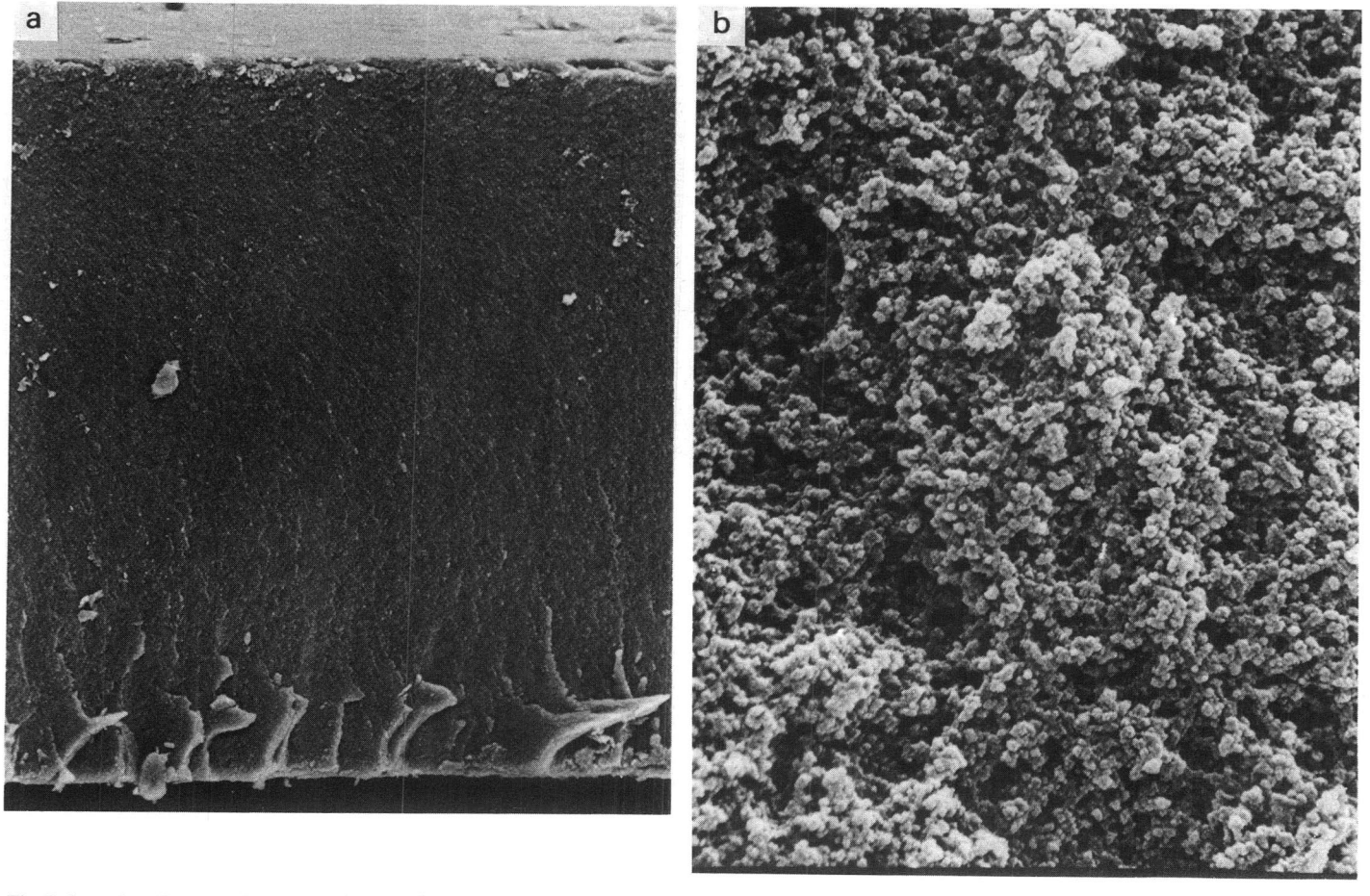

Fig. 2. Scanning electron microscopy pictures of a standard poly[glycidyl methacrylate-co-ethylene dimethacrylate] membrane. Magnification (a) 800 and (b) 5400.

matography resembles perfusion chromatography, in which the column packing also contains two kinds of pores: through pores and diffusion pores [19,20].

Fig. 2 shows a scanning electron microscopy (SEM) picture of the membrane cross-section at two magnifications. The globular structure characteristic of macroporous polymers is distinct, especially at the higher magnification, and large voids (transport canals) are seen between agglomerates of globules.

An exceptional advantage of glycidyl methacrylate copolymers is the possibility of preparing, from a single initial membrane, a whole set of chromatographic membranes containing groups commonly used in column ion-exchange chromatography or hydrophobic interaction chromatography, or, *i.e.* sulpho, diethylamino, butyl, octyl and phenyl groups, and many others:

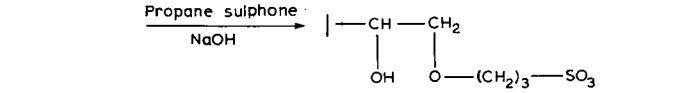

(1)

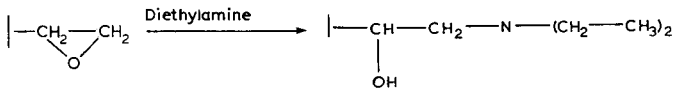

(2)

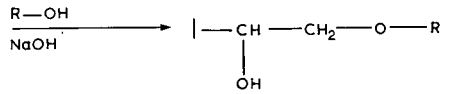

(3)

where R is an alkyl or aryl group.

The oxirane group (if any) remaining after the modification can be readily removed within 3 h by acid catalysed hydrolysis in a 0.1 mol/l sulphuric acid solution at 60–80°C. As shown schematically in eqn. 4, hydrolysis increases the hydrophility of the macroporous membrane surface and reduces the probability of non-specific interactions. At the same time, the absence of reactive oxirane groups also rules out chemical reactions in which the separated proteins could be covalently immobilized on the sorbent, particularly in alkaline medium:

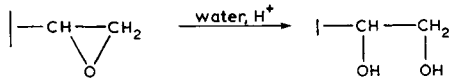

(4)

Experiments with albumin, chymotrypsinogen, lysozyme and ribonuclease A adsorbed from a solution containing 0.5 mg/ml protein proved that with the hydrolysed membranes in which the fraction of the cross-linking agent (ethylene dimethacrylate) is less than 60%, almost no interactions take place between proteins and the polymer. The protein recovery exceeds 96%. Table II summarizes the data on the sorption capacity of a membrane modified with butyl groups. The adsorption was determined by frontal analysis with a high excess of protein by following the decrease in concentration photometrically. Loading of the membrane reaches 20–40 g of protein per square metre of the 1 mm thick membrane. As the volume of 1 m^2 of a 1 mm thick macroporous membrane is 100 ml, the loading is up to 40 mg/ml. This corresponds to the loading capacities of leading commercially available chromatographic packing materials [24]. However, the dynamic capacity calculated from flow-through experiments is considerably lower.

TABLE II

STATIC AND DYNAMIC CAPACITIES OF C_4 MODIFIED MEMBRANES FOR SORPTION OF PROTEINS

Protein	Amount sorbed (mg/g)		Covering of surface (%)		Specific capacity (g/m^2)	
	Static	Dynamic	Static	Dynamic	Static	Dynamic
Ribonuclease	17.6	4.4	17	4.3	20	5
Lysozyme	22.1	–	20	–	26	–
Ovalbumin	41.2	4.4	18	1.9	47	5

Chromatography

The mixture of proteins is separated using liquid chromatography equipment, but instead of the column a specially designed cell, as described under Experimental, is used.

A simple calculation assuming that the polymer has a porosity of approximately 50% [12] (the volume fraction of pores) reveals that solvent regain in a 2 cm diameter membrane 1 mm thick is only 0.15 ml. The retention time of this volume in the membrane is 9 s when the flow-rate is 1 ml/min. Hence the composition of the eluent inside the membrane is almost homogeneous and the concentration gradient between the top and bottom of the membrane is negligible. This means that the dissolution of the protein is simultaneous throughout the whole membrane, and occurs just as the capacity factor k' reaches a sufficiently low values. This results in a narrow peak. An increase in the flow-rate accelerates the changes in the composition

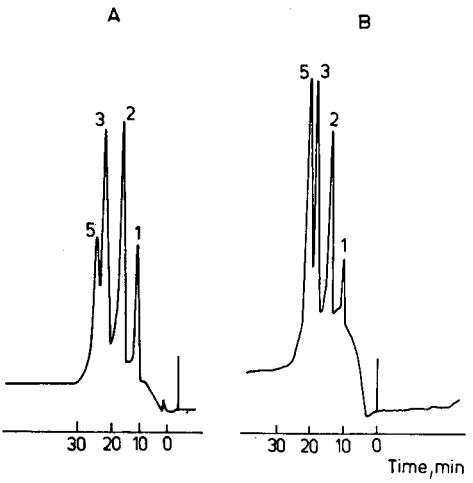

Fig. 3. Separation of a mixture of (1) myoglobin, (2) ovalbumin, (3) lysozyme and (4) chymotrypsinogen using a G-50-C8 membrane. Membrane 1 mm thick, 20 mm diameter, total loading (A) 5 mg or (B) 1.2 mg of proteins, elution rate 1 ml/min, mobile phase gradient from 2 mmol/l ammonium sulphate in 0.02 mol/l phosphate buffer solution (pH 6.8) to buffer solution only in 20 min.

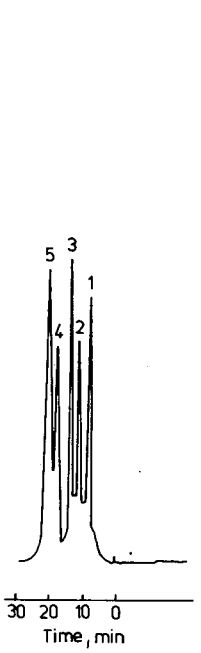

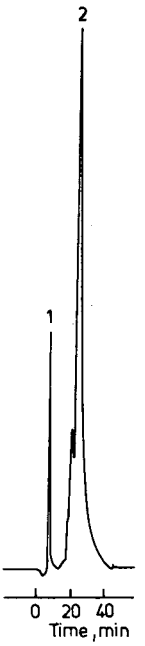

Fig. 4. Separation of a mixture of (1) myoglobin, (2) ovalbumin, (3) ribonuclease A, (4) lysozyme and (5) chymotrypsinogen using a G-50-C4 membrane. Gradient time 10 min, total loading 5 mg of proteins. Other conditions as in Fig. 3.

Fig. 5. Separation of (1) ribonuclease A and (2) lysozyme using a G-50-SP membrane. Membrane 1 mm thick, 20 mm diameter, elution rate 1 ml/min, mobile phase gradient from 0.02 phosphate buffer (pH 6.8) to 0.5 mol/l solution of sodium chloride in the buffer, loading 0.1 mg of each protein.

of the eluent, but the retention time in the membrane is shorter and the difference in concentration between the inlet and outlet does not change very much. The shape of the peaks remains almost unchanged.

The mechanism of separation does not change considerably when the thickness of the membrane is doubled or even tripled. The volume retained is still very low and represents 1–1.5% of the total eluent volume. Unless the thickness of the layer matches the length of a column, no typical chromatographic separation mechanism (repeated sorption–desorption steps) can take place and the separation proceeds by simple gradient elution.

Fig. 3 shows the separation of a model mixture of proteins on a G-50-C8 membrane with octyl groups. This can be compared with the separation of a similar mixture in a column 20 cm × 4.6 mm I.D. packed with specially treated C_{18}-silica [25]. Separations with membrane loadings of 1.5 and 5 mg are satisfactory and are fully comparable with column separation at a pressure 8 MPa. Recalculated dynamic loading gives 20 g/m^2 of proteins (20 mg/ml). The similar membrane G-50-C4 gives a fast separation of a mixture of five proteins (Fig. 4).

A chromatographic separation of proteins using a membrane modified with ionogenic sulphopropyl groups (Fig. 5) shows the feasibility of the ion-exchange mode of membrane chromatography.

CONCLUSIONS

The chromatographic data reported here demonstrate that a membrane may be used instead of a column for the separation of proteins. The separations are comparable with HPLC using standard chromatographic columns, but the membrane chromatography possesses the following advantages over traditional column methods:

(1) The membrane is synthesized directly at the final size from any combination of monomers in a mould; classical chromatographic supports prepared by suspension processes have to be size-classified.

(2) In the fabrication of beads, many are produced which are not of the desired size, which causes considerable waste. The membranes are prepared efficiently in almost the correct shape and are used after only minor mechanical treatment.

(3) The cell is simple and the membrane is easily positioned, whereas the packing of an efficient column requires substantial experience of packing procedures.

(4) The price of a quality column is relatively high, making long-term use necessary, whereas a membrane cartridge is cheaper may be economically disposed of much earlier.

(5) Flow-rates in membrane chromatography are obtained using pressures which are at least one order of magnitude lower than those used in analytical columns, thus making the use of highly efficient pump unnecessary.

(6) Scale-up in membrane chromatography is achieved by enlargement of the membrane area. This can be achieved either by enlarging the size of cartridge or by using several small cartridges connected in parallel. In preparative HPLC scale-up gives rise to specific problems of column packing and radial gradients and requires the use of heavy duty equipment.

These advantages show that membrane chromatography, although not necessarily exceeding the efficiency of HPLC, is still a competitive separation method. It has a wide range of uses in less challenging analytical separations and in preparative applications. Owing to the number of advantages and the simplicity of synthesis and use, this separation method may be appropriately called high-performance membrane chromatography.

ACKNOWLEDGEMENT

The authors are indebted to Dr. Z. Pelzbauer for this kind cooperation and SEM pictures of the membranes.

REFERENCES

1 G. B. Cox, *Ind. Chromatogr. News*, 1 (1989) 19.
2 *Ion-Exchange Membranes for Fast Separations, Application Sheet*, Bio-Rad Chemical Division, Richmond, CA.
3 M. S. Le and J. A. Sanderson, *GB Patent Appl.* 87/3 471 (1987); *C.A.* 111 (1989) 93 470b.
4 CUNO Corp., *US Pat.*, (1986) 4 663 163 and 4 639 513.
5 R. Fahnestock, *J. Bacteriol.*, 167 (1986) 870.
6 L. R. Snyder and M. A. Stadalius, in Cs. Horváth (Editor) *High-Performance Liquid Chromatography —Advances and Perspectives*, Vol. 4, Academic Press, New York, 1986, p. 293.
7 L. R. Snyder, M. A. Stadalius and M. A. Quarry, *Anal. Chem.*, 55 (1983) 1412A.
8 M. A. Quarry, R. L. Grob and L. R. Snyder, *Anal. Chem.*, 58 (1986) 907.

9 M. A. Quarry, M. A. Stadalius, T. H. Mourey and L. R. Snyder, *J. Chromatogr.*, 327 (1986) 1, 17.
10 J. M. DiBussolo and J. R. Gant, *J. Chromatogr.*, 327 (1985) 67.
11 C. H. Lochmuller, S. J. Breiner, C. E. Reese and M. N. Koel, *Anal.Chem.*, 61 (1989) 367.
12 F. Švec, J. Hradil, J. Čoupek and J. Kálal, *Angew. Makromol. Chem.*, 48 (1975) 135.
13 W. F. Blatt, in P. Mears (Editor), *Membrane Separation Processes*, Elsevier, Amsterdam, 1976, p. 127.
14 F. Švec, H. Hrudková, D. Horák and J. Kálal, *Angew. Makromol. Chem.*, 63 (1977) 23.
15 C. M. A. Ribeiro, J. Hradil, F. Švec and J. Kálal, *Angew. Makromol. Chem.*, 87 (1980) 119.
16 Z. Pelbauer, J. Lukáš, F. Švec and J. Kálal, *J. Chromatogr.*, 171 (1979) 101.
17 F. Švec, M. Bleha, T. B. Tennikova and B. G. Belenkii, *US Pat.*, 4 889 632 (1989); *US Pat.*, 4 923 610 (1990).
18 T. B. Tennikova, B. G. Belenkii and F. Švec, *J. Liq. Chromatogr.*, 135 (1990) 63.
19 F. E. Regnier, presented at the *14th International Symposium on Column Liquid Chromatography, Boston, MA, May 21–25, 1990*, Abstracts, Vol. 1, p. 15.
20 N. Afeyan, N. Gordon, I. Maszaroff, L. Varady, S. Fulton, Y.B. Yang and F. E. Regnier, *J. Chromatogr.*, 519 (1990) 1.
21 D. Horák, F. Švec, M. Ilavský, M. Bleha, J. Baldrian and J. Kálal, *Angew. Makromol. Chem.*, 95 (1981) 117.
22 J. Hradil, M. Jelínková, M. Ilavský and F. Švec, *Angew. Makromol. Chem.*, 185/186 (1991) 275.
23 T. B. Tennikova, D. Horák, F. Švec, M. B. Tennikov, E. F. Kever and B. G. Belenkii, *J. Chromatogr.*, 475 (1989) 187.
24 E. P. Kroeff, R. A. Owens, E. L. Campbell, R. D. Johnsom and H. I. Marks, *J. Chromatogr.*, 461 (1989) 45.
25 K. M. Gooding and M. N. Schmuck, *J. Chromatogr.*, 296 (1984) 321.

Journal of Chromatography, 555 (1991) 109–124
Elsevier Science Publishers B.V., Amsterdam

CHROM. 23 250

Anion-exchange chromatography of DNA restriction fragments

MARK A. STREGE and AVINASH L. LAGU*
Eli Lilly and Company, Lilly Research Laboratories, Indianapolis, IN 46285 (USA)
(First received June 25th, 1990; revised manuscript received February 28th, 1991)

ABSTRACT

The abilities of several high-performance liquid chromatography (HPLC) anion-exchange packings to separate DNA restriction fragments, ranging in size from 50 to 23 000 base pairs, were studied. The ion exchangers investigated include the porous packings Protein-Pak DEAE-5PW, Nucleogen-DEAE 4000-7, Poros-Q and BakerBond WP-PEI, and the non-porous packings TSK Gel DEAE-NPR, Gen-Pak FAX, and ProPac PA1. The results indicated that the non-porous packings could separate all 18 fragments (< 600 base pairs) in a pBR322 DNA-HaeIII digest, while of the porous packings, only Nucleogen-DEAE 4000-7 could resolve DNA fragments in this size range. Only Gen-Pak FAX and TSK Gel DEAE-NPR could significantly resolve the very large DNA fragments (125–23 000 base pairs) of a λ DNA-HindIII digest. The chromatographic parameters governing this separation by Gen-Pak FAX were optimized so that six of eight fragments were resolved. Split-peak phenomena were observed at low flow-rates when employing non-porous packings, but were eliminated by the incorporation of organic modifiers or surfactants, suggesting that, under certain conditions, hydrophobicity may play a significant role in separations on this packing. Gen-Pak FAX also separated 21 of 23 fragments in a 1000-base pair DNA ladder, a performance which, in addition to the quantitative capabilities of HPLC, makes anion-exchange chromatography a powerful method complementary to slab-gel electrophoresis, and perhaps preferable over agarose gel electrophoresis for applications such as the confirmation of plasmid integrity.

INTRODUCTION

Improvements in the manipulation and analysis of DNA have facilitated many of the achievements of the recent biotechnological revolution. Following the discovery of restriction endonucleases [1], techniques for the separation and characterization of large molecules have been developed. Since individual restriction enzymes cleave at specific DNA base sequences, separation and analysis of individual fragments provide important information regarding the structure of the DNA.

Restriction mapping, a method of separation and analysis of DNA fragments, is currently a major application of slab gel electrophoresis. Agarose gel electrophoresis in particular has been found to be applicable to the analysis of restriction enzyme digests containing DNA fragments within the size range of 500–15 000 base pairs (bp). At the present time, agarose gel electrophoresis is employed to confirm the integrity of plasmids utilized in the fermentation of recombinant DNA products.

While successful as a qualitative procedure, agarose gel electrophoresis is a long (>2 h), tedious, non-quantitative process prone to error, particularly in regard to the incomplete detection of small fragments and the resolution of fragments larger than 15 000 bp.

The analytical separation of DNA restriction fragments by anion-exchange chromatography is a technique offering several advantages compared to agarose gel electrophoresis. Potentially, ion-exchange high-performance liquid chromatography (HPLC) offers rapid separation and quantitation when combined with reliable area integration. In addition, DNA fragments can be recovered easily following separation for further analysis if so desired.

DNA fragments of different sizes have proven to be difficult to separate chromatographically, primarily due to the fact that large DNA molecules possess similar charge densities [2]. Early attempts at the separation of restriction fragments by ion-exchange chromatography exploited the binding of the negatively charged DNA to the weak anion-exchange functionality, diethylaminoethyl (DEAE). Covalent attachment of DEAE to chemically modified silica gels resulted in physically stable microparticles possessing properties ideal for many chromatographic applications. Using a commercially available silica-based anion-exchange support, Nucleogen-DEAE, Hecker *et al.* [3] were able to resolve DNA fragments between 25 and 1500 bp in size. Westmann *et al.* [4] reported resolution of fragments of up to 600 bp in size by employing a wide pore polymer-based resin, Mono-Q. Both of these separations required times of 1–8 hours. More recently, Stowers *et al.* [5] reported separations of a wide range of nucleic acids, including large DNA fragments up to 23 000 bp in size, requiring 40–60 min, through the use of a polymer-based DEAE anion-exchange packing, Gen-Pak FAX. Using the same packing, Merion *et al.* [6] were able to resolve the majority of the large restriction fragments in a λ DNA-HindIII digest in less than 15 min. Kato *et al.* [7] also recently demonstrated the high-resolution separation of large DNA restriction fragments in a very short time (<15 min) by utilizing a non-porous anion exchanger, TSK Gel DEAE-NPR. If these columns perform as claimed, they could efficiently replace agarose gel electrophoresis for certain applications. It, therefore, became necessary to compare commercially available anion-exchange packings in their potential to separate large DNA fragments. The influence of various parameters such as buffer, pH, eluting salt, gradient, temperature, flow-rate, organic modifiers and surfactants on the resolution of DNA fragments was also investigated.

EXPERIMENTAL

Chromatography was performed with a Gilson gradient HPLC system (Models 303 and 305 pumps, Model 811B dynamic mixer, Model 116 variable-wavelength UV detector, and a Model 231 sample injector equipped with a 20-μl sample loop). Analog data were collected directly from the absorbance detector (260 nm) on an in-house centralized chromatography computer system based on the Hewlett-Packard Model 1000 minicomputer. The packings employed in this investigation were the TSK Gel DEAE-NPR (Lot DENPM0012) (35 mm × 4.6 mm I.D.) (Toso-Haas) and the Gen-Pak FAX (Lot T90561) (10 cm × 4.6 mm I.D.) (Waters), both of which were packed with non-porous spherical hydrophilic resin particles of 2.5-μm diameter whose sur-

faces were chemically bonded with DEAE groups [5–7]; the Protein-Pak DEAE-5PW (7.5 cm × 7.5 mm I.D.) (Waters) packed with DEAE-bonded hydrophilic porous (1000 Å pore size) polymer particles 10 μm in size; the ProPac PA1 (25 cm × 4 mm I.D.) (Dionex) packed with 10-μm non-porous polystyrene–divinylbenzene resin particles derivatized with a quaternary amine; the BakerBond WP-PEI Scout (50 mm × 4.6 mm I.D.) (J. T. Baker) packed with porous (300 Å pore size) 5-μm silica particles coated with polyethyleneimine; Poros-Q (50 mm × 4.6 mm I.D.) (Perseptive Biosystems), a polymeric porous (500–1000 Å diffusive pores, 6000–8000 Å connective pores) packing consisting of crosslinked polystyrene–divinylbenzene derivatized with fully quaternized crosslinked polyethylenimine and an 8–10 μm particle size; Nucleogen-DEAE 4000-7 (125 mm × 6 mm I.D.), a silica gel-based diethylamine anion exchanger with a hydrophilic surface, a 7-μm particle size, and a 4000 Å pore size. Tetra-*n*-butylammonium hydroxide was purchased from BDH (Poole, UK) and Brij-35 was obtained from Fisher Scientific. Analytical-grade acetonitrile and 2-propanol (HPLC grade) were purchased from Burdick & Jackson Laboratories (Muskegon, MI, USA). Analytical-reagent-grade sodium phosphate and sodium hydroxide were purchased from EM Science (Gibbstown, NJ, USA). Acidic and neutral pH phosphate buffers were prepared using monobasic sodium phosphate, while dibasic sodium phosphate was employed for the preparation of pH 8 and 9 buffers. Phosphate buffers were adjusted to the specified pH by adding 6 *M* sodium hydroxide or dilute phosphoric acid as needed. All eluents were filtered through a 0.22-μm (Millipore) membrane filter. Unless otherwise specified, DNA fragments were separated by various gradient elutions of sodium chloride in 25 m*M* phosphate pH 7.0 at ambient temperature (25°C). Phosphate is a buffer salt recommended in the literature for the ion-exchange separation of DNA restriction fragments, using both porous [3,8–10] and non-porous packings [5–7]. The initial conditions employed for each separation were those suggested in the literature, when applicable [5–8], or by the manufacturers of the packings. The gradients and flow-rates were altered from the initial conditions if better separations could be achieved.

A pBR322 DNA-HaeIII digest (Sigma, St. Louis, MO, USA), a λ DNA-EcoRI digest and a λ DNA-HindIII digest (Promega, Madison, WI, USA), and a 1000-bp DNA ladder (BRL, Gaithersburg, MD, USA) were obtained from their manufacturers as protein-free sources of DNA restriction fragments. The pBR322 DNA-HaeIII digest contains 22 fragments of 7, 11, 18, 21, 51, 57, 64, 80, 89, 104, 123, 124, 184, 192, 213, 234, 267, 434, 458, 504, 540 and 587 base pairs. The λ DNA-EcoRI digest contains six fragments of 3410, 4800, 5540, 5930, 7520 and 21 800 base pairs. The λ DNA-HindIII digest contains eight fragments of 125, 564, 2028, 2322, 4371, 6557, 9419 and 23 130 base pairs. The 1000-bp DNA ladder contains 23 fragments of 75, 134, 154, 201, 220, 298, 344, 396, 506, 517, 1018, 1636, 2036, 3054, 4072, 5090, 6108, 7126, 8144, 9162, 10 180, 11 198 and 12 216 bp. The DNA standards were diluted with 25 m*M* sodium phosphate pH 7 (prior to injection) to concentrations between 0.025 and 0.10 μg/μl, so that between 0.5 and 2.0 μg of DNA were injected for each separation. These amounts are considered to be well below the loading capacities of all packings investigated.

DNA present in the HPLC fractions was ethanol-precipitated using the standard procedure for the recovery of nucleic acids larger than 100 nucleotides [11]. The DNA was then redissolved in TBE buffer (89 m*M* Tris–borate pH 8.3, 2.5 m*M*

Na_2EDTA), and electrophoresed on 1% agarose gels. The loading buffer contained 50 m*M* EDTA, 70% (v/v) glycerol and 0.05% bromophenol blue. Electrophoresis was performed at 68–70 mA for 2–3 h. The gels were stained with ethidium bromide in TBE buffer and photographed with a Polaroid type 57 film using a Polaroid 545 camera. The UV light source was a Transilluminator Chromato-Vue Cabinet Model CC-60 (Ultraviolet Products).

RESULTS AND DISCUSSION

Investigations of ion-exchange packings

Chromatograms of 0.5 μg of a pBR322 DNA-HaeIII digest, which consists of DNA fragments up to 587 bp in size, were obtained using various column packings. Of the porous packings, Protein-Pak 5PW, Poros-Q and BakerBond WP-PEI were unable to resolve any of the fragments using a 40-min 0.0–1.0 *M* NaCl gradient at 0.5

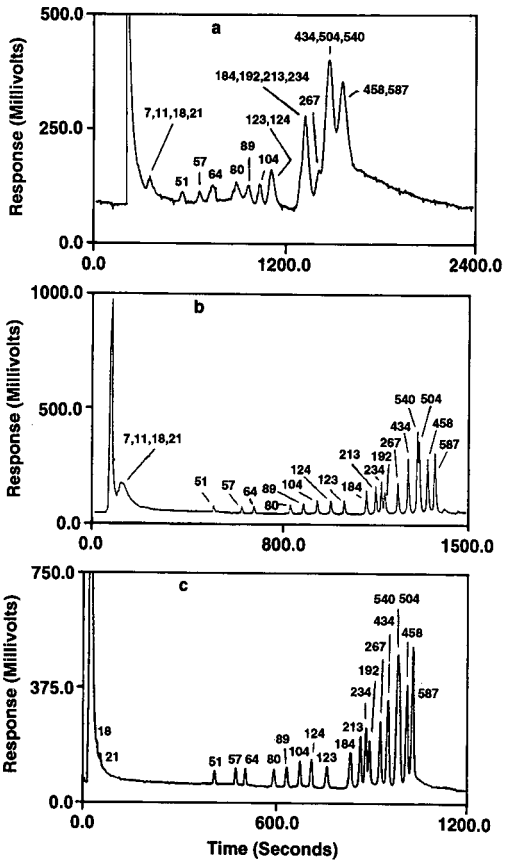

Fig. 1. Separations of 0.5 μg pBR322 DNA-HaeIII digest obtained using 25 m*M* sodium phosphate pH 7.0 buffer as mobile phase at 25°C, and the following packings, flow-rates and gradients: (a) Nucleogen DEAE 4000-7, 1.0 ml/min, 60 min 0.35–0.6 *M* NaCl (mobile phase also contained 6 *M* urea); (b) Gen-Pak FAX, 0.5 ml/min, 40 min 0.45–0.70 *M* NaCl; (c) TSK Gel DEAE-NPR, 1.5 ml/min, 60 min 0.45–1.0 *M* NaCl.

ml/min, and attempts using Poros-Q in conjunction with a 10-min 0.0–1.0 *M* NaCl gradient at 4.0 ml/min were also unsuccessful. These results may reflect the effects of pore size, as size exclusion and slow mass diffusion may contribute to the observed lack of separation in packings possessing pores 1000 Å or smaller. However, significant resolution of the digest was achieved by Nucleogen-DEAE (7 μm particle size, 4000 Å pore size) and a 60-min 0.35–0.6 *M* NaCl gradient in a mobile phase containing 6 *M* urea (Fig. 1a). The fragment sizes are indicated in base pairs [8,10]. The non-porous packings, Gen-Pak FAX (40 min 0.45–0.70 *M* NaCl, 0.5 ml/min), TSK Gel DEAE-NPR (60 min 0.45–1.0 *M* NaCl, 1.0 ml/min), and ProPac PA1 (40 min 0.57–0.68 *M* NaCl, 1.2 ml/min) were also able to resolve the digest. The separations obtained with these three packings were nearly identical (Figs. 1b and c and 2). The shoulders on the leading side of many of the peaks present in the ProPac PA1 separation (Fig. 2a) may be due to hydrophobic interactions with the packing. These distortions disappeared in the presence of 10% 2-propanol in the mobile phase, used in conjunction with a 40-min 0.45–0.60 *M* NaCl gradient (the gradient was adjusted to obtain the same ionic strength following the incorporation of the organic modifier), as displayed in Fig. 2b. The peaks in Figs. 1 and 2 were labeled as indicated by considering that DNA restriction fragments are mainly eluted in order of increasing size, although base composition also appears to have an effect upon elution and the peak areas are approximately proportional to the chain lengths [12]. These assignments agree with the reported separation of the pBR322 DNA-HaeIII digest on a

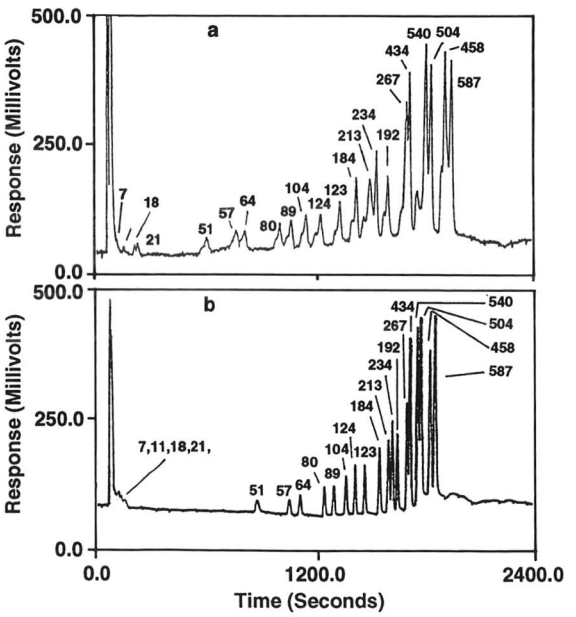

Fig. 2. Separations of 0.5 μg pBR322 DNA-HaeIII digest by ProPac PA1 at 25°C using (a) 25 m*M* sodium phosphate pH 7.0 buffer as mobile phase and a 40-min 0.57–0.68 *M* NaCl gradient, 1.2 ml/min; (b) 25 m*M* sodium phosphate pH 7.0, 10% 2-propanol as mobile phase and a 40-min 0.45–0.60 *M* NaCl gradient, 1.2 ml/min.

porous ion exchanger, where peaks were assigned by polyacrylamide gel electrophoresis [4].

The large fragments in the λ DNA-EcoR1 digest were partially resolved by the ProPac PA1 packing using a 40-min 0.6–1.0 *M* NaCl gradient and a 0.5 ml/min flow-rate (Fig. 3a). The digest was separated into three peaks, the first of which was revealed via agarose gel electrophoresis to be comprised of several of the smaller fragment components (Fig. 3c). Interestingly, the two later-eluting peaks were both found to contain only the 21 800 bp fragment. "Split-peak" phenomena such as this have been found to occur in the chromatography of macromolecules, where adsorption kinetics and mass transfer tend to be slow [13]. For a reversed-phase, ion-pair separation, Low and Haddad [14] have suggested that peak splitting is the result of a composite interplay of two retention mechanisms which are mutually competitive under certain conditions. The split peaks encountered in this study were observed to disappear (Fig. 3b) when 10% 2-propanol was incorporated into the mobile phase (40 min 0.5–0.9 *M* NaCl gradient), or when the flow-rate through the ProPac PA1 packing was increased to 1.2 ml/min.

The separation of 1.0 μg λ DNA-EcoR1 digest obtained using the Gen-Pak

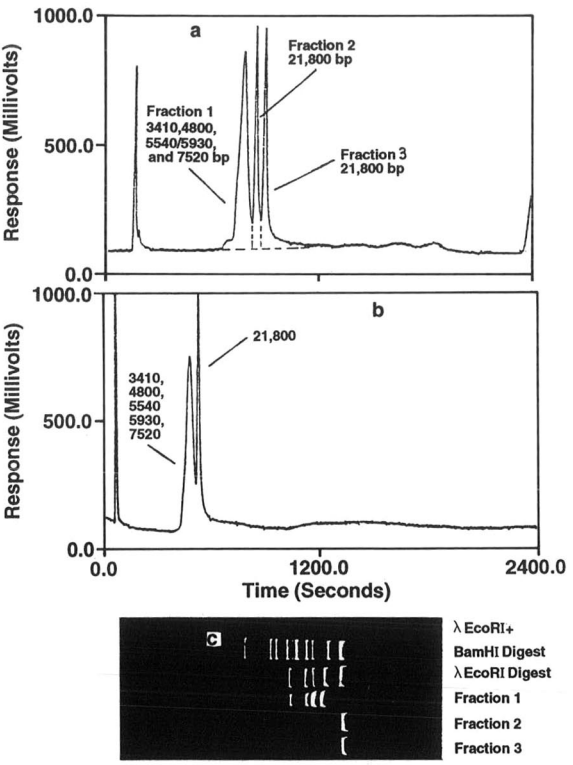

Fig. 3. Separations of 1.0 μg λ DNA-EcoR1 digest obtained using ProPac PA1, a flow-rate of 0.5 ml/min at 25°C and (a) 25 m*M* sodium phosphate pH 7.0, and a 40-min 0.6–1.0 *M* NaCl gradient; (b) 25 m*M* sodium phosphate, 10% 2-propanol, and a 40-min 0.5–0.9 *M* NaCl gradient; (c) agarose gel electrophoresis analysis of the fractions collected during elution of the λ DNA-EcoRI digest represented in (a).

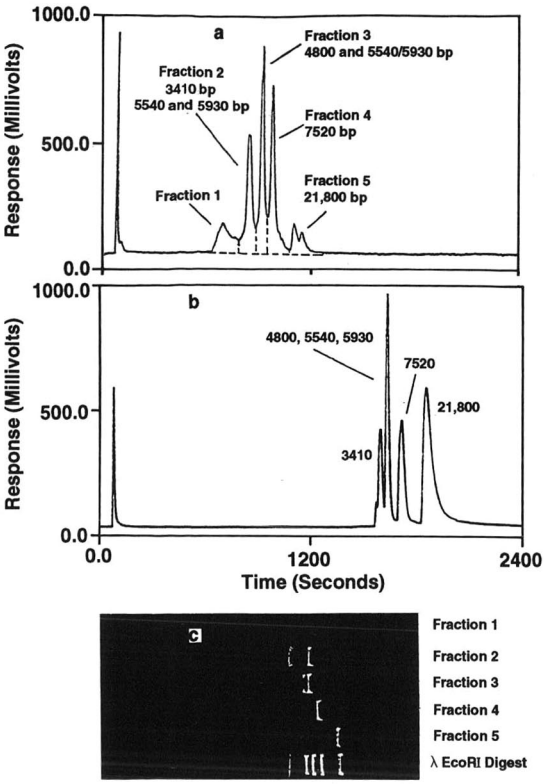

Fig. 4. Separations of 1.0 μg λ DNA-EcoR1 digest obtained using Gen-Pak FAX, a flow-rate of 0.5 ml/min at 25°C and (a) 25 m*M* sodium phosphate pH 7.0, and a 40-min 0.55–0.70 *M* NaCl gradient; (b) 25 m*M* sodium phosphate pH 7.0, 10% 2-propanol, and a 40-min 0.45–0.60 *M* NaCl gradient; (c) agarose gel electrophoresis analysis of the fractions collected during elution of the λ DNA-EcoR1 digest represented in (a).

FAX packing (Lot T90561) is displayed in Fig. 4a. The peaks in this chromatogram were identified through agarose gel electrophoresis of the collected fractions (the mass of the 125-bp fragment was too low to permit detection, Fig. 4c). Fraction 1 of the λ DNA-EcoR1 digest was not found to contain any DNA. Fraction 2 contained the 3410-bp fragment and the 5540/5930-bp fragments (unresolved on the agarose gel). Fraction 3 contained the 4800 and 5540/5930-bp fragments, while the peaks in fractions 4 and 5 were determined to be the 7520 and 21 800-bp fragments, respectively. Together with the fact that the 5540/5930-bp fragments appear in multiple chromatographic peaks, the elution profile of the largest fragment (doublet) is further evidence of the peak-splitting phenomenon. Separation of 1.0 μg λ DNA-HindIII digest is depicted in Fig. 5a. Fraction 1 of the λ DNA-HindIII digest was identified as the 564-bp fragment (Fig. 5c). Fraction 2 did not contain any DNA. The peak corresponding to fraction 3 was determined to be comprised of the 2028, 2322 and 4371-bp fragments. Fractions 4 and 5 were primarily the 6557 and 9419-bp fragments, respectively. The 9419-bp fragment was also the primary component of fraction 6, while

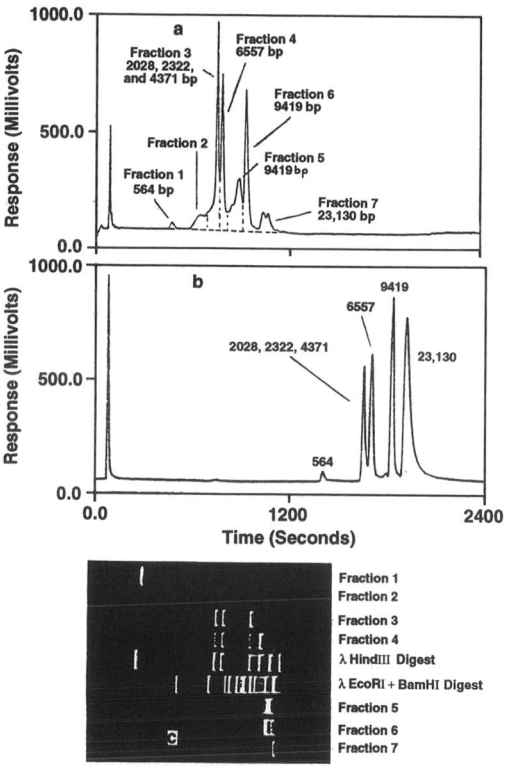

Fig. 5. Separations of 1.0 μg λ DNA-HindIII digest obtained using Gen-Pak FAX, a flow-rate of 0.5 ml/min at 25°C and (a) 25 m*M* sodium phosphate pH 7.0, and a 40-min 0.55–0.70 *M* NaCl gradient; (b) 25 m*M* sodium phosphate pH 7.0, 10% 2-propanol and a 40-min 0.45–0.60 *M* NaCl gradient; (c) agarose gel electrophoresis analysis of the fractions collected during elution of the λ DNA-EcoR1 digest represented in (a).

fraction 7 contained only the 23 130-bp fragment. The two largest fragments exhibited peak splitting. The peak-splitting phenomenon was reproducible on a second Gen-Pak FAX column (Lot T90531), where the occurrence of peak splitting of both λ DNA digests by Gen-Pak FAX could be eliminated by the presence of 10% 2-propanol (see Figs. 4b and 5b). It is also interesting to note that the recovery of the fragments > 20 000 bp is markedly enhanced in the presence of 10% 2-propanol. This may occur because hydrophobic interactions can prevent complete desorption of these molecules at low flow-rates in the absence of organic modifiers. Although denaturation of the double-stranded DNA may also enhance the UV absorption of the sample [15], spectrophotometric scans of 20 μg λ DNA-HindIII digest in water and in 10% 2-propanol revealed no significant difference. These results suggest that the enhanced UV response of the >20 000-bp fragments may not be due to melting of the DNA strands.

TSK Gel DEAE-NPR was also able to significantly resolve the DNA fragments in the λ DNA digests. Using a 40-min 0.55–0.70 *M* NaCl gradient at 0.5 ml/min, this packing was able to separate the λ DNA-HindIII digest into five peaks (Fig. 6a). To

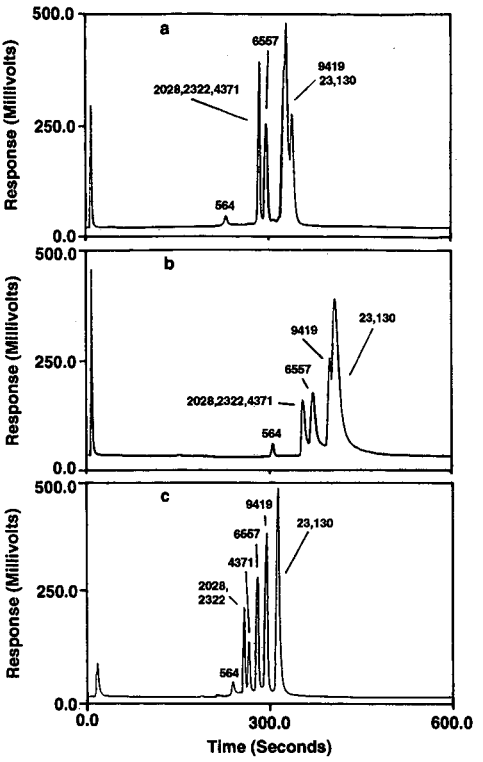

Fig. 6. Separations of 1.0 μg λ DNA-HindIII digest obtained using TSK Gel DEAE-NPR at 25°C and (a) 25 m*M* sodium phosphate pH 7.0, a flow-rate of 0.5 ml/min and a 40-min 0.55–0.70 *M* NaCl gradient; (b) 25 m*M* sodium phosphate pH 7.0, 10% 2-propanol, a flow-rate of 0.5 ml/min, and a 40-min 0.45–0.60 *M* NaCl gradient; (c) 25 m*M* sodium phosphate pH 7.0, a flow-rate of 1.0 ml/min and a 10-min 0.5–1.0 *M* NaCl gradient.

determine if hydrophobic interactions were responsible for any part of this elution profile, the digest was separated under identical conditions in a mobile phase containing 10% 2-propanol (Fig. 6b). The shoulder on the back side of the largest peak in Fig. 6a disappeared in the presence of the organic modifier. This shoulder may be representative of a peak splitting of the 23 130-bp fragment, a component of the digest which was found to possess a tendency for hydrophobic interaction on both Gen-Pak FAX (a packing very similar to TSK Gel DEAE-NPR) and ProPac PA1. The shoulder on the early-eluting side of the largest peak of Fig. 6b is probably the 9416-bp fragment, since hydrophobic interactions and peak splitting were eliminated in this separation. Using a steep gradient (10 min 0.5–1.0 *M* NaCl) and a faster flow-rate (1.0 ml/min) recommended by Kato *et al.* [7] six of the eight fragments in this digest were separated in only 6 min (Fig. 6c).

Size-exclusion effects and slow mass diffusion appear to cause reduced resolution when porous packings are employed to separate the λ DNA digests. Nucleogen-DEAE 4000-7 displayed very limited separation of the λ DNA digests, while the Protein-Pak DEAE 5PW, BakerBond WP-PEI Scout and Poros-Q packings provided no resolution at all.

From this series of investigations, it can be concluded that non-porous anion-exchange packings can provide greater resolution of a wide size range of DNA restriction fragments than the porous packings that were investigated in this study. In regard to the non-porous packings, Gen-Pak FAX and TSK Gel DEAE-NPR provided greater resolution of the large fragments present in λ DNA digests than ProPac PA1.

Optimization of chromatographic parameters

In order to optimize the separation of DNA restriction digests by non-porous anion-exchange packings, the effects of various chromatographic parameters upon the resolution of the λ DNA-HindIII digest were investigated. The TSK Gel DEAE-NPR packing (Lot DENPM0012) employed in this investigation was obtained through personal communication with Toso-Haas [16], and was anticipated to be commercially available in October 1990 [a TSK Gel DEAE-NPR column (Lot DENPRK0075) purchased January 1990 had provided comparatively poorer separations of the λ DNA digests]. Therefore, the following optimization studies were performed using the Gen-Pak FAX packing.

Although the protein standards utilized in this study were claimed by their manufacturers to be protein-free, it was felt necessary to determine if the presence of protein could interfere with the elution profiles of the DNA digests. Therefore, a digest buffer "blank" containing only restriction enzymes was chromatographed on Gen-Pak FAX (0.5 ml/min at 25°C, 40 min 0.55–0.70 *M* NaCl gradient, 25 m*M* sodium phosphate pH 7). No peaks eluted later than 100 s, indicating that protein does not interfere with the chromatography of DNA fragments on this packing.

Gradient

The shallow gradient slopes employed throughout the investigation of the ion-exchange packings (0.3–10 m*M* NaCl/min) (see Figs. 1–4) were employed, as suggested in the literature [3,4,9,10], to facilitate optimum baseline separation. However, sharper gradient slopes (30–50 m*M* NaCl/min) have recently been recommended for the separation of large restriction fragments on non-porous packings [6,7]. The λ DNA-HindIII digest was chromatographed using a 10-min, 0.40–0.75 *M* NaCl gradient at 0.5 ml/min, and is displayed in Fig. 7b. Consecutive injections of the λ DNA digest and a buffer blank revealed the absence of sample carry-over under these chromatographic conditions. Comparison of this separation to that obtained earlier through the use of a 40-min 0.55–0.70 *M* NaCl gradient (see Fig. 5a) reveals a change in the elution profile when the steeper gradient is employed. In addition to the partial resolution between the 2322/2028-bp fragments and the 4361-bp fragment, the 6557-bp fragment was baseline resolved. The two peaks observed to comprise the 9419-bp fragment have coalesced into one peak, although the 23 130-bp fragment still displays the split-peak phenomenon.

Flow-rate

To investigate the effects of flow-rate upon the resolution of DNA restriction digests by Gen-Pak FAX, the λ DNA-HindIII digest was chromatographed, using a 10-min 0.40-0.75 *M* NaCl gradient, at flow-rates of 0.25, 0.5, 0.8 and 1.1 ml/min (Fig. 7). To maximize resolution and improve mass-transfer kinetics, ion-exchange col-

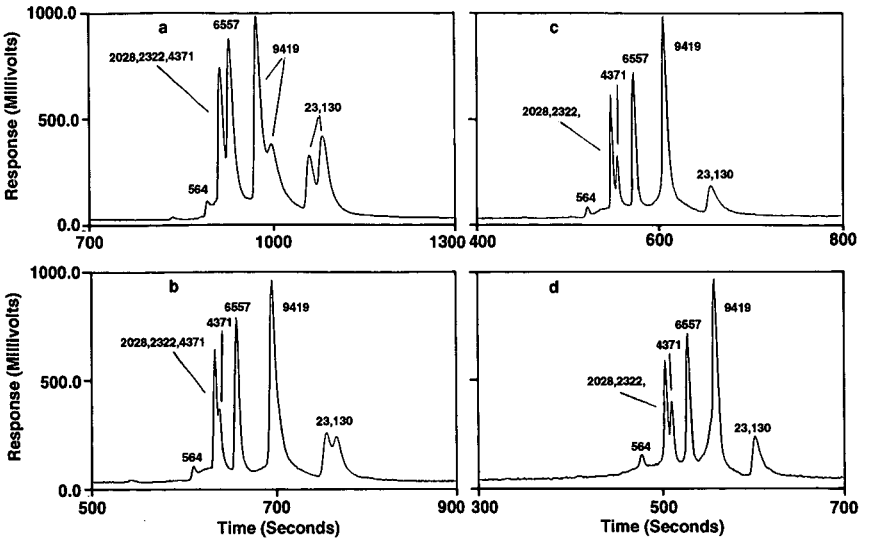

Fig. 7. Gen-Pak FAX separations of 1.0 μg λ DNA-HindIII digest obtained using 25 mM phosphate pH 7.0 buffer as mobile phase, a 10-min 0.40–0.75 M NaCl gradient at 25°C and the following flow-rates: (a) 0.25; (b) 0.50; (c) 0.80; (d) 1.10 ml/min.

umns have often been operated at flow-rates slightly lower than in other HPLC methods [17]. Resolution between DNA fragments less than 600 bp in size has been found to either decrease with an increase in flow-rate [3,4], or to be insignificantly affected by flow-rate [9]. However, the elution profiles presented in Fig. 7 reveal that resolution of the digest components by Gen-Pak FAX improved as the flow-rate was increased from 0.25 ml/min to 0.8 ml/min, especially in regard to the enhancement of the resolution of the 4371 and 6557-bp fragments. Peak splitting of the 9419 and 23 130-bp fragments is highly evident at 0.25 ml/min, but diminishes as the flow-rate is increased to 0.8 ml/min, where the phenomenon is absent. However, the recovery of the 23 130-bp fragment remains considerably less than expected. The separation presented in Fig. 7c was complete in 12 min, twice the time required by TSK Gel DEAE-NPR for a similar separation (Fig. 6c). The separation achieved at a flow-rate of 1.1 ml/min was equivalent to that obtained at 0.8 ml/min, and since the back-pressures at flow-rates greater than 1.0 ml/min were very high, *ca.* >2500 p.s.i., 0.8 ml/min appeared to be the optimum flow-rate for the separation of large restriction fragments.

pH

Ion-exchange selectivity can often be adjusted by varying the pH of the mobile phase. Changing the pH may modify both the character of the ion-exchange media and the acid–base equilibria and ionization of the sample. In regard to anion-exchange chromatography using weak anion exchangers such as DEAE, retention generally decreases with an increase in pH, and small changes in pH can have a large influence on separation selectivity. On porous diethylamino- and diethylamine-bound silica packings, Colpan and Riesner [9] found the resolution of large nucleic acids to be optimum at pH 6.5–7.0, while pH 5.5 yielded the best resolution of oligonucleo-

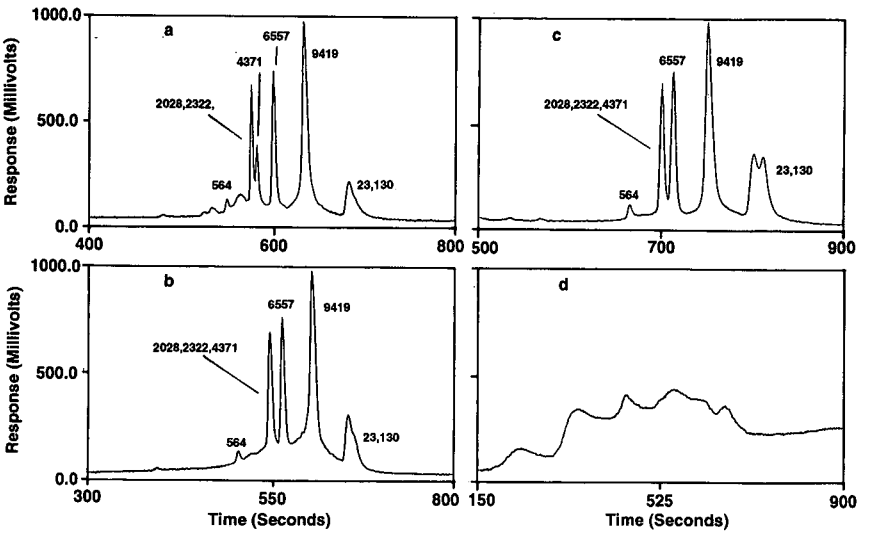

Fig. 8. Gen-Pak FAX separation of 1.0 μg λ DNA-HindIII digest obtained using 25 mM phosphate pH 7.0 buffer as mobile phase, a 10-min 0.40–0.75 M NaCl gradient and a 0.8-ml/min flow-rate at the following temperatures: (a) 25; (b) 45; (c) 60; (d) 5°C.

tides. Other studies found DNA fragment resolution to be independent of pH in the neutral pH range when employing either strong or weak amino groups as ion exchangers [3,4]. Gen-Pak FAX, a DEAE-derivatized non-porous packing, is stable within a pH range of 1.5 to 12 [18]. However, to protect DNA from depurination, the pH should be higher than pH 4 [3]. The λ DNA-HindIII digest was chromatographed on Gen-Pak FAX over a pH range from 5 to 9. Fragment separation remained insensitive to pH in the range between pH 5 and pH 8, but a decline in resolution occurred at pH 9, where a decrease in retention was also evident. Therefore, it appeared that the entire range between pH 5 and pH 8 may be employed to facilitate separation of large DNA fragments on this packing.

Temperature

To improve solute diffusion and mass transfer, ion-exchange columns are often operated at elevated temperatures. In addition to increasing column efficiency, an increase in column temperature usually results in low binding capacity factor values [17]. Muller [10] found that an increase in temperature from ambient to 60°C greatly improved the resolution of DNA fragments less than 600 bp in size on the porous strong ion exchanger Mono-Q. However, Colpan and Riesner [9] determined that elevated temperatures did not affect fragment resolution by the porous ion exchanger Nucleogen, but did shift elution to higher ionic strengths. The λ DNA-HindIII digest was separated under optimum conditions at elevated temperatures (Fig. 8b and c). In comparison to the separation obtained at ambient temperature (25°C) (Fig. 8a), the resolution of the digest decreased very subtly at both 45°C and 60°C, as the 4371-bp peak had merged with the 2322/2027-bp peak. At 60°C, the 23 130-bp fragment displayed peak splitting. In addition, the UV response of the 23 130-bp peak relative to

the 9419-bp peak was observed to increase at elevated temperatures. This effect may be due to partial denaturation of the larger fragment, since the intramolecular hydrogen bonding of the DNA strands is weaker at elevated temperatures [19]. It is known that the UV response of partially unwound double-stranded DNA is higher than that for a fully wound double-stranded DNA molecule [15]. Retention can also be affected by changes in temperature. At high temperatures, because the structure of DNA is more open or relaxed, a greater number of the ionic groups on the phosphate backbone might interact with the packing [18]. This effect, in addition to higher ion-exchange strength caused by increased desolvation of charged sites, results in greater retention. Chromatography of the digest at 5°C (the column and mobile phase reservoirs were cooled in an ice bath) reveals an extreme decrease in both retention and resolution (Fig. 8d). It appears that ambient temperature is an optimum parameter for separation of large restriction fragments on Gen-Pak FAX.

Eluting salt

In ion-exchange chromatography, solvent strengths and selectivity are influenced by the nature of the eluting salt counterion present in the mobile phase. Buffer salts, such as sodium phosphate or Tris–HCl, have been found to possess no influence on resolution of DNA restriction fragments [8]. Many reports of the separation of restriction fragments by ion-exchange chromatography on a variety of packings list chloride as the eluting counterion of choice [3–7,10,12,18,20,21]. Sodium chloride and potassium chloride have been found to promote equivalent resolution of small restriction fragments, although differences in eluting salt concentration were noted [3,10]. To investigate the effects of employing eluting salts other than sodium chloride upon the Gen-Pak FAX separation of large restriction fragments, attempts were made to elute the λ DNA-HindIII digest by ammonium sulfate or sodium acetate. 40-min gradients of 0.0–0.5 *M*, 0.0–1.0 *M* and 0.0–2.0 *M* ammonium sulphate failed to elute the DNA fragments, while a 40-min 0.0–0.6 *M* sodium acetate gradient failed to provide separation.

Surfactant additives

Many ion-exchange packings possess hydrophobic regions which may interact with similar regions on sample molecules, resulting in retention times longer than would be predicted if only a purely electrostatic mechanism were involved. The presence of a non-ionic surfactant can serve to reduce hydrophobic interactions, as surfactant may preferentially adsorb to the packing, thereby facilitating the release of sample molecules as the eluting salt concentration is increased. To determine if hydrophobic regions on Gen-Pak FAX affect the separation of DNA restriction digests, two surfactants, tetra-*n*-butylammonium hydroxide and Brij-35, were incorporated into the mobile phase as 0.5% solutions. The chromatograms of the λ DNA-HindIII digest revealed that the presence of surfactants eliminated the hydrophobic interactions causing peak splitting, but provided no additional separation benefits.

Organic modifiers

Ion-exchange solvent strength generally increases with the volume percent of organic modifier, its effect most evident when hydrophobic mechanisms contribute significantly to retention. The presence of an organic modifier can also alter both the

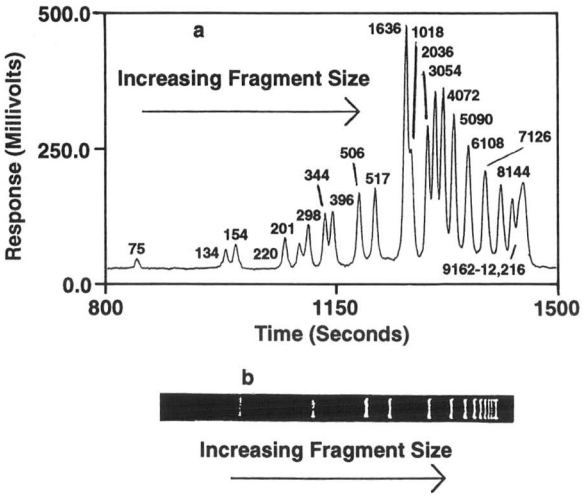

Fig. 9. (a) Gen-Pak FAX separation of 2.0 μg 1000-bp DNA ladder obtained using a flow-rate of 0.8 ml/min at 25°C and a 25 m*M* phosphate pH 7.0 buffer with a 30-min 0.40–0.75 *M* NaCl gradient. (b) agarose gel electrophoresis separation of the 1000-bp DNA ladder.

mobile phase viscosity and the solute mass-transfer kinetics. Therefore, organic modifiers were utilized to determine if they might serve to enhance DNA digest resolution. Mobile phases containing 20% acetonitrile or 10% 2-propanol were employed to obtain elution profiles of the λ DNA-HindIII digest. Similar to surfactants, organic modifiers can serve to reduce hydrophobic interactions, promoting a simple ion-exchange retention mechanism. As was observed earlier, peak splitting is eliminated in the presence of organic modifiers, and as for surfactants, no additional effects were observed.

Employing the conditions optimized for the separation of the large fragments present in the λ DNA-HindIII digest (0.8 ml/min at 25°C, 10-min 0.04–0.75 *M* NaCl gradient, 25 m*M* phosphate pH 7 buffer), 2 μg of the 1000-bp DNA ladder were chromatographed. At least 18 of the 23 fragments present in the sample were resolved. 21 fragments were resolved when the gradient time was increased from 10 to 30 min (Fig. 9a), the improvement in the separation particularly evident in regard to the smaller fragments. This performance is superior to the qualitative separation which is achieved via agarose gel electrophoresis (Fig. 9b), where only the 13 largest of the 23 fragments are visible as fluorescing bands.

CONCLUSIONS

The four porous packings, Protein-Pak DEAE-5PW, BakerBond WP-PEI, Nucleogen DEAE 4000-7, and Poros-Q, appear to possess limited applicability in regard to the separation of a wide size range of DNA restriction fragments. This characteristic may reflect the effects of pore size, as size exclusion and slow mass diffusion may contribute to minimal DNA fragment separation by porous packings, especially those possessing pores 1000 Å or smaller. Only Nucleogen DEAE 4000-7, possessing

the largest pore size (4000 Å) of these packings, could significantly separate the small fragments (< 500 bp) in a pBR322 DNA digest, but its separation of the larger fragments in a λ DNA-HindIII digest was minimal. Non-porous packings provided the best separation of the wide size range of restriction fragments present in the pBR322 DNA and λ DNA digests. Gen-Pak FAX and TSK Gel DEAE-NPR could completely resolve a pBR322 DNA-HaeIII digest. ProPac PA1 could comparably separate the pBR322 DNA-HaeIII digest, but its resolution of the large fragments in a λ DNA digest did not compare as favorably. Depending upon the size differences among the fragments to be fractionated, other investigations [6] have found that as much as 50 to 100 μg of DNA could be applied to Gen-Pak FAX, with a total recovery of 98.5%, and separations seemed to require at least 12 min. In our study, however, it appeared that the incorporation of an organic modifier may be necessary to achieve such high recoveries of fragments larger than 20 000 bp from this packing. Comparable separations were attained using TSK Gel DEAE-NPR in about one half of the time required by Gen-Pak FAX. Other studies have achieved recoveries greater than 85% by TSK Gel DEAE-NPR, but resolution by this packing was found to decrease significantly when sample loads greater than 10 μg were applied [7]. It appears that while TSK Gel DEAE-NPR can offer faster analyses, Gen-Pak FAX may be the column of choice for preparative work.

The chromatographic parameters governing the separation of large DNA restriction fragments by the non-porous packing Gen-Pak FAX were optimized to the following conditions: 0.8 ml/min at 25°C, 10-min 0.40–0.75 *M* NaCl gradient, 25 m*M* phosphate pH 7 buffer. Hydrophobic interactions seemed to promote peak-splitting phenomena at low flow-rates, since these effects could be eliminated by the incorporation of organic modifiers or surfactants into the mobile phase. Under the optimized conditions, Gen-Pak FAX could resolve six of the eight fragments in a λ DNA-HindIII digest. When using a 30-min gradient, 21 of the 23 fragments in a 1000-bp DNA ladder were separated and detected. In regard to run time and fragment detection, this performance exceeded that obtainable via agarose gel electrophoresis. When combined with the additional benefit of reliable quantitation that is offered by HPLC, these advantages suggest that anion-exchange HPLC using non-porous packings is a powerful complement to slab gel electrophoresis, and may be a superior alternative for applications such as the analysis of plasmid DNA integrity.

ACKNOWLEDGEMENTS

We thank Mr. P. R. Rostek, Jr. for helpful discussions, and Mr. Dan Alexander for his assistance with agarose gel electrophoresis.

REFERENCES

1 D. Nathans, *Science*, 206 (1979) 903.
2 P. Serwer and J. L. Allen, *Biochemistry*, 23 (1984) 922.
3 R. Hecker, M. Colpan and D. Riesner, *J. Chromatogr.*, 326 (1985) 251.
4 E. Westman, S. Eridsson, T. Laas, P. A. Pernemalm and S. E. Skold, *Anal. Biochem.*, 166 (1987) 158.
5 D. J. Stowers, J. M. B. Keim, P. S. Paul, Y. S. Lyoo, M. Merion and R. M. Benbow, *J. Chromatogr.*, 444 (1988) 47.
6 M. Merion, W. Warren, C. Stacey and M. E. Dwyer, *BioTechniques*, 6 (1988) 246.

7 Y. Kato, Y. Yamasake, A. Onaka, T. Kitamura, T. Hashimoto, T. Murotso, S. Fukushige and K. Matsubara, *J. Chromatogr.*, 478 (1989) 264.
8 R. Hecker and D. Riesner, *J. Chromatogr.*, 418 (1987) 97.
9 M. Colpan and D. Riesner, *J. Chromatogr.*, 296 (1984) 339.
10 W. Muller, *Eur. J. Biochem.*, 155 (1986) 203.
11 T. Maniatis, E. Fritch and J. Sambrook (Editors), *Molecular Cloning: A Laboratory Manual*, Cold Spring Harbor Laboratory, Cold Spring Harbor, NY, 1989.
12 Y. Kato, M. Sasaki, T. Hashimoto, T. Murotsu, S. Fukushige and K. Matsubara, *J. Chromatogr.*, 265 (1983) 342.
13 J. Wade and P. Carr, *J. Chromatogr.*, 449 (1988) 53.
14 G. Low and P. Haddad, *J. Chromatogr.*, 336 (1984) 15.
15 R. McGilvery and G. Goldstein, *Biochemistry: A Functional Approach*, W. B. Saunders, Philadelphia, PA, 1979.
16 R. Eksteen, personal communication, March 1990.
17 C. F. Poole and S. A. Schuette, *Contemporary Practice of Chromatography*, Elsevier, Amsterdam, 1984.
18 *Gen-Pak FAX Care and Use Manual*, Waters, Milford, MA, Revision 1, Draft 4, 1990.
19 D. Rickwood and B. Hames (Editors), *Gel Electrophoresis of Nucleic Acids: A Practical Approach*, IRL Press, Oxford, 1982.
20 Y. Kato, T. Kitamura, A. Mitsui and T. Hashimoto, *J. Chromatogr.*, 398 (1987) 327.
21 M. M. Merion, presented at the *7th International Symposium on High-Performance Liquid Chromatography of Proteins, Peptides, and Polynucleotides, Washington, DC, November 2–4, 1987.*

Journal of Chromatography, 555 (1991) 125–136
Elsevier Science Publishers B.V., Amsterdam

CHROM. 23 384

High-performance liquid chromatography of the phenolic compounds in the juice of some French cider apple varieties

ELISABETH DELAGE*

Faculté de Pharmacie, Laboratoire de Botanique (Professeur P. Cillard), Université de Rennes I, 35043 Rennes Cedex (France)

and

G. BOHUON, A. BARON and J.-F. DRILLEAU

Institut National de la Recherche Agronomique, Station de Recherches Cidricoles, Biotransformation des Fruits et Légumes, B.P. 29, 35650 Le Rheu (France)

(Received March 19th, 1991)

ABSTRACT

The phenolic compounds chlorogenic acid, *p*-coumaric acid, protocatechuic acid, (+)-catechin, (−)-epicatechin, phloridzin and di-, tri- and tetrameric procyanidins in apple juice were separated by reversed-phase high-performance liquid chromatography on a C_{18} column using a methanol–dilute hydrochloric acid solvent gradient. Absorbance ratios and UV spectrometry were used to identify the separated phenolic compounds and to check their purity.

INTRODUCTION

The phenolic compounds in apple juice are involved in enzymic browning and haze formation and they also contribute to bitterness and astringency [1]. A knowledge of the phenolic composition of the different apple varieties would be useful in juice processing.

High-performance liquid chromatography (HPLC) has been used for separating a wide range of phenolic acids [1–6] and also the most common substituted benzoic and cinnamic acids occurring naturally in plant materials [7,8]. Polymeric procyanidins, which provide a large proportion of the apple juice phenolics [9], and cider procyanidins have been analysed by both reversed-phase and normal-phase HPLC [10,11]; however, these techniques gave only partial resolution.

In this study we used an HPLC method coupled with UV spectrometry (photodiode-array detector) as reported previously [12–15]. Separation, detection and quantification of phenolic acid derivatives and flavonoids present in the juices of French cider apple cultivars were performed. The authentic compounds studied included two benzoic acids, two cinnamic acids, three flavanols and four individual procyanidins with different degrees of polymerization, (di-, tri- and tetrameric forms).

All the phenolic compounds in the juices were identified by matching the reten-

0021-9673/91/$03.50

tion times and the spectral characteristics of their peaks against those of standards. Absorbance ratios were also measured.

EXPERIMENTAL

Preparation of crude apple juice

Single-variety juices were extracted from four typical apple cider varieties: two sharp varieties (Petit Jaune and Judor) and two bitter sweet varieties (Bedan and Kermerrien). After harvest, the apples were stored for 2 weeks at 10°C, then crushed and the pulp was pressed with a rack-and-cloth laboratory device (50-kg batches). Samples of the running juices were frozen and stored at −30°C until needed.

Industrial juice was made from a blend of typical bitter and bitter sweet cider apple varieties. The processing was the same as above except that 1000-kg batches were pressed.

Standards

The phenolic standards benzoic acid derivatives, cinnamic acid derivatives, (+)-catechin, (−)-epicatechin and phloridzin were obtained from Sigma (St. Louis, MO, USA); procyanidins (trimer C_1 and tetramer) were a gift from Dr. A. Lea (Cadbury Schweppes, Reading, UK). Analyses were carried out with standard solutions containing 3 m*M* of each phenolic acid or 5 m*M* of each flavonoid.

Preparation of a total phenolic extract of apple juice

Apple juice (10 ml) was adjusted to pH 7 with sodium hydroxide solution (0.1 *M*), then extracted three times with 10 ml of ethyl acetate [16]. After centrifugation at 1000 *g* for 10 min, the pooled organic phases to which α-naphthol (100 μl of a solution at 3.2 g/l) was added as an internal standard [17] were evaporated to dryness in a rotary evaporator at 40°C. The residue was dissolved in 1 ml of methanol–acetic acid (99:1, v/v). This extract (E7) should contain flavonoids.

The remaining aqueous fraction was adjusted to pH 2 with hydrochloric acid (0.1 *M*). Preparation of the extract was performed as described above. This extract (E2) was likely to contain phenolic acid derivatives. Volumes of 20 μl of each extract were injected separately onto the column.

Apparatus

The analytical equipment consisted of a Model 2152 HPLC gradient controller, Model 2156 solvent conditioner and a Model 2150 pump, coupled with a Model 2140 rapid spectral detector (all from LKB).

The analytical separations were performed at 40°C on a Spherisorb ODS 2 reversed-phase C_{18} (5 μm) column (25 cm × 4.6 mm I.D.) (Waters). The same elution programme was used for both the phenolic acids and the flavonoids, at a flow-rate of 1.8 ml/min, with solvent A, water–hydrochloric acid (1 *M*) (99.8:0.2), and solvent B, methanol–hydrochloric acid (1 *M*) (99.8:0.2), the solvent gradient being increased from 0 to 50% B in 85 min. All solvents were of HPLC grade and degassed with helium at room temperature.

RESULTS AND DISCUSSION

Data obtained with standards

In Table I, the eleven phenolic compounds used as standards are listed, with retention times and absorbance ratios. All these standards were determined by their spectral properties (Fig. 1). Each group exhibited different absorption maxima: benzoic acids (gallic and protocatechuic) at 260–270 nm, cinnamic acids (chlorogenic and *p*-coumaric) at 310 nm with a shoulder that extended to 270–290 nm and flavonoid compounds between 275 and 285 nm; only chalcone derivatives also showed an absorption at 320 nm.

The results show that the use of several absorbance ratios at suitable wavelengths permit one to distinguish between benzoic acid derivatives, cinnamic acid derivatives and flavonoids. Regardless of peak shape, flow-rate and retention time, the ratios obtained were characteristic of each compound in a given mobile phase [13]. We propose the use of 275 nm as the denominator wavelength for the absorbance-ratio analysis of benzoic and cinnamic acid derivatives (Table I), because at this wavelength the absorptions of nearly al the compounds tested were the weakest. Although the flavonoid spectra showed a maximum absorption near 275 nm, we retained this wavelength because the use of 255 nm (minimum absorption) for calculating absorbance ratios did not allow good identification of the standards.

The numerator wavelength for the absorbance ratio should be close to the absorption maxima, so we adopted 255 nm for the benzoic acids and 290 and 320 nm for the cinnamic acids (Table I). For the flavonoids we need only one absorbance ratio, $A_{220\ nm}/A_{275\ nm}$; although at 220 nm the spectra of flavonoids showed a shoulder (Fig. 1), the resolutuion for specific identification was better than that using 280 nm.

Fig. 2 shows the elution pattern of phenolic standards. Elution is in order of decreasing polarity, as reported previously [7,8]. Loss of polar hydroxy groups and/or

TABLE I

RETENTION TIMES AND ABSORBANCE RATIOS OF STANDARD PHENOLICS

Type	Compound	t_r (min)	Absorbance ratio			
			220/275 nm	255/275 nm	290/275 nm	320/275 nm
Benzoic acids	1b Gallic acid	7.00		0.7	0.6	
	2b Protocatechuic acid	10.00		2.1	1.12	
Cinnamic acids	1c Chlorogenic acid	31.00			1.58	2.15
	2c *p*-Coumaric	39.30			1.5	1.3
Flavonoids	1p (+)-Catechin	21.00	7.65			
	2p Dimer B_2 procyanidin	32.79	8.03			
	3p Trimer procyanidin	34.95	9.11			
	4p (−)-Epicatechin	41.35	7.88			
	5p Trimer C_1 procyanidin	52.80	8.54			
	6p Tetramer procyanidin	55.00	9.06			
	7p Phloridzin	72.80	1.34			

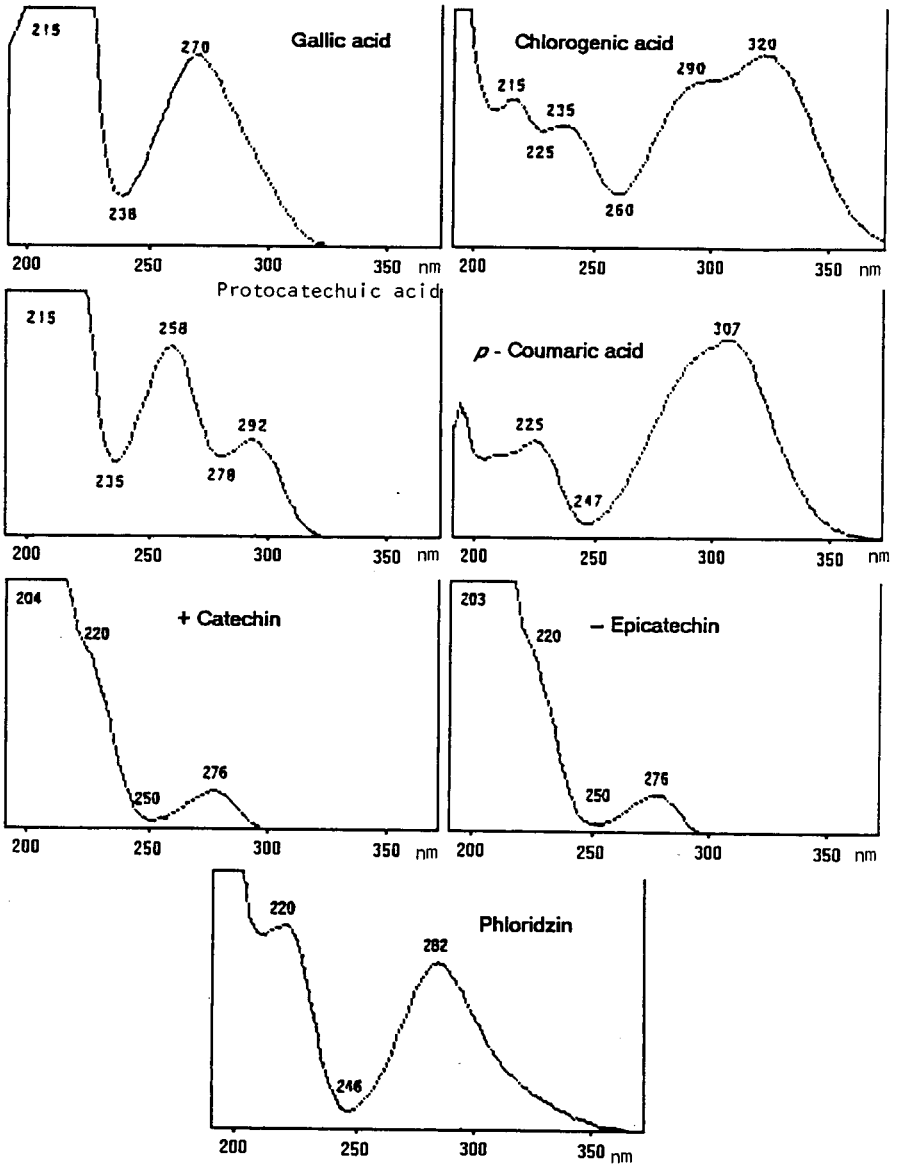

Fig. 1. UV spectra of standard phenolics.

addition of methoxy groups decreased the polarity within each class (benzoic acid *vs.* cinnamic acid). The presence of the ethylenic side-chain in the cinnamic acids reduced their polarity compared with similarly substituted benzoic acids. In the HPLC of standard flavonoids, phloridzin was eluted later, as reported previously [6]. For all these studies different mixtures of standards were injected.

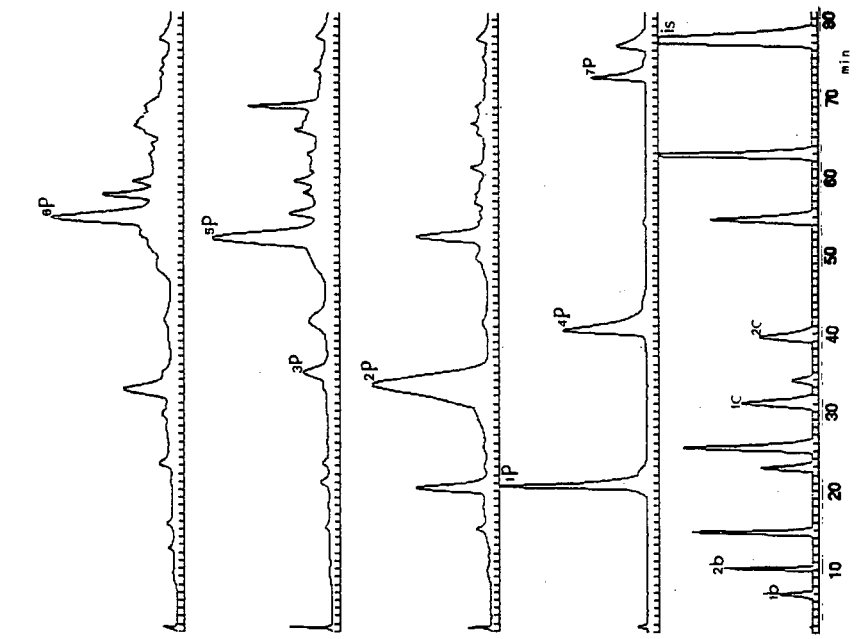

Fig. 2. Liquid chromatograms of standard phenolics. Detection at 235 nm. 1b–7p, see Table I; IS = internal standard.

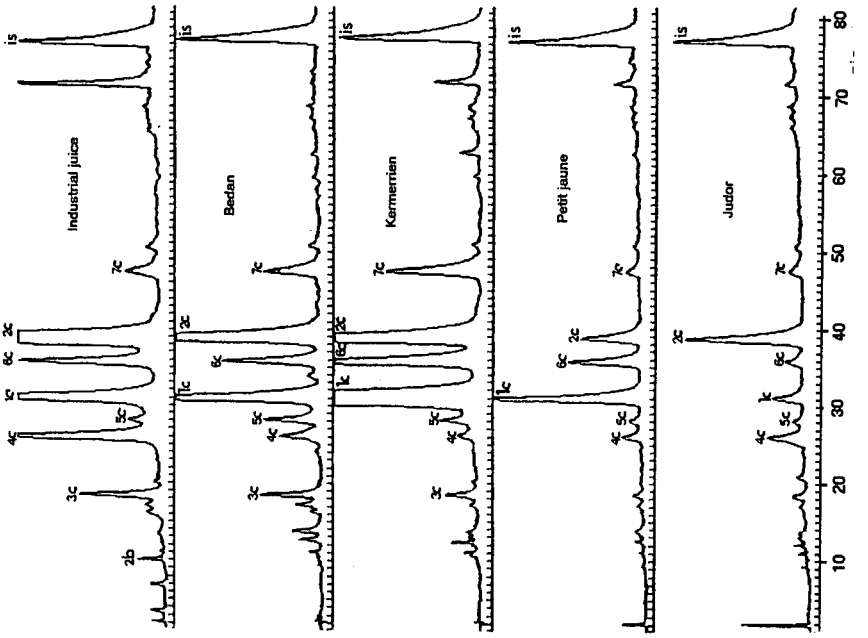

Fig. 3. Separation of phenolic acid derivatives from varietals (extract pH = 2). Detection at 280 nm. 2b–7c, see Table II; IS = internal standard.

TABLE II

RETENTION TIMES AND ABSORBANCE RATIOS OF PHENOLIC ACID DERIVATIVES FROM EXTRACTS (E2)

t_r = Retention time; $a_1 = A_{290\ nm}/A_{275\ nm}$; $a_2 = A_{320\ nm}/A_{275\ nm}$.

Phenolics compound	Industrial juice			Bedan			Kermerrien			Petit Jaune			Judor		
	t_r	a_1	a_2	t_r	a_1	a_2	t_r	a_1	a_2	t_r	a_1	a_2	t_r	a_1	a_2
2b Protocatechuic acid	10.09	1.17	1.17	–	–	–	–	–	–	–	–	–	–	–	–
Benzoic acid derivatives	–	–	–	11.15	0.8	0.7	–	–	–	–	–	–	–	–	–
(unidentified)	–	–	–	12.37	0.8	0.4	–	–	–	–	–	–	–	–	–
	–	–	–	13.89	1.1	0.9	–	–	–	–	–	–	–	–	–
3c *p*-Coumaric acid derivative	18.55	1.36	1.6	18.55	1.53	1.53	18.59	1.2	1.2	–	–	–	–	–	–
4c *p*-Coumaric acid derivative	25.85	1.3	1.1	26.15	1.40	1.16	26.19	1.4	1.6	26.09	1.28	1.14	26.05	1.32	1.2
5c Cinnamic acid derivative	28.05	1.28	1.9	28.25	1.38	2	28.19	1.18	1.91	–	–	–	–	–	–
1c Chlorogenic acid	30.85	1.64	2.11	30.85	1.65	2.15	30.52	1.66	2.15	30.95	1.67	2.12	31.12	1.77	2.11
6c Cinnamic acid derivative	35.65	1.31	1.45	35.79	1.40	1.45	35.79	1.31	1.46	35.75	1.36	1.5	35.92	1.29	1.29
2c *p*-Coumaric acid	38.42	1.66	1.73	38.69	1.68	1.73	38.79	1.65	1.70	38.79	1.58	1.64	38.72	1.58	1.70
7c *p*-Coumaric acid derivative	47.21	1.8	1.8	47.25	1.8	1.86	47.23	1.7	1.75	47.19	2	2	47.37	1.5	0.75

HPLC of phenolic compounds in apple juice

Identification. Typical separations of apple phenolic compounds in sharp varieties such as Petit Jaune and Judor or bitter sweet varieties such as Bedan and Kermerrien are shown in Figs. 3 and 4. Good resolution of the major monomeric phenolics was achieved; they were identified by comparing the retention times and spectral characteristics of their peaks with those of standards (Table II and III). Simultaneously, the absorbance ratio was measured; for phenolic acids, additional ratio plots were used as indicated in Table II: a_1 ($A_{290\ nm}/A_{275\ nm}$) and a_2 ($A_{320\ nm}/A_{275\ nm}$). For the flavonoid compounds the measurement of the absorbance ratio was adopted as 220/275 nm (Table III), as was previously indicated for the standards.

In the extracts E2, (Fig. 3) chlorogenic acid (peak 1c) is a major component, as already found in apple extracts [1,4,11,14]. Similarly, the presence of *p*-coumaric acid (peak 2c) was verified. The accuracy of the identity of these compounds is evident from the agreement of the absorbance ratios. Inspection of the data for other compo-

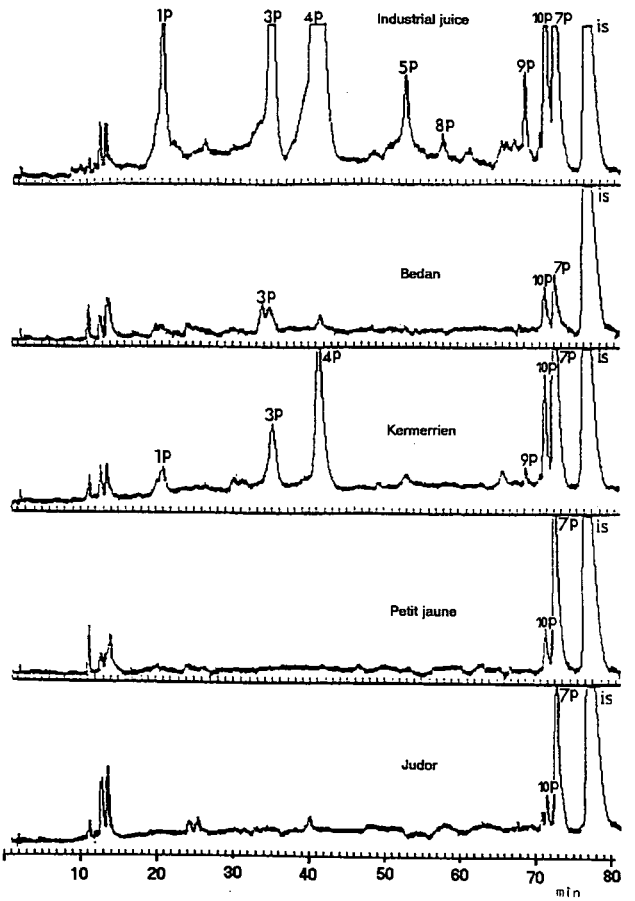

Fig. 4. Separation of flavonoid derivatives from varietals (extract pH = 7). Detection at 220 nm. 1p–10p, see Table III; IS = internal standard.

TABLE III

RETENTION TIMES AND ABSORBANCE RATIOS OF FLAVONOID DERIVATIVES FROM EXTRACTS (E7)

Phenolic compound	Industrial juice		Bedan		Kermerrien		Petit Jaune		Judor	
	220/275 nm	t_r (min)	220/275 nm	t_r (min)	220/275 nm	t_r (min)	220/275 nm	t_r (min)	220/275 nm	t_r (min)
1p Catechin	7.8	20.95	–	–	9.8	20.99	–	–	–	–
3p Trimer	9.94	34.95	8.71	35.12	10	35.12	–	–	–	–
4p Epicatechin	7.9	40.65	–	–	8.1	41.42	–	–	–	–
5p Trimer C1 procyanidin	9.3	53.02	9.25	52.95	–	–	–	–	–	–
8p Unidentified procyanidin	7.8	57.92	–	–	–	–	–	–	–	–
9p Unidentified procyanidin	9.6	69.15	–	–	8	69.19	–	–	–	–
10p Chalcone	1.4	71.79	1.25	71.72	1.2	71.82	1.21	71.75	1.12	71.82
7p Phloridzin	1.3	73.09	1.12	73.09	1.3	73.05	1.29	73.05	1.2	73.15

nents should be made with care. The accuracy of the identities was demonstrated by both retention times and spectral data. A minor component (peak 2b), present only in the industrial juice, was protocatechuic acid, as shown by its retention time and absorbance ratio values (Table II). Most of the *p*-coumaric acid or cinnamic acid derivatives appeared to give the theoretical values for the absorbance ratios, but did not show the actual spectra. For the others, it was not possible to calculate absorbance ratios because of the small amounts present.

In the extracts E7 (Fig. 4), some major components were present. Peak 1p and 4p are (+)-catechin, and (−)-epicatechin, respectively. Peak 10p is a chalcone derivative and peak 7p is phloridzin. They were identified by their retention times and spectral data.

Identification of a trimer procyanidin (peak 3p) and trimer C_1 procyanidin (peak 5p) was based on the retention times of standards (Table I) and on the typical catechin spectrum. This is in agreement with previous results [1,10,11,14,15,18]. Procyanidin tetramer was not identified, although other workers have done so [1,14]. However, a number of minor peaks (up to eight) that showed typical catechin spectra were considered to be unknown procyanidins.

TABLE IV

PRECISION OF THE RESULTS FOR DIFFERENT PHENOLIC COMPOUNDS FOUND IN THE JUICE OF BEDAN APPLES AND IN THE INDUSTRIAL JUICE

3c, 4c, 5c, 1c, 6c, 2c: see Table II. 1p, 3p, 4p, 7p: see Table III.

Phenolic acids (Bedan)	3c	4c	5c	1c	6c	2c
t_r (min)	18.49	26.02	28.08	30.84	35.70	38.60
Phenolics content (μM)	23.70	26.66	24.08	129.84	46.88	171.86
	22.20	25.49	27.16	134.24	49.07	171.70
	26.24	27.05	26.91	136.37	47.93	180.35
	22.89	25.48	25.07	134.93	48.85	174.28
	22.04	23.58	26.44	137.94	48.42	177.64
Degrees of freedom	4	4	4	4	4	4
Mean values (μM)	23.41	25.65	25.93	134.66	48.23	175.17
Standard deviation (μM)	1.71	1.35	1.31	3.05	0.87	3.76
Relative standard deviation (%)	7.30	5.27	5.06	2.26	1.81	2.15
Standard error (P = 95%) (%)	20.26	14.64	14.04	6.28	5.01	5.96

Flavonoids (industrial juice)	1p	3p	4p	7p
t_r (min)	21.00	35.63	39.85	71.67
Phenolics content (μM)	36.11	94.22	411.44	14.41
	38.18	90.71	422.65	14.78
	34.65	90.17	400.57	15.39
	37.10	90.55	401.35	14.66
	34.69	93.88	412.16	14.36
	36.25	90.96	426.62	15.30
Degrees of freedom	5	5	5	5
Mean values (μM)	36.15	91.91	409.63	14.72
Standard deviation (μM)	1.54	1.97	9.08	0.41
Relative standard deviation (%)	4.25	2.14	2.22	2.80
Standard error (P = 95%) (%)	10.92	5.51	5.70	7.19

Quantification. Calculation of concentrations was based on the internal standard method. Dilutions (10:0, 8:2, 6:4, 4:6 and 2:8) of a methanolic solution containing 3 m*M* chlorogenic acid, 2.5 m*M* *p*-coumaric acid and 3 m*M* protocatechuic acid were used to fit a calibration graph (peak area *vs.* concentration in m*M*), with linear regression for each individual compound. *p*-Coumaric acid derivatives were measured as *p*-coumaric acid and 3,4-cinnamic acid derivatives as chlorogenic acid.

Similar dilutions of an aqueous solution containing 5 m*M* catechin, 5 m*M* epicatechin and 5 m*M* phloridzin were used for the determination of catechins and procyanidins. All procyanidins were expressed as catechin and the chalcone derivative as phloridzin.

A compromise value was required to choose the wavelength for the calculation of concentrations in apple juice. It was chosen as 320 nm for phenolic acids as it resulted in a smaller recorder baseline shift during the elution programme due to changing solvent composition. For the determination of flavonoids it was chosen as 220 nm for the same reason as indicated previously when measuring the absorbance ratio. Concentration values expressed in μmol/l are presented in Table IV for the two extracts (E2 and E7).

All HPLC analysis were replicated. The precision of the results obtained by the chosen method (extraction + chromatography) was studied for phenolic acids in the juice of Bedan apples and for flavonoids in the industrial juice (Table V). The values must not be compared with those given in Table IV for the later considered juices extracted at a different harvest time.

Although the precision was not calculated for the flavonoids corresponding to

TABLE V

PHENOLIC ACID AND FLAVONOID CONTENTS IN APPLE JUICES

Phenolic compounds	Concentration (μ*M*)				
	Industrial juice	Bedan	Kermerrien	Petit Jaune	Judor
Phenolic acids					
2b Protocatechuic acid	5.3	1.4			1.2
3c *p*-Coumaric acid derivative	70.3 ± 14.2[a]	12.6 ± 2.6	2.3 ± 0.5	7.2 ± 1.5	17.6 ± 3.6
4c *p*-Coumaric acid derivative	15.6 ± 2.3	26.2 ± 3.8	19.6 ± 2.9	6.9 ± 1.0	6.3 ± 0.9
5c Cinnamic acid derivative	61.1 ± 8.6	36.8 ± 5.2	97.6 ± 13.7	34.3 ± 4.8	7.4 ± 1.0
1c Chlorogenic acid	180.0 ± 11.3	139.4 ± 8.8	702.8 ± 44.1	98.5 ± 6.2	20.6 ± 1.3
6c Cinnamic acid derivative	19.3 ± 1.0	27.7 ± 1.4	51.2 ± 2.6	9.0 ± 0.5	8.8 ± 0.4
2c *p*-Coumaric acid	394.3 ± 23.5	141.5 ± 8.4	181.3 ± 10.8	33.5 ± 2.0	73.9 ± 4.4
Flavonoids					
1p Catechin	156.8 ± 17.1	11.5 ± 1.3	23.6 ± 2.6	2.4 ± 0.3	1.5 ± 0.2
3p Trimer	349.5 ± 19.3	11.8 ± 0.7	80.0 ± 4.4	1.2 ± 0.1	0.6 ± 0.0
4p Epicatechin	854.4 ± 48.7	11.2 ± 0.6	137.5 ± 7.8	2.6 ± 0.1	1.3 ± 0.1
5p Trimer C1 procyanidin	137.2	2.9	19.2	2.0	2.4
8p Unidentified procyanidin	36.2	0.8	2.7	2.7	0.7
9p Unidentified procyanidin	71.0	2.2	14.2	2.1	4.6
10p Chalcone	75.6	14.3	25.2	11.8	9.9
7p Phloridzin	81.3 ± 5.8	11.0 ± 0.8	60.4 ± 4.3	49.9 ± 3.6	35.1 ± 2.5

[a] The ± values are absolute errors.

peaks 5p, 8p, 9p and 10p, their amounts are reported in Table IV; the great difference between the industrial juice and the different variety juices is evident.

Chlorogenic acid was the major phenolic acid present in all varieties. This agrees with Lea [11] and Spanos *et al.* [14], who reported that this acid is one of the main phenolics of apple juice; the highest concentration occurred in Kermerrien (702 μmol/l) and the lowest in Judor (20.6 μmol/l). It has been reported that the range of levels of chlorogenic acid is very wide: Lee and Wrolstad [19] found levels ranging from 1.5 mg/l (4.2 μmol/l) to 228 mg/l (644 μmol/l) in Golden Delicious, McIntosh, Jonathan and Granny Smith apple juices.

p-Coumaric acid was present in a significant amount in the industrial juice (394 μmol/l) and in minor amounts in all varieties, particularly in Petit Jaune (33.4 μmol/l). Low levels of other cinnamic and *p*-coumaric acid derivatives were present in all varieties; some of them, such as protocatechuic acid, present in the industrial juice could not be determined accurately because their amounts were too low.

In the extracts E7, epicatechin was a major component; the highest concentration was found in the industrial juice (854 μmol/l) and the lowest in Petit Jaune (2.6 μmol/l) and Judor (1.3 μmol/l). (+)-Catechin, which was abundant in the industrial juice (157 μmol/l), appeared as a minor component in the varieties (between 1.5 and 23 μmol/l).

It is interesting that only one major procyanidin *viz.*, procyanidin trimer C_1, has been reported in apples [10]; however, it is apparent from Table IV that significant proportions of the unidentified procyanidins (peaks 5p, 8p, 9p) were observed in the industrial juice.

Peak 10p appeared to be a chalcone derivative. Apart from phloridzin (peak 7p), another phloretin derivative was characterized; these two derivatives were found in both the industrial and the single-variety juices. Other workers [14,20] have reported that another phloretin derivative, phloretin xyloglucoside, is also present in apples [1,5,21].

CONCLUSIONS

Each variety showed the same qualitative phenolic acid and flavonoid pattern. Quantification was not very easy: in the preparation of the total phenolic extract, the method of extraction did not allow a good separation of phenolic compounds; it was observed that the amounts of the phenolics studied were different in the different juices. In Petit Jaune and Judor, the phenolic compounds were present only in trace amounts; in bitter sweet varieties, mainly Kermerrien, chlorogenic acid, *p*-coumaric acid and epicatechin were present in important concentrations. The industrial juice showed the highest concentrations of (+)-catechin, procyanidin trimer, *p*-coumaric acid and epicatechin but not chlorogenic acid.

The separation, identification and quantification of plant tissue phenolics represent a difficult challenge. However, our experience suggests that some improvements should be made, particularly for extraction by use of different chromatographic techniques, such as with Sephadex LH-20, Phenyl-Sepharose and C_{18} (Sep-Pak), and also for the identification of phenolic glycosides by acid and/or enzymic hydrolysis.

ACKNOWLEDGEMENTS

The authors thank Dr. A. G. H. Lea for a gift of procyanidins, and the Comité des Fruits à Cidre et des Productions Cidricoles (Paris) for financial assistance.

REFERENCES

1 E. L. Wilson, *J. Sci. Food Agric.*, 32 (1981) 257.
2 A. B. Durkee and P. A. Poapst, *J. Agric. Food Chem.*, 13 (1965) 137.
3 A. J. Dick, P. R. Redden, A. C. DeMarco, P. D. Lidster and T. B. Grindley, *J. Agric. Food Chem.*, 35 (1987) 529.
4 A. Bilyk, K. B. Hicks, D. D. Bills and G. M. Sapers, *J. Liq. Chromatogr.*, 11 (1988) 2829.
5 G. C. Whiting and R. A. Coggins, *J. Sci. Food Agric.*, 26 (1975) 1833.
6 L. W. Wulf and C. W. Nagel, *J. Chromatogr.*, 116 (1976) 271.
7 J. B. Murphy and C. A. Stutte, *Anal. Biochem.*, 86 (1978) 220.
8 K. Vande Casteele, H. Geiger and C. F. Van Sumere, *J. Chromatogr.*, 258 (1983) 111.
9 A. G. H. Lea, *J. Sci. Food Agric.*, 30 (1979) 833.
10 A. G. H. Lea, *J. Chromatogr.*, 194 (1980) 62.
11 A. G. H. Lea, *J. Chromatogr.*, 238 (1982) 253.
12 D. Schaufelberger and K. Hostettmann, *J. Chromatogr.*, 389 (1987) 450.
13 K. H. Law and N. P. Das, *J. Chromatogr.*, 388 (1987) 225.
14 G. A. Spanos, R. E. Wrolstad and D. A. Heatherbell, *J. Agric. Food Chem.*, 38 (1990) 1572.
15 A. W. Jaworski and C. Y. Lee, *J. Agric. Food Chem.*, 35 (1987) 257.
16 M. H. Salagoïty-Auguste and A. Bertrand, *J. Sci. Food Agric.*, 35 (1984) 1241.
17 T. Adzet and M. Puigmacia, *J. Chromatogr.*, 348 (1985) 447.
18 J. Oszmianski and J. C. Sapis, *J. Agric. Food Chem.*, 37 (1989) 1297.
19 H. S. Lee and R. E. Wrolstad, *J. Assoc. Off. Anal. Chem.*, 71 (4) (1988) 789.
20 A. G. H. Lea and C. F. Timberlake, *J. Sci. Food Agric.*, 25 (1974) 1537.
21 W. Oleszck, C. Y. Lee, A. W. Jaworski and K. R. Price, *J. Agric. Food Chem.*, 36 (1988) 430.

Journal of Chromatography, 555 (1991) 137–145
Elsevier Science Publishers B.V., Amsterdam

CHROM. 23 353

Determination of triazines and organophosphorus pesticides in water samples using solid-phase extraction

J. C. MOLTÓ, Y. PICÓ, G. FONT* and J. MAÑES
Laboratory of Food Chemistry and Toxicology, Faculty of Pharmacy, University of Valencia, Blasco Ibañez 13, 46010 Valencia (Spain)

(First received September 21st, 1990; revised manuscript received March 28th, 1991)

ABSTRACT

Octadecyl (C_{18})-bonded porous silica was evaluated for the extraction of triazine and organophosphorus pesticides from natural water. The extraction results showed an effective performance when 1 l of water was passed through small glass columns containing 500 mg of 50–100-μm C_{18} bonded porous silica. The adsorbed compounds were removed with ethyl acetate, evaporated to 200 μl and determined by gas chromatography. The overall average recoveries were greater than 85% except for dimethoate and trichlorfon. Application of this procedure to the analysis of natural water samples gave results that agree well with those obtained by solvent extraction methods.

INTRODUCTION

In recent years, the need for increased agricultural productivity has led to pesticide residues in natural waters at greater than ppb levels. Organophosphorus pesticides and triazine herbicides are currently the major types used on a worldwide scale as most organochlorine pesticides have been withdrawn from use because of their toxicity, persistence and bioaccumulation in the environment. Hence there is a need for methods suitable for detecting large numbers of those water pollutants at concentrations less than EEC the limit of 0.1 ng/l.

Several methods have been developed. The traditional approach involving solvent partition [1,2] is time consuming and expensive because of the high cost of the solvents. To reduce the analysis time and costs in multi-residue determinations [3], liquid–solid extraction methods were first introduced in 1974 [4] and more recently improved upon [5–8]. Among the solid supports available for solid-phase extraction of organic components from aqueous solution, octadecyl-bonded porous silica has become the most popular [9–15]. Its availability in inexpensive cartridges from several suppliers has contributed to an increase in the application of solid-phase extraction methods. However, when gas chromatography (GC) with electron-capture detection is used, some extraneous peaks appear that interfere in the analysis [16], caused by the plastics used for the cartridges. The use of glass microcolumns has the great advantage of avoiding contamination of the sample with plasticizers [17]. We report

0021-9673/91/$03.50

here the application of this technique to the determination of several pesticides in field studies of both surface and ground waters.

EXPERIMENTAL

Reagents

The organophosphorus pesticides used were cumaphos, purity 98% (Chemical Services), diazinon, purity 98.5% (Inquinasa), dimethoate, purity 97% (Argos), formothion, purity 96% (Sandoz), phorate, purity 93.5% (Chemical Services), piridafenthion, purity 99% (Inagra), pyrazophos, purity 99.2% (Hoechst), quinalphos, purity 99.5% (Sandoz), tetrachlorvinphos, purity 98.3% (Shell), triazophos, purity 93% (Hoechst), and trichlorfon, purity 92% (Afrasa). Triazine herbicides (prometryne, propazine and simazine) were obtained from Polyscience with purities of 99%. Stock solutions of the pesticides were prepared in ethyl acetate and diluted as required with distilled water.

Preparative octadecylsilica (55–105 μm) was obtained from Waters–Millipore.

Dichloromethane, ethyl acetate, diethyl ether, *n*-hexane, methanol and light petroleum (b.p. 40–60°C) were glass distilled and free from interfering residues as tested by GC (concentration 100:1). Buffer solutions of pH 2–9 were prepared [18].

Apparatus

A Konik 2000-C gas chromatograph equipped with a splitless injector, alkali flame ionization detector and a Spectra-Physics SP 4290 integrator was used. Two fused-silica capillary columns, one 25 m × 0.22 mm I.D., BP-5 (0.25 μm), provided by Scientific Glass Engineering, and the other 30 m × 0.24 mm I.D., DB-17 (0.25 μm), provided by J & W Scientific, with helium as the carrier gas were used to separate the pesticides. The injector and detector temperatures were 280 and 300°C, respectively. Splitless injection at 50°C was employed, followed by a 0.8-min delay before heating the column to 140°C at 30°C/min. The column temperature was maintained at 140°C for 2 min followed by further heating to 280°C at 5°C/min, the final temperature being maintained for 5 min.

Procedure

Microcolumn preparation. A 0.5-g amount of actadecylsilica was inserted in a Vidrafoc glass column (100 mm × 9 mm I.D.) with a sintered-glass coarse frit (No. 3) and covered with a plug of 0.1 g of silanized glass-wool. The microcolumn was conditioned with 5 ml of methanol and 10 ml of distilled water.

Sample extraction. The microcolumn was connected to a separating funnel with glass joints. A volume of 1 l of water sample was passed though the microcolumn. Vacuum by water aspiration was applied in order to obtain a flow-rate of about 40–45 ml/min. The C_{18}-bonded porous silica was then dried by drawing room air through the cartridge using a vacuum. The adsorbed residues were eluted with 5 ml of ethyl acetate by water aspiration at a flow-rate of 2–3 ml/min. The organic layer was concentrated to 0.2 ml using a gentle stream of nitrogen. Samples of 2 μl were injected into the gas chromatograph.

RESULTS AND DISCUSSION

Fig. 1 shows the simultaneous determination of the fourteen pesticides after solid-phase extraction from water. The BP-5 capillary column provided excellent resolution at the picogram level with baseline separation of all the pesticides and with a run time of *ca.* 30 min.

To confirm the results obtained, an additional capillary column of different

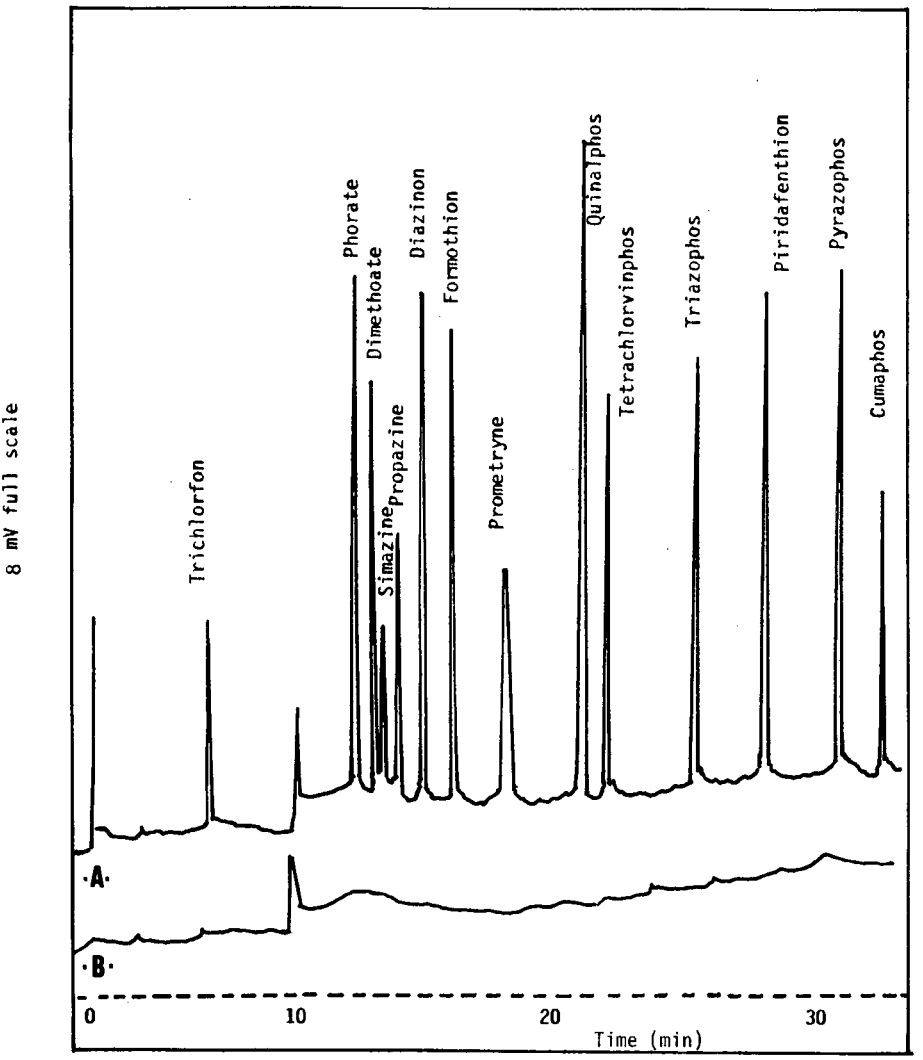

Fig. 1. (A) Gas chromatogram showing the separation of triazine herbicides and organophosphorus pesticides. Volume injected: 1 μl. Amounts injected (ng): trichlorfon 54, phorate 3, dimethoate 4, simazine 33, propazine 22, diazinon 1, formothion 3, prometryne 50, quinalphos 4, tetrachlorvinphos 4, triazophos 6, piridafenthion 2, pyrazophos 4 and cumaphos 7. For original concentrations, see Table I. (B) Chromatogram of a laboratory water blank.

polarity was employed for each real sample. The differences in elution order and retention times of the pesticides between the semipolar DB-17 and non-polar BP-5 columns aloowed the use of the two columns to confirm the identities of the pesticides.

In previous work [17], several pesticides were conveniently extracted and concentrated from water samples using a glass microcolumn containing 500 mg of C_{18}-bonded porous silica. Several additional herbicides and insecticides were included in the present study in order to examine further the effect of pH, salinity and eluent on the recovery efficiency.

The recoveries reported represent the means of five analyses. The pesticide concentrations in water were maintained constant throughout all the tests (see Table I).

The results given in Table I show the effect of the eluent on the recoveries of the fourteen pesticides at pH 7. Ethyl acetate was found to be the best eluting solvent.

Table II shows the effect of the pH of the spiked water samples on the performance of the octadecyl-bonded porous silica column. The results indicated that pH values between 6.0 and 8.0 give the best recoveries. The use of sea water had a negligible effect on the performance.

The effect of the volume of eluent (1–10 ml) was investigated. The maximum recovery was obtained with 4 ml for all the pesticides; 5 ml was adopted because it was found that the relative standard deviation was slightly lower.

Test were also performed to determine whether the sample volume affected the recovery of the pesticides. The recoveries for all compounds were satisfactory with 1 l

TABLE I

RECOVERIES OF PESTICIDES FROM SPIKED WATER USING DIFFERENT ELUENTS FOR SOLID-PHASE EXTRACTION

Pesticide	Amount added (μg/l)	Recovery (%)[a]		
		Ethyl acetate	*n*-Hexane	Light petroleum
Triazine herbicides				
Prometryne	10.00	94.8 ± 8.2	6.9 ± 18.1	6.8 ± 26.6
Propazine	5.00	79.6 ± 9.7	8.7 ± 28.6	5.5 ± 17.8
Simazine	7.00	75.6 ± 9.7	2.2 ± 17.4	0.4 ± 23.5
Organophosphorus pesticides				
Cumaphos	1.40	98.4 ± 8.1	36.4 ± 11.4	36.8 ± 10.8
Diazinon	0.20	84.9 ± 9.3	70.2 ± 8.0	78.7 ± 9.8
Dimethoate	10.00	16.2 ± 23.0	–	–
Formothion	0.80	65.1 ± 15.0	8.3 ± 29.6	11.1 ± 31.3
Phorate	1.00	59.4 ± 10.1	43.5 ± 10.1	52.0 ± 9.9
Piridafenthion	0.40	97.7 ± 7.9	–	–
Pyrazophos	0.80	93.5 ± 8.3	11.3 ± 33.6	11.9 ± 25.9
Quinalphos	0.80	89.8 ± 9.0	75.6 ± 8.9	78.7 ± 8.7
Triazophos	1.20	90.6 ± 8.7	5.5 ± 15.8	–
Tetrachlorvinphos	0.80	97.2 ± 7.4	4.1 ± 23.6	2.6 ± 26.9
Trichlorfon	180.00	6.9 ± 20.8	–	–

[a] Mean ± R.S.D. (%) ($n = 5$).

TABLE II

EFFECT OF pH ON ADSORBENT PERFORMANCE

Pesticides	Recovery (%)						
	pH 2.0	pH 3.5	pH 4.8	pH 6.1	pH 7.0	pH 8.0	pH 9.0
Triazine herbicides							
Prometryne	80.3	79.8	80.3	100.5	94.8	91.7	85.8
Propazine	10.4	45.1	66.6	90.2	79.6	71.1	72.0
Simazine	34.2	36.0	35.7	69.8	75.6	65.0	53.0
Organophosphorus pesticides							
Cumaphos	78.3	84.1	95.6	98.4	97.3	89.1	80.9
Diazinon	80.7	82.9	84.2	84.9	82.0	81.6	79.0
Dimethoate	8.1	8.8	10.8	8.9	16.2	8.3	–
Formothion	36.6	37.6	72.8	60.3	65.1	–	–
Phorate	–	–	8.7	17.7	59.4	69.3	74.4
Piridafenthion	22.7	47.7	69.9	99.9	89.8	78.7	75.1
Pyrazophos	36.0	50.1	66.6	92.5	93.5	32.0	4.0
Quinalphos	8.1	16.0	47.7	99.4	89.8	78.7	75.1
Triazophos	29.1	33.4	72.3	93.6	90.6	92.2	95.6
Tetrachlorvinphos	81.8	81.0	82.2	100.6	97.2	83.5	76.6
Trichlorfon	–	–	–	4.2	6.9	2.5	–

of sea, tap and lake water samples. When large amounts (10 l) of water samples containing the same amounts of pesticides were passed trichlorfon, phorate, prometryne, dimethoate, formothion, piridafenthion and pyrazophos were not recovered. Under the same conditions, the recoveries of quinalphos, triazophos and cumaphos decreased to 20, 65 and 16%, respectively. The recoveries of all the other pesticides studied showed no significant differences when 10-l samples were used.

Therefore, the optimum conditions for maximum recoveries of the pesticides were established as volume of water used for the extraction, 1 l; pH of the water, 7.0; and 5 ml of ethyl acetate as the extraction solvent.

As a low volume of organic eluent is finally obtained (200 μl), a high preconcentration ratio is achieved (1:5000), allowing a detection limit of lower than 0.1 μg/l, except for trichlorfon (see Table III), which shows a lower recovery and strong variations. The limit of detection was calculated by extrapolation from diluted samples that produced a chromatographic peak having a height equal to three times the standard deviation of the baseline noise [19].

A comparison of the recoveries obtained with C_{18} and with the solvent extraction procedures is shown in Fig. 2.

The application of the proposed method was tested on natural water samples, which were subjected to the trace-enrichment procedure described here. Albufera lake waters were very muddy, requiring filtration through a 1-μm glass filter prior to elution through the microcolumn, whereas the Mediterranean sea and tap waters were eluted directly through the adsorbent. The recoveries obtained for spiked waters demonstrate the applicability of the method (Table III).

The water samples analysed were collected in the Comunitat Valenciana during 1989–1990. Forty lake, irrigation and sea-water samples from different locations were

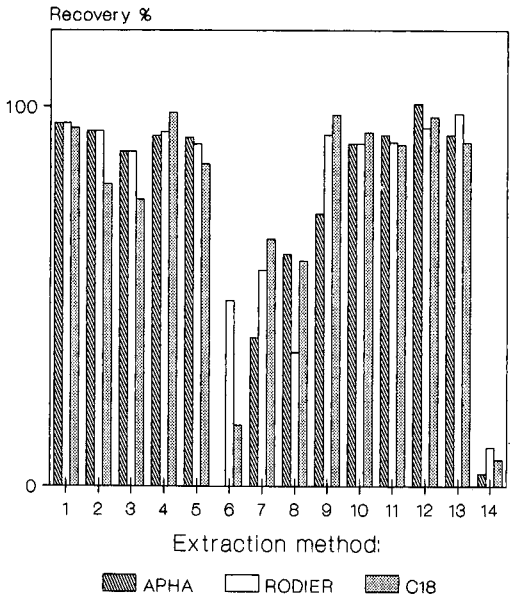

Fig. 2. Comparison of recoveries between the APHA [2] and Rodier [1] solvent extraction methods and the present (C_{18}) method. Pesticides: 1 = prometryne; 2 = propazine; 3 = simazine; 4 = cumaphos; 5 = diazinon; 6 = dimethoate; 7 = formothion; 8 = phorate; 9 = piridafenthion; 10 = pyrazophos; 11 = quinalphos; 12 = tetrachlorvinphos; 13 = triazophos; 14 = trichlorfon.

TABLE III

RECOVERY OF ORGANOPHOSPHORUS PESTICIDES AND TRIAZINE HERBICIDES ADDED TO 1 l OF DIFFERENT WATER SAMPLES AND DETECTION LIMITS OBTAINED

Pesticide	Detection limit (μg/l)	Recovery (%)		
		Tap water	Lake water	Sea water
Triazine herbicides				
Prometryne	0.052	99.6	97.3	96.4
Propazine	0.037	98.3	95.2	96.7
Simazine	0.092	71.0	71.4	59.9
Organophosphorus pesticides				
Cumaphos	0.045	82.4	98.4	90.0
Dimethoate	0.089	9.0	10.2	6.4
Diazinon	0.001	90.4	89.1	89.1
Formothion	0.016	61.0	64.2	60.9
Phorate	0.001	51.0	61.9	46.0
Piridafenthion	0.024	87.6	81.2	80.7
Pyrazophos	0.007	97.2	96.3	92.0
Quinalphos	0.002	81.3	90.0	89.0
Triazophos	0.048	87.0	86.9	84.0
Tetrachlorvinphos	0.010	88.7	84.7	86.2
Trichlorfon	0.729	5.5	5.7	6.3

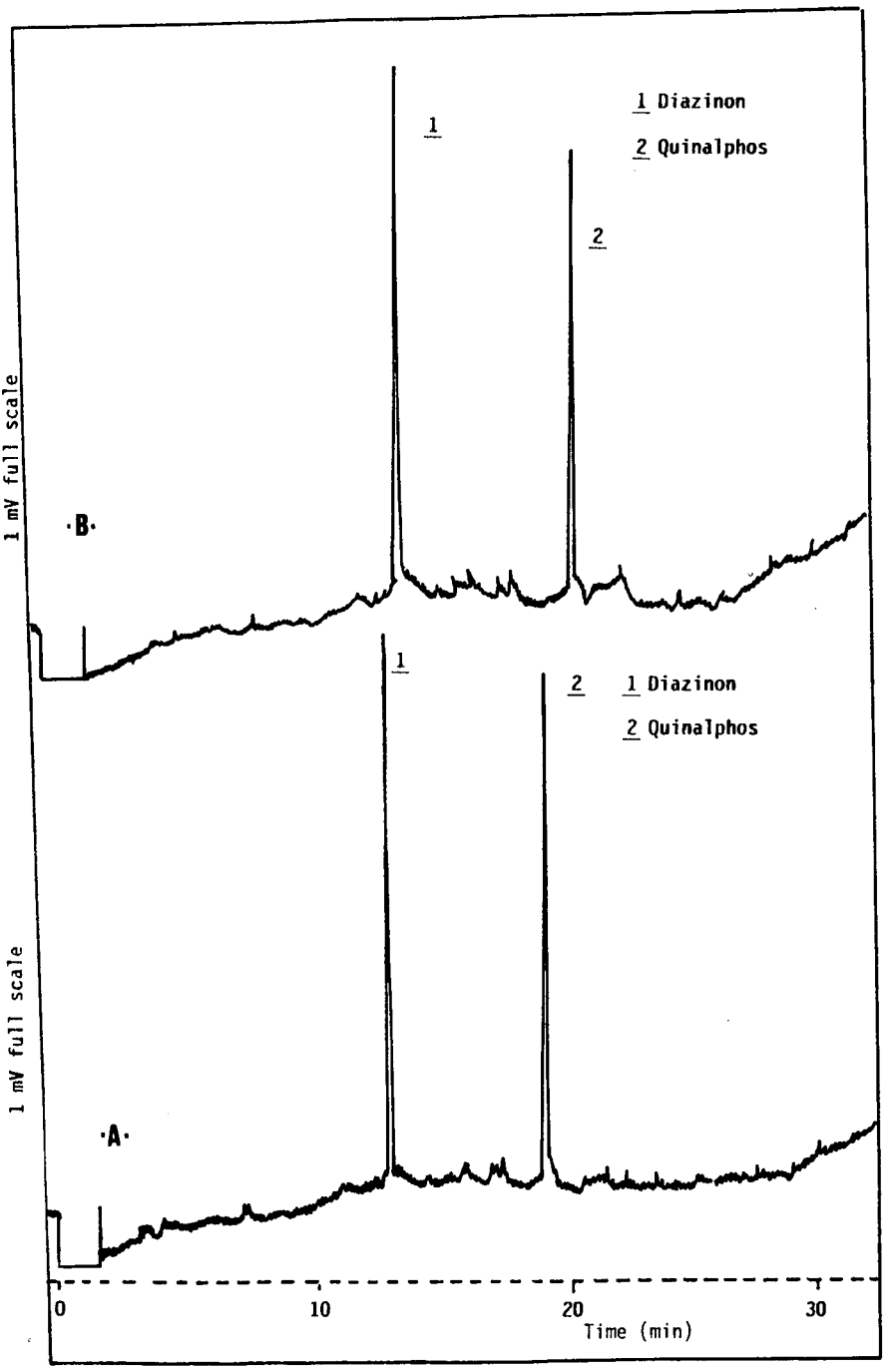

Fig. 3. Chromatograms for a 1-l irrigation channel water sample from Sueca, Valencia. (A) BP-5 column; (B) DB-17 column. Peaks: 1 = diazinon; 2 = quinalphos.

TABLE IV

LEVELS OF ORGANOPHOSPHORUS AND TRIAZINE COMPOUNDS IN NATURAL WATERS OF THE COMUNITAT VALENCIANA

Location	Compound	Level (μg/l)
Albufera lake	Diazinon	0.007
Irrigation channel, Marjal Pego	Cumaphos	0.152
Irrigation channel, Cullera	Simazine	0.308
Irrigation channel, Sueca	Diazinon	0.032
	Quinalphos	0.012
Irrigation channel, Sueca	Prometryne	0.176
	Tetrachlorvinphos	0.074
Irrigation channel, Perello	Prometryne	0.176
	Simazine	0.629
Irrigation channel, Mareny de les Barraquetes	Propazine	0.444
	Tetrachlorvinphos	0.036
Serpis river	Atrazine	0.734
	Triazophos	0.069
Irrigation channel, Sueca	Piridafenthion	0.053
Irrigation channel, Sueca	Piridafenthion	0.048
Irrigation channel, Mareny de Sant Llorens	Piridafenthion	0.039

analysed. Cumaphos, diazinon, piridafenthion, prometryne, propazine, quinalphos, simazine and tetrachlorvinphos were detected in 30% of the samples. The levels of pesticides found in the waters are given in Table IV.

Fig. 3 shows the chromatograms of irrigation channel water from Sueca. The pesticides found were diazinon and quinalphos.

In conclusion, the use of solid-phase extraction provides a rapid, efficient and reproducible method for the simultaneous determination of various pesticides in waters. The two-step extraction and concentration procedure minimizes residue losses and contamination problems. The simplicity of the analysis is complemented by good GC results.

The widespread occurrence of pesticide residues in the natural waters of the Comunitat Valenciana indicates pollution as a result of agricultural activity.

ACKNOWLEDGEMENT

The authors thank CICYT (GR85-0036) for financial support of this project.

REFERENCES

1 J. Rodier, *L'Analyse de l'Eau*, Dunod, Paris, 1984, pp. 414–416.
2 *Standard Methods for the Examination of Water and Wastewater*, American Public Health Association, Washington, DC, Supplement to the 15th ed., 1981, pp. 51–57.
3 J. Sherma, *Anal. Chem.*, 61 (1989) 154R.
4 G. A. Junk, J. J. Richard, M. D. Griesser, D. Witiak, J. L. Witiak, M. D. Arguello, R. Vick, H. J. Svec, J. S. Fritz and G. V. Calder, *J. Chromatogr.*, 99 (1974) 745.
5 P. A. Greve and C. E. Gowie, *Int. J. Environ. Anal. Chem.*, 20 (1985) 309.
6 A. Agostiano, M. Caselli and M. Provenzano, *Water Air Soil Pollut.*, 19 (1983) 309.
7 M. Popl, V. Tatar and Z. Voznakova, *Fresenius' Z. Anal. Chem.*, 313 (1982) 137.

8 D. Levesque and V. Mallet, *Int. J. Environ. Anal. Chem.*, 16 (1983) 1939.
9 J. J. Richard and G. A. Junk, *Mikrochim. Acta, Part I*, (1986) 387.
10 J. Putzien, *Wasser*, 68 (1987) 33.
11 J. Mañes, J. C. Moltó, C. Igualada and G. Font, *J. Chromatogr.*, 472 (1989) 365.
12 G. A. Junk and J. J. Richard, *Anal. Chem.*, 60 (1988) 451.
13 U. Oechmichen, F. Karrenbrock and K. Hoberer, *Fresenius' Z. Anal. Chem.*, 327 (1987) 715.
14 H. W. Brooks, J. Jenkins, M. Jimenez, T. Quin and J. M. Clark, *Analyst (London)*, 114 (1989) 405.
15 Z. Frobe, V. Drevenkar and B. Stengl, *Anal. Chim. Acta*, 206 (1988) 299.
16 G. A. Junk, M. J. Avery and J. J. Richard, *Anal. Chem.*, 60 (1988) 1347.
17 J. C. Moltó, C. Albelda, G. Font and J. Mañes, *Int. J. Environ. Anal. Chem.*, 41 (1990) 21.
18 J. Lurie, *Handbook of Analytical Chemistry*, Mir, Moscow, 1978.
19 J. E. Knoll, *J. Chromatogr. Sci.*, 23 (1985) 422.

Journal of Chromatography, 555 (1991) 147–154
Elsevier Science Publishers B.V., Amsterdam

CHROM. 23 401

Rapid on-line precolumn high-performance liquid chromatographic method for the determination of benomyl, carbendazim and aldicarb species in drinking water

CHRIS H. MARVIN[a] and IAN D. BRINDLE
Department of Chemistry, Brock University, St. Catharines, Ontario L2S 3A1 (Canada)
C. DAVID HALL
Ontario Ministry of the Environment, Rexdale, Ontario M9W 5L1 (Canada)
and
MIKIO CHIBA*
Research Station, Agriculture Canada, Vineland Station, Ontario L0R 2E0 (Canada)
(First received January 17th, 1991; revised manuscript received April 24th, 1991)

ABSTRACT

A reversed-phase high-performance liquid chromatographic (HPLC) method has been developed for the determination of trace concentrations of benomyl, carbendazim, aldicarb, aldicarb sulphoxide and aldicarb sulphone in drinking water. A 10-ml sample of water is passed through a 3-cm precolumn, packed with 5-μm C_8 sorbent, at a flow-rate of 5 ml/min. The HPLC system is then switched to an acetonitrile–water gradient elution program. The preconcentrated analytes are eluted from, and separated by, the 3-cm C_8 precolumn and determined by UV absorption. The total analytical time is 25 min. The lowest detectable concentrations are in the range of $2.5 \cdot 10^{-9} - 11.0 \cdot 10^{-9}$ g/ml for the five analytes investigated with 10 ml of sample.

INTRODUCTION

The use of solid sorbents for the preconcentration of organic pollutants in water is well documented [1,2]. When any of these solid sorbents is contained in a precolumn, and connected directly to an analytical column in a high-performance liquid chromatographic (HPLC) instrument, a technique known as on-line preconcentration results [3]. This method has received much recognition in the past several years owing to its relative simplicity, good sensitivity, and adaptability to automation [4,5].

Prior to the development of the combined technique, in which a precolumn and an analytical column were connected in series, sample water was passed through an analytical column in order to concentrate analytes at the head of the column packing.

[a] Present address: Department of Chemistry, McMaster University, Hamilton, Ontario L8S 4L8, Canada.

0021-9673/91/$03.50

Subsequent application of mobile phase to the analytical column resulted in the separation and determination of analytes [6,7]. This technique, a precursor to on-line preconcentration, is known as on-column preconcentration. Later analysts found it unwise to pass large volumes of aqueous sample through an analytical column as degradation of the column packing occurred. As a result, separate precolumns were installed to preconcentrate the analytes in the sample water [8].

A wide variety of commercially packed precolumns are now available. Goewie *et al.* [9] have shown that these precolumns can provide large numbers of theoretical plates. This fact presents the possibility of developing a rapid on-column preconcentration technique, employing a short precolumn, for both the preconcentration and separation of analytes.

In this paper, we report the development of an automated on-column preconcentration method for the determination of benomyl, its degradation product carbendazim (MBC), aldicarb, and its degradation products aldicarb sulphoxide and aldicarb sulphone. These analytes are of concern in Ontario environmental samples. Aldicarb (manufactured by Union Carbide under the tradename Temik) is quite toxic as evidenced by its LD_{50} value (for rats) of 0.6 mg/kg. Aldicarb sulphoxide and aldicarb sulphone are relatively polar and difficult to separate owing to their short retention times on reversed-phase material [10]. Residues of intact benomyl are difficult to determine because of its instability in organic solvent [11], and its low solubility in water [12]. Marvin *et al.* [13] have reported an automated on-line preconcentration technique or the determination of benomyl and MBC in water, and Chaput [10] has reported an on-line preconcentration method for the determination of aldicarb species in water.

Also reported in this paper are the factors affecting the use of the short precolumn for both the preconcentration and separation of the aforementioned analytes from water. These factors included: (1) size of packing material used in the precolumn; (2) properties of the solid sorbent phase; (3) sample volume; (4) minimum detectable concentrations; and (5) sample matrix.

EXPERIMENTAL

Solvents

Acetonitrile was of HPLC grade from Fisher Scientific (Fairlawn, NJ, USA), and Caledon Laboratories (Georgetown, Canada). Water used for preparation of standards was distilled in glass in the laboratory.

Pesticides

Solid aldicarb, aldicarb sulphoxide, and aldicarb sulphone standards were obtained from Union Carbide Agriculture Products (Research Triangle Park, NC, USA). Analytical standard of MBC and benomyl was obtained from Du Pont. Benomyl formulation was purchased commercially as Benlate wettable powder (WP) (Wilson Labs., Laval, Canada, 50% active ingredient). Using the method developed by Chiba and Singh [14], the active ingredient in the Benlate WP was determined to be 54.5%, of which 86% was benomyl and 14% was MBC.

The pesticides, listed in the order in which they appear in the chromatograms, are (**1**) aldicarb sulphoxide; (**2**) aldicarb sulphone; (**3**) aldicarb; (**4**) MBC; and (**5**) benomyl.

Preparation of stock standard solutions

Solid standards (with the exception of benomyl) were dissolved in methanol and diluted in methanol. Benomyl was prepared as a suspension of Benlate WP in distilled water.

As benomyl decomposes in water at room temperature [15], and the rate of decomposition is temperature dependent [16], benomyl standard solutions should be refrigerated. Benomyl standard suspensions containing more than its solubility in water, should be thoroughly stirred before dilution to ensure an even distribution of particulate matter in any aliquot removed.

The individual stock standard solutions were diluted with water at different concentrations because of their varying sensitivities to ultraviolet (UV) detection.

Water samples

Standard water samples were prepared by diluting the combined standard solutions (prepared as above) to 1000 ml with distilled water from the laboratory unless otherwise noted.

HPLC apparatus

The HPLC system consisted of a Waters Model 600 Powerline solvent delivery system, a Waters WISP Model 710B sample processor, a Waters Model 484 tunable absorbance UV detector, a Fisher Recordall series 5000 strip chart recorder, and an NEC Powermate 2 computer system (NEC Information Systems, Boxborough, MA, USA) incorporating Waters 810 chromatography software (Waters Assoc., Millford, MA, USA).

The factory-packed precolumns were 5-μm Spherisorb C_{18} (80 Å pore size), 5-μm C_8 (80 Å pore size), 7-μm C_{18} (300 Å pore size), and 5-μm CN (80 Å pore size) 3 cm × 4.6 mm I.D. cartridges from Brownlee Labs. (Santa Clara, CA, USA)[a]. The 10-μm C_{18} (300 Å pore size) 3-cm precolumns were laboratory packed using 10-μm Vydac Reverse Phase TP-201 (Separations Group, Hesperia, CA, USA).

The on-line preconcentration apparatus (Fig. 1) incorporated a high-pressure in-line filter with a 0.5-μm frit from Mandel Scientific (Guelph, Canada), and a Rheodyne Model 7000 two-position six-port switching valve, which was equipped with a Rheodyne Model 5701 air actuator controlled by a Rheodyne Model 7163 solenoid valve kit (Rheodyne, Cotati, CA, USA).

HPLC operating conditions

Wavelength, 220 nm; chart speed, 0.5 cm/min; detector sensitivity, 0.200 a.u.f.s. (1 mV = $1 \cdot 10^{-3}$ a.u.); recorder range, 10 mV f.s.; column temperature, ambient.

On-line preconcentration

A 10-ml volume of water sample was passed through the precolumn while the apparatus was in the "load" position unless otherwise noted.

---

[a] The stationary phases currently available from Brownlee Labs. may differ from those used in this study.

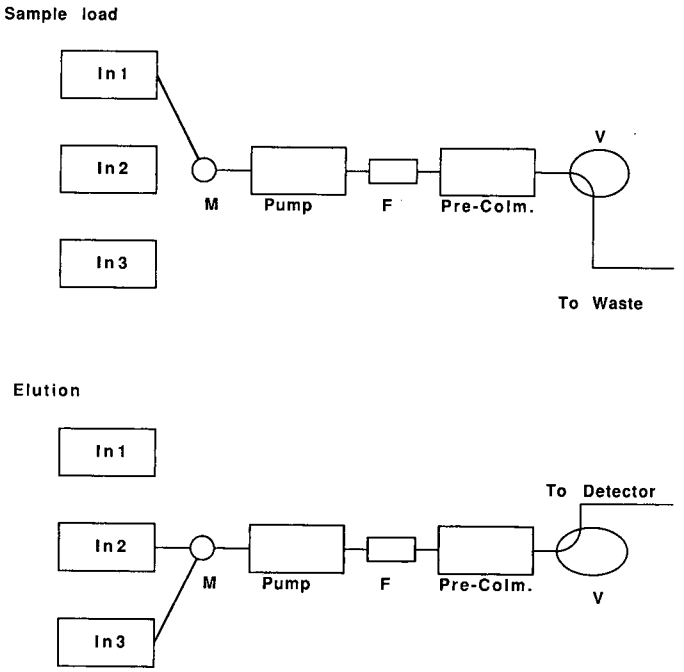

Fig. 1. Schematic diagram of the valve switching system and the directions of liquid flow. V, M, In and F = Valve, mixer, solvent inlets and filter, respectively; Pre-colm. = precolumn. During the sample loading step, In1 dispenses sample water. During the elution steps, In2 dispenses water, and In3 dispenses acetonitrile as part of the mobile phase.

Elution

The following gradient program was run after switching the valves of the "elute" position from the "load" position:

Elapsed time (min)	Flow-rate (ml/min)	Acetonitrile (%)	Water (%)	Curve
Initial	1.0	10	90	
2.5	1.0	10	90	
10.0	1.0	60	40	6
10.5	1.5	60	40	11
15.0	1.5	70	30	6
20.0	1.0	10	90	6

Curve 6 denotes a linear change and curve 11 denotes an immediate change to the described conditions.

RESULTS AND DISCUSSION

The on-line preconcentration valving apparatus is shown in Fig. 1. This apparatus is a modification of the one described in previous papers by Marvin and co-

workers [5,13], but is substantially simpler as only unidirectional elution is required. A simple valving apparatus employing only one valve is sufficient.

A 5-μm C_8, a 5-μm C_{18}, a 7-μm C_{18}, and a 5-μm CN sorbent were investigated for both their retention properties and their abilities to provide adequate separation of the analytes. There was little difference in the degree of retention of the analytes on the 5-μm C_8 and C_{18} precolumns, but the C_8 packing demonstrated superior resolution of MBC and aldicarb. The use of a 5-μm CN or a 7-μm C_{18} resulted in very poor seperation of aldicarb sulphoxide and aldicarb sulphone. A 10-μm C_{18} stationary phase was also investigated, but dit not provide enough theoretical plates to result in adequate separation of the aldicarb sulphoxide and aldicarb sulphone.

Table I shows the pesticides used in the study, their retention times, a comparison of peak areas between those obtained from a preconcentration sample and those obtained by a straight injection of a concentrated standard containing an equal amount of the pesticides, the sample pesticide concentrations, and the minimum detectable concentrations for a 10-ml sample. The minimum detectable concentrations (MDC values) were calculated using a 5:1 signal-to-baseline-noise ratio. The peak-area standard deviations for five replicate samples averaged approximately 3% for each of the analytes.

A sample volume of 7.5 ml was found to result in the best resolution of aldicarb sulphoxide and aldicarb sulphone. Volumes greater than 10 ml result not only in the loss of aldicarb sulphoxide and aldicarb sulphone due to breakthrough, but also gave poorer separation of the two early-eluting analytes. These results are in agreement with those of Chaput [10]. Chaput calculated a 50% loss in theoretical plate number for sample volumes of 20 ml compared with volumes of 10 ml. This theoretical plate loss is due to broadening of the weakly retained analyte peaks as the volume of sample passed through the precolumn increases. This results in little or no separation of the aldicarb sulphoxide and aldicarb sulphone when the maximum sample volume of 10 ml is exceeded.

On the basis of these observations, we judged that a sample volume of 10 ml,

TABLE I

SELECTED PESTICIDES, THEIR RETENTION TIMES (t_R) AVERAGE PERCENTAGE PEAK AREAS ± S.D. AS COMPARED WITH THOSE OBTAINED FROM A STRAIGHT INJECTION OF EQUAL AMOUNTS OF THE PESTICIDES, SAMPLE CONCENTRATIONS AND MDC VALUES FOR A 10-ml SAMPLE AT 220 nm

The data were obtained from five replicate 10-ml samples using the described method and a 5-μm C_8 precolumn. The MDC values were calculated using a 5:1 signal-to-baseline-noise ratio.

No.[a]	Pesticide	t_R (min)	Percentage peak area ± S.D. (%)	Sample concentrations (10^{-9} g/ml)	MDC (10^{-9} g/ml)
1	Aldicarb sulphoxide	4.1	92±2	138	7.0
2	Aldicarb sulphone	4.7	102±3	117	9.0
3	Aldicarb	9.2	104±1	112	11.0
4	MBC	10.3	95±4	47	2.5
5	Benomyl	12.7	94±5	68	9.0

[a] The pesticides are numbered to correspond with those in the figures.

loaded at 5 ml/min onto a 5-μm C_8 precolumn, to be the best combination of experimental conditions. Fig. 2 shows a chromatogram resulting from a distilled water sample containing the five compounds of interest. The sample was analyzed under the aforementioned conditions. The total analytical time is 25 min for one sample. It is interesting to note that MBC can be determined without the use of a buffered mobile phase, which had been necessary in the past to produce a sharp MBC peak for accurate quantitation [13].

Other analysts studying on-line preconcentration [5,10,17,18] have observed that the chromatograms resulting from the analysis of municipal tap waters or natural groundwaters are characterized by large peaks resulting from early-eluting impurities. This was of concern as aldicarb sulphoxide and aldicarb sulphone are eluted on the downslope of these impurities. It was found that this problem could be partially overcome by using UV detection at wavelengths greater than 220 nm. The impurities are much less sensitive to UV detection at wavelengths greater than 230 nm. With the exception of aldicarb sulphone, the other four analytes could be determined at longer wavelengths with substantially less interference from sample matrix impurities. Fig. 3 compares two chromatograms resulting from the analysis of a municipal tap water sample containing 25 ppb (10^{-9} g/ml) of MBC and 100 ppb of benomyl at 220 and 280 nm. The compounds are well separated as sharp peaks in both chromatograms, but the background is substantially better in Fig. 3b (produced at 280 nm) compared to Fig. 3a (produced at 220 nm). Relative peak heights of MBC and benomyl at 280 nm are 60.3 and 94.3%, respectively, of those at 220 nm. Similarly, at 254 nm peak

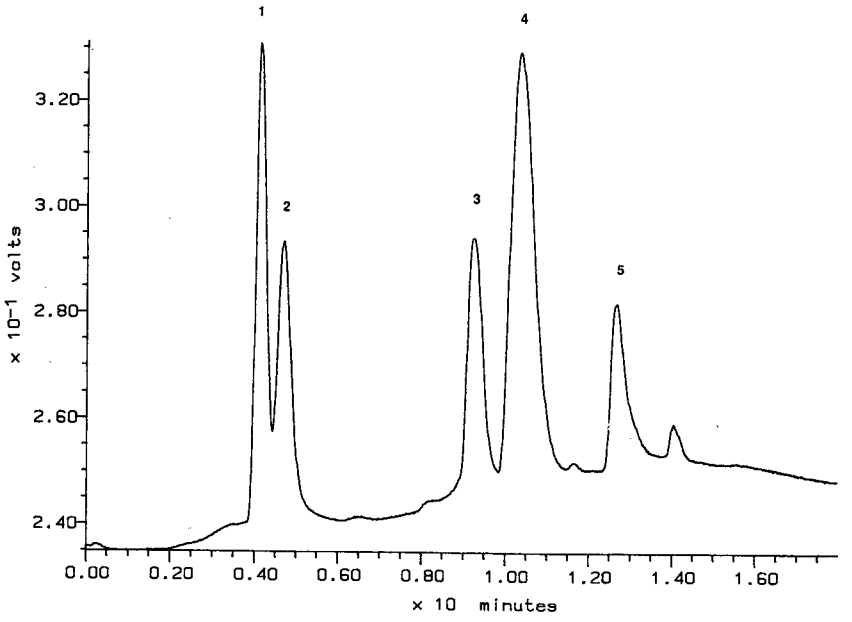

Fig. 2. Chromatogram resulting from the analysis of a 10-ml sample containing the five analytes. The analysis was performed on a 5-μm C_8 precolumn using the described method. The concentrations of the individual pesticides are those listed in Table I. For peak identification, see text.

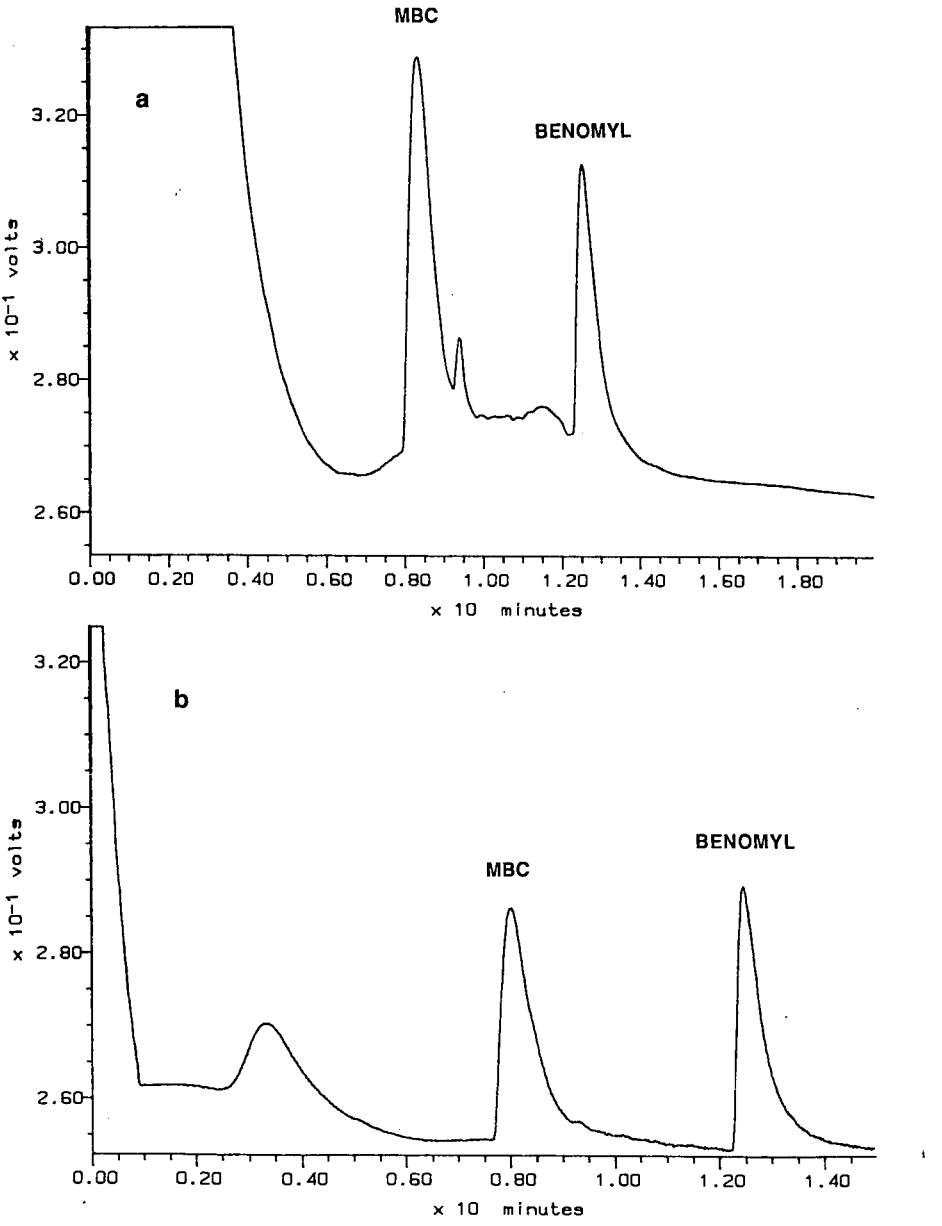

Fig. 3. A comparison of samples containing residues of MBC and benomyl only, at two different UV wavelengths: (a) 220; (b) 280 nm. The samples were analyzed using the described method.

heights of aldicarb sulphoxide and aldicarb were 96.0 and 78.0%, respectively, of those at 220 nm.

Additional experiments with sample water containing only two of the less polar analytes, MBC and benomyl, have shown that sample sizes of the order of 100 ml can

be analyzed using the described method. Even with these larger sample sizes, separation of the analytes was good and the peak profiles were sharp enough for accurate quantitation. The larger sample sizes result in significantly lower MDC values, although the period of time required for analysis becomes longer.

CONCLUSIONS

Our results indicate that a 3-cm precolumn packed with 5-μm C_8 is best. Precolumns packed with 5-μm C_{18}, 10-μm C_{18}, 5-μm CN and 7-μm C_{18} precolumns were less effective. Under the described conditions, the analytes can be detected at the 10 ppb level using 10 ml of sample water. The total analysis time is 25 min.

The on-line preconcentration method described in this paper using a 3-cm precolumn is applicable as a simple, rapid, inexpensive, qualitative and quantitative procedure for all five analytes of interest. Even difficult separations, such as that of aldicarb sulphoxide and aldicarb sulphone, can be accomplished effectively. The method is sensitive and will provide reliable and reproducible results for practical applications. The method also offers the possibility of complete automation for the analysis of many samples.

ACKNOWLEDGEMENT

The authors wish to thank the Research and Technology Branch of the Ontario Ministry of the Environment for financial support.

REFERENCES

1 G. A. Junk and J. J. Richard, *Anal. Chem.*, 60 (1988) 451.
2 E. Chladek and R. S. Maranaro, *J. Chromatogr. Sci.*, 22 (1984) 313.
3 M. C. Harvey and S. D. Stearns, in J. F. Lawrence (Editor), *Liquid Chromatography in Environmental Analysis*, Humana Press, Clifton, NJ, 1984, Ch. 7,pp. 332–338.
4 K. A. Ramsteiner, *J. Chromatogr.*, 465 (1989) 410.
5 C. H. Marvin, I. D. Brindle, C. D. Hall and M. Chiba, *J. Chromatogr.*, 503 (1990) 167.
6 J. J. Kirkland, *Analyst (London)*, 99 (1974) 859.
7 J. N. Little and G. J. Fallick, *J. Chromatogr.*, 112 (1975) 389.
8 K. Ogan, E. Katz and W. Slavin, *J. Chromatogr. Sci.*, 16 (1978) 517.
9 C. E. Goewie, M. W. F. Nielen, R. W. Frei and U. A. Th. Brinkman, *J. Chromatogr.*, 301 (1984) 325.
10 D. Chaput, *J. Assoc. Off. Anal. Chem.*, 69 (1986) 6.
11 M. Chiba, *J. Agric. Food Chem.*, 25 (1977) 368.
12 R. P. Singh and M. Chiba, *J. Agric. Food Chem.*, 33 (1985) 63.
13 C. H. Marvin, I. D. Brindle, R. P. Singh, C. D. Hall and M. Chiba, *J. Chromatogr.*, 518 (1990) 242.
14 M. Chiba and R. P. Singh, *J. Agric. Food Chem.*, 34 (1986) 108.
15 R. P. Singh, I. D. Brindle, C. D. Hall and M. Chiba, *J. Agric. Food Chem.*, 38 (1990) 1758.
16 J. Northover and M. Chiba, *J. Agric. Food Chem.*, 37 (1989) 1416.
17 W. Golkiewicz, C. E. Werkoven-Goewie, U. A. Th. Brinkman and R. W. Frei, *J. Chromatogr. Sci.*, 21 (1983) 27.
18 R. J. Bushway, *J. Chromatogr.*, 211 (1981) 135.

Journal of Chromatography, 555 (1991) 155–162
Elsevier Science Publishers B.V., Amsterdam

CHROM. 23 397

Reversed-phase high-performance liquid chromatographic determination of linear alkylbenzenesulphonates in river water at ppb[a] levels by precolumn concentration

YUKIO YOKOYAMA* and HISAKUNI SATO

Laboratory of Analytical Chemistry, Faculty of Engineering, Yokohama National University, 156 Tokiwadai, Hodogaya-ku, Yokohama 240 (Japan)

(First received December 27th, 1990; revised manuscript received April 24th, 1991)

ABSTRACT

A high-performance liquid chromatography method for the determination of linear alkylbenzenesulphonates (LASs) in river waters has been developed. The ppb levels of LASs can be determined by reversed-phase high-performance liquid chromatography with ultraviolet detection after on-line anion-exchange concentration and successive injection. LASs were quantitatively concentrated on the anion-exchange precolumn and easily cleaned up from river water matrix, because of its specific affinity, for the anion-exchange resin. A weak non-polar reversed-phase column was useful for the determination of LASs. The relationships between concentration and summation of peak areas were linear from 10 to 200 ppb for total LAS concentrated from 5 ml of standard solutions. Overall recovery for total LAS was found to be 99%. Total LAS in the Tama River waters was determined to be around 100 ppb by the proposed method.

INTRODUCTION

Synthetic anionic surfactants are extensively used as detergents, and their subsequent direct disposal into waste water causes environmental pollution. In particular, linear alkylbenzenesulphonates (LASs), a major constituent of laundry detergents, are consumed in great quantity and discharged into environmental waters. Thus various kinds of techniques for the determination of trace levels of LASs in environmental samples such as river waters have been proposed by many workers.

Colorimetric methods [1], which provide information on total anionic surfactants in aqueous samples, are not specific for LAS.

Gas chromatography techniques have been used for the specific determination of LASs in environmental samples; however, complicated desulphonation [2,3] or derivatization [4,5] is required to convert LASs into volatile compounds.

Recently a ^{13}C NMR technique [6] has been proposed. This is, however, a qualitative method for the confirmation of LAS-type compounds.

High-performance liquid chromatography (HPLC) is widely accepted as a spe-

[a] Throughout this article, the American billion (10^9) is meant.

0021-9673/91/$03.50

cific method for the determination of LASs in various environmental samples. Nakae *et al.* have proposed a reversed-phase HPLC technique, using an ODS silica gel column, for the separation of LASs consisting of a mixture of homologues of various alkyl chain length and their phenyl position isomers [7], and for the determination of trace amounts of LASs in river waters [8]. The method seems to be useful for relatively clean samples because no clean-up procedures have been described. Ion-exchange HPLC has also been applied to the separation and determination of mixtures of ionic surfactants [9,10]. However, the methods are not suitable for the determination of LASs in environmental samples.

In order to extend the column life, the injection of environmental samples such as river waters directly into the analytical column should be avoided. In addition, it is necessary to concentrate trace levels of analytes in water for their microdetermination. Thus, several concentration and clean-up procedures prior to HPLC determination of trace levels of LASs have been proposed recently. Solvent extraction procedures [11,12] are somewhat cumbersome. Because of its simplicity, solid-phase extraction is frequently used for the prepurification of LASs from various environmental matrices [5,13–15].

This paper presents a newly developed on-line precolumn concentration and clean-up procedure prior to reversed-phase HPLC determination of LASs in river waters. Ion-exchange precolumns were successfully employed for the pretreatment of such anionic surfactants. Adequate conditioning of the precolumn was necessary for the on-line introduction of LASs into the reversed-phase analytical column. The application of this procedure to other types of anionic and cationic surfactants is also described.

EXPERIMENTAL

Chemicals

Sodium linear 4-alkylbenzenesulphonates (laundry analysis grade, C_{10}–C_{14}) as LAS standards were obtained from Wako (Osaka, Japan), hard sodium alkylbenzenesulphonates (branched ABSs) from Tokyo Kasei Kogyo (Tokyo, Japan), sodium alkylsulphates (ASs, C_{12}–C_{15}) from Asahi Denka Kogyo (Tokyo, Japan), alkyltrimethylammonium salts (ATMAs) —*n*-dodecyl-, *n*-tetradecyl- and *n*-hexadecyltrimethylammonium bromide— from Tokyo Kasei Kogyo, and sodium perchlorate and acetonitrile of guaranteed grade from Wako. Water and acetonitrile were distilled before use.

Analytical columns

A Wakosil 5C4 (150 × 4.6 mm I.D., butyl silica gels, particle size 5 μm, weak non-polar reversed-phase column) obtained from Wako was used for all analytical separations.

Precolumns

A TSK precolumn IC-Conc-A (Tosoh, anion-exchange precolumn, 10 × 3 mm I.D., capacity 2.1 μequiv. per column) was used for the concentration of LASs (or ASs), and a TSK precolumn IC-Conc-C1 (Tosoh, cation-exchange precolumn, 10 × 3 mm I.D., 0.85 μequiv. per column) was used for the concentrations of ATMAs.

Instruments

The chromatography system consisted of an Erma (Tokyo, Japan) Model ERC-3510 degasser, a Tosoh (Tokyo, Japan) Model CCPE pump, a Rheodyne (Cotati, CA, USA) 7125 sample loop injector, a Gasukuro Kogyo (Tokyo, Japan) Model 502T variable-wavelength UV detector and a Hitachi (Tokyo, Japan) Model D-2000 integrator. A Shimadzu (Kyoto, Japan) Model RID-6A refractive index (RI) detector was used for detecting UV-transparent ASs and ATMAs. The two detectors were set in series. A line filter (Gasukuro Kogyo, with a 2-μm stainless-steel frit) was located between pump and injector to remove insoluble substances resulting from abrasion of plunger seals in the pump heads and/or insoluble substances from the eluent reservoir. A column inlet filter (Rheodyne 7335) was also placed between injector and analytical column.

Chromatography conditions

Acetonitrile–water (50:50, v/v) containing 0.1 *M* sodium perchlorate was used as the mobile phase, which was sonicated for 5 min after preparation. All separations were carried out by isocratic elution at ambient temperature. The flow-rate of the mobile phase was kept at 1.0 ml/min throughout the experiments. The wavelength of the UV detector was adjusted to 220 nm for the detection of LASs.

Concentration and clean-up procedure

(1) The anion-exchange precolumn was connected to the proper valve ports of the Rheodyne 7125 injector in place of a sample loop.

(2) At the LOAD position of the valve, 1 ml of 0.1 *M* sodium perchlorate was passed through the precolumn from the needle port with a 2.5-ml gas-tight syringe (Hamilton, Reno, NV, USA) to convert the anion exchanger into ClO_4^- form.

(3) The precolumn was rinsed with 1 ml of distilled water.

(4) A 5.0-ml aliquot of sample water, previously filtered through a 0.2-μm disposable cellulose acetate filter (Advantec, Tokyo, Japan), was repeatedly introduced into the precolumn with the 2.5-ml gas-tight syringe from the needle port of the Rheodyne valve at the rate of about 5-ml/min.

(5) The needle port and the precolumn were rinsed with 1 ml of distilled water.

(6) A 1-ml sample of 0.1 *M* sodium perchlorate was passed through the precolumn. In the case of a standard or a clean solution of LASs, this step can be omitted.

(7) The precolumn was rinsed with 1 ml of distilled water.

(8) A 1-ml volume of acetonitrile–water (50:50, v/v) was passed through the precolumn.

(9)The valve was turned to the INJECTION position, and the concentrated LAS on the precolumn was introduced into the analytical column.

RESULTS AND DISCUSSION

Precolumn concentration and clean-up

Reversed-phase silica gel cartridges have been used to concentrate LASs in environmental samples [5,13]. However, it is thought, that several kinds of neutral compounds act together with LASs on the reversed-phase cartridge and therefore probably interfere with the determination of LASs. The specific concentration and clean-up of LASs seem to be difficult.

In the method presently described, the anion-exchange precolumn was efficiently used for the concentration and clean-up of LASs in river waters.

In stage 4 of the concentration procedure, described in the Experimental section, LASs were quantitatively adsorbed and concentrated on the anion-exchange resin of ClO_4^- form by means of both ion-exchange interaction and hydrophobic interaction. A 5.0-ml portion of the sample solution was injected into the precolumn correctly with using a 2.5-ml syringe with less than 0.1% deviation in the sum of the volumes. Inorganic cations and very polar compounds were removed from the precolumn by water in stage 5. In stage 6, hydrophilic anions were completely eluted from the precolumn by 0.1 *M* sodium perchlorate. LASs remain in the precolumn because of their hydrophobicity. In stage 8, non-polar compounds, non-ionic surfactants and cationic surfactants were eluted from the precolumn by the aqueous, salt-free, acetonitrile solution. LASs are never eluted from the precolumn because of ion-exchange interaction between LASs and anion-exchange resin.

The last conditioning step (stage 8) just before the injection of concentrated LASs should never be omitted. The acetonitrile concentration of the conditioning solution must be the same as that of the mobile phase used for the analytical HPLC. If this step is omitted, a large volume (the dead volume of the precolumn) of aqueous solution of different composition from that of the mobile phase containing acetonitrile is injected into the analytical column. Consequently, the equilibrium between the mobile phase and the stationary phase is destroyed, and a large number of pseudo peaks appear on the chromatogram. It then becomes difficult to differentiate the analyte peaks from the pseudo peaks. This is because of the difference in UV absorptivity between water and acetonitrile at low wavelengths such as 220 nm. In contrast, there is no baseline problem at detection wavelengths higher than 260 nm, which are unavailable for the detection of LASs. In such a case, analytes are often dissolved in the mobile phase. However, the present method does not, of course, allow rinsing of the precolumn with the mobile phase. Since 0.1 *M* sodium perchlorate is transparent to UV radiation at 220 nm, the salt-free mobile phase was adequate for the conditioning solvent of the precolumn.

Aliphatic anionic surfactants such as ASs, also concentrated in the precolumn, could be cleaned up and determined as well as LASs.

The present procedure can be applied to the prepurification of cationic surfactants such as ATMAs by using a cation-exchange precolumn in the same way.

Although non-ionic surfactants such as polyoxyethylenenonylphenylether could be concentrated into an ODS precolumn, the determination was not successful because of the loss of the analytes at the final conditioning step.

Analytical column for LAS determination

Reversed-phase HPLC with an ODS silica gel column is widely used for the qualitative analysis of LAS homologues and phenyl position isomers [7,15]. It is thought, however, that such a non-polar column is not suitable for the determination of LASs because the detection sensitivity of LASs is decreased due to the peak distribution. Recently, a weak non-polar reversed-phase column, providing a single peak for the individual homologues, has been used for the determination of LASs [15].

As a result of examining several commercially available columns for the present method, a 15-cm Wakosil 5C4 column was found to be adequate for the purpose,

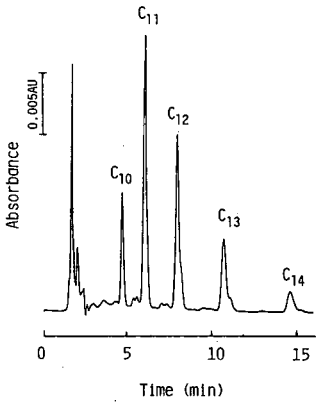

Fig. 1. Chromatogram of an LAS standard. Column: Wakosil 5C4, 150 × 4.6 mm I.D. Mobile phase: 0.1 *M* sodium perchlorate in acetonitrile–water (50:50, v/v). Flow-rate: 1 ml/min. Detection: UV 220 nm. Sample size: 100 ppb × 5.0 ml.

giving a simple chromatogram for LASs, as shown in Fig. 1. Each peak corresponds to an LAS homologue of alkyl chain length between C_{10} and C_{14}. No separation of their phenyl isomers is observed. The mobile phase system used was based on the procedure previously reported by Nakae *et al.* [7,8].

On the other hand, it seems difficult to determine branched ABSs because it gives irregularly complicated peaks at retention times between 3 and 8 min.

Quantification

It was necessary to concentrate 5 ml of a sample solution for the determination of ppb levels of LASs. Calibration plots were constructed from measurements of peak areas *versus* known concentrations of total LAS in the standard solutions. The distribution of LAS homologues was dependent on the standard LAS reagent used.

The calibration data are summarized in Table I. The total peak area calculated by the summation of areas of individual homologues was reproducible. Total

TABLE I

CALIBRATION DATA FOR LAS DETERMINATION

Alkyl chain length	C.V. (%) of peak area ($n=5$)	Regression line (10–200 ppb)[a]	Regression coefficient (r)
C_{10}	0.7	$y=0.352\cdot10^3x-0.04\cdot10^3$	0.9999
C_{11}	1.1	$y=1.004\cdot10^3x-0.01\cdot10^3$	0.9999
C_{12}	2.2	$y=0.798\cdot10^3x-0.12\cdot10^3$	0.9997
C_{13}	7.0	$y=0.463\cdot10^3x-0.64\cdot10^3$	0.9975
C_{14}	21.0	$y=0.184\cdot10^3x-1.16\cdot10^3$	0.9871
Total LAS	3.0	$y=2.800\cdot10^3x-1.94\cdot10^3$	0.9997

[a] y = Peak area (integration units); x = concentration (ppb).

TABLE II

RECOVERY DATA FOR LAS DETERMINATION ($n=3$)

	Alkyl chain length					Total LAS
	C_{10}	C_{11}	C_{12}	C_{13}	C_{14}	
Recovery (%)	96	97	98	105	104	99

amounts of LASs could be determined with a coefficient of variation (C.V.) of 3%, although the C.V. values of the peak areas of C_{13} and C_{14} homologues were relatively large. The relationship between the total LAS concentration and the total peak areas was linear from 10 to 200 ppb, although there were some differences in the linearity of the calibration plots for individual homologues. The recovery of total LAS, examined by 100 ppb standard LAS solution, was calculated to be 99%, as shown in Table II.

The method can be applied to other anionic and cationic surfactants. Typical chromatograms of ASs and ATMAs concentrated from 5 ml of sample volume are shown in Figs. 2 and 3, respectively. ATMAs concentrated on the cation-exchange precolumn were separated under the same eluting conditions as used in the LAS determination. The regression coefficients for calibration plots of ASs and ATMAs are listed in Table III. Since these surfactants have less UV detectability, their detection sensitivities are considerably lower than those of LASs. Sub-ppm to ppm levels could be determined by means of concentration of a 5 ml sample.

Interference for LAS determination

Aliphatic anionic surfactants such as ASs probably interfere in the determina-

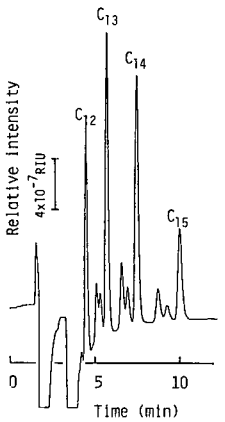

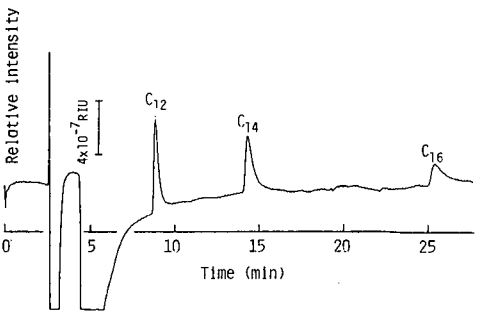

Fig. 2. Chromatogram of an AS standard. Column: Wakosil 5C4, 150 × 4.6 mm I.D. Mobile phase: 0.1 *M* sodium perchlorate in acetonitrile–water (50:50, v/v). Flow-rate: 1 ml/min. Detection: RI. Sample size: 5 ppm × 5.0 ml.

Fig. 3. Chromatogram of an ATMA standard. Column: Wakosil 5C4, 150 × 4.6 mm I.D. Mobile phase: 0.1 *M* sodium perchlorate in acetonitrile–water (50:50, v/v). Flow-rate: 1 ml/min. Detection: RI. Sample size: 500 ppb each × 5.0 ml.

TABLE III

REGRESSION COEFFICIENTS (r) OF CALIBRATION LINES FOR ASs AND ATMAs

	r					Total
	C_{12}	C_{13}	C_{14}	C_{15}	C_{16}	
AS (0.2–5 ppm)	0.999	0.999	0.999	0.996		0.999
ATMA (0.1–1 ppm)	0.997		0.996		0.973	

tion of LASs, because they act like LASs in the precolumn and are chromatographed as shown in Fig. 2. However, the amounts of intact aliphatic anionic surfactants in environmental waters are thought to be smaller than those of LASs, and their UV sensitivity is two orders of magnitude lower than that of LASs. Therefore, the influence of aliphatic anionic surfactants on the determination of LASs is negligible unless they coexist in large quantities with LASs.

Application to river waters

The total amount of LASs in the Tama River in Tokyo (sampling points: Gasu Bridge and Maruko Bridge) was determined by the proposed method. A typical chromatogram of the Tama River water (Gasu Bridge) is shown in Fig. 4. The composition of LAS homologues in Tama River was consistent with that previously reported by Nakae *et al.* [8], *i.e.* LASs in the river water consisted of shorter alkyl chain length homologues compared with the standard LASs shown in Fig. 1. The

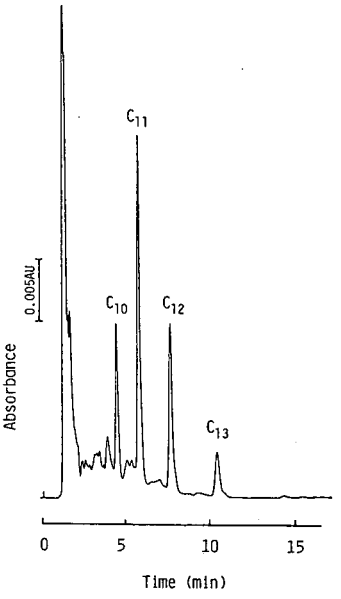

Fig. 4. Chromatogram of Tama River water (Gasu Bridge). Column: Wakosil 5C4, 150 × 4.6 mm I.D. Mobile phase: sodium perchlorate in acetonitrile–water (50:50, v/v). Flow-rate: 1 ml/min. Detection: UV 220 nm. Sample size: 5.0 ml.

alkyl chain distribution was not related to the location of the sampling point.

Total LAS was determined to be 86 ppb and 91 ppb for the river waters from Gasu Bridge and Maruko Bridge, respectively. The results were obtained 5 h after sampling.

The concentration of LASs in the Tama River waters gradually decreased after sampling, and the chromatographic peaks corresponding to LASs disappeared after 72 h at room temperature. In contrast, the 100 ppb standard LASs, which was dissolved in distilled water and stored in a polypropylene bottle at room temperature, was stable and its concentration was unchanged for a long time. Although the concentration of 100 ppb LASs dissolved in tap water did not change after 72 h, the concentration of LASs dissolved in water from the Shiraito Falls (a relatively clean environment in Japan) decreased to 70% of the initial concentration at 72 h after preparation. This may have been the result of biodegradation. The results clearly show that measurements must be made immediately after sampling if LASs in environmental waters are to be quantified accurately.

The above discussion shows that the precolumn concentration procedure presently described is useful for the immediate fixation of LASs, being easy to execute at the site of sampling. The proposed method is useful for the microdetermination of LASs in river waters.

REFERENCES

1 S. Motomizu, S. Fujiwara, A. Fujiwara and K. Toei, *Anal. Chem.*, 54 (1982) 392.
2 Q. W. Osburn, *J. Am. Oil Chem. Soc.*, 63 (1986) 257.
3 J. Waters and J. T. Garrigan, *Water Res.*, 17 (1983) 1549.
4 H. Hon-nami and T. Hanya, *J. Chromatogr.*, 161 (1978) 205.
5 M. L. Trehy, W. E. Gledhill and R. G. Orth, *Anal. Chem.*, 62 (1990) 2581.
6 E. M. Thurman, T. Willoughby, L. B. Barber, Jr. and K. A. Thorn, *Anal. Chem.*, 59 (1987) 1798.
7 A. Nakae, K. Tsuji and M. Yamanaka, *Anal. Chem.*, 53 (1981) 1818.
8 A. Nakae, K. Tsuji and M. Yamanaka, *Anal. Chem.*, 52 (1980) 2275.
9 H. Yoshimura, S. Tanaka, Y. Fujiyama, T. Sugiyama and T. Nagai, *Hippon Kagaku Kaishi*, (1984) 445.
10 J. Weiss, *Tenside Surfactants Deterg.*, 23 (1986) 237.
11 T. Matsueda, Y. Osaki and S. Shigee, *Bunseki Kagaku*, 31 (1982) 59.
12 A. Marcomini and W. Giger, *Anal. Chem.*, 59 (1987) 1709.
13 M. Kikuchi, A. Tokai and T. Yoshida, *Water Res.*, 20 (1986) 643.
14 E. Matthijs and H. de Henau, *Tenside Surfactants Deterg.*, 24 (1987) 193.
15 M. A. Castles, B. L. Moore and S. R. Ward, *Anal. Chem.*, 61 (1989) 2534.

Journal of Chromatography, 555 (1991) 163–171
Elsevier Science Publishers B.V., Amsterdam

CHROM. 23 394

Correlation analysis in liquid chromatography of metal chelates

II. One-dimensional retention–mobile phase composition (physicochemical property) models in reversed-phase liquid chromatography

A. R. TIMERBAEV*, I. G. TSOI and O. M. PETRUKHIN
Mendeleev Moscow Institute of Chemical Technology, 125190 Moscow (USSR)
(First received December 28th, 1990; revised manuscript received April 24th, 1991)

ABSTRACT

The applicability of linear correlation models for describing the effect of mobile phase composition and properties on the retention of metal chelates in reversed-phase liquid chromatography is demonstrated. The macroscopic (dielectric constant, surface tension, viscosity, concentration of organic modifier, distribution constant in an *n*-octanol–water system, etc.) and microscopic (characteristics of donor and acceptor ability) parameters of binary water–organic mixtures are used as variables. Although each of the studied parameters alone is somewhat limited in application, together they allow retention values to be estimated and the chromatographic behaviour of metal chelates to be predicted. The dominant influence of mobile phase composition and proton-donating ability on chelate retention in reversed-phase liquid chromatography is confirmed.

INTRODUCTION

The complex polyfunctional structure of metal chelates requires an extensive application of mathematical modelling to describe their liquid chromatographic behaviour at the quantitative level [1–4]. In a previous paper [1] we confirmed the necessity for the development of multiparametric correlation models based both on the structural parameters of chelates and on the parameters of a chromatographic system. This paper deals with the effect of mobile phase composition and physicochemical properties on metal chelate retention in reversed-phase liquid chromatography (RPLC) and is the next stage in developing such models.

EXPERIMENTAL

The synthesis of metal chelates (dialkyldithiocarbamates and dialkyldithiophosphates) and the conditions of the chromatographic experiments are described in

0021-9673/91/$03.50

ref. 1. Parameters for organic solvents and the corresponding binary water–organic mixtures were taken from refs. 5–11.

RESULTS AND DISCUSSION

Correlation dependences of the general type:

$$\log k' = a + bx \tag{1}$$

where k' is the capacity factor and x is the eluent parameter (or its logarithmic function), are widely used in RPLC of organic compounds to describe the effect of the mobile phase and to optimize its composition. There is every reason to believe that one-dimensional models of the type in eqn. 1 may be used to estimate retention parameters of the sulphur-containing chelates under consideration. Firstly, owing to the covalent character of metal–ligand bonds and the small effective charge of the metal atom, the major contribution to the intermolecular interactions within a chromatographic system is made by the organic part of the molecule. Secondly, most chelates of a given type are relatively stable in a chromatographic process, *i.e.* the interphase distribution may be considered to be the main type of physico-chemical equilibrium. Moreover, as was shown in ref. 12, the behaviour of sulphur-containing chelates in RPLC is well described in terms of the solvophobic theory [13]. Therefore the effect of the mobile phase may be evaluated by such parameters as surface tension, dielectric constant, characteristics of donor–acceptor ability, etc.

The mobile phase parameters as well as structural parameters of chelates [1] should not be selected formally. For example, determination of the parameters most closely connected to retention values provides additional information for the theoretical understanding of the retention mechanism. On the other hand, the readily accessible x parameters affect the selection, since the main purpose of the correlation analysis is a practical one —to obtain the means of predicting relative changes of retention and to optimize separation. One final task of this study was to confirm that the principles of liquid chromatography of organic compounds may be applied to metal chelates.

All studied parameters x may be conditionally divided into two groups: macroscopic parameters characterize the properties of the mobile phase as a continuous medium, and molecular parameters reflect the ability of the mobile phase to participate in intermolecular interactions of different types. The former comprise such physical–chemical properties of solvents as surface tension, viscosity, dielectric permeability, hydrophobicity, etc., and the latter parameters of electron- and proton-donating ability.

Macroscopic parameters of mobile phase

Concentration of organic modifier. The concentration of the organic component (the simplest characteristic of mobile phase composition) was experimentally shown to be indicative of eluent strength in RPLC with regard to compounds of the most diverse nature, including metal chelates [14,15].

According to the theoretical calculations of free energies of intermolecular interactions of metal chelates in RPLC systems determined by the mathematical treatment of solvophobic theory [16] (for more details see ref. 12), the dependence of $\log k'$

values on the volume ratio of the organic solvent is almost linear (Fig. 1; the model system is mercury diethyldithiophosphate–octadecylsilanized silica gel–dioxane–water) over a wide range of compositions (from 40 to 100% in the case under consideration). The experimental dependences of capacity factors *vs.* composition of mobile phases modified by various organic solvents (Fig. 2a) are fairly well described by the model:

$$\log k' = a - bc \tag{2}$$

(r = 0.973–0.998; s = 0.06–0.08). A mobile phase of water–isopropanol is the only exception. In this case another approach is necessary, based on the replacement model developed by Snyder [17]. According to this model, at high concentrations of the organic modifier the following linear correlation applies:

$$\log k' = a - b\log C \tag{3}$$

where C is molar concentration of the organic solvent. In the above example, changing the coordinates system from eqn. 2 to eqn. 3 results in better linear correlation (Fig. 2b). This shows that solvation processes are most marked when mobile phases are modified by isopropanol. This is consistent with the fact that isopropanol is the most hydrophobic of all solvents studied.

Hydrophobicity. According to both the solvophobic theory and the concept of competitive adsorption (the basis of our study of the behaviour of metal chelates in

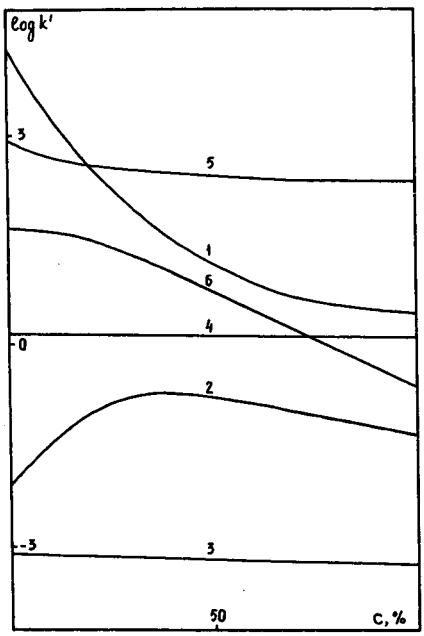

Fig. 1. Energetic contributons of the various parameters to log k' values at different mobile phase compositions. 1,2 = Formation of cavity in mobile phase [$\Delta A\gamma N$ and $(k^e\text{-}1)A_s\gamma N$, respectively], 3 = Van der Waals interactions; 4 = dipole–dipole interactions; 5 = changes of mobile phase free volume; 6 = total dependence. A and A_s are the surface area of the cavity and a solvent molecule, respectively; γ is the surface tension value; N is Avogadro's number and k^e is the dimensionless value.

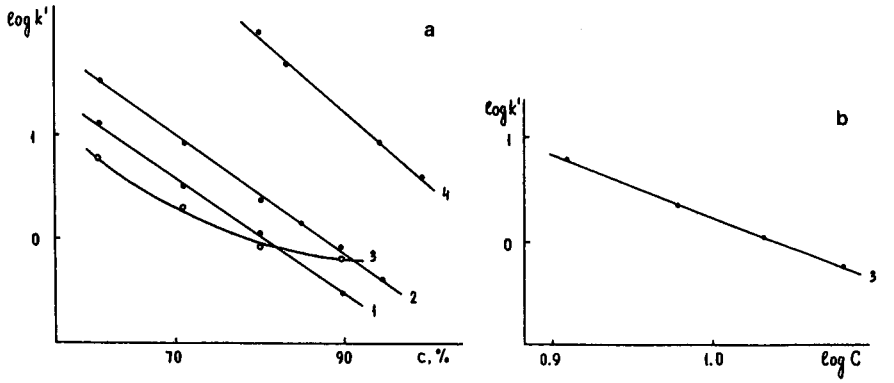

Fig. 2. Dependence of the retention parameters of cobalt (1, 2) and mercury (3, 4) diethyldithiocarbamates on (a) volume and (b) molar concentration of organic modifier in mobile phase. 1 = Dioxane; 2 = acetonitrile; 3 = isopropanol; 4 = methanol. Stationary phase: octadecylsilanized silica gel.

RPLC) chelate retention should depend on the hydrophobic properties of the mobile phase. The hydrophobicity of eluent was evaluated by measuring the same parameter as was used for the sorbate [1] – the distribution constant in an *n*-octanol–water system (P_S) [18]. The dependence of log k' of metal diethyldithiocarbamates on the P_S values of water–methanol and water–acetonitrile mixtures (Fig. 3) is well described by the equation:

$$\log k' = a - b \log P_S \tag{4}$$

but only for large contents of organic component, *i.e.* at weak eluent structuring. The non-linearity region for water–methanol mobile phases is extended, apparently because methanol molecules are capable of entering the hydrated structures of the associated mobile phase without destroying them.

Methylene selectivity. Another parameter which affects mobile phase relative hydrophobicity is methylene selectivity, log α_{CH_2}, defined as the difference in retention

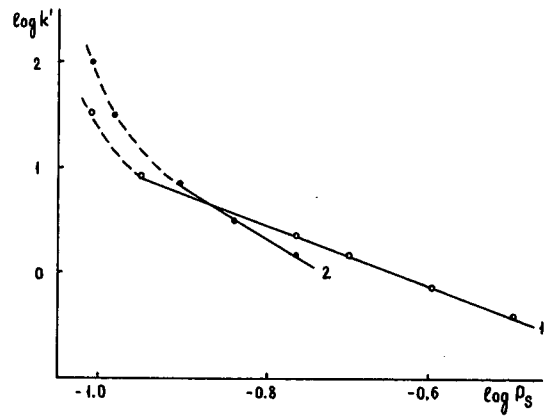

Fig. 3. Effect of mobile phase hydrophobicity on retention of mercury diethyldithiocarbamate. 1 = Methanol–water; 2 = acetonitrile–water.

of two adjacent alkyl homologues. It is a convenient measure of the influence of mobile phase composition on metal chelates with various alkyl substituents. The calculated log α_{CH_2} values agree well with the data calculated from retention parameters of various classes of organic compounds (Table I). The effect of the methylene selectivity of a dioxane–water mobile phase on the retention of metal dithiocarbamates is described by the equation:

$$\log k' = a + b \log \alpha_{CH_2} \tag{5}$$

with good correlation (r = 0.990–0.997; s = 0.04–0.06).

Surface tension. The solvophobic theory of RPLC established the linear correlation between retention parameters and the surface tension of the mobile phase [19]. For mixtures of water and aprotic solvents (acetonitrile, dioxane) the log k' *vs.* γ dependences (Fig. 4) take the shape of a linear function (r = 0.991–0.998; s = 0.04–0.08). Deviations from linearity are observed for water–alcoholic eluents; these are less pronounced for methanol than for isopropanol. Nevertheless, the importance of γ as a measure of mobile phase eluting strength in relation to metal chelates is beyond doubt.

Viscosity. The molecular properties affecting viscosity are volume, polarizability, dipole moment, molecular weight, etc. Most of these properties determine simultaneously the specific interactions of sorbate within the mobile phase. Thus, the relation between log k' and viscosity (η) must also reflect the intermolecular interactions of metal chelate with eluent components. However, the majority of dependences are non-linear (Fig. 5). This may be attributed to the fact that changes in viscosity with changing water–organic solution composition are non-monotonous [5]. The peak dependence is determined by the concentration of the organic component and by its hydrophobicity. Therefore the heuristic properties of η values apply only over a limited range of component ratios that correspond to the region of monotonous viscosity changes (as a rule, the range in which the organic component does not exceed 60%).

Dielectric constant (ε). The experimental data show the increase in chelate retention with increasing dielectric permeability of the mobile phase (Fig. 6). In general the obtained dependences have a high degree of correlation (r = 0.998–0.999; s = 0.01–0.04) regardless of the type of mobile phase. This may be interpreted as a prevalence of solvophobic over specific interactions for the metal chelates studied. Conversely, owing to the growth in specific solvation with increasing eluent polarity (proportional to ε values) the log k' values were assumed to decrease.

TABLE I

ELUTION ABILITY OF ACETONITRILE–WATER MOBILE PHASE IN TERMS OF METHYLENE SELECTIVITY VALUES

Composition acetonitrile–water (v/v)	Log α_{CH_2}		
	Alkylbenzenes [8]	Nitroalkanes [8]	Copper dialkyldithiocarbamates
65:35	0.167	0.165	0.165
80:20	0.133	0.129	0.130

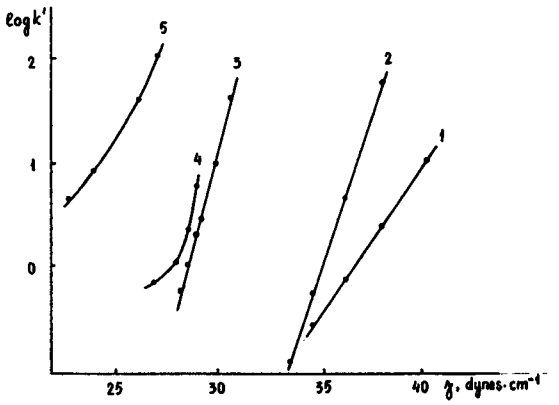

Fig. 4. Dependence of the capacity factors of copper (1, 3) and mercury (4, 5) diethyldithiocarbamates and copper di-*n*-butyldithiophosphate (2) on the surface tension of mobile phase. 1, 2 = Dioxane–water; 3 = acetonitrile–water; 4 = isopropanol–water; 5 = methanol–water.

Molecular parameters

The chromatographic behaviour of metal chelates in RPLC is affected by specific interemolecular interactions with components of the mobile phase (mostly hydrogen bonds and donor–acceptor interactions [20]). However, it is difficult to describe in terms of macroscopic parameters how the solvation processes affect chelate retention. Therefore we turned to a large class of empiric parameters that characterize the proton- and electron-donating ability of solvents and that are widely used to evaluate the elution strength of the mobile phase in RPLC [9–11].

All parameters studied (Kamlet–Taft basicity parameter π^*, Dimroth–Reichardt acceptor strength parameter E_T, Kosower and Brounstein's parameters z and S) are more or less able to predict chelate retention in terms of one-dimensional

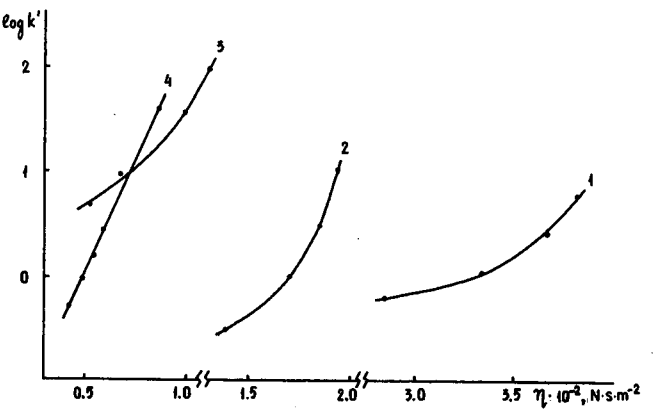

Fig. 5. Plots of log k' and dynamic viscosity coefficient of mobile phase for mercury (1, 3), copper (2) and cobalt (4) diethyldithiocarbamates. 1 = Isopropanol–water; 2 = dioxane–water; 3 = methanol–water; 4 = acetonitrile–water.

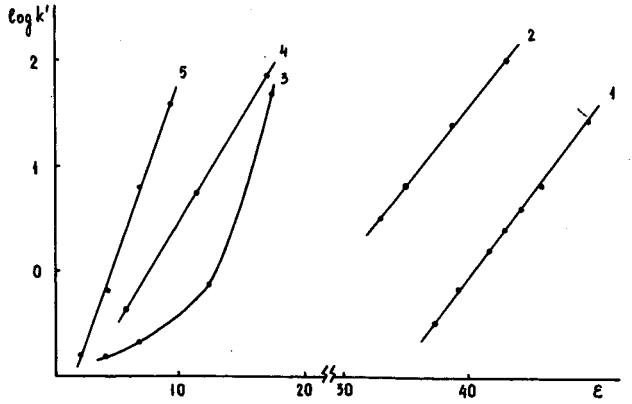

Fig. 6. Log k' values of mercury (1) and cobalt (2) diethyldithiocarbamates and mercury diethyl (3), dibutyl (4) and dioctyl (5) dithiophosphates *vs.* dielectric constants. Mobile phase: 1 = methanol–water; 2 = acetonitrile–water; 3–5 = dioxane–water.

linear models. However, as one would expect, no one of them is universal. Thus, the dependence of log k' on π^* values is linear only when mobile phases are modified by aprotic solvents (Fig. 7), because π^* parameters fail to reflect the solvent's ability to form hydrogen bonds. On the other hand, the E_T parameter is sensitive to the proton-donating properties of the mobile phase. Therefore, it is linearly correlated with log k' values only for water–alcoholic eluents. The z and S parameters, which characterize the solvation capacity of a solvent as a proton donor, exhibit linear correlation only for mobile phases containing aprotic solvents (Fig. 8). This may be due to the fact that the proton-donating ability of such mixtures decreases proportionally to the increase in the organic component, while for water–alcoholic eluents (both components are proton donors of different strength) there is no such proportional relationship.

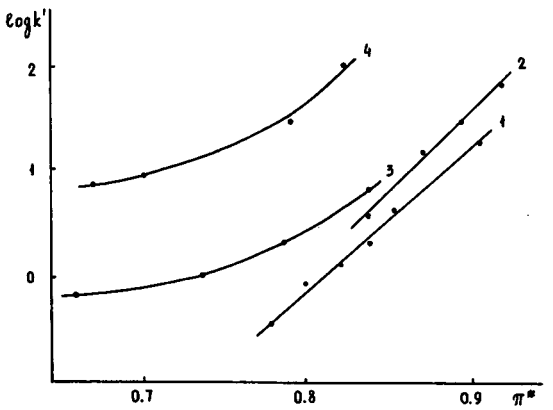

Fig. 7. Dependence of log k' values of lead (1) and mercury (2–4) diethyldithiocarbamates on the basicity parameter of the mobile phase. 1 = Acetonitrile–water; 2 = tetrahydrofuran–water; 3 = isopropanol–water; 4 = methanol–water.

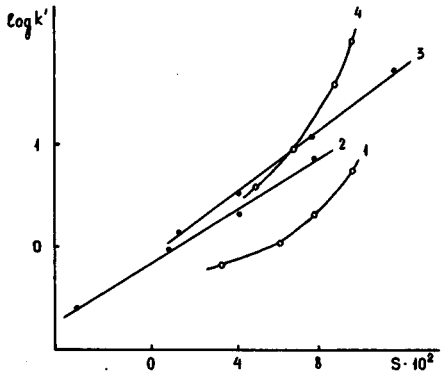

Fig. 8. Dependence of retention on mobile phase electron-accepting ability (by Kosower) for mercury (1, 3, 4) and antimony (2) diethyldithiocarbamates. 1 = isopropanol–water; 2,3 = dioxane–water 4 = methanol–water.

It must be stressed that as the mobile phase solvation capacity increases as measured by the above-mentioned parameters, the retention does not decrease (as it would if specific sorbate–eluent interactions mostly contributed to retention) but increases. This can be explained if the ability of mobile phase to form hydrogen bonds is considered as a reason for its association or, in other words, its solvophobic effect.

Other possible parameters used to estimate the elution strength of mobile phase in RPLC, like Snyder's P' parameter [21] of solvent polarity or Hildebrand's δ_T parameter [22], proved to be ineffective in evaluating metal chelate retention. They may only be applied for rather ideal solutions. However, this condition is rarely observed for polar water–organic eluents, especially when sorbates (like metal chelates) undergo specific intermolecular interactions with components of these mobile phases.

The above retention models can be applied to the optimization of metal chelate separation by the interpretive strategy approach. We use the single-parametric opti-

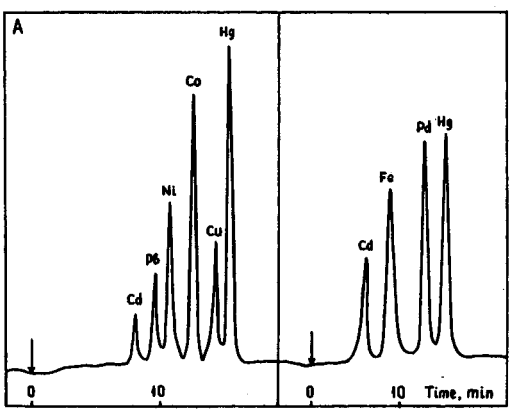

Fig. 9. Optimized separation of metal diethyldithiocarbamates by RP-HPLC. Column: 64 × 2 mm. Stationary phase: Separon C_{18} (5 μm). Mobile phase: acetonitrile–water (70:30, v/v) containing 2% chloroform. Flow-rate: 50 μl/min. UV-detection (280 nm).

mization procedure based on the analysis of window diagrams and α_{min} as an optimization criterion [23]. The selected optimal eluent was applied to separation of metal diethyldithiocarbamates under high-performance liquid chromatography (HPLC) conditions. Fig. 9 depicts two chromatograms obtained with the predicted mobile phase composition and indicates that the optimization was rather successful.

CONCLUSIONS

Thus, one-dimensional models based on the principle of free energy linear relations may be widely applied for the *a priori* estimation of retention parameters and the prediction of chromatographic retention behaviour of metal chelates, especially when the macroscopic parameters of the mobile phase are used as variables. As a rule, the molecular parameters are only limited to certain types of solvent or certain component ratios since such eluent properties as proton- or electron-donating ability characterize specific interactions of only one type. It is obvious that the analysis of retention–mobile phase composition (or physico-chemical property) models also provides valuable data for establishing the nature of intermolecular interactions and understanding the retention mechanism of metal chelates.

REFERENCES

1 A. R. Timerbaev, I. G. Tsoi and O. M. Petrukhin, *J. Chromatogr.*, 498 (1990) 337.
2 V. V. Salov, A. R. Timerbaev and O. M. Petrukhin, *J. Planar Chromatogr.*, 3 (1990) 73.
3 A. R. Timerbaev, A. Yu. Malykhin, T. A. Bol'shova and O. M. Petrukhin, *Zh. Anal. Khim.*, 45 (1990) 1113.
4 A. R. Timerbaev, I. G. Tsoi and O. M. Petrukhin, presented at the *18th International Symposium on Chromatography, Amsterdam, september 23–28, 1990.*
5 J. Timmermans, *The Physico-Chemical Constants of Binary Systems in Concentrated Solutions*, Vol. 4, Interscience, New York, 1960.
6 K. A. Connors and J. L. Wright, *Anal. Chem.*, 61 (1989) 194.
7 H. B. Patel and T. M. Jefferies, *J. Chromatogr.*, 389 (1987) 21.
8 B. P. Johnson, M. G. Khaledi and J. G. Dorsey, *J. Chromatogr.*, 384 (1989) 221.
9 M. G. Kamlet, J. L. Abboud and R. W. Taft, *J. Am. Chem. Soc.*, 98 (1976) 377.
10 B. P. Johnson, M. G. Khaledi and I. G. Dorsey, *Anal. Chem.*, 58 (1986) 2354.
11 K. Burger, *Solvation, Ionic and Complex Formation Reactions in Non-aqueous Solvent*, Akademiai Kiado, Budapest, 1983.
12 I. G. Tsoi, *Ph.D. Thesis*, Mendeleev Moscow Institute of Chemical Technology, Moscow, 1990.
13 W. Melander and Cs. Horváth, in Cs. Horváth (Editor), *High Performance Liquid Chromatography–Advances and Perspectives*, Vol. 2, Academic Press, New York, London, 1980, pp. 113–319.
14 F. Vlačil and V. Hamplova, *Coll. Czechosl. Chem. Commun.*, 50 (1985) 2221.
15 W. Schunk and G. Schwedt, *Chromatographia*, 1 (1983) 37.
16 Cs. Horváth, W. Melander and I. Molnar, *J. Chromatogr.*, 125 (1976) 156.
17 F. Murakami, *J. Chromatogr.*, 178 (1979) 393.
18 H. B. Patel and T. M. Jefferies, *J. Chromatogr.*, 389 (1987) 21.
19 Cs. Horváth, W. Melander and I. Molnar, *J. Chromatogr.*, 125 (1976) 129.
20 A. R. Timerbaev and O. M. Petrukhin, *Zhidkostnaya Adsorbtsionnaya Khromatographiya Khelatov*, Nauka, Moscow, 1989.
21 L. R. Snyder, *J. Chromatogr.*, 92 (1974) 223.
22 J. H. Hildebrand and A. L. Scott, *The Solubility of Non-Electrolytes*, Dover, New York, 1964.
23 P. J. Schoenmakers, *Optimization of Chromatographic Selectivity – A Guide to Method Development*, Elsevier, Amsterdam, 1986.

Journal of Chromatography, 555 (1991) 173–182
Elsevier Science Publishers B.V., Amsterdam

CHROM. 23 319

Theoretical and experimental comparison of serially linked and mixed-packing gas–liquid chromatography columns

J. H. PURNELL* and M. H. WATTAN
Department of Chemistry, University College of Swansea, Singleton Park, Swansea SA2 8PP (UK)
(First received November 22nd, 1990; revised manuscript received March 13th, 1991)

ABSTRACT

Theory developed in this laboratory allows accurate prediction of solute capacity factors for serial operation of columns A and B from basic data for A and B alone. Window analysis then identifies the relative and total column lengths required for baseline resolution of all mixture components. The relative lengths required depend on column sequence, A (front)/B (back) or B (front)/A (back), and normally differ significantly although the resulting chromatograms are identical. Provided the theoretical plate height (H) carrier velocity ($\bar{u}$) relationships for A and B are not too dissimilar, the total column length required is the same in either mode. It is shown theoretically that an optimised mixed packing (A + B) provides exactly the same chromatogram, though the necessary packing ratio does not correspond to either optimised serial column length ratio. Thus, depending on the packing (length) ratio used, an experimental comparison may indicate that the mixed packing approach is superior, or *vice versa*.

Where the $H/\bar{u}$ relationships of A and B differ greatly, total column lengths may vary from one mode to the other to produce the same optimised separation. Generally, the effect is more marked for the serial systems. However, even in this situation, total analysis time will, in certain circumstances, be less for the serial system.

The experimental results presented confirm the theoretical arguments.

INTRODUCTION

In seeking controlled improvement in selectivity of separation in gas–liquid chromatography (GLC) by the use of two (or more) liquid substrates (solvents), three practical routes are open to us:

(a) the use of mixed liquids (A + B) on a single solid support (S); or,

(b) of intimately, mixed or highly striated, packings (A + S) and (B + S) in a single column; or,

(c) serial operation of two columns, (A + S) and (B + S).

We have shown [1–4] that for a number of commonly used GLC solvents, the results obtained with mixed solvents and mixed packings are essentially identical, which implies independent action by A and B when mixed. However, we would generally expect interaction of A with B, hence, some change in solvent properties on mixing. Mode a is, therefore, generally less reliable than mode b and since the one approach is as technically easy as the other, the latter is generally to be preferred. Since

0021-9673/91/$03.50

the solvents A and B must act independently in a mixed packing the net retention volume (V'_R) of any analyte (solute) must be the sum of the independent contributions (V'_{RA} and V'_{RB}),

$$V'_R = V'_{RA} + V'_{RB} = w_A V^0_{gA} + w_B V^0_{gB} \tag{1}$$

where w represents a solvent weight and V^0_g is the specific retention volume of the solute with the relevant solvent. The overall specific retention volume $V^0_g = [V'_R/(w_A + w_B)]$ is thus [5,6],

$$V^0_g = W_A V^0_{gA} + W_B V^0_{gB} \tag{2}$$

where W represents a solvent weight fraction ($w/\Sigma w$). It is a simple matter to show that this can alternatively be written,

$$K^0_R = \varphi_A K^0_{RA} + \varphi_B K^0_{RB} \tag{3}$$

where K^0_R represents the stoichiometric partition coefficient and φ is the volume fraction of one or other solvent ($V_l/\Sigma V_l$).

Thus, measurements of either V^0_g or K^0_R for any solute with test columns containing either solvent A or B allows immediate calculation of the corresponding quantity for any known mixture of A and B packings. The retention of each solute is clearly simply linearly related to the quantity of each solvent or packing present.

In decided contrast, the retention parameters of any solute eluted from the same pair of columns linked in series are not simply related to substrate composition. This arises because the two columns do not operate over the same pressure (flow velocity) regime and so, compressibility of the carrier gas contributes to the overall retention. Further, the overall retention of any given solute depends upon the mode of operation *i.e.* whether A precedes B or *vice versa*. The general equation for the serial operation of two columns, now designated for convenience, front (F) and back (B), where front defines the inlet end of the system, is [7–14]

$$k' = \left[\frac{Pk'_F + k'_B}{P + 1}\right] \tag{4}$$

where k' represents the capacity factor for a solute with either column and $P = t_{dF}/t_{dB}$, where t_d is the dead time (elution of unsorbed component). Using columns of A and B, either of course, may be F or B. Only if $P = 1$ is k' the arithmetic average of k'_F and k'_B and the same in alternative modes, [A(F)/B(B)] and [B(F)/A(B)].

Values of k'_A and k'_B for solutes are readily determined with test columns exactly as in mixed packing applications. P, however, cannot be calculated without further experimental information. First, we need to know the value of the junction pressure p arising when we run the system with column A at the inlet ($p_i \rightarrow p$) and column B at the outlet ($p \rightarrow p_o$), or *vice versa*. Secondly, because there may be differences in packing density or column dimensions, we need to know the relevant column dead volumes (V_M) and resistance to flow factors, R_F, the latter being defined by [15]

$$R_F = \frac{[p_i^2 - p_o^2]}{p_o u_o} = \frac{[p_i^2 - p_o^2]}{\bar{p}\bar{u}} \tag{5}$$

where $\bar{p}$ and $\bar{u}$ are the compressibility averaged pressure and gas velocity, respectively. While we can use eqn. 5 to evaluate R_F it is much more convenient to use the equation

$$t_d = \frac{2LR_F}{3}\left[\frac{(p_i^3 - p_o^3)}{(p_i^2 - p_o^2)^2}\right] \tag{6}$$

A plot of t_d against the bracketted function gives a straight line of slope $(2LR_F/3)$ and if flow-rates, corrected to column temperature (F_c) are measured simultaneously with t_d, V_M can be also be calculated.

For any column pair, the junction pressure is then given by [9,14]

$$p^2 = \left[\frac{p_i^2 - l_F[p_i^2 - (V_{MB}R_{FF}/V_{MF}R_{FB})p_o^2]}{1 - l_F[1 - (V_{MB}R_{FF}/V_{MF}R_{FB})]}\right] \tag{7}$$

where l_F is the length fraction of the front column $[L_F/(L_F + L_B)]$. We note that this equation is, as also are subsequent equations presented, independent of any assumption of, or need to measure, other column parameters such as column diameters or phase ratios, a considerable advantage.

Finally, we can calculate P for any solute for any column lengths and inlet pressure *via.* [9,14]

$$P = \left[\frac{L_B R_{FB}}{L_F R_{FF}}\right]\left[\frac{V_{MF}}{V_{MB}}\right]^2\left[\frac{p_i^3 - p^3}{p^3 - p_o^3}\right] \tag{8}$$

and, so, can calculate k' for all solutes in either mode A(F)/B(B) or B(F)/A(B).

We turn now to the matter of analytical interest, the choice of mixed packing ratio, or of relative column lengths in serial operation, that will provide the desired separation of the mixture to hand. The method of choice is the window analysis method developed by Laub and Purnell [16]. For mixed packings this is a straightforward procedure. From eqns. 2 and 3 we see that V_g^0 and K_R^0 are both linear functions of controllable column variables, so, we need know only the values of either for the solutes measured with the columns of the pure solvents, A and B, and can then use the relevant equation to calculate k' for all mixture components at any value of W_A or φ_A. Alternatively, we may construct a plot by simply connecting the relevant values for a solute with solvents A and B with a straight line on a scale of W_A or $\varphi_A = 0$ to 1. It is clearly a simple matter to evaluate the relevant retention parameter for each solute at a number of intermediate values of W_A or φ_A by interpolation from the plot or by use of the appropriate equation and so, for all pairs of solutes, the ratios $V_{g2}^0/V_{g1}^0 = K_{R2}^0/K_{R1}^0 = \alpha$, the relative retention. The plot has the merit of indicating immediately which pairs offer no difficulty of separation and so can be left out of the calculations. The values of α are then plotted against W_A (or φ_A) and, since we are uninterested at this point in the order of elution we choose to keep $\alpha \geqslant 1$. Typically then, the lower envelope of the plot takes the form of a number of approximate triangles (windows), the highest of which defines the largest value of the lowest value of α among all solute pairs. and the corresponding value of W_A or φ_A. Knowing α at the optimum window

peak, we then calculate the number of theoretical plates required (N_{req}) to provide base-line separation of all components *via* [17]

$$N_{req} = 36\left[\frac{\alpha}{\alpha - 1}\right]^2\left[\frac{1 + k'}{k'}\right]^2 \tag{9}$$

where k' is now the capacity factor of the second to elute of the most difficult pair to separate. Clearly, if this pair is separated, so too are all others.

During the test experiments that yielded the basic data, we can determine the attainable theoretical plate height (H) and, hence, from N_{req}, the total column length needed for base-line separation. We thus know all that is necessary to achieve the optimisation of the desired separation with the chosen packings at the test temperature. Given further information the optimisation can be extended [18–20] to solvent choice, temperature, analysis time, and so forth. Window analysis is now widely employed to optimise various aspects of chromatographic, or other, analysis although it is frequently designated by some other name.

As eqn. 4 shows, in serial column operation, k' is not a simple linear function of the controllable variable, l_F. Thus, to apply the technique of window analysis as described above would now appear to require measurements of k' for all mixture components at a number of values of l_F. This would be tedious. Fortunately, as Purnell and Williams [9] have shown, we can get around this problem as follows.

Let us identify a quantity $f(f_F + f_B = 1)$ which linearises k', thus,

$$k' = f_F k'_F + f_B k'_B \tag{10}$$

Equating the right hand side with that of eqn. 4 shows that

$$P = f_F/(1 - f_F) \tag{11}$$

Substituting in eqn. 8 and rearranging gives

$$p^3 = \left[\frac{p_i^3 - f_F(p_i^3 - \gamma p_o^3)}{1 - f_F(1 - \gamma)}\right] \tag{12}$$

where

$$\gamma = \left[\frac{L_F R_{FF}}{L_B R_{FB}}\right]\left[\frac{V_{MB}}{V_{MF}}\right]^2 = \left[\frac{\bar{R}_{FF}}{\bar{R}_{FB}}\right]\left[\frac{\bar{V}_{MB}}{\bar{V}_{MF}}\right]^2 \tag{13}$$

the superior bars defining a quantity per unit column length.

This then leads, finally, to an expression for the value of l_F that corresponds to any given value of f_F, and P at specified p_i and p_o (eqn. 12) *viz*

$$l_F^{-1} = \left[\frac{\bar{R}_{FF}\bar{V}_{MB}}{\bar{R}_{FB}\bar{V}_{MF}}\left[\frac{(p^2 - p_o^2)}{(p_i^2 - p^2)}\right] + 1\right] \tag{14}$$

We can now proceed with the window analysis as before by plotting k' as a linear function of f_F and so identify the highest window and the corresponding value of f_F. Fixing on values of p_i and p_o we then calculate the corresponding value of p (eqn. 12) and, thence, evaluate l_F *via* eqn. 14.

The foregoing allows us to draw an important conclusion regarding the relative merits of mixed packings and the analogous serial columns. For the same packings the two methods share the same window peak, *i.e.*, α at the optimum is the same in either approach and so provided we work at the same H, the total column length needed for base-line resolution of the mixture is exactly the same although the relative amounts of packing needed may be very different. But, further, since the value of α at the optimum occurs at the same values of k' for the most difficult pair to separate, all other k' must also be the same in either mode. That is, the optimised chromatograms will be identical in every respect. This is an important observation in the context of choice or comparison of method. It also explains why the few attemps to compare the methods experimentally [21–25] have produced conflicting conclusions. They produce identical chromatograms only when operated so as to optimise separation. In other experimental conditions, *e.g.* if a pair of serial test columns were run, then unpacked and repacked as a mixed packing column, the experiments would yield different chromatograms and, depending on circumstances, column sequence in the serial mode for instance, would indicate that one or other method was superior in terms of resolution.

In what follows we provide experimental proof of the foregoing.

EXPERIMENTAL

The experiments were all conducted with a Perkin-Elmer F.33 chromatograph equipped with flame ionization detection. The carrier gas was nitrogen and mixture components (0.1–1.0 μl) were eluted separately to establish the relevant capacity factors and methane was used to measure dead times. The column packings used were 10% (w/w) of squalane (SQ) and of diisobutylphthalate (DBP) supported on 100–120 mesh Chromosorb G AW DCMS and were packed in stainless steel tube of 0.32 cm outside diameter. Carrier flow-rates were measured with a soap-bubble meter and corrected for water vapour pressure and to column temperature (90°C) to yield fully corrected values (F_c). All values of t_d, k' and V_M reported are averages of a number of measurements.

The solvents were obtained from Phase Separations (Queensferry, UK) and the mixture components from BDH (Poole, UK). All were used as delivered. Solvent/support loadings were doubly checked by thermogravimetric analysis (TGA) and Soxhlet extraction.

RESULTS

Table I lists values of k' for twelve hydrocarbons eluted by nitrogen at 90°C from both the SQ and DBP columns. With each solvent there is at least one solute pair that cannot be separated at any realistic column length.

The pressure, dead time and flow-rate studies yielded the values of R_F and V_M listed in Table II while concurrent measurements of H as a function of flow-rate

TABLE I

k' FOR NAMED SOLUTES ELUTED AT 90°C BY NITROGEN FROM 10% (w/w) COLUMNS OF SQUALANE (SQ) (180 cm) AND DIISOBUTYLPHTHALATE (DBP) (170 cm) ON 100–120 MESH CHROMOSORB G AW DCMS

Component	Solute	k'(SQ)	k'(DBP)
1	*n*-Hexane	4.92	1.24
2	Benzene	8.80	5.37
3	*n*-Heptane	11.6	3.48
4	Methylcyclohexane	15.5	6.32
5	Toluene	18.7	15.1
6	*n*-Octane	26.6	8.05
7	Ethyl benzene	39.3	30.6
8	Non-1-ene	52.3	20.4
9	*o*-Xylene	52.3	39.5
10	*n*-Propyl benzene	78.7	58.1
11	Dec-1-ene	113.8	43.3
12	*n*-Decane	130.4	39.5

provided good Van Deemter plots the minima for both columns occurring at $H_{min} = 0.065$ cm and $\bar{u} = 4.3$ cm s^{-1}.

Fig. 1 shows plots of k' against f_{SQ} constructed simply by connecting the values of k' at $f_{SQ} = 0$ and $f_{SQ} = 1$. We see a number of values of f_{SQ} at which lines cross ($\alpha = 1$) and so expect to find numerous windows on the α/f_F plot. Fig. 2 shows that there are seven with one outstandingly superior to all others ($f_{SQ} = 0.872$; $\alpha = 1.12$). This value of α with the relevant $k' \approx 12$ (see Fig. 1) gives, via eqn. 9, the value $N_{req} = 3260$. At $H = 0.065$ cm (the Van Deemter minimum for both columns) the total column length required is thus 212 cm to provide baseline separation of all components.

We calculate the corresponding relative column lengths, as described earlier, as follows:

Mode 1: SQ(F)/DBP(B); $f_F = 0.872$; $P = 6.812$; $\gamma = 1.288$ and, with $p_o = 14.6$ p.s.i. and $p_i = 34.6$ p.s.i., $p = 19.14$ p.s.i. giving $l_F = 0.813$ ($L_{SQ} = 172$ cm; $L_{DBP} = 40$ cm).

Mode 2: DBP(F)/SQ(B); $f_F = 0.128$; $P = 0.146$; $\gamma = 0.776$ and, with $p_o = 14.6$ p.s.i. and $p_i = 34.6$ p.s.i., $p = 33.46$ p.s.i. giving $l_F = 0.0915$ ($L_{SQ} = 192.5$ cm; $L_{DBP} = 19.5$ cm).

TABLE II

R_F AND V_M VALUES FOR COLUMNS AND CONDITIONS OF TABLE I

Column	$10^{-6}R_F$ (Nsm^{-3})	V_M (ml)	$10^{-6}\bar{R}_F$ (Nsm^{-4})	$\bar{V}_M$ (ml m^{-1})
SQ	5.56	3.86	3.09	2.14
DBP	4.71	3.99	2.77	2.34

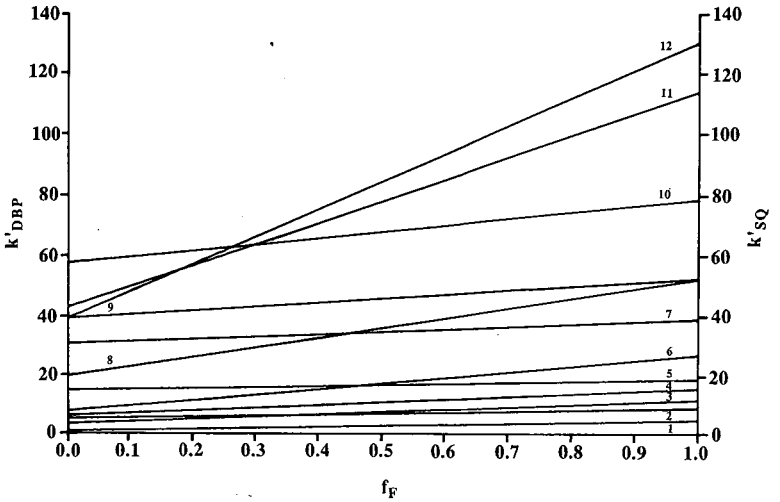

Fig. 1. Plots of k' against f_{SQ} constructed by plotting data of Table I at $f_{SQ} = 0$ and 1 and connecting with straight line. Note numerous cross-overs which indicate a value of $\alpha = 1$ so that separation of all components cannot be achieved.

Fig. 3 shows the chromatograms obtained in the alternative modes. They are clearly baseline resolved and identical, as theory demands.

Turning now to the mixed packing alternative. Provided that the free volumes per g of each packing are not too dissimilar then eqn. 2 can be represented as

$$k' = W_A k'_A + W_B k'_B \tag{15}$$

For the two packings used here the free volume discrepancy is not more than 5% so that eqn. 15 can be used with little approximation. Thus, had we represented Fig. 1 as

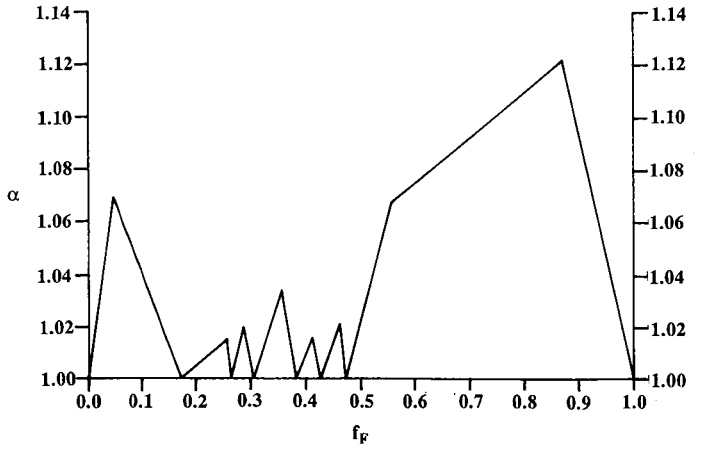

Fig. 2. Window diagram constructed from data of Table I (eqn. 10). Each window defines a region of f_F wherein total separation of all components is possible. Highest window defines most favourable α (shortest column) and corresponding f_F.

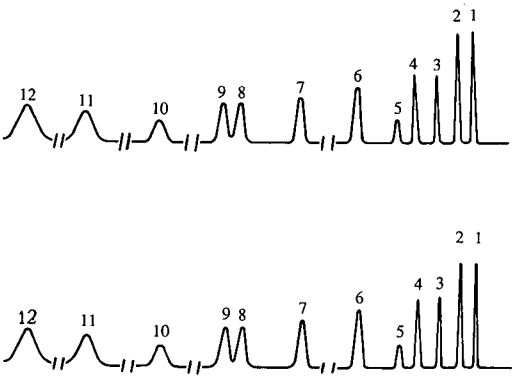

Fig. 3. Optimised serial separations at 90°C. Upper: SQ(F) 172 cm/DBP(B) 40 cm; lower: DBP(F) 19.5 cm/SQ(B) 192.5 cm. Time scale interrupted for convenience of presentation.

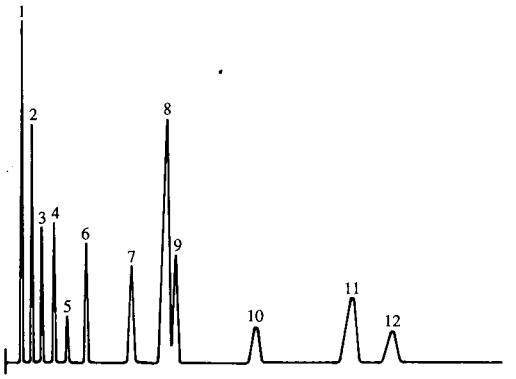

Fig. 4. Optimised mixed column separation at 90°C. Column, 212 cm; weight ratio of 10% (w/w) packings SQ/DBP = 6.81.

TABLE III

k' FOR ALL SOLUTE COMPONENTS WITH SERIAL COLUMNS, WITH MIXED PACKING AND AS THEORETICALLY CALCULATED FOR CONDITIONS OF OPTIMISED SEPARATION

Component	Serial columns average k'	Mixed packing k'	Any mode calculated k'
1	4.92	4.90	4.45
2	8.00	7.80	8.40
3	11.1	11.5	11.2
4	15.0	14.8	14.7
5	18.6	18.5	18.3
6	24.6	24.7	24.3
7	38.1	38.3	38.2
8	47.8	47.9	48.2
9	50.7	50.8	50.7
10	75.7	75.7	76.1
11	106	106	104
12	120	120	119

a plot of k' against W_{SQ}, the numerical value of the weight fraction at the best window peak would have equalled that of f_F cited earlier (0.872). Thus, to complete the comparison sought we now require a 212 cm mixed packing column with the 10% packings in the ratio SQ:DBP = 6.81. Fig. 4 shows the chromatogram obtained with this column at the same p_i and p_o as employed with the serial systems. To all intents and purposes, baseline resolution is again achieved and the three chromatograms are visually identical. The most telling information, however, is that detailed in Table III where we list the average values of k' for the two serial modes, those for the mixed packing and those calculated *via* the equations presented earlier. The agreement is seen to be virtually exact.

DISCUSSION

The theoretical arguments advanced earlier are fully confirmed. They allow us to calculate precisely the capacity factors arising in mixed packing or serial operation in either mode and, further, tell us that in the conditions of optimised separation the actual chromatograms obtained are identical. As indicated, provided the theoretical plate heights attainable are not too dissimilar in the two approaches, the overall column length needed for the optimised separation is also the same for the mixed packing and either serial mode. This situation will be encountered fairly frequently in practice. Thus, choice of method will commonly depend on other criteria. One obvious factor is that associated with solvent volatility. In the serial array, solvent from both columns will be transported but that from the front column will be deposited initially in the back column. Thus, the basic retention characteristics of both front and back columns will change with time. As this happens the system moves away from the optimum and progressive loss of resolution will be observed. There will also be transfer in the mixed packing bed but here, as indicated earlier, the deposition of *e.g.* A in B, will lead to little change in α in most cases. Thus, the mixed packing is likely to maintain resolution far longer. If, therefore, one or other of the chosen solvents is excessively volatile, the operating lifetime of the mixed packing column should be superior.

The most significant effect that influences choice of method, however, arises where $H/\bar{u}$ differs significantly from column to column. There are two cases to consider. First, if the van Deemter curves for the serial and mixed packings are very different, not only will different total column lengths be needed but different gas velocities may be necessary. Whilst this will not influence k' values in the optimised separation it may lead to significant difference in the total time of analysis. Where the $H/\bar{u}$ differences between the separate packings are significant the situation is more complex. This aspect has been treated theoretically by Purnell and Williams [5,6] but no experimental study has yet been reported. They showed that in certain circumstances the value of $H/\bar{u}$ for a serial column could be significantly greater than the corresponding values of $H/\bar{u}$ for either column alone. Broadly, this arises when the columns are of disparate length and the shorter column is both more retentive and substantially less efficient. In contrast, all published evidence is that $H/\bar{u}$ for a mixed packing lies between the values characterising the separate test columns. The mixed packing column would then be superior to the serial column in terms of the length required for optimised analysis. Extention of their analysis allowed comparison of the alternative modes when the optimised separation is conducted in conditions yielding

minimum analysis time (far above the Van Deemter minimum). In this situation, it emerges that, notwithstanding the efficiency issue illustrated above, conditions could exist in which either mode, serial or mixed, might provide faster analysis. Clearly, any future experimental comparison involving analysis time as one criterion of optimisation must take this observation into account.

Where the main aim is to achieve separation the foregoing clearly indicates that the mixed packing approach will normally be preferred in GLC–GLC since, if nothing else, it is more convenient. However, it cannot be used with confidence with GLC–gas–solid chromatography combinations due to potential deactivation of the gas–solid component following solvent transfer. Equally, with open-tube columns, mixed substrates present practical problems and serial operation will be preferred.

Finally, it is evident that serial systems provide opportunity to operate the columns at different temperatures. This developing technique, for which commercial equipment is already available, is subject to exactly the theory and procedures described here, as we have shown earlier [14]. Since, in this case, separate temperature regimes are superimposed on the compressibility effect, the empirical approach to optimisation is tedious, and possibly unrewarding and a theoretically based procedure becomes even more desirable.

REFERENCES

1 R. J. Laub and J. H. Purnell, *Anal. Chem.*, 48 (1976) 799.
2 R. J. Laub and J. H. Purnell, *Anal. Chem.*, 48 (1976) 1720.
3 R. J. Laub, J. H. Purnell and P. S. Williams, *Analytica Chim. Acta*, 95 (1977) 135.
4 R. J. Laub, J. H. Purnell, D. M. Summers and P. S. Williams, *J. Chromatogr.*, 155 (1978) 1.
5 R. J. Laub and J. H. Purnell, *J. Chromatogr.*, 161 (1978) 59.
6 J. H. Purnell, *Proc. Anal. Div. Chem. Soc.*, 16 (1979) 136.
7 J. H. Purnell and P. S. Williams, *J. High Resolut. Chromatogr. Chromatogr. Commun.*, 6 (1983) 569.
8 J. H. Purnell and P. S. Williams, *J. Chromatogr.*, 292 (1984) 197.
9 J. H. Purnell and P. S. Williams, *J. Chromatogr.*, 321 (1985) 249.
10 J. H. Purnell, M. Rodriguez and P. S. Williams, *J. Chromatogr.*, 323 (1985) 402.
11 J. H. Purnell and P. S. Williams, *J. Chromatogr.*, 325 (1985) 1.
12 J. H. Purnell, M. Rodriguez and P. S. Williams, *J. Chromatogr.*, 358 (1986) 39.
13 J. H. Purnell, J. R. Jones and M. H. Wattan, *J. Chromatogr.*, 399 (1987) 99.
14 J. R. Jones and J. H. Purnell, *Anal. Chem.*, 62 (1990) 2300.
15 G. P. Hildebrand and C. N. Reilley, *Anal. Chem.*, 36 (1964) 47.
16 R. J. Laub and J. H. Purnell, *J. Chromatogr.*, 112 (1975) 71.
17 J. H. Purnell, *J. Chem. Soc.*, (1960) 1268.
18 R. J. Laub and J. H. Purnell, *J. Chromatogr.*, 161 (1978) 49.
19 W. K. Al-Thamir, R. J. Laub and J. H. Purnell, *J. Chromatogr.*, 142 (1977) 3.
20 J. H. Purnell, *J. Chromatogr.*, Library, 32 (1985) 363.
21 W. H. McFadden, *Anal. Chem.*, 30 (1958) 479.
22 J. A. Barnard and H. W. D. Hughes, *Nature (London)*, 183 (1959) 250.
23 G. R. Primavesi, *Nature (London)*, 184 (1959) 2010.
24 H. J. Maier and O. C. Karpathy, *J. Chromatogr.*, 8 (1962) 308.
25 A. A. Zhukhovitskii, M. S. Selenkia and N. M. Turkel'taub, *Zh. Fiz. Khim.*, 36 (1962) 993.

Journal of Chromatography, 555 (1991) 183–190
Elsevier Science Publishers B.V., Amsterdam

CHROM. 23 382

Study of microporous carbons by gas chromatographic determination of heats of physisorption

X. L. CAO*
Environmental Science Division, Lancaster University, Lancaster LA1 4YQ (UK)
and
B. A. COLENUTT and K. S. W. SING
Department of Chemistry, Brunel University, Uxbridge, Middlesex UB8 3PH (UK)
(First received December 27th, 1990; revised manuscript received April 15th, 1991)

ABSTRACT

Gas chromatography has been used to measure low-coverage isosteric heats of adsorption (q^{st}) of *n*-alkanes (C_1 to C_9), *n*-alkenes (C_2 to C_4), isopentane, cyclohexane, benzene, 2-methylpentane and 2,2-dimethylbutane on different microporous carbons. The similar q^{st} values between *n*-alkanes and *n*-alkenes, cyclohexane and benzene show the non-polar or slight polar surfaces of these adsorbents. The q^{st} values of the molecules with branch chains or bulky shapes are smaller than those of corresponding straight-chain molecules, which may indicate the molecular sieving properties of these slit-shaped microporous carbons. It is also shown that there may be an enhancement of adsorption energy for adsorption of some molecules in wider micropores.

INTRODUCTION

Gas chromatography (GC) can be used not only as a means of chemical analysis, but also as a means of physicochemical measurement. Over the past twenty years GC has become an unique means of studying the adsorption characteristics of surface by the determination of isosteric heats of adsorption (q^{st}) at very low surface coverage [1], provided that certain conditions are fulfilled. By using saturated molecules of different size and shape, for example alkanes, it is possible to investigate the non-specific adsorbate–adsorbent interactions and avoid any specific effects which may contribute to the energitics of adsorption of polar molecules [2,3]. The magnitude of the specific adsorbate–adsorbent interaction can be estimated by the differences between the corresponding values for unsaturated and saturated linear hydrocarbons [4,5].

GC can also be used to study the enhancement of adsorption energy associated with the physisorption of molecules in very narrow pores [2,3], *i.e.*, the process of primary micropore filling [6]. It is known that the energy of adsorption is considerably enhanced when physisorption takes place in very narrow pores, and the maximum enhancement is given when the width of the pore is slightly larger than the

0021-9673/91/$03.50

diameter of the adsorbed molecule [7]. Thus the determination of the enhancement of adsorption energy at very low surface coverage should provide an effective method for the estimation of the width of narrow pores of a given shape [8]. Carrott and Sing [3] found that the isosteric heats of adsorption are weighted in favour of the narrowest pores in the adsorbent, the observed differences in the values of isosteric heats of adsorption given by different microporous carbons can be regarded as reflecting not only differences in pore width, but also differences in the homogeneity of the micropore structure.

In this paper, the results of a study of isosteric heats of adsorption of molecular probes with different sizes, shapes and polarity on different microporous carbons were reported in order to have a better understanding of the relationships between the isosteric heats of adsorption and the microporous carbons' pore structures and the surface properties. The q^{st} values of these molecular probes on these adsorbents were compared with those on the non-specific adsorbent, graphitized carbon black (GCB).

EXPERIMENTAL

GC measurements were made using a Perkin-Elmer F30 gas chromatograph fitted with a flame ionization detector. The carrier gas was nitrogen at a flow-rate of 35 cm^3/min which was controlled by the make-up needle valve throughout the course of the experiment. The column inlet pressure was measured by a septum pressure gauge and the outlet pressure was assumed to be atmospheric. Retention measurements were made over the temperature range 40–380°C. The gas-hold-up time (t_0) was determined by the homologous series method.

The adsorptive vapours were injected into the carrier gas stream by means of a gas-tight syringe. The on-line computer was started simutaneously when injecting. The specific retention volume, V_g, was calculated from the equation

$$V_g = 273\,(t_R - t_0)F_c/(Tw) \tag{1}$$

where t_R is the retention time of the adsorptive, t_0 is the gas hold-up time, T is the column temperature, w is the weight of adsorbent in the column, and F_c is the volumetric flow-rate reduced to column temperature and mean pressure.

The molecular probes used were *n*-alkanes (methane to *n*-nonane), *n*-alkenes (ethene to *n*-butylene), cyclohexane, benzene, 2-methylpentane, 2,2-dimethylbutane and isopentane. Two 1% calibration standards (from Phase Separations) for *n*-alkanes (methane to *n*-butane) and *n*-alkenes (ethene to *n*-butylene) were used after diluting them to 1–10 ppm in nitrogen. The other samples were prepared by injecting 1 μl liquid of each into a 1-l Pyrex glass flask which had been purged with dry nitrogen. The range of masses of molecular probes injected was 1–80 ng.

The following adsorbents were studied. Carbosieve B is a polymer-based molecular sieve carbon, obtained from JJ's Chromatography, Hardwick Trading Estate (King's Lynn, UK). The two charcoal cloths, CC1, a high burn off charcoal cloth with a much wider range of pore size, and CC2, a low burn off charcoal cloth, were kindly supplied by Dr. J. J. Freeman of Brunel University. The surface properties of the adsorbents are summarized in Table I.

The Carbosieve B column was made of glass tube with dimensions of 35 cm × 2

TABLE I

SURFACE PROPERTIES OF ADSORBENTS

A_{BET} = BET specific surface area; A_s = external area; V_p and V_s = primary and secondary micropore volumes from nitrogen α_s-plot, respectively.

Adsorbent	A_{BET} (m^2/g)	A_s (m^2/g)	V_p [cm^3(liq.)/g]	V_s [cm^3(liq.)/g]
Carbosieve B	1174	51.5	0.45	0
CC1	2074	60.5	0.23	0.98
CC2	1039	16.5	0.41	0

mm I.D., which was filled with glass beads (80–100 mesh) and Carbosieve B (80–100 mesh). The charcoal cloth columns were constructed using the method mentioned in Carrott and Sing's work [3]. Before use, columns were heated overnight at 380°C in an nitrogen flow of 35 cm^3/min.

RESULTS AND DISCUSSION

It was found that under the conditions employed almost all molecular probes gave nearly symmetrical chromatographic peaks with specific retention volumes independent of flow-rate or sample size, except a few cases, such as 2,2-dimethylbutane on Carbosieve B and *n*-octane and *n*-nonane on Carbosieve B and CC2. Thus it could be

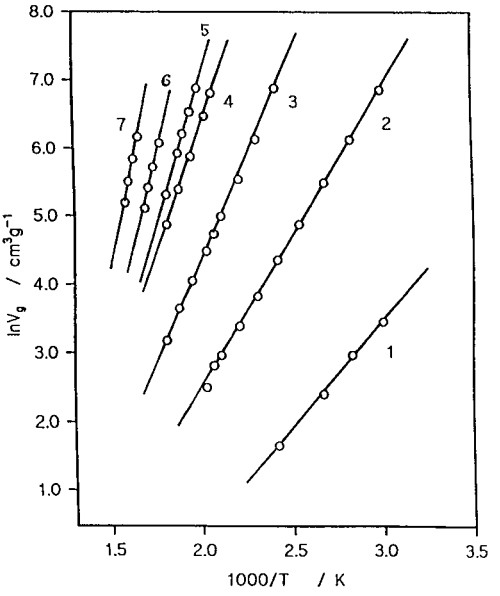

Fig. 1. Variation of specific retention volume with temperature for *n*-alkanes on Carbosieve B. Numbers on lines indicate number of carbon atoms.

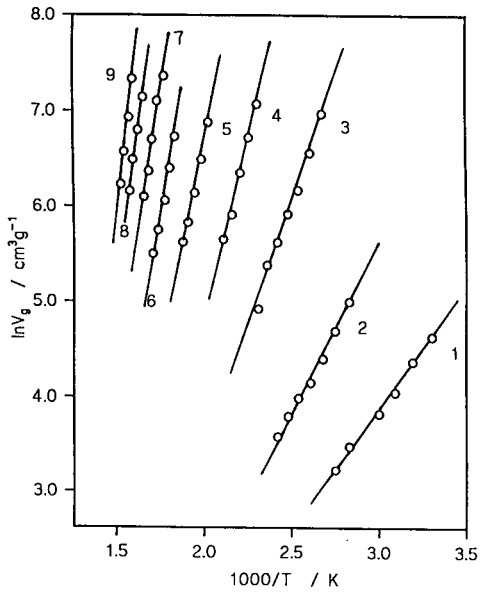

Fig. 2. Variation of specific retention volume with temperature for *n*-alkanes on CC1. Numbers on lines indicate number of carbon atoms.

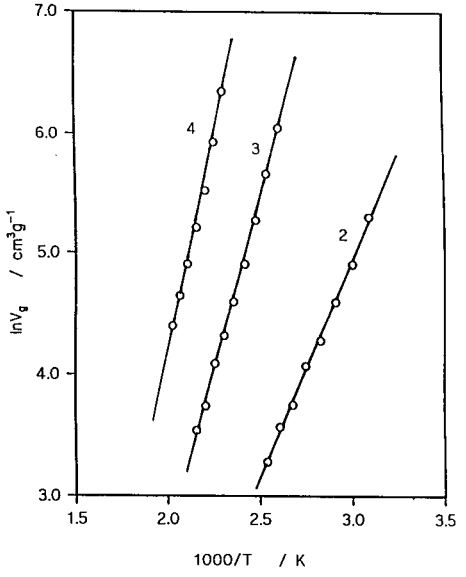

Fig. 3. Variation of specific retention volume with temperature for *n*-alkenes on CC2. Numbers on lines indicate number of carbon atoms.

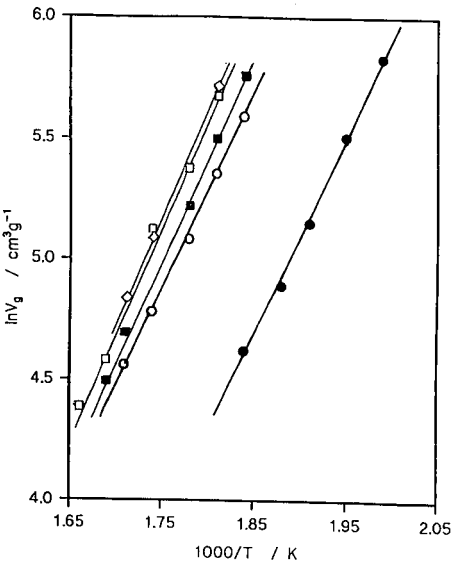

Fig. 4. Variation of specific retention volume with temperature for hydrocarbons on CC2. ○ = 2,2-Dimethylbutane; ● = isopentane; □ = benzene; ■ = cyclohexane; ◇ = 2-methylpentane.

assumed that adsorption occurred at very low surface coverage, and use may then be made of the equation

$$q^{st} = R\, d(\ln V_g)/d(1/T) \quad (2)$$

in order to calculate q^{st}, the isosteric heats of adsorption at zero uptake, from the variation of $\ln V_g$ with $1/T$ (R is the universal gas constant).

Representatives $\ln V_g$ *vs.* $1/T$ plots of different molecular probes for Carbosieve B, CC1 and CC2 are shown in Figs. 1–4, respectively. These plots are almost all linear over a wide range of temperature, although there is a slight curvature in some cases.

The derived values of q^{st} for each adsorbent are listed in Table II, and the q^{st} vs. n_c (the number of carbon atoms in the *n*-alkanes or *n*-alkenes adsorptive molecules) plots for *n*-alkanes and *n*-alkene are shown in Figs. 5 and 6. The estimated uncertainty in the values of q^{st} is about ± 1 kJ/mol. The q^{st} values for 2,2-dimethylbutane on Carbosieve B and *n*-octane and *n*-nonane on Carbosieve B and CC2 cannot be determined because of the severe asymmetry of the chromatographic bands (tailing) and the problems of irreproducible retention data.

The linearity of the plots of q^{st} *vs.* n_c for *n*-alkanes and *n*-alkenes show that there is a fairly steady increase in the adsorbent–adsorbate interaction energy with increase in chain length of *n*-alkanes and *n*-alkenes. The values of q^{st} for *n*-alkanes, given by microporous samples, are considerably higher than the corresponding values given by GCB, which is an indication of porous nature or polar surface of these adsorbents.

The corresponding q^{st} values for *n*-alkanes generally have the following order: Carbosieve B > CC2 ≥ CC1, *i.e.*, Carbosieve B which possesses a homogeneous pore structure gives higher q^{st} values than CC1 which has a much broader range of pore

TABLE II

ISOSTERIC HEATS OF ADSORPTION FOR VARIOUS HYDROCARBONS ON ADSORBENTS

Adsorptive	q^{st} (kJ/mol)		
	Carbosieve B	CC1	CC2
Methane	22.2	20.9	21.4
Ethane	36.6	33.0	33.8
Propane	49.5	44.3	46.2
n-Butane	62.9	58.6	57.6
n-Pentane	75.4	69.7	71.8
n-Hexane	88.9	82.1	82.7
n-Heptane	100.4	93.6	93.4
n-Octane	–	104.7	–
n-Nonane	–	115.2	–
Ethylene	36.4	29.4	33.9
Propylene	48.9	45.2	47.4
n-Butylene	60.3	59.4	61.3
Isopentane	69.2	66.5	68.3
Cyclohexane	75.7	73.9	69.7
Benzene	74.9	72.6	70.7
2-Methylpentane	83.3	79.4	75.8
2,2-Dimethylbutane	–	75.1	68.4

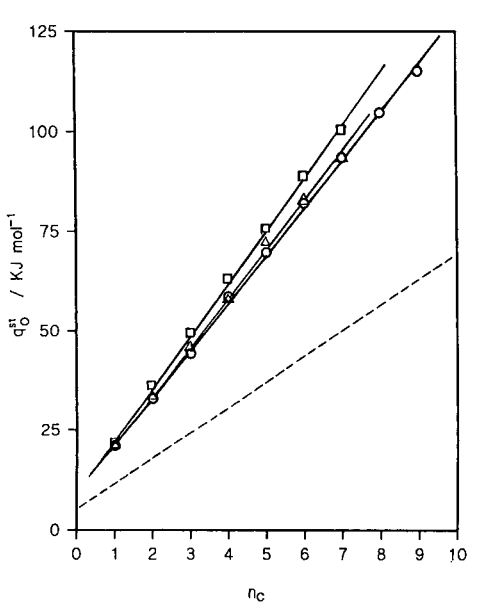

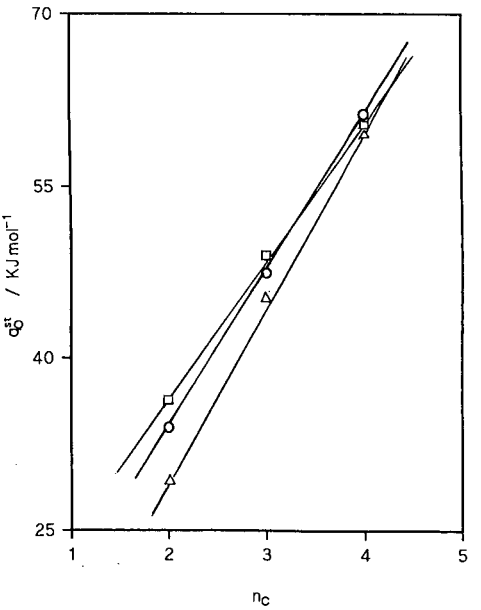

Fig. 5. Variation of q^{st} with *n*-alkane chain length for various adsorbents. ○ = CC1; □ = Carbosieve B; △ = CC2. Dashed line: GCB [9].

Fig. 6. Variation of q^{st} with *n*-alkene chain length for various adsorbents. ○ = CC2; □ = Carbosieve B; △ = CC1.

TABLE III

DIFFERENCES BETWEEN THE q^{st} VALUES OF *n*-ALKANES AND *n*-ALKENES ON ADSORBENTS

Adsorbents	Δq^{st} (kJ/mol)		
	Ethylene and ethane	Propylene and propane	*n*-Butylene and *n*-butane
Carbosieve B	−0.1	−0.5	−2.5
CC1	−3.6	0.9	0.7
CC2	0.2	1.3	1.6

sizes. This results show, as Carrott and Sing [3] reported, that the isosteric heats of adsorption are weighted in favour of the narrowest pores in the adsorbent. It is interesting to note that the q^{st} values of *n*-alkanes on CC1 which has much broader range of pores are similar to those on CC2, but the q^{st} values for molecular probes with branched or bulky shapes on CC1 are higher than those on CC2. This may be due to the wider micropores in CC1 in which there may be an enhancement of the adsorption energy for adsorption of bulkier molecules.

Table III shows differences between the isosteric heats of adsorption of *n*-alkanes and *n*-alkenes on the adsorbents. It can be seen that for each adsorbent the q^{st} values of *n*-alkanes are similar to those obtained with the corresponding *n*-alkenes, which shows the non-polar or slightly polar surfaces of these adsorbents, and that the adsorption of *n*-alkenes was dependent primarily on non-specific dispersion forces. The non-polarity of these adsorbents can also be shown by the similar q^{st} values of benzene and cyclohexane for these adsorbents.

The differences between the q^{st} values of different-shape molecular probes are shown in Table IV. It can be seen that the q^{st} values of straigth-carbon-chain hydrocarbons are higher than those of hydrocarbons with branch chains or bulky shape, which may show the molecular sieving properties of these adsorbents. For all adsorbents, the q^{st} values obey the following order: *n*-pentane > isopentane, hexane > 2-methylpentane > 2,2-dimethylbutane > cyclohexane $\approx$ benzene. This may be explained by assuming that generally a linear conformation will allow greatest inter-

TABLE IV

DIFFERENCES BETWEEN THE q^{st} VALUES OF DIFFERENT-SHAPE MOLECULES

Adsorptive	Δq^{st} (kJ/mol)		
	Carbosieve B	CC1	CC2
Between *n*-hexane and 2-methylpentane	5.5	2.7	6.9
2,2-dimethylbutane	–	6.9	14.3
cyclohexane	13.2	8.1	12.9
benzene	13.9	9.5	11.9
Between *n*-pentane and isopentane	6.2	3.2	3.6

actions between surface and adsorbate, while in branched structure the interaction between surface and adsorbate is weakened because some carbon atoms are relatively far away from the surface. It may also be an indication of slit-shaped micropores in these adsorbents to which the straight-chain molecules will be more accessible than those with bulky shapes.

CONCLUSIONS

GC has been shown to be useful for characterizing adsorbents by the determination of isosteric heats of adsorption at low surface coverage. For all adsorbents, the derived values of isosteric heats of adsorption of *n*-alkanes and *n*-alkenes generally increase linearly with the increase of the carbon number. The q^{st} values of *n*-alkenes are similar to those obtained with the corresponding *n*-alkanes, which shows the non-polar or slightly polar surface of these adsorbents. The q^{st} values of the molecules with branch chains or bulky shapes are smaller than those of corresponding straight-chain molecules, which may indicate the molecular sieving properties and the slit-shaped microporous structures of these adsorbents. The q^{st} values of hydrocarbons on these adsorbents were higher than those on GCB. The results also show that there may be an enhancement of adsorption energy for adsorption of some molecules in wider micropores.

REFERENCES

1 A. V. Kiselev, *Adv. Chromatogr.*, 4 (1967) 113.
2 P. J. M. Carrott and K. S. W. Sing, *Chem. Ind.*, (1986) 360.
3 P. J. M. Carrott and K. S. W. Sing, *J. Chromatogr.*, 406 (1987) 139.
4 T. Ahsan, B. A. Colenutt and K. S. W. Sing, *J. Chromatogr.*, 464 (1989) 416.
5 T. Ahsan, B. A. Colenutt and K. S. W. Sing, *J. Chromatogr.*, 479 (1989) 17.
6 S. J. Gregg and K. S. W. Sing, *Adsorption, Surface Area and Porosity*, Academic Press, London, 2nd ed., 1982.
7 D. H. Everett and J. C. Powl, *J. Chem. Soc., Faraday Trans. 1*, 72 (1976) 619.
8 D. H. Everett, in S. J. Gregg, K. S. W. Sing and H. F. Stoeckli (Editors), *Characterization of Porous Solids*, Society of Chemical Industry, London, 1979, p. 99.
9 N. N. Avgul and A. V. Kiselev, in P. L. Walker (Editor), *Chemistry and Physics of Carbon*, Marcel Dekker, New York, 1965, p. 1.

Journal of Chromatography, 555 (1991) 191–204
Elsevier Science Publishers B.V., Amsterdam

CHROM. 23 380

Gas chromatographic retention behaviour of some solutes on structurally similar polar and non-polar stationary phases

JEAN-CLAUDE DUTOIT[a]

Laboratoire de Chimie Technique, École Polytechnique Fédérale de Lausanne, CH-1015 Lausanne (Switzerland)

(First received December 12th, 1990; revised manuscript received April 18th, 1991)

ABSTRACT

A selection of 135 solutes, chosen to represent most chemical families, were characterized by *I*, the retention index of the solute on a pure polar phase and on a pure non-polar phase. Apart from the analysis of all the injected substances on the two pure extreme phases, a great number of the compounds were also measured on phases of variable polarity by modifying the mixtures of the two stationary phases available in well-defined proportions. Some correlations such as *I* as a function of the temperature and of the composition of the stationary phase were established.

INTRODUCTION

Alkanes are recognized as non-polar stationary phases in gas chromatography [1]. Their retention characteristics are the basis for the comparison of all other stationary phases. In order to obtain a non-polar model stationary phase, a high-molecular-weight branched hydrocarbon with very low polarity, $C_{78}H_{158}$, has already been synthesized [2].

Modification of the polarity of the reference stationary phase, 19,24-dioctadecyl dotetracontane (structure I), called hereafter "C_{78}", is achieved by replacing a methyl group with a unique hydroxyl group. This causes only a small change in the molecular weight and the global volume of the molecule [3].

Thus, the effect on the solute molecules of a change in only the polarity of the polar phase can be studied. The influence of molecular weight in the paraffin series of 1,1,6,6-tetraalkylhexane skeleton being already well documented [4], a single change in the structure of a molecule from this series changes only its polar part. In other words, having practically eliminated the effect of molecular weight, the effect of the polarity of the phase due to the one and only hydroxyl group of 19-(17′-hydroxy heptadecyl) 24-octadecyl dotetracontane (structure II), "C_{77}-OH", can be measured. Moreover, this –OH group, situated at the end of a chain, like a primary alcohol, is in an extremely

[a] Present address: Institut de Police Scientifique et de Criminologie, Place du Château 3, CH-1005 Lausanne, Switzerland.

0021-9673/91/$03.50

isolated situation, facing the rest of the molecule, represented by an enormous hydrocarbon ensemble.

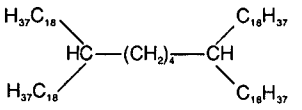

I

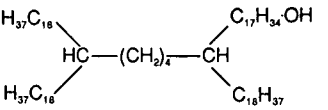

II

The retention index [5] of a solute (j) is defined as:

$$I_j = 100 \cdot \frac{\log X_j - \log X_z}{\log X_{z+1} - \log X_z} + 100 \cdot z \qquad (1)$$

where X represents any net retention value, j refers to the solute to be examined and X_z is the paraffin whose peak comes out before the solute and whose carbon atom number is z. X_{z+1} is the net retention value of the paraffin with $z + 1$ carbon atoms, which comes out after the solute.

The value of the retention index is affected by: (i) the solute; (ii) the stationary phase; and (iii) weakly by temperature.

EXPERIMENTAL

Materials

The solutes used for the chromatographic measurements were purchased either from Fluka (Buchs, Switzerland) or from Aldrich-Chemie (Steinheim, Germany). The compounds $C_{78}H_{158}$ [2] and $C_{77}H_{155}$-OH [3] were employed as stationary phases on Chromosorb G-HP (high performance), acid-washed and treated with dimethyl-chlorosilane, AW-DMCS, 80–100 mesh, from Supelco (Bellefonte, PA, USA). The commercial support was passed through a sieve and the fraction with particle diameter (d_p) 150–180 μm (between filters DIN Nos. 30 and 50) was dried overnight in an oven at 100°C.

Column packings

The columns were 370 cm long circular Pyrex tubes with a spiral diameter of 16.0 cm and an internal diameter of 0.40 cm.

The columns were filled with a support impregnated with 5.00% (w/w) liquid phase. This was measured by weighing both support and liquid phase with a precision of ± 0.0001 g. (Preparation of the filling: the fine white crystals were dissolved in distilled cyclohexane and the homogeneous solution was added to an exact quantity of support. The solvent was evaporated under a slight vacuum in an argon stream at about 180°C.)

The Pyrex glass columns, washed, dried and weighed with a precision of ± 0.01 g, were filled using a water pump and vibrations. They were kept overnight under argon.

The weight of packing in the column was measured as the difference between the

TABLE I

COLUMN PACKING CHARACTERISTICS

w is the ponderal fraction of C_{77}-OH in the stationary liquid, m_r is the packing mass, P_θ is the liquid internal weight (%) and $m_\theta = m_r \cdot P_\theta/100$ is the stationary liquid mass in the column.

w	m_r (g)	P_θ (%)	m_θ (g)
0.000	32.06	4.766	1.528
0.333	31.38	4.767	1.496
0.667	30.17	4.760	1.436
1.000	30.16	4.764	1.458

empty and packed columns (see Table I). The amount of liquid phase was calculated from the total weight of the packing. Since the two stationary phases were pure C_{78} and C_{77}-OH, two mixtures consisting of 33.3% and 66.7% C_{77}-OH could be precisely measured, to pack two further columns.

Apparatus

A Packard-Becker (Delft, Netherlands) Model 419 gas chromatograph was used for the retention data determination. This instrument was equipped with a platinum resistance thermometer, a flowmeter and a precision manometer for more precise measurements.

The flow-rate was measured and regulated with a thermal flowmeter from Brooks (Veenendaal, Netherlands), composed of two essential units: a mass flow sensor Type 5850 TR and a regulator Model 4251-IA2B1E0. The flowmeter, originally calibrated at 2 Bars (1500.12 mmHg) and 20°C, was adjusted to give digital display of the volumic flow-rate of the carrier gas (helium) at 760 Torr and 0°C.

The column temperature was determined taking into account the temperature gradient inside the chromatograph oven. To measure this gradient, a cube-shaped wire skeleton was built smaller than the oven size. A chromel wire was fixed on the skeleton, and an alumel wire was soldered at each of its corners. The temperature differences between the corners of the cube were measured by means of a digital microvoltmeter, Type Trendicator 400A (Doric, San Diego, CA, USA). The absolute temperature was measured with a platinum resistance thermometer, which was calibrated by Dr. M. Wittwer (Eidg. Amt für Mass und Gewichte, Wabern/Berne, Switzerland) between 0°C and 400°C with a precision of ± 0.1°C in absolute temperature. The column temperature ($\overline{T_c}$) was calculated as described in ref. 6, taking the gradient in the oven into consideration. A middle temperature value was calculated for the column centre, located at 1/4 and 3/4 of the total distance between the cube front and back sides.

The inlet pressure of the chromatographic system, $P_i' = \Delta P' + P_{atm}$, was measured via a Heise Type 710B digital manometer (Dresser Europe, Werk Baesweiler, Germany), where

$$\Delta P' = \Delta P + \Delta P_i + \Delta P_o \tag{2}$$

was the pressure drop in the chromatographic system. The average pressure in the column was calculated considering the inlet resistance at the capillary tubes' injector

(R_i) and the outlet resistance at the detector (R_o). The inlet resistance (R_i) was determined at different temperatures and flow-rates by measuring the flow-rate, $\dot{V}_i$, after the injector and the pressure drop (ΔP_i), in the absence of column (NTP = normal temperature and pressure):

$$R_i = \Delta P_i / \dot{V}_i \tag{3}$$

$$\dot{V}_i = (\dot{V}_c/\text{NTP}) \cdot (\overline{T_c}/273.15)[760/(P_{atm} + \Delta P_i/2)] \tag{4}$$

where $\dot{V}_c$ is the flow-rate in the column at NTP.

To measure the outlet resistance (R_o), an empty column was placed in the apparatus and the resistance was determined by measuring the carrier gas flow at the detector outlet ($\dot{V}'_o$).

$$R_0 = \Delta P_o / \dot{V}'_o \tag{5}$$

$$\dot{V}'_o = (\dot{V}_c/\text{NTP}) \cdot (\overline{T_c}/273.15) \cdot [760/(P_{atm} + \Delta P_o/2)] \tag{6}$$

and

$$\Delta P_o = \Delta P' - P_i \tag{7}$$

Both resistances (R_i and R_o) were constant with temperature. A mean value was therefore used [6].

The definition of the retention volume only becomes applicable if the flow at the column outlet, $\dot{V}_o$, is replaced by the average gas flow along the column [7], which is ${}^2_3J \cdot \dot{V}_o$. The James and Martin factor (${}^2_3J$) [8], which depends on the inlet and the outlet pressures of the column, respectively P_i and P_o, is ($p = P_i/P_o$):

$${}^2_3J = 3/2\ (p^2 - 1)/(p^3 - 1) \tag{8}$$

Practically, an average volumic flow of the carrier gas through the column, taking the charge loss into account, is defined by:

$$\overline{\dot{V}_c} = {}^2_3J \cdot \dot{V}_o \tag{9}$$

The gross retention time t_R was determined with two HP 3390A integrators (Hewlett-Packard) at a precision of ± 0.001 min. The various regression coefficients listed in Table II were obtained by computer (Digital Equipment Corp., Maynard, MA, USA; Model Pro. 380). The data evaluation system RS/1 was conceived by the firm Bolt Beranek and Newmann (Cambridge, MA, USA). The tables were printed by an LA50 printer and the graphs traced with an LVP16 plotter (both Digital).

RESULTS

Using the retention time t_R and the "retention time of a non-retained compound" [7] such as neon, $\overline{t_R}$(Ne), we determined the net retention time, t_N:

$$t_N = t_R - \overline{t_R}(\text{Ne}) \tag{10}$$

Considering eqn. 1, the retention index can then be calculated by:

$$I_j = 100 \cdot \frac{\log t_N - \log t_N(z)}{\log t_N(z+1) - \log t_N(z)} + 100 \cdot z \tag{11}$$

The retention index I is determined at an experimental temperature, T_{exp}, which is near the column nominal temperature, *i.e.*, 90.0°C, 110.0°C, 130.0°C, 150.0°C and 170.0°C. The I average and T_{exp} average were determined at each experimental temperature. After regression of the experimental I, the slope was adjusted for I experimental to I at the nominal temperature.

The resulting general equation of the retention index as a function of the temperature interval around 130°C, ΔT, and of the C_{77}-OH mass fraction, w, is therefore:

$$\begin{aligned} I = I_{130} &+ d_T \cdot \Delta T + d_{TT} \cdot \Delta T^2 + d_{TTT} \cdot \Delta T^3 + \\ &+ d_L \cdot w + d_{LL} \cdot w^2 + d_{LT} \cdot w \cdot \Delta T + \\ &+ d_{LLT} \cdot w^2 \cdot \Delta T + d_{LTT} \cdot w \cdot \Delta T^2 + d_{LLTT} \cdot w^2 \cdot \Delta T^2 \end{aligned} \tag{12}$$

where the coefficients for d_X are expressed by T for the temperature and L for the stationary phase composition, and where:

$$\Delta T = \{-40, -20, 0, +20, +40\} \tag{13}$$

and

$$w = \{0, 1/3, 2/3, 1\} \tag{14}$$

The stationary phase consisting of only pure C_{78} was taken as the reference, and thus I_{130} is the index at 130°C on C_{78} ($w = 0$).

An equation analogous to eqn. 12 can be put for I by considering, this time, the b_x coefficients of the orthogonal polynomials in P:

$$\begin{aligned} I = b_o &+ b_T \cdot P_T + b_{TT} \cdot P_{TT} + b_{TTT} \cdot P_{TTT} + \\ &+ b_L \cdot P_L + b_{LL} \cdot P_{LL} + b_{LT} \cdot P_L \cdot P_T + \\ &+ b_{LLT} \cdot P_{LL} \cdot P_T + b_{LTT} \cdot P_L \cdot P_{TT} + b_{LLTT} \cdot P_{LL} \cdot P_{TT} \end{aligned} \tag{15}$$

Considering that a five-temperature (T source) and four-phases composition (L source) system is available, the coefficient values of the orthogonal polynomials are defined [9] as follows:

$$P_T = \frac{\Delta T}{20} = \{-2, -1, 0, +1, +2\} \tag{16}$$

$$P_{TT} = P_T^2 - 2 = \{+2, -1, -2, -1, +2\} \tag{17}$$

$$P_{TTT} = P_T^3 - 3.4\, P_T = \frac{6}{5}\{-1, +2, 0, -2, +1\} \tag{18}$$

TABLE II

RETENTION INDICES ON STRUCTURALLY SIMILAR STATIONARY PHASES

The coefficients in eqn. 12 are evaluated by the orthogonal polynomials method applied to the measured chromatographic data. The values marked "−" are not calculable because measurements for these solutes were carried out only on the two extreme phases. On the other hand, "ϕ" means that the coefficient was not significant, and the values were therefore not retained. Δ_{95} is the confidence limit at the 95% confidence level.

Solute	Experimental conditions		I_{130}	$d_T \cdot 10$ (K^{-1})	$d_{TT} \cdot 10^3$ (K^{-2})	d_L	d_{LL}	$d_{LT} \cdot 10$ (K^{-1})	$d_{LLT} \cdot 10$ (K^{-1})	$d_{LTT} \cdot 10^3$ (K^{-2})	Δ_{95}
	T (°C)	L^a									
Isoalkanes											
2,2-Dimethylbutane	90–170	(2)	541.3	0.94	ϕ	−0.3	−	0.05	−	ϕ	1.08
2,2-Dimethylpentane	90–170	(2)	628.3	0.78	ϕ	−0.1	−	0.05	−	ϕ	0.77
2,4-Dimethylpentane	90–170	(2)	629.5	0.35	ϕ	−0.8	−	0.06	−	ϕ	0.85
2,2,3-Trimethylbutane	90–170	(2)	652.1	1.60	ϕ	−0.1	−	0.12	−	ϕ	0.82
2,2-Dimethylhexane	90–170	(2)	719.4	0.48	ϕ	−0.6	−	0.10	−	ϕ	0.69
2,4-Dimethylhexane	90–170	(2)	733.1	0.52	ϕ	−0.2	−	0.01	−	ϕ	0.55
3,4-Dimethylhexane	90–170	(2)	780.3	1.04	ϕ	0.2	−	0.03	−	ϕ	0.61
2,3,4-Trimethylpentane	90–170	(2)	764.8	1.45	ϕ	0.3	−	0.07	−	ϕ	0.53
2,2,4-Trimethylpentane	90–170	(2)	694.5	1.05	ϕ	−0.2	−	0.01	−	ϕ	0.50
2,2,4,6,6-Pentamethylheptane	90–170	(2)	989.7	2.08	ϕ	−0.5	−	−0.01	−	ϕ	1.08
Alkenes											
1-Hexene	90–170	(2)	588.1	0.88	ϕ	2.9	−	−0.37	−	ϕ	1.56
1-Heptene	90–170	(2)	686.5	0.58	ϕ	3.3	−	−0.26	−	ϕ	1.04
1-Octene	90–170	(2)	785.6	0.51	ϕ	3.7	−	−0.18	−	ϕ	0.69
1-Nonene	90–170	(2)	885.5	0.52	ϕ	4.0	−	−0.16	−	ϕ	0.44
1-Decene	90–170	(2)	985.2	0.50	ϕ	4.3	−	−0.25	−	ϕ	1.00
Alkynes											
1-Hexyne	90–170	(4)	589.7	0.67	ϕ	15.3	ϕ	−0.18	ϕ	ϕ	1.30
1-Heptyne	90–170	(4)	689.1	0.43	ϕ	15.6	ϕ	−0.17	ϕ	ϕ	1.03
1-Octyne	90–170	(4)	788.7	0.42	ϕ	16.0	ϕ	−0.08	ϕ	ϕ	0.87
1-Nonyne	90–170	(4)	889.0	0.47	ϕ	16.1	ϕ	−0.03	ϕ	ϕ	0.90
1-Decyne	110–170	(2)	988.9	0.54	ϕ	16.3	−	−0.10	−	ϕ	1.30
Cycloalkanes											
Cyclopentane	90–170	(2)	588.2	2.11	ϕ	2.1	−	−0.09	−	ϕ	0.90
Cyclohexane	90–170	(2)	694.0	3.08	ϕ	1.6	−	−0.13	−	ϕ	1.27
Cycloheptane	90–170	(2)	837.2	4.24	ϕ	3.0	−	−0.05	−	ϕ	0.59
Cyclooctane	90–170	(2)	965.2	5.25	ϕ	3.8	−	−0.10	−	ϕ	0.46

Alkylbenzenes											
Benzene	90–170	(4)	677.6	3.24	0.84	10.5	5.5	−0.08	ϕ	−1.13	1.01
Toluene	90–170	(4)	785.8	3.19	0.58	12.4	4.0	0.03	ϕ	−0.84	0.77
Ethylbenzene	90–170	(4)	875.4	3.52	0.63	12.9	3.4	−0.03	ϕ	−1.11	0.72
Propylbenzene	90–170	(2)	963.9	3.72	0.27	15.8	–	0.09	–	−0.89	1.56
1-Chloroalkanes											
1-Chlorobutane	90–170	(4)	639.7	1.93	0.75	13.7	2.7	−0.45	0.36	−1.09	0.75
1-Chloropentane	90–170	(4)	742.4	1.90	0.32	14.1	2.4	−0.42	0.44	−0.70	0.53
1-Chlorohexane	90–170	(4)	843.8	2.00	0.22	14.7	2.0	−0.44	0.46	−0.62	0.52
1-Chloroheptane	130–170	(2)	945.2	2.13	ϕ	16.8	–	−0.20	–	ϕ	0.88
1-Chlorooctane	130–170	(2)	1046.4	1.93	ϕ	16.2	–	0.00	–	ϕ	0.19
1-Bromoalkanes											
1-Bromopropane	90–170	(2)	628.8	2.67	0.36	17.1	–	−0.02	–	−0.29	1.33
1-Bromobutane	90–170	(2)	732.0	2.74	0.34	17.1	–	0.02	–	−0.30	1.13
1-Bromopentane	90–170	(2)	834.4	2.94	0.30	17.2	–	−0.03	–	−0.16	1.02
1-Bromohexane	130–170	(2)	935.4	3.28	ϕ	17.5	–	−0.15	–	ϕ	1.28
1-Bromoheptane	130–170	(2)	1036.3	3.38	ϕ	17.6	–	−0.20	–	ϕ	0.88
1-Cyanoalkanes											
1-Cyanopropane	90–170	(4)	593.8	1.24	ϕ	53.7	2.5	−1.40	4.16	ϕ	0.94
1-Cyanobutane	90–170	(4)	697.0	1.54	ϕ	53.7	4.4	−2.13	1.13	ϕ	1.34
1-Cyanopentane	90–170	(4)	798.8	1.67	ϕ	55.1	4.1	−2.18	1.26	ϕ	1.08
1-Cyanohexane	90–170	(4)	899.8	1.60	ϕ	55.0	4.2	−1.73	1.05	ϕ	1.13
1-Cyanoheptane	130–170	(2)	1000.7	1.80	ϕ	60.2	–	−1.17	–	ϕ	0.62
1-Nitroalkanes											
Nitroethane	90–170	(4)	571.9	1.62	ϕ	39.4	9.9	−0.88	0.36	ϕ	1.17
1-Nitropropane	90–170	(4)	664.6	1.98	ϕ	38.4	9.1	−1.40	0.87	ϕ	1.29
1-Nitrobutane	90–170	(4)	767.0	2.19	ϕ	39.7	8.3	−1.37	1.00	ϕ	1.15
1-Nitropentane	90–170	(4)	868.6	2.26	ϕ	41.8	6.7	−1.01	0.78	ϕ	1.42
1-Nitrohexane	130–170	(2)	970.1	2.38	ϕ	48.5	–	−0.55	–	ϕ	0.64
1-Acetoxyalkanes											
1-Acetoxypropane	90–170	(4)	639.8	−0.56	ϕ	45.8	−3.8	−2.12	1.14	ϕ	1.16
1-Acetoxybutane	90–170	(4)	741.0	−0.54	ϕ	46.7	−3.7	−2.21	1.28	ϕ	1.06
1-Acetoxypentane	90–170	(4)	841.3	−0.53	ϕ	47.8	−4.1	−1.88	0.97	ϕ	1.07
1-Acetoxyhexane	130–170	(2)	940.5	−0.28	ϕ	44.2	–	−1.17	–	ϕ	2.21
1-Acetoxyheptane	130–170	(2)	1040.4	−0.23	ϕ	44.1	–	−1.20	–	ϕ	2.47

(*Continued on p. 198*)

TABLE II *(continued)*

Solute	Experimental conditions		I_{130}	$d_T \cdot 10$ (K^{-1})	$d_{TT} \cdot 10^3$ (K^{-2})	d_L	d_{LL}	$d_{LT} \cdot 10$ (K^{-1})	$d_{LLT} \cdot 10$ (K^{-1})	$d_{LTT} \cdot 10^3$ (K^{-2})	Δ_{95}
	T (°C)	L^a									
1-Alkanols											
1-Butanol	90–170	(4)	596.7	0.97	1.32	57.6	12.0	−6.43	ϕ	4.59	2.84
1-Pentanol	90–170	(4)	700.0	0.85	0.76	60.6	10.7	−6.39	ϕ	5.29	2.75
1-Hexanol	90–170	(4)	801.6	0.98	0.77	63.5	9.1	−6.46	ϕ	5.37	2.78
1-Heptanol	130–170	(2)	903.2	1.33	ϕ	73.2	–	−4.51	–	ϕ	4.19
1-Octanol	130–170	(2)	1004.1	1.35	ϕ	73.5	–	−4.55	–	ϕ	4.34
2-Alkanols											
2-Butanol	90–170	(4)	549.7	0.75	0.20	46.7	12.3	−5.38	ϕ	4.94	3.40
2-Pentanol	90–170	(4)	647.8	0.87	0.38	50.3	9.5	−5.67	ϕ	4.63	3.10
2-Hexanol	90–170	(4)	747.3	0.90	0.31	53.6	8.0	−5.73	ϕ	4.74	3.00
2-Heptanol	90–170	(4)	837.2	0.99	0.33	55.7	6.9	−5.80	ϕ	4.82	2.94
2-Octanol	110–170	(2)	948.8	1.01	ϕ	63.6	–	−4.46	–	ϕ	3.58
2-Methylalkan-2-ols											
2-Methylbutanol-2	90–170	(4)	600.2	1.19	1.20	50.2	5.9	−5.30	ϕ	3.38	3.11
2-Methylpentanol-2	90–170	(4)	691.9	0.92	1.10	51.4	5.4	−5.22	ϕ	3.21	3.07
2-Methylhexanol-2	90–170	(4)	787.0	0.94	1.05	53.3	4.6	−5.26	ϕ	3.28	2.92
2-Methylheptanol-2	90–170	(4)	884.7	0.97	1.05	55.1	3.4	−5.31	ϕ	3.15	3.04
Thiols											
Butanethiol	90–170	(2)	722.5	3.15	−1.11	19.3	–	0.23	–	2.05	5.52
Pentanethiol	90–170	(2)	823.8	3.22	−0.89	18.1	–	0.59	–	2.25	2.00
Hexanethiol	130–170	(2)	924.7	2.83	ϕ	17.7	–	1.57	–	ϕ	1.00
Heptanethiol	130–170	(2)	1024.5	3.00	ϕ	18.5	–	1.45	–	ϕ	2.29
2-Alkanones											
2-Pentanone	90–170	(4)	631.6	0.77	0.66	47.9	ϕ	−3.32	1.98	−0.92	1.05
2-Hexanone	90–170	(4)	732.8	0.79	0.63	49.5	ϕ	−3.34	2.04	−0.93	0.99
2-Heptanone	90–170	(4)	832.8	0.88	0.68	50.2	ϕ	−3.57	2.27	−0.98	1.06
2-Octanone	130–170	(2)	932.6	1.25	ϕ	50.6	–	−1.75	–	ϕ	1.03
2-Nonanone	130–170	(2)	1032.7	1.23	ϕ	50.8	–	−1.78	–	ϕ	0.76
Ethers											
Dipropyl ether	90–170	(4)	657.1	0.29	0.58	17.1	0.8	−2.65	1.67	−0.79	1.08
Dibutyl ether	90–170	(4)	854.5	0.10	0.30	20.4	−2.1	−1.87	1.22	−0.64	0.61
Dipentyl ether	130–170	(2)	1051.1	0.20	ϕ	18.9	–	−0.85	–	ϕ	0.50

Halogenomethanes											
Dichloromethane	90–170	(4)	508.0	1.70	ϕ	15.9	9.9	0.05	ϕ	ϕ	1.87
Trichloromethane	90–170	(4)	610.1	2.57	ϕ	16.4	9.2	−0.47	ϕ	ϕ	1.25
Tetrachloromethane	90–170	(4)	680.2	3.07	ϕ	3.1	5.5	−0.02	ϕ	ϕ	0.91
Aldehydes											
Pentanal	90–170	(2)	651.6	1.12	−0.84	40.5	–	−2.17	–	1.80	3.50
Hexanal	90–170	(2)	751.8	1.17	−0.36	42.4	–	−1.98	–	1.13	1.41
Heptanal	90–170	(2)	852.7	1.26	−0.21	43.2	–	−1.89	–	1.04	0.93
Octanal	110–170	(2)	953.3	1.36	ϕ	43.8	–	−1.60	–	ϕ	0.67
Halogenobenzenes											
Fluorobenzene	90–170	(2)	666.4	2.49	ϕ	17.7	–	−0.07	–	ϕ	1.76
Chlorobenzene	90–170	(2)	865.7	4.46	ϕ	19.8	–	−0.04	–	ϕ	1.29
Bromobenzene	90–170	(2)	960.9	5.63	ϕ	21.5	–	0.04	–	ϕ	0.91
Alkylpyridines											
Pyridine	90–170	(4)	725.5	3.47	0.82	66.9	−1.3	−6.17	2.90	ϕ	2.22
2-Picoline	90–170	(4)	803.4	2.99	1.04	72.9	−6.6	−6.98	3.33	ϕ	1.93
3-Picoline	90–170	(4)	846.0	3.73	1.04	76.6	−3.1	−7.25	3.34	ϕ	2.16
4-Picoline	90–170	(4)	845.1	3.79	1.21	81.1	−4.0	−8.02	3.83	ϕ	2.49
2,3-Lutidine	130–170	(2)	936.6	3.70	ϕ	70.6	–	−3.85	–	ϕ	0.36
2,4-Lutidine	130–170	(2)	921.8	3.03	ϕ	76.7	–	−4.48	–	ϕ	0.88
2,5-Lutidine	130–170	(2)	921.3	3.30	ϕ	71.9	–	−4.05	–	ϕ	2.46
2,6-Lutidine	130–170	(2)	873.8	2.25	ϕ	62.6	–	−3.68	–	ϕ	2.46
3,4-Lutidine	130–170	(2)	988.1	4.55	ϕ	86.0	–	−4.98	–	ϕ	1.41
3,5-Lutidine	130–170	(2)	966.1	3.88	ϕ	80.7	–	−4.61	–	ϕ	3.34
2-Ethylpyridine	130–170	(2)	888.5	3.35	ϕ	57.2	–	−2.95	–	ϕ	1.05
3-Ethylpyridine	130–170	(2)	928.9	4.18	ϕ	73.0	–	−3.83	–	ϕ	1.23
4-Ethylpyridine	130–170	(2)	943.4	4.10	ϕ	76.9	–	−4.07	–	ϕ	0.71
2-Propylpyridine	130–170	(2)	976.8	3.35	ϕ	56.4	–	−2.87	–	ϕ	3.51
4-Propylpyridine	130–170	(2)	1033.6	4.38	ϕ	76.0	–	−3.90	–	ϕ	2.64
sym-Collidine	130–170	(2)	988.2	2.30	ϕ	72.3	–	−4.23	–	ϕ	1.41
2,3,6-Collidine	130–170	(2)	1002.2	2.80	ϕ	66.3	–	−3.95	–	ϕ	0.36
4-*t*-Butylpyridine	130–170	(2)	1069.8	4.78	ϕ	76.7	–	−3.98	–	ϕ	0.19
3-Chloropyridine	110–170	(2)	886.7	4.57	ϕ	47.9	–	−1.59	–	ϕ	0.93
Silane derivatives											
Hexamethyldisilane	90–170	(2)	686.2	0.27	ϕ	−0.3	–	−0.07	–	ϕ	1.82
Hexamethyldisiloxane	90–170	(2)	597.8	−2.49	ϕ	0.2	–	−0.11	–	ϕ	2.54

(*Continued on p. 200*)

TABLE II *(continued)*

Solute	Experimental conditions		I_{130}	$d_T \cdot 10$ (K^{-1})	$d_{TT} \cdot 10^3$ (K^{-2})	d_L	d_{LL}	$d_{LT} \cdot 10$ (K^{-1})	$d_{LLT} \cdot 10$ (K^{-1})	$d_{LTT} \cdot 10^3$ (K^{-2})	Δ_{95}
	T (°C)	L^a									
Primary amines											
Butylamine	90–170	(2)	610.4	0.84	0.57	71.4	–	−5.36	–	−3.52	19.96
Pentylamine	90–170	(2)	713.8	0.76	0.14	68.1	–	−5.83	–	2.36	8.18
Hexylamine	90–170	(2)	815.6	0.89	0.41	66.7	–	−5.83	–	4.18	4.58
Heptylamine	130–170	(2)	917.5	0.95	ϕ	66.2	–	−3.85	–	ϕ	2.22
Secondary amines											
Diethylamine	90–170	(2)	555.8	−0.25	−1.27	55.1	–	−5.51	–	4.98	1.78
Dipropylamine	90–170	(2)	743.6	0.19	−0.75	42.5	–	−4.26	–	3.02	1.03
Dibutylamine	130–170	(2)	943.0	0.18	ϕ	44.4	–	−3.61	–	ϕ	4.35
Tertiary amines											
Triethylamine	90–170	(2)	676.4	0.47	−0.64	29.6	–	−3.28	–	1.77	1.66
Tripropylamine	110–170	(2)	918.5	0.68	ϕ	10.2	–	−0.76	–	ϕ	1.03
Miscellaneous											
Tetrahydrofuran	90–170	(4)	611.3	1.99	ϕ	43.5	−4.9	−1.45	ϕ	ϕ	1.80
1,4-Dioxane	90–170	(4)	670.8	2.31	ϕ	50.1	−2.3	−1.20	ϕ	ϕ	1.59
Thiophene	90–170	(2)	685.6	3.57	ϕ	18.6	–	−0.11	–	ϕ	1.89
1,1,1-Trifluorodecane	110–170	(2)	922.1	−2.44	ϕ	9.5	–	0.01	–	ϕ	2.11
Miscellaneous cyclic compounds											
Cyclopentanone	90–170	(2)	743.5	3.00	ϕ	60.0	–	−1.59	–	ϕ	0.98
Cyclohexanone	90–170	(2)	857.2	4.52	ϕ	61.5	–	−1.77	–	ϕ	0.36
Cyclohexanol	110–170	(2)	855.3	4.05	ϕ	68.2	–	−4.72	–	ϕ	4.48
Cyclohexylamine	110–170	(2)	863.2	4.23	ϕ	72.1	–	−5.69	–	ϕ	3.74
Pyrrolidine	90–170	(2)	679.5	2.08	−1.21	78.3	–	−10.18	–	8.77	1.98
Piperidine	90–170	(2)	766.4	3.35	−0.96	72.1	–	−7.32	–	4.86	1.86
Miscellaneous aromatics											
Aniline	110–170	(2)	939.4	4.98	ϕ	59.1	–	−1.75	–	ϕ	0.95
Nitrobenzene	130–170	(2)	1053.9	5.48	ϕ	46.1	–	−0.53	–	ϕ	1.06
Benzylic alcohol	130–170	(2)	981.4	4.33	ϕ	89.7	–	−4.86	–	ϕ	5.38
2-Phenylethanol	130–170	(2)	1060.4	4.93	ϕ	85.2	–	−4.50	–	ϕ	3.28
Anisol	130–170	(2)	910.7	3.00	ϕ	28.3	–	−0.20	–	ϕ	2.12
Phenetol	130–170	(2)	979.6	2.43	ϕ	27.1	–	−0.25	–	ϕ	2.52

[a] $L = 2$: tested with the two pure phases. $L = 4$: tested with the two pure phases, as well as with the two mixtures (1:3; 2:3).

$$P_L = 3\left(w - \frac{1}{2}\right) = \frac{1}{2}\{-3, -1, +1, +3\} \quad (19)$$

$$P_{LL} = P_L^2 - \frac{5}{4} = \{+1, -1, -1, +1\} \quad (20)$$

Substituting eqns. 16–20 into eqn. 15, and comparing with eqn. 12, we then obtain the d_x conversion coefficients, connected algebraically by the calculation method of the orthogonal polynomials, to b_x:

$$I_{130} = b_o - 2\,b_{TT} - \frac{3}{2}\,b_L + b_{LL} + 3\,b_{LTT} - 2\,b_{LLTT} \quad (21)$$

$$d_T = \frac{1}{2}\,b_T - 1.7\,b_{TTT} - \frac{3}{4}\,b_{LT} + \frac{1}{2}\,b_{LLT} \quad (22)$$

$$d_{TT} = \frac{1}{4}\,b_{TT} - \frac{3}{8}\,b_{LTT} + \frac{1}{4}\,b_{LLTT} \quad (23)$$

$$d_{TTT} = \frac{1}{8}\,b_{TTT} \quad (24)$$

$$d_L = 3\,b_L - 9\,b_{LL} - 6\,b_{LTT} + 18\,b_{LLTT} \quad (25)$$

$$d_{LL} = 9\,b_{LL} - 18\,b_{LLTT} \quad (26)$$

$$d_{LT} = \frac{3}{2}\,b_{LT} - \frac{9}{2}\,b_{LLT} \quad (27)$$

$$d_{LLT} = \frac{9}{2}\,b_{LLT} \quad (28)$$

$$d_{LTT} = \frac{3}{4}\,b_{LTT} - \frac{9}{4}\,b_{LLTT} \quad (29)$$

$$d_{LLTT} = \frac{9}{4}\,b_{LLTT} \quad (30)$$

The treatment by orthogonal polynomials gives us a variance analysis. Each coefficient of eqn. 12 is thus examined separately for the significance of its effect. Although all the solutes are considered individually, the coefficients with a significant effect are taken into consideration with regard to a global analysis at the chemical family level. The coefficient is accepted as long as the significance level is within 5% of the maximum for each source and for at least half the solutes of a single family. The variance of each source is tested not against the total residue after the elimination of ten

b_x coefficients, but on the residual variance of the LT source having still $8 = [(4 - 1) \times (5 - 1)] - 4$ degrees of freedom. The test allows a b_x effect to be retained when the $F_{1/8}$ is greater or equal to 5.

For the cases of the incompletely measured solutes, that is on only two phases and at three temperatures (130.0–170.0°C) or four temperatures (110.0–170.0°C), only the treatment on each of the two phases taken separately was considered. The variance analysis considered only the T source effects. Consideration of the complete chemical family assumes that the effects of the T and LT sources are the same for each of its members. In this case, the coefficient $d_{LT} = d_T(C_{77}\text{-OH}) - d_T(C_{78})$ and $d_{LTT} = d_{TT}(C_{77}\text{-OH}) - d_{TT}(C_{78})$. Only the LL and LLT sources are not accessible for these incomplete situations (Table II).

DISCUSSION

From the measurements of the indices, some examples can be extracted. In Fig. 1, the difference in behaviour of solutes on the two pure stationary phases is compared. The retention index of 1-cyanopropane, a rather non-polar solute, increases linearly with temperature, whereas I values are higher on C_{77}-OH, because of the interactions, as expected. For a polar solute like 1-butanol, I is similar to that of the cyano compound on C_{78}, but on C_{77}-OH its behaviour is quite different, because I decreases with temperature.

At a constant temperature such as $T = 130$°C, as shown in Fig. 2, I increases going from a non-polar to a polar stationary phase. I of both of the two solutes increases as the polar phase concentration increases.

The two graphs in Figs. 3 and 4 show that the solutes can have very different behaviour when the phase composition is modified. If the solute is 1-cyanopropane (Fig. 3), I increases linearly with the temperature whatever the stationary phase composition w may be.

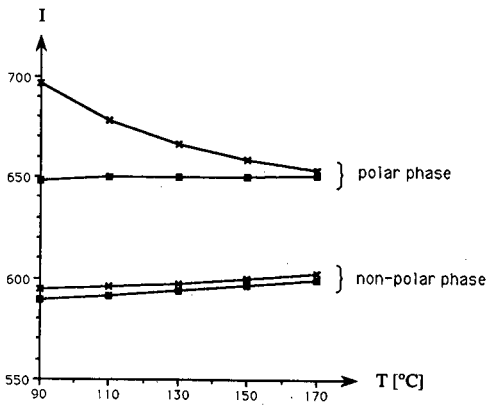

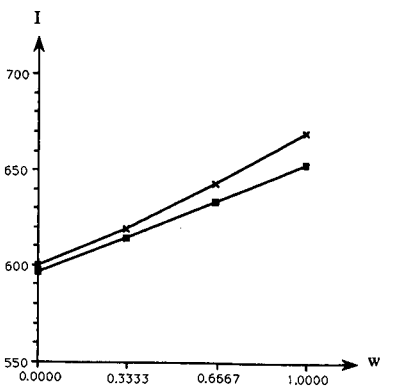

Fig. 1. I values as a function of column temperature (90, 110, 130, 150 and 170°C) on the pure stationary phases. Solutes: ◘ = 1-cyanopropane; × = 1-butanol.

Fig. 2. I values as a function of w = stationary phase composition, at constant temperature $T = 130$°C. Solutes: ◘ = 1-cyanopropane; × = 1-butanol.

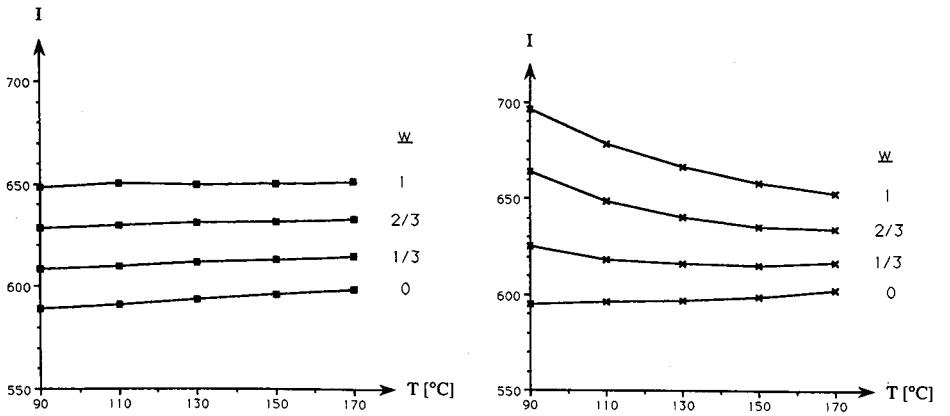

Fig. 3. I values as a function of column temperature (90, 110, 130, 150 and 170°C). w is the stationary phase composition. Solute: 1-cyanopropane.

Fig. 4. I values as a function of column temperature (90, 110, 130, 150 and 170°C). w is the stationary phase composition. Solute: 1-butanol.

For 1-butanol as the solute (Fig. 4), I increases linearly with the temperature on C_{78} but decreases as w increases, *i.e.*, with increased polarity of the stationary phase.

In conclusion, we can say that the I values are well adapted for a comparison between two stationary phases.

All the above data can also be compressed and reduced to an explicit three-dimensional diagram [10] using I, T and w as coordinates.

CONCLUSIONS

It should be noted that the results of the investigation on column packings prepared with two pure substances combined in different proportions allow the characterization of these two phases.

Finally, the retention indices obtained in this study will allow the determination of thermodynamic parameters useful for a further explanation of molecular interactions in gas chromatography [11].

ACKNOWLEDGEMENTS

This paper reports part of a project supported by the Fonds National Suisse de la Recherche Scientifique, Project No. 69.02. I thank Professor E. sz. Kováts for his continuous support and supervision, and Dr. Chr. de Reyff for his help with the calculations.

REFERENCES

1 F. Riedo, D. Fritz, G. Tarján and E. sz. Kováts, *J. Chromatogr.*, 126 (1976) 63.
2 P. Zeltner, G. A. Huber, R. Peters, F. Tátrai, L. Boksányi and E. sz. Kováts, *Helv. Chim. Acta*, 62 (1979) 2495.

3 J.-C. Dutoit and K. Fóti, in preparation.
4 G. A. Huber and E. sz. Kováts, *Anal. Chem.*, 45 (1973) 1155.
5 E. sz. Kováts, *Helv. Chim. Acta*, 41 (1958) 1915.
6 D. F. Fritz, A. Sahil and E. sz. Kováts, *J. Chromatogr.*, 186 (1979) 63.
7 J. Tranchant, *Manuel Pratique de Chromatographie en Phase Gazeuse*, Masson, Paris, 3rd ed., 1982, p. 11.
8 A. S. Said, *Theory and Mathematics of Chromatography*, Hüthig, Heidelberg, 1981, p. 65.
9 R. A. Fisher and F. Yates, *Statistical Tables for Biological, Agricultural and Medical Research*, Longman, London, 6th ed., 1963, p. 98.
10 J.-C. Dutoit, *Doctoral Thesis No. 717*, École Polytechnique Fédérale de Lausanne, Lausanne, 1988.
11 J.-C. Dutoit, *J. Chromatogr.*, submitted for publication.

Journal of Chromatography, 555 (1991) 205–210
Elsevier Science Publishers B.V., Amsterdam

CHROM. 23 395

Attempts to use Laffort's solubility factors as polarity parameters for organic compounds in inverse gas chromatography

ADAM VOELKEL* and JAROSŁAW JANAS

Poznań Technical University, Institute of Chemical Technology and Engineering, Pl. M. Sklodowskiej-Curie 2, 60-965 Poznań (Poland)

(First received January 31st, 1991; revised manuscript received April 18th, 1991)

ABSTRACT

Solubility factors were applied to characterize organic compounds used as the stationary phase in a gas chromatographic column. A procedure for their determination is proposed and the physico-chemical meaning is discussed. Relationships between solubility factors and appropriate retention index increments ΔI_i for McReynolds solutes are presented. The influence of the structure of thioethylene derivatives on the parameters examined is discussed.

INTRODUCTION

Rohrschneider [1,2] expressed the polarity of the stationary phase as a polynomial, where the variables represent increments prescribed for different solute–solvent intermolecular interactions. Hartkopf *et al.* [3,4] discussed the validity of *a priori* selected standard solutes and indicated some contradictions existing in the Rohrschneider–McReynolds system. They showed, by means of solubility parameters, that each standard solute will act in different types of intermolecular interactions, not only the selected ones. Laffort and co-workers [5,6] introduced semi-empirical solubility factors calculated from retention data for standard solutes measured on five selected stationary phases of different polarity. They assumed that the retention index (I_i) of a given solute could be expressed as

$$I_i = \alpha A + \omega O + \varepsilon E + \pi P + \beta B + 100 \quad (1)$$

where α, ω, ε, π and β represent the properties of a solute i and A, O, E, P and B are solubility factors that characterize the stationary phase.

Patte *et al.* [6] described the physico-chemical meaning of the solute parameters as follows: α = apolar factor, ω = orientation factor proportional to the dipole moment, ε = electron factor, π = proton donor factor or acidity factor and β = proton acceptor factor or basicity factor. However, they discussed only one

0021-9673/91/$03.50

solvent solubility factor. They indicated the existence of a relationship between factor E and the density of the stationary phase at its boiling point.

The physico-chemical characteristics of liquid stationary phases in gas chromatography (GC) are far from completely known. We have applied inverse GC for the characterization of non-ionic surface-active agent and metal extractants [7–12]. Different polarity parameters have been used, including retention indices for polar standards [7–12], dispersive force parameters [10], thermodynamic parameters [9–12] and parameters that represent electrical intermolecular interactions [8]. The proposal of Laffort and co-workers offers the possibility of describing more completely the properties of stationary phases.

The formal similarity of Rohrschneider's equation and eqn. 1 induced us to search for relationships between McReynolds "constants" and solvent solubility factors determined for various stationary phases.

EXPERIMENTAL

Eight thioalkanes of the general formula $RSCH_2CH_2S(CH_2)_nSCH_2CH_2SR$, where R = C_4H_9, C_6H_{13}, C_8H_{17}, $C_{12}H_{25}$ and n = 2, 3, 4, 5 and 6 were used as stationary phases. These compounds were synthesized by the group of Professor Beger at the Mining Academy, Freiberg (Germany), and kindly donated for our investigation.

The chromatographic conditions were as follows: column, 1 m × 3 mm I.D.; column temperature, isothermal at 90°C; column packing, 25% (w/w) surfactant on Celite (80–120 mesh); carrier gas, helium; flow-rate, 40 ml/min; detector, flame ionization; gas chromatograph, Chrom 5 (Kovo, Czechoslovakia); non-polar standards, C_5–C_9, n-alkanes; polar agents, McReynolds solutes, *i.e.*, 1-butanol, 2-pentanone, benzene, pyridine and 1-nitropropane, and additionally methanol, ethanol, propanol and 2-butanone were used.

Retention indices of the polar solutes were measured for all the stationary phases examined. Solubility factors for the solutes were taken from ref. 6. We measured the Kováts retention indices of nine selected solutes on each stationary phase. For any stationary phase compound j we have the general form of eqn. 1:

$$I_{ij} - 100 = \alpha_i A_j + \omega_i O_j + \varepsilon_i E_j + \pi_i P_j + \beta_i B_j \quad (2)$$

where I_{ij} denotes the retention index of the solute i as measured on stationary phase j; α_i–β_i are solubility factors for solute i and A_j–B_j are Laffort solubility factors for stationary phase j. In our case, i = 1–9 and j = 1–8.

For one stationary phase, we have a series of nine equations in the form

$$I_i - 100 = \alpha_i A + \omega_i O + \varepsilon_i E + \pi_i P + \beta_i B \quad (3)$$

where α_i–β_i have the same meaning as in eqn. 2 and I_i is the retention index of solute i. It is possible to solve this set of equations if we have $i \geqslant 5$ retention data (I_i) for different solutes. We calculated Laffort's solubility factors by the use of eqn. 2 separately for each stationary phase (j = 1–8), *i.e.*, we used the form of eqn. 3. The solubility factors are given in Table II.

RESULTS AND DISCUSSION

It is obvious that an increase in the hydrocarbon part of the molecule will decrease the polarity of a compound. The compound's polarity could be expressed, *e.g.*, by polarity indices commonly used for the characterization of surfactants (Table I) [7–12]. Solubility factors *O*, *E* and *P* decrease with increase in the number of carbon atoms in the stationary phase, as shown as an example for factor *O* in Fig. 1. Phase 3 does not fit this relationship, probably owing to experimental error. The influence of the methylene group in the central hydrocarbon chain is much weaker than those in the alkyl side-group. The central methylene groups are screened by thioethylene units and their influence on estimated parameters is relatively smaller. For example, each methylene units decreases factor *O* by 13.78 i.u., compared with 12.89 i.u. for the those in the alkyl side-chain.

Similar relationships exist between the sum of the first five McReynolds solutes, $\sum_{i=1}^{5} \Delta I_i$, and the number of carbon atoms (Fig. 2). This supports the idea that solubility factors could be discussed as polarity parameters in the characterization of organic compounds. They are sensitive to changes in the structure of stationary phases. However, the question of their physico-chemical meaning remains open. The density of the stationary phase discussed by Patte *et al.* [6] as the quantity which may be correlated with factor *E* is not the most important property of a stationary phase. Possibly the solvent solubility factors are the only invariable mathematical parameters in multivariate equations. The solvent solubility factor *E* is highly correlated with ΔI_{Bz} for benzene (Table II, Fig. 3). The value of ΔI_{Bz} is used for the description of intermolecular interactions caused mainly by the presence of π-electrons. It means that the factor *E* could characterize the ability of a stationary phase to take part in such interactions. Rohrschneider chose 2-butanone for the description of dipole orientation forces while McReynolds [13] introduced the higher homologue 2-pentanone. However, Hartkopf *et al.* [3,4] showed that a ketone as a polar standard does not

TABLE I

RETENTION AND POLARITY PARAMETERS FOR EXAMINED COMPOUNDS AT 90°C

No.	Stationary phase		ΔI^b					Polarity index		Criterion *A*
	R[a]	*n*[a]	Bz	MPK	Bu	Py	Np	CH_3OH	C_2H_5OH	
1	C_6	2	118	149	192	180	212	518	567	2.240
2	C_8	2	81	136	175	164	189	614	562	2.261
3	C_{12}	2	68	114	163	135	149	501	545	2.297
4	C_4	2	135	183	228	200	244	557	621	2.100
5	C_4	3	119	180	223	200	243	553	613	2.110
6	C_4	4	129	174	224	200	243	550	607	2.116
7	C_4	5	113	168	215	200	231	549	602	2.130
8	C_4	6	112	165	212	199	226	547	597	2.141

[a] In the general formula $RSCH_2CH_2S(CH_2)_nSCH_2CH_2SR$.

[b] ΔI = difference in Kováts retention indices as measured on a given stationary phase and on squalane at 90°C. Bz = benzene; MPK = 2-pentanone; Bu = 1-butanol; Py = pyridine; Np = 1-nitropropane.

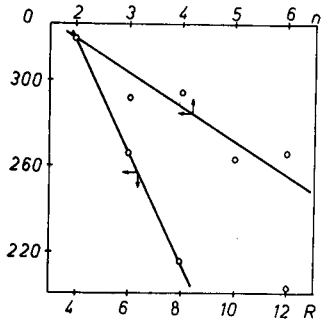

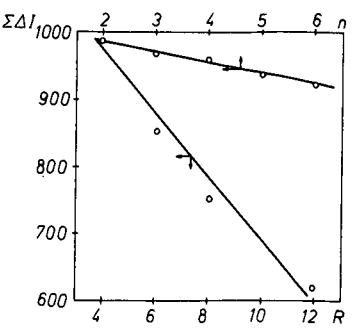

Fig. 1. Influence of the number of carbon atoms in the central (n, upper horizontal axis) and peripheral (R, lower horizontal axis) hydrocarbon chains on the solubility factor O for the examined compounds.

Fig. 2. Influence of the number of carbon atoms in the central (n, upper horizontal axis) and peripheral (R, lower horizontal axis) hydrocarbon chains on the sum of the first five McReynolds solutes, $\Sigma \Delta I_i$, for the examined compounds.

properly and selectively characterize this type of interaction. The correlation coefficient for the relationship ΔI_{MPK} *vs.* factor O is relatively high (Fig. 4). We can discuss factor O as a dipole orientation factor bearing in mind the limitations of 2-pentanone as a standard.

Factors A and B could be correlated with any of the ΔI_i values (Table III). Golovnya and Mišarina [14] indicated that the interactions of methylene groups in the alkyl chain are omitted in the Rohrschneider–McReynolds system. Criterion A [15] defined as

$$\text{criterion } A = \frac{t'_{\mathrm{R}n+1} - t'_{\mathrm{R}n}}{t'_{\mathrm{R}n} - t'_{\mathrm{R}n-1}} \tag{4}$$

where $t'_{\mathrm{R}n+1}$, $t'_{\mathrm{R}n}$ and $t'_{\mathrm{R}n-1}$ are adjusted retention times for n-alkanes having $n + 1$, n and $n - 1$ carbon atoms, respectively, was used as a dispersive force parameter for

TABLE II

SOLUBILITY FACTORS

Stationary phase[a]	Solubility factor				
	A	*O*	*E*	*P*	*B*
1	197	264	274.6	216.1	71.6
2	192.4	214.1	247	175	222.8
3	198.2	204.2	237.3	186.1	179.9
4	197.2	317.8	285.5	261.2	−20.6
5	195.6	290.8	274.4	234.1	71.6
6	198.2	297.2	280.8	244	31.1
7	193.2	262.3	268.9	212.3	151.1
8	195.7	267.6	268	217.7	122.1

[a] See Table I.

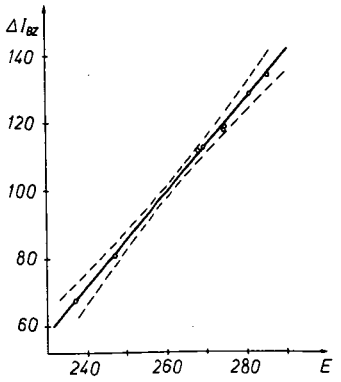

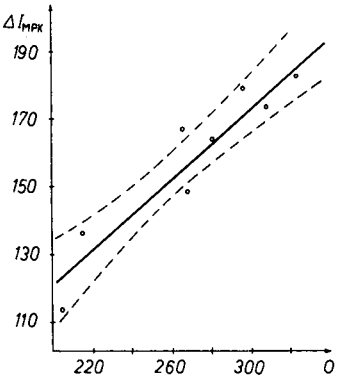

Fig. 3. Relationship between ΔI_{Bz} and solubility factor E (confidence limit for $\alpha = 0.05$).

Fig. 4. Relationship between ΔI_{MPK} and solubility factor O (confidence limit for $\alpha = 0.05$). MPK denotes methyl propyl ketone, *i.e.*, 2-pentanone.

the characterization of apolar interactions. Criterion A was correlated with the solubility factor A, but the correlation coefficient is low (Table III). This means that the solubility factor A could not be considered as interchangeable with the criterion A. Ševčik and Löwentap's criterion A [15] has a different origin to Laffort's factor A.

Relationships between solubility factor P and different ΔI_i values are characterized by very moderate correlation coefficients ($R = 0.9$) and we cannot decide on the best one, *i.e.*, that which has the strongest physico-chemical meaning. The ΔI_i values refer to the behaviour of selected solutes on given liquid phases, while Laffort's solubility factors characterize essentially the properties of the liquid phase. These groups of parameters could be correlated or not, as shown here.

TABLE III

CORRELATION COEFFICIENTS FOR LINEAR RELATIONSHIPS $\Delta I_Y = a + bX$

Y = McReynolds solute; X = solubility factor.

Parameter	A	O	E	P	B
ΔI_{Bz}	Low	0.9722	0.9990	0.9247	Low
ΔI_{Bu}	Low	0.9480	0.9129	0.8952	Low
ΔI_{MPK}	Low	0.9421	0.9160	0.8698	Low
ΔI_{Np}	Low	0.9252	0.9351	0.8342	Low
ΔI_{Py}	Low	0.8717	0.8943	0.7683	Low
Criterion A	Low	−0.8988	−0.8393	−0.8469	0.6879

CONCLUSIONS

Semi-empirical solubility factors could be used in the physico-chemical characterization of organic compounds used as GC stationary phases. It has been shown that

at least two Laffort solubility factors could be correlated with McReynolds constants and therefore they could be considered as a measures of π-electron (E factor) and orientation forces (O factor). For example, the high value of E indicates that a given organic compound could interact with a solute by π-electron forces. The larger the value of the solubility factor, the stronger are the interactions measured by that parameter. Solubility factors decrease with increase in the number of carbon atoms both in the central methylene chain and in alkyl end-groups. Factors E and O decrease with increase in the number of crabon atoms in the central hydrocarbon chains and as in the peripheral groups.

REFERENCES

1 L. Rohrschneider, *J. Chromatogr.*, 17 (1965) 1.
2 L. Rohrschneider, *J. Chromatogr.*, 22 (1966) 6.
3 A. Hartkopf, *J. Chromatogr. Sci.*, 12 (1974) 113.
4 A. Hartkopf, S. Grunfeld and R. Delumeya, *J. Chromatogr. Sci.*, 12 (1974) 119.
5 P. Laffort and F. Patte, *J. Chromatogr.*, 406 (1987) 51.
6 F. Patte, M. Etcheto and P. Laffort, *Anal. Chem.*, 54 (1982) 2239.
7 J. Szymanowski, A. Voelkel, J. Beger and H. Merkwitz, *J. Chromatogr.*, 330 (1985) 61.
8 A. Voelkel, *Chromatographia*, 25 (1988) 95.
9 A. Voelkel, J. Szymanowski, J. Beger and K. Ebert, *J. Chromatogr.*, 409 (1987) 29.
10 A. Voelkel, *J. Chromatogr.*, 435 (1988) 29.
11 A. Voelkel, J. Szymanowski, J. Beger and H. Rüstig, *J. Chromatogr.*, 448 (1988) 219.
12 A. Voelkel, J. Szymanowski, J. Beger and H. Rüstig, *J. Chromatogr.*, 454 (1988) 51.
13 W. O. Reynolds, *J. Chromatogr. Sci.*, 8 (1970) 685.
14 R. V. Golovnya and T. A. Mišarina, *J. Chromatogr.*, 190 (1981) 1.
15 J. Ševčik and M. S. H. Löwentap, *J. Chromatogr.*, 217 (1981) 139.

Journal of Chromatography, 555 (1991) 211–220
Elsevier Science Publishers B.V., Amsterdam

CHROM. 23 347

Reliability assessment of a gas chromatographic method for polycyclic aromatic hydrocarbons in olive oil

EDOARDO MENICHINI*, ALESSANDRO DI DOMENICO and LUCA BONANNI
Istituto Superiore di Sanità, Viale Regina Elena 299, 00161 Rome (Italy)
and
ERNESTO CORRADETTI, LILIANA MAZZANTI and GOFFREDO ZUCCHETTI
Presidio Multizonale di Sanità Pubblica, 63100 Ascoli Piceno (Italy)
(Received January 21st, 1991)

ABSTRACT

A quality control test was developed for a gas chromatographic method to determine polycyclic aromatic hydrocarbons in olive oil. Fifteen oil specimens were fortified with eight three- to six-ring polycyclic aromatic hydrocarbons at levels of between 3.0 (approximate detection limit) and 360 μg/kg. Three sets of five equally fortified specimens were obtained and assayed at random by three operators. For each fortification level, the means of recovery yield were in the range 56–107%, and were independent of the polycyclic aromatic hydrocarbon congener specificity and the operator's capability. Excluding subsets of data associated with both the fortification level at the detection limit and a deviant polycyclic aromatic hydrocarbon term (benzo[*ghi*]perylene), an overall mean accuracy of 96% and a precision of 7% were achieved.

INTRODUCTION

The determination of polycyclic aromatic hydrocarbons (PAHs) in evironmental samples is currently of major interest, owing to their ubiquitousness and to the carcinogenic and mutagenic activity shown by many of them [1,2]. PAHs result from the combustion, pyrolysis and pyrosynthesis of organic matter. They have been inplicated as possible contaminants of foodstuffs mainly through polluted air, sorption from water and soil, or food preparation methods. This topic has been extensively reviewed by Fazio and Howard [3]. In particular, PAHs appear to be generally present in vegetable oils at trace levels. For such foods, biochemical synthesis has been suggested as a possible additional source of contamination; however, according to the reviewers, this route seems to be considerably controversial.

Identification and assessment of PAHs in commercial olive oil have previously been carried out by UV and fluorescence spectrophotometry [4–8] and, more recently, by gas chromatography–mass spectrometry [9] and high-performance liquid chromatography [10,11]. PAHs have been extracted from oil by various liquid–liquid partition schemes [4,6,9,10], in some cases preceded by a saponification step [8,11] or even by a caffeine–formic acid complexation [10]. Clean-up of the extract has been per-

0021-9673/91/$03.50

formed by column chromatography on silica gel [9–11], alumina [6,7], XAD-2 resin [10], and Florisil, alone [8] or followed by two-step thin-layer chromatography (TLC) on cellulose and cellulose acetate [4].

In a previous paper [12], results were reported of an investigation carried out to assess the PAH content of "extra-virgin" olive oil derived from plants contaminated with industrial pitch condensate. (The "extra-virgin" oil is an unrefined quality obtained traditionally from the olive-pressing process or alternatively, in recent times, by centrifugation in presence of warm water.) In that paper, a procedure was developed which enabled determination of complex mixtures of PAHs in a relatively short time and with limited amounts of reagent. The procedure is reported here below. The aim of this paper is to present the results of a quality control test carried out to evaluate the reliability of the procedure, especially in terms of accuracy and precision, at contamination levels of practical interest (from a few μg/kg to a few hundreds of μg/kg).

EXPERIMENTAL[a]

Reagents

Reference PAHs were selected to cover a wide range of gas chromatographic retention times and had three to six rings (see Table I). PAHs were obtained from Analabs (Norwalk, CT, USA) and Fluka (Buchs, Switzerland). *p*-Terphenyl (p-T) and β,β′-binaphthyl (bNA) were purchased from Fluka and K&K Labs (Plainview, NY, USA), respectively, and used as internal standards; reference solutions were made in cyclohexane at 219 and 314 μg/ml, respectively.

All solvents were obtained from Carlo Erba (Milan, Italy). *n*-Pentane and dimethyl sulfoxide (DMSO) were UV-spectroscopy grade. The other solvents were of analytical grade; however, acetone, cyclohexane and dichloromethane (DCM) were distilled in a glass apparatus prior to use.

Silica gel 70–230 mesh was purchased from Merck (Darmstadt, Germany). TLC was performed on 20 × 20 cm, 1-mm-thick layer, ready-for-use silica gel plates provided by Merck; plates were washed with acetone before use.

Analytical procedure

A scheme of the analytical procedure is presented in Fig. 1. Each oil specimen (10.0 g) was spiked with 5.0 μl of the p-T solution, dissolved in 20 ml *n*-pentane, and partitioned three times with 10 ml DMSO, according to a procedure adapted from Natusch and Tomkins [13]. The combined DMSO extracts were diluted with 60 ml water (caution: considerable heat can be generated when mixing DMSO and water) and back-partitioned three times with 50 ml cyclohexane. The combined cyclohexane extracts were washed with 100 ml distilled water and filtered through an 8-cm-diameter funnel containing (from bottom to top): a glass wool plug, a 1-cm silica gel layer and a 2-cm anhydrous sodium sulphate layer. After filtration, the funnel was washed with an additional 10 ml of cyclohexane and two 5-ml portions of DCM. The filtrate

---

[a] *Precautions.* Many PAHs have carcinogenic activity, for which there are different degrees of experimental evidence [1,2]. Every possible precaution must be taken to avoid human exposure when handling PAHs as a class. Spent samples and unused standards should be disposed of safely.

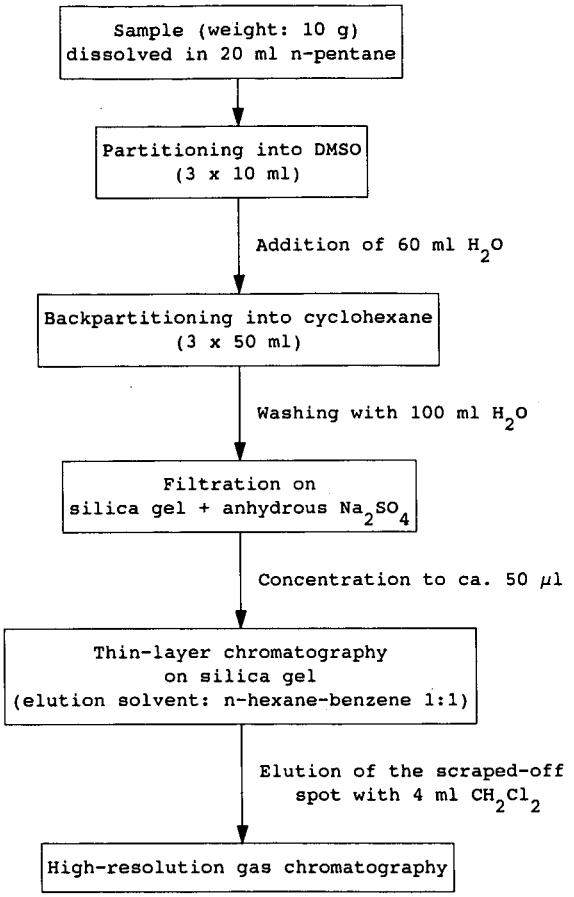

Fig. 1. Scheme of the analytical procedure to assess PAHs in olive oil.

and washings were combined, concentrated to about 50 µl, and subjected to TLC. The TLC plate was developed with 1:1 (v/v) *n*-hexane–benzene to a height of 12 cm. The PAH spot (R_F: *ca.* 0.8) was detected with 366-nm UV light. The silica gel spot was then scraped off, quantitatively transferred to a 2.5-cm I.D. glass tube equipped with a sintered glass disc, and eluted in three successive stages with a total of 4 ml DCM. The eluate was gently evaporated to dryness under nitrogen, then 5.0 µl of the bNA solution were added, and the solution was made up to 100 µl volume with cyclohexane.

Instrumental determination

A Carlo Erba Model 2960 gas chromatograph, equipped with a cold on-column injector (temperature at initial oven temperature), a 30 m × 0.32 mm I.D. fused-silica SPB-1 capillary column and a flame ionization detector (temperature 300°C), was employed for quantitative assessment. A Hitachi Model D-2000 integrator was used

for data acquisition and processing. The oven temperature was held at 85°C for 1 min, raised to 180°C at 25°C/min, and then to 300°C at a rate of 7°C/min, where it was held isothermally. Helium was used as a carrier gas at a flow-rate of 5 ml/min. PAH identification and quantification were carried out by comparing sample chromatograms against calibration solutions. Integrator peak height measurements were used for quantifications; they were corrected against the mean value of the internal standard bNA, obtained by averaging all its determinations carried out during this study. The estimated detection limit in specimens was about 3 μg/kg.

Quality control program

PAHs were weighed (approximately 2.5 mg each; precision ±0.01 mg) and dissolved in 25 ml cyclohexane to obtain eight individual standard solutions. Working solutions were prepared at concentrations of about 1 and 10 ng/μl. Fifteen 10.0-g specimens of blank olive oil were spiked with known quantities of the working solutions, so that three sets of five equally fortified specimens each were obtained (Table I). Added volumes ranged from 29.3 to 334.6 μl. Blank oil was an "extra-virgin" olive oil previously analyzed and found to contain few PAHs at relatively low background levels [mean values (n = 3): AN, 6 μg/kg; FA, 19; PY, 18; BaF, 3; TRI, 5. For PAH abbreviations, see Table I].

The fortified oil specimens were shipped to another laboratory, together with three blank unspiked specimens (10.0 g) and a PAH standard mixture (each PAH approximately 50 ng/μl). All specimens were kept refrigerated from the time of their preparation until analysis. Fortified and blank oil specimens were analyzed by three operators of the receiving laboratory. The operators were not informed of specimen identities. In addition, three reagent blanks were also analyzed. Three calibration solutions were prepared from the PAH standard mixture at concentration levels of 0.5, 5 and 20 ng/μl to obtain analytical levels of 5, 50 and 200 μg/kg: for each compound, calibration graphs were found to be linear over the whole range of concentrations.

TABLE I

FORTIFICATION LEVELS OF OIL SPECIMENS (μg/kg)

Each set includes five equally fortified specimens.

Compound[a]	Abbreviation	Mol. wt.	Number of rings	Set A	Set B	Set C
Anthracene	AN	178	3	15	50	80
Fluoranthene	FA	202	4	60	120	160
Pyrene	PY	202	4	50	180	120
11H-benzo[*a*]fluorene	BaF	216	4	3	35	18
Triphenylene	TRI	228	4	30	70	220
Benzo[*e*]pyrene	BeP	252	5	20	20	300
Perylene	PE	252	5	8	140	40
Benzo[*ghi*]perylene	BPE	276	6	5	9	360
Total 8 PAHs				191	624	1298

[a] Ranked according to increasing molecular weight and, for isomers, increasing gas chromatographic retention time.

RESULTS AND DISCUSSION

Table II shows the results of the study with reference to each PAH term. Results were corrected for background (see *Quality control program* section). The recovery yields, per individual PAH and fortification level (FL), are means of five independent determinations which vary between 56 and 107%. The higher figure is associated with an FL at the detection limit (3.0 μg/kg for BaF), the lower figure with the highest FL adopted in the study (360 μg/kg for BPE). However, BPE also exhibits lower mean recovery yields (76%) at the other two FLs (for which signal-to-noise ratio ≥ 5), and at 360 μg/kg FL its recovery yield may drop to as low as 39%. Based on these findings, it may be presumed that BPE exhibits a certain degree of deviance with respect to the other congeners. If, in the light of the above, the data associated with BPE and with the only level at the detection limit (five-datum subsets 1, 2, 4 and 24) are neglected, then the remaining 20 subsets exhibit mean recovery yields between 78 and 106% (see also Table III, "all operators"). Coefficients of variation (C.V.) vary between 8 and 20%, except for one case (PE at a 40 μg/kg FL: C.V. = 30%). Lastly, if individual recovery yield figures are averaged by a specific congener ($n = 15$ for each mean), *i.e.* regardless of FLs, the new means are very similar from congener to congener (except for BPE) and range between 89 and 95%.

Table III shows the recovery yields rearranged to show their dependence on FL (see also Fig. 2) and on the operator's capability (operator's repeatability). The three operators seem to perform differently with respect to accuracies and precisions (Table III, lower section). When the entire set of data ($n = 120$) is considered, deviance from expectancy is 5% for operator III, 10% for operator I and 20% for operator II; when the set of data omitting subsets 1, 2, 4 and 24 ($n = 100$) is considered, the deviance is 4, 8 and 18%, respectively. Inter-operator precision shows even greater variations: based on C.V. values, operator III is about two-fold more precise than operators I and II. In general, this is true with both data sets, *i.e.* for $n = 120$ and $n = 100$. Each operator provides Gaussian-distributed findings, although operators I and II exhibit distributions (unshown) which are broader than that of operator I.

The recovery data set ($n = 120$) has a Gaussian distribution (Fig. 2). The overall mean of recovery yield data is 88%; when subsets 1, 2, 4 and 24 are excluded the mean improves to 90%.

CONCLUSIONS

The analysis of the results obtained makes it possible to conclude that the tested procedure is a reliable tool for assessing PAHs in olive oil. This is borne out by the individual recovery yields ($n = 120$) which are all within the range 39–133%: this approximately 1:3 variation appears to be small if one considers the number of variables dealt with, *i.e.* FL, PAH congener specificity and operator capability. It would also be acceptable in risk assessment analysis. Moreover, if one considers the set of recovery yield means estimated at each FL, (five-datum subsets 1–24), then the overall variation is only from 56 to 107%, *i.e.* it improves to somewhat less than 1:2.

The procedure can provide a high degree of accuracy (within 4% of expectancy) and very good precision (C.V. $\pm$ 7%). These figures, taken from the "best" operator's selected ($n = 100$) results, are independent of FL and the congener specificity.

TABLE II

RECOVERY YIELDS OF PAHs ADDED TO BLANK OLIVE OIL FOR QUALITY CONTROL TEST: EFFECT OF CHEMICAL COMPOUND

PAH[a]	Fortification level (μg/kg)	Recovery yield (%)[b]														$\bar{x}$	S.D.	C.V.	All samples		
		Set A					Set B					Set C									
		I	I	II	II	III	II	III	II	III	III	III	II	II	I	I				$\bar{x}$	S.D.	C.V. (%)
AN	15	100	93	73	87	93											89	10	11			
	50						78	94	72	94	106						89	14	15			
	80											91	65	93	90	101	88	14	15			
																				89	12	13
FA	60	105	85	100	87	97											95	9	9			
	120						78	101	87	91	98						91	9	10			
	160											92	61	89	89	99	86	15	17			
																				90	11	12
PY	50	106	88	94	94	104											97	8	8			
	120											96	67	88	90	98	88	13	14			
	180						73	88	76	81	94						82	9	11			
																				89	11	12

BaF	3.0	133	100	100	67	133											107	28	26			
	18										89	56	94	72	89		80	16	20			
	35						69	97	89	91	94						88	11	13			
																				92	22	24
TRI	30	113	90	97	70	103											95	16	17			
	70						76	100	89	84	99						89	10	11			
	220											99	60	90	76	84	82	15	18			
																				89	14	16
BeP	20	120	105	110	90	105											106	11	10			
	20						85	110	105	100	110						102	10	10			
	300											89	65	90	65	80	78	12	16			
																				95	17	17
PE	8.0	100	113	100	75	100											98	14	14			
	40											108	53	108	65	83	83	25	30			
	140						76	100	89	94	92						90	9	10			
																				90	17	19
BPE	5.0	80	80	80	60	80											76	9	12			
	9.0						67	78	78	78	78						76	5	7			
	360											67	49	70	39	56	56	13	22			
																				69	13	19

[a] For abbreviations, see Table I.
[b] As obtained by three operators identified by I, II and III.

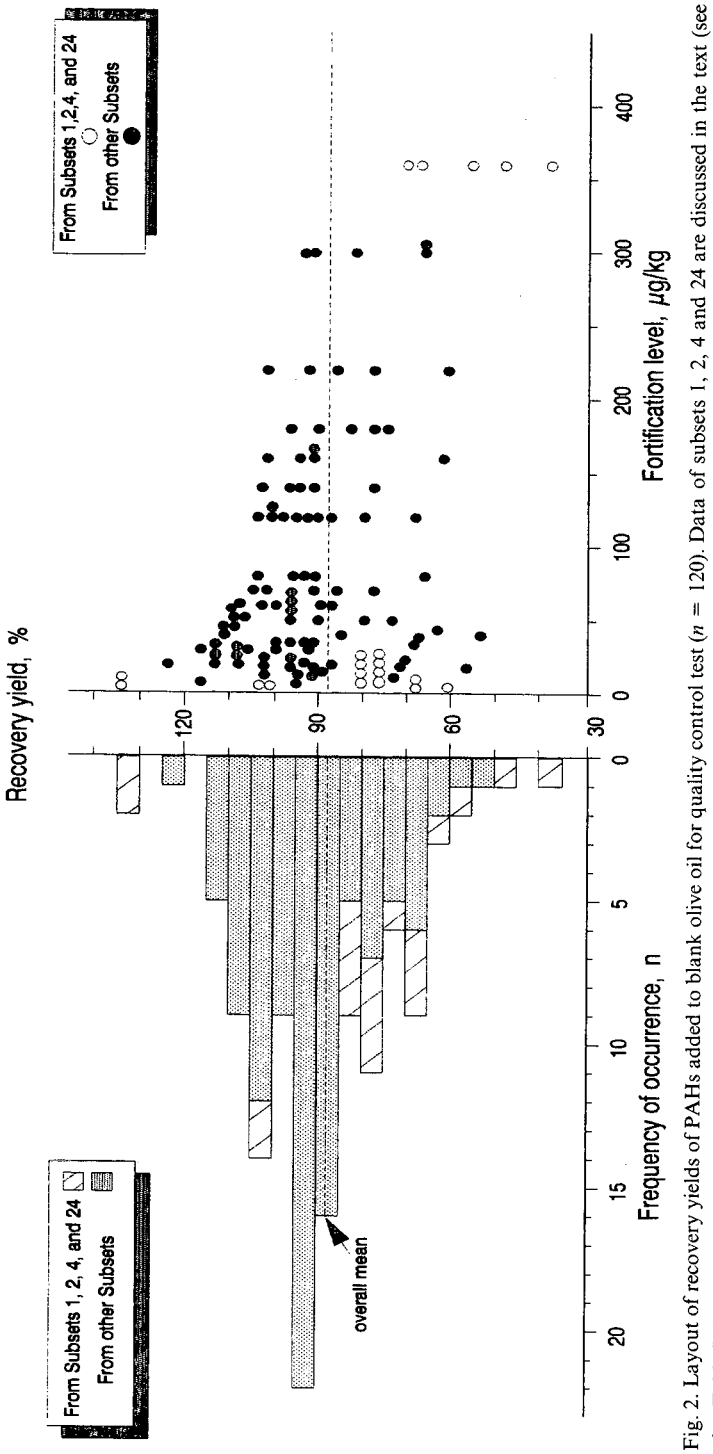

Fig. 2. Layout of recovery yields of PAHs added to blank olive oil for quality control test (n = 120). Data of subsets 1, 2, 4 and 24 are discussed in the text (see also Table III).

TABLE III

RECOVERY YIELDS OF PAHs ADDED TO BLANK OLIVE OIL FOR QUALITY CONTROL TEST: EFFECT OF FORTIFICATION LEVEL AND OPERATOR

Subset[a]	Fortification level (μg/kg)	PAH[b]	Recovery yield (%)[c]									
			Operator I		Operator II		Operator III			All operators		
										$\bar{x}$	S.D.	C.V. (%)
1	3.0	BaF	133	100	100	67	133			107	28	26
2	5.0	BPE	80	80	80	60	80			76	9	12
3	8.0	PE	100	113	100	75	100			98	14	14
4	9.0	BPE			67	78	78	78	78	76	5	7
5	15	AN	100	93	73	87	93			89	10	11
6	18	BaF	72	89	56	94	89			80	16	20
7	20	BeP	120	105	110	90	105			106	11	10
8	20	BeP			85	105	110	100	110	102	10	10
9	30	TRI	113	90	97	70	103			95	16	17
10	35	BaF			69	89	97	91	94	88	11	13
11	40	PE	65	83	53	108	108			83	25	30
12	50	AN			78	72	94	94	106	89	14	15
13	50	PY	106	88	94	94	104			97	8	8
14	60	FA	105	85	100	87	97			95	9	9
15	70	TRI			76	89	100	84	99	89	10	11
16	80	AN	90	101	65	93	91			88	14	15
17	120	FA			78	87	101	91	98	91	9	10
18	120	PY	90	98	67	88	96			88	13	14
19	140	PE			76	89	100	94	92	90	9	10
20	160	FA	89	99	61	89	92			86	15	17
21	180	PY			73	76	88	81	94	82	9	11
22	220	TRI	76	84	60	90	99			82	15	18
23	300	BeP	65	80	65	90	89			78	12	16
24	360	BPE	39	56	49	70	67			56	13	22
$\bar{x}$			90		80		95			88		
S.D.			19		15		11			16		
C.V.(%)			21		18		12			18		
n			32		48		40			120		
$\bar{x}^d$			92		82		96			90		
S.D.			14		14		7			14		
C.V.(%)			15		17		7			15		
n			26		40		34			100		

[a] Subsets 1 and 2: fortification levels at, or near to, detection limit; subsets 2, 4 and 24 associated with a deviant PAH term (see text).

[b] For abbreviations, see Table I.

[c] Same values as reported in Table II, but ranked according to increasing fortification level and grouped according to operators.

[d] Estimates not including subsets 1, 2, 4 and 24.

Finally, although a mean recovery greater than 50% may be accepted for the assessment of the environmental contaminants (risk analysis), the study shows that as far as possible particular care should be taken when analyzing the heavier congeners such as BPE.

REFERENCES

1 IARC, *Polynuclear Aromatic Compounds, Part 1, Chemical, Environmental and Experimental Data (Monographs on the Evaluation of the Carcinogenic Risk of Chemicals to Humans*, Vol. 32), IARC, Lyon, 1983.
2 IARC, *Overall Evaluations of Carcinogenicity: An Updating of IARC Monographs Volumes 1 to 42 (Monographs on the Evaluations of Carcinogenic Risk to Humans*, Suppl. 7), IARC, Lyon, 1987.
3 T. Fazio and J. W. Howard, in A. Bjorseth (Editor), *Handbook of Polycyclic Aromatic Hydrocarbons*, Marcel Dekker, New York, 1983, Ch. 11, pp. 461–505.
4 J. W. Howard, E. W. Turicchi, R. H. White and T. Fazio, *J. Assoc. Off. Anal. Chem.*, 49 (1966) 1236.
5 B. Fábián, *Arch. Hyg. Bakteriol.*, 152 (1968) 231; C.A., 69 (1968) 95209m.
6 W. Ciusa, V. D'Arrigo and G. Marchesini, *Riv. Ital. Sostanze Grasse*, 47 (1970) 114; C.A., 73 (1970) 44081p.
7 A. Morgante, *Quad. Merceol.*, 12 (1973) 49, C.A., 81 (1974) 24236e.
8 F. L. Joe Jr., E. L. Roseboro and T. Fazio, *J. Assoc. Off. Anal. Chem.*, 62 (1979) 615.
9 A. Hopia, H. Pyysalo and K. Wickström, *J. Am. Oil Chem. Soc.*, 63 (1986) 889.
10 P. Welling and B. Kaandorp, *Z. Lebensm.-Unters.-Forsch.*, 183 (1986) 111.
11 T. Stijve and C. Hischenhuber, *Dtsch. Lebensm.-Rundsch.*, 83 (1987) 276.
12 E. Corradetti, C. Abbondanza, L. Mazzanti and G. Poli, *Boll. Chim. Ig. Parte Sci.*, 39 (1988) 297.
13 D. F. S. Natusch and B. A. Tomkins, *Anal. Chem.*, 50 (1978) 1429.

Journal of Chromatography, 555 (1991) 221–228
Elsevier Science Publishers B.V., Amsterdam

CHROM. 23 363

Simultaneous separation and determination of hydrocarbons and organochlorine compounds by using a two-step microcolumn

O. M. RODRIGUEZ
Department of Chemistry, University of Costa Rica, San José (Costa Rica)
and
P. G. DESIDERI*, L. LEPRI and L. CHECCHINI
Department of Public Health, Epidemiology and Environmental Analytical Chemistry, University of Florence, Via G. Capponi, 9-50121 Florence (Italy)
(First received December 21st, 1990; revised manuscript received April 3rd, 1991)

ABSTRACT

The simultaneous separation and determination of a mixture of hydrocarbons and organochlorine compounds was successfully carried out by using sorption chromatography on a two-step microcolumn of silica and aluminium oxide for their fractionation, and a dual detector system. In addition to the separation and identification of hydrocarbons and heterocompounds containing nitrogen, oxygen and sulphur atoms, separation and identification of chlorinated hydrocarbons (dichlorobenzenes, *p*-chlorotoluene, hexachlorobutadiene, 1,2,4-trichlorobenzene and 2-chloronaphthalene), pesticides (chlorpicrin, aldrin, lindane, α- and β-benzene hexachloride (BHC), endrin, dieldrin, endosulphan, methoxychlor) and herbicides (propanil, dichlobenil, trifluralin, difolatan) were achieved in mixtures containing polychlorinated biphenyl, strobane and chlordane.

INTRODUCTION

Investigations on the organochlorides [*i.e.* pesticides, benzene hexachloride (BHC) isomers and polychlorinated biphenyl (PCB) congeners] are of great importance in environmental studies since, as is well known, these compounds are persistent, have cumulative effects in human tissues, and occur widely in the environment [1–5].

Recent data [6–9] on the presence of untransformed 1,1,1-trichloro-2,2-bis(*p*-chlorophenyl)ethane (*p,p'*-DDT) analogues in rain, snow, soil and peat samples indicate that, although their use is forbidden by law, there is a new input of DDTs even in regions where there is no evidence that direct applications are taking place.

The organochlorine compounds are a vast class of organic molecules which show similar chemical–physical properties. Pesticides for instance are chemically related to PCBs: this is a serious disadvantage to their identification and quantification because if simultaneously present in the same sample they will interfere with each

0021-9673/91/$03.50

other. A preliminary separation of these compounds is thus essential, and a great many papers on the subject are available in the literature; however, the problem has still not been definitely settled [10–11].

The present work investigates the possibility of extending the separation method already adopted for the analysis of hydrocarbons and heterocompounds containing nitrogen, oxygen and sulphur atoms [12] to mixtures that also contain organochlorine compounds. Our aim was to analyse the complex mixtures of organic compounds usually present in the environmental matrices [13–14] by using a single separation of the sample in homogeneous fractions by means of a two-step microcolumn coupled with gas chromatographic (GC) determinations using a dual detector system [flame ionization detection–electron-capture detection (FID–ECD)].

EXPERIMENTAL

Reagents and materials

The solvents used, *n*-hexane, methylene chloride, carbon tetrachloride, acetone and methanol, all supplied by Merck (Darmstadt, Germany), were for pesticide analysis. The hydrocarbons, pesticides, herbicides and chlorinated phenols were from Polyscience (IL, USA). The PCB standards, Arochlors 1016, 1232, 1242, 1248, 1260 and 1268, were from Supelco (St. Louis, MO, USA). Standards solutions of all compounds and several mixtures were prepared in *n*-hexane. The concentrations of hydrocarbons and of organochlorides were 0.2 mg/ml and 2 μg/ml for each compound, respectively. The volume of solution used for analysis was 50 μl. The silica gel 60 (70–230 mesh) and the basic aluminium oxide E type (70–230 mesh) supplied by Merck were activated at 120°C for 12 h.

Apparatus

A Carlo Erba (Milan, Italy) HRGC-5160 Mega Series gas chromatograph was used to identify simultaneously hydrocarbons and organochlorides in the different fractions. This instrument was equipped with both a flame ionization detector and an electron-capture detector, working in parallel by means of a split in the capillary column.

The injection was made using a cold split–splitless liquid injector according to the following temperature program: injection at 40°C, then an immediate increase of temperature to 300°C. After 30 s the split was automatically switched on. A capillary column (30 m × 0.25 mm I.D.), SPB-5 (Supelco), was used. The column temperature program was 40°C for 1 min then a linear increase to 300°C at 6°C/min. The carrier gas was hydrogen.

Identification of organic compounds

Eight substances were selected as reference standards for the hydrocarbons and eight for organochlorides. For the organochlorine compounds the chosen substances were: chlorobenzene, hexachloroethane, dacthal and the hexyl, octyl, decyl, palmityl and stearyl esters of trichloroacetic acid. The standards used in the identification of hydrocarbons were the *n*-alkanes *n*-C_8, *n*-C_{12}, *n*-C_{16}, *n*-C_{20}, *n*-C_{24}, *n*-C_{28}, *n*-C_{32} and *n*-C_{34}. The identification of organic compounds was realized by using a Lotus 1-2-3 spreadsheet program based on the retention index calculated with respect to the reference standards [15].

Fractionation

Mixtures containing the organochlorides and the hydrocarbons were separated into five fractions indicated by roman numbers, I, II, III, IV and V, using the sorption chromatography on a two-step microcolumn of silica gel and aluminium oxide. The microcolumn was formed by a first semi column of silica gel and by a second of aluminium oxide, separated by a glass frit [12].

Every fraction was then concentrated to 100 μl at 25°C under a stream of nitrogen. The volume injected into the GC column was 1 μl.

RESULTS AND DISCUSSION

Fig. 1 shows the complete scheme of separation of the different classes of organic compounds studied. A standard mixture of PCBs, hydrocarbons, chlorinated hydrocarbons, pesticides, herbicides, fatty acid esters, phthalic acid diesters with 1–12 carbon atoms and other polar compounds (alcohols, ketones, aldehydes, phenols and chlorophenols) was eluted on the silica gel semicolumn with 2 ml of *n*-hexane; in this way the aliphatic hydrocarbons and chlorinated hydrocarbons were completely recovered in fraction I (see Table I).

The highest-molecular-weight alkanes could not be eluted from a mixed column of silica gel and aluminium oxide using *n*-hexane since such compounds are strongly adsorbed on aluminium oxide. By combining the two semi columns and eluting with solvent mixtures of increasing polarity a further fractionation of the compounds was obtained. The following modifications to the original scheme [12] were made:

(1) The eluent *n*-pentane was substituted with *n*-hexane without apparent variations of the hydrocarbons in the different fractions.

(2) *n*-Pentane–carbon tetrachloride (8:2, v/v) and *n*-pentane–methylene chloride (9:1, v/v), used to separate aromatic hydrocarbons with one and two rings into two fractions [12], were substituted by a solution of *n*-hexane–methylene chloride (9:1, v/v). This meant that such compounds were found in a single fraction (see Fig. 1). This replacement was necessary because carbon tetrachloride interferes negatively

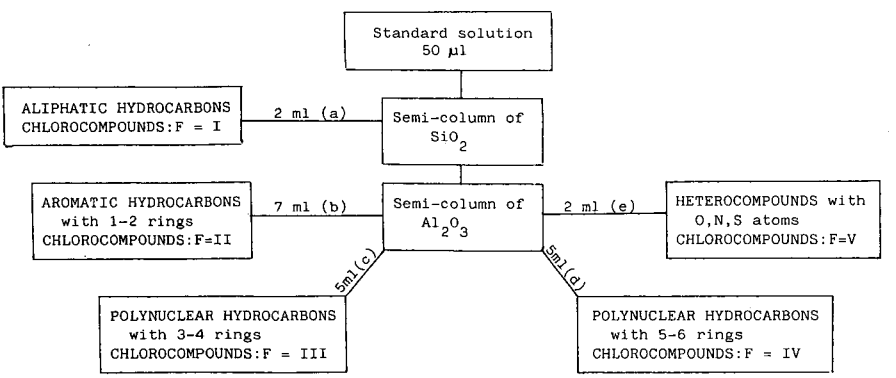

Fig. 1. Fractionation scheme. Eluents: (a) *n*-hexane; (b) *n*-hexane–methylene chloride (9:1, v/v); (c) *n*-hexane–methylene chloride (7:3, v/v); (d) *n*-hexane–methylene chloride (2:8, v/v); (e) acetone–methanol (2:1, v/v). For the identification of chlorocompounds, see Table I.

TABLE I

RECOVERY PERCENTAGE OF CHLORINATED COMPOUNDS WITH DUAL COLUMN FRACTIONATION[a]

Compound	Fraction				
	I	II	III	IV	V
Chlorinated hydrocarbons					
Chlorotoluene	100	–	–	–	–
2-Chloronaphthalene	90	10	–	–	–
Dichlorobenzene	100	–	–	–	–
1,2,4-Trichlorobenzene	100	–	–	–	–
Hexachlorobutadiene	100	–	–	–	–
Hexachlorobenzene	100	–	–	–	–
Arochlors (PCBs)					
1016	10	90	–	–	–
1232	10	90	–	–	–
1242	10	90	–	–	–
1248	15	85	–	–	–
1254	35	65	–	–	–
1260	40	60	–	–	–
1262	80	20	–	–	–
1268	100	–	–	–	–
Pesticides					
Chloropicrin	100	–	–	–	–
Aldrin	85	15	–	–	–
Heptachlor	–	100	–	–	–
o,p'-DDT	–	100	–	–	–
p,p'-DDT	–	100	–	–	–
1,1-Dichloro-2,2-bis(*p*-chlorophenyl)ethylene (*p,p*-DDE)	–	100	–	–	–
o,p'-DDE	–	100	–	–	–
1,1-Dichloro-2,2-bis(*p*-chlorophenyl)ethane (*p,p*-DDD)	–	–	100	–	–
o,p'-DDD	–	55	45	–	–
Chlordane	–	40	60	–	–
Strobane	–	35	65	–	–
α-BHC	–	–	100	–	–
Lindane (γ-BHC)	–	–	100	–	–
β-BHC	–	–	–	100	–
Methoxychlor	–	–	–	100	–
Endrin	–	–	–	100	–
Dieldrin	–	–	–	100	–
Endosulphan	–	–	–	75	25
Herbicides					
Trifluralin	–	–	100	–	–
Dichlobenil	–	–	–	100	–
Propanil	–	–	–	–	100
Difolatan	–	–	–	–	100
Chlorinated phenols					
2,3-Dichlorophenol	–	–	–	–	80
2,4,5-Trichlorophenol	–	–	–	–	–
2,3,4,5-Tetrachlorophenol	–	–	–	–	–

[a] The recoveries are average values from five determinations. The absolute error for these measurements is 5%. The standard deviations are between 2 and 5%.

with the ECD of organochlorides. In any case the identification and quantitation of all the aromatic hydrocarbons with one and two rings posed no problems, as this mixture is easily resolved by GC.

(3) Methanol used for polar heterocompounds was substituted with a mixture of acetone and methanol (2:1, v/v) to cut down the interference while using ECD.

A careful inspection of the scheme clearly shows that the organochlorides are divided according to their chemical characteristics in all the five fractions. The organochlorine compounds present in the different fractions together with the relative percentages are reported in Table I.

Fraction I

This fraction shows a complete recovery of the chlorinated hydrocarbons with the sole exception of 2-chloronaphthalene, but even for this component the recovery is quite good.

The Arochlors show instead a non-homogeneous behaviour because the relative percentage of the various mixtures increases with the degree of chlorination, reaching 100% only for Arochlor 1268. Of the pesticides, only chlorpicrin and aldrin are present in this fraction, both in very high percentages.

The chromatographic analysis of this fraction shows that the chlorinated hydrocarbons are visibly separated from all the other eluted compounds and so they can be always determined without problems regardless of the complexity of the mixture. The Arochlor compounds on the other hand, generally interfere with each other and

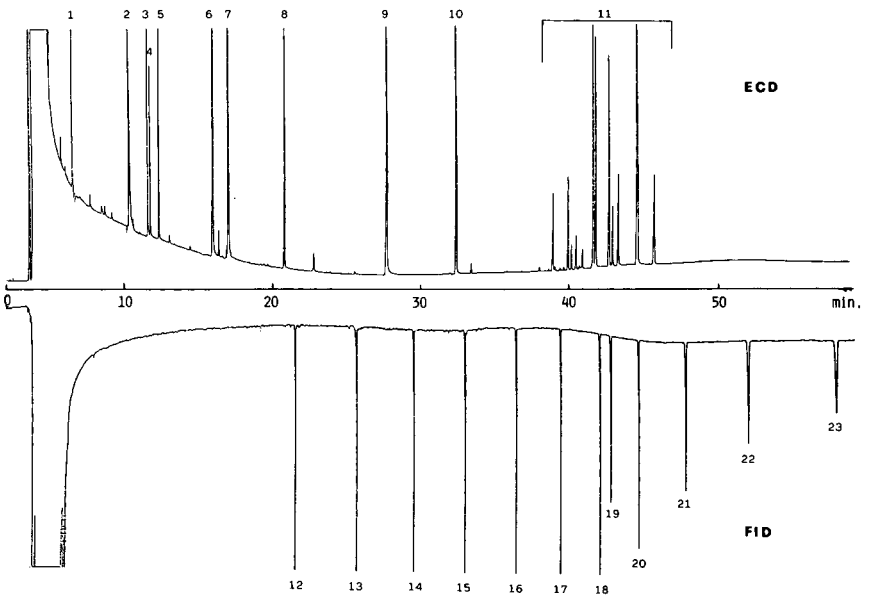

Fig. 2. Fraction I,. GC–ECD: 1 = chlorpicrin; 2 = *p*-chlorotoluene; 3 = 1,3-dichlorobenzene; 4 = 1,4-dichlorobenzene; 5 = 1,2-dichlorobenzene; 6 = 1,2,4-trichlorobenzene; 7 = hexachlorobutadiene; 8 = 2-chloronaphthalene; 9 = hexachlorobenzene; 10 = aldrin; 11 = Arochlor 1268. GC–FID: 12 = *n*-C_{14}; 13 = *n*-C_{16}; 14 = *n*-C_{18}; 15 = *n*-C_{20}; 16 = *n*-C_{22}; 17 = *n*-C_{24}; 18 = *n*-C_{26}; 19 = squalane; 20 = *n*-C_{28}; 21 = *n*-C_{30}; 22 = *n*-C_{32}; 23 = *n*-C_{34}.

with aldrin, with the exception of Arochlor 1268, for which no interferences occur. Fig. 2 shows the simultaneous determination of chlorinated compounds, chlorpicrin, aldrin and Arochlor 1268 (GC–ECD) and of aliphatic hydrocarbons (GC–FID).

Fraction II

The second fraction has some limitations from the analytical point of view because most of its components are found in other fractions too. Chlordane, strobane and PCBs show a very complex GC pattern that seriously interferes with the determination of the other pesticides contained in 100% recovery percentages in this fraction. As a consequence these pesticides can be determined only when the intererences are absent.

Fraction III

In this fraction the PCBs are missing. This is why the possible interferences in the determination of the pesticides present and of trifluoralin are associated with the presence of chlordane and strobane. When chlordane and strobane are absent the determination of the trifluoralin and pesticides is easily achieved even if their concentrations in the analysed mixture are at ppt (10^{-12}) levels. This fraction, on the other hand, allows the determination of strobane and chlordane even when they are simultaneously present in the mixture. It is interesting to note that the α- and γ-BHC isomers were completely recovered in this fraction, while the β isomer was not eluted from the column.

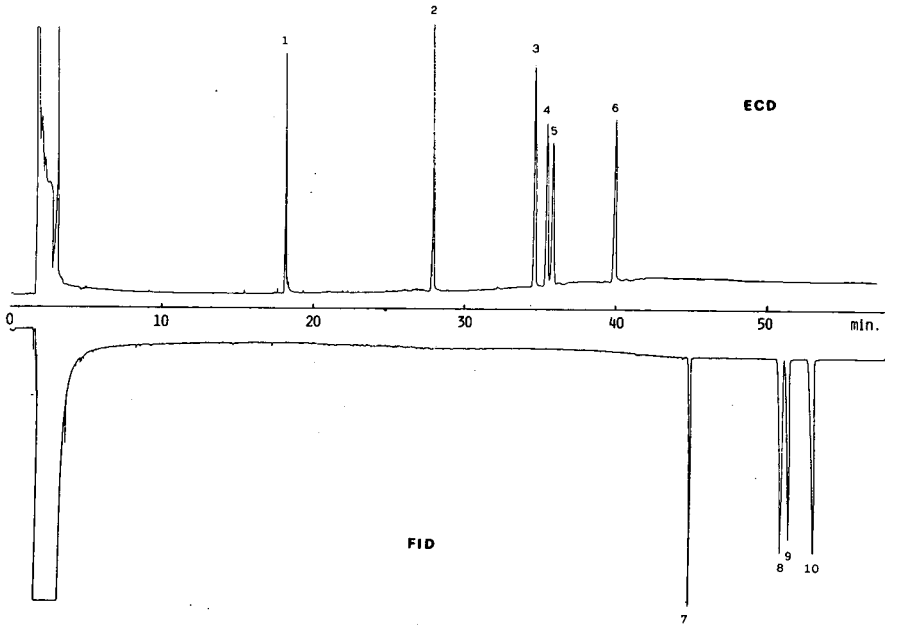

Fig. 3. Fraction IV. GC–ECD: 1 = dichlobenil; 2 = β-BHC; 3 = dieldrin; 4 = endrin; 5 = endosulphan; 6 = methoxychlor. GC–FID: 7 = benzo[a]pyrene; 8 = indeno [1,2,3-*cd*]pyrene; 9 = dibenzo[*a,h*]anthracene; 10 = benzo[*g,h,i*]perylene.

Fraction IV

This fraction contains a few important pesticides (β-BHC, endrin, dieldrin, methoxychlor, endosulphan) and the herbicide dichlobenil. These compounds are completely separated and easily identified, as the GC–ECD trace in Fig. 3 shows. The GC–FID trace in the same figure shows the simultaneous determination of four-ring polynuclear aromatic hydrocarbons. Fraction IV is very important because the above-mentioned compounds can be identified even in very complex mixtures containing PCBs, chlordane and strobane.

Fraction V

This fraction contains the other two herbicides examined (propanil and difolatan) and the 2,3-dichlorophenol, although this was not completely recovered; the loss in recovery can be ascribed to its affinity for the aluminium oxide support that prevents its complete elution from the column. The increase in the number of the chlorine atoms in the ring enhances the acidity of the compound and a greater affinity for the basic alumina semicolumn results.

In fact, neither 2,4,5-trichlorophenol nor 2,3,4,5-tetrachlorophenol is eluted from the column. This fraction is the only one of the five in which there occurs interference due to the simultaneous presence of organochlorides and heterocompounds containing oxygen, nitrogen and sulphur atoms, detectable with ECD.

CONCLUSIONS

The proposed fractionation method is an implementation of that successfully applied to the analysis of real complex mixtures of hydrocarbons and heterocompounds [12], taking also into account the organochlorides. It offers good potential for the fractionation and determination of a great variety of organic compounds.

Only some eluents and their total volumes were changed from those used previously, without any effect on the identification and determination of the hydrocarbons and heterocompounds containing nitrogen, oxygen and sulphur atoms.

These results were not obtained using the single column of silica gel or aluminium oxide. In fact, silica gel is commonly used to clean up samples containing organochlorides, which are very slightly retained even when eluted with hydrophobic solvents such as *n*-hexane [16–18]. This support cannot be used if the organochlorine compounds must be divided into several fractions eluting with mixtures of increasing polarity (*i.e.* *n*-hexane–methylene chloride). On the other hand, using aluminium oxide a quantitative recovery of aliphatic hydrocarbons with high molecular weight is not possible because of its strong affinity for these compounds.

REFERENCES

1 R. W. Risebrough, P. Rieche, S. G. Herman, D. B. Peakall and M. N. Kirven, *Nature (London)*, 220 (1968) 1099–1102.
2 F. J. Biros, A. Walker and A. Medbery, *Bull. Environ. Contam. Toxicol.*, 5 (1970) 317–323.
3 M. R. Bleavins and J. Aulerich, *Residue Rev.*, 90 (1983) 57–67.
4 M. Splinder, *Residue Rev.*, 90 (1983) 1–34.
5 A. L. Jensen, *Environ. Pollut. Ser. A*, 34 (1984) 73–82.
6 R. A. Rapaport, N. R. Urban, P. D. Capel, J. E. Baker, B. B. Looney, S. J. Einsenreich and E. Gorham, *Chemosphere*, 14 (1985) 1167–1173.

7 R. Tatsukawa, *Eisei Kagaku*, 31 (1985) 1–7.
8 H. Shiraishi, N. H. Oilkington, A. Otsuki and K. Fuwa, *Environ. Sci. Technol.*, 19 (1985) 585–589.
9 L. Morselli, S. Zappoli, A. Donati, *Ann. Chim. (Rome)*, 79 (1989) 677–688.
10 D. R. Thielen, G. Olsen, *Anal. Chem.*, 60 (1988) 1332.
11 J. Sherma, *Anal. Chem.*, 61 (1989) 153R.
12 P. G. Desideri, L. Lepri, D. Heimler, S. Giannessi and L. Checchini, *J. Chromatogr.*, 284 (1984) 167–178.
13 P. G. Desideri, L. Lepri, M. Canovaro and L. Checchini, in L. Pawloski, E. Mentasti, W. L. Lacy and C. Sarzanini (Editors), *Chemistry for Protection of the Environment 1987*, Elsevier, Amsterdam, 1988.
14 P. G. Desideri, L. Lepri and L. Checchini, *Ann. Chim. (Rome)*, 79 (1989) 589.
15 S. B. Tejada and J. E. Sigsby Jr., *J. Chromatogr. Sci.*, 26 (1988) 494.
16 H. Hidaka, S. Tanabe and R. Tatsukawa, *Agric. Biol. Chem.*, 47 (1983) 2009.
17 D. E. Gaskin, R. Frank and M. Holdrinet, *Arch. Environ. Contam. Toxicol.*, 12 (1983) 211.
18 B. D. Gardner, *S. Afr. J. Science*, 80 (1984) 43.

Journal of Chromatography, 555 (1991) 229–237
Elsevier Science Publishers B.V., Amsterdam

CHROM. 23 362

Gas chromatography–mass spectrometry and high-performance liquid chromatographic analyses of thermal degradation products of common plastics

VĚRA PACÁKOVÁ
Department of Analytical Chemistry, Charles University, Albertov 2030, 128 40 Prague 2 (Czechoslovakia)
and
PIET A. LECLERCQ*
Laboratory of Instrumental Analysis, Department of Chemical Engineering, Eindhoven University of Technology, P.O. Box 513, 5600 MB Eindhoven (Netherlands)
(First received January 4th, 1991; revised manuscript received April 12th, 1991)

ABSTRACT

The thermo-oxidation of five commonly used materials, namely low-density polyethylene, retarded polyethylene, paper with a polyethylene foil, a milk package and filled polypropylene, was studied. Capillary gas chromatography and gas chromatography–mass spectrometry were used to analyze the volatile degradation products, while high-performance liquid chromatography was employed to measure polycyclic aromatic hydrocarbons. The results are discussed from the point of view of toxicity of the products.

INTRODUCTION

A great variety of products is formed by thermal degradation of polymeric materials. Many of the degradation products are toxic to living organisms. Carbon monoxide and hydrogen cyanide are among the most important products, but many other compounds are produced during combustion at high temperatures, *e.g.* organic nitriles, dioxanes, polycyclic aromatic hydrocarbons (PAHs), etc. Detailed analysis of these products is, therefore, of great importance [1–7].

The composition of the product mixtures formed during combustion of various materials depends strongly on the experimental conditions. Therefore, standard methods must be used for the evaluation of the toxicity of the products. The thermal degradation process can be studied in a combustion chamber [1,2] with a constant volume, enabling precise control and measurement of the temperature. In this way, reproducible reaction conditions can be realized, yielding degradation product mixtures of constant composition. Samples of different sizes can be used, and the equipment allows experiments with mice for biological tests.

Volatile products are best analyzed by capillary gas chromatography (GC), especially in combination with mass spectrometry (GC–MS) [3–7]. Modern fused-

0021-9673/91/$03.50

silica columns are very well suited for the separation of complex mixtures of substances, and the retention indexes measured on standard stationary phases can be useful for the identification of unknown products [8,9].

PAHs are formed during incomplete combustion of organic materials, especially at higher temperatures. PAHs represent the largest known group of chemical carcinogens with mutagenic and teratogenic effects [10]. Although capillary GC and GC–MS can be applied to the analysis of PAHs [11–13], high-performance liquid chromatography (HPLC) is the method of choice [14–19]. Either UV photometric or fluorimetric detection can be applied, the latter being more sensitive and selective [18,19].

The present paper reports on the results of the analyses of the thermal degradation products of five materials which are used in every day life. Capillary GC and GC–MS were employed to analyze the volatile products, while HPLC was used for the analyses of PAHs. The results of biological tests [20,21] are included, and the toxicity of the combustion products is evaluated.

EXPERIMENTAL

Combustion chamber

The combustion chamber [1–3] consisted of separate compartments for the sample combustion (volume 1.8 l) and for biological tests with mice (volume 2.3 l). In the combustion compartment, the sample was placed in a crucible that was electrically heated to the required temperature. A ventilator forced the combustion products into the smoke compartment, from which samples were taken by syringe and directly injected into a gas chromatograph or were swept by an inert gas into vessels placed in solid carbon dioxide. The frozen-out samples were diluted with methanol before analysis. The overall volume of the chamber was 4.2 l; the void volume was 0.1 l.

Analyzed materials

Low-density polyethylene (sample 1), retarded polyethylene (2), paper with a polyethylene coating (3) and milk packages (4) were burnt at temperatures below and above their flash points. Sample 5, filled polypropylene (Taboren), was heated for 35 min at 260°C. The manufacturer did not grant permission to publish the composition of the filler.

Analytical equipment

A CHROM 4A gas chromatograph (Laboratorní Přístroje, Prague, Czechoslovakia) was used with a flame ionization detector. A 25 m × 0.22 mm I.D. fused-silica column coated with 0.32-μm OV-1 stationary phase, was temperature programmed from 50°C, after a 3-min hold time, at 5°/min up to 300°C. A 50 m × 0.2 mm I.D. stainless-steel capillary column, coated with squalane and operated isothermally at 70°C, was used additionally for the analysis of sample 5. Nitrogen was the carrier gas. Of the gaseous products, 100 μl were injected with a split ratio of 1:100.

For GC–MS analyses an HP 5970A MSD quadrupole instrument was directly coupled to an HP 5790A gas chromatograph (Hewlett-Packard, Palo Alto, CA, USA). A 25 m × 0.22 mm I.D. HP-UP column, coated with 0.32-μm OV-1 stationary phase, was employed with helium as carrier gas. The frozen-out samples, dissolved in

methanol, were injected splitless in 1-μl portions (samples 1–4) or with a split ratio of 1:100 (sample 5, 0.1 μl). The column was temperature programmed as described above.

An LKB 2500 liquid chromatograph (Bromma, Sweden) was employed with a UV–VIS detector, a Rheodyne 7120 sampling valve with a 20-μl loop, an LKB 220 integrator and a 150 mm × 3.3 mm I.D. 7-μm Separon SGX C_{18} column (Tessek, Prague, Czechoslovakia). The fluorescence was measured with an RF-535 detector (Shimadzu, Japan) at an excitation and emission wavelength of 260 and 430 nm, respectively. The mobile phase consisted of methanol–water mixtures (80:20 or 90:10) and had a flow-rate of 0.3 ml/min and a temperature of 20 ± 2°C.

RESULTS AND DISCUSSION

Five samples of routinely used materials were examined: low-density polyethylene (1), retarded polyethylene (2), paper with a polyethylene foil (3), a milk package (4) and filled polypropylene (5). Samples 1–4 were degraded in the combustion chamber in air under flameless (500°C) conditions. Sample 5 was degraded at 260°C, *i.e.* the

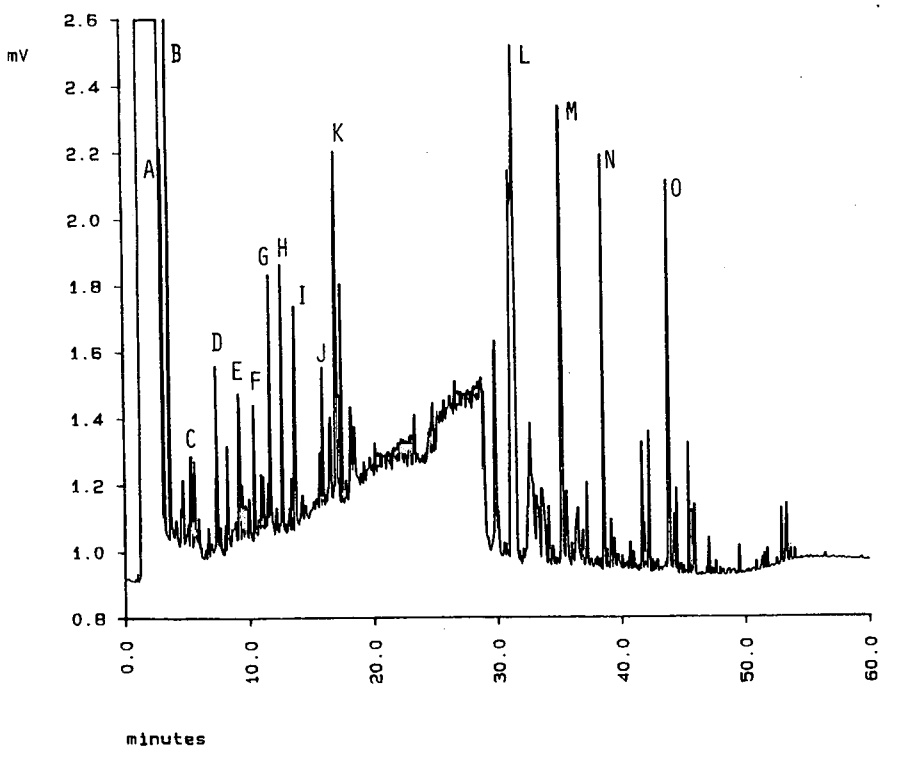

Fig. 1. Gas chromatogram (OV-1) of sample 3 (polyethylene-coated paper). Compounds identified by GC–MS: A = acetone alcohol; B = trimethoxymethane; C = 2-furfural; D = furanone; E = 5-methoxy-2(5H)-furanone; F = phenol; G, H = cresols; I, J = dimethylphenols; K = trimethylphenol; L = 1,3-diphenylpropane; M = diphenylbutene; N, O = phthalates.

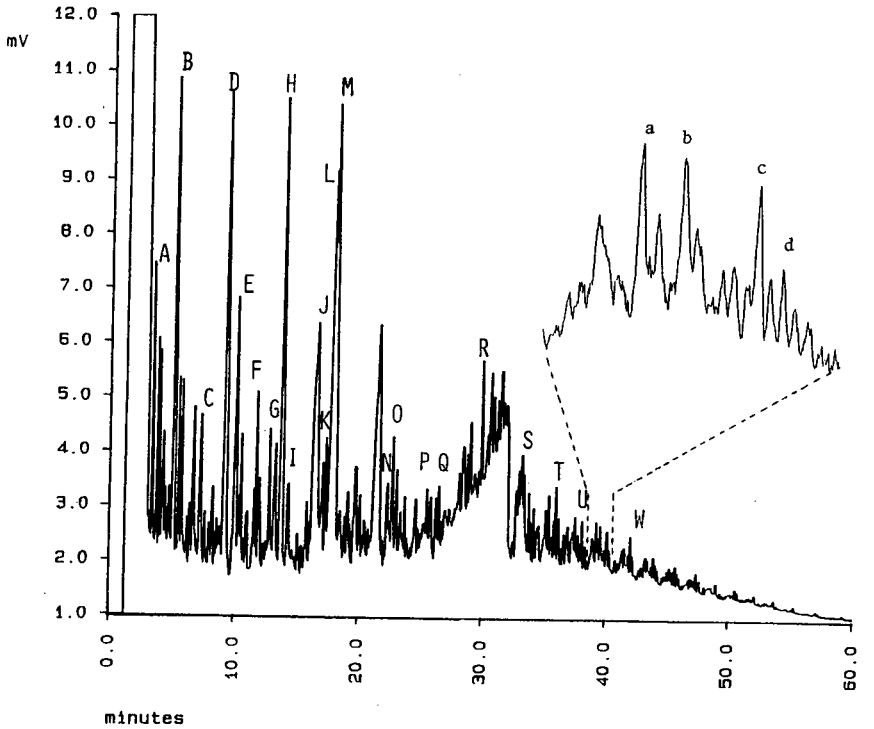

Fig. 2. Gas chromatogram (OV-1) of sample 4 (milk package). Compounds identified by GC–MS: A = trimethoxymethane; B = 2-furfural; C = 5-methyl-2-furfural; D = 1-decene + 2-hydroxy-1-methoxyethyl-1-furan; E = *n*-decane; F = cresol; G = 1,1-dimethoxyheptane; H = 1-undecene; I = *n*-undecane; J = 2-dimethoxymethyl-2,3-dihydrofuran; K = trimethylphenol; L = 5-hydroxymethyl-2-furfural; M = 1-dodecene; N = 1,1-dimethoxynonane; O = 1-tridecene; P = 1,1-dimethoxydecane; Q = 1-tetradecene; R, S, T, U, W = 1-pentadecene through 1-eicosene. Inset: exploded view of C_{19} fraction. a = 1,1-Dimethoxypentadecane; b = 1,18-nonadecadiene; c = 1-nonadecene; d = *n*-nonadecane.

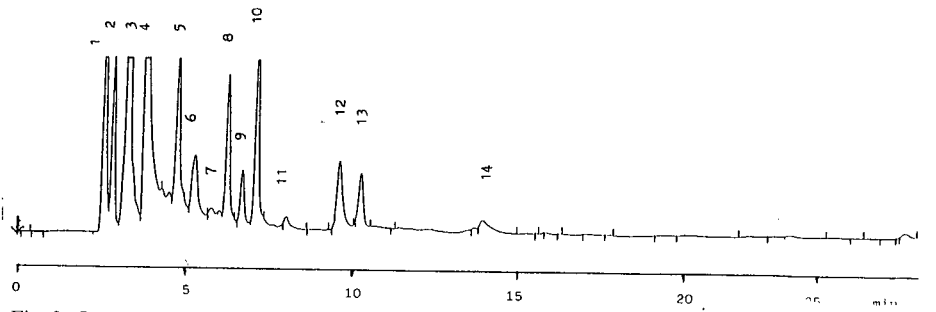

Fig. 3. Gas chromatogram (squalane, 70°C) of sample 5 (filled polypropylene). Compounds identified by retention index matching: 1 = methane + ethane + ethene; 2 = propene; 3 = butene + 1,3-butadiene; 4 = acetone + propionaldehyde; 5 = pentane; 6 = 1-*trans*-3-pentadiene; 7 = 3-buten-2-one; 8 = 4-methyl-1-pentene; 9 = 2,5-dihydrofuran; 10 = 2-butanol; 11 = *n*-hexane; 12 = 2-pentanone; 13 = acetone alcohol; 14 = 1-heptene.

temperature used for the production of automobile dashboards from this material. The products were analyzed by GC, GC–MS and HPLC. The results are summarized in Figs. 1–5 and Table I.

Biological tests, involving measurements of the lethal dose, LD_{50}, the carboxyhemoglobin content (HS value), and calculation of the toxicity index I_{tox}, were carried out at the Biological Departments of Charles University, within the framework of a systematic study of the dangerous effects of the combustion products of various materials [21]. These results are summarized in Table II.

GC and GC–MS

Sample 1 yielded the simplest spectrum of products. Compounds typical of the thermal degradation of polyethylene were found, *i.e.* characteristic gas chromatographic triplets of homologous 1-alkenes (present in the largest amounts) and the corresponding α,ω-alkadienes and *n*-alkanes. The only other substance present was trimethylphenol.

Similar degradation products were found in the gas chromatogram of sample 2 (retarded polyethylene). In addition to the hydrocarbons, 1,1-dimethoxyalkanes were present among the products. The origin of these compounds can be explained by the

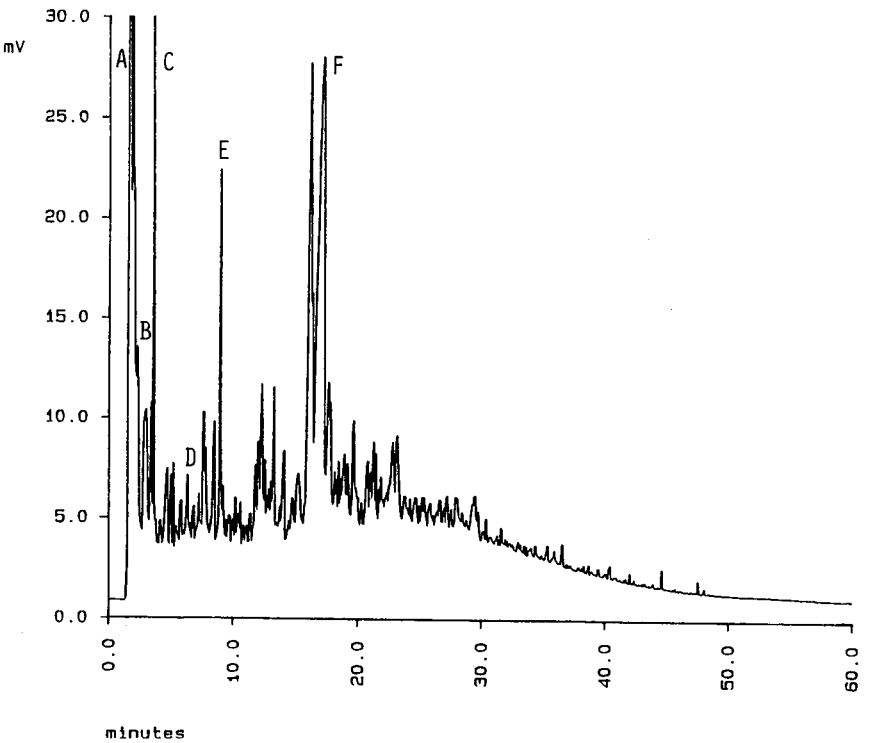

Fig. 4. Gas chromatogram (OV-1) of sample 5 (filled polypropylene). Compounds identified by GC–MS: A = acetone; B = acetone alcohol; C = 3-penten-2-one; D = diacetone alcohol; E = (tetrahydro-2H-pyran-2-yl)oxyacetone; F = dimethoxymethyl-2,3-dihydrofuran.

reaction of alkylaldehydes with the solvent methanol. The initially formed aldehydes are very unstable and degrade before analysis. They can be stabilized by the formation of methoxy derivatives, as was proven by the analyses of sample 2 with and without methanol added to the sample.

The GC–MS analyses of sample 3 revealed no characteristic polyethylene degradation products. The main components found were phenols, and diphenylalkanes and -alkenes (see Fig. 1).

The largest spectrum of products was obtained when burning sample 4 (milk package). The gas chromatogram of the degradation products of this sample is given in Fig. 2. The characteristic products of burning of polyethylene were formed, *i.e.* the 1-alkenes, α,ω-alkadienes and *n*-alkanes. The corresponding alkylaldehydes, and derivatives of furfurals, were present as compounds stabilized by reaction with methanol.

Sample 5, filled polypropylene, was heated to 260°C. During this procedure, this material is partially decomposed, causing an unpleasant smell and irritation of the eyes and skin of the workers. The degradation products were analyzed by capillary GC (Fig. 3) and GC–MS (Fig. 4). The compounds shown in Fig. 3 were identified by comparing their retention indexes, obtained at two temperatures, with values published for standard substances [8]. Many compounds were found, including saturated and unsaturated hydrocarbons, various oxygen-containing compounds, saturated and unsaturated ketones, alcohols, cyclic ethers, ketoalcohols, etc.

Analyses of PAHs by HPLC

The stationary phase and the mobile phase composition were selected on the basis of literature data. The separation conditions were optimized. The best resolution of a standard PAH mixture on a given C_{18} column was attained with a methanol–water mobile phase at volume ratios between 8:2 and 9:1.

The PAHs contained among the degradation products were identified by comparing the capacity factors of the unknown components with those of standard compounds, measured with two different mobile phases. Fluorescence detection was employed to improve the selectivity and sensitivity of the analyses.

All samples produced the same PAHs, *i.e.* naphthalene, phenanthrene, anthracene, pyrene, benzo[*a*]anthracene and benzo[*a*]pyrene (see Fig. 5), except for sample 4, from which phenanthrene was absent. However, the relative content of individual PAHs in the samples was different (see Table I). Anthracene was present in the highest amount, especially in the degradation products of sample 3, paper impregnated with polyethylene. Similar PAHs were found in refinery effluents [18], environmental dust and grass samples [17,19], and during combustion of polystyrene [12].

Toxicity tests

The toxicity of the combustion products, characterized by the LD_{50}, the carboxyhemoglobin content (HS value) and the toxicity index I_{tox}, for the materials studied is given in Table II. The toxicity is not very high, but there are various effects connected with the identified substances.

Aliphatic aldehydes exhibit strong irritating effects, especially on the eyes, and may cause allergies. The same is true of ketones, which also have narcotic properties. Unsaturated ketones, such as 3-buten-2-one (methylvinylketone) and 4-methyl-3-

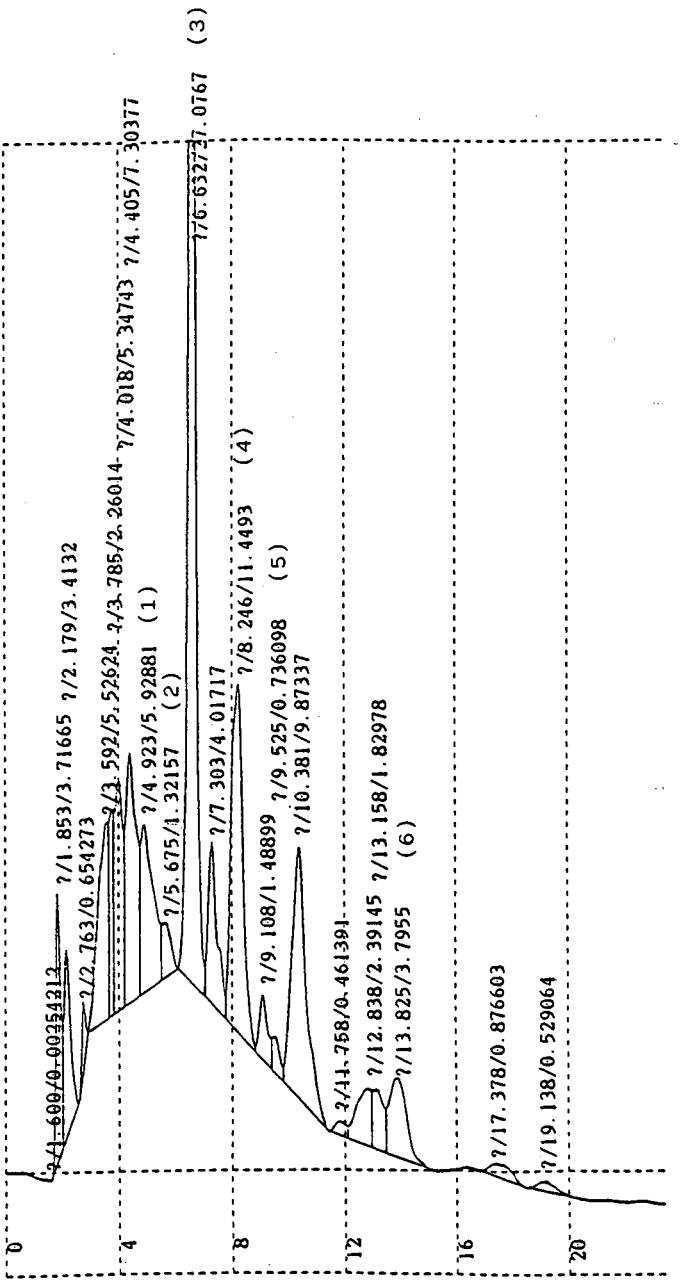

Fig. 5. Liquid chromatogram of sample 1 (low-density polyethylene). Compounds identified by capacity factor matching: 1 = naphthalene; 2 = phenanthrene; 3 = anthracene; 4 = pyrene; 5 = benzo[*a*]anthracene; 6 = benzo[*a*]pyrene.

TABLE I

RELATIVE AMOUNTS OF POLYCYCLIC AROMATIC HYDROCARBONS (%)

Compound	Sample No.			
	1	2	3	4
Naphthalene	1.4	11.7	11.2	30.6
Phenanthrene	0.4	4.1	2.6	–
Anthracene	91.4	34.8	53.9	30.2
Pyrene	2.7	17.3	1.4	17.6
Benzo[*a*]anthracene	3.0	17.1	1.3	17.5
Benzo[*a*]pyrene	1.2	9.3	7.6	3.3

TABLE II

BIOLOGICAL TOXICITY TESTS

HS = The carboxyhemoglobin content in mouse blood causing death of the animal (%); LD_{50} = lethal dose, *i.e.* the sample weight in mg/l of the chamber volume causing death of 50% of mice; I_{tox} = toxicity index: $I_{tox} = 10^4/[LD_{50}\,(1 + HS \cdot 10^{-2})]$.

Sample No.	HS	LD_{50}	I_{tox}
1	75	58	99
2	54	58	115
3	71	71	82
4	72	56	105

penten-2-one (mesityloxide), strongly irritate the eyes and skin. Hydrocarbons exhibit narcotic effects that are stronger for unsaturated compounds, and further adversely influence the nervous system, blood production and respiration. The toxicity index of the degradation product mixture of sample 5 was not measured, but the analysis of this mixture confirmed the presence of toxic compounds. Therefore, the original polymer had to be modified to decrease the danger to the workers during its treatment.

Many aromatics, especially PAHs, are proven or suspected carcinogens. Carcinogenic effects of naphthalene, anthracene and phenanthrene are still open to discussion, but pyrene, benzo[*a*]anthracene and benzo[*a*]pyrene are definitely carcinogenic.

REFERENCES

1 J. Michal, *Fire Mater.*, 7 (1983) 163.
2 J. Michal, *Fire Mater.*, 7 (1983) 169.
3 V. Pacáková, P. A. Leclercq, S. Holotík and I. Beroun, *Anal. Lett.*, 18 (1985) 1759.
4 R. S. Lehrle, *J. Anal. Appl. Pyrolysis*, 11 (1987) 55.
5 T. P. Wampler and E. J. Levy, *J. Anal. Appl. Pyrolysis*, 12 (1987) 75.
6 T. P. Wampler, *J. Anal. Appl. Pyrolysis*, 16 (1989) 291.
7 V. Pacáková, R. Dieckmann, P. A. Leclercq and K. Hoch, *Coll. Czech. Chem. Commun.*, 54 (1989) 934.
8 V. Pacáková and L. Feltl, *Retention Indices in Chromatography*, E. Horwood, Chichester, in press.

9 *The Sadtler Standard Retention Index Data Base*, Sadtler Research Laboratories, Philadelphia, PA.
10 R. Freudenthal and P. W. Jones (Editors), *Polynuclear Aromatic Hydrocarbons Chemistry, Metabolism and Carcinogenesis*, Raven Press, New York, 1976.
11 R. A. Hawley-Fedder, M. L. Parsons and F. W. Karasek, *J. Chromatogr.*, 314 (1984) 263.
12 R. A. Hawley-Fedder, M. L. Parsons and F. W. Karasek, *J. Chromatogr.*, 315 (1984) 201.
13 R. A. Hawley-Fedder, M. L. Parsons and F. W. Karasek, *J. Chromatogr.*, 315 (1984) 211.
14 D. W. Grant and R. B. Meiris, *J. Chromatogr.*, 203 (1981) 293.
15 K. Jinno and K. Kawasaki, *Chromatographia*, 17 (1983) 445.
16 K. Jinno and K. Kawasaki, *Chromatographia*, 18 (1984) 103.
17 E. P. Lankmayer and K. Müller, *J. Chromatogr.*, 170 (1979) 139.
18 R. K. Symons and I. Crick, *Anal. Chim. Acta*, 151 (1983) 237.
19 J. W. M. Wegener and M. J. M. van Schaick, presented at the *18th International Symposium on Chromatography, Amsterdam, September 1990*, Poster Mo-P-109.
20 H. Blahušková, J. Mácha, A. Markoš, Z. Procházková, B. Štefl and J. Michal, *Fire Mater.*, 10 (1986) 1.
21 *Catalogue of Technical Properties of Materials for Fire Protection*, Ministry of Interior, Bratislava, 1990.

Journal of Chromatography, 555 (1991) 239–245
Elsevier Science Publishers B.V., Amsterdam

CHROM. 23 400

High-performance thin-layer chromatographic and high-performance liquid chromatographic determination of abscisic acid produced by cyanobacteria

HELENA ZAHRADNÍČKOVÁ*
Laboratory of Analytical Chemistry, Czechoslovak Academy of Sciences, Branišovská 31, 370 05 České Budějovice (Czechoslovakia)
BLAHOSLAV MARŠÁLEK
Institute of Soil Biology, Czechoslovak Academy of Sciences, Branišovská 31, 370 05 České Budějovice (Czechoslovakia)
and
MARIE POLIŠENSKÁ
Institute of Plant Molecular Biology, Czechoslovak Academy of Sciences, Branišovská 31, 370 05 České Budějovice (Czechoslovakia)
(First received February 13th, 1991; revised manuscript received April 24th, 1991)

ABSTRACT

Methods for the determination of abscisic acid released by cyanobacteria into culture media based on high-performance thin-layer chromatographic densitometry and high-performance liquid chromatography have been developed. Abscisic acid exogenously released from cyanobacterial culture was separated and purified in only one step by using Sep-Pak C_{18} cartridges. In the case of high-performance thin-layer chromatography, a mobile phase of toluene–ethyl acetate–acetic acid (25:15:2, v/v/v) and silica gel plates with fluorescent label were used with absorbance measurements; for high-performance liquid chromatography, a mobile phase methanol–1% acetic acid (1:1, v/v) and a reversed-phase column were used. Comparison of the methods is included. Both methods were applied to the determination of abscisic acid in stressed and non-stressed cultures of the cyanobacteria *Trichormus variabilis* (Kom. Anag.) syn. *Anabaena variabilis* strain A 215. The salt stress (0.05 *M*) significantly increased the release of abscisic acid into the culture medium after only 2 under h the influence of stress.

INTRODUCTION

Abscisic acid (ABA) is an important plant growth hormone involved in various processes during the life cycle of higher plants. However, the occurrence and role of ABA in lower plants remains obscure. It is not at all clear whether ABA synthesized by algae, fungi, bryophyta, etc., is merely a product of secondary metabolism or if it is involved in the regulation of growth and development of lower plants. So far, the majority of ABA determinations in higher plants has been based on gas chromatography (GC) [1,2], GC–mass spectrometry (MS) both with and without single ion monitoring (SIM) [3,4], high-performance liquid chromatography (HPLC) [5–8], radio-

0021-9673/91/$03.50

immunoassay (RIA) and enzyme-linked immunosorbent assay (ELISA) [9–10]. In our previous work we developed a high-performance thin-layer chromatographic (HPTLC) method for the quantification of ABA produced by stressed green algae [11].

Most of the above-mentioned procedures employ an initial extraction of the plant material with an aqueous organic solvent. The non-selective nature of these solvent systems yields a highly complex sample containing many polar and non-polar compounds, including many plant pigments and polyphenolic components [1,12]. The high concentrations of impurities relative to ABA content means that extensive purification is required before most analytical techniques can be performed. In the course of purification of ABA many workers used solvent partitioning and TLC with or without different liquid chromatography systems (open column chromatography and HPLC). Time-consuming purification steps have been greatly simplified by using chromatographic cartridges that reduce the time necessary for sample preparation [1,8]. Purification steps can also be decreased by using water as extraction solvent [11,13].

The aim of this study was to devise a simplified sample preparation method (especially with a shortened purification step) and to develop and compare HPTLC and HPLC in the determination of ABA produced by cyanobacteria and, after comparison of the studied methods, to find the most convenient one.

EXPERIMENTAL

Plant material

Trichormus variabilis (Kom. Anag.) syn. *Anabaena variabilis* strain A 215, obtained from the collection of autotrophic organisms in the Institute of Botany, Czechoslovak Academy of Sciences, Třeboň, was used as the experimental organism. The cyanobacterium was cultivated in Bold's basal medium [14] in suspended culture with a 12-h photoperiod at 21°C for 13 days. After 13 days of cultivation 0.05 *M* sodium chloride was applied to one part of cultures. The stressing factor was applied to the cultures for 2 h, 48 h and 6 days. The fresh weight of cyanobacterium was established by centrifugation of the suspension; the volume of the suspension was measured before the centrifugation.

Chemicals

All chemicals and solvents were of analytical grade. Organic solvents and water were freshly distilled prior to use. Ethyl acetate, methanol, toluene and acetic acid were from Lachema (Brno, Czechoslovakia). (±)-2-*cis*-4-*trans*-Abscisic acid was obtained from Aldrich (Steinheim, Germany) and Sep-Pak C_{18} cartridges from Waters Associates (Milford, MA, USA).

HPTLC system

Apparatus: Linomat IV, CAMAG (Muttenz, Switzerland); TLC Scanner II, CAMAG; integrator SP 4270, Spectra Physics (San Jose, CA, USA); twintrough developing chamber, CAMAG. Chromatographic plates: Precoated silica gel 60 F254 HPTLC plates (10 × 10 cm, Merck, Darmstadt, Germany). Plates were cleaned before use by developing in methanol. The developing system was toluene–ethyl acetate–acetic acid (25:15:2, v/v/v).

HPLC system

A Varian 5500 liquid chromatographic system equipped with a Rheodyne 7126 injection valve with 10-μl loop, DS 604 data station and UV - 200 detector was used. The column used was an analytical Separon TM SGX RPS column (250 mm × 4 mm I.D.), 5 μm (Tessek, Prague, Czechoslovakia).

Purification procedure

The supernatant from centrifuged (2260 *g*, 20 min) cyanobacterial culture (usually 100 ml) was frozen, slowly thawed and centrifuged again (2260 *g*, 10 min). To one half of the supernatant a known amount of ABA standard was added to determine the ABA recovery, and both halves were processed in the same way. The supernatant after adjusting its pH to 2.5 with acetic acid was passed through a Sep-Pak C_{18} cartridge consecutively preconditioned with 10 ml of water 10 ml of methanol and 10 ml of 0.2 *M* acetic acid (rate 1 ml/min, the peristaltic pump was used). The cartridge was washed with 10 ml of 0.2 *M* acetic acid and 10 ml of 10% methanol; ABA was eluted with 5 ml of methanol–0.2 *M* acetic acid (3:2, v/v). The eluate was evaporated at 35°C to dryness with a stream of nitrogen; the residue was dissolved in 500 μl of methanol and used for HPTLC and HPLC ABA determination after centrifugation.

HPTLC method

Samples of 10 μl (triplicate) were applied in 3-mm stripes at 2-mm intervals in a nitrogen stream, at a rate of 5 s per 1 μl, alternating with 15, 10, 5 and 2 μl of standard ABA solution (1 μg/ml methanol, duplicate). Both standards and samples were applied to both halves of the plates, 8 mm from the lower edge of the plate. One-dimensional developments were performed vertically at ambient temperature (approximately 25°C) in saturated twin-trough chambers; the developing path was 5 cm. The developed plates were completely dried in a stream of air and immediately scanned under these conditions: λ = 270 nm (chosen after recording the absorbance spectrum of ABA on HPTLC plates – the optimum wavelength found concurs with that in ref. 15); absorption mode; deuterium lamp; monochromator bandwidth, 10 mm; slit width, 0.4 mm; slit length, 2 mm; scanning speed 1 cm/min. Calibration was based on peak heights obtained from the application of ABA standards to each plate.

HPLC method

Isocratic elution with a solvent mixture of methanol–1% acetic acid (1:1, v/v) was caried out for 11 min, followed by a linear gradient to 100% methanol over 3 min. At 6 min the column was washed isocratically with 100% methanol [16]. The solvents were carefully degassed prior to use. A constant flow of 0.8 ml/min and temperature of 40°C were maintained during the analysis. The injection volume was 10 μl, the detection wavelength 268 nm. Calibration was based on peak heights of standard solutions of ABA (1–15 ng of ABA injected).

RESULTS

HPTLC method

The reproducibility of the sample application was checked. Four series of standards, 2, 5, 10 and 15 ng of ABA, two series on one half of the plate, two on the other,

TABLE I

RELATIVE STANDARD DEVIATIONS OF DENSITOMETRIC RESPONSES TO ABA ON HPTLC PLATES

ABA (ng)	Relative standard deviation (%)
2	5.33
5	4.61
10	5.27
15	5.12

were applied to three HPTLC plates. The average relative standard deviations calculated from densitometric responses are listed in Table I. R_F of ABA was 0.43, the detection limit being 2 ng of ABA on the HPTLC plate. In a similar way we measured the reproducibility of the sample application of series of standards of cinnamic acid, which has been used by some authors [5] as an internal standard. Because the results showed great differences and were not easily reproducible, cinnamic acid could not be used to determine the recovery of ABA (in HPTLC or in HPLC).The linear regression equation calculated from densitometric responses on three plates with four series of ABA contents in the range 2–15 ng was as follows: $y = 5.075\,x + 1.681$ ($r^2 = 0.9836$). The data obtained confirmed the linearity of the calibration curves at the concentrations of ABA used.

The repeatability of absorbance measurements in reflectance mode was also evaluated by repeated scanning of strips of ABA standards. From each of three HPTLC plates two strips of different ABA content from different halves of the plate were scanned ten times. Relative standard deviations of the densitometer responses were in the range 0.58–1.69%.

The recovery of ABA by HPTLC was 95 ± 3% (determined from a known added amount of ABA in one half of each sample).

HPLC method

The reproducibility of the peak heights was studied. Four series of standards (1, 5, 10 and 15 ng of ABA in injection) were injected three times in a day and again on

TABLE II

RELATIVE STANDARD DEVIATIONS OF PEAK HEIGHTS OF ABA STANDARDS MEASURED BY HPLC

ABA (ng)	Relative standard deviation (%)			
	Day 1	Day 2	Day 3	Within 3 days[a]
1	0	6.15	3.54	12.59
5	4.11	1.64	3.29	4.20
10	3.82	4.45	3.93	6.83
15	2.09	3.37	0	4.23

[a] Relative standard deviation calculated from all results obtained by measuring ABA standards responses on three successive days.

TABLE III

DETERMINATION OF ABA IN SUPERNATANT FROM SUSPENSION OF *TRICHORMUS VARIABILIS* CULTIVATED UNDER SALT STRESS

Time of stress	Kind of stress	Fresh weight (g)	ABA (ng) per ml susp.		ABA (ng) per g fresh weight		HPLC as a percentage of HPTLC
			HPTLC	HPLC	HPTLC	HPLC	
2 h	None[a]	1.94	1.1	0.85	45.4	35.1	77.3
	0.05 *M* sodium chloride	1.93	1.9	1.55	78.8	64.2	81.6
48 h	None[a]	1.86	0.64	0.48	34.4	25.8	75
	0.05 *M* sodium chloride	1.93	2.8	2.5	145	129	89
6 d	None[a]	1.88	0.6	0.47	31.9	25	78.4
	0.05 *M* sodium chloride	1.91	4.6	3.4	240.8	178	73.9

[a] Control.

two successive days. The relative standard deviations calculated from peak heights are listed in Table II. The retention times of ABA ranged between 7.3 and 7.7 min and the detection limit was 1 ng of ABA injected.

The linearity of the calibration curves was tested using four solutions of ABA of concentrations 0.0001, 0.0005, 0.001 and 0.0015 mg per millilitre of methanol (corresponding to 1, 5, 10 and 15 ng of injected ABA). The results were evaluated by linear regression analysis. The linear regression equation calculated from peak heights measured three times or three successive days was as follows: $y = 5.714\,x + 1.119$ ($r^2 = 0.99497$). The data obtained confirm the linearity of the calibration curves at the concentrations of ABA used.

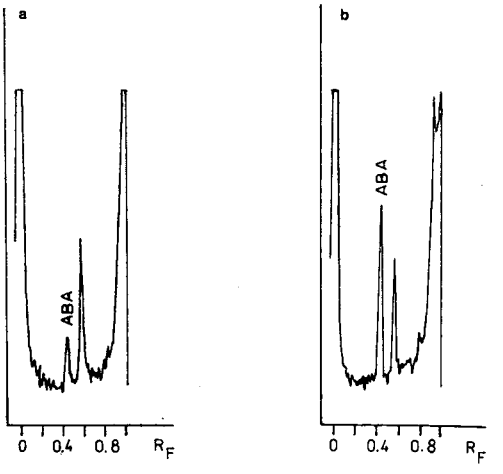

Fig. 1. Densitograms of stressed cyanobacterial samples (48 h, 0.05 *M* sodium chloride). Conditions: detection wavelength, 270 nm; mobile phase, toluene–ethyl acetate–acetic acid (25:15:2, v/v/v). (a) Original sample (2 ng of ABA); (b) sample spiked with 10 ng of ABA.

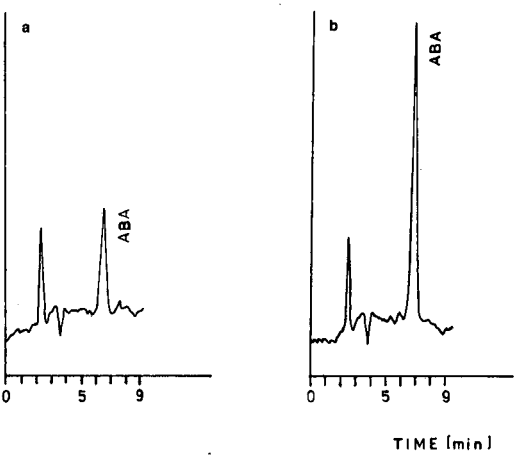

Fig. 2. HPLC chromatograms of stressed cyanobacterial samples (48 h, 0.05 *M* sodium chloride). Conditions: detection wavelength, 268 nm; mobile phase, methanol–1% acetic acid (1:1, v/v). (a) Original sample (5 ng); (b) sample spiked with 10 ng of ABA.

Both HPTLC and HPLC were used for ABA determination in cyanobacterium suspension cultures placed under stress by the addition of sodium chloride solution. The results (the averages of three analyses of three parallel determinations, *i.e.* of nine values) are listed in Table III. Examples of the densitograms and HPLC chromatograms of sample from cyanobacterial suspension after sodium chloride stress are given in Fig. 1a and b (densitograms) and Fig. 2a and b (HPLC chromatograms) both without (Figs. 1a, 2a) and with (Figs. 1b, 2b) spiked ABA.

DISCUSSION

The detection limit was nearly the same in HPTLC (2 ng on HPTLC plates) and HPLC (1 ng injected). The relative standard deviations of chromatographic responses ranged in HPTLC from 4.61% to 5.33% (Table I) and in HPLC from 0 to 6.12% in one day and from 4.20% to 12.59% (Table II) after several days. It is evident from Table II that measurements of the lowest standard concentration (1 ng) are subject to the greatest errors. As concerns the speed of analyses, HPTLC has a significant advantage over HPLC. The application of nine samples and two series of standards on both sides of an HPTLC plate, development and densitometric scanning takes at most 3 hours, while in HPLC one analysis lasts half an hour, and so to measure the same number of samples takes the whole day. In HPTLC we could apply more than 10 μl of sample (25 μl was possible without any deterioration of ABA differentiation) if the peak height was too small. The HPLC column was overloaded by impurities when more than 10 μl was injected. In HPTLC the impurities mostly remain at the start of chromatogram and do not interfere with peak of ABA; in HPLC columns the impurities must be washed away after each analysis. The results obtained by HPLC were lower than those obtained with HPTLC, - HPLC results being 82 $\pm$ 7% of HPTLC ones. A decrease in ABA as determined by HPLC has also been reported by other investigators [17]. In biological materials the comparison of results obtained by

different methods is very difficult due to different errors in the measurements. From to our results we consider HPTLC to be better than HPLC for the determination of ABA produced by cyanobacteria.

The results in Table III indicate that the cyanobacterium *Trichormus variabilis* is able to produce ABA. Cyanobacteria subjected to sodium chloride stress for six days increased their production of ABA six times; after two days of stress the production of ABA was increased 3–4 times. These methods are able to determine ABA production after only 2 hours (usually an 80% increasing in ABA production). This phenomenon —the occurence of ABA in lower plants– is under investigation and results will be published in the near future. Our finding, that cyanobacteria are able to produce ABA, is very interesting, because it is known that bacteria do not contain ABA [18]. Moreover, in another cyanobacterium, *Nostoc muscorum*, exogenous application of 10 mg/l ABA stimulated a response (exogenous ABA increased the utilization of molecular nitrogen from air six times) [19]. These facts indicate that ABA in cyanobacteria may also play some role in regulatory processes.

REFERENCES

1 F. T. Addicot, *Abscisic Acid*, Praeger, New York, 1983.
2 E. Vermeer, E. Knegt and J. Bruisma, *J. Chromatogr.*, 404 (1987) 346–351.
3 W. Dathe, O. Miersch and J. Schmidt, *Biochem. Physiol. Pflanzen*, 185 (1989) 83–92.
4 G. Guinn, J. R. Dunlap and D. L. Brummett, *Plant Physiol.*, 93 (1990) 1117–1120.
5 E. Bousquet, N. A. Santagati and G. Romeo, *J. Chromatogr.*, 354 (1986) 503–506.
6 Ph. Label, B. Sotta and E. Miginiac, *Plant Growth Regul.*, 8 (1989) 325–333.
7 D. M. Cahill and E. W. B. Ward, *Phytopathology*, 79 (1989) 1238–1242.
8 A. M. Carrasquer, I. Casals and L. Alegre, *J. Chromatogr.*, 503 (1990) 459–465.
9 E. Vernieri, P. Perata, D. Armellini, M. Bugnoli, R. Presentini, R. Lorenzi, N. Ceccarelli, A. Alpi and F. Tognoni, *J. Plant Physiol.*, 134 (1989) 441–446.
10 J. Soejima, M. Watanabe and T. Moriguchi, *J. Japan. Soc. Hort. Sci.*, 58 (1990) 819–826.
11 H. Zahradníčková, B. Maršálek and M. Polišenská, *J. Planar Chromatogr.*, 3 (1990) 243–248.
12 J. R. Dunlap and G. Guin, Plant Physiol., 90 (1989) 197–201.
13 B. R. Loveys and H. M. van Dijk, *Aust. J. Plant Physiol.*, 15 (1988) 421–427.
14 B. Brown and H. C. Bold, *Phycol. Studies*, 6417 (1964) 8–9.
15 S. V. Savinskii, I. Sh. Kofman, V. I. Kofanov and I. P. Stasevskaia, *Fiziol. Biokhim. Kult. Rastenii*, 19 (1987) 195–200.
16 S. N. Norman, V. P. Maiev and L. C. Echols, *J. Liq. Chromatogr.*, 5 (1982) 81–91.
17 S. Marx, W. Grosse and H. A. W. Schneider-Poetsch, *J. Plant Physiol.*, 133 (1988) 475–479.
18 M. Muller, C. Diegel and H. Ziegler, *Z. Pflanzen. Boden K.*, 152 (1989) 247–254.
19 B. Maršálek, M. Šimek and A. Lukešová, *Fifth International Symposium on Nitrogen Fixation with Non-Legumes, Florence, September 10–14, 1990*, Programme and abstracts, p. 156.

Journal of Chromatography, 555 (1991) 247–253
Elsevier Science Publishers B.V., Amsterdam

CHROM. 23 399

Dilution effect of carbonate ion on isotachophoretic zones observed with scanning UV photometric detection

TAKESHI HIROKAWA*, TOMOHIRO TAKA, YASURO YOKOTA and YOSHIYUKI KISO
Applied Physics and Chemistry, Faculty of Engineering, Hiroshima University, Kagamiyama 1, Higashi-hiroshima 724 (Japan)
(First received February 13th, 1991; revised manuscript received April 23rd, 1991)

ABSTRACT

A problem in the isotachophoretic analysis of anions at high pH is the so-called 'dilution effect' originating from aerial carbon dioxide dissolved in the terminating electrolyte. Elongation of isotachophoretic zones due to this dilution effect was studied with a scanning UV photometric detector, varying the carbonate concentration in the terminating electrolyte from 0 to 3 m*M*. The zone of a component with a smaller effective mobility than that of carbonate ion was elongated in proportion to the carbonate concentration, and the present system was still isotachophoretic, although it had two criteria of migration velocity. A practical example of the dilution effect in protein analysis at high pH using a model mixture of globulin, transferin and albumin is presented.

INTRODUCTION

In the isotachophoretic separations of anions, a problem encountered at relatively high pH (> 7) is disturbance due to carbonate ions from the terminating electrolyte solution. The carbonate ions originate from aerial carbon dioxide dissolved in water, and cause the elongation of sample zones and a decrease in the step heights in isotachopherograms due to the dilution of the sample (dilution effect). The carbonate zone can be suppressed to some extent by adding barium hydroxide to the terminating electrolyte [1]. This conventional technique may sometimes cause unwanted complex formation and blocking of the separation tube due to the precipitation of barium carbonate. As discussed by Verheggen *et al.* [2], the use of an isotachophoretic analyser with a complete closed system is useful for preventing the dilution effect; doubly distilled water is used to fill the electrode compartments, which are separated from the separation compartment by a semi-permeable membrane placed at the boundary between the electrolyte compartment and the separation compartment. The system was especially useful when the operational electrolytes were prepared in a closed system under a nitrogen atmosphere [2].

Fidler *et al.* [3] discussed several situations that may occur when the operational electrolyte system contains impurities. The dilution effect is one of these situations and is the most frequently encountered effect in the analysis of anions at high pH. Although a method for coping with the dilution effect is available [2], the theoretical

0021-9673/91/$03.50

approach [3] based on the simulation of the transient state should be confirmed by experiment and the feature of this unusual migration should be studied in detail from a dynamic viewpoint.

In this work, the mechanism of the elution and the degree of the dilution effect in relation to the concentration of carbonate in the terminating electrolyte was investigated by the use of a scanning UV photometric zone detection system [4], which permitted the observation of the transient state of electrophoretic migration. The dynamic feature of the elution is briefly discussed and a practical sample of the dilution effect in protein analysis at high pH is presented.

EXPERIMENTAL

Apparatus

The scanning UV photometric detection system used was equipped with a scanning assembly of a UV lamp and a detector. The assembly was driven by a linear head with a stepping motor [4]. The separation tube, a fused-silica capillary (I.D. 0.53 mm, O.D. 0.66 mm), was scanned over a length of 32 cm. A single scanning cycle took 7.027 s and 5333 photometric signals (a UV position spectrum) were acquired. The practical resolution was 0.15 mm and the detection limit of picric acid was 20 pmol. The migration current was 50 μA throughout. No special care was taken to prevent carbon dioxide from the air. The electrolyte compartments were conventionally filled with each electrolyte.

Samples and electrolyte system

The model sample used to study the dilution effect was a mixture of 4,5-dihydroxy-3-(*p*-sulphophenylazo)-2,7-naphthalenedisulphonic acid (SPADNS) and picric acid from Tokyo Kasei Kogyo (Tokyo, Japan). The dilution effect in the actual analysis was demonstrated using a model mixture of globulin, transferin and albumin. Transferin (molecular weight (MW) 70 000–90 000, p*I* 5.8) and albumin (MW 66 000, p*I* 4.7) were obtained from Midori Juji (Tokyo, Japan) and globulin (MW) 90 000–150 000, p*I* 6.3–8.4) from Sigma (St. Louis, MO, USA). The other chemicals for the electrolyte system were obtained from Tokyo Kasei Kogyo in the purest form available.

The leading electrolyte was 10 m*M* hydrochloric acid buffered by adding 2-amino-2-methyl-1,3-propanediol (ammediol, pH of leading electrolyte pH_L = 8.6). Hydroxypropylcellulose (HPC) was added to the leading electrolyte (0.2%). The terminator was 10 m*M* β-alanine. In order to clarify the dilution effect, sodium carbonate was added to the terminating electrolyte in the concentration range 1–4 m*M*. Water was distilled once after being processed by an anion exchanger.

In the analysis of globulin, transferin and albumin, the terminating electrolyte (10 m*M* β-alanine) was prepared in a conventional manner: the pH was adjusted to 10 by adding barium hydroxide and sodium carbonate was not added. The pH measurements were carried using a Horiba (Tokyo, Japan) Model F7ss expanded pH meter. Data processing was carried out with an NEC PC9801VX microcomputer.

RESULTS AND DISCUSSION

Fig. 1A illustrates the normal separation diagram of a two-component mixture of SPADNS (S) and picric acid (P). After the constituents had been separated, the zone length of the separated samples did not change, as shown in Fig. 1A, *i.e.*, all of the boundaries migrate at constant speed. Fig. 1B shows the migration model of SPADNS and picrate zones when carbonate ions were contained only in the terminating zone (CT) before starting electrophoretic migration. When SPADNS and picric acid are separated at pH_L = 8.6, the effective mobility of carbonate ions is higher than that of picrate and smaller than that of SPADNS. At this pH, most of carbonic acid (pK_a = 6.352 and 10.329, mobility = 46.1 × 10^{-5} and 71.8 × 10^{-5} cm^2 V^{-1} s^{-1}) is in the form of hydrogencarbonate ion, HCO_3^-. The abundance of carbonate ion, CO_3^{2-}, is negligibly small. The simulated effective mobility was 42.7 × 10^{-5} cm^2 V^{-1} s^{-1} at pH_L = 8.6. After the migration had started, the carbonate ions were eluted from the terminating zone (zone electrophoresis). It forms a pure carbonate zone (C) behind the SPADNS zone (S) after penetrating the picrate zone (CP).

As indicated by Fig. 1B, the SPADNS zone (S) will never be influenced by the carbonate ions from the terminating zone, but the picrate zone will be seriously affected: the zone length will be elongated and the conductivity of the zone will be decreased by the dilution due to carbonate ions. The extent of the dilution effect may depend on the concentration of carbonate ions in the terminating electrolyte, as the concentration in the picrate zone depends on it.

Zone elongation effect

Fig. 2 shows the observed transient isotachopherograms of an equimolar mixture of SPADNS and picric acid at pH_L = 8.6. In all experiments, the amount of sample was kept constant (total amount 20 nmol). On the other hand, the concentration of the added carbonate ions in the terminating electrolyte was varied in the range

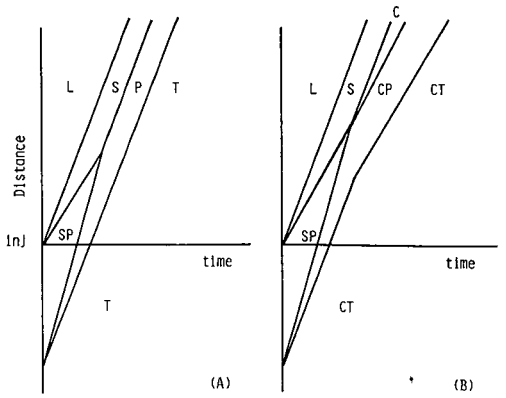

Fig. 1. (A) Normal separation process of two-component system of SPADNS and picrate ions. (B) Separation process with elution of carbonate from the terminating electrolyte. L = leading zone; S = SPADNS zone; P = picrate zone; T = terminating zone; SP = mixed zone of SPADNS and picrate ions; CP = mixed zone of carbonate and picrate ions; CT = terminating zone containing carbonate ion; inj = sample injection point.

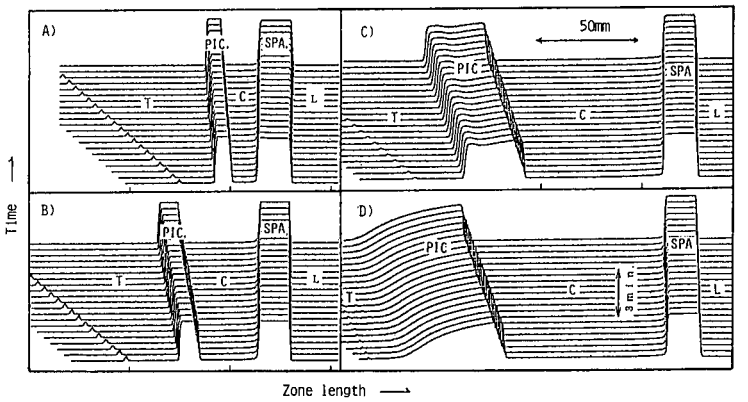

Fig. 2. Observed transient isotachopherograms of SPADNS (SPA) and picric acid (PIC) by the use of the scanning UV photometric zone detection system. L = leading zone; C = carbonate zone; T = terminating zone. The concentration of carbonate ion added to the terminating electrolyte was (A) 0, (B) 1, (C) 2 and (D) 3 m*M*. Leading electrolyte: 10 m*M* HCl–ammediol (pH_L = 8.6). Terminating electrolyte: 10 m*M* β-alanine. The migation current was 50 μA.

of 0–3 m*M*. In Fig. 2, the boundaries between the leading and SPADNS zones were rearranged at the same abscissa position to demonstrate the change in the individual zone lengths at the transient state. It is apparent from Fig. 2 that the length of the picrate and carbonate zones increased with increasing concentration of carbonate ion in the terminating electrolyte, although the increment was not linearly related to concentration.

Fig. 3 shows the concentration dependence of the ratio of zone length of SPADNS and picrate ions. Although the change in the zone length was negligible when the carbonate concentration was low, serious disturbances were observed at high concentrations. According to our simulation, the concentration of the pure

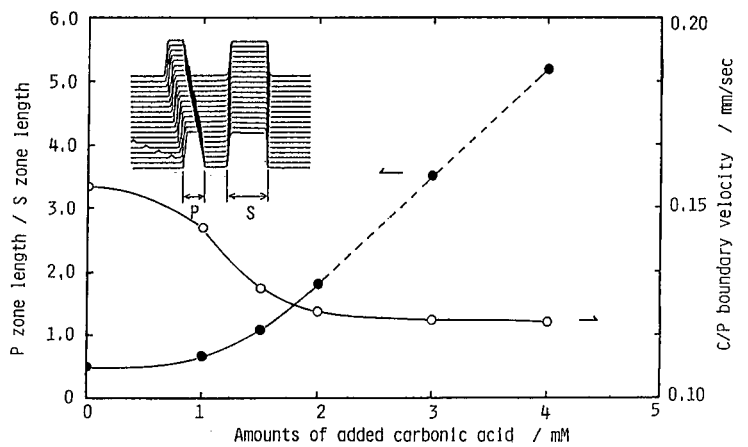

Fig. 3. Observed elongation of the zone length of picrate and the observed velocity of the boundary between carbonate and picrate zones. Operational conditions as in Fig. 2.

picrate zone was 6.8 m*M*. The concentration of picrate coexisting with carbonate ion was estimated from the value and the concentration ratio in Fig. 3 as 5.7, 3.1 and 1.8 m*M* for the terminating electrolyte containing 1, 1.5 and 2 m*M* carbonate ion, respectively.

Verheggen *et al.* [2] suggested that the calibration line was distorted owing to the dilution effect. It should be noted that the degree of the distortion depends on the carbonate concentration in the terminating zone.

Migration mode

Table I summarizes the evaluated boundary velocity. As estimated from the constant zone length in Fig. 2, the velocity of the boundary of the leading and SPADNS zone (L/S) and that of the SPADNS and carbonate zone (S/C) agreed with each other, suggesting that SPADNS migrated isotachophoretically and reached the steady state without any disturbance by the eluted carbonate ions. An interesting observation was that the boundary velocity of the carbonate and picrate zone (C/P) and that of the picrate and terminating zone (P/T) agreed with each other, within experimental error. This suggested that the zone length of the picrate zone was also constant during detection, in spite of the significant dilution effect. Hence the picrate zone also reached the steady state, although the boundary velocity was smaller than that of SPADNS. The migration in the present system is not isotachophoresis, in the sense that the criteria of migration velocity should be unique in isotachophoresis. However, it should be noted that the present system was still isotachophoretic in the sense that all sample zones reached the steady state, although it had two criteria of migration velocity, namely L/S and C/P boundaries.

As shown in Fig. 3, the velocity of the C/P boundary decreased and reached a constant value. Moreover, the boundary between the carbonate and the terminating zones was obscure at high concentrations of the carbonate ion. This might be caused by the similar potential gradient of the zones owing to the addition of carbonate. The simulated R_E values of the pure carbonate zone and the pure picrate zone were 1.73

TABLE I

BOUNDARY VELOCITIES OBSERVED WITH THE USE OF THE SCANNING UV DETECTION SYSTEM

L = Leading zone (Cl^-); S = SPADNS zone; C = carbonate zone; P = picrate zone; T = terminating zone [(β-alanine)$^+$].

Amount of carbonate (m*M*)[a]	Boundary velocity × 10^2 (cm s^{-1})			
	L/S	S/C	C/P	P/T
0	1.504	1.498	1.373	1.371
1	1.547	1.544	1.311	1.303
1.5	1.519	1.520	1.145	1.136
2	1.529	1.533	1.098	1.080
3	1.476	1.476	1.040	–
4	1.522	1.525	1.071	–

[a] Added to the terminating electrolyte.

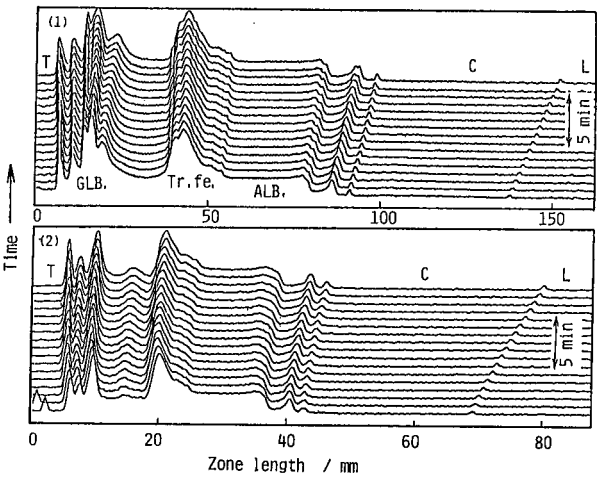

Fig. 4. Observed transient isotachopherograms of albumin (ALB), transferin (Tr.fe.) and globulin (GLB) by the use of the scanning UV photometric zone detection system. Total amount: (1) 553 μg and (2) 267 μg. The constituent ratio was 5:1:10. L = leading zone; C = carbonate zone; T = terminating zone. No carbonate ion was added to the terminating electrolyte (10 m*M* β-alanine; pH adjusted to 10 by adding barium hydroxide. The migration current was 50 μA.

and 2.61, respectively. The R_E value of the picrate zone with eluted carbonate ions may decrease to 1.73 with increase in the amount of eluted carbonate ion.

Migration of proteins with elution of carbonate

In the analysis of protein anions and amino acid anions, the pH of the leading electrolyte is usually chosen in the range *ca.* 8–10. Under such pH conditions, the carbonate zone migrates before the sample zones. Fig. 4 shows the observed transient isotachopherograms of a mixture of albumin, transferin and globulin (5:1:10, w/w/w). Apparently a zone of eluted carbonate was observed. Although the 553-μg mixture did not reach the steady state during the observation, it seemed that the 267-μg sample reached the steady state in spite of the dilution effect.

In a conventional isotachophoretic analyser, a potential gradient detector and a UV detector are used simultaneously. If the dilution effect exists, the zone lengths found in the recorder traces do not agree with each other even if the separation is complete. The reason is obvious from the above discussion. In protein analysis the patterns of the isotachopherograms were compared with each other. However, it must be noted that the difference, if it exists, may be caused by the dilution effect. Also, it should be noted that such an unfavourable effect is not restricted to carbonate ion, but can be caused by any mobile impurity in the terminating electrolyte, as generally discussed in ref. 3, if the abundance is significant.

If the leading electrolyte contains carbonate ion, a similar dilution effect will be observed for the sample zones sandwiched by the carbonate zone and the leading zone. However, the magnitude of the effect will be much smaller than that caused by the carbonate ions in the terminating electrolyte if the carbonate concentration in both electrolyte solutions is the same.

REFERENCES

1 F. M. Everaerts, J. L. Beckers and Th. P. E. M. Verheggen, *Isotachophoresis*, Elsevier, Amsterdam, 1976.
2 Th. P. E. M. Verheggen, J. C. Reijenga and F. M. Everaerts, *J. Chromatogr.*, 260 (1983) 471.
3 Z. Fidler, V. Fidler and J. Vacik, *J. Chromatogr.*, 320 (1985) 175.
4 T. Hirokawa, Y. Yokota and Y. Kiso, *J. Chromatogr.*, 538 (1991) 403.

Journal of Chromatography, 555 (1991) 254–259
Elsevier Science Publishers B.V., Amsterdam

CHROM. 23 434

Short Communication

Preparation of a chiral matrix

Resolution of (6*R,S*)-N^5-formyltetrahydrofolate

ROBERT J. MULLIN* and DAVID S. DUCH
Division of Cell Biology, Wellcome Research Laboratories, 3030 Cornwallis Road, Research Triangle Park, NC 27709 (USA)

(First received October 31st, 1990; revised manuscript received May 6th, 1991)

ABSTRACT

Combination chemotherapy involving (6*R,S*)-N^5-formyltetrahydrofolate and 5-fluorouracil has raised considerable speculation concerning the effects of the unnatural (6*R*) diastereomer. The inability to obtain quantities of the individual diastereomers has greatly limited work in this area. Commercially available chiral columns, suitable for diastereomer analysis, are inadequate for preparative work. We report here on the use of epoxide-activated media in the construction of a bovine serum albumin-based high-performance liquid chromatography matrix capable of resolving the diastereomers of (6*R,S*)-N^5-formyltetrahydrofolate in milligram quantities. Similar columns based upon alternative protein matrices may prove useful for the resolution of additional materials.

INTRODUCTION

Chemical synthesis of compounds containing a chiral center generally results in the production of a racemic mixture. Studies in biological systems using racemic mixtures raise numerous questions concerning the relative contribution of each of the stereoisomers present to the observed biological response. The development of chemotherapeutic protocols targeted against thymidylate synthase involving the combination of (6*R,S*)-N^5-formyltetrahydrofolate and 5-fluorouracil can be used as an example. Optimal response to this protocol is dependent upon the use of (6*S*)-N^5-formyltetrahydrofolate as a folate source for increasing intracellular levels of the cofactor for thymidylate synthase N^5,N^{10}-methylenetetrahydrofolate [1–5]. Considerable speculation has been raised concerning the effects of the unnatural (6*R*) diastereomer on the utilization of (6*S*)-N^5-formyltetrahydrofolate as a result of pharmacokinetic studies which have shown that the two diastereomers of (6*R,S*)-N^5-formyltetrahydrofolate differ with respect to plasma half-life. (6*R*)-N^5-

0021-9673/91/$03.50

formyltetrahydrofolate, the unnatural diastereomer, has a plasma half-life of 451 min, considerably longer than the half-life of 32 min for the natural isomer. Due to these differences in half-lives the (6*R*)/(6*S*) ratio increases dramatically with time [6,7]. Since the potentiation of 5-fluorouracil requires the uptake and metabolism of (6*S*)-N^5-formyltetrahydrofolate, the increasing (6*R*)/(6*S*) ratio may be less than optimal for therapeutic response. The difficulty of obtaining adequate amounts of the individual isomers of (6*R,S*)-N^5-formyltetrahydrofolate has greatly limited studies in this area. The introduction of Resolvosil high-performance liquid chromatography (HPLC) columns and their use in resolving (6*R,S*)-N^5-formyltetrahydrofolate [8,9] has offered an approach to the production of the isomers of (6*R,S*)-N^5-formyltetrahydrofolate in quantities suitable for biological studies. Unfortunately, the low capacity of these columns does not allow their use in isomer preparation. Employing epoxide (EP)-activated HPLC support media, we have prepared bovine serum albumin (BSA)-based chiral HPLC matrices capable of resolving the isomers of (6*R,S*)-N^5-formyltetrahydrofolate in milligram quantities.

EXPERIMENTAL

Reagents

Folate standards other than tetrahydrofolate were prepared as previously described [10]. Tetrahydrofolate was prepared by the enzymatic reduction of H_2PteGlu [11]. (6*R,S*)-5-CHO-H_4PteGlu was from Burroughs Wellcome, Research Triangle Park, NC, USA. BSA was purchased from Sigma (St. Louis, MO, USA) as a charcoal-treated and dialyzed preparation. Hydropore EP columns were purchased from Rainin (Wobourn, MA, USA). Ultraffinity-EP columns were purchased from Beckman (San Ramon, CA, USA). Diethylaminoethyl cellulose (DE-52) was purchased from Whatman Biosystems (Clifton, NJ, USA).

Cells

WiDr cells, derived from a human colon adenocarcinoma, were obtained from the American Type Culture Collection and were maintained in folate-free RPMI 1640 medium supplemented with 10% dialyzed fetal calf serum, 20 μM thymidine and 50 μM hypoxanthine.

Column derivatization

BSA-EP columns were prepared by coupling BSA to the activated epoxide function on either Hydropore EP or Ultraffinity-EP HPLC columns (100 mm × 10 mm I.D.) by recycling a 50-ml solution containing 3 g of BSA for 18 h. Prior to coupling, this solution was dialyzed overnight against 1 *M* potassium phosphate buffer, pH 7.0, and then passed trough a 0.2-μ filter to remove particulates. In addition to the above columns, a Rain Dynamax preparative HPLC column with Hydropore EP column packing (120 mm × 41.4 mm I.D.) was also derivatized. For this column, a 62-g sample of BSA in 500 ml was employed as the coupling solution. This material, which had also been dialyzed against 1 *M* potassium phosphate buffer, pH 7.0, and filtered, was recycled at a rate of 14 ml/min for 18 h. Based upon the manufacturer's specifications, all of the BSA-EP columns described in this report were derivatized with a tenfold excess of BSA relative to the expected binding capacity. No

attempt was made to quantitate the actual quantity of BSA coupled to these columns. It is not known if unreacted EP groups remained following coupling.

Chromatography

HPLC was carried out using a Waters 712 WISP autoinjector (Waters Chromatography Division, Milford, MA, USA), an LDC/Milton Roy Constametric 3000 pump, and an LDC Spectromonitor III detector (Laboratory Data Control, Rivera Beach, FL, USA). Data were collected and analyzed with a DS-80 microcomputer (Digital Specialties, Chapel Hill, NC, USA). The preparative chromatography was carried out using modified Waters 6000A pumps driven with a Waters 600 solvent programmer. The Resolvosil (Macherey-Nagel) column and the 100 mm × 10 mm I.D. BSA-EP columns were eluted isocratically with 10 m*M* sodium phosphate pH 7.0. The larger preparative column was eluted isocratically with 20 m*M* sodium phosphate pH 7.0. The ionic strength of the mobile phase for the larger column was adjusted to allow for a run time of 1 h. Reversed-phase analysis of folates was performed on a C_{18} column according to previously published methods [10].

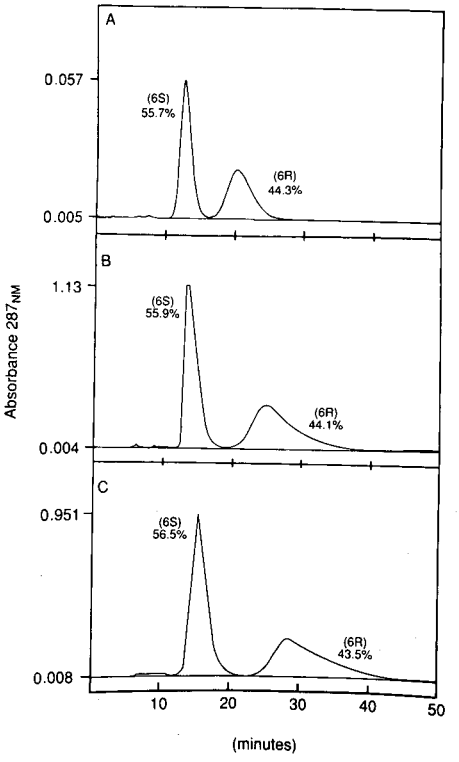

Fig. 1. Resolution of the isomers of (6*R*,*S*)-N^5-formyltetrahydrofolate. (A) 10-μg sample on a 150 mm × 4 mm I.D. Resolvosil column; (B) 100-μg sample on a 100 mm × 10 mm I.D. Hydropore BSA-EP column; (C) 100-μg sample on a 100 mm × 10 mm I.D. Ultraffinity BSA-EP column. All three columns were eluted with a mobile phase of 10 m*M* sodium phosphate, pH 7.0, and a flow-rate of 1 ml/min. Detection at 287 nm.

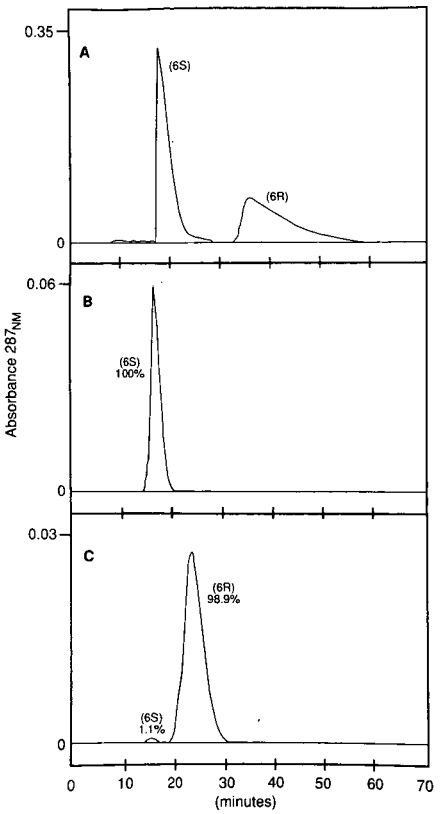

Fig. 2. (A) Resolution of 3 mg of N^5-formyltetrahydrofolate on a 120 mm × 41.1 mm I.D. Hydropore BSA-EP column; (B) Resolvosil analysis of (6*S*)-N^5-formyltetrahydrofolate prepared with the 120 mm × 41.1 mm I.D. Hydropore BSA-EP column; (C) Resolvosil analysis of (6*R*)-N^5-formyltetrahydrofolate prepared with the 120 mm × 41.1 mm I.D. Hydropore BSA-EP column.

RESULTS AND DISCUSSION

Hydropore EP and Ultraffinity-EP columns, folowing derivatization with BSA, could be used to effectively resolve N^5-formyltetrahydrofolate. Fig. 1 compares the elution of (6*R,S*)-N^5-formyltetrahydrofolate samples from a commercially available BSA-based Resolvosil column and two BSA-EP columns prepared by the method described in this manuscript. The 150 mm × 4 mm I.D. Resolvosil columns are capable of baseline resolution of a 10-μg sample of N^5-formyltetrahydrofolate. The capacity of Resolvosil columns has been variable in our hands with two columns in series often being required to achieve baseline resolution. This variability was the initial stimulus in our effort to prepare BSA resins. Improper column handling, resulting in BSA denaturation, may have been associated with the observed variability. Functional columns, flushed with 50 m*M* phosphate buffer, pH 7.0, containing 0.02% NaN_3, showed no sign of deterioration with long-term storage at 4°C. A 100 mm × 10 mm I.D. BSA-EP column is routinely capable of resolving a 100-μg sample. This represents a more than twofold increase in capacity following correction for the

TABLE I

GROWTH OF WiDr CELLS ON THE ISOMERS OF N^5-FORMYLTETRAHYDROFOLATE

Cell number × 10^{-6}. Cells, grown in folate-free RPMI 1640 medium with 10% dialyzed fetal calf serum, supplemented with 50 μM hypoxanthine and 20 μM thymidine, were transferred to medium containing 10% dialyzed fetal calf serum and either 5 nM (6*S*) or (6*R*)-N^5-formyltetrahydrofolate, 10 nM (6*R,S*)-N^5-formyltetrahydrofolate, or 50 μM hypoxanthine (H) and 20 μM thymidine (T).

Time	(6*S*)	(6*R*)	(6*R,S*)	H + T
24h	0.26	0.21	0.23	0.24
48h	0.70	0.22	0.64	0.48
72h	1.40	0.21	1.25	0.88

difference in internal volume between the Resolvosil and BSA-EP columns. In addition to the above columns, a Rainin Dynamax preparative HPLC column with Hydropore-EP column packing (120 mm × 41.4 mm I.D.) was also successfully derivatized and was capable of baseline resolution of 3 mg of (6*R,S*)-N^5-formyltetrahydrofolate using a mobile phase of 20 mM sodium phosphate, pH 7.0, and a flow-rate of 13.5 ml/min (Fig. 2). Baseline resolution of the isomers was not obtained with larger sample size. A 40-mg amount of each of the isomers of N^5-formyltetrahydrofolate was prepared by repetitive use of the 120 mm × 41.4 mm I.D. Hydropore-BSA-EP column. These samples were concentrated using a DE-52 cellulose column eluted with a linear gradient of 50–750 mM ammonium bicarbonate with a total gradient volume equal to 10 times the column bed volume (100 ml). The pooled fractions from the DEAE column were freeze-dried twice to remove the ammonium bicarbonate buffer. Analysis of these materials on a Resolvosil column indicated that on a chrial basis, the (6*S*) material was 100% pure and the (6*R*) material was 98.9% pure (Fig. 2). The identification of the diastereomers as (6*R*) or (6*S*) was based upon the ability to support the growth of the human colon adenocarcinoma cell line, WiDr (Table I). The order of elution and peak shape was in agreement with previous reports [8]. The identification of these products as N^5-formyltetrahydrofolate was based upon spectral data and reversed-phase HPLC analysis [10] (data not shown). The affinity of BSA for (6*R*)-N^5-formyltetrahydrofolate is of interest and may be a contributing factor to the plasma protein binding of (6*R*)-N^5-formyltetrahydrofolate, which appears to be the mechanism for the long plasma half-life of this isomer [7].

None of the other reduced folates examined (tetrahydrofolate, N^{10}-formyltetrahydrofolate or N^5-methyltetrahydrofolate) maintained structural integrity during chromatography on the BSA-EP columns. Chromatography on the larger columns led to degradation which could not be prevented by degassing and helium purging of the mobile phase. (6*R,S*)-N^5-methyltetrahydrofolate could be resolved on the Resolvosil columns with only minor degradation; however, significant breakdown was seen on the BSA-EP columns. Reversed-phase analysis indicated that degradation was typically a result of oxidation and C^9-N^{10} cleavage as tetrahydrofolate eluted as dihydrofolate and *para*-aminobenzoylglutamate. N^{10}-formyltetrahydrofolate eluted as N^{10}-formyldihydrofolate and *para*-aminobenzoylglutamate. The mechanism for this degradation is unknown.

In conclusion, commercially available epoxide-activated HPLC supports, designed for affinity chromatography, were easily derivatized with BSA to generate matrices capable of resolving the optical isomers of (6*R,S*)-N^5-formyltetrahydrofolate. The low capacity of this matrix was compensated for by scale-up of column size. No complications in this scale-up were observed in operation of this larger column following adjustment for the increased column cross-sectional area. This has allowed the separation of the diastereomers of (6*R,S*)-N^5-formyltetrahydrofolate in quantities suitable for tissue culture studies. The use of Resolvosil columns for the resolution of a variety of compounds has been described in the literature [12]. Presumably, the columns described in this report could also be used for the preparation of the isomers of these and related chemicals in milligram quantities, which should prove adequate for initial studies examining the contribution of the individual isomers to the biochemical properties of the mixture. The employment of these activated epoxide matrices should also allow for the simple coupling of alternative proteins as chiral stationary phases; α_1 acid glycoprotein is an example of such an alternative protein that has already been employed as a chiral matrix for a variety of compounds [13].

REFERENCES

1 B. Ullman, M. Lee, D. W. Martin and D. V. Santi, *Proc. Natl. Acad. Sci.*, 75 (1978) 980.
2 R. M. Evans, J. D. Laskin and M. T. Hakala, *Cancer Res.*, 41 (1981) 3288.
3 J. A. Houghton, S. J. Maroda, J. O. Phillips and P. J. Houghton, *Cancer Res.*, 41 (1981) 144.
4 D. Machover, L. Schwarzenberg, E. Goldschmidt, J. M. Tourane, B. Michalski, M. Hatat, T. Dorval, J. I. Misset, C. Jasmin, R. Maral and G. Mathe, *Cancer Treat. Rep.*, 66 (1982) 1803.
5 E. Mini, F. Trave, Y. M. Rustum and J. R. Bertino, *Pharmac. Ther.*, 47 (1990) 1.
6 J. A. Straw, D. Szapary and W. T. Wynn, *Cancer Res.*, 44 (1984) 3114.
7 E. M. Newman, J. A. Straw and J. H. Doroshow, *Cancer Res.*, 49 (1989) 5755.
8 K. E. Choi and R. L. Schilsky, *Anal. Biochem.*, 168 (1988) 398.
9 I. W. Wainer and R. M. Stiffin, *J. Chromatogr.*, 424 (1988) 158.
10 D. S. Duch, S. W. Bowers and C. A. Nichol, *Anal. Biochem.*, 130 (1983) 385.
11 C. K. Mathews and F. M. Huennekens, *J. Biol. Chem.*, 235 (1960) 3304.
12 S. Allenmark, *J. Liq. Chrom.*, 9 (1986) 425.
13 I. W. Wainer, S. A. Barkan and G. Shill, *LC·GC*, 4 (1986) 422.

Journal of Chromatography, 555 (1991) 260–266
Elsevier Science Publishers B.V., Amsterdam

CHROM. 23 426

Short Communication

Improved accuracy in the determination of field-flow fractionation elution volumes

JIANMIN LI and KARIN D. CALDWELL*
Department of Bioengineering, University of Utah, Salt Lake City, UT 84112 (USA)
(First received February 21st, 1990; revised manuscript received May 6th, 1991)

ABSTRACT

Conventional operation of field-flow fractionation (FFF) systems involves carrying out the analysis at a constant flow of carrier; the flow is temporarily interrupted after injection of a sample in order to permit its equilibration under the applied field. Retention is calculated as the ratio of elution times for a non-retained species and the sample of interest, respectively. Such time-based retentions are only valid if the flow-rate is precisely known at all times during the run. The peristaltic pumps often used with FFF equipment are shown to have an output which varies unpredictably in time. Furthermore, initiation of flow after relaxation is shown to result in significant periods of transient behaviour while the system adjusts to the operating pressure. These and other variations in flow-rate can be eliminated as sources of error by basing the retention measurement on effluent weight, rather than on time. For this purpose, an electronic balance is interfaced with the system's computer, so that detector response/effluent weight data pairs are continuously monitored during the course of the FFF analysis.

INTRODUCTION

Elution volumes in field-flow fractionation (FFF), as in ordinary column chromatography, are generally determined from observed elution times at what is assumed to be constant rates of delivery of carrier, or mobile phase. These times are measured either directly, from the run-time associated with the peak maximum for an eluting component, or indirectly, from measurements of the distance on a chart recording between points representing the start of the separation process and the location of the peak maximum, respectively. Since the fundamental parameter of thermodynamic significance in these quasi-equilibrium processes is the elution volume, which directly relates to elution time only at a constant or well-controlled flow-rate, it is evident that significant errors may be introduced into the measurements if the mobile phase is delivered at an unstable or uncontrolled rate [1].

Characteristic for the FFF columns is their open geometry which provides little resistance to liquid flow; in fact, under normal operating conditions, the column

0021-9673/91/$03.50

pressure rarely exceeds 15 p.s.i. The carrier is, therefore, often successfully delivered to these columns by means of relatively inexpensive, low-pressure peristaltic pumps. Despite the many conveniences offered by these pumps, such as a wide range of flow-rates, the potential for electronic control of the pump speed, and the low cost, they have a clear disadvantage in that their output tends to vary with time. Factors such as temperature fluctuations in the laboratory, slight obstacles in the flow path, and ageing of the pump tubing, all have a significant influence on this output. Even the more elaborate pumping systems normally used in high-performance liquid chromatography are known to occasionally generate flow-rates which vary in time [1–3]. Retention data from FFF experiments using peristaltic or other pumps with non-constant output should, therefore, ideally be based directly on recorded elution volumes, rather than on elution times as is commonly done.

A parameter of utmost importance to any FFF analysis is the void volume, V^0, which is the reference point in any determination of retention ratio R [4,5]. Often, V^0 is determined from the elution volume of a non-retained compound mixed in with the injected sample. Since the void volume is small compared to most practical elution volumes of retained compounds for which analytical information is sought, any error in this number is of particularly large consequence for the accuracy of such retention-derived characteristics as the particle diameter or molecular weight.

Very often, the field-induced relaxation of a sample into its equilibrium distribution is allowed to occur in the absence of carrier flow [6]. As pumping is resumed, there is likely to be a certain lag period during which the system's pressure builds up to the steady state level associated with a desired flow rate. If the flow is assumed to be constant during this period, and elution volumes are calculated from elution times, serious errors could result. In particular, if the lag period is comparable in length to the time required to sweep out one column volume, such errors would strongly affect the measured void volume and, by implication, the accuracy of any analytical information gained from the FFF experiment.

In the present work, we have chosen to replace the time-based measurements of elution volume with a direct read-out of effluent weight via an inexpensive electronic balance interfaced to the system's computer. The advantages of this approach are illustrated in runs of both short (void volume) and long duration.

Upon injection into the FFF channel a sample is exposed to the applied field, which in the present context is a sedimentation field. Several other fields have been used successfully to accomplish separation in the FFF mode [5], and the experimental approach described here is generally applicable to any FFF system. Under the influence of the field, the different sample components migrate to that channel wall where their potential is minimized. After a certain relaxation time [6] the field-induced migration to the wall is exactly balanced by diffusion; at this point, each component has established a unique equilibrium distribution in the channel the thickness of which is reflected in the observed retention. From measurements of the volume V_e needed to sweep out the sample, and the void volume, V^0, one can therefore determine this thickness which, in turn, leads to information about the appropriate sample property, *e.g.* molecular mass or particle size in the case of sedimentation FFF [4].

During their migration through the channel, the sample zones will broaden due to a variety of causes. For a monodisperse material, the most important factor is generally the velocity-dependent non-equilibrium effect [7], which results from the fact

that the laminar flow of carrier will move different layers of the sample cloud at different velocities, thus disturbing its equilibrium distribution. Diffusive corrections to these disturbances are not instantaneous, and the non-equilibrium zone broadening (H_{neq}) will therefore increase with increasing carrier velocity. In the limit of high retention,

$$H_{neq} = 24\lambda^3[w^2 < v > /D] \quad (1)$$

where parameter λ [approximately equal to $(V^0/V_e)/6$] represents the dimensionless thickness of the sample layer [4]. Here, w is the channel thickness and D is the sample's diffusion coefficient. From this expression it is easily seen that the reduced efficiency resulting from fast channel flow $< v >$, can well be offset by operation at higher retention (smaller λ values). Early on, this condition suggested that rapid, high-resolution separations could be obtained at constant field, using a carrier flow which is programmed to increase during the course of the run [8]. The use of this promising approach will require precise knowledge of the magnitude of the flow-rate throughout the entire separation process.

METHODS

The overall experimental arrangement is shown in Fig. 1. Here, three items are of particular importance, namely the valve A, which permits by-passing the column

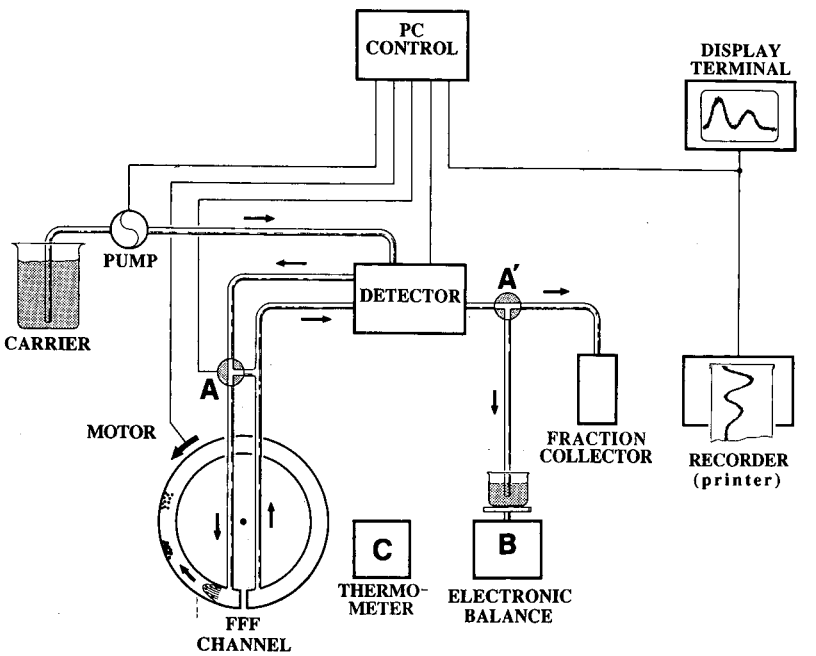

Fig. 1. Experimental arrangement involving the use of an electronic balance to measure flow-rates. A and A' are two magnetic valves under computer control, which determine the directions of flow before the inlet to the channel and after the detector, respectively. A read-out of the temperature from the thermometer C is fed into the computer before the program begins. Aside from controlling the pump, the system's computer also controls the centrifuge motor, and thus the channel's spin rate, via a feed-back mechanism. See also text.

during relaxation, the balance B which monitors the weight of effluent from the system, and the digital thermometer C. The first two items are interfaced with the system's computer, as indicated in the figure, and the third provides a separate record of the ambient temperature to enable a correct assessment of the carrier density. At no time was the temperature fluctuation larger than ± 0.25°C during the course of a 2-h run.

The sedimentation FFF system was built in house, essentially according to descriptions published previously [9]; the length, breadth, and thickness dimensions of the separation channel are 94.0 cm, 2.0 cm, and 0.0254 cm, respectively, and both ends are tapered with an angle of 60°. The void volume V^0 is 4.78 ml, as determined from the elution volume for non-retained acetone. Carrier (0.1% aqueous FL-70 from Fisher Scientific) is fed to the system via a peristaltic pump of type Minipuls 3 from Gilson, which is controlled by the computer. The optical density of the effluent is monitored at 254 nm by means of a Linear Model 106 UV detector, the signal of which is fed to the system's IBM-compatible AT personal computer (PC), which stores the output as amplitude/time pairs of data. The effluent is collected in a vented polythylene receptacle which is placed on top of an OHAUS electronic balance Model C501 with an interface port, designed to weigh with an accuracy of 0.1 g in the 0–500 g range. The output port from this balance is connected to the computer's RS-232 port, which stores its signal as weight/time pairs of data. By-pass valve A is likewise connected to the computer. A digital thermometer of type Sigma, Model HH22 is reporting the temperature of the experiment with an accuracy of 0.1°C. The samples used to establish Table I are polystyrene latex standards with a density of 1.057 g/ml, obtained from the BASF Corporation.

The following is an outline of the course of the analysis: The pump is instructed by the computer to deliver carrier at a low rate (0.5 ml/min) in preparation for the injection (commonly 1–25 μl), which is made directly at the head of the channel. In order to ensure that the sample fully enters the separation chamber, the pump is allowed to deliver carrier for an additional 15 s before being turned off. At this point valve A is automatically closed, and the rotor accelerated to a specified spin rate; as this

TABLE I

REPRODUCIBILITY OF PARTICLE SIZE ASSIGNMENTS UNDER DIFFERENT EXPERIMENTAL CONDITIONS

Sample: polystyrene latex spheres with a density of 1.057 g/ml. Carrier: 0.1% (v/v) aqueous FL-70 with a density at 25°C of 0.9973 g/ml. Average flow-rate was 3.10 ml/min.

No.	Diameter (nm)						Average diameter (nm)
	RPM						
	1000	1100	1200	1300	1400	1500	
1	257	248	254	251	253	253	253 ± 3
2	308	300	303	301	301	300	302 ± 3
3	357	349	352	347	344	342	349 ± 5
4	425	421	421	409	—[a]	—[a]	420 ± 5

[a] Data excluded due to the strong wall effects seen at high retention.

rate is reached, the computer starts the count-down towards the end of the relaxation period; 2 min prior to reaching this end, while the channel is still being by-passed, the pump is automatically adjusted and starts delivering carrier at the faster flows desired for elution. This pressurizes all parts of the system with the exception of the channel itself. At the end of the relaxation period the computer opens valve A, now shunting all flow through the channel whose effluent is being collected in the receptacle on the balance. The detector signal, recorded by the computer as a function of effluent weight, is plotted versus the computed elution volume V_e on the computer screen, which also displays the instantaneous rate of flow through the channel. Data analysis is performed at the end of the run. The valve labelled A′ in the figure permits a temporary interruption of the flow-rate measurements to allow the collecting of fractions.

RESULTS AND DISCUSSION

Peristaltic pumps are inexpensive tools for delivering mobile phase to low-pressure chromatographic systems, and their output is, in principle, easily controlled by an external voltage regulator. In practice, however, the output is not fully predictable, but shows fluctuations both of high [3] and low frequency. The high-frequency pulsing is inherent in the operation of these pumps; however, its time constant is such that it has no effect on flow-rates measured during a typical FFF run, which lasts several tens of minutes. By contrast, slow changes over long periods of time, such as those recorded in Fig. 2, tend to introduce errors in retention ratios R based on measured elution times rather than on elution volumes. The figure displays the weight-based flow-rate at time t_n, $V(t_n)$, computed as the arithmetic mean of five consecutive weight/time data pairs:

$$V(t_n) = \frac{1}{5} \sum_{i=n-4}^{n} \frac{(w_i - w_{i-1})}{(t_i - t_{i-1})} \tag{2}$$

Here, w_i is the weight of the collected effluent at time t_i. Whether the variations in flow-rate are undesired, as those displayed in Fig. 2, or intended, as in the case of operation under programmed flow [8], the continuous measurement of effluent weight

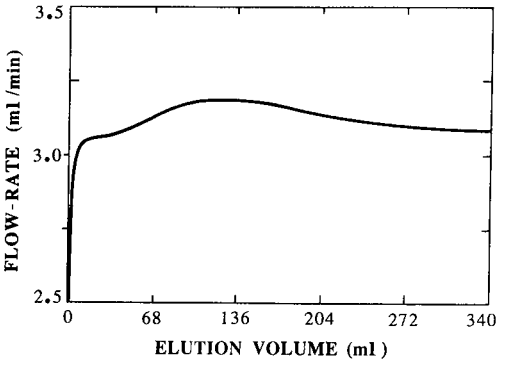

Fig. 2. An illustration of the flow-rate variations observed during a typical 2-h run.

offers clear analytical advantages, due to its direct proportionality to V_e at constant temperature.

Short-term fluctuations in flow-rate have a particularly severe impact on the determination of the small void volumes V^0 (typically less than 5 ml), which relate linearly to the retention ratio R from which particle diameters, d, or molecular weights are determined [4,5]. In the limit of high retention, R becomes a linear function of λ. Under these conditions, the sedimentation FFF technique generates retentions proportional to d^{-3}, while the flow FFF analogue retains particles in proportion to d^{-1}; thus, an error of *e.g.* 20% in V^0 translates into an error of 6% in d for a sedimentation FFF analysis, while diameters determined by flow FFF, with its lowersize selectivity, will have an error similar to that of V^0.

The measurement of effluent weights, in lieu of elution times, immediately highlighted a source of error that had previously been neglected. Traditionally, resumption of carrier flow at the end of the relaxation period is made by letting the start of pumping coincide with the beginning of separation. From the flow-rate–time relationship shown in Fig. 3 it became obvious that a significant number of seconds elapse between the onset of flow and the establishment of a steady-state of carrier delivery. By assuming that the flow had remained constant throughout, at the steady-state level, the observed elution time for the void peak of 1.3 min translated into a value for V^0 of 3.70 ml. This value is 23% below the weight-based value, determined to be 4.78 ml in good agreement with the 4.76 ml known from the channel geometry. In case one determines the void volume from the elution time of a non-retained compound admixed with the sample, as is commonly done, the sedimentation FFF analysis may therefore yield diameters in error of more than 6% as discussed above. It should be noted that, although R is the ratio of two elution volumes which are both affected by the transient behavior at the beginning of separation, the sample elution volumes, which ideally should be in excess of five column volumes [10], are much less in error than is V^0.

The effect illustrated in Fig. 3 led to the installation of by-pass valve A, as described above under Methods. By starting the pump and pressurizing the system before allowing flow into the channel it is now possible to significantly reduce the time required to reach a steady flow, as shown in Fig. 4. The oscillating behavior seen in these graphs is an artifact introduced by the low precision of the balance (0.1 g) in combination with the high sampling frequency, and persists despite use of the five-point smoothing routine described in eqn. 2.

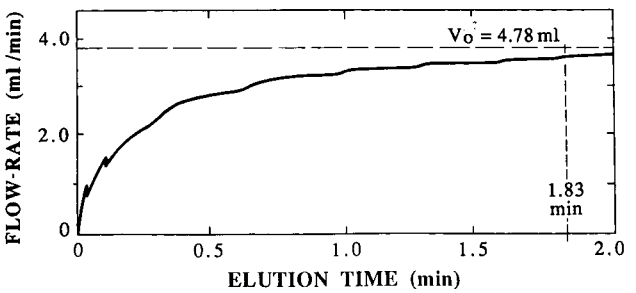

Fig. 3. The time course of effluent weight shows the slow approach to a steady flow during the early stage of a run in the absence of by-pass valve A.

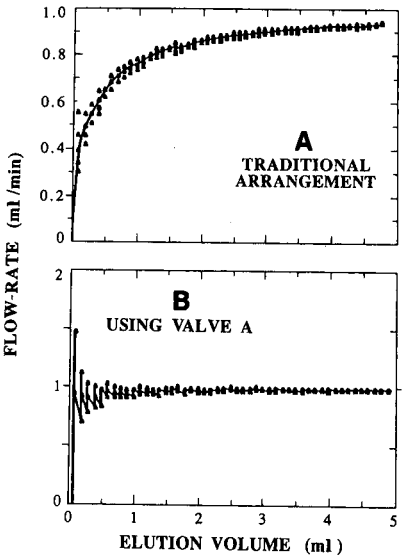

Fig. 4. (A) In the absence of by-pass valve A, the flow is slowly approaching the set level of 1 ml/min. (B) Operation of the by-pass valve as described in the text ensures a rapid establishment of steady flow.

By introducing the operational procedures described above, *i.e.* by weighing the effluent, and pressurizing the system prior to supplying carrier to the separation channel, it is now possible to determine particle diameters under widely varying field strengths, *i.e.* retention times, with a standard deviation of just above 1%, as seen in Table I.

While illustrated by samples from FFF analysis, the use of electronic balances to measure flow-rates is generally applicable to all liquid chromatography techniques, particularly where the system operates under computer control. By incorporating a high-precision balance into the system, one would thus be able to correct such discrepancies as those discussed in ref. 1.

ACKNOWLEDGEMENT

Support via grant No. GM 38008-02 from the National Institutes of Health is gratefully acknowledged.

REFERENCES

1 J. D. Dolan, *LC·GC.*, 8 (1990) 842.
2 K. D. Caldwell and M. N. Myers, *Anal. Chem.*, 58 (1986) 1583.
3 J. D. Dolan, *LC·GC*, 8 (1990) 916.
4 J. C. Giddings, *J. Chem. Ed.*, 50 (1973) 667.
5 J. C. Giddings and K. D. Caldwell, in B. W. Rossiter (Editor), *Physical Methods of Chemistry*, Vol. IIIB, Wiley-Interscience, New York, 1989, p. 867.
6 F. J. Yang, M. N. Myers and J. C. Giddings, *Anal. Chem.*, 49 (1977) 659.
7 M. Martin, M. N. Myers and J. C. Giddings, *J. Liq. Chromatogr.*, 2 (1979) 147.
8 J. C. Giddings, K. D. Caldwell, J. F. Moellmer, T. H. Dickinson, M. N. Myers and M. Martin, *Anal. Chem.*, 51 (1979) 30.
9 J. C. Giddings, M. N. Myers, K. D. Caldwell and S. R. Fisher, in D. Glick (Editor), *Methods of Biochemical Analysis*, Vol. 26, Wiley, New York, 1980, p. 19.
10 M. R. Schure, *Anal. Chem.*, 60 (1988) 1109.

Journal of Chromatography, 555 (1991) 267–271
Elsevier Science Publishers B.V., Amsterdam

CHROM. 23 386

Short Communication

Use of N-acetylpsychosine as internal standard for quantitative high-performance liquid chromatographic analysis of glycosphingolipids

OLIVIERO CECCONI, SALVATORE RUGGIERI and GABRIELE MUGNAI*
Istituto di Patologia Generale, Università degli Studi di Firenze, Viale Morgagni 50, I-50134 Florence (Italy)
(First received January 30th, 1991; revised manuscript received April 15th, 1991)

ABSTRACT

The use of N-acetylpsychosine as an internal standard for the quantitative high-performance liquid chromatography (HPLC) of *p*-nitrobenzoyl derivatives of glycosphingolipids is described. It is suitable because the chromogen reacts on equimolar basis with both N-acetylpsychosine and sample glycosphingolipids. The use of N-acetylpsychosine as an internal standard was validated by determining the glycosphingolipid content of a system of metastatic variants selected from a murine fibrosarcoma line (T3 cells). Reproducible results were obtained throughout several quantitative analyses of cellular glycosphingolipids and it was possible to determine the glycosphingolipid content of as few as $5 \cdot 10^6$ cells.

INTRODUCTION

The use of high-performance liquid chromatography (HPLC) for determination of glycosphingolipids (GSLs) gives a better resolution and recovery than techniques based on column or thin-layer chromatography (TLC). However, the spectrophotometric detection of GSLs eluted from HPLC columns is precluded by the strong UV absorbance of the organic solvents (*e.g.*, chloroform recommended for the separation of GSLs. This difficulty has been only partially overcome by the conversion of GSLs into UV-absorbing derivatives [1–5], owing to the incompleteness of the derivatization reactions. Although this problem could be solved by including an internal standard in the derivatization reaction, there are no reports on the use of an appropriate molecule for the HPLC determination of GSL derivatives.

This paper reports the use of N-acetylpsychosine as an internal standard for the HPLC determination of *p*-nitrobenzoyl derivatives [2,3] of GSLs from a system of metastatic fibrosarcoma cell lines, *viz.*, the T3 cells and T3a1:p clone. GSLs of these cell lines were composed of glucosyl-, lactosyl- and globotriaosylceramides [6]. The use of N-acetylpsychosine was considered particularly advantageous for this purpose

0021-9673/91/$03.50

because the chromogen reacts with both the internal standard and sample GSLs on an equimolar basis as both GSLs and N-acetylpsychosine contain a common reactive group, the amidic linkage. In addition, N-acetylpsychosine exhibits the same physicochemical properties as those of the GSLs under study, and can therefore be added to the sample before starting the reaction.

EXPERIMENTAL

Preparation of N-p-nitrobenzoyl derivatives of N-acetylpsychosine and glycolipid standards

Psychosine was obtained from rat brain galactosylceramide, which was hydrolysed with butanolic 1 *M* potassium hydroxide under reflux for 2.5 h. Psychosine was freed from hydrolysis products by partition in an equal volume of water and then purified by silica gel column chromatography [7]. Psychosine was converted into N-acetylpsychosine by acetylation in pyridine–acetic anhydride (3:2) followed by *O*-deacetylation with sodium methoxide [8]. N-Acetylpsychosine and standards of glucosylceramide (GlcCer), lactosylceramide (LacCer), globotriaosylceramide (Gb3ose) and globoside (Gb4ose) were used to construct calibration graphs of peak area ratio *versus* concentration. GlcCer, LacCer and Gb3ose were prepared from a fibrosarcoma grown in CBA mice and Gb4ose was prepared from human erythrocyte ghosts. Total lipids were extracted according to Folch *et al.* [9] and then submitted to Florisil column chromatography [8] in order to separate GSLs from other lipid classes. GSLs were fractionated by TLC on 0.25-mm silica gel H plates (Merck, Darmstadt, Germany) in chloroform–methanol–water (60:25:4). After detection with primuline spray reagent [10], individual GSLs were identified by the gas chromatographic analysis of their carbohydrate groups [11].

N-Acetylpsychosine and GSL standards were acetylated according to Saito and Hakomori [8] and converted into *p*-nitrobenzoyl derivatives by reaction with *p*-nitrobenzoyl chloride (70 mg/ml) in pyridine at 60°C for 6 h [4]. These derivatives were recovered from the reaction mixture by solvent partitioning followed by solid-phase extraction on Sep-Pak C_{18} cartridges (Waters Assoc., Milford, MA, USA) [5].

HPLC conditions

p-Nitrobenzoyl derivatives were dissolved in 50 μl of carbon tetrachloride and injected into a Perkin-Elmer silica B5 column (25 × 0.46 cm I.D.) mounted in a Perkin-Elmer Series 3B HPLC apparatus equipped with a Model LC75 spectrophotometric detector set at 254 nm. Chromatography was performed at a flow-rate of 1.1 ml/min with a linear gradient from 1% to 5% 2-propanol in hexane–chloroform (2:1) over 26 min, then from 5% to 10% 2-propanol in hexane–chloroform (2:1) over 8 min, and finally with the final solvent mixture for 10 min.

Analysis of glycolipid composition of murine fibrosarcoma cell lines

T3 cells and T3a1:p clone were cultured as described [6]. Cells from subconfluent cultures were harvested by means of a "rubber policeman", washed in phosphate-buffered saline and sonicated. Proteins were assayed by the method of Lowry *et al.* [12]. Lipids were extracted according to Folch *et al.* [9] and the extracts were acetylated together with 5 μg of N-acetylpsychosine and submitted to Florisil column

chromatography [8] in order to separate the GSLs from the other lipid classes. Acetylated GSLs were converted into their *p*-nitrobenzoyl derivatives and analysed as described above.

RESULTS AND DISCUSSION

Fig. 1 shows that the calibration graph for *p*-nitrobenzoyl-N-acetylpsychosine is linear between 0.5 and 55 nmol of the standard. This line differed only by 15% from that obtained after converting weighed amounts of N-acetylpsychosine into its *p*-nitrobenzoyl derivative, indicating an almost quantitative conversion of the standard into its derivative. Quantitative conversion of GlcCer and Gb4ose into *p*-nitrobenzoyl derivatives was also reported by Suzuki *et al.* [3].

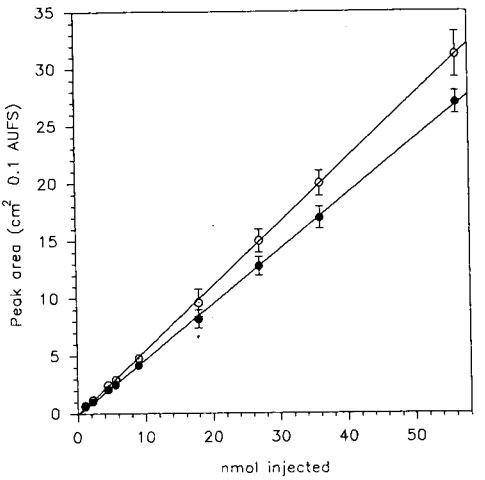

Fig. 1. Recovery of N-acetylpsychosine after conversion into its *p*-nitrobenzoyl derivative. The top line (○) was constructed with the peak areas produced with increasing amounts of *p*-nitrobenzoyl-N-acetylpsychosine. The molar response factor was 0.556 cm^2/nmol (r = 0.999). The bottom line (●) was obtained by converting known amounts of N-acetylpsychosine into its *p*-nitrobenzoyl derivative, then measuring the resultant peak areas after HPLC. The molar response factor was 0.479 cm^2/nmol (r = 0.998). For both lines, the experimental points represent the mean ± S.D. of eight determinations. Peak areas are expressed as cm^2 at 0.1 a.u.f.s. (25 cm) and at a chart speed of 0.5 cm/min.

As shown in Fig. 2, the determination of known amounts of GlcCer, LacCer and Gb3ose standards together with N-acetylpsychosine (54 nmol) gave similar peak-area ratio calibration graphs, indicating that, under the experimental condition used, there was no difference in the recoveries of all three of the GSLs. A value close to unity for the slopes of these curves demonstrates that the recovery of the GSL standards is identical with that of N-acetylpsychosine. The slope for Gb4ose was twice those for GlcCer, LacCer and Gb3ose, which is accounted for by the two groups present in Gb4ose, *i.e.*, the amidic bond of the ceramide and the acetamidic bond of the terminal N-acetylgalactosamine, which can react with the chromogen.

The use of N-acetylpsychosine as an internal standard in the HPLC of GSLs was validated by determining the GSL content of two fibrosarcoma cell lines grown in

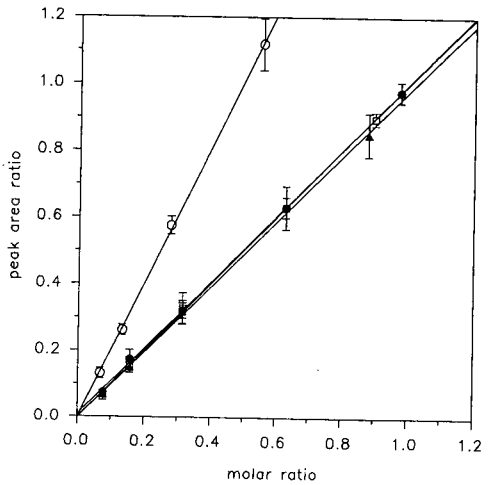

Fig. 2. Peak-area ratio calibrations for GlcCer, LacCer, Gb3ose and Gb4ose with N-acetylpsychosine as internal standard. Known amounts of an equimolar mixture of glycolipid were derivatized in the presence of 54 nmol of N-acetylpsychosine and determined. The lines were obtained by plotting the peak-area ratio *versus* the molar ratio between each glycolipid standard and N-acetylpsychosine. Slopes of the lines: (●) GlcCer = 0.993; (□) LacCer = 1.003; (▲) Gb3ose = 0.981; (○) Gb4ose = 2.023. For lines, the experimental points represent the mean ± S.D. of eight determinations.

tissue culture: T3 cells and T3a1:p clone. Gb3ose was the prevalent GSL in T3 cells (10.6 nmol/mg protein), followed by LacCer (2.5 nmol/mg protein), while the major GSL component of T3a1:p clone was LacCer (13.9 nmol/mg proteins) (Table I). Fairly reproducible results were obtained throughout several quantitative HPLC analyses of cellular GSLs, and it was possible to determine the GSL content of as few as $5 \cdot 10^6$ cells, *i.e.*, 0.5 nmol in the case of the least represented GSLs, *i.e.*, GlcCer.

TABLE I

GLYCOSPHINGOLIPID CONTENT OF T3 CELLS AND T3a1:p CLONE AS DETERMINED BY HPLC WITH N-ACETYLPSYCHOSINE AS INTERNAL STANDARD

Cell line	Glycosphingolipid[a]		
	GlcCer	LacCer	Gb3ose
T3	1.2 ± 0.3	2.5 ± 0.4	10.6 ± 1.4
T3a1:p	1.3 ± 0.3	13.9 ± 0.6	3.1 ± 0.4

[a] Values, reported as nmol/mg proteins, are the means ± S.D. of nine determinations. The protein content per 10^6 cells averaged 130 and 110 μg in T3 cells and T3a1:p clone, respectively.

ACKNOWLEDGEMENTS

This study was supported by grants from the Consiglio Nazionale delle Ricerche (Special Project: Oncologia), from the Associazione Italiana per la Ricerca sul Cancro and from the Ministero della Pubblica Istruzione (40 and 60%). The authors thank Dr. A. Fonnesu, Chairman of the Institute of General Pathology, University of Florence, for his interest in this research.

REFERENCES

1 M. D. Ullmann and R. H. McCluer, *J. Lipid Res.*, 18 (1977) 371.
2 T. Yamazaki, A. Suzuki, S. Handa and T. Yamakawa, *J. Biochem.*, 86 (1979) 803.
3 A. Suzuki, S. K. Kumar and D. M. Marcus, *J. Lipid Res.*, 21 (1980) 473.
4 H. Nakabayashi, M. Iwamori and Y. Nagai, *J. Biochem.*, 96 (1984) 977.
5 K. Miyazaki, N. Okamura, Y. Kishimoto and Y. C. Lee, *Biochem. J.*, 235 (1986) 755.
6 G. Mannori, O. Cecconi, G. Mugnai and S. Ruggieri, *Int. J. Cancer*, 45 (1990) 984.
7 T. Taketomi and T. Yamakawa, *J. Biochem.*, 54 (1963) 444.
8 T. Saito and S. Hakomori, *J. Lipid Res.*, 12 (1971) 257.
9 J. Folch, M. Lees and J. M. Sloane-Stanley, *J. Biol. Chem.*, 226 (1957) 497.
10 V. P. Skipski, *Methods Enzymol.*, 35 (1975) 396.
11 G. Mugnai, R. Coppini, D. Tombaccini, A. Fallani and S. Ruggieri, *Biochem. J.*, 193 (1981) 1025.
12 O. H. Lowry, N. J. Rosebrough, A. L. Farr and J. R. Randall, *J. Biol. Chem.*, 193 (1951) 265.

Journal of Chromatography, 555 (1991) 272–277
Elsevier Science Publishers B.V., Amsterdam

CHROM. 23 383

Short Communication

Application of ligand-exchange chromatography to the assay of L-alanine from DL-aspartic acid by *Pseudomonas dacunhae*

CHEANYEH CHENG* and LI-HUEI HUANG
Department of Chemistry, Chung Yuan Christian University, Chung-Li 32023 (Taiwan)
(First received November 15th, 1990; revised manuscript received March 19th, 1991)

ABSTRACT

A direct chiral ligand-exchange chromatographic method was developed to monitor L-alanine production by fermentation. A mobile phase containing aqueous 0.25 m*M* Zn^{2+} solution is utilized to separate amino acids in the fermentation medium. The detection limit for L-alanine is 0.5 ppm and the analysis time for one sample is about 8 min. As sample preparation is simple and the matrix effects are minimal, the assay is fast and convenient. The results indicate that the method has potential for the analysis of complicated fermentation media.

INTRODUCTION

Although the amino acid analyser is routinely used for the determination of amino acids in various biological fluids, ligand-exchange chromatographic methods, pioneered by Davankov and co-workers [1,2], have been developed for analysing amino acid enantiomers with a chiral stationary phase [3,4] and the high selectivity and specificity of ligand-exchange chromatography has led to many applications. Recently, the resolution of DL-amino acids on MCI GEL CRS10W and CRS10WD columns based on the ligand-exchange reactions between the copper complex of an optically active ligand adsorbed on the column matrix and the amino acid to be separated has been reported [5]. The enantiomers of amino acids were determined with the aid of ligand-exchange chromatography in chiral complex-containing mobile phases by Duchateau *et al.* [6]. Fukuhara and Yuasa [7] demonstrated that fourteen DL-amino acids can be resolved by using a chiral cyanocobalamin-coated ligand-exchange column with a mobile phase containing copper complexes of ADP, NAD or FAD as a chiral additive [8]. Racemic α-alkyl-α-amino acids can be analysed by ligand-exchange chromatography with L-3-carboxy-1,2,3,4-tetrahydroquinoline as the bonded chiral selector [9]. Moreover, even α-CF_3AA enantiomers can be separat-

0021-9673/91/$03.50

ed on L-proline and L-hydroxyproline sorbents with Cu^{2+} ions in the aqueous mobile phase [10]. However, the application of ligand-exchange chromatography to the analysis of fermentation media containing amino acids has received little attention.

In our laboratory, the direct ligand-exchange separation of α-amino acid enantiomers without any derivatization has been found useful for monitoring the amino acid fermentation system [11]. The developed method used a commercially available column with silica gel modified with a chiral aliphatic amino acid–Cu^{2+} complex as the stationary phase and an achiral aqueous solution containing Zn^{2+} ion as the mobile phase. The separation of L-alanine from other amino acids in a complicated fermentation medium can thus characterize the applicability of ligand-exchange chromatography.

EXPERIMENTAL

Materials

DL-Aspartic acid, D-aspartic acid, L-aspartic acid and L-alanine were purchased from Sigma (St. Louis, MO, USA). $ZnSO_4 \cdot 7H_2O$, $MgSO_4 \cdot 7H_2O$, KH_2PO_4, K_2HPO_4, extract of dried meat and sodium L-glutamate were obtained from Merck (Darmstadt, Germany). The high-performance liquid chromatographic (HPLC) column (25 cm × 4.6 mm I.D.) was packed with a chemically bonded aliphatic amino acid–Cu^{2+} complex on silica gel (5 μm) (Tosoh, Tokyo, Japan). Water was deionized and filtered before use.

Instrumentation

The HPLC system consisted of a Shimadzu (Kyoto, Japan) LC-9A dual-piston solvent-delivery module with a high-sensitivity filter unit, a Rheodyne (Cotati, CA, USA) Model 7125 injection valve with a 20-μl sampling loop, a Shimadzu Chromatopac CR-6A data processor and a Shimadzu Model SPD-6A variable-wavelength UV detector. The detection wavelength was at 254 nm and the column operating temperature was at 26°C. The isocratic elution rate of the mobile phase was at 1.0 ml/min.

Fermentation

Pseudomonas dacunhae (CCRC 12623; Hsinchu, Taiwan) was incubated with the following growth medium [11]: 8 g of sodium L-glutamate, 1.25 g of extract of dried meat, 0.125 g of KH_2PO_4, 0.81 g of K_2HPO_4 and 0.025 g of $MgSO_4 \cdot 7H_2O$ in 250 ml of water. The bacteria were grown in this medium for 4 days, then about 50 ml of the medium were transferred into 100 ml of fermentation medium, consisting of 0.125 g of KH_2PO_4, 0.81 g of K_2HPO_4, 0.025 g of $MgSO_4 \cdot 7H_2O$ and 2.5 g of DL-aspartic acid per 250 ml of water. The inoculated fermentation medium was incubated in an orbital incubator–shaker (Model 702, Hotech, Taipei, Taiwan) for 7 days at 30°C with a shaker speed 120 rpm. No foaming was observed during fermentation.

Sample preparation

Stock standard amino acid solutions were prepared by measuring suitable amounts of analytical-reagent grade amino acids and dissolving them in water, and successive dilutions were utilized to obtain lower concentrations. Mild heating was

needed to dissolve both D- and L-aspartic acid. A 0.20-μm microporous membrane filter (Gelman Science, Ann Arbor, MI, USA) was used to filter off the bacterial cells from the fermentation medium. The filtered medium was diluted with water to a concentration range suitable for analysis.

RESULTS AND DISCUSSION

Qualitative separation

L-Alanine produced in the fermentation medium can be separated from DL-aspartic acid by using aqueous eluents containing Zn^{2+} ion or Cu^{2+} ion or their mixture. As the formation constant of $Cu(NH_3)_4^{2+}$ is larger than that of $Zn(NH_3)_4^{2+}$, the free amino acid–Zn^{2+} complexes should be less stable than the free amino acid–Cu^{2+} complexes. Cu^{2+} (with a d^9 electron configuration) uses a dsp^2 hybrid orbital to form stable square-planar complexes with amino acids, whereas Zn^{2+} (with a d^{10} electron configuration) usually forms tetrahedral complexes via an sp^3 hybrid orbital. Therefore, the separation of amino acids by different metal ions is mainly based on the different stability of the complexes formed. The structure of the amino acid is a determining factor in the separation.

Fig. 1 shows that the best resolution between L-alanine and DL-aspartic acid is represented by chromatogram A, obtained by elution with an aqueous mobile containing 0.25 m*M* Zn^{2+}. Also, only the aqueous mobile phase containing Zn^{2+} can resolve the L-glutamic acid and DL-aspartic acid. The separation of L-glutamic acid and DL-aspartic acid is not successful with the aqueous mobile phase containing Cu^{2+}.

The experiment was repeated many times with an aqueous mobile phase con-

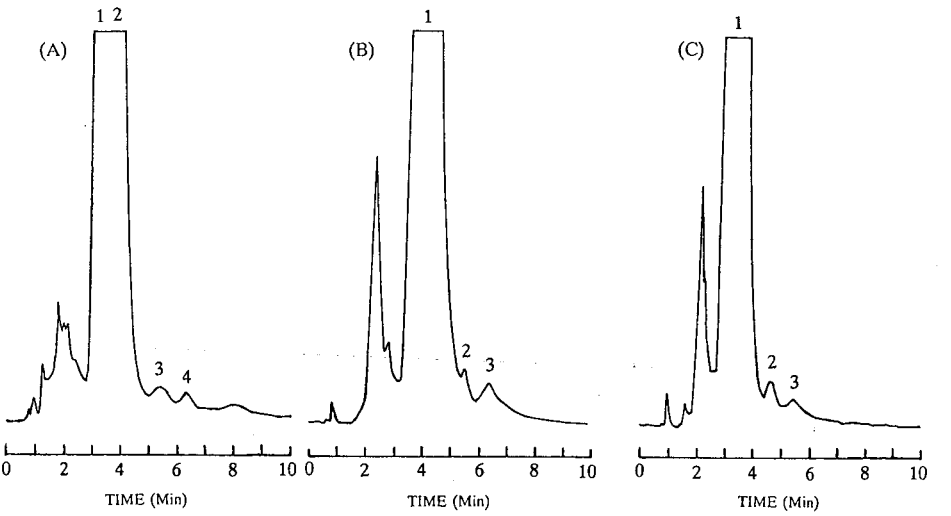

Fig. 1. Effect of mobile phase on the separation of the 10-fold diluted fermentation medium. (A) Mobile phase: 0.25 m*M* Zn^{2+}; peaks: 1 = L-glutamic acid; 2 = DL-aspartic acid; 3 = L-alanine; 4 = unknown. (B) Mobile phase: 0.125 m*M* Cu^{2+}; peaks: 1 = L-glutamic acid and DL-aspartic acid; 2 = L-alanine; 3 = unknown. (C) Mobile phase: 0.125 m*M* Cu^{2+}–0.25 m*M* Zn^{2+} (45:55); peaks: 1 = L-glutamic acid and DL-aspartic acid; 2 = L-alanine; 3 = unknown.

taining Zn^{2+} and demonstrated good detection sensitivity at UV wavelength of 254 nm and good stability of the column. There is no problem with replacement of Cu^{2+} ions bonded on the silica gel surface by a Cu–Zn exchange equilibrium. Thus, the eluent selected at present stage is 0.25 m*M* aqueous Zn^{2+} solution [12]. Verification of peaks was achieved by adding standard amino acid solutions to the medium. A very small peak is produced by the medium that cannot be identified.

After fermentation the pH of the fermentation medium was 8.42 and with 100-fold dilution it was 8.38. DL-Aspartic acid enantiomers in the medium cannot be resolved under basic conditions, as shown in Figs. 1 and 2A. The fermentation medi-

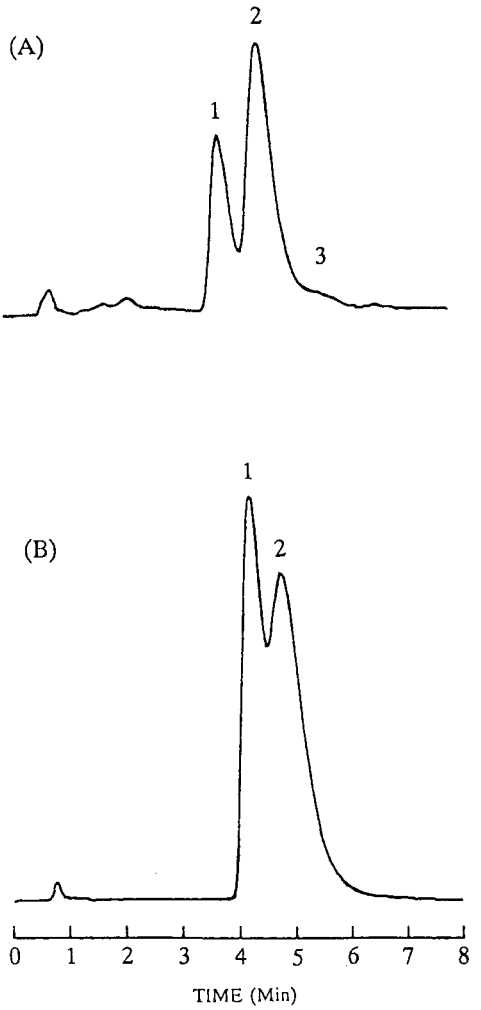

Fig. 2. Effect of pH on the separation of DL-aspartic acid with 0.25 m*M* Zn^{2+} aqueous solution as mobile phase. (A) Medium: sodium L-glutamate, DL-aspartic acid, extract of dried meat, KH_2PO_4, K_2HPO_4, $MgSO_4 \cdot 7H_2O$; 100-fold dilution; pH 8.38; peaks: 1 = L-glutamic acid; 2 = DL-aspartic acid; 3 = L-alanine. (B) Medium: DL-aspartic acid, KH_2PO_4, K_2HPO_4, $MgSO_4 \cdot 7H_2O$; 100-fold dilution; pH 3.74; peaks: 1 = D-aspartic acid; 2 = L-aspartic acid.

um without DL-aspartic acid and without a fermentation process occurring had a pH of 7.11. The pH of the medium containing DL-aspartic acid, $MgSO_4 \cdot 7H_2O$ and KH_2PO_4–K_2HPO_4 buffer measured before fermentation was 3.37. After 100-fold dilution, the former medium had a pH 3.74, as shown in Fig. 2B. DL-Aspartic acid enantiomers can be separated slightly under acidic conditions with 0.25 m*M* Zn^{2+} aqueous mobile phase. We also found that DL-aspartic acid enantiomers dissolved in water alone were better separated under the same chromatographic conditions [12]. Therefore, the simultaneous determination of D-aspartic acid, L-aspartic acid and L-alanine is possible under acidic conditions. However, substances present in or the ionic strength of the fermentation medium may have crucial effects on the separation of L-alanine and DL-aspartic acid enantiomers. We do not intend to consider the detailed separation mechanism of DL-amino acid enantiomers here, but we believe that molecular distortion of amino acids toward different irregular tetrahedral structures may play an important role in their separation.

Quantitation

The amount of L-alanine produced by fermentation was determined by using external calibration. Experimental data for D-aspartic acid, L-aspartic acid and L-alanine were fitted to the linear relationship $y = ax + b$ by non-linear regression (NLR) analysis. The regression procedure is based on the Marquart algorithm which utilizes an interpolation technique to combine the Gauss–Newton and steepest descent search method [13]. The slope of the calibration graph for L-alanine was 3423.0 ± 87.74 and the intercept was −4407.2 ± 1971 at the 95% confidence level. The precision for L-alanine determination was usually about 2 within the concentration range 50–5 ppm. The amount of L-alanine produced by the fermentation was about 104.2 ppm. The accuracy of this value is slightly affected by tailing, as shown in Fig. 1, and a correction should be made by analysing standard material. However, here we only want to know whether the developed ligand-exchange chromatographic procedure is adequate for monitoring an amino acid fermentation system or not. The yield of L-alanine in the medium is low, indicating a low activity of the enzyme L-aspartate β-decarboxylase. Shibatani *et al.* [14] reported that the optimum pH for L-aspartate β-decarboxylase was 5.3 and the maximum decarboxylation temperature was 47°C. Utilizing the whole cell of *Pseudomonas dacunhae* for fermentation, we prefer to keep the pH at 6.2 and maintain a temperature at 37°C [10,11]. Nevertheless, the detection limit for L-alanine is 0.5 ppm with a recorder attenuation of 2^5. The results indicate that ligand-exchange chromatography is applicable to the trace determination of L-alanine. The determination of L-glutamic acid in the fermentation medium is also possible.

CONCLUSIONS

The time required for the determination of L-alanine produced by DL-aspartic acid fermentation is about 8 min. The background medium shows no interference with the determination L-alanine and has a minimum effect in analysis with of the fermentation medium dilution. As no derivatization of the amino acids is necessary for detection, sample preparation is simple. Thus, the direct separation of amino acids by using an achiral aqueous mobile phase containing only Zn^{2+} makes the

proposed ligand-exchange chromatographic method fast and convenient. The procedure needs to be improved but it has potential for monitoring amino acid production systems.

ACKNOWLEDGEMENTS

The authors gratefully acknowledge the National Science Council of Taiwan for supporting this study. Dr. Andrew Yeh's laboratory is thanked for providing purified water.

REFERENCES

1 V. A. Davankov and S. V. Rogozhin, *J. Chromatogr.*, 60 (1971) 280.
2 V. A. Davankov, S. V. Rogozhin, A. V. Semechkin and T. P. Sachkova, *J. Chromatogr.*, 82 (1973) 359.
3 R. W. Souter, *Chromatographic Separations of Stereoisomers*, CRC Press, Boca Raton, FL, 1985, Ch. 3, p. 152.
4 V. A. Davankov, *Pure Appl. Chem.*, 54 (1982) 2159.
5 H. Katoh, T. Ishida, Y. Boba and H. Kiniwa, *J. Chromatogr.*, 473 (1989) 241.
6 A. Duchateau, M. Crombach, M. Aussems and J. Bongers, *J. Chromatogr.*, 461 (1989) 419.
7 T. Fukuhara and S. Yuasa, *J. Chromatogr. Sci.*, 28 (1990) 114.
8 G. Jeanneret-Gris, J. Porret and K. Bernauer, *Chromatographia*, 29 (1990) 449.
9 S. V. Galushko, I. P. Shishkina, V. A. Soloshonok and V. P. Kukhar, *J. Chromatogr.*, 511 (1990) 115.
10 M. Senuma, O. Otsuki, N. Sakata, M. Furui and T. Tosa, *J. Ferment. Bioeng.*, 67 (1989) 233.
11 K. Yamamoto, T. Tosa and I. Chibata, *Biotechnol. Bioeng.*, 22 (1980) 2045.
12 C. Cheng, *Technical Report*, NSC79-0208-M033-23, National Science Council, Taipei, 1990.
13 A. Constantinides, *Applied Numerical Methods with Personal Computers*, McGraw-Hill, New York, 1987.
14 T. Shibatani, T. Kakimoto, J. Kato, N. Nishimura and I. Chibata, *J. Ferment. Technol.*, 52 (1974) 886.

Journal of Chromatography, 555 (1991) 278–284
Elsevier Science Publishers B.V., Amsterdam

CHROM. 23 452

Short Communication

Utility of dansyl derivatization to the high-performance liquid chromatographic analysis of 2-phenylethylamine drugs

ROBERT W. ROOS*
New York Regional Laboratory, Food and Drug Administration, 850 Third Avenue, Brooklyn, NY 11232 (USA)
and
CESAR A. LAU-CAM
St. John's University, College of Pharmacy and Allied Health Professions, Jamaica, NY 11439 (USA)
(First received July 6th, 1990; revised manuscript received May 13th, 1991)

ABSTRACT

This paper describes the utility of dansyl derivatization in the high-performance liquid chromatographic separation of a number of 2-phenylethylamines of pharmaceutical interest. The derivatives were formed in an alkaline acetone–aqueous sodium carbonate solution, and injected into the chromatograph without the need for their extraction from the reaction mixture. Separations were accomplished on an octadecylsilane column using methanol–water–acetic acid–triethylamine mobile phases and photometric detection at 249 or 335 nm. Comparison of the retention data for the non-dansylated and dansylated 2-phenylethylamines indicated the achievement of favorable alterations in the elution orders. The applicability of dansyl derivatization to the detection of an impurity was demonstrated with a sample of epinephrine containing norepinephrine at the 2% level.

INTRODUCTION

The 2-phenylethylamines are a group of drugs of pharmaceutical and pharmacological interest because of their widespread occurrence in commercial dosage forms and the diversity of their biological actions [1]. These compounds are primary or secondary amines of low molecular weight, often also containing one or more phenolic groups [2]. Owing to the close similarities of their structural features, the chromatographic resolutions of mixtures of 2-phenylethylamines is sometimes challenging, particularly when dealing with diastereomeric pairs such as ephedrine and pseudoephedrine [3,4].

Our laboratory is investigating the use of 5-dimethylaminonaphthalene-1-sulfonyl (dansyl) chloride as a derivatizing reagent for the high-performance liquid chromatographic (HPLC) analysis of drugs of pharmaceutical importance. In addition to

0021-9673/91/$03.50

imparting strong ultraviolet and fluorescent properties, the introduction of a dansyl moiety into the structure of an organic analyte will result in a derivative of higher molecular weight and lower polarity, effects which are all desirable in chromatographic separations [5,6]. Hence, it is not surprising to find that this reagent has been extensively used for the identification, detection and separation of a wide variety of drugs by thin-layer chromatography (TLC) [7–10] and HPLC [11–15]. However, HPLC methods for the analysis of those 2-phenylethylamines that are present in pharmaceutical dosage forms, and which make use of a dansylation step, appear to be limited to only a few compounds [16–19].

The purpose of this communication is to describe the general utility of dansyl derivatization for the HPLC separation of eighteen phenolic and non-phenolic 2-phenylethylamine drugs found in pharmaceutical samples and of which all but two, methamphetamine and norpseudoephedrine, are listed in the United States Pharmacopeia [20]. Furthermore, the applicability of this approach to the simultaneous detection of these compounds when they occur in mixtures in which one of the 2-phenylethylamine derivatives is present in much smaller concentrations than another one is also demonstrated.

EXPERIMENTAL

Apparatus and experimental conditions

The liquid chromatograph consisted of a Spectra-Physics (Santa Clara, CA, USA) Model 3500B solvent delivery system and a Model 770 variable-wavelength detector. Samples were injected through a Valco (Houston, TX, USA) injector valve fitted with a 10-μl sample loop. Elutions were monitored at 254 or 335 nm. Chromatograms were recorded with a Hewlett-Packard (Avondale, PA, USA) Model 3380A recording integrator. The chromatographic column was a Waters Assoc. (Milford, MA, USA) 10-μm μBondapak C_{18}, 300 × 3.9 mm I.D., protected by a Whatmann (Clifton, NJ, USA) 30–40-μm Co:Pell C_{18}, 70 × 2.1 mm I.D. guard column. The mobile phases were combinations of HPLC-grade methanol, reagent-grade acetic acid and triethylamine (TEA) (J. T. Baker, Phillipsburg, PA, USA) and water that had been doubly distilled in glass. All analyses were performed at ambient temperature, and with the mobile phases delivered at the flow-rate of 1.5 ml/min.

Chemicals

2-Phenylethylamines used were laboratory working standard samples of levonordefrin, hydroxyamphetamine hydrobromide, the sulfate salts of amphetamine and mephentermine, the bitartrate salts of epinephrine, metaraminol and norpinephrine, and the hydrochloride salts of dopamine, ephedrine, ethylnorepinephrine, methamphetamine, methoxamine, norephedrine (phenylpropanolamine), norpseudoephedrine, phenoxyphenamine, phentermine, phenylephrine and pseudoephedrine. Standard solutions of 2-phenylethylamines (1 mg/ml) were prepared by dissolving the individual compounds in methanol–water–acetic acid–TEA (50:38:1.5:0.5). Reagents for derivatization reactions were analytical-grade dansyl chloride (Aldrich, Milwaukee, WI, USA) and certified anhydrous sodium carbonate and spectroanalyzed acetone (Fisher Scientific, Fair Lawn, NJ, USA).

Reagents

The dansyl chloride solution was prepared in acetone to contain 5 mg/ml. After filtering, this solution was stored in an amber glass container. The basic solution was prepared by dissolving 0.367 g of sodium carbonate in 300 ml of water, adding 150 ml of acetone, and mixing.

Dansylation procedure

To the 2-phenylethylamine compound (*ca.* 5 mg), contained in a 50-ml glass-stoppered erlenmeyer flask, 10 ml of dansyl chloride solution and 15 ml of basic solution were added in succession. After dissolving the sample with swirling, the flask was stoppered and allowed to stand in the dark and at room temperature for at least 2 h. The solution was then injected into the chromatograph.

RESULTS AND DISCUSSION

The dansylation procedure described in the present study is based on the experimental conditions used by Fishman [21] for the dansylation of the phenolic groups of estrogen compounds. Such experimental conditions are especially advantageous for the derivatization of the *o*-diphenolic functionalities of 2-phenylethylamine compounds like the catecholamines because, once dansyl moieties become attached to these positions, the possibility of their fast base-catalyzed oxidative degradation to non-reactive quinone artifacts is precluded [22]. However, since the dansylation of the amino group of 2-phenylethylamines by this procedure has not been previously described, we conducted first a reaction-rate study using model compounds. Based on the temporal changes in detector responses at 335 nm, the non-phenolic 2-phenylethylamines, phenylpropanolamine and pseudoephedrine, were dansylated more slowly than phenolic estrogens. Moreover, the reaction rates for both compounds became maximal in about 2 h and remained fairly constant thereafter. Similar results were obtained with those 2-phenylethylamines capable of forming di- and tridansylated derivatives.

Table I lists the capacity ratio, k', values of the non-dansylated and dansylated forms of the 2-phenylethylamines studied. As expected, the data show that the dansyl derivatives are more strongly retained than the corresponding non-dansylated parent compounds, a situation that made necessary the use of a higher concentration (65 *vs.* 5%) of methanol in the mobile phase to bring about their elution. Furthermore, dansylation altered the order of elution of several groups of 2-phenylethylamines. For instance, whereas the non-dansylated compounds were retained in the increasing order non-phenolic > monophenolic > diphenolic, dansylation caused the order of retention to change to that of diphenolic > monophenolic > non-phenolic. The same effect was noted with the diastereomeric pair phenylpropanolamine–norpseudoephedrine. In addition, the dansyl derivative of methoxamine was eluted ahead of the dansyl derivatives of non-phenolic 2-phenylethylamines even though they were similarly retained when in the non-dansylated state. This change in elution behavior is probably related to structural differences among these compounds since methoxamine in the only one possessing an alkoxy group.

Fig. 1. shows the HPLC separation of a mixture of several non-phenolic 2-phenylethylamines known to undergo dansylation only at a primary or secondary

TABLE I

COMPARISON OF k' VALUES OF 2-PHENYLETHYLAMINES AND THEIR CORRESPONDING DANSYL DERIVATIVES

$k' = (t_R/t_0) - 1$, where t_R = retention time and dead time t_0 = 2.0 min. Mobile phases: methanol–water–acetic acid–TEA (non-dansylated = 5:93:1.5:0.5; dansylated = 65:33:1.5:0.5).

Compounds	k'	
	Non-dansylated (254 nm)	Dansylated (335 nm)
Diphenolic		
Norepinephrine	0.2	23.0
Levonordefrin	0.2	27.4
Ethylnorepinephrine	0.2	31.0
Epinephrine	0.3	39.1
Dopamine	0.3	45.7
Monophenolic		
Metaraminol	0.6	8.6
Phenylephrine	0.6	10.7
Hydroxyamphetamine	1.1	15.1
Non-phenolic		
Phenylpropanolamine	1.6	1.8
Norpseudoephedrine	2.0	1.7
Ephedrine	2.3	2.5
Pseudoephedrine	2.9	3.0
Methoxamine	3.3	1.6
Amphetamine	3.7	3.7
Methamphetamine	5.0	5.5
Phentermine	7.6	6.1
Methoxyphenamine	8.7	6.6
Mephentermine	9.8	7.6

amino group. Relative to their non-dansylated forms, dansylation generally led to improved peak symmetry and, as in the case of the diastereomeric pair ephedrine and pseudoephedrine, also to improved resolution (R_s = 2.67 *vs.* 2.00) in spite of the closeness of their relative retention values (α = 1.25 for the dansylated form; α = 1.23 for the non-dansylated form). However, in the case of the related compounds amphetamine and methamphetamine it was surprising to find that both resolution (R_s = 7.03 *vs.* 3.70) and relative retention (α = 1.70 *vs.* 1.38) were improved since these compounds differ from each other by only one N-methyl group. A similar trend was noted with the pair phentermine–mephentermine, for which the difference is just one methyl group.

Fig. 2 shows the separation of the dansyl derivatives of representative 2-phenylethylamines capable of adding from one to three dansyl groups to their structures. As expected, the order of elution was found to be directly related to the number of dansyl groups added, with the monodansylated derivatives eluting the earliest and the tridansylated derivatives eluting the latest. As with the mixture of dansyl derivatives

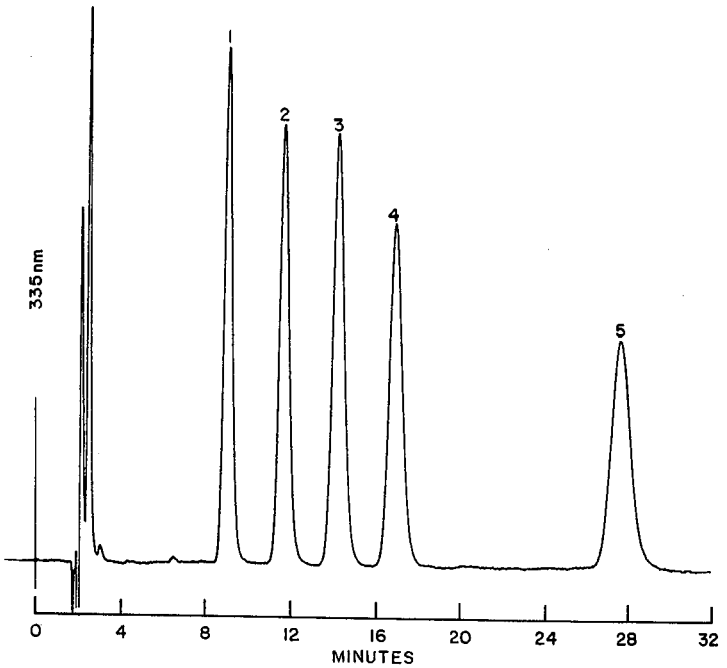

Fig. 1. Chromatographic separation of the monodansyl derivatives of: 1 = phenylpropanolamine; 2 = ephedrine; 3 = pseudoephedrine; 4 = amphetamine; 5 = methamphetamine. Mobile phase: methanol–water–acetic acid–TEA (60:38:1.5:0.5).

shown in Fig. 1, the separation was only achievable when the concentration of methanol in the mobile phase was raised even further, namely to 70%. An interesting finding was the order of elution of the pair materaminol–phenylephrine, two monophenolic compounds differing only in the position of the methyl group in the alkyl side chain, and whose mixture was not resolvable when in the underivatized form. After dansylation, metaraminol, a primary amine, eluted ahead of phenylephrine, an N-methylated secondary amine.

To test the applicability of the dansylation reaction to the simultaneous analysis of a mixture of two or more 2-phenylethylamines, and in which one of the components is present in much smaller concentrations relative to another, a sample of epinephrine found to contain less than 4% of norepinephrine by the compendial TLC procedure [20], was analyzed by the HPLC method with dansylation. By comparison with the results obtained with a solution of pure epinephrine that had been spiked with different concentrations of norepinephrine, and on the basis of the ratio of the norepinephrine peak area to the sum of the norepinephrine plus epinephrine peak areas, the suspected epinephrine sample was found to contain about 2% norepinephrine (duplicate analyses). Hence, the proposed dansylation procedure may also prove valuable in the HPLC detection and quantitation of very low levels of 2-phenylethylamine compounds that may be present as contaminants of other 2-phenylethylamines.

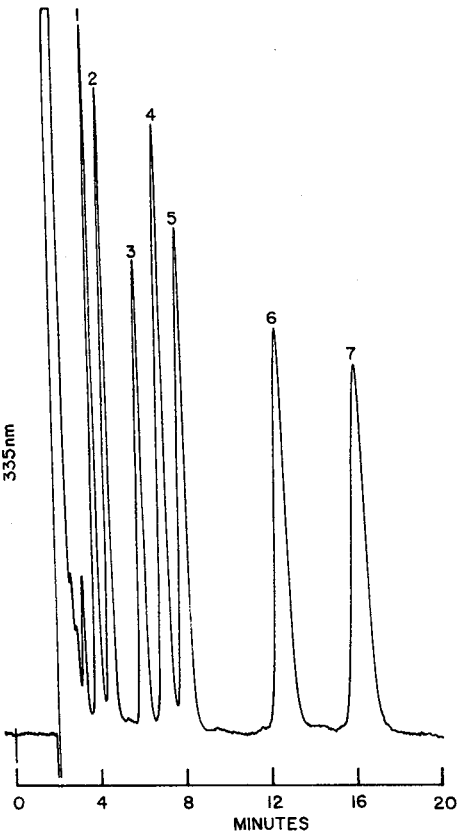

Fig. 2. Chromatographic separation of the mono-, di- and tridansylderivatives of: 1 = phenylpropanolamine; 2 = ephedrine; 3 = metaraminol; 4 = phenylephrine; 5 = hydroxyamphetamine; 6 = norepinephrine; 7 = epinephrine. Mobile phase: methanol–water–acetic acid–TEA (70:28:1.5:0.5).

In summary, dansylation is a simple and effective means of improving the detectability and resolution of 2-phenylethylamines of pharmaceutical interest during their HPLC analysis. In addition, comparison of the retention times of the dansylated and non-dansylated forms of a given 2-phenylethylamine may provide the analyst with additional confirmatory evidence on the identity of these compounds.

REFERENCES

1 N. Weiner, in A. Goodman Gilman, L. S. Goodman, T. Rall and F. Murad (Editors), *Goodman and Gilman's The Pharmacological Basis of Therapeutics*, Macmillan, New York, 7th ed., Ch. 8.
2 R. Gill, S. P. Alexander and A. C. Moffat, *J. Chromatogr.*, 218 (1981) 639–646.
3 S. Barkan, J. D. Weber and E. Smith, *J. Chromatogr.*, 219 (1981) 81–88.
4 G. K. C. Low, P. R. Haddad and A. M. Duffield, *J. Liq. Chromatogr.*, 6 (1983) 311–323.
5 N. Seiler and L. Demisch, in K. Blau and G. S. King (Editors), *Handbook of Derivatives for Chromatography*, Heyden, Philadelphia, PA, 1979, Ch. 9.
6 L. A. Sternson, in R. W. Frei and J. F. Lawrence (Editors), *Chemical Derivatization in Analytical Chemistry*, Vol. 1, Plenum, New York, 1981, Ch. 3.

7 N. Seiler and M. Wiechmann, in A. Niederwieser and G. Pataki (Editors), *Progress in Thin-Layer Chromatograpy and Related Methods*, Vol. 1, Ann Arbor–Humphrey Sciences Publishers, Ann Arbor, MI, 1970, Ch. 4.
8 L. Penzes and G. W. Oertel, *J. Chromatogr.*, 51 (1970) 325–327.
9 N. Seiler, *J. Chromatogr.*, 63 (1971) 97–112.
10 H. H. Loh, I. K. Ho, W. R. Lipscomb. T. M. Cho and C. Selewski, *J. Chromatogr.*, 68 (1972) 289–293.
11 R. Bongiovanni, K. D. Burman, R. K. Garis and T. Boehm, *J. Liq. Chromatogr.*, 4 (1981) 813–824.
12 W. Dünges, G. Naundorf and N. Seiler, *J. Chromatogr. Sci.*, 12 (1974) 655–660.
13 P. J. Meffin, S. Harapat and D. C. Harrison, *J. Pharm. Sci.*, 66 (1977) 583–586.
14 J. P. Sommadossi, M. Lemar, J. Necciari, Y. Sumirtapura, J. P. Cano and J. Gaillot. *J. Chromatogr.*, 228 (1982) 205–213.
15 L. L. Needham and M. M. Kochhar, *J. Chromatogr.*, 114 (1975) 220–222.
16 R. W. Frei, W. Santi and M. Thomas, *J. Chromatogr.*, 116 (1976) 365–377.
17 G. Schwedt and H. H. Bussemas, *Z. Anal. Chem.*, 283 (1977) 23–28.
18 R. W. Roos, *J. Pharm. Sci.*, 67 (1978) 1735–1739.
19 A. Kaukinen, J. Hamekoski and H. Auterhoff, *Arch. Pharm.*, 311 (1978) 469–475.
20 *The United States Pharmacopeia*, United States Pharmacopeial Convention, Rockville, MD, 22nd revision, 1990.
21 S. Fishman, *J. Pharm. Sci.*, 64 (1975) 674–680.
22 E. Vidal-Ollivier, G. Schwadrohn, C. Maillard, G. Balansard and B. Ollivier, *J. Chromatogr.*, 396 (1987) 421–424.

Journal of Chromatography, 555 (1991) 285–290
Elsevier Science Publishers B.V., Amsterdam

CHROM. 23 396

Short Communication

Analysis of commercial hesperidin methyl chalcone by high-performance liquid chromatography

J. CASTILLO, O. BENAVENTE and F. BORREGO
Department of Research and Development, Zoster SA (Ferrer Group International), Raiguero 143, Zeneta, 30588 Murcia (Spain)
and
J. A. DEL RIO*
Department of Plant Biology, Faculty of Biology, University of Murcia, Espinardo, 30071 Murcia (Spain)
(First received October 22nd, 1990; revised manuscript received April 19th, 1991)

ABSTRACT

A high-performance liquid chromatographic procedure for the determination of the different components present in commercial samples of hesperidin methyl chalcone (HMC) was developed. It employs a C_{18} column and an elution gradient with a mixture of methanol and 0.01 *M* aqueous phosphoric acid and a diode-array detector. Eighteen compounds were detected and their UV spectra characterized. The spectra indicate that HMC is a mixture of flavanones and chalcones with different degrees and/or positions of methylation.

INTRODUCTION

Hesperidin methyl chalcone (HMC) is widely used in the pharmaceutical industry as vasodilatator [1], vascular permeability modifier [2], capillary resistence enhancer [3] and prostaglandin E stabilizer [4]. The use of HMC as a colouring agent in cosmetics has also been reported [5].

HMC is usually synthesized by methylation of hesperidin with dimethyl sulphate in alkaline media [6]. However, the structures of the products formed in the reaction are not well known and some attempts have been made to identify the large number of compounds that are formed in the synthesis of HMC. For example, six methylhesperidin derivatives with different degrees of methylation were found by partition and adsorption chromatography [6].

This paper describes a high-performance liquid chromatographic (HPLC) method for the separation of hesperidin methyl derivatives in order to study the methylation reaction and elucidate all the products formed. Eighteen compounds were separated and their spectra analysed with the aid of a diode-array detector.

0021-9673/91/$03.50

EXPERIMENTAL

Chromatography

HPLC analysis was performed using a Beckman liquid chromatograph with a Model 110B solvent-delivery module and a System Gold Module 168 diode-array detector. An IBM Model 30 286 computer was used for all computations.

A 250 × 4 mm I.D. μBondapak C_{18} (Waters Assoc., Milford, MA, USA) column with an average particle size of 5 μm was used.

Separation was performed by gradient elution with a mixture of solvent A (methanol) and solvent B (0.01 *M* aqueous phosphoric acid). The gradient profile being 30% of A for 20 min, then increasing to 45% of A in 30 min, remaining constant there for 30 min at a flow-rate of 1 ml/min.

Reagents

Commercially available HMC was obtained from Merck (Barcelona, Spain), Takeda (Tokyo, Japan) and Zoster (Murcia, Spain).

Procedure

HMC (40 mg) was dissolved in 10 ml of dimethyl sulphoxide and the solution was filtered through a 0.45-μm nylon membrane and injected into the liquid chromatograph. Peaks were monitored at both 345 and 280 nm.

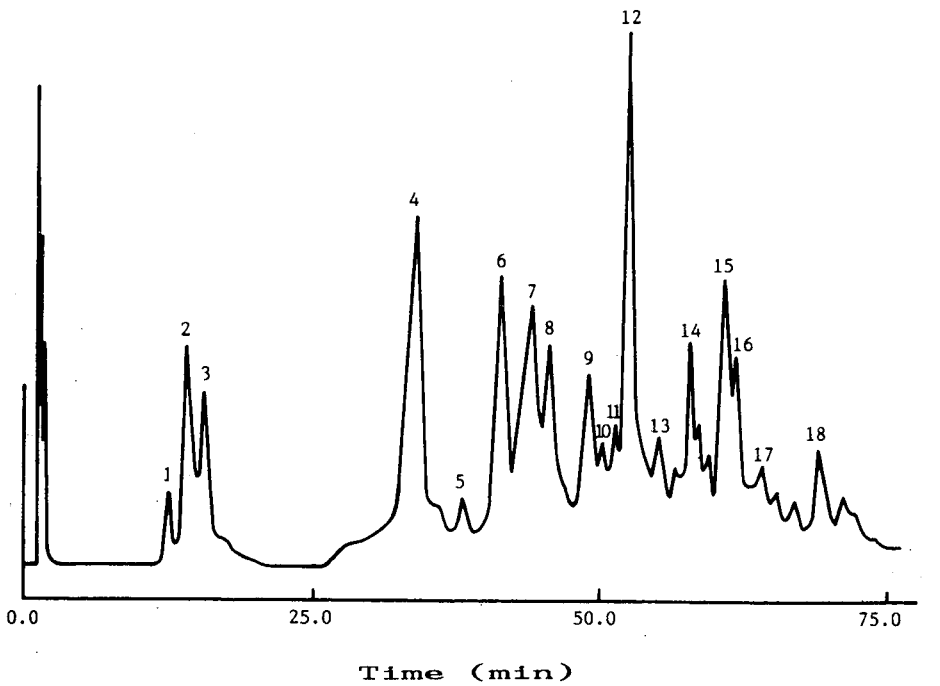

Fig. 1. High-performance liquid chromatogram of commercial HMC from Zoster. See text for eluents and elution profile. Column, μBondapak C_{18} (5 μm) (250 × 4 mm I.D.). Detection: 280 nm. Peak identification as in Table I.

RESULTS AND DISCUSSION

Owing to the complex composition of commercial HMC, the different chromatographic system mentioned in the literature [7–16] were not able to attain the complete resolution of the different compounds present. Chromatographic systems that use direct stationary phases, used for the resolution of flavonoids of high molecular weight, generally polymethoxylated and polybenzoylated flavones, and which employ mobile phases of low polarity [7–9] such as heptane–isopropanol or chloroform–methanol–water, did not permit a good resolution of the samples of commercial HMC analysed, since peaks 1–3 and 4–12 in Fig. 1 overlapped. C_8 and C_{18} reversed-phase columns were tried [10], the latter showing greater peak resolution, for which reason it was used in the following assays. Acetonitrile–water mixtures [11–14] presented problems of resolution, producing grouping of peaks 1–3, 4–5, 6–8, 9–12 and 14–16. Methanol–water combinations (acedified with acetic or phosphoric acid) [10,15], although resolving a greater numbers of peaks than acetonitrile–water combinations, were not capable of resolving all the species later found in HMC because peaks 1–3, 6–8 and 13–16 overlapped. The use of mixtures of water and other alchols such as *tert.*-butanol [16] did not improve the resolutions obtained with methanol–water mixtures (acidified with acetic and phosphoric acid).

Because methanol–water mixtures (acidified with acetic and phosphoric acid) showed a greater capacity to resolve the different species present in commercial HMC, different gradients of methanol–0.01 *M* aqueous phosphoric acid were tried, complete resolution of all peaks being obtained when the gradient profile was 30% methanol–70% 0.01 *M* phosphoric acid for 20 min, rising to 45% methanol in 30 min and remaining constant there for 30 min, at a flow-rate of 1 ml/min. Fig. 1 shows the results for a commercial sample of HMC from Zoster. Other samples from different manufacturers, showed the same distribution of peaks, although their relative proportions differed slightly (data not shown).

Spectral analysis of the peaks in Fig. 1 by means of a diode-array detector showed three UV patterns for methyl derivatives of hesperidin (Fig. 2). The first (Fig. 2a) was a typical flavanone spectrum with a maximum at 280 nm and a low-intensity maximum at 320 nm. The peaks designated F in Table I corresponded to this pattern. The second group of peaks, designated C, had a chalcone spectrum with a maximum at 345 nm (Fig. 2b). The remaining peaks, designated O, had an unidentified spectrum, with a maximum at 285 and others between 330 and 345 nm (Fig. 2c). All the compounds listed in Table I showed spectra similar although unidentified, to one of the three spectra shown in Fig. 2.

Bearing in mind the spectral characteristics of structures F and C, the absorption ratios between 280 and 345 nm were used to compare the different compounds resolved in the chromatogram in Fig. 1. This ratio was higher than 1 for the F compounds, owing to their characteristic maximum at 280 nm. However, this ratio was not constant, varying between a maximum of 7.85 for compounds 2 and 3 and 1.60 for compound 9. Identical 280/345 nm ratios and different retention times suggest an identical degree of methylation but distinct positions [9]. On the other hand, the different ratios suggest different degrees of methylation. The chalcone-type structures, C, with a maximum at 345 nm, showed 280/345 nm ratios lower than 1 (Table I), varying between a maximum of 0.7 (compound 16) and 0.32 (compound 4).

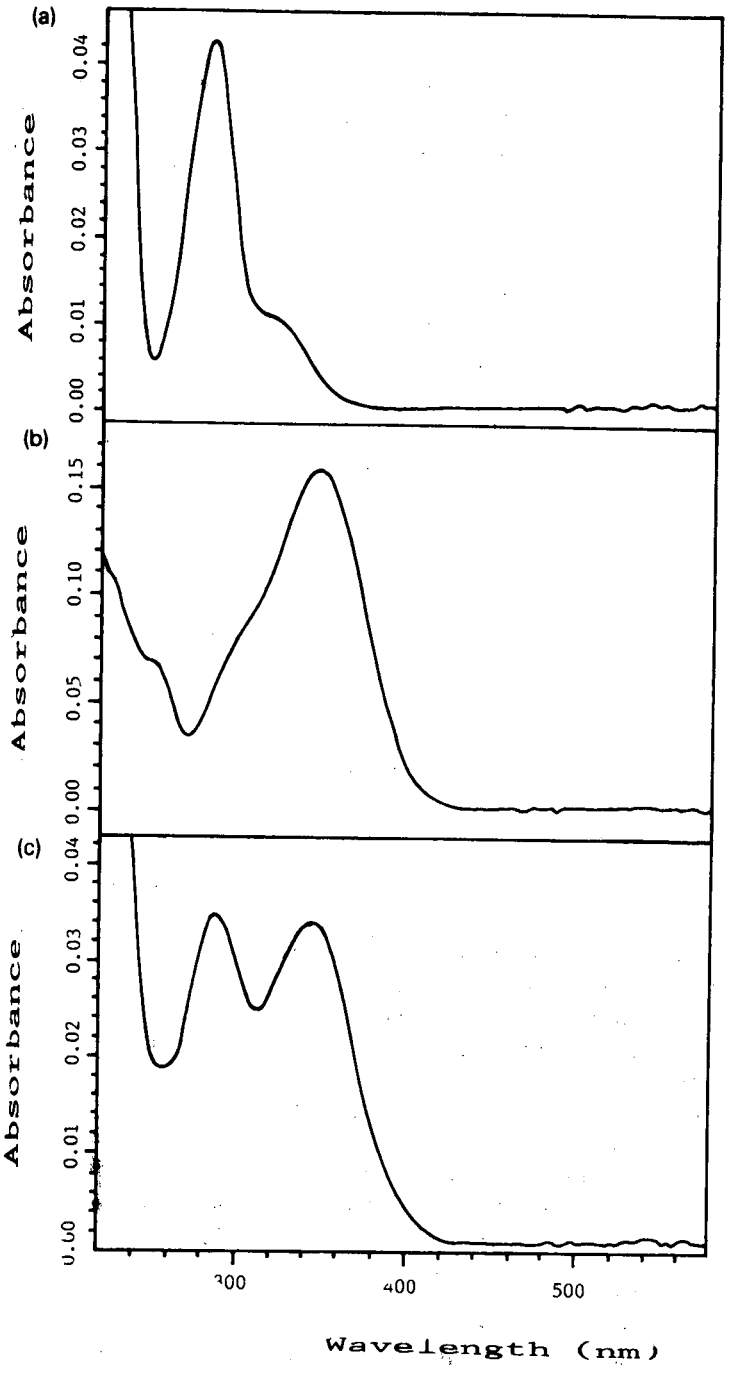

Fig. 2. UV spectrum of different methyl derivatives of hesperidin. (a) Flavanone species (F); (b) chalcone species (C); (c) others species (O).

TABLE I

RETENTION TIMES, SPECTRAL CHARACTERISTICS AND 280/345 nm ABSORPTION RATIOS OF METHYLHESPERIDIN DERIVATIVES IN COMMERCIAL HMC ON μBONDAPAK C_{18} USING A DIODE-ARRAY DETECTOR

No.	t_R (min)	Spectrum	Absorbance ratio (280/345 nm)
1	13.21	F	7.84
2	15.47	F	7.85
3	17.82	F	7.85
4	33.83	C	0.32
5	38.24	C	0.63
6	41.43	F	4.10
7	43.85	O	1.23
8	45.53	F	1.61
9	49.05	F	1.60
10	50.07	F	2.70
11	51.24	F	1.83
12	52.20	C	0.38
13	54.86	O	1.04
14	57.56	C	0.54
15	60.50	F	5.18
16	61.38	C	0.70
17	63.71	O	1.00
18	68.54	O	1.04

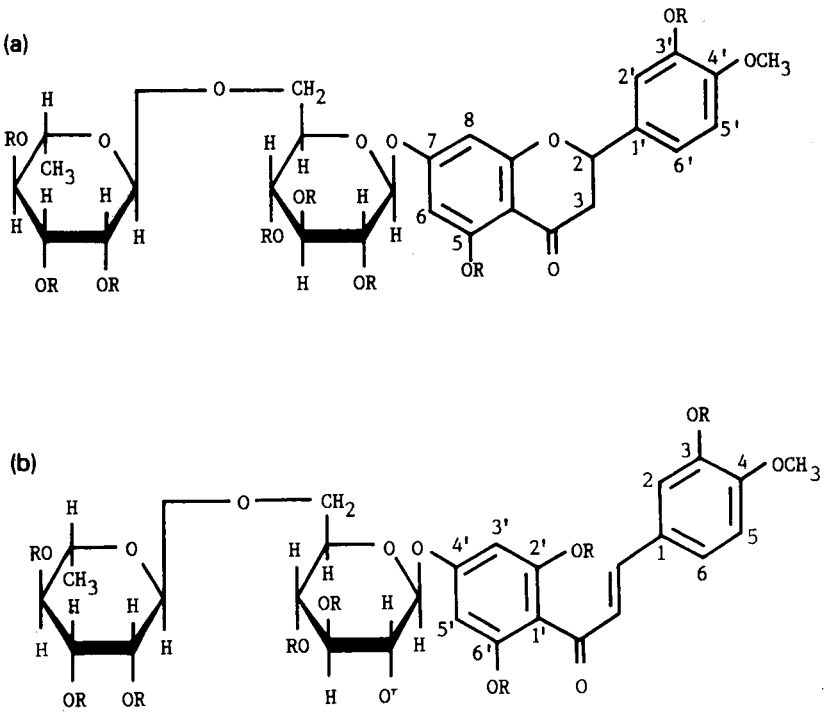

Fig. 3. Structures of methylhesperidines. (a) Flavanone; (b) chalcone. R = H or CH_3.

No differences were observed in the peak distribution at either wavelength. All peaks included in Tabl I were detected was pure compounds by the diode-array detector. The purity criteria employed, included in the spectrum-treatment program, were based on the comparison of the spectra at the half-height of each peak. When these and their derivatives coincided, the peak was considered to be pure. The peaks not considered did not fulfil this criterion.

The different chalcone–flavanone spectra were caused by methylation of the free hydroxyl groups at the 2′-position of chalcone compounds (Fig. 3). This conclusion is based on the equilibrium between the flavanone and chalcone structures, which depends on the pH, and with the eluent employed (pH 3.3) the chalcone structure cannot be maintained if the hydroxyl group at C-2′ is not methylated.

This work demonstrates that commercial HMC is a mixture of chalcone and flavanone species with an unspecified pattern of methylation. Further, no compound predominantes. HPLC with diode-array detection provides an excellent method of detecting not only the presence of distinct methylhesperidines in commercial HMC but also their chalcone–flavanone structure.

Details of the isolation and identification of the different peaks in Fig. 1 will be reported elsewhere.

REFERENCES

1 Q. Chem and G. Feng, *Zhongguo Yaoli Xuebao*, 8 (1987) 344.
2 J. P. Tarayre, H. Lauressergues, M. Vidal, M. Barbara, C. Tailhan and F. Menard, *Ann. Pharm. Fr.*, 34 (1976) 375.
3 M. Gabor, A. Antal and Z. Dirner, *Acta Physiol.*, 34 (1968) 221.
4 M. Naruto, K. Ohno and N. Naruse, *Aust. Patt.*, Au 7840682 (1978).
5 Ihara Chem. Ind., Jpn Patt., JP 60127370 (1985).
6 I. Sakieki, *Nippon Kagaku Zasshi*, 79 (1958) 733.
7 J. P. Bianchini and E. M. Gaydou, *J. Chromatogr.*, 190 (1980) 233.
8 J. P. Bianchini and E. M. Gaydou, *J. Chromatogr.*, 211 (1981) 61.
9 J. P. Bianchini and E. M. Gaydou, *J. Chromatogr.*, 259 (1983) 150.
10 J. B. Harborne and M. Boardley, *J. Chromatogr.*, 299 (1984) 377.
11 K. H. Law and N. P. Das, *J. Chromatogr.*, 388 (1987) 225.
12 P. Pietta and A. Calatroni, *J. Chromatogr.*, 280 (1983) 172.
13 R. L. Rouseff and S. V. Ting, *J. Chromatogr.*, 176 (1979) 75.
14 R. V. Tamma and G. C. Miller, *J. Chromatogr.*, 322 (1985) 236.
15 L. W. Wulf and C. W. Nagel, *J. Chromatogr.*, 116 (1976) 271.
16 M. Bernardi, E. Uberti and G. Vidari, *J. Chromatogr.*, 284 (1984) 269.

Journal of Chromatography, 555 (1991) 291–296
Elsevier Science Publishers B.V., Amsterdam

CHROM. 23 398

Short Communication

N-(Hydroxymethyl)thioamide resin as stationary phase in ion-exchange chromatography for metal ion separation

C. Y. LIU*, M. J. CHEN and T. J. CHAI
Department of Chemistry, National Taiwan University, Taipei (Taiwan)
(Received April 24th, 1991)

ABSTRACT

The sorption properties of Ag(I), Au(III), Cd(II), Co(II), Cu(II), Fe(III), Hg(II), Ni(II), Pb(II), Pt(IV) and Zn(II) on N-(hydroxymethyl)thioamide resin using perchloric acid and hydrochloric acid at various concentrations were studied. The effect of foreign ligands on the retention of metal ions was also investigated. The chromatographic properties of this resin as a stationary phase in ion-exchange chromatography for the separation of cobalt, copper, gold, iron, mercury, platinum, silver and zinc are described. Separations were achieved in many instances by using a mineral acid containing chloride or sulphate anions. Quantitative chromatographic analysis was possible for a variety of sample types. The suitability of the resin for metal preconcentration for both single elements and metal ion mixtures is also described.

INTRODUCTION

To determine metal ions at low levels in complex matrices, three different methods using high-performance liquid chromatography (HPLC) can be applied. The ion chromatographic method is the most common, but often requires the use of a metal complexing additive in the buffered eluent [1]. Reversed-phase HPLC is also popular, but the sample mixture to be separated must be converted into neutral metal chelates [2–7]. Another method is a hybrid of the above two methods, and a more direct approach. Pretreatment of the sample solution is generally not necessary, and a simple mobile phase can be used because selectivity is designed into the stationary phase. A chelating resin used as stationary phase is an example [8].

In ion chromatography, originally the suppressed approach was mainly used, but published results with the non-suppressed column technique subsequently encouraged its application, as conventional LC equipment can be used. Columns other than the normal ion-exchange type can also be used for the technique of ion chromatography [1]. A reliable method for the preparation of a chelating resin containing sulphur and oxygen donors from an acrylonitrile–divinylbenzene co-

0021-9673/91/$03.50

polymer and studies of the chelating behaviour of the resin have previously been reported [9]. The chelate-forming properties of this resin appeared to be promising, and the work has now been extended to apply it as the stationary phase in ion-exchange chromatography in the separation of some metal ions.

EXPERIMENTAL

Apparatus

A Dionex Model 2000i ion chromatograph and a Dionex UV–VIS detector were used. A sample loop of 50 μl was employed, and a Chem Inert glass column (50 mm × 6 mm I.D.) packed with 100–200-mesh N-(hydroxymethyl)thioamide resin was used for separations.

Preparation of resin

The N-(hydroxymethyl)thioamide resin was synthesized in our laboratory. Detailed procedures for the preparation and some of the properties of this resin have been described in a previous paper [9].

Determination of sorption properties in strongly acidic solution

Air-dried resin samples (0.03 g) were equilibrated by mechanical shaking with 25 ml of 4×10^{-4} mol l^{-1} solutions of the individual metal salts in a strongly acidic medium, using either perchloric acid or hydrochloric acid. After a shaking time of 24 h at 25 ± 0.02°C, aliquots were taken from the aqueous solutions and analysed spectrophotometrically. The distribution coefficients D were calculated in the usual way.

General chromatographic conditions

Chromatograms were generally run at ambient temperature of a flow-rate of 1 ml min^{-1}. All mobile phases were degassed ultrasonically before use. Prior to sample injection, the column was equilibrated with the eluent for at least 0.5 h at 1 ml min^{-1}. The columns were considered to be equilibrated when the acidity of the effluent matched that of the entering mobile phase to within ±0.02 pH unit, when a stable baseline was obtained and when two successive injections of sample yielded the same retention time.

The 4-(2-pyridylazo)resorcinol (PAR) flow-rate was generally half that of the mobile phase, the latter being 1.0 ml min^{-1}. The detector was set at 520 nm or direct UV detection of the chloride complexes at 215 nm was applied.

Suitability of resin for metal preconcentration

The ability of the resin to preconcentrate metal ions was tested. Volumes of 10 ml of solutions with metal ion concentrations of 10^{-4}–10^{-7} M at the desired pH value were passed through the resin column at a flow-rate of 1.0 ml min^{-1}. Borosilicate glass columns were used. The resin column was 10 × 0.63 cm I.D. Recovery of the metal ion was achieved by treating the resin with 5 ml of a suitable stripping agent. After elution, the resin was rinsed twice with 2 ml of high-purity water; both washings were collected in a 10-ml calibrated flask and then made up to volume. The metal ion concentrations were determined spectrophotometrically.

RESULTS AND DISCUSSION

Sorption of metal ions by batch operation

The sorption of metal ions on N-(hydroxymethyl)thioamide resin at higher concentrations of mineral acid was studied, as that of noble metal ions was previously found to be nearly independent of pH in a higher pH medium [9]. The results (Table I) indicate that the distribution coefficients of the auric ion were larger than 10^5 even with 5 *M* perchloric acid solution. Those of silver, mercury and platinum were somewhat lower, while those of the other metal ions such as Cd(II), Co(II), Cu(II), Fe(III), Ni(II), Pb(II) and Zn(II), showed almost no adsorption on this resin. For further studies, hydrochloric acid was used instead of perchloric acid; the distribution coefficients obtained (Table I) showed a larger decrease for silver, mercury and platinum, whereas those of gold did not decrease so much and were still large at 3 *M* hydrochloric acid, but obviously decreased at higher concentrations of hydrochloric acid. These results indicate that the synthesized resin was highly selective for noble metal ions in strongly acidic solution, and the competition of the chloride ion with the functional group of the resin increased as the acid concentration increased. These results also suggest that hydrochloric acid could be used as an eluent for the separation of noble metal ions from other transition metal ions.

TABLE I

DISTRIBUTION COEFFICIENTS OF SOME METAL IONS ON N-(HYDROXYMETHYL)THIOAMIDE RESIN AT DIFFERENT CONCENTRATIONS OF MINERAL ACID SOLUTION

Amount of resin: 0.3 g. Amount of each metal ion: 0.01 mmol. Volume of solution: 25 ml.

Metal ion	Acid	Acid concentration (*M*)			
		0.1	2	4	5
Ag(I)	$HClO_4$	317	229	145	51
	HCl	–	6	3	0
Au(III)	$HClO_4$	$>10^5$	$>10^5$	$>10^5$	$>10^5$
	HCl	$>10^5$	$>10^5$	79	25
Cd(II)	$HClO_4$	9	5	<3	<3
	HCl	<1	<0.5	<0.5	<0.5
Co(II)	$HClO_4$	4	<3	<0.5	<0.5
	HCl	<1	<1	<0.5	<0.5
Cu(II)	$HClO_4$	4	<2	<0.5	<0.5
	HCl	<2	<0.5	<0.5	<0.5
Fe(III)	$HClO_4$	<0.5	<0.5	<0.5	<0.5
	HCl	<1	<0.5	<0.5	<0.5
Hg(II)	$HClO_4$	$>10^3$	$>10^3$	$>10^2$	$>10^2$
	HCl	148	26	16	12
Ni(II)	$HClO_4$	<3	<0.5	<0.5	<0.5
	HCl	<1	<0.5	<0.5	<0.5
Pb(II)	$HClO_4$	<1	<0.5	<0.5	<0.5
	HCl	<1	<0.5	<0.5	<0.5
Pt(II)	$HClO_4$	533	103	103	–
	HCl	153	73	32	–
Zn(II)	$HClO_4$	<1	<0.5	<0.5	<0.5
	HCl	<0.5	<0.5	<0.5	<0.5

TABLE II

EFFECT OF FOREIGN LIGANDS ON THE RETENTION OF METAL IONS ON N-(HYDROXYMETHYL)THIOAMIDE RESIN[a]

Volume of solution: 25 ml. Amount of resin: 0.3 g. Amount of metal ion: 0.01 mmol.

Ligand	Retention (%)								
	Cu(II)	Fe(III)	Co(II)	Ni(II)	Zn(II)	Pb(II)	Cd(II)	Hg(II)	Ag(I)
Tartaric acid[b]	1.5	4.5	2.4	~0	~0	5.7	8.4	6.4	45.0
Glycine[c]	91.2	70.3	90.0	100	92.4	100	85.7	73.8	53.1
Glycine[d]	94.4	72.4	91.0	100	95.0	100	88.4	79.3	56.3
EDTA[c]	0.6	~0	2.5	~0	23.5	5.8	7.4	~0	45.6
EDTA[d]	69.3	32.2	76.5	73.2	80.1	73.8	67.2	66.4	54.4
Thiourea[c]	60.3	57.6	77.5	41.9	84.0	97.8	90.4	54.4	14.4
Thiourea[d]	92.8	64.4	87.1	92.1	91.0	97.8	92.4	59.2	20.0
Citrate[c]	99.0	18.6	97.0	92.7	75.4	89.6	97.0	55.4	46.2
Citrate[d]	99.0	53.3	100	100	84.2	97.8	98.0	61.9	46.9

[a] Means of triplicate determinations.
[b] [L] = 0.1 *M*.
[c] [L] = 10^{-3} *M*.
[d] [L] = 10^{-4} *M*.

Table II shows the effect of foreign ligands on the retention of metal ions on N-(hydroxymethyl)thioamide resin. The ligands chosen were those most probably competitive with the functional group of the resin. In the presence of 0.1 *M* tartaric acid and 10^{-3} *M* EDTA, most of the metal ions were hardly adsorbed by the resin. Therefore, tartaric acid or EDTA might be the best eluent for the separation of these metal ions. Thiourea was chosen as representative of a sulphur ligand. The results also showed that the sorption increased considerably when the concentration of these ligands was decreased to 10^{-4} *M*. As EDTA might be a very strong ligand in natural water and 10^{-7} *M* EDTA might be a reasonable upper limit to the possible ligand concentration in nature, it can be concluded that the synthesized resin would be very useful in natural water analysis.

Analytical applications

As the synthesized resin showed fast kinetics and selective, strong binding of noble metal ions, the application of this resin in the chromatographic separation of noble metals from base metals or noble metal ion mixtures should be promising.

Separation of metal ion mixture

The resin column has been used for the separation of aqueous metal ion mixtures of Cu–Ag, Cu–Au, Hg–Fe–Cu, Au–Co–Cu–Zn and Au–Hg–Pt–Fe–Cu. Through the use of step gradients with 0.0036–0.036 *M* sulphuric acid, the noble metal ion could be separated from base metal ions with a resolution ranging from 0.75 to 2.5, and with 0.1–1 *M* hydrochloric acid, the noble metal ions could be separated from each other with a resolution ranging from 0.6 to 1.5.

TABLE III

RECOVERY OF CADMIUM(II), COPPER(II) AND LEAD(II) WITH N-(HYDROXYMETHYL)-THIOAMIDE RESIN COLUMN

Resin column: 10 cm × 0.63 cm I.D. Volume of solution: 10 ml. Conditions: 0.1 *M*, pH 5 (acetic acid–sodium acetate buffer). Flow-rate: 1.0 ml min^{-1}. Eluent for Cu(II): 0.1 *M* HNO_3. Eluent for Pb(II) and Cd(II): 0.1 *M* tartaric acid. No. of measurements for each sample: 3.

Metal ion	Metal ion added (μg)	Metal ion found (μg)	Recovery (%)
Cu(II)	0.128	0.128 ± 0.003	100 ± 3
Cd(II)	1.31	1.24 ± 0.03	95 ± 2
Pb(II)	2.07	1.99 ± 0.04	86 ± 2

TABLE IV

RECOVERY OF METAL ION MIXTURES WITH N-(HYDROXYMETHYL)THIOAMIDE RESIN COLUMN

Resin column: 10 cm × 0.63 cm I.D. Volume of solution: 10 ml for Ag–Cu and 500 ml for Ag–Cu–Fe. Flow-rate: 1.0 ml min^{-1}. Eluent for copper(II) or copper(II) and iron(III): 0.2 *M* $HClO_4$. Eluent for gold(III): 12 *M* HCl. Eluent for silver(I): 6 *M* HCl. No. of measurements for each sample: 3.

Metal ion mixture	Metal ion	Metal ion added (μg)	Metal ion found (μg)	Recovery (%)
Au–Cu	Au	39.4	39.0 ± 0.8	99 ± 2
	Cu	63.5	63.5 ± 0.1	100 ± 0
Ag–Cu–Fe	Ag	13.6	10.1 ± 0.5	74 ± 4
	Cu	1.59×10^3	$(1.69 \pm 0.04) \times 10^3$	106 ± 3
	Fe	43.8	43.0 ± 0.9	98 ± 2

Suitability of resin for metal preconcentration

A preliminary investigation was made of the recovery of Ag(I), Au(III), Cu(II), Cd(II), Fe(III) and Pb(II) from dilute solutions at pH 5 and a flow-rate of 1.0 ml min^{-1}. Some metal ions are strongly retained by this resin, and the release procedure involves elution with a strong acid. Table III shows the recoveries of single elements with this resin column. Copper ion was eluted with 0.1 *M* nitric acid, while lead and cadmium ions were eluted with tartaric acid.

Table IV shows the recoveries of metal ion mixtures with the resin column. Mixtures of Au–Cu and Ag–Cu–Fe were tested. Samples of 10 ml of Au–Cu solution showed a satisfactory recovery for both elements. This result indicates the potential of the proposed method for the recovery of gold from Cu–Au mixtures. The anomalously low recoveries obtained for silver ion from Ag–Cu–Fe mixtures could be attributed to the presence of some reduced form of silver ion in the resin column.

ACKNOWLEDGEMENT

The financial support of this study by the National Science Council of the Republic of China is gratefully acknowledged.

REFERENCES

1 J. Weiss, *Fresenius' Z. Anal. Chem.*, 327 (1987) 451.
2 B. Willeford and H. Veening, *J. Chromatogr.*, 251 (1982) 61.
3 J. O'Laughlin, *J. Liq. Chromatogr.*, 7 (1984) 127.
4 G. Nickless, *J. Chromatogr.*, 313 (1985) 129.
5 B. Steinbrech, *J. Liq. Chromatogr.*, 10 (1987) 1.
6 A. R. Timberbaev, O. M. Petrukhin and Y. A. Zolotov, *Fresenius' Z. Anal. Chem.*, 327 (1987) 87.
7 M. V. Main and J. S. Fritz, *Anal. Chim. Acta*, 229 (1990) 101.
8 C. Y. Liu, *J. Chin. Chem. Soc.*, 36 (1989) 389.
9 C. Y. Liu, H. T. Chang and C. C. Hu, *Inorg. Chim. Acta*, 172 (1990) 151.

Journal of Chromatography, 555 (1991) 297–301
Elsevier Science Publishers B.V., Amsterdam

CHROM. 23 393

Short Communication

Trace determination of volatile organic compounds in soil based on thermal vaporization followed by Tenax-GC trapping and capillary gas chromatography–mass spectrometry

YOKO YOKOUCHI*
National Institute for Environmental Studies, 16–2, Onogawa, Tsukuba, Ibaraki 305 (Japan)
and
MASAFUMI SANO
Shiga Prefectural Institute for Public Health and Environmental Science, 13–45, Gotenhama, Otsu, Shiga 520 (Japan)
(Received April 23rd, 1991)

ABSTRACT

A simple method for the determination of trace volatile organic compounds in the soil was developed, based on the thermal vaporization of the volatile organics from the sample (1–3 g) and their entrapment on Tenax-GC adsorbent, followed by capillary gas chromatography–mass spectrometry. Using this method, volatile hydrocarbons, aldehydes, sulphides and ketones could be measured in garden soil.

INTRODUCTION

Many kinds of organic compounds are present in soil naturally and/or anthropogenically. They have been studied from the viewpoint of soil contamination [1] and soil chemistry [2], but might also be important in atmospheric chemistry, as volatile organics would be expected to migrate from the soil into the air.

Organics in the soil have usually been determined by gas chromatography (GC) or GC–mass spectrometry (MS) after extraction and concentration with a rotary evaporator. However, volatile organics are likely to be lost through the process of evaporative concentration, and for compounds having similar boiling points to solvents, solvent extraction cannot be applied.

We have therefore developed a technique for the determination of volatile organics in soil based on thermal vaporization from the sample under a flow of nitrogen and entrapment on Tenax-GC adsorbent, followed by capillary GC–MS. The use of a

0021-9673/91/$03.50

Poraplot Q analytical capillary column made it possible to refocus the organics introduced into the capillary without the necessity to cool them below 0°C, thus preventing the formation of ice. This method has been successfully used to determine volatile organics in garden soil.

EXPERIMENTAL

Apparatus

Fig. 1 shows the preconcentration–capillary GC–MS system. The preconcentration unit consists of a soil sample, a cold trap, a Tenax-GC trap and two six-port valves (VL1 and VL2) and is a form of the analytical system for atmospheric organics described elsewhere [3]. The soil sample is placed inside a 5-ml screw-capped vial sealed with a PTFE-lined silicone-rubber septum and an aluminium open-top screw cap, and is inserted into an aluminium heater block. The cold trap is an empty screw-capped vial maintained at 0°C with ice–water. The adsorption trap is a stainless-steel tube (4 cm × 3.2 mm), packed with 0.04 g of Tenax-GC and is set inside a PTFE tube (8 cm × 14 mm O.D.). The temperature around the trap can be regulated in the range from −60 to 300°C by a temperature regulator which controls both liquid carbon dioxide cooling and a heater. All the connections except for the soil sample and the water trap are of 1.6 mm O.D. stainless-steel tubing which is as short as possible. The soil sample and the cold trap are connected with a stainless-steel needle (7 cm long), and are connected to the valve VL1 with 1.6 mm O.D. PTFE tubing and 1.6 mm O.D. stainless-steel tubing, respectively, through the needle end. Screw vials, septa and needles were precleaned by heating at 150°C in an evacuated oven before use.

To avoid any adsorption of the compounds on the transfer lines, the valves and the stainless-steel tubes downstream of the cold trap were warmed at 115°C by wrapping with a flexible heater.

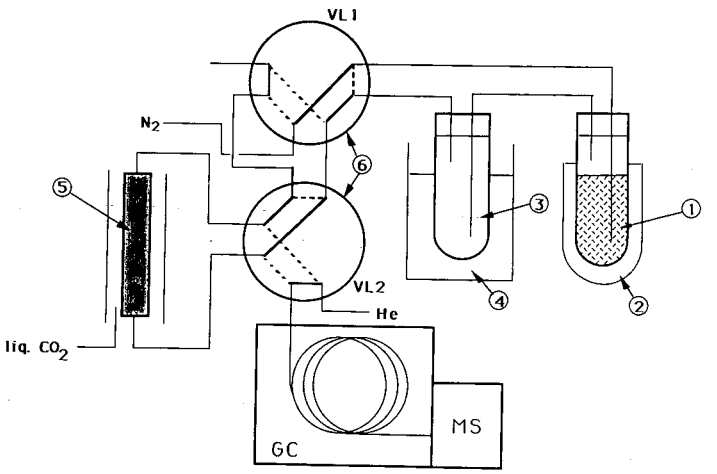

Fig. 1. Analytical set-up for the determination of volatile organic compounds in soil. 1 = Soil sample; 2 = heater block; 3 = cold trap; 4 = ice-water; 5 = Tenax-GC trap; 6 = six-port switching valve.

Computerized GC–MS analyses were carried out on Finnigan MAT 90 with a Varian 3400 gas chromatograph.

Procedure

The soil sample is collected *in situ* by directly inserting the sample into 5-ml vials, which are subsequently sealed tightly with PTFE-lined silicone-rubber septa. The vial is connected to the valve by inserting the needle ends as shown in Fig. 1. The following analytical process is a variation of the purge-and-trap method. On purging, the positions of the two switching valves are at the position of the solid line, and the vial is heated at a preset temperature (150°C) for 7 min. Nitrogen purge gas at a flow-rate of 20 ml/min sweeps the evaporated compounds from the soil sample onto the Tenax-GC trap, which is maintained at 10°C, passing the cold trap where most of the water vapour is removed to avoid interference. The lines are then directly connected by removing the sample and the cold trap, and by inserting the two needle ends into an empty vial, and only nitrogen is passed through the Tenax-GC trap for 5 min to purge water from the adsorbent. After the purge, the switching valve VL2 is changed to the position of the broken line and the Tenax-GC trap is heated to a preset temperature (210°C). Helium carrier gas at a flowrate of 1.4 ml/min transfers the adsorbed compounds onto the analytical capillary column for 7 min. The GC oven temperature is maintained at 55°C during this transfer and then programmed to 220°C at 12°C/min. MS measurements are started immediately after the transfer. The conditions are summarized in Table I. During GC–MS measurements, the valve VL2 is kept in the position of the solid line to allow pure nitrogen to flow through the Tenax-GC trap to remove any remaining trace contaminants.

Calibration is performed by analysing standards (0.1–100 ng of authentic samples dissolved in 0.5 μl of methanol) injected into the vial in place of the soil sample in Fig. 1.

RESULTS AND DISCUSSION

Recovery and precision

The breakthrough volume for *n*-pentane on the Tenax-GC adsorbent was found to be 25 l per gram of Tenax-GC (1 l per 0.04 g of Tenax-GC) at 10°C. As the total amount of nitrogen purge gas flowing from the soil sample into the Tenax-GC trap is only 140 ml, *n*-pentane and less volatile hydrocarbons are considered to be trapped without any loss.

Studies on recovery and reproducibility were done for eleven volatile halogenated hydrocarbons (the most volatile being dichloromethane and the least volatile

TABLE I

GC–MS CONDITIONS

Column	Poraplot Q, 10 m × 0.32 mm I.D.
Oven temperature	Programmed from 55 to 220°C at 12°C/min
Ionization	Electron impact
Scan range	*m/z* 35–500

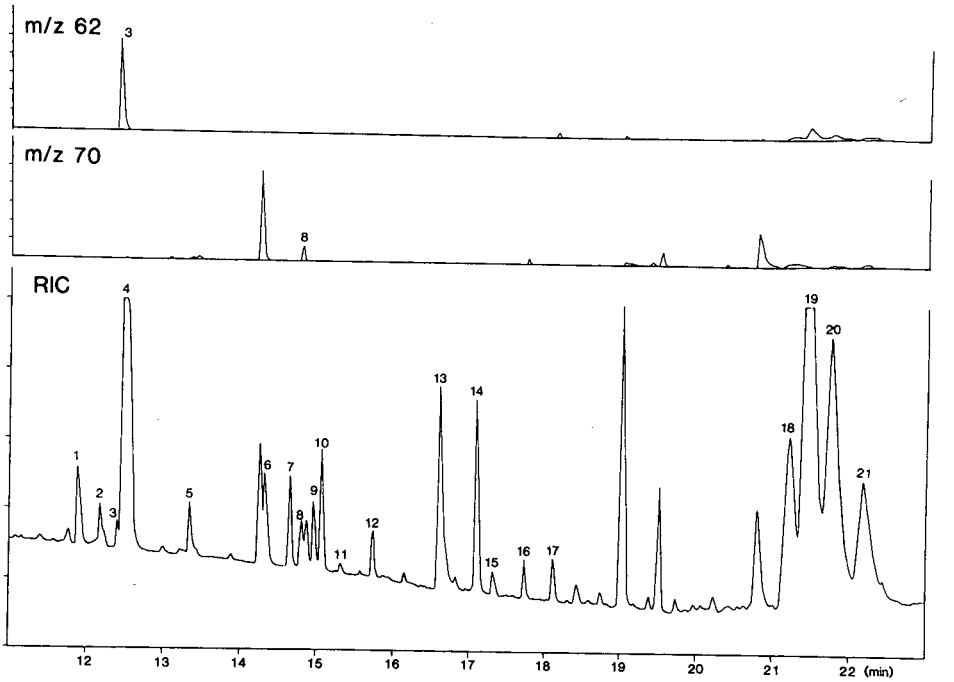

Fig. 2. Reconstructed ion chromatogram (RIC) and ion chromatogram (IC) traces for *m/z* 62 and 70 obtained from a garden soil sample.

tetrachloroethylene), where soil sample, standard (16 ng of each halogenated hydrocarbon in 0.5 μl of methanol) and standard added soil sample were analysed, and the results were compared [4]. A quantitative recovery (90–101%) was obtained for each of the tested components. The relative standard deviation (five repetitions) for each component was in the range 1–5%.

TABLE II

TENTATIVELY IDENTIFIED COMPOUNDS IN THE SOIL

Compound	Peak No.[a]	Retention time (min:s)	Compound	Peak No.[a]	Retention time (min:s)
Acrolein	1	11:52	Hexane	12	15:44
Propanal	2	12:11	3-Methylbutanal	13	16:36
Dimethyl sulphide	3	12:24	Pentanal	14	17:06
Acetone	4	12:28	Dimethyl disulphide	15	17:19
Pentane	5	13:21	Heptane	16	17:45
2-Methylpropanal	6	14:19	Toluene	17	18:06
2-Methylfuran	7	14:39	$C_{10}H_{16}$	18	21:12
Methyl vinyl ketone	8	14:48	α-Pinene	19	21:35
Butanedione	9	14:57	Camphene	20	21:43
Methyl ethyl ketone	10	15:04	$C_{10}H_{16}$	21	22:11
2-Methylpentane	11	15:19			

[a] See Fig. 2.

Blank

A blank test with a pre-baked vial showed no detectable contamination.

Analysis of garden soil

Garden soil (2–3 g), collected in the grounds of the National Institute for Environmental Studies, was analysed by the proposed method. Fig. 2, which is an example of a reconstructed ion chromatogram (RIC) obtained for these soil samples, shows good chromatographic separation. Compounds identified tentatively on the basis of their mass spectra are summarized in Table II with the corresponding peak numbers and retention times in Fig. 2. A variety of volatile compounds, including hydrocarbons, aldehydes, ketones, ethers and sulphides, were found to be present in the soil. Most of these compounds have not been reported previously. Several other soil samples showed different compositions, but acetone was always the major component.

Regarding their sources, monoterpene hydrocarbons ($C_{10}H_{16}$) such as α-pinene and camphene are well known secondary products of higher plants. Aldehydes, ketones and sulphides are also likely to be derived from terrestrial plants and/or bacterial production [5], although very little is known about their behaviour.

Ion chromatography (IC) can be used for the selective detection of overlapping compounds. In Fig. 2, IC traces for ions of m/z 62 and 70 show the selective peaks of dimethyl sulphide and methyl vinyl ketone, respectively. For known compounds, more sensitive MS analysis can be done using selected ion monitoring.

A significant feature of the compounds detected with the present method is that all of them seem to migrate easily into the atmosphere owing to their high volatility. This suggests that they participate in atmospheric chemistry. For example, dimethyl sulphide emitted from the soil might contribute to the production of sulphate, in addition to that from the oceans [6]. The amount of dimethyl sulphide detected in the soil was in the range of several nanogram per gram, which is higher than its average concentration in the oceans [6].

REFERENCES

1 J. S. Warner, M. C. Landes and L. E. Slivon, in R. A. Conway and W. P. Gulledge (Editors), *Hazardous and Industrial Solid Waste Testing, Second Symposium* (*ASTM STP* 805), Amercian Society for Testing and Materials, Philadelphia, 1983, p. 203.
2 G. Eglinton and M. T. J. Murphy (Editors), *Organic Geochemistry*, Springer, Berlin, 1969.
3 Y. Yokouchi, Y. Ambe and T. Maeda, *Anal. Sci.*, 2 (1986) 571.
4 Y. Sano, *Master Thesis*, Tsukuba University, Tsukuba, 1991.
5 T. E. Graedel, D. T. Hawkins and L. D. Claxton, *Atmospheric Chemical Compounds—Sources, Occurrence and Bioassay*, Academic Press, Orlando, 1986, Ch. 6, 7.
6 M. O. Andreae and H. Raemdonck, *Science* (*Washington, D.C.*), 221 (1983) 744.

Journal of Chromatography, 555 (1991) 302–305
Elsevier Science Publishers B.V., Amsterdam

CHROM. 23 349

Short Communication

Use of a Sep-Pak cartridge for preparative collection in gas chromatography

HAN-CHAO WEI and CHIA-LI WU*
Department of Chemistry, Tamkang University, Tamsui 25137 (Taiwan)
(First received December 3rd, 1990; revised manuscript received April 4th, 1991)

ABSTRACT

Commercial Sep-Pak cartridges (Si or C_{18}) with a piece of short PTFE tubing could be used directly without any cooling or heating as a convenient and efficient collection device for preparative gas chromatography. Four sets of experimental results are presented.

INTRODUCTION

Conventionally, cold-bath (dry-ice–acetone or NaCl–ice–water) cooling or certain types of alternative heating and cooling devices have been used for preparative collections in gas chromatography (GC) [1–5]. However, in our hands these methods suffered several drawbacks, such as the inconvenient supply of dry-ice, the liability to breakage of the long glass collection tubes and the often low recovery yields. We recently found that commercial Sep-Pak cartridges (Si or C_{18}) with a piece of short PTFE tubing could be used directly without any cooling or heating as a very convenient and efficient collection device. In this paper, four sets of experimental results are presented.

EXPERIMENTAL

Materials

Ethyl acetate was of analytical reagent grade. α-Pinene was purchased from TCI (Janpan, Taiwan); all other chemicals were obtained from Fluka, (Buchs, Switzerland). The properties of the test samples and international standards are given in Table I. Both silica and C_{18} Sep-Pak cartridges were products of Waters Assoc. (Milford, MA, U.S.A.).

0021-9673/91/$03.50

TABLE I

PROPERTIES OF TEST SAMPLES (TS) AND INTERNAL STANDARDS (IS)

Group	Compound	B.p. (°C)[a]	Formula	M.W.
I	Isolongifolol (TS)	113–114 (m.p.)	$C_{15}H_{26}O$	222.37
	Globulol (IS)	87–88 (m.p.)	$C_{15}H_{26}O$	222.37
II	Longifolene (TS)	258–260	$C_{15}H_{24}$	204.36
	Ledene (IS)	268–270	$C_{15}H_{24}$	204.36
III	Pulegone (TS)	223–224	$C_{10}H_{16}O$	152.24
	Carvone (IS)	228–230	$C_{10}H_{14}O$	150.22
IV	α-Pinene (TS)	154–156	$C_{10}H_{16}$	136.24
	α-Phellandrene (IS)	171–174	$C_{10}H_{16}$	136.24

[a] Taken from Fluka Catalogue.

Gas chromatography

All collections were carried out on a Shimadzu GC-8A gas chromatograph with a 5% SE-30 (methylsilicone) packed column (3 m × 3 mm I.D.) and under the following conditions, unless specified otherwise: injector temperature, 220°C; column temperature, programmed from 50 to 200°C at 5°C/min; detector (thermal conductivity) temperature, 220°C; and carrier gas (nitrogen) flow-rate, 25 ml/min.

All determinations were performed on a Hewlett-Packard HP 5890A gas chromatograph equipped with fused-silica capillary columns of DB-Wax (bonded phase, polyethylene glycol), (30 m × 0.25 mm I.D., 0.25 μm film thickness) (J&W Scientific) or SP-2250 [methyl–phenylsilicone (50:50)] (60 m × 0.25 mm I.D., 0.2 μm film thickness) (Supelco) and a flame ionization detector. The carrier gas (nitrogen) flow-rate was 2 ml/min and the make-up gas flow-rate was 30 ml/min. The splitting ratio was 1:80. The injector and detector temperatures were 250°C. The oven temperature was programmed from 150 (DB-Wax) or 50°C (SP-2250) to 220°C at 5°C/min. A Shimadzu Model C-R3A integrator was used.

Collection device

As shown in Fig. 1, a 6 cm × 4.2 mm O.D. PTFE tube connecting with a Sep-Pak cartridge was used as the collection device. The PTFE tube was snugly inserted into the outlet of the gas chromatograph for about 3–4 cm and fixed with a silicone-rubber septum screw-cap.

Sample collection and recovery

All injected samples were weighed (*ca.* 10 mg) and dissolved in 100–200 μl of ethyl acetate. The same set of Sep-Pak cartridge and PTFE tube was used for collection for the same sample during three or four injections performed on each sample.

The collected material was washed out with ethyl acetate from the bottom side of the cartridge, with the PTFE tube still connected, into a 5-ml calibrated flask. The final volume was precisely adjusted to 5 ml. An internal standard of the same kind as the test sample was chosen for comparison. The weighed standard was also dissolved in a 5-ml calibrated flask. By using a 1-ml pipette, 1 ml was taken from both the

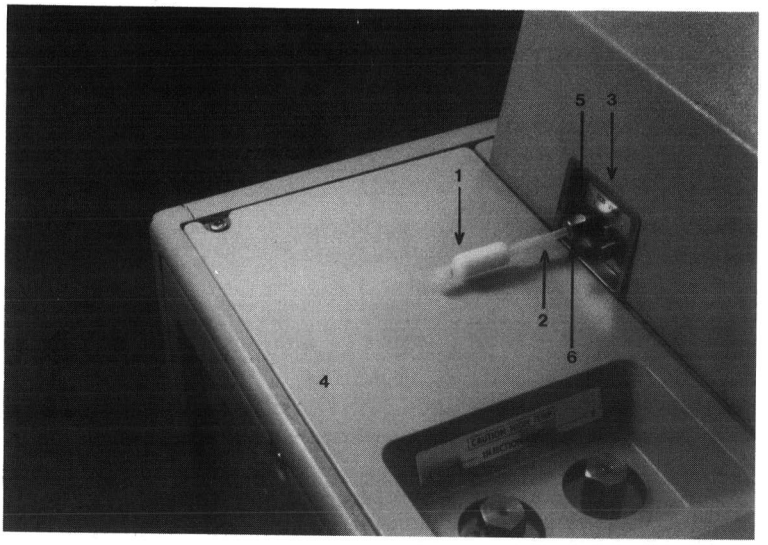

Fig. 1. Preparative GC collection device. 1 = Sep-Pak cartridge; 2 = PTFE tube (ca. 6 cm); 3 = GC thermal conductivity detector outlet; 4 = gas chromatograph; 5 = screw-cap; 6 = silicone-rubber septum (inside the screw-cap).

collected sample and the corresponding standard to make a mixture for GC quantification. The area ratio of the two peaks and the number of moles of the internal standard were used to calculate the recovery of the sample.

TABLE II

RESULTS OF PREPARATIVE GC COLLECTION USING SEP-PAK CARTRIDGES

Group[a]	Sep-Pak cartridge	Amount injected (mg)	Amount of internal standard (mg)	Calculated recovery (mg)	Recovery (%)
I	Silica	13.1	7.9	12.6	96.18
	C_{18}	10.6	6.6	10.1	95.25
II	Silica	11.2	8.6	10.8	96.43
	C_{18}	10.2	8.6	9.7	95.10
III	Silica	9.7	10.9	9.1	93.81
	C_{18}	9.4	10.7	8.5	90.43
IV	Silica:				
	Run 1	17.9	15.9	14.4	80.45
	Run 2[b]	9.8	6.6	8.2	83.67
	C_{18}:				
	Run 1	17.7	15.5	5.8	32.77
	Run 2[b]	8.4	9.7	6.5	77.38
	Run 3[b,c]	10.7	9.9	8.8	82.24

[a] See Table I.

[b] Both injector and detector temperature were lowered to 180°C.

[c] Two Sep-Pak cartridges were connected in parallel, but the yield was based on the ethyl acetate wash from the first cartridge only.

RESULTS AND DISCUSSION

Except for α-pinene, the recoveries were all better than 90%, whichever cartridge (Si of C_{18}) was used. As shown in Table II, for the sesquiterpenes and monoterpenes tested, the silica Sep-Pak gave slightly better yields in all instances. For α-pinene, the low recovery from run 1 on the C_{18} cartridge was improved considerably when both the injector and detector temperatures were lowered from 250 to 180°C (run 2) and improved still further when two cartridges were connected in parallel (run 3). In run 3, however, nothing could be washed out from the second cartridge, and the recovery was based on the ethyl acetate wash from the first cartridge only.

During nearly all collections, either white solid or oil droplets were observed in the PTFE tube near the cartridge end. In run 1 on the C_{18} cartridge for α-pinene, however, nothing could be seen in the PTFE tube and the recovered material (32.77%) was obviously trapped in the cartridge. It seems that the Sep-Pak cartridge works mainly as a very efficient stopping device to slow the fast gas stream from the outlet of the gas chromatograph, but if this stopping function fails, the packing in the cartridge may also work as an adsorbent to trap the material. The lower recoveries for α-pinene illustrate that both the stopping and absorbing functions of the packing in the cartridge do not work as efficiently for small and non-polar molecules. However, adding a third cartridge in parallel may further improve the recovery for such compounds. The slightly better recovery with the silica cartridge in all instances is probably due to the stronger adsorbing property of silica particles.

In conclusion, for reasonably sized molecules ($\geqslant C_{10}$), Sep-Pak cartridges can be used for very convenient and efficient preparative GC collections.

REFERENCES

1 C. F. Poole and S. A. Schutte, *Contemporary Practice of Chromatography*, Elsevier, New York, 1984.
2 D. L. Pavia, G. M. Lampman, G. S. Kriz and R. G. Engle, *Introduction to Organic Laboratory Techniques, a Contemporary Approach*, Saunders, Philadelphia, 1976.
3 S. Smith, *J. Chem. Educ.*, 67 (1990) 615.
4 G. Magnusson, *J. Chromatogr.*, 109 (1975) 393.
5 A. A. Casselman and R. A. B. Bannard, *J. Chromatogr.*, 90 (1974) 185.

Journal of Chromatography, 555 (1991) 306–310
Elsevier Science Publishers B.V., Amsterdam

CHROM. 23 387

Short Communication

Determination of volatile thiols by gas chromatography using separation as tributyltin mercaptides

MIECZYSŁAW WROŃSKI

Department of Chemical Technology and Environmental Protection, University of Łódź, Pomorska 18, Łódź (Poland)

(Received February 15th, 1991)

ABSTRACT

Thiols were converted with a 0.01 *M* solution of tributyltin hydroxide in hexane to tributyltin mercaptides. Part of the hexane solution was evaporated in a small test tube on a water bath, hexane vapour was removed and the remaining mercaptides were decomposed with 3 *M* hydrochloric acid saturated with ammonium sulphate. A sample of 1.2 ml from the total headspace of 1.3 ml was applied on the column of a gas chromatograph using nitrogen gas and flame ionization defection. The average relative standard deviation of the peak height for 10 nmol of each of seven different thiols was 11%. The method is illustrated by analysis of thiols separated from cigarette smoke.

INTRODUCTION

In the course of investigation of sulphur compounds in the environment it became apparent that it was necessary to develop a reliable analytical method for volatile thiols in air, smoke, water, food, soil and biological materials. The resolution of thiols by gas–liquid chromatography is well established [1], but the isolation is difficult to perform or not at all suitable for trace amounts. The thiols can be isolated from the gas phase as mercury [2,3], cadmium [3] and mercuribenzoic acid [4] mercaptides. The disadvantage of these reagents however is that the precipitates are troublesome to deal with and they easily deompose into metal sulphide and thioether.

Although flame photometric detection combined with gas chromatography has been found to be very valuable for the determination of a few sulphur compounds in air [5], the results for complex mixtures cannot be regarded as satisfactory. The analysis of sulphur compounds in tobacco smoke is virtually limited to carbon disulphide, carbonyl sulphide, hydrogen sulphide, sulphur dioxide, dimethylsulphide, dimethyldisulphide, diethylsulphide and thiophene [6–8]. About 30 peaks remain unknown, and no results concerning the thiol composition have been reported.

Another approach to gas chromatographic analysis of thiols is based on deri-

0021-9673/91/$03.50

vatization either to pentafluorobenzyl ethers [9] or to dinitrophenylalkyl thioethers [10].

The method suggested in this paper involves conversion of thiols to tributyltin mercaptides dissolved in hexane, evaporation of hexane with other volatile compounds, if any, decomposition with hydrochloric acid and application of the gas from the headspace to the chromatograph. By this approach the thiols are completely separated from other volatile compounds, apart from hydrogen sulphide, which however does not interfere when flame ionization detection is used.

EXPERIMENTAL

A Chrom 4 gas chromatograph (Laboratorni Přistroje, Prague, Czechoslovakia) equipped with a flame ionization detector and a glass column (2.5 m × 3 mm I.D.) packed with 5% tricresylphosphate on Chromosorb G AW 60–80 mesh was used. The column was operated at 37°C with a nitrogen carrier gas flow-rate of 16 ml/min, a hydrogen flow-rate of 25 ml/min and an air flow-rate of 300 ml/min. The sensitivity was 1:1 (full sensitivity), and the detector response 5 mV = 25 cm.

To prepare a stock solution of *o*-hydroxymercuribenzoic acid (HMB), dissolve 0.321 g of *o*-hydroxymercuribenzoic acid anhydride in 10 ml of 2 *M* potassium hydroxide and dilute to 200 ml with water. To 10 ml of the stock solution ($5 \cdot 10^{-3}$ *M*) add 1 ml of dibutylamine and dilute with methanol to 500 ml, the concentration being 10^{-4} *M*.

To prepare a stock solution of tributyltin (TBT) hydroxide, dissolve 3 ml of tributyltin chloride in 100 ml of hexane and shake for 5 min with 25 ml of 2 *M* potassium hydroxide. Leave aside overnight, remove the aqueous phase and filter through paper. To obtain 0.01 *M* TBT hydroxide, dilute the stock solution with hexane in a ratio of 1:10.

The prepared solutions of thiols in hexane were analysed by titration with HMB (sample + a few millilitres of *n*-propanol + 0.5 ml of 2 *M* potassium hydroxide, dithizone as indicator) and diluted to obtain 10^{-5}–10^{-4} *M* concentrations in 0.01*M* TBT in hexane.

Separation of thiols from aqueous samples

To 100 ml of the sample add 0.5 ml of 2 *M* potassium hydroxide, 2 g of sodium sulphite and 1 ml of 0.1 *M* Na_2EDTA and shake for 2 min with 5 ml of 0.01 *M* TBT in hexane. To reduce vaporization of hexane cool the sample to 5°C. Use the hexane phase for analysis.

Separation of thiols from water-miscible solvents

Shake together 5 ml of the sample, 5 ml of 0.01 *M* TBT in hexane and 10 ml of a 4% aqueous solution of ammonium sulphate; separate the hexane phase and wash it with water and with 0.1 *M* potassium hydroxide.

Separation of thiols from gases

The thiols are absorbed in a small gas-washing bottle containing 5 ml of 0.01 *M* TBT in hexane and 5 ml of 0.1 *M* potassium hydroxide and cooled with iced water.

Thiols are always separated with hydrogen sulphide and the total concentration can be determined by titration with HMB.

TABLE I

DETERMINATION OF THIOLS BY GAS CHROMATOGRAPHY AND HEADSPACE METHOD

Thiol	Amount taken (nmol)						Relative peak area with regard to methanethiol	Retention time (min)	Average peak height per nmol (mm)
	5	10	15	5	10	15			
	Average peak height (mm)			Relative standard deviation for $n = 5$ (%)					
Methanethiol	15	33	48	21	7	8	1.0	2.4	3.2 ± 0.2
Ethanethiol	27	60	95	14	4	4	3.1	4.0	5.9 ± 0.5
2-Propanethiol	43	89	142	26	9	8	5.3	5.6	9.0 ± 0.5
2-Methyl-2-propanethiol	79	138	236	6	6	18	9.8	6.4	15 ± 1.5
1-Propanethiol	14	31	49	15	18	11	3.6	9.4	3.1 ± 0.3
2-Butanethiol	19	35	55	22	13	14	4.6	14.2	3.7 ± 0.2
2-Methyl-1-propanethiol	10	17	29	29	22	17	3.7	15.8	1.9 ± 0.2

Determination of thiols dissolved in 0.01 M TBT in hexane by gas chromatography

Place a test tube of 11 cm length and 0.75 cm I.D. in boiling water and slowly add 2 ml of hexane solution. Small amounts of pulverized glass or ceramic can be added. In order to remove the hexane vapour, pass argon or nitrogen through the test tube at a flow-rate 100 ml/min for 3 min. Cool the tube and cover it with a plug containing a 0.3 cm I.D. hole. Through the hole fill the test tube with a solution prepared by saturation of 3 *M* hydrochloric acid with ammonium sulphate, until the distance to the plug is 3 cm. Close the hole with a glass rod and, keeping it tightly closed, place for 1 min in boiling water. Shake vigorously, remove the glass rod, take from the head space a 1.2-ml sample and apply it to the column.

RESULTS AND DISCUSSION

The suggested method has been extensively examined using solutions of seven thiols of concentration 10^{-5} *M* in 0.01 *M* TBT in hexane (1 ml = 10 nmol), standardized by titration with HMB. As may be seen from the results summarized in Table I, relative standard deviation varies from 4 to 29%, with an average value of about 17% for 5 nmol and 11% for 10 and 15 nmol. The proportionality between the amount of thiol taken and peak height is well confirmed within ± 10%. The relative peak area increases sharply from methanethiol to 2-methyl-2-propanethiol and then decreases. The response expressed as peak area and peak height is proportional to the amount of

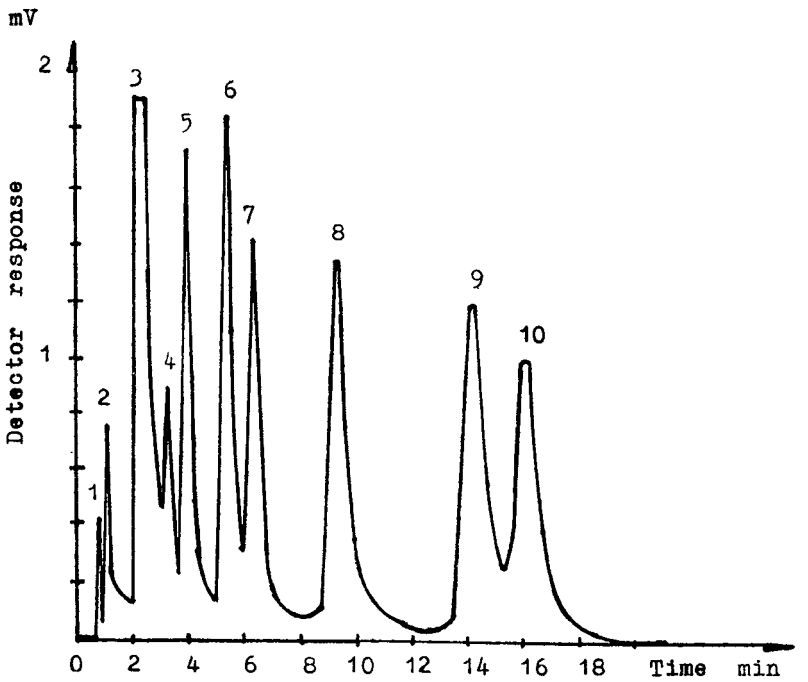

Fig. 1. Gas chromatogram of thiols separated from cigarette smoke. Peaks: 1 = methane; 2 = butane; 3 = methanethiol; 4 = hexane; 5 = ethanethiol; 6 = 2-propanethiol; 7 = 2-methyl-2-propanethiol; 8 = 1-propanethiol; 9 = 2-butanethiol; 10 = 2-methyl-1-propanethiol.

thiol taken and to its molar response for flame ionization detector. The last value increases with increasing number of carbon atoms in the molecule [11]. The volume of the headspace amounts to 1.3 ml and the volume taken for analysis 1.2 ml. When the headspace air is taken by the syringe with a simultaneous inflow of fresh air, the part of thiol taken from the head space amounts to

$$1 - \exp(-1.2/1.3) = 0.60$$

The concentration of thiol in the headspace is determined by its partition coefficient and increases with increasing temperature. The part of the total thiol content taken by the syringe as suggested in the method can be determined by absorption in alkaline alcohol solution and titration with HMB. The following results were obtained: methanethiol 12%, ethanethiol 20%, 2-propanethiol 22% and 2-butanethiol 16%.

As an illustration of the great usefulness of the suggested method, an investigation of the thiol content of the cigarette smoke was performed. A cigarette containing 0.8 g of tobacco was smoked in a stream of air, and the smoke after passing a cotton filter was absorbed, as described above, in 5 ml of 0.01 *M* TBT in hexane and 2 ml taken for analysis. The result is demonstrated on Fig. 1. It may be concluded that by this approach the thiol composition of the smoke can be clearly established. Apart from thiols traces of methane resulting from air contamination in the laboratory, butane produced by decomposition of TBT in acid solution and some remaining hexane can be seen.

REFERENCES

1 M. R. E. Asworth, *The Determination of Sulphur-Containing Groups, Vol. 2, Analytical Methods for Thiol Groups*, Academic Press, London, New York, San Francisco, CA, 1976.
2 J. F. Carson, W. J. Weston and J. W. Rulls, *Nature (London)*, 186 (1960) 801.
3 M. Feldstein, S. Balestrieri and D. A. Levaggi, *J. Air Pollution Control. Assoc.*, 15 (1965) 215.
4 B. Zygmunt and R. Staszewski, *J. Chromatogr.*, 119 (1976) 599.
5 R. K. Stefens, J. D. Mulik and A. E. O'Keeffe, *Anal. Chem.*, 93 (1971) 827.
6 P. J. Groenen and L. J. van Genert, *J. Chromatogr.*, 57 (1971) 239.
7 A. D. Horton and M. R. Guerin, *J. Chromatogr.*, 90 (1974) 63.
8 L. Blomber, *J. Chromatogr.*, 125 (1976) 389.
9 F. K. Kawahara, *Anal. Chem.*, 40 (1968) 1009.
10 J. Korolczuk, M. Daniewski and Z. Mielniczuk, *J. Chromatogr.*, 100 (1974) 165.
11 F. Raulin and G. Toupance, *J. Chromatogr.*, 90 (1974) 218.

Journal of Chromatography, 555 (1991) 311–314
Elsevier Science Publishers B.V., Amsterdam

CHROM. 23 327

Short Communication

Determination of 3-chloropropane-1,2-diol in liquid hydrolysed vegetable proteins by capillary gas chromatography with flame ionization detection

W. J. PLANTINGA, W. G. VAN TOORN and G. H. D. VAN DER STEGEN*
Research & Development, Koninklijke Douwe Egberts B.V., Keulsekade 143, P.O. Box 2, 3500 CA Utrecht (Netherlands)
(First received October 10th, 1990; revised manuscript received March 18th, 1991)

ABSTRACT

An improved method for determination of 3-chloropropane-1,2-diol in liquid hydrolysed vegetable proteins using capillary gas chromatography with flame ionization detection is presented. A phenylboronic acid derivative was prepared and extracted with hexane. The identity of the derivative was confirmed by gas chromatography–mass spectrometry. The method showed a standard deviation of 0.019 ppm and a repeatability of 0.05 ppm at a level of 0.84 ppm. The limit of detection was 0.2 ppm.

INTRODUCTION

3-Chloropropane-1,2-diol (3-MCPD) is a contaminant which can be formed in the manufacture of protein hydrolysates. A routine gas chromatographic (GC) determination of 3-MCPD in such liquid hydrolysed vegetable proteins (HVPs) has not yet been published. As monochloropropanediols often show unsatisfactory chromatographic properties, they are frequently derivatizatized for analysis. Schurig and Wistuba [1] derivatized 3-MCPD in non-aqueous media using *n*-butylboronic acid. Pesselman and Feit [2] showed that quantitative measurements of the diol in standard aqueous solutions is possible, using such a derivatization combined with a hexane extraction. Rodman and Ross [3] described the preparation of a phenylboronic acid derivative of 3-MCPD in a non-aqueous medium and characterized the derivative by Fourier transform infrared spectrometry and its mass spectrum. The phenylboronic acid derivatization and solvent extraction were further explored to develop an analysis suitable for routine purposes in liquid HVPs.

EXPERIMENTAL

Apparatus

For GC–flame ionization detection (FID) analyses a Packard Model 439 gas chromatograph equipped with a split injection port and a flame ionization detector was used. For GC–mass spectrometric (MS) identification of the 3-MCPD-phenylboronic acid derivative, a Hewlett-Packard Model 5890A gas chromatograph with a split injection port and a Model 5970B mass-selective detector was used. For both GC–FID and GC–MS analyses the chromatographic separation was carried out using a 50 m × 0.32 mm I.D. CP-SIL 5 CB fused-silica column with 0.12-μm film (Chrompack). The GC operating conditions were as follows: carrier gas, helium; head pressure, 150 kPa; detector make-up gas, nitrogen at 30 ml/min; split flow, 10 ml/min. The oven temperature program was: initial temperature 40°C for 1 min, oven temperature rise 1 = 7.5°C/min for 19 min, oven temperature rise 2 = 39.99°C/min at 20 min for 2.45 min, oven final temperature 280°C for 13 min. The injector and detector temperatures were 200 and 280°C, respectively.

Reagents

3-MCPD and phenylboronic acid were obtained from Aldrich Chemie, acetone (pro analisi grade) from J. T. Baker and *n*-hexane (pro analisi grade), sodium chloride (pro analisi grade) and *n*-heptadecane from E. Merck.

Solutions

The internal standard solution contained 0.01 mg/ml *n*-heptadecane in hexane. The derivatization solution contained 250 mg/ml phenylboronic acid and was prepared by dissolving 5 g phenylboronic acid in 19 ml acetone plus 1 ml distilled water. The sodium chloride solution contained 200 g/l sodium chloride. All solutions except the sodium chloride solution were kept chilled (5°C).

PROCEDURE

Sample preparation

Into an 100-ml volumetric flask a 75.0-g sample was weighed and diluted with 20% sodium chloride solution.

Preparation of standards

A stock solution of 3-MCPD was prepared by weighing 10.0 mg 3-MCPD into a 100-ml volumetric flask and filling up to volume with 20% sodium chloride solution; 10 ml of the prepared stock solution were diluted to 100 ml with 20% sodium chloride solution (solution 1). Solution 1 contained 10. μg/ml 3-MCPD, which, taking into account the predilution of samples, corresponds to 13.3 ppm 3-MCPD in samples. Calibration solutions corresponding to 0.53, 1.33 and 5.3 ppm 3-MCPD in samples were prepared by dilution of solution 1 using 20% sodium chloride solution.

Derivatization and extraction

Volumes of 5.0 ml of each of the calibration and sample solutions were pipetted into sample vials. After addition of 1.0 ml of derivatization solution, the vials were

sealed with vial caps and left for 20 min at 90°C. After cooling to room temperature, the vial caps were removed, 3.0 ml of internal standard solution in hexane were added and the vials were sealed with a new cap. The vials were shaken for 30 s using a vortex and, after separation of the organic and water layers, 2 μl of the hexane layer were injected.

RESULTS AND DISCUSSION

Confirmation and identification of the penylboronic acid derivative of 3-MCPD in a sample chromatogram was achieved by matching its mass spectrum with a literature spectrum [3] and by comparing the retention time of the suspected peak with that of the derivatized pure 3-MCPD. The phenylboronic acid derivative of 2-MCPD was identified by interpretation of its mass fragmentation pattern only. The peak gave ions at m/z 196 and 104 suggestive of the proposed structure. Using the described chromatographic conditions, the phenylboronic acid derivative of 3-MCPD has a Kovats retention index of 1413 and that of the derivative of 2-MCPD is 1426.

Two different extraction solvents (*n*-hexane and toluene) were evaluated for their influence on the recovery of 3-MCP-phenylboronate in HVP samples. An internal standard (*n*-heptadecane) was added to the extraction solvent to compensate for possible variations in the injection volume. A sample spiked with 21 ppm 3-MCPD was extracted up to six times after derivatization, and each time the 3-MCPD content in the extraction solvent was measured. Toluene proved to have the best recovery: 84% in the first, 13% in the second and 3% in the third extraction step. *n*-Hexane had a lower recovery: about 45% in the first, 27% in the second and 15% in the third step. However, although toluene had the best recovery, its extract produced more peaks with reduced resolution in the chromatogram, which hindered accurate integration and reliable quantification at levels around 1 ppm 3-MCPD. The hexane

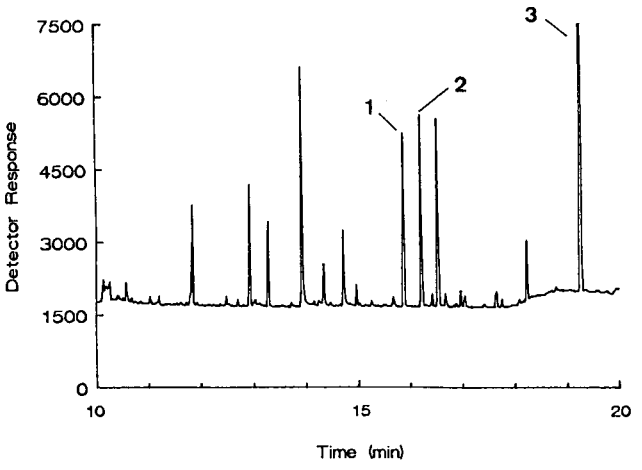

Fig. 1. Chromatogram of MCPD-phenylboronic acid derivatives in a liquid HVP sample containing 5.2 ppm 3-MCPD. 1 = 3-MCPD-phenylboronate; 2 = 2-MCPD-phenylboronate; 3 = *n*-heptadecane.

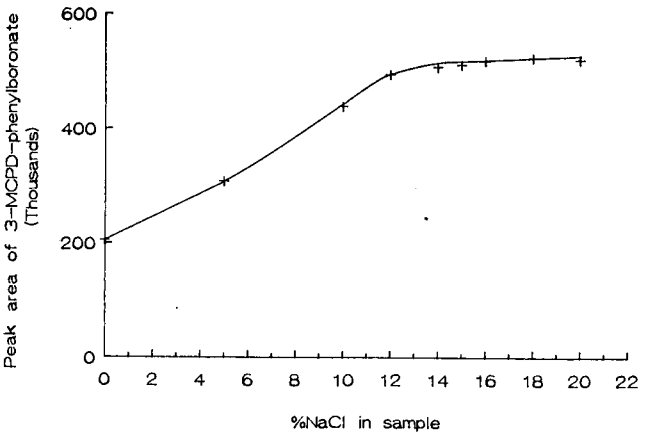

Fig. 2. Influence of the sodium chloride concentration in a sample on the extraction of the 3-MCPD-phenylboronic acid derivative with hexane.

extraction produced a rather clean chromatogram without interfering peaks (Fig. 1). Therefore hexane was selected as the extraction solvent.

The salt concentrations in both test sample and reference sample proved to be quite relevant as there is a clear desalting effect observable in the hexane extraction. A salt concentration in the range 12–20% has been found to be essential. At increasing salt concentrations, the recovery of the phenylboronic derivative of 3-MCPD also increases, reaching a constant level at 12% (Fig. 2). Because most of the samples contain between 13 and 14% salt, dilution of these samples with a 20% sodium chloride solution results in a salt concentration which is always higher then 12%.

The effect of shaking time on extraction was determined. A shaking time of 30 s using a vortex proved to be sufficient.

Linear regression analyses performed on the calibration curve generated when analysing calibration solutions under the described chromatographic conditions revealed excellent linearity (correlation coefficient 0.9999) over the range tested (0.53–13.7 ppm). For sample analyses the standard deviation obtained for 3-MCPD was 0.019 ppm and the repeatability (the maximum absolute difference between two test results, with a probability of 95%, obtained under the same test conditions) was 0.05 ppm, both assessed by eight replicate analyses of a sample containing 0.84 ppm 3-MCPD. The detection limit for the method was 0.2 ppm 3-MCPD.

In conclusion, this proposed method is rapid, sensitive and precise, suited for fast routine determination of 3-MCPD in HVPs.

REFERENCES

1 V. Schurig and D. Wistuba, *Tetrahedron Lett.*, 25 (1984) 5633–5636.
2 R. L. Pesselman and M. J. Feit, *J. Chromatogr.*, 439 (1988) 448–452.
3 L. E. Rodman and R. D. Ross, *J. Chromatogr.*, 369 (1986) 97–103.

Journal of Chromatography, 555 (1991) 315–320
Elsevier Science Publishers B.V., Amsterdam

CHROM. 23 442

Short Communication

Development of a screening method for five sulfonamides in salmon muscle tissue using thin-layer chromatography

GERRY J. REIMER* and AGRIPINA SUAREZ
CanTest Ltd., 1523 West 3rd Avenue, Vancouver, British Columbia V6J 1J8 (Canada)
(First received February 13th, 1991; revised manuscript received May 7th, 1991)

ABSTRACT

A thin-layer chromatographic (TLC) method was developed for the analysis of five sulfonamides [sulfadiazine (SDZ), sulfamerazine (SMRZ), sulfamethazine (SMTZ), sulfadimethoxine (SDMX) and sulfapyridine (SP)] in salmon muscle tissue. "Matrix solid-phase dispersion" was employed whereby the tissue sample was ground with C_{18}-derivatized silica gel. This material was packed into a column and washed with 10% toluene in hexane (discarded) followed by dichloromethane which was evaporated. The residue was chromatographed on a high-performance TLC plate using ethyl acetate–*n*-butanol–methanol–aqueous ammonia (35:45:15:2, v/v). Sulfonamides were detected after spraying the plate with a solution of fluorescamine. Method parameters were determined by analyzing spiked salmon muscle tissue samples. The method detection limits at the 99% confidence level were 0.11, 0.44, 0.07, 0.13 and 0.13 ppm for SDZ, SMRZ, SMTZ, SDMX and SP, respectively. The lowest-detectable levels were approximately 0.04 ppm for SDZ, SMTZ, SDMX and SP, and 0.10 ppm for SMRZ. The average recoveries of analytes were 61, 63, 60, 63 and 57% for SDZ, SMRZ, SMTZ, SDMX and SP, respectively, and were found to be analyst-dependent. The method was found to give linear detector responses for all analytes over spiking levels ranging from 0 to 2 ppm.

INTRODUCTION

The objective of this work was to develop a rapid screening method for the fives sulfonamides sulfadimethoxine (SDMX), sulfadiazine (SDZ), sulfamerazine (SMRZ), sulfamethazine (SMTZ) and sulfapyridine (SP) in salmon muscle tissue. Several methods were reported for the analysis of sulfonamides in other animal tissue using solvent extraction with ion exchange [1] and reveresed-phase column cleanup [2], and also using ion-pair extraction [3]. The major problem with these methods when applied to salmon muscle tissue was the appearance of a pigmented (orange) oil in the final extract, as well as inconsistent recoveries for the above group of sulfonamides.

A method reported by Long *et al.* [4], for the analysis of sulfonamides in pork

0021-9673/91/$03.50

using "matrix solid-phase dispersion"[5] appeared more promising. This paper reports the results of the application of this method to salmon muscle tissue.

EXPERIMENTAL

Materials

Sulfonamides were obtained from Sigma (St. Louis, MO, USA) and Burroughs Wellcome (Kirkland, Canada). Stock (1000 ppm) solutions were prepared as follows: SDZ: Dissolve 0.05 g in 15 ml methanol plus three drops concentrated ammonia. Dilute to 50.0 ml with methanol; SMRZ: dissolve 0.05 g in 15 ml methanol plus 1 ml deionized water; dilute to 50.0 ml with methanol; SMTZ, SDMX and SP: dissolve 0.05 g in 50.0 ml methanol. Working solutions were prepared by diluting the stock solutions with methanol. C_{18}-derivatized silica gel (40 μm, Analytichem, Harbor City, CA, USA) was washed twice with hexane, dichloromethane and methanol. In each wash, the material was placed in a beaker and enough solvent was added to make a free-flowing slurry. This was filtered, and the damp material was placed in the beaker for the next wash. The second dichloromethane slurry was allowed to sit for 20 min to overnight before filtering. After the last methanol wash, the material was partially airdried, so that is was clumpy, but not dripping with methanol, and not a free-flowing powder. This material was placed in a foil-covered beaker and used immediately. Plastic columns were supplied by Brinkman Instruments (Rexdale, Canada); 10-ml plastic syringe barrels may also be used. High-performance thin-liquid chromatographic (HPTLC) plates (Merck; silica gel 60 F_{-254}, 0.25 mm, 10 × 20 cm) were supplied by BDH, Vancouver, Canada. Fluram solution was prepared by dissolving 0.01 g of fluorescamine (Sigma, St. Louis, MO, USA) in 100 ml of acetone and was stored in a freezer. All solvents were HPLC grade. Farmed salmon muscle tissue was obtained from a local market. (We found that wild salmon tissue gave a higher background.)

Extraction procedure

Salmon muscle tissue (0.50 ± 0.08 g) was placed in a glass mortar (*ca.* 236 ml). Spiking solution (10–100 μl) was placed on the tissue (methanol on tissue blanks). One "scoop" (2 g dry weight; *ca.* 5 ml) of methanol-damp C_{18} material was added and the sample was ground with the pestle. After grinding for approximately 20 s the mortar contents were scraped into the center (to ensure thorough mixing) and grinding was continued for approximately 30 s. The contents of the mortar were transferred to a Brinkman column (a 10-ml plastic syringe barrel may also be used) and tightly compacted with a glass rod (4-mm diameter).

The column was placed on a vacuum manifold and washed with 8 ml of 10% toluene in hexane (≈ 1 drop/s; discard), and aspirated dry. A glass test tube, containing a folded Wathmann No. 1 filter paper (4.25 cm) inserted ≈ 2 cm below the top of the tube, was placed under the column, and the analytes were eluted with 8 ml of dichloromethane (≈ 1 drop/s). The filter paper served to catch any C_{18} material from the column. (In-line PTFE syringe filters clogged when dichloromethane was added.) The dichloromethane eluate was transferred to a plastic centrifuge tube (15 ml) and evaporated to dryness under a stream of nitrogen using a 40°C water bath. The wall of the tube was washed wit 2 × 1 ml methanol; each wash was evaporated to dryness.

TLC analysis

Methanol (50 μl) was added to the sample residue and the contents were vortex-mixed (10 s) and sonicated (5 min). The solution (*ca.* 7 μl) was spotted on an activated (65°C, 12 h) HPTLC plate using a glass capillary tube (75 mm × 0.56 mm I.D.). During spotting the plate was warmed to *ca.* 70°C. The sports (diameter less than 4 mm) were "focused" by developing the plate in a methanol bath to ≈ 2 mm above the origin. The plate was airdried in a fume hood for ≈ 10 min. During this time the chromatography bath was prepared: ethyl acetate–*n*-butanol–methanol–aqueous ammonia (30%) (35:45:15:2, v/v). The plate was developed to a height of 8.5 cm, airdried for *ca.* 10 min (fume hood), and sprayed evenly (side-to-side motion) with Fluram solution, such that the plate was saturated, but not dripping. The sprayed plate was airdried for *ca.* 30 min and scanned with a Camag II densitometer (equipped with an IBM XI-compatible computer) in the fluorescence mode (366 nm excitation). The dried plate could be covered with a glass plate and stored in a freezer overnight before scanning.

Quantitation

The method detection limit (MDL) was determined from the equation

$$\mathrm{MDL} = St$$

where t is the students' "t" value appropriate for the desired confidence level and number of observations ($t = 3.143$ for $n = 7$, and 99% confidence level [6]), and S is the standard deviation of the analytical results of a group of samples spiked at one level. Seven tissue samples were spiked with all analytes at 0.1 ppm, and analyzed concurrently with seven samples spiked with methanol only (tissue blanks). Analyte peak arreas were corrected for tissue interferences by subtracting the average ($n = 7$) peak areas of the interferences found in the tissue blanks.

Recoveries of analytes from salmon muscle tissue were determined using a single-point calibration method. A standard containing all five sulfonamides was spotted on the same plate as the samples, such that groups of three to four samples were bracketed by pairs of standards spots. The amounts of analytes in each standard spot corresponded to that of 100% recovery from the spiked tissue samples.

RESULTS AND DISCUSSION

Chromatography

Baseline resolution of all analytes was achieved at a tissue spiking level of 0.1 ppm as shown in Fig. 1. The resolution of SDMX and SP was sensitive to the age of the TLC bath. Best results were obtained if the bath was prepared just before use. A tissue interference was observed for SMRZ (Fig. 1) which resulted in a higher detection limit for this analyte. Smaller interferences were observed for SDMX and SP.

MDL

With the exception of SMRZ, MDL values ranged from 0.07 to 0.13 ppm (Table I). The high MDL of SMRZ (0.44 ppm) was due to the tissue interference observed for this analyte (Fig. 1), the area of which was found to be quite variable in

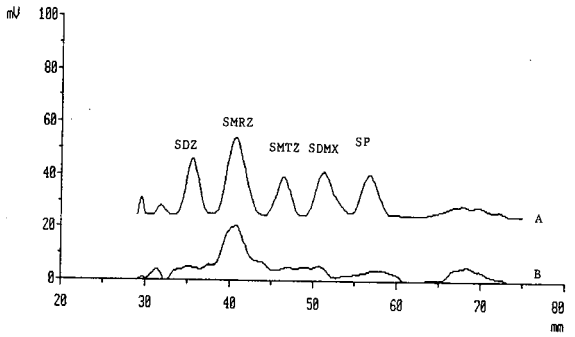

Fig. 1. Chromatograms (densitometer traces) of spiked salmon muscle tissue samples. (A) Spiking level = 0.1 ppm (all analytes); (B) 0 ppm (tissue blank). Detection at 366 nm.

the tissue blanks (coefficient of varation = 79%). These MDL values were calculated using a high confidence level (99%). The lowest-detectable levels, on the other hand, were approximately 0.04 ppm for SDZ, SMTZ, SDMX and SP, and 0.1 ppm for SMRZ.

Before scanning, plates were visually assessed under long-wavelength UV light. Spiking levels down to approximately 0.1 ppm could be observed in this manner.

Recovery

Recoveries of analytes from salmon muscle tissue were determined at two spiking levels: 0.5 and 2.0 ppm. with five replicates at each level. Recoveries did not vary significantly with spiking level. The overall average recoveries ranged from 57 to 63% for the five sulfonamides (Table I). On closer examination, it was found that recovery was analyst-dependent. The steps of sample grinding and column compacting were performed by two analysts, denoited as A and B. Analyst A used a larger and heavier pestle, and was also physically larger and heavier than analyst B. Recoveries of ana-

TABLE I

ANALYTICAL RESULTS FOR THE FIVE SULFONAMIDES IN SPIKED SALMON MUSCLE TISSUE

Compound	MDL[a] (ppm)	Correlation coefficient[b]	Average recoveries[c]		
			Analyst A ($n=5$)	Analyst B ($n=5$)	Overall ($n=10$)
SDZ	0.11	0.983	73 ± 7	50 ± 3	61 ± 12
SMRZ	0.44	0.983	76 ± 7	50 ± 3	63 ± 14
SMTZ	0.07	0.949	71 ± 5	49 ± 2	60 ± 12
SDMX	0.13	0.858	72 ± 8	54 ± 3	63 ± 11
SP	0.13	0.946	69 ± 6	45 ± 3	57 ± 12

[a] Calculated at the 99% confidence level.
[b] Spiking levels: 0.10, 0.20, 0.30, 0.40, 1.0, 2.0 ppm. Two replicate samples analyzed per level.
[c] See text.

lyst A were consistently higher than those of analyst B (Table I). The average recoveries of analyst A were approximately 10% higher than the overall averages, ranging from 69 to 76% for the five sulfonamides (Table I). It was also observed that the extracts of analyst A, after evaporation of dichloromethane, contained slightly less fat/oil than those of analyst B.

It was speculated that analyst A applied a larger force to the pestle during grinding, resulting in more efficient distribution of the tissue sample over the C_{18} surface, and more efficient partitioning of the analytes (and endogenous substances) between the solvent and stationary phase furing column chromatography. Recoveries were not improved by using a more polar elution solvent (20% ethyl acetate in dichloromethane).

In the analysis of pork tissue (results not shown) it was found that recovery was influenced by the methanol content of the C_{18} material, and by the type of mortar and pestle used. Lower recoveries were observed using: (1) dry (free-flowing) C_{18} compared to methanol-damp material, and (2) a procelain mortar and pestle compared to a glass apparatus. In addition, it was shown that the duration of grinding (between 30 s and 2 min) did not affect the recovery of sulfonamides from prork tissue. These results were not validated for salmon musle tissue.

Recoveries of the five sulfonamides from wild trout (a salmonid) musle tissue were found to be 10–20% higher than from salmon muscle tissue (data not shown). This may be related to the relatively high cholesterol level in salmon muscle tissue [7], although its higher fat/oil content [8] may also be important.

Precision

The observed analyst dependency of recovery affected the precision of the results. The standard deviations of average recoveries of samples processed by a single analyst ranged from 2 to 8% (average = 5%), whereas the overall standard deviations of both sets of recoveries (analysts A and B) were significantly higher, ranging from 11 to 14% (average = 12%) (Table I).

Method linear range

Detector response was found to be linear for eacht analyte over a spiking range of 0.10 to 2.0 ppm, with correlation coefficients ranging from 0.858 to 0.983 (average = 0.944) (Table I).

ACKNOWLEDGEMENTS

This work was funded by the Department of Health and Welfare. Discussions with Dr. S. A. Barker were very helpful during method development work. Janet Milton assisted with the preparation of this manuscript.

REFERENCES

1 N. Haagsma, R. J. Nooteboom, B. G. M. Gortemaker and M. J. Mass, *Z. Lebesm.-Unters.-Forsch.*, 181 (1985) 194–197.
2 M. Horie, K. Saito, Y. Hoshino, N. Nose, N. Hamada and H. Nakazawa, *J. Chromatogr.*, 502 (1990) 371–378.
3 G. Weiss, P. D. Duke and L. Gonzales, *J. Agric. Food Chem.*, 35 (1987) 905–909.

4 A. R. Long, L.C. Hsieh, M. S. Malbrough, C. R. Short and S. A. Barker, *J. Agric. Food Chem.*, 38 (1990) 423–426.
5 A. R. Long, C. R. Short and S. A. Barker, *J. Chromatogr.*, 502 (1989) 87–94.
6 *Federal Register*, Environmental Protection Agency, Washington, D.C., 49 (209) 1984, appendix B to part 136, revision 1.11.
7 J. A. Walisser, H. M. Burt, T. A. Valg, D. D. Kitts and K. M. McErlane, *J. Chromatogr.*, 518 (1990) 179–188.
8 J. A. Nettleton, *Aquacult. Mag.*, January–February (1990) 34.

Journal of Chromatography, 555 (1991) 321–328
Elsevier Science Publishers B.V., Amsterdam

CHROM. 23 392

Short Communication

Isotachophoretic analyser with options for operational electrolyte selection and repeated analysis

TAKESHI HIROKAWA*, YASURO YOKOTA, HITOSHI TAKABA, KIYOSHI NAKAHARA and YOSHIYUKI KISO

Applied Physics and Chemistry, Faculty of Engineering, Hiroshima University, Kagamiyama 1, Higashi-hiroshima 724 (Japan)

(First received February 13th, 1991; revised manuscript received April 23rd, 1991)

ABSTRACT

A prototype of an isotachophoretic analyser with options for electrolyte selection and repeated analysis was constructed, which might be useful for the optimization of separation and the measurement of qualitative indices at different pH values for mobility and pK_a evaluation. After a sample mixture had been injected into the system it was separated and pushed back to the original position, and this cycle was repeated varying the leading electrolyte. The sample was pushed back by the use of the counter flow technique. The process of repeated analysis was monitored by the use of a 32-channel UV photometric zone detection system. It was found that the flow-rate of push-back was decisively important for good reproducibility in repeated analysis. The efficiency of the apparatus was demonstrated with a model mixture of anions.

INTRODUCTION

In electrophoresis it frequently happens that some of the sample constituents cannot be separated owing to their similar effective mobilities with the operational electrolyte system used. If the constituents are weak electrolytes, the separability might be improved by applying another appropriate electrolyte system of different pH [1,2]. On the other hand, in order to evaluate mobility and pK_a isotachophoretically, the quantitative indices must be measured under various pH conditions.

In such instances the sample must be injected and separated again after changing the operational electrolyte. Usually this process is carried out manually and it is time consuming because the electrode compartment has to be rinsed thoroughly, even if the electrolyte was ready. Recently Pospichal *et al.* [3] reported a convenient method for changing the operational pH conditions by using a three-pole column (a separation column with three electrodes), where the required operational leading electrolyte can be generated. The migration current was fed via two electrolyte

0021-9673/91/$03.50

compartments filled with solutions of different pH and the fraction of the current controlled the pH of the new leading electrolyte. A similar technique was also applied in capillary zone electrophoresis [4]. The advantage is that numerous leading electrolytes with different pH values can be generated from two basic electrolytes.

This paper describes another method for changing the electrolyte conditions, selecting from several kinds of the leading solutions prepared beforehand. The analysis of the same sample as the initially injected one can be repeated: after a sample mixture has been injected into the system, the mixture is separated and subsequently pushed back to the injection position, and the procedure is repeated varying the leading electrolyte. A well established counter-flow technique [1] is utilized for this purpose. In this paper, the design and functioning of a prototype of an isotachophoretic analyser with such a repeating option is described.

EXPERIMENTAL

Apparatus

A schematic diagram of the apparatus is shown in Fig. 1. The construction of the apparatus was not very different from the ordinary one, except for a pump to supply leading electrolyte and three T-branches (J1, J2 and J3) being added to the separation tube. The other feature of this apparatus is the electrolyte supply system: in this apparatus the electrode compartment (E in Fig. 1), which is usually the leading electrolyte compartment, no longer contains the leading solution but an arbitrary high-conductivity solution. A 10 m*M* sodium chloride solution was used in this experiment. The actual leading electrolyte was the solution filled between J1 and J2 in the PTFE separation tube (30 cm × 1 mm I.D.). The leading electrolyte selected from reservoirs 1–6 can be flowed continuously from J1 to J2 during the analysis by the use of a micropump [Model PUD-008 double-plunger type; Gasukuro Kogyo (Tokyo, Japan)]. The flow-rate was 6.4 μl/min and the linear velocity of the flow (8.2 cm/min)

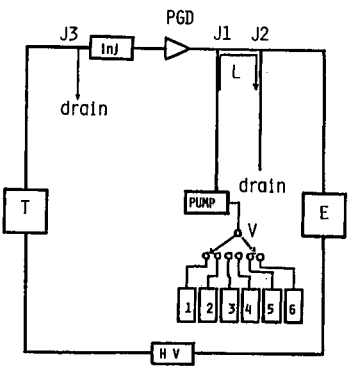

Fig. 1. Schematic diagram of isotachophoretic analyser equipped with operational electrolyte exchange system. E = electrolyte solution compartment (the actual leading electrolyte was filled between J1 and J2); T = terminating electrolyte compartment; inj = injection port; PGD = potential gradient detector; J1 = leading electrolyte inlet; J2 = leading electrolyte outlet; J3 = drain; V = valves to change operational leading electrolyte; 1–6 = leading electrolyte reservoirs; PUMP = double-plunger pump; HV = high-voltage power supply.

was 2.5 times greater than the migration velocity of sodium ions. The overflow was discarded from J2. As sodium ions migrating in the opposite direction to the samples are swept away by the flow, the isotachophoretic equilibrium was not disturbed by the use of sodium chloride solution. Consequently, the leading electrolyte in the tube connecting J1 and J2 (20 cm × 1 mm I.D.) regulated the isotachophoretic separation of the samples.

The valves and the electrolyte compartments used were those of a Shimadzu IP-1B isotachophoretic analyser. A potential gradient detector instrument (PGD) and the power supply was those for a Shimadzu IP-2A.

Method of leading electrolyte exchange

As the inner volume of the tube (J1–J2) was very small, the exchange of the electrolyte was very rapid and smooth compared with the case when the leading electrolyte was filled in the electrode compartment of E in Fig. 1. It took 5 min at the above flow-rate.

Fig. 2 illustrates the principle of the repeated separation. At time $t1$, sample (S) was separated using the leading electrolyte solution L1 and the first detection was just finished. The solution L1 was fed continuously from J1 and was drained from J2, while J3 was closed except when the counter flow technique [1] was utilized to improve the separation. The leading electrolyte L1 was replaced with the different electrolyte L2 as follows: first J3 was closed and L1 in the separation tube (J1–J2) was replaced with L2. Then at time $t2$, J3 was opened and the sample zone was pushed back on applying the migration current. At time $t3$, the sample zone was pushed back to the end of the separation tube. After J3 had been closed, the separation was repeated under the electrolyte condition of L2. The second detection was finished at time $t4$. Thus the same sample can be analysed repeatedly using different leading electrolytes. Under a typical operation, the time necessary for the electrolyte exchange and the push-back of the initial sample zone was 5–10 min.

Apparently from Fig. 1, at time $t1$ the present system has a restriction on the amount of sample, which depends on the volume of the separation tube between PGD and J1. If the leading side of the sample zone reached one of side channels J1,

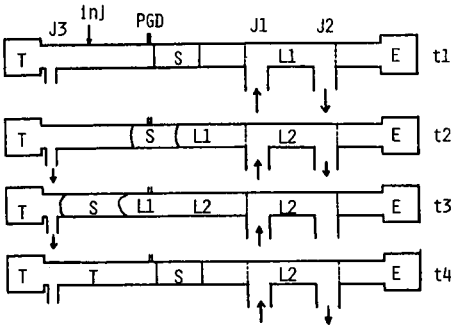

Fig. 2. Principle of the leading electrolyte exchange and repeated separation. E = NaCl solution; L1 = leading electrolyte 1; L2 = leading electrolyte 2; S = sample zone; T = terminating electrolyte. J1, J2 and J3 as in Fig. 1.

the sample would be swept away from the separation tube. Similarly at time $t3$, if the sample was pushed back too far, part of it would be drained away from J3. In the present experiment, this situation was avoided by using coloured samples. For general samples, however, an appropriate "tell-tale" detector should be placed at the leading side of J3.

The mixing of L1 and L2 in the separation tube was inevitable. However, it caused no serious problem if the pH of the leading electrolyte (pH_L) was changed appropriately, as discussed later.

Samples and electrolyte system

Two anionic model mixtures were used. One contained 4,5-dihydroxy-3-(*p*-sulphophenylazo)-2,7-naphthalenedisulphonic acid (SPADNS), monochloroacetic acid (MCA) and picric acid (PIC). The separation behaviour in repeated analysis of the mixture was monitored by the use of a Shimadzu potential gradient detector and the 32-channel UV photometric zone detection system [5]. In the latter detection system, the array of 32 photometric cells was set along the separation tube. The cell interval was *ca.* 5 mm (16.6 cm for 32 channels).

The other model mixture obtained ten constituents, oxalic acid, bromic acid, hypophosphorous acid, bromoacetic acid, succinic acid, 2-hydroxyisobutyric acid, benzoic acid, acetic acid, glutamic acid and butyric acid. The separation efficiency of the present apparatus was examined for this rather complex mixture.

The leading electrolytes were 10 m*M* hydrochloric acid buffered by adding β-alanine (pH 3.6 and 4) and ε-aminocaproic acid (pH 4.4). Hydroxypropylcellulose (HPC) was added to the leading electrolyte (0.02%). The terminator was 10 m*M* caproic acid.

Chemicals were obtained from Tokyo Kasei Kogyo (Tokyo, Japan) in the purest form available. pH measurements were carried using a Horiba Model F7ss expanded pH meter. Data processing was carried out with an NEC PC9801VX microcomputer.

RESULTS AND DISCUSSION

Reproducibility of zone length

First the reproducibility of the time-based zone length was examined for the repeated analysis of the same kind of sample and the leading electrolyte (pH 3.6). Fig. 3 shows the PGD trace of the repeated separation of SPADNS, MCA and PIC. When the counter flow-rate for push-back was 12.2 μl/min, the total zone length agreed with that of the initial separation. On the other hand, when the counter flow-rate was 43.8 μl/min, the total zone length decreased to 80% of the initial length. This suggested that when the flow-rate for push-back was high, the separated samples mixed with the leading and/or terminating electrolytes and the initial sample amount could not be fully recovered until the next detection.

In order to establish what happened in the push-back process with a high flow-rate, the repeated analysis of SPADNS, MCA and PIC was monitored by use of the 32-channel UV photometric detector. Fig. 4 shows the isotachopherogram obtained. The base lines of the UV signals show the position of the detectors. The migration order was SPADNS (S), MCA (M) and PIC (P). It should be noted that

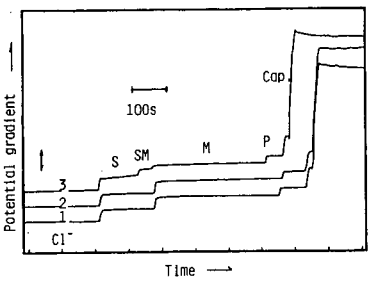

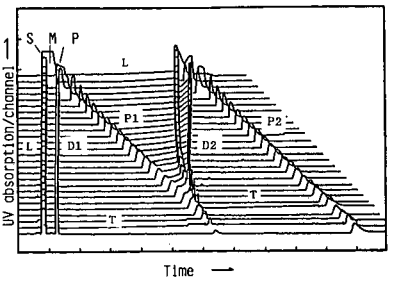

Fig. 3. Observed isotachopherograms of SPADNS (S), monochloroacetic acid (M) and picric acid (P). (1) First detection; (2) second detection (counter flow-rate for push-back = 12.2 μl/min); (3) third detection (counter flow-rate for push-back = 43.8 μl/min). The sample amounts were 7.2 nmol (S), 35.7 nmol (M) and 6.7 nmol (P). The migration current was 100 μA.

Fig. 4. Observed transient isotachopherograms of SPADNS (S), monochloroacetic acid (M) and picric acid (P) by the use of the 32-channel UV photometric zone detection system. D1 = First detection; P1 = first push-back; D2 = second detection; P2 = second push-back (counter flow-rate for push-back = 40.7 μl/min). The sample amounts were 5.8 nmol (S), 28.8 nmol (M) and 5.4 nmol (P). The migration current was 100 μA.

MCA (M) was UV transparent. In Fig. 4, D1 shows the first detection of the isotachophoretically separated steady zones. The boundaries between the leading and SPADNS zones were rearranged at the same abscissa position to demonstrate the exchange of the individual zone length at the transient state.

After the sample zones had reached to the final cell (No. 32), the zones were pushed back to cell No. 2 by applying a counter flow. A migration current (100 μA) was also applied during the push-back. The flow-rate was 40.7 μl/min. P1 shows the above process. Then the counter flow for push-back was stopped and the separation was restarted. D2 shows the second detection and P2 the second push-back.

Apparently from the patterns of the push-back processes (P1 and P2), the SPADNS, MCA and PIC zones, once separated, merged into a mixed zone. The gradual decrease in the UV absorption in the P1 process suggested that the concentrations of SPADNS and PIC decreased significantly, *i.e.*, the separated zones were perturbed and diluted by the counter flow. In the P1 and P2 process in Fig. 4, the left-hand side of the peaks corresponds to the boundary between the terminating zone (T) and the pushed zone. The boundary was steeper than the boundary between the leading zone (L) and the pushed zone. Moreover, the base lines of the leading zone drifted during the push-back, suggesting that the unrecovered samples existed mainly in the leading zone. This observation could explain the shortening of the zone length in Fig. 3 when the counter flow-rate was high. Considering these results, the counter flow-rate for the push-back of sample zones was in the range 10–20 μl/min, depending on the sample constituents. If a higher migration current was applied, the counter flow-rate might be increased because of the increase in the self-correction effect of the sample zone.

Counter flow technique to improve separation

When the sample amount was relatively large, the so-called counter flow technique is useful for improving the separability [1]. As the capillary length was fixed in

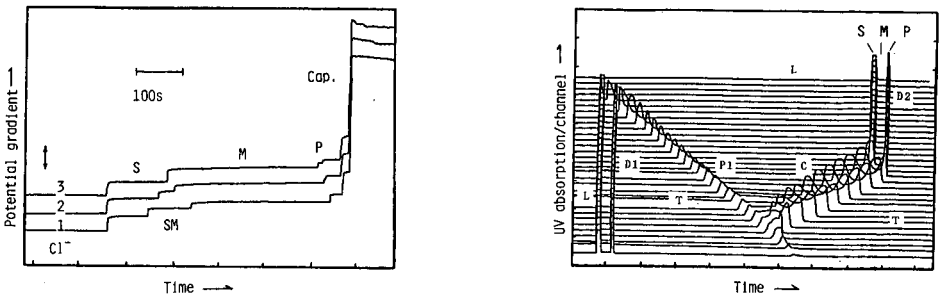

Fig. 5. Observed isotachopherograms of SPADNS (S), monochloroacetic acid (M) and picric acid (P). (1) First detection without counter flow; (2) second detection with 63% counter flow (2.2 μl/min, 8 min); (3) third detection with 17-min counter flow. The sample amounts were 28.6 nmol (S), 142.8 nmol (M) and 26.6 nmol (P). The migration current was 100 μA.

Fig. 6. Observed transient isotachopherograms of SPADNS (S), monochloroacetic acid (M) and picric acid (P) by the use of the 32-channel UV photometric zone detection system. D1 = First detection; P1 = first push-back; C = counter flow applied to improve the separability; D2 = second detection. The sample amounts were 5.8 nmol (S), 29.1 nmol (M) and 5.8 nmol (P). The migration current was 100 μA.

this apparatus, this technique was utilized. Fig. 5 shows the effect of the counter flow for a mixture of SPADNS (28.6 nmol), MCA (142.8 nmol) and PIC (26.6 nmol). As shown by trace 1 in Fig. 5, a mixed zone of SPADNS and MCA was formed (SM) when the counter flow was not applied. Then the sample zones were pushed back and separated again by applying a 63% counter flow (2.2 μl/min) for 8 min. On the trace obtained (2 in Fig. 5), however, the mixed zone still existed. Analysis was repeated by applying a counter flow for 17 min. The separation was complete, as shown by trace 3 in Fig. 5.

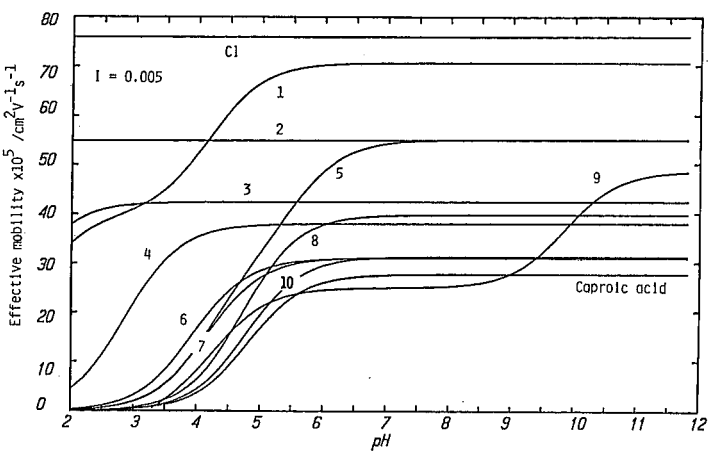

Fig. 7. Calculated effective mobility *vs.* pH curves for (1) oxalic acid, (2) bromic acid, (3) hypophosphorous acid, (4) bromoacetic acid, (5) succinic acid, (6) 2-hydroxyisobutyric acid, (7) benzoic acid, (8) acetic acid, (9) glutamic acid and (10) butyric acid. The effective mobility of the leading chloride ion and the terminating caproate ion was also plotted. Temperature = 25°C; ionic strength, 0.005.

The improvement of the separability by this method was observed by use of the 32-channel UV photometric detector for the same samples. Fig. 6 shows the observed transient isotachopherogram. D1 shows the first detection of the isotachophoretically separated zones and P1 shows the push-back process. After the sample zones had reached cell No. 2, the counter flow was reduced to 63% and the separation was restarted (C). D2 shows the second detection after the counter flow process. Apparently the separability was increased by applying the counter flow technique.

Repeating analysis using different operational systems

Finally, the isotachophoretic separation was repeated varying the leading electrolyte. Fig. 7 shows the effective mobility–pH curves for ten anionic constituents together with caproic acid as the terminator and chloride ion as the leading ion. The ionic strength was 0.005. As the curves cross each other at low pH, it seemed that complete separation with one electrolyte system was difficult. In this experiment, the pH of the leading electrolyte (pH_L) used was 3.6, 4.0 and 4.4 and was changed in the above order. As the mixing of the different leading electrolytes was inevitable in the present method, this pH_L order was very important for minimizing unfavourable effects. The buffers used were β-alanine (pK_a = 3.552, pH_L = 3.6 and 4) and ε-aminocaproic acid (pK_a = 4.373, pH_L = 4.4). Although these buffers coexisted in the separation tube when the pH_L was changed from 4.0 to 4.4, β-alanine has no serious effect on the sample zone because of its small effective mobility at pH 4.4.

Fig. 8 shows isotachopherograms observed with the use of a PGD. D1, D2 and D3 show the first, second and third detections and P1 and P2 show the PGD traces of the push-back process. The counter flow technique was utilized in order to improve the separability after changing the leading electrolyte (*ca.* 20 min). The observed isotachopherograms agreed well with those obtained individually in the usual way, confirming the smooth exchange of the electrolyte conditions in the present apparatus. Apparently from Fig. 8, the separability of the samples varied depending on the pH of the leading electrolyte. For example, the separation of samples 8 and 9 at pH 3.6, 1 and 2 at pH 4.0 and 5 and 6 at pH 4.4 could be improved at the different pH values.

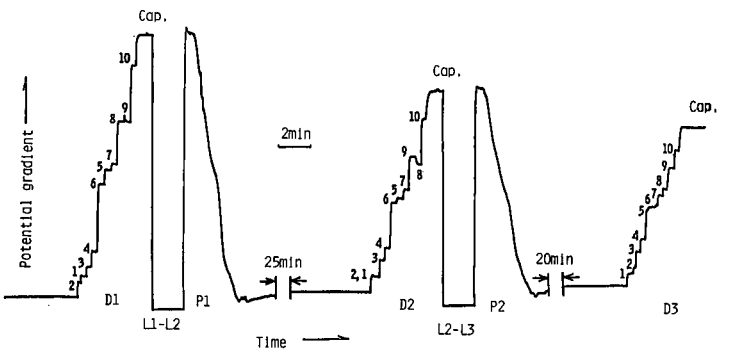

Fig. 8. Isotachopherograms observed for samples 1–10 shown in Fig. 7 obtained by the use of a PGD. The separation was repeated for the same sample, changing the leading electrolyte (pH 3.6, 4.0 and 4.4). D1, D2 and D3 = first, second and third detection, respectively; P1 and P2 = push-back process. Cap. = caproic acid (terminator). For the details, see text.

In high-performance liquid chromatography, the use of various types of eluents in a run is a common technique. Undoubtedly this technique contributes to the high separability. Similarly in electrophoresis, a new option for repeated analysis by varying the leading electrolyte might improve the separability. A fully automated repeating analyser might be possible on the basis of the proposed method in combination with a leading electrolyte generator [3].

REFERENCES

1 F. M. Everaerts, J. L. Beckers and Th. P. E. M. Verheggen, *Isotachophoresis*, Elsevier, Amsterdam, 1976.
2 P. Bocek, M. Deml, P. Gebauer and V. Dolnik, *Analytical Isotachophoresis*, VCH, Weinheim, 1988.
3 J. Pospichal, M. Deml, P. Gebauer and P. Bocek, *J. Chromatogr.*, 470 (1989) 43.
4 P. Bocek, M. Deml, J. Pospichal and J. Sudor, *J. Chromatogr.*, 470 (1989) 309.
5 T. Hirokawa, K. Nakahara and Y. Kiso, *J. Chromatogr.*, 463 (1989) 39.

Journal of Chromatography, 555 (1991) 329
Elsevier Science Publishers B.V., Amsterdam

CHROM. 23 451

Book Review

Ion exchange in analytical chemistry, by H. E. Walton and R. D. Rocklin, CRC Press, Boca Raton, FL, 1990, VII + 229 pp., price £ 52.50, ISBN 0-8493-6199-0.

The stated purpose of this book is to evaluate the role of ion exchange and ion-exchanging materials in chemical analysis. It describes some of the advances in high-performance ion-exchange chromatography, now known simply as ion chromatography. It also reviews some of the older methods of separation and preconcentration of metallic species that unfortunately are often ignored these days.

The book starts with an interesting historic review of early ion-exchange techniques in Chapter 1. Chapters 2 and 3 provide rather detailed descriptions on modern ion-exchanging materials and their properties. This is followed by a long chapter on ion chromatography. Chapter 5 briefly touches on ion-pair chromatography while Chapter 6 provides a very interesting review on the less popular ligand-exchange chromatography. The applications of ion-exchange chromatography to the separation of biological molecules are summarized in Chapter 7. Chapters 8 and 9 review methods for separation and preconcentration of metal ions using ion-exchange materials. The book ends with miscellaneous analytical uses of ion exchange in Chapter 10.

Almost no material is included on the hardware or experimental details of ion exchange. This is a wise choice because it permits coverage of many interesting and useful topics in this relatively short book. The book is generally well written and very readable. The topics are presented in a logical order. At times, more modern material could have been selected to illustrate the relevant principles. For example, the only numerical data on ion-exchange selectivity (p. 49) are quite old and apply to resins that no longer find much use in modern chromatography. The discussion in Chapter 4 strongly stresses Dionex methods and philosophy of ion chromatography. More examples from other sources would have made this chapter more scientific and convincing.

Ames, IA (USA)

JAMES S. FRITZ
JIAN CHEN

Author Index

PUBLICATION SCHEDULE FOR 1991

Journal of Chromatography and Journal of Chromatography, Biomedical Applications

MONTH	D 1990–M 1991	J	J	A	S	O	N	D
Journal of Chromatography	Vols. 535–545/1	545/2 546/1 + 2 547/1 + 2	548/1 + 2 549/1 + 2 550/1 + 2	552/1 + 2 553/1 + 2 554/1 + 2 555/1 + 2	556/1 + 2 557/1 + 2 558/1	558/2 559/1 + 2		
Cumulative Indexes, Vols. 501–550				551/1 + 2				
Bibliography Section	560/1	560/2			561/1			561/2
Biomedical Applications	Vols. 562–566	567/1	567/2 568/1	568/2	569/1 + 2 570/1	570/2	571/1 + 2	572/1 + 2

INFORMATION FOR AUTHORS

(Detailed *Instructions to Authors* were published in Vol. 522, pp. 351–354. A free reprint can be obtained by application to the publisher, Elsevier Science Publishers B.V., P.O. Box 330, 1000 AH Amsterdam, The Netherlands.)

Types of Contributions. The following types of papers are published in the *Journal of Chromatography* and the section on *Biomedical Applications:* Regular research papers (Full-length papers), Review articles and Short Communications. Short Communmications are usually descriptions of short investigations, or they can report minor technical improvements of previously published procedures; they reflect the same quality of research as Full-length papers, but should preferably not exceed six printed pages. For Review articles, see inside front cover under Submission of Papers.

Submission. Every paper must be accompanied by a letter from the senior author, stating that he/she is submitting the paper for publication in the *Journal of Chromatography*.

Manuscripts. Manuscripts should be typed in double spacing on consecutively numbered pages of uniform size. The manuscript should be preceded by a sheet of manuscript paper carrying the title of the paper and the name and full postal address of the person to whom the proofs are to be sent. As a rule, papers should be divided into sections, headed by a caption (*e.g.*, Abstract, Introduction, Experimental, Results, Discussion, etc.). All illustrations, photographs, tables, etc., should be on separate sheets.

Introduction. Every paper must have a concise introduction mentioning what has been done before on the topic described, and stating clearly what is new in the paper now submitted.

Abstract. All articles should have an abstract of 50–100 words which clearly and briefly indicates what is new, different and significant.

Illustrations. The figures should be submitted in a form suitable for reproduction, drawn in Indian ink on drawing or tracing paper. Each illustration should have a legend, all the *legends* being typed (with double spacing) together on a *separate sheet*. If structures are given in the text, the original drawings should be supplied. Coloured illustrations are reproduced at the author's expense, the cost being determined by the number of pages and by the number of colours needed. The written permission of the author and publisher must be obtained for the use of any figure already published. Its source must be indicated in the legend.

References. References should be numbered in the order in which they are cited in the text, and listed in numerical sequence on a separate sheet at the end of the article. Please check a recent issue for the layout of the reference list. Abbreviations for the titles of journals should follow the system used by *Chemical Abstracts*. Articles not yet published should be given as "in press" (journal should be specified), "submitted for publication" (journal should be specified), "in preparation" or "personal communication".

Dispatch. Before sending the manuscript to the Editor please check that the envelope contains four copies of the paper complete with references, legends and figures. One of the sets of figures must be the originals suitable for direct reproduction. Please also ensure that permission to publish has been obtained from your institute.

Proofs. One set of proofs will be sent to the author to be carefully checked for printer's errors. Corrections must be restricted to instances in which the proof is at variance with the manuscript. "Extra corrections" will be inserted at the author's expense.

Reprints. Fifty reprints of Full-length papers and Short Communications will be supplied free of charge. Additional reprints can be ordered by the authors. An order form containing price quotations will be sent to the authors together with the proofs of their article.

Advertisements. Advertisement rates are available from the publisher on request. The Editors of the journal accept no responsibility for the contents of the advertisements.